NASA Technical Memorandum 102254

Final Reports of the U.S. Experiments Flown on the Soviet Biosatellite Cosmos 1887

February 1990

(NASA-TM-102254) THE US EXPERIMENTS FLOWN ON THE SOVIET BIOSATELLITE COSMOS 1887 Final Reports (NASA) 501 p CSCL 06C

N90-26452
--THRU--
N90-26478
Unclas
G3/51 0280467

NASA
National Aeronautics and Space Administration

NASA Technical Memorandum 102254

Final Reports of the U.S. Experiments Flown on the Soviet Biosatellite Cosmos 1887

Edited by
James P. Connolly, Richard E. Grindeland, and Rodney W. Ballard
Ames Research Center, Moffett Field, California

February 1990

National Aeronautics and
Space Administration

Ames Research Center
Moffett Field, California 94035

TABLE OF CONTENTS

PRECEDING PAGE BLANK NOT FILMED

PREFACE

On September 29, 1987, the Soviet Union launched Cosmos 1887, an unmanned spacecraft carrying biological and radiation physics experiments from nine countries. This mission included 26 U.S./U.S.S.R. joint experiments and involved more than 50 NASA-sponsored scientists.

Cosmos 1887 represents the sixth consecutive Soviet biosatellite mission involving U.S./U.S.S.R. joint experiments. Earlier flights included Cosmos 782 in November 1975 (NASA TM 78525), Cosmos 936 in August 1977 (NASA TM 78526), Cosmos 1129 in September 1979 (NASA TM 81289), Cosmos 1514 in December 1983 (NASA TM 88223) and Cosmos 1667 in July 1985. These previous Cosmos biosatellite missions, involving experiments with monkeys, rats, plants and insects, have provided scientists with information on how the basic biology of living organisms is affected by the space environment.

Though the goals of Cosmos 1887 were similar in many respects to the five previous flights, the task of coordinating and performing this large number of experiments required extensive cooperation and communication among U.S. and U.S.S.R. representatives. The science and engineering specialists within the United States' academic community, the Soviet Union's Institute of Biomedical Problems and NASA worked together as a team with dedication and good will, enabling both countries to achieve scientific results which are contributing to man's further understanding of space biology and radiation physics.

It has been a pleasure to be part of this Cosmos 1887 team and to work closely with our Soviet colleagues. On behalf of all those who participated in the Cosmos 1887 Biosatellite Mission, both from the U.S. science community and from NASA, I wish to thank the Soviet Union for making this opportunity possible; and, especially, may I express sincere appreciation to our Soviet counterparts, and to all their staff, who assisted with the execution of these joint experiments.

James P. Connolly
Cosmos Project Manager
NASA Ames Research Center

PRECEDING PAGE BLANK NOT FILMED

SUMMARY

Cosmos 1887 was launched on September 29, 1987, containing biological and radiation experiments from the Soviet Union, the United States and seven other countries. The biological payload included two young male Rhesus monkeys, ten adult male Wistar rats, Drosophila, Indian Grasshoppers, beetles, guppies, Hynobiidae, Chlorella ciliates, newts and corn.

One Rhesus monkey's feeder stopped working two days into the flight and extra juice had to be provided for partial nourishment. The monkey's condition was carefully monitored by Soviet specialists and eventually a decision was made to terminate the mission after 12 1/2 days. The biosatellite returned to Earth on October 12, 1987.

A system malfunction, during the reentry procedure, caused the Cosmos 1887 spacecraft to land approximately 1800 miles beyond the intended landing site. All specimens were recovered, except for the guppies, and returned to the planned landing site. This delayed the start of the postflight procedures by approximately 44 hours. Further information on the conditions at landing and on postflight activities is included in the Mission Operations portion of this document.

U.S. and U.S.S.R. specialists jointly conducted 26 experiments on this mission, including the postflight transfer of data, hardware and biosamples to the United States. The U.S. responsibilities for this flight included the development of flight and ground-based hardware, development of rat tissue sampling procedures and techniques, verification testing of hardware and experimental procedures, and postflight transfer of tissue and data to the United States for analysis. The U.S. experiments examined the effect of spaceflight on adaptation of the musculoskeletal, nervous, immune, cardiovascular, hepatic and endocrine systems. In addition to the biological experiments, the United States placed eight radiation detector packages inside and outside the spacecraft to measure total radiation doses during the flight and to evaluate spacecraft shielding.

A description of the Cosmos 1887 mission is presented in this document including preflight, on-orbit, and postflight activities, and Final Science Reports for each of the U.S./U.S.S.R. joint experiments.

PRECEDING PAGE BLANK NOT FILMED

I. COSMOS 1887 MISSION DESCRIPTION

A. INTRODUCTION

The Cosmos 1887 biosatellite was launched on September 29, 1987, at 1550 hours Moscow time with recovery at 0703 hours on October 12th for a total mission duration of 12 1/2 days. More than fifty NASA-sponsored scientists from Ames Research Center (ARC) and from universities throughout the nation were involved directly in 26 U.S./U.S.S.R. joint experiments conducted on this flight. This mission was the sixth consecutive Soviet Biosatellite with joint U.S./U.S.S.R. experiments onboard. Pertinent information about these past U.S./U.S.S.R. joint biosatellite missions is included in Table I. The 1887 mission carried two young Rhesus monkeys, ten adult rats, and a variety of other specimens. The well-being of the two monkeys was a primary concern of the mission and, in spite of a malfunction in one of the monkey feeders, the monkeys were judged to be in good condition shortly after recovery.

Besides the experiments conducted by the United States and the Soviet Union, the biosatellite also carried experiments from Poland, Czechoslovakia, German Democratic Republic, France, Rumania, Bulgaria and Hungary. The European Space Agency (ESA) also sponsored some experiments on this mission.

MISSION MANAGEMENT PLAN

The U.S. responsibilities for this flight included: 1) development of flight and ground-based hardware; 2) conduct of hardware environmental and performance verification tests; 3) development, along with Soviet specialists, of procedures and techniques for the collection and preservation of rat tissues; and 4) the postflight transfer of tissues and data to the United States for analysis. The U.S. experiments investigated the effects of microgravity on major body systems and included musculoskeletal, neural, immunological, cardiovascular, hepatic, endocrine and plasma measurements. Furthermore, to evaluate radiation exposure during the flight and the shielding effectiveness of the spacecraft, the United States placed eight radiation detector packages inside and outside the spacecraft for measurement of radiation doses.

1. Hardware Development

The radiation dosimeters were the only flight hardware developed by the United States for this mission. The development of this hardware was closely coordinated with Soviet physicists to ensure trouble-free integration with other radiation measurement hardware. To support preflight and postflight radiograph measurements for the Primate Skeleton Experiment, both U.S. and Soviet X-ray equipment were used. In addition, biotransporters for transporting tissue samples and fixatives at various controlled temperatures were designed and fabricated by the United States. All hardware inspections and testing were under the surveillance of NASA Quality Assurance personnel. A detailed discussion of this hardware is included as a separate chapter in this report.

2. Training

To establish the procedures required for conducting each experiment, U.S. and Soviet experiment development teams were in communication regularly by telephone over a period of nine months prior to launch and met on two occasions at the Institute of Biomedical Problems in Moscow. The primary training requirement was for the extensive postflight rat tissue processing, which included dissection and tissue preservation procedures.

3. Hardware and Experiment Verification Tests

A prototype of a U.S. external dosimetry package was taken to the Soviet Union in July 1987, to verify its compatibility with Soviet hardware and to establish a mounting scheme for these dosimeters on the spacecraft.

A portable X-ray developer was tested in the U.S. principal investigator's laboratory before it was shipped to the Soviet Union.

All U.S.-developed biotransporters, designed to support postflight tissue preservation and shipment to the United States, were tested at Ames Research Center prior to being sent to the Soviet Union.

4. Data/Specimen/Hardware Transfer for Postflight Analysis

The primary data and specimens transferred postflight were skeletal radiographs of Rhesus monkeys, flight and ground-control radiation dosimeters, and rat tissues.

5. Documentation

The critical information required for conducting each experiment was contained in a document titled the Experiment Management Plan (EMP). Each EMP included: 1) a description of the experiment objectives; 2) a listing of the joint investigators (U.S./U.S.S.R.) and their general responsibilities; 3) the protocols for the flight and control experiments; 4) the experiment verification tests; 5) the procedures for specimen collection and labelling; 6) the procedures for animal preparation/tests; 7) the log sheets for experimental data; 8) the requirements/procedures for data transfer and analysis; and 9) an equipment list with specifications and procedures for operation. The EMP was the major document used to define each experiment for both U.S. and Soviet specialists.

The EMP for the Radiation Dosimetry and Spectrometry experiment, in particular, outlined the specifications for all equipment, listed experiment materials, and detailed methods and instructions for assembly.

For the coordination of science reporting by both countries, the United States submitted postflight science reports to the Soviets prior to submission to science journals for publication. Preliminary Science Reports were submitted to the Soviets six months postflight and Final Science Reports one year after the flight. A Cosmos 1887 Final Results Symposium was held in Moscow November 29 - December 3, 1988, to review the science results from all countries participating in the Cosmos 1887 mission. Eight

U.S. scientists, representing the 26 U.S./U.S.S.R. joint experiments, attended the symposium. A list of papers presented for review at this symposium is included in Table 2.

SPACECRAFT DESCRIPTION

The Cosmos 1887 mission utilized a modified Vostok spacecraft of a design used for previous Cosmos biosatellite flights. The spherical craft of approximately 2.5 meters in diameter had a gross weight of approximately 2250 kg with a 900-kg payload (Fig. 1). The atmospheric pressure within the craft approximated sea level and averaged 758 mm Hg. The air temperature within the flight capsule ranged between 20.5 and 24.0°C (the temperature in the primate BIOS capsule was more tightly controlled, ranging between 24.0 and 25.0°C). The pO_2 varied between 150 to 210 mm Hg, and pCO_2 was kept below 1.5 mm Hg. Relative humidity was kept between 30 and 50%. The lighting cycle for flight was 16 hours light and 8 hours dark with light beginning at 0800 Moscow time. The illumination level was approximately 60 ± 10 lux during light and less than 1 lux during the dark phase. Spacecraft power was supplied by onboard batteries. The biosatellite had an orbital inclination of 62.8°, an apogee of 406 km and a perigee of 224 km.

1. Primate BIOS

Each Soviet monkey BIOS capsule (Fig. 2) included a life support system and an experiment system. Each monkey was seated in a primate restraint couch equipped with upper and lower arm restraint straps, as shown in Figures 3 and 4, a lap-restraint plate with a leg separator, and a waste collection system, which used unidirectional airflow to deflect excreta toward a receptacle underneath the chair, as shown in Figures 3 and 5. The degree of thoracic restraint could be varied by ground command. The primate chair was designed to provide adequate support to the monkey for the shock experienced at ground impact after parachute descent. Paste diet and juice were separately presented to the monkeys by a ground-control signal which allowed eating and drinking by monkey-activated bite switches in the spouts of the dispensers, as shown in Figure 6. The two capsules were oriented in the spacecraft to allow the monkeys to view each other and a television camera allowed the inflight behavior of subjects to be viewed from the ground.

The BIOS capsule was equipped with a psychomotor test system, which included a leg response lever, as shown in Figure 5, and an eye-tracking light display, with which limb muscle and vestibular measurements were obtained. A motorized device attached to the restraint couch provided further vestibular stimulation by elevating the restraint couch, followed by a spring return to its original position.

2. Rodent BIOS

The ten male rats were group-housed in a single cage equipped with 10 nozzles for delivery of a paste diet, as shown in Figure 7, and with 10 nozzles for dispensing of water. The atmospheric pressure in the cage was 760 mm, the humidity averaged 58%, and the ambient temperature was 22-23°C. Lights were on from 0800-2400 and off from 2400-0800 hours for a 16:8 light/dark cycle. Light intensity was 4-8 lumens at the cage floor. An incandescent lamp was placed over each of the 10 feeders.

U.S. EXPERIMENTS

Of the 26 U.S./U.S.S.R. joint experiments included in Cosmos 1887, three experiments were designed to measure radiation inside and outside the spacecraft, one experiment used monkey subjects and the remaining experiments were designed for rats. The subjects for these U.S. experiments were two male Rhesus monkeys (*Macaca mulatta)* laboratory-bred at the Soviet Primate Center in Sukumi, and five of ten specific pathogen-free male rats of Czechoslovakia-Wistar origin from the Institute of Endocrinology, Bratislava, Czechoslovakia.

1. Rat Experiments

Many of the U.S. investigators who proposed rat experiments for this flight had previously conducted similar experiments as part of NASA's Spacelab 3 Mission of 7 days duration in April 1985. Several of the Cosmos 1887 experiments were an extension of studies on Spacelab 3. Of the 10 flight rats on Cosmos 1887, five rats, designated 6-10, were devoted to joint U.S./U.S.S.R. experiments. Rats 1-5 were to be sacrificed and dissected from 4 to 8 hours after landing, and rats 6-10 were to be processed 8 to 12 hours after landing. The Soviet scientists' rationale for giving the United States rats 6-10 was that the 8- to 12-hour delay before sacrifice was closer to the sacrifice schedule for Spacelab 3. The U.S. experiments studied the effects of weightlessness on bone, muscle, brain tissue, blood chemistry and various other organs of the rat.

2. Primate Skeleton Experiment

The objective for this experiment was to take preflight and postflight radiographs of flight candidate primates for matching skeletal age of flight and control subjects, and for monitoring subtle changes in cortical thickness and intracortical resorption of specific bones.

3. Radiation Dosimetry and Spectrometry Experiment

Radiation experiments were designed to measure the efficacy of shielding depth against different doses and types of incoming radiation. The three experiments required flying radiation dosimeters located both inside and outside the spacecraft. The high inclination orbit (62°) on this mission provided a radiation environment seldom available to U.S. investigators.

In one experiment, the radiation levels inside the spacecraft were measured using three separate detectors—plastic nuclear track detectors (PNTD), nuclear emulsions and thermoluminescent detectors (TLD).

The second experiment measured absorbed radiation doses as a function of very thin shielding on the outside of the spacecraft. This measurement distinguished which fraction of dose was due to low-energy electrons as opposed to heavy charged particles. To accommodate these measurements, the shielding of the outermost detectors was no more than a few mg/cm^2 and the detectors themselves were very thin. Two identical flight units, each containing three stacks of TLDs, were used.

In the third experiment, linear energy transfer (LET) spectra as a function of shielding depth were examined by measuring the low-energy, heavy particles (excluding electrons) through various depths of

shielding starting from zero shielding (outside the spacecraft). In addition, information regarding the neutron energy spectra was obtained by placement of ^{59}Co activation foils outside the craft and a single ^{59}Co activation foil inside the satellite.

B. MISSION OPERATIONS

GENERAL MISSION DESIGN

The overall Soviet design for Cosmos 1887 was similar to earlier missions and included basal, flight, synchronous, and vivarium control experiments. In general, the synchronous control was designed to duplicate the flight experiment except for factors unique to the external spacecraft environment, such as weightlessness. The vivarium control was designed to accumulate as much data as possible from subjects housed closer to normal laboratory conditions but exposed to environmental factors characteristic of the internal spacecraft. These control experiments are described in more detail below.

Rat Experiments

Subjects for the rat experiments were ten 12-week-old, male, SPF Wistar rats weighing about 300 grams at launch. These animals were flown in a normal state and all tissue analyses were performed postflight. Four groups of 10 rat subjects each were established to provide animals for Flight, Basal, Vivarium and Synchronous control groups.

The Basal control group provided tissue specimens from which preflight control data could be obtained. Diet, temperature, humidity and lighting for this control group were kept consistent with conditions expected inflight.

The Vivarium control group was caged in standard laboratory cages under standard conditions. They were fed the same quantity of food per day but in a single feeding. Postflight conditions (e.g., temperature) were not mimicked for this group.

In addition to being adapted to flight cages and diet, the Synchronous control group experienced conditions which closely simulated the actual flight. This simulation included the G-force and vibration of launch, the 42-hour food deprivation experienced postflight, and the disrupted lighting regimen and temperature variations experienced by flight rats after the off-target landing. Sacrifice of Synchronous control rats, furthermore, was postponed for the same period as the delay for the sacrifice of Flight rats. The reentry G-force and postflight transportation conditions of the Flight animals were not mimicked for the Synchronous controls.

The composition of the paste diet fed to the rats is shown in Table 3. This diet was of a similar consistency to that of the Rhesus diet and included a preservative, as well.

Soviet specialists sacrificed all ten flight rats at the recovery site, prepared the specimens and preserved them as required, and then transferred them to Moscow. The U.S. investigator team in Moscow assumed responsibility for the continuation of rat experiments upon the arrival of tissue samples. These

procedures entailed culturing of cells from tissues, isolation and transplantation of pituitary cells into hypophysectomized rats, fixative changes for processing of flight samples, and packaging of tissues and cells in biotransporters for shipment back to the United States.

PREFLIGHT EVENTS

1. Primate Skeleton Experiment

Soviet specialists started with eight monkeys for preflight measurements. Four films were taken per animal at two months preflight, and then again at one month preflight. These films were of the right and left arms and the right and left legs as described in the U.S. investigator's Experiment Management Plan.

2. Rat Experiments

All rats were acclimated to flight-type cages and paste diet beginning 19 days before launch.

The subjects of the Basal rat experiment were sacrificed at L–5. Tissues obtained from the Basal control study were frozen in liquid nitrogen or maintained at 4 to 5°C, as required, and held by the Soviets for postflight shipment to the United States.

Flight rats were transported to the launch site and installed in the spacecraft 46 hours before launch.

3. Radiation Dosimetry and Spectrometry Experiments

All dosimeter units were for single exposure and therefore no preflight testing was performed. The batches of materials from which some of the dosimeters were taken (PNTDs and TLDs) were tested preflight to determine that they were of the quality necessary for accurate measurements. The U.S. investigator conducted final assembly of units in his laboratory with NASA oversight. All detectors were hand-carried to Moscow in a specially designed lead-lined transport carrier. The flight dosimeters were transported to the launch site for direct placement into the biosatellite by Soviet specialists. Detectors were placed in external and internal locations of the spacecraft prior to launch. Photographs of the spacecraft were taken to document the arrangement of dosimeters around the satellite.

LAUNCH, ON-ORBIT, REENTRY EVENTS

Soviet data from earlier missions have indicated that accelerations are 4 g at launch (+Gz), and 8 g (+Gz) during reentry.

1. Rat Experiments

There were no special inflight procedures for the rodent BIOS. For details regarding lighting and internal environmental specifications during flight see previous section on Spacecraft Description.

The average daily consumption of the pastelike diet by the flight rats was 50 grams. This quantity of food contained approximately 35 ml of water. The rats had an additional daily water intake of approximately 2.5 ml.

Seven days following launch of the flight rats the Synchronous Control experiment was begun.

2. Radiation Dosimetry and Spectrometry Experiment

Detectors located external to the spacecraft were mounted on the spacecraft exterior inside a flat container equipped with a closeable lid. The lid was opened during launch and throughout orbit to expose the dosimeters but closed to protect the detectors before reentry into Earth's atmosphere.

POSTFLIGHT EVENTS

The malfunction of one of the monkey feeders led to the intended 14-day flight mission being curtailed by 1 1/2 days. Prior to reentry on October 12, 1987, the normal dark cycle was interrupted at 0500 hours so the monkeys would awaken before landing. Landing occurred at 0703 hours (Moscow time) about 1800 miles from the anticipated recovery site. Landing G-force was estimated to be 3 to 4 g. When the spacecraft was eventually located in Siberia, approximately 3 hours after landing in weather ranging between –5 to 20°C, a heated tent (23°C) was placed around the vehicle in order to warm the specimens. The lights had extinguished at landing and the animals remained in the dark until they were put into transport cages. While the biosatellite was on the ground, the ventilation system continued to work so the animals received an adequate air supply.

Twenty hours elapsed after landing before the animals were transferred to transport cages. They were then carried by bus (3 hours), airplane (6 1/2 hours) and a van (1/2 hour) before arriving at the designated recovery site at 1800 hours (R+30 hours) on October 13, 1987.

1. Primate Skeleton Experiment

Brief postflight clinical and physiological examinations of the monkey subjects were conducted at the recovery site (R+0 days). The monkeys were shipped by air in transport cages to Moscow and returned to their vivarium cages. Additional clinical and physiological examinations were carried out on the flight animals from R+2 through R+12 days. A Postflight Control Study was conducted from R+42 to R+56.

There was a 25% weight loss for the monkey (Yerosha) with the inoperable feeder. The smaller monkey (Drema), who received food throughout the flight, showed a weight gain of 140 grams.

At R+9 days, four radiographs were taken per animal of the six Control monkeys. At R+16, eight films per animal (duplicate of each film) were taken of the two flight animals according to the protocol completed preflight. Final films of the flight animals and four control animals were taken at R+37 and R+72 days, before and after the Postflight Control Study. These radiographs were transferred to the U.S. investigator at approximately 120 days after recovery.

2. Rat Experiments

The temperature of the rat cage was not recorded after landing, but postflight calculations indicated that the temperature decreased slowly to a minimum of +12 to +15°C. Because the rats neither huddled nor were cold to touch when the cage was first opened, the rats appeared not to be affected by the cold

temperature. A photograph taken at the recovery site revealed that the animals were well-groomed and appeared healthy.

The rats were fed last in flight at 0200 hours (Moscow time) on October 12 and not again until 2000 hours, on October 13. At the recovery site, they were fed 28 grams of food at the end of the 42-hour starvation period. It is uncertain if water was available to the rats after landing. The rats, however, did not appear to be interested in water when it was provided to them in the transport cages. They were given water ad libitum at 2000 hours on October 13. The 105-day-old flight rats were sacrificed according to protocol on the morning of October 14, 48 to 56 hours after landing, and the tissues were delivered to Moscow on October 15.

The Basal experiment began at Launch–19 days (L–19) with the subjects sacrificed at L–5 days.

The Vivarium and Synchronous control experiments were begun at L+4 and L+7 days respectively, at the Institute of Biomedical Problems in Moscow. The Vivarium control group was sacrificed at 108 days of age on October 17, approximately 72 hours after the sacrifice of the Flight group. The Synchronous control group was sacrificed 72 hours later at 111 days of age.

As reported by the Soviets, the mean weight gain of the Flight rats during the on-orbit period was only one-fourth the weight gained by the Synchronous control rats in the comparable time period and feeding regimen (9 grams vs. 37 grams, Flight vs Synchronous).

3. Radiation Dosimetry and Spectrometry Experiment

The U.S. dosimetry packages were returned to the United States in the lead-lined transfer box 10 days after recovery. According to the reentry profile of the spacecraft, the Soviets determined that some high temperatures were experienced in the vicinity of the external radiation dosimeters.

The U.S. investigator received the dosimeters in generally good condition and the exposure of the detectors to high temperatures (<88°C in the worst case) was believed brief enough so as not to induce any significant differences in the detector response. Collaborative ground-based experiments were performed for the interpretation of flight results and the calibration of detectors. These experiments were conducted by the U.S. investigator at the BEVALAC accelerator in Berkeley, California. The results of these studies are under current analysis.

RAT BIOSPECIMEN TRANSFER

Sacrifice, dissection and initial tissue preservation (freezing, fixation or storage in sterile media at 4 or 23°C) were performed by a team of Soviet specialists at the planned recovery site.

All biological specimens were delivered to U.S. scientists in Moscow, where they performed the culturing of tissues in a Soviet laboratory. A total of 2000 tissue samples were subsequently delivered in two separate shipments from Moscow to San Francisco in temperature-controlled biotransporters.

The U.S.-supplied biotransporters enabled the packaging of tissues at shipping temperatures specified by individual investigators in their respective Experiment Management Plans. Shipment #1 consisted of two

biotransporters, one at –70°C and another at 4°C. Shipment #2 contained samples in a –23°C biotransporter. Biotransporters and samples were periodically inspected and/or repackaged during the transfer process to ensure the maintenance of desired shipping temperatures. Both shipments (accompanied by U.S. personnel) were met in San Francisco by a courier from Ames Research Center (ARC). After delivery to ARC, samples were checked and repacked in –70°C (dry ice) and 4°C (frozen water) "shippers" for overnight delivery to investigators located throughout the United States.

Most reports from investigators, which stated the condition of tissue samples upon receipt, concluded that the processing and transfer of tissues by the Soviets and the subsequent transport to the United States were successful. All tissues arrived in good condition.

TABLE 1 - COSMOS BIOSATELLITE MISSIONS WITH U.S. PARTICIPATION

Mission Parameters	782	936	1129	1514	1667	1887
Launch	25 Nov '75	3 Aug '77	25 Sep '79	14 Dec '83	10 Jul '85	29 Sep '87
Recovery	15 Dec '75	22 Aug '77	14 Oct '79	19 Dec '83	17 Jul '85	12 Oct '87
Duration (Days)	19.5	18.5	18.5	5.0*	7.0	12.5
Orbital Period (Min)	90.5	90.7	90.5	89.3	89.4	90.7
Apogee (Km)	405	419	406	288	270	403
Perigee (Km)	226	224	226	226	211	222
Inclination (Deg)	62.8	62.8	62.8	82.3**	82.4**	62.3

* Mission Duration shortened for first Rhesus monkey flight.

** Higher orbital inclination for radiation experiments.

TABLE 2 - EXPERIMENTS FLOWN ON COSMOS-1887 AND RELATED GROUND-BASED EXPERIMENTS

GROWTH, DEVELOPMENT AND ENVIRONMENTAL PROBLEMS

Reproductive Functions of Male Rats in Real and Simulated Spaceflight
L.A. Denisova, Yu. V. Ivanov, L.V. Serova (USSR)

The Effect of Spaceflight on the Morphology of Rat Testes
D. Philpott (USA)

Morphometric Analysis of Yellow Body Cells of the Ovaries of Pregnant Rats Exposed to Hypergravity
E. Jankowska, W. Baranska, W. Baran (Poland), L.V. Serova (USSR)

The Effect of Hypergravity on Various Stages of Mammalian Development
L.V. Serova, Z.I. Apanasenko, S.Ya. Ivanova (USSR), Z. Dragota (Czechoslovakia)

The Effect of Hypergravity on Liver Regeneration After Partial Hepatectomy
E. Misurova, K. Kropaceva (Czechoslovakia), L.V. Serova, E.V. Snetkova (USSR)

The Effect of Hypergravity on Hormonal Reactions of Rats During Liver Regeneration After Partial Hepatectomy
I.M. Lartina, V.M. Ivanov, I.V. Belowsava (USSR)

The Use of P Substance as an Antistressful Drug in Intact and Pregnant Animals
P. Oheine, K. Hecht, E. Wachte. (GDR), L.V. Serova, L.A. Dentsova, A.M. Pustynnikova (USSR)

Guppy Embryogenesis in Microgravity
L. R. Palmbakh, T.V. Ostroumova, E.M. Cherdantseva, (USSR)

Formation of the Hydrostatic Apparatus in the Guppy Fry During COSMOS-1887 Flight
L.P. Palmbakh, V.I. Tsvetkov (USSR)

Ontogenesis of Carausius Morosus During COSMOS-1887 Flight
I.A. Ushakov, A.M. Alpatov, Yu. A. Zakhvatkin (USSR), H. Bucker, D. Messland, G. Horneck, G. Reis, R. Fazius, W. Ruter, W. Heinrich, R. Bojan, W. Enge (FRG)

The Effect of Spaceflight Factors on Lens and Limb Regeneration in Newts
E.N. Grigoryan, E.A. Orgenblick, S. Ya. Tuchkova, I.E. Malchevskaya, V.I. Mitashov (USSR)

Regeneration of the Flat Worm Planaria in Space
A.M. Morozov (USSR)

TABLE 2 - CONTINUED

Growth, Development and Reproduction of Algae in Spaceflight
M.A. Levinskikh, V.N. Sychev (USSR)

Growth, Development and Reproduction of Higher Plants in Spaceflight
A.L. Mashinsky (USSR)

Biocenosis in Microgravity: Aquarium Experiment
G.I. Meleshko, V.V. Antipov, V.K. Golov, M.A. Levinskikh, L.R. Palmbakh, V.N. Sychev, E.Ya. Shepelev (USSR)

Metabolism of Higher Plants in Spaceflight
A.L. Mashinsky, A.N. Bezhke, T.P. Alekhina, E.I. Ivanova, L.S. Chernova (USSR)

Metabolism of Unicellular Algae in Spaceflight
A.A. Antonyan, G.I. Meleshka, N.I. Sukhova (USSR)

Fatty Acids of Lipids in Chlorella Grown in Microgravity
A.A. Antonyan, V.P. Naidina (USSR)

Quantitative and Qualitative Analysis of Pigments of Chlorella Grown in Microgravity
A.A. Solontsova (USSR)

Chlorella Cell Ultrastructure in a Multicomponent System in Spaceflight
A.F. Kordyum, K.M. Sytnik (USSR)

Lipid Peroxidation and Ultrastructure of Maplopappus Tissue Cell Culture Flown on COSMOS-1887
S.I. Zhadke, A.D. Klimchak, E.L. Kordyum, K.M. Sytnik, P.G. Sidosenko, V.A. Baraboy (USSR)

Cell Ultrastructure of the Root Cap and Meristem of Impatiens Balsamina Seedlings Grown in Microgravity
V.G. Chuchkin, V.N. Filippenko, V.B. Ivanov, E.L. Kordyum, L.A. Denevin, A.G. Podlutsky (USSR)

Cell Ultrastructure of Cotyledons, Hypacetyls and the Apical Meristem of Impatiens Balsamina Seedlings Flown on COSMOS-1887
E.M. Nedukha, V.G. Chuchkin, V.N. Filippenko (USSR)

Qualitative and Quantitative Composition of the Bacterial Component of the Algae-Bacteria-Fish System in Microgravity
I.V. Maksimova, M.N. Smirnova, M.A. Levinskikh, O.A. Sidorova, V.G. Prokhorov (USSR)

Ultrastructure of Layers of the Motor and Visual Cortex of the Brain
L.N. Dyachkova (USSR)

TABLE 2 - CONTINUED

NERVOUS SYSTEM MORPHOLOGY

Morphometric Analysis of Nerve Cell Dendrites of the Visual Cortex and the Gigantocellular Nucleus of the Reticular Formation
T.A. Leotovich, M.A. Makhanov, P.V. Belichenko (USSR)

Histological Examination of the Cerebellum and Spinal Cord Vessels
I.G. Lyudkovskaya, V.A. Morgunov (USSR)

Structure and Function of Spinal Cord Motoneurons of Rats at an Early Stage of Readaptation After COSMOS-1887 Flight
V.I. Drobyshev, V.V. Makarov, I.V. Polyakov (USSR)

Morphology and Histochemistry of the Visual Cortex and Retina
A.N. Kardenko (USSR)

Ultrastructure of Layers of the Cerebellar Nodulus Cortex
I.B. Krasnov (USSR)

Effect of Microgravity on Metabolic Enzymes, Neurotransmitter Amino Acids, and Associated Neurotransmitter Enzymes in the Motor and Somatosensory Cerebral Cortex
O. Lowry (USA)

Study of Muscarinic and GABA Receptors in the Sensory-Motor Cortex of Rats Flown on COSMOS-1887
N. Daunton (USA)

Pineal Physiology in Microgravity and Its Relation to the Gonadal Function
D. Holley (USA)

Pineal Morphology
P. Groza (Rumania)

Growth Hormone Regulation and Secretion in Response to Microgravity
R. Grindeland (USA)

Effect of Spaceflight on Pituitary Oxytocin and Vasopressin Content
L. Keil (USA)

Effect of Microgravity on Contractile Properties and Composition of Proteins of Rat Skeletal Muscles
T. Szilagyie, A. Soor, M. Rapcsak, F. Guba (Hungary)

TABLE 2 - CONTINUED

MUSCULOSKELETAL SYSTEM: FUNCTION, METABOLISM AND STRUCTURE

Sarcoplasmic Reticulum and Calcium Transport in Rat Skeletal Muscles After 13-Day Spaceflight
I. Mounier, X. Holy (France)

COSMOS-1887: Contractile Properties of Rat Myofibers
S.A. Skuratova, L.M. Murashko, V.S. Oganov (USSR)

Morphohistochemical Study of Skeletal Muscles in COSMOS-1887 Rats
E.I. Ilyina-Kakueva (USSR)

Metabolic and Morphologic Properties of Rat Muscles Flown on COSMOS-1887
R. Edgerton (USA)

Skeletal Muscle (Vasius Medialis) Atrophy in Response to 12.5 Days of Weightlessness
X.J. Musacchia, J.M. Steffen, R.D. Fell (USA)

Electron Microscopic, Histochemical and biochemical Investigation of Microgravity-Induced Muscle, Nerve and Blood Vessel Breakdown
D. Riley, S. Ellis (USA)

Electron Microscopic Examination of Nerve-Muscle Synapses and Myofibers of Rats Flown on COSMOS-1887
O.M. Pozdnyakov, L.L. Babakova, M.S. Demorjee, E. I. Illyina-Kakuava (USSR)

Effects of Zero Gravity on Myofibril Protein Content and Isomyosin Distribution in Rodent Skeletal Muscle
K.M. Baldwin (USA)

Effects of Spaceflight on Messenger RNA Levels in Skeletal Muscle
F. Booth, D.B. Thomason, P.R. Morrison (USA)

Histometry and Morphometry of Rat Myofibers After COSMOS-1887 Spaceflight
C. Gharib, D. Desplanches (France)

Content and Distribution of Inorganic Cations in Rat Skeletal Muscles
V.P. Nesterov, I.V. Burovina, I.N. Denisova, A.F. Sidorov, V.K. Tembitsky (USSR)

Content and Enzyme Activity of Proteins of Different Fractions in the Quadriceps Muscle of COSMOS-1887 Rats
L.I. Kurkina, E.G. Vetrova, T.E. Drozdova, L.B. Zattseva, I.V. Zabolotskaya (USSR)

TABLE 2 - CONTINUED

Morphological Mechanisms of Calcium Metabolism Regulation in Newts Exposed to Microgravity
S.V. Savelyev, N.V. Besova, E.A. Olgenblick (USSR)

COSMOS-1887: Primate Bone Densitometry
S.L. Dubonos, A.S. Rakhmanov (USSR)

Muscle Adaptability of COSMOS-1887 Rats
D. Desplanches, M.Maye, S. Sempur, R. Flangre (France)

Effect of Microgravity on Metabolic Enzymes of Type 1 and Type 2 Myofibers
O. Lowry (USA)

Analysis of Radiographs from COSMOS-1887 Primate Studies
C. Cann (USA)

Production of the Osteoclast Activating Factor by Immunocompetent Cells of COSMOS-1887 Rats
A.T. Lesnyak, I.V. Serov, A.G. Kolesnik, I.V. Konstantinova (USSR)

Histomorphometric Examination of Bones of COSMOS-1887 Rats
G. N. Durnova, A.S. Kaplansky, Z.F. Sakharova, E.I. Ilyina-Kakueva (USSR)

Bone Metabolism of COSMOS-1887 Rats
I.A. Popova, N.Yu. Fedotova (USSR)

Comparative Analysis of the Mineral Composition of Bones, Muscles and Viscera of COSMOS-1887 Rats
L.A. Denisova, E.A. Lovrova, Yu. V. Natochin, L. V. Serova (USSR)

Effect of Microgravity on Collagenic and Noncollagenic Proteins of Rat Bones and Skin
M. Pospishil (Czechoslovakia)

COSMOS-1887: Mechanical Characteristics of Rat Bones
A.V. Bakulin, V.E. Novikov, L.A. Rezaeva, K.V. Smirnov (USSR)

X-Ray Flourescence Examination of Rat Bones
Baca (Hungary)

Histomorphological Modification of Bone Examination of Two Rhesus-Monkeys and Five Rats in Microgravity
E. Zerath, M. Armand, A. Kolombani, C. Nogues (France)

TABLE 2 - CONTINUED

Effect of COSMOS-1887 Flight on the Trabecular Bone Mass and Construction in Growing Rats
L. Vico, S. Bourrin, D. Chappard, C. Alexander (France)

Effect of COSMOS-1887 Flight on Osteoclasts and Osteoids of Rats
L. Vico, S. Bourrin, D. Chappard, C. Alexander (France)

Distribution and Biochemistry of Mineral and Matrix in the Femora of Rats Flown on COSMOS-1887 Mission
S. Arnaud, E. Katz, P. Buckendahl, G. Mechanic (USA)

Dense, Fibrous Connective Tissues Response to 13-Day Spaceflight
A. Vailas, R. Zernicke (USA)

Microgravity and Skeletal Growth
E. Morey-Holton, S. Doty, E. Roberts, D. Berretta (USA)

Trace Element Balance in Rats During Spaceflight
C. Cann (USA)

Morphometry and Electron Microscopy Analyses of Tibial Epiphyseal Plates from COSMOS-1887 Rats
J. Duke (USA)

Maturation of Bone and Dentin Matrices in COSMOS-1887 Rats
D. Simmons, W. Rosenberg, M. Grynpas (USA)

Changes in the Concentration of Carbonic Apatites in Rat Teeth and Jaws Under the Influence of Microgravity of Varying Duration
M. Kleber, O. Volgt, H. Veingard, E. Wachtel (GDR), L. A. Dentsova, M.A. Dotsenko (USSR)

Histomorphometric Analysis of Pituitary Somatotrophic Hormones
E.I. Alekseev (USSR)

Morphological State of Calcium-Regulating Systems (C-Cells, Parathyroid Cells) of Rats After COSMOS-1887 Flight
G.I. Plakhuta-Plakutina, N.A. Dmitrieva, E.A. Amirkhanyan (USSR)

Growth Hormone Regulation: Synthesis and Secretion in Microgravity
R. Grindeland (USA)

Biochemical Investigation of Rat Jaws and Teeth in Microgravity
A.I. Votoshin (USSR)

TABLE 2 - CONTINUED

Histomorphometric Examination of Rat Bone
I. Foldes (Hungary)

BEHAVIOR, SLEEP AND BIORHYTHMS

Investigation of Primate Conditioned Reflexes in Real and Simulated Microgravity
G.G. Shlyk, M.A. Shirvinskaya, V.I. Korolkov, T.G. Urmancheeva, N.F. Kolpakova, M. Ye Efimova, O.I. Zavadskaya (USSR)

Methods for Assessing the Cortical Function of Primates in Ground-Based Simulation Studies
G. D. Kuznetsova, T.B. Shvets, G.G. Shlyk, M. A. Shirvinskaye (USSR)

Emotional Reactivity of Primates During the Development of Conditioned Reflexes in the Process of Preflight Training
T.G. Urmancheeva, A.A. Ozhockua, N.F. Kolpakova, V.M. Ellova, Z.K. Beridze (USSR)

Investigation of the Higher Nervous Activity of Primates Based on Their Sleep and Behavior in Real and Simulated Flights
G.G. Shlyk, M.A. Shirvinakaya, V.S. Rottenberg, V.I. Korolkov, M.Ya. Efimova. O. I. Zavadskaya (USSR)

Analysis of Biorhythmic Components of Sleep During Adaptation to Spaceflight
E. Wachtel, G.J. Baltzer (GDR), E.A. Ilyin, V.I. Korolkov, G.G. Shlyk, V.S. Magedov (USSR)

Computer-Aided Analysis of Biorhythmic Components of Sleep
G.J. Baltzer, K. Evgenov, J. Fitze (GDR), V.N. Stepnoy (USSR)

Electroencephalographic Investigation of Sleep of Two Rhesus-Monkeys in Microgravity
D. Loggard, K. Miyo, G. Anton (France)

Biorhythmic Variations in Skin-Galvanic Reactivity as Correlates of Emotional Parameters in Primates
K. Hecht, E. Wachtel, G.J. Baltzer (GDR), M.A. Shirvinskaya (USSR)

Spaceflight Effects on the Free Run of Circadian Rhythms in Tenebrionidae Beetles
Yu. A. Evstratov, A.M. Alpatov, V.B. Chernyshev, M.I. Lebedev, V.A. Zotov (USSR)

Do Primates Suffer From Desynchronosis in Spaceflight?
A.M. Alpatov, V. Ya. Klimovitsky, Yu. A. Evstratov (USSR)

Thermometric Data from Primate Experiments as Related to the Assessment of Their Health Condition in Spaceflight
V. Ya. Klimovitsky, A.M. Alpatov, Yu. A. Evstratov (USSR)

TABLE 2 - CONTINUED

RADIATION DOSIMETRY

Measurement of Absorbed Doses on the Outer Surface of COSMOS Biosatellites by Glass Thermoluminescent Detectors
Yu. A. Akatov, V.V. Arkhangelsky, E.E. Kovalev (USSR), F. Spurny, J. Votockova (Czechoslovakia)

Measurement of Cosmic Ray Heavy Ions by Solid-State Tracking Detectors on COSMOS-1468, 1514, 1667, 1837, and 1887 Satellites
I. Cige, G. Somogy, I. Hunagy (Hungary), A.M. Marennyi, G.P. Herzen (USSR)

Attenuation of the Multicomponent Flux of Cosmic Ray Heavy Ions in Matter
G.P. Herzen, A.M. Marennyi, R.A. Nymmik (USSR), J. Harvat (Czechoslovakia)

Investigation of Cosmic Ray Low Energy Nuclei Onboard Earth Artificial Satellites of the COSMOS Series
G.P. Herzen, A.M. Marrennyi, R.A. Nymmik (USSR)

Dosimetric Examinations of Radiobiology Experiments in Outer Space
Yu A. Akatov (USSR)

Dosimetric Data From COSMOS-1887 Experiments
H. Reitz (FRG)

Radiation Experiments on COSMOS-1887
E. Benton (USA)

COSMOS-1887 Dosimetric Measurements by Thermoluminescent Detectors
J. Fellinger (GDR)

VESTIBULAR APPARATUS (STRUCTURE AND FUNCTION) VESTIBULO-OCULOMOTOR INTERACTION

Responses of the Vestibular Receptors of Primates to the Otolith Stimulation
B. M. Babaev, I.N. Beloozerova, M.G. Sirota, A.M. Ivanov, A.N. Nyrova, S.B. Yakushin, I.B. Kozlovskaya (USSR)

The Effect of Microgravity on the Characteristics of Eye and Head Movements of Primates Performing Eye-Head Coordination Task
S.B. Yakushin, B.M. Babaev, I.N. Beloozerova, M.G. Sirota, A.M. Ivanov, AN. Nyrova, I.B. Kozlovskaya (USSR)

TABLE 2 - CONTINUED

Neuronal Activity of Vestibular Structures of the Brain Stem and Cerebellum of Primates Performing Various Motor Tasks in Ground-Based Experiments
S.B. Yakushin, B.M. Babaev, I.N. Beloozerova, M.G. Sirota, A.M. Ivanov, A.N. Nyrova, I.B. Kozlovskaya, (USSR)

Neuronal Activity of Vestibular Structures of the Brain Stem and Cerebellum of Primates Performing Eye-Head Coordination Task
M.G. Sirota, I.N. Beloozerova, S.B. Yakushin, B.M. Babaev, A.M. Ivanov, A.N. Nyrova, I.B. Kozlovskaya (USSR)

The Effects of 13-Day Exposure to Microgravity on the Vestibulo-Motor Function of Primates
I.B. Kozlovskaya, M.G. Sirota, I.N. Beloozerova, B.M. Babaev, S.B. Yakushin (USSR)

Ultrastructure of Receptor Cells of the Utriculus
I.B. Krasnov (USSR)

Vestibular Responses of Newts After the 13-Day Orbital Flight
G.P. Gorgiladze, E.A. Digenblick (USSR)

HEMODYNAMICS AND BODY FLUIDS

Study of the Cardiac Function of Primates Based on Electrocardiographic Data
A.N. Truzhennikov, Yu. V. Gordev, N.I. Vikhrov, G.V. Ivanov (USSR)

Electrocardiographic Examinations of Two Rhesus-Monkeys in Microgravity
G. Florence, K. Miyo, L. Lemaine, N Vidalnake (France)

The Effect of 13-Day Flight on the Circulation System of Primates
V.I. Lobachik, S.V. Abrosimov, D.K. Endeka, V.V. Zhidkov (USSR)

The Effect of 13-Day Flight on Body Fluids of Primates
V.I. Lobachik, V.V. Zhidkov, S.V. Abrosimov (USSR)

Study of Acceleration (12 G in the Head-To-Feet Direction) Tolerance in Monkeys
I.F. Vil-Vilyams, A.V. Opryshko, A.N. Truzhennikov, Yu V. Gordeev (USSR)

Investigation of Fluid-Electrolyte Metabolism in Primates
M.A. Dotsenko, R.I. Rudneva, Yu A. Sukhanov, V.I. Korolkov (USSR)

State of Mineral Metabolism in Rats and Primates
P. Luderitz, D. Marquart, Z. Lappin (GDR), M.A. Dotsenko (USSR)

TABLE 2 - CONTINUED

CELL BIOLOGY

The Effect of Spaceflight on the Induction of Phage Production of the Lysogenic Culture
S.V. Kamarov, A.V. Letarov, M.P. Bragina, V.K. Illyin (USSR)

Amplification of rDNA Genes in Ovocytes of COSMOS-1887 Newts
N.L. Delone, T.V. Ostroumova, L.V. Belousov, V.V. Antipov (USSR)

Cytogenetic Examination of Lymphocytes of COSMOS-1887 Primates
S.M. Kuzin, V.P. Zhvalikovskaya, N.L. Delone, V.V. Antipov (USSR)

The Effect of COSMOS-1887 Flight on Mitosis in Cells of the Rat Corneal Epithelium
G.V. Galaktionova (USSR)

Mechanisms of Chromosome Recombinations of COSMOS-1887 Drosophila Females
A.V. Smirnova, S.Yu Danilyuk (USSR)

Recombinogenesis in Drosophila Males Exposed to an Altered Gravity
L.P. Filatova, E.N. Vaulina, N. Sh. Lapleva, T.Ya Grozdeva (USSR)

The Effect of Microgravity on Unicellular Eucaryotic Organisms
M.G. Tairbekov, I.B. Raikov, I.S. Irlina, A.V. Gabova, V.K. Golov (USSR)

The Effect of COSMOS-1887 Flight on Haplopappus Cultured Cells
E.L. Kordyum, A.V. Papova, E.T. Nedukha, D.A. Klimchuk, S.I. Zhadko, A.G. Podlutsky (USSR)

IMMUNOLOGY, HEMATOLOGY AND MICROBIOLOGY

Functional Activity of Natural Killers and Their Characterization at the Level of Formation of Killer-Target Conjugates in the Rat Spleen and Bone Marrow After COSMOS-1887 Flight
M.P. Rykova, D.O. Meshkov (USSR)

Production of Interleukin-2 and Alpha and Gamma Interpherons by Rat Spleen Cells in COSMOS-1887 Flight
I.V. Serov, A.T. Lesnyak, E.P. Golovtseva, F.I. Ershov (USSR)

Effect of Spaceflight on Levels and Function of Immune Cells
G. Sonnenfeld, A. Mandel, G. Taylor (USA)

Characterization of Primate Cell-Mediated Immunity Before and During COSMOS-1887 Experiments
A.T. Lesnyak, I.V. Serov, M.P. Rykova, D.O. Meshkov, P.N. Uchakin, V.I. Korolkov (USSR)

TABLE 2 - CONTINUED

Study of Spontaneous and Induced IL-2 Proliferative Activity, Spontaneous and Induced Production of Cytotoxic Factors and Natural Cytotoxicity of Spleen Cells in COSMOS-1887 Rats
B.B. Fuks, A.L. Rahhmilevich, A.E. Medvedev, I.S. Rakhimova (USSR)

Electron Microscopic Examination of Natural Killers of COSMOS-1887 Rats
A.M. Bykov, A.F. Bykovsky, M.P. Rydova, D.O. Meshkov (USSR)

Parameters of Humoral Immunity of Rhesus-Monkeys in Response to Extreme Effects
M.A. Pochkhua, E.K. Ozhekidze, V.I. Korolkov, V.M. Knyazev (USSR)

Production of the Osteoclast-Activating Factor and Proliferative Activity of Spleen and Bone Marrow Cells of COSMOS-1887
A.T. Lesnyak, I.V. Serov, I.V. Konstantinova (USSR)

Blood and Bone Marrow Analysis in COSMOS-1887 Rats
N.A. Chelnaya (USSR)

Changes of Stem Clone-Forming Hemopoietic Cells of Rats After 13-Day Flight
A. Vacek, D. Rolkoyska, A. Bartonickova (Czechoslovakia), T.V. Michurina, F. N. Domoradskaya, O.N. Pryanishnikova (USSR)

Ultrastructure of Red Blood Cells of COSMOS-1887 Rats
L.A. Sidorenko (USSR)

Red Blood Cell Metabolism and Membrane Function of COSMOS-1887 Rats
S. N. Ivanova, S.S. Brantova, O.I. Labetskaya, T.I. Turkina (USSR)

Morphofunctional State of Erythron of COSMOS-1887 Primates
I.I. Britvan, G.J. Kozinets, V.I. Korolkov (USSR)

Effect of 13-Day Flight on Primate Bone Marrow Metabolic Activity
V.I. Lobachik, D.K. Endeka, V.V. Zhidkov, S.V. Abrosimov (USSR)

Intestinal Lactoflora in Healthy Primates
A.A. Lentsner, H.P. Lentsner, M.E. Mikelsaar, M.E. Turie, M.A. Toom, V.M. Knyazev, V.I. Korolkov, L.N. Petrova, M.A. Pochkhua (USSR)

Intestinal Lactoflora in COSMOS-1887 Primates
A.A. Lentsner, H.P. Lentsner, M.E. Mikelsaar, M.E. Turie, V.M. Knyazev, V.I. Korolkov, L.N. Petrova, M.A. Pochkhua (USSR)

Adhesive Properties of Intestinal Lactoflora of Rhesus-Monkeys
A.A. Lentsner, V.I. Brilis, L.A. Levkov, H.P. Lentsner, V.M. Knyazev, V.I. Korolkov, L.N. Petrova (USSR)

TABLE 2 - CONTINUED

Bacterial Treatment as Part of Primate Preparation for Biomedical Experiments
V.N. Frolov, N.N. Lizko (USSR)

Intestinal Microecology of Primates in COSMOS Experiments
N.N. Lizko, V.N. Frolov, R.A. Pechenkina, V.I. Korolkov (USSR)

Intestinal Microorganisms of SPF Animals in COSMOS Experiments
N.N. Lizko, L.N. Petrova, A.A. Naumov (USSR)

Microflora of the Upper Respiratory Tract of Rhesus-Monkeys Exposed to Extreme Effects
M.A. Pochkhua, E.K. Ozhekidze, V.I. Korolkov, V.M. Knyazev (USSR)

METABOLISM AND ITS REGULATION

Chromatin and Nucleic Acids in Rat Tissues After COSMOS-1887 Flight
E. Misurova, K.Krokaceva (Czechoslovakia), I.A. Popova (USSR)

Intensity of Glycolysis in COSMOS-1887 Rat Muscles and Liver
S.M. Ivanova, O.I. Labetskaya, I.A. Popova, U.M. Ivanov (USSR)

Morphological and Biochemical Examination of Heart Tissues from COSMOS-1887 Rats
D. Philpott (USA)

Content of Cyclic Nucleotides in Heart Tissues from COSMOS-1887 Rats
L.M. Kurkina, I.V. Zabolotskaya (USSR)

Creotine Kinase in the Cytosol and ATPase in Myofibers of the Heart of COSMOS-1887 Rats
T.E. Drozdova, E.A. Nosova (USSR)

Morphometric Evaluation of Cardiomyocytes of COSMOS-1887 Rats
W. Baranska, P. Skopinski (Poland), A.S. Kaplansky (USSR)

Morphometric Studies of Atrial Granules and Hepatocytes from COSMOS-1887 Rats
L. Kraft, L.C. Keil, W. Savage (USA)

Hepatic Function in Rats After Spaceflight
A. Merrill, D. Jones, G. Hargrave, R. Mullins (USA)

Lipid Peroxidation in Rats After COSMOS-1887 13-Day Flight
A.A. Markin, N.V. Delenyan (USSR)

Measurement of Plasma Proteins of COSMOS-1887 Rats by Two-Dimensional Electophoresis
O.N. Larina (USSR)

TABLE 2 - CONTINUED

Amino Acids of Plasma of COSMOS-1887 Rats
N. Yu. Fedorova (USSR)

Changes in Lipids and Saccharides of Rats After COSMOS-1887 Flight
E. Alersova, I. Alers (Czechoslovakia), I.A. Popova (USSR)

Physiological, Biochemical and Morphological Investigations of the Gastrointestinal Tract of COSMOS-1887 Rats
K.V. Smirnov, N.K. Permyakov, L.G. Goncharova, I.A. Morozov, G.P. Titava, E.I. Alekseev (USSR)

Histochemical Changes in the Gastrointestinal Tract of COSMOS-1887 Rats
P. Groza, A. Bordeianu, A Boka (Rumania)

Structural Changes and Cell Turnover in the Small Intestine Cells of Rats Exposed to Spaceflight
R. Phillips, H. Sawyer (USA)

Hormonal Regulation of Individual Functions of the Animal Body After 13-Day Flight
I.M. Larina, E.A. Zagarskava, Yu V. Sukhanov, T.V. Sokolov (USSR)

Functional State of the Rat Pituitary Somatotrophic Hormones
E.I. Alekseev (USSR)

Metabolism of Catecholamines in Primates After COSMOS-1887 Flight
N.A. Davydova, M.A. Datsenko (USSR)

Morphological Examination of the Rat Thyroid Gland
E.N. Kabitsky, G.I. Plakhuta-Plakutina (USSR)

Activity of Adenylate Cyclase in the Cortical and Modullary Layers of Rat Kidneys After COSMOS-1887 Flight
L.M. Kurkina, I.V. Zabolotskaya (USSR)

Activity of the Sympathoadrenal System and Adrenergic Receptors in COSMOS-1887 Rats
R. Kvetnansky, T. Torda, R. Vlasicek, J. Jurovicova, D. Ezhova, M. Vigas (Czechoslovakia), I. A. Popova, L.V. Serova, (USSR)

Insulin Receptors and Enzyme Activity in Liver of COSMOS-1887 Rats
L. Macho, S. Nemeth, E. Slabova, M. Fiskova, S. Zorad (Czechoslovakia)

Morphometric Evaluation of Adrenal Cells of COSMOS-1887 Rats
W. Baranska, P. Skopinski (Poland), A.S. Kaplansky (USSR)

TABLE 2 - CONTINUED

RADIATION BIOLOGY

Effect of HZE Particles on Lactuca Sativa Seeds Exposed Outside the COSMOS-1887 Biosatellite
L. V. Nevzgodina, E.N. Maksimova, E.V. Kaminskaya, A.I. Vikhrov, A.M. Marennyl (USSR)

Radiobiological Experiments with Crepis Capillaris and Arabidopsis Thaliana Seeds Exposed on COSMOS-1887
L.N. Kostina, I.D. Anikeeva, E.N. Vautina, A.M. Marennyl (USSR)

Effect of HZE Particles on Bacteria Brevis Vegetative Cells and Spores Exposed on COSMOS-1887
I.M. Parkhomenka, N.A. Romanova, M.M. Sidyakina, A.P. Zorubina (USSR)

Effect of Accelerated Carbon Ions on Rat Cortical Neurons
B.S. Fedorenko, R.A. Kabitsina, G.N. Krivitskaya, V.I. Derevyagina (USSR)

A New Object for Studying the Effect of HZE Particles - Wolfia Errihus
V. M. Abramova, I.G. Vasilyeva, A.M. Marrennyl (USSR)

Ablogenic Synthesis and Degradation of Nucleosides Under the Action of Ultraviolet Radiation on COSMOS-1887
E.A. Kuzicheva, I.L. Maiko, N.Ya Dodonova (USSR)

Biological Effects of Cosmic Radiation and Microgravity
N. Bucker (FRG)

Radiobiological Effect of Hze Particles on Carausius Morosus Embryogenesis and Organogenesis in COSMOS-1887 Flight
G. Reitz, W. Ruter (FRG)

Measurement of HZE Particle Hits of Lettuce Seeds Flown on COSMOS-1887
R. Fazius (FRG)

General Aspects of Radiation Effects at Low Doses, Including Heavy Ions
E.H. Graul (FRG)

TABLE 3 - COMPOSITION OF RAT DIET

Component	% of Total Calories
casein	18.2
sunflower oil	24.2
sucrose	57.4
yeast, salt, vitamins	< 0.8

The paste diet for the rats contained 70% water and was made up of the above components as a percentage of total calories. The paste diet contained 1.72 k cal/g.

ORIGINAL PAGE
BLACK AND WHITE PHOTOGRAPH

Figure 1. Cosmos spacecraft.

Figure 2. Soviet monkey BIOS.

ORIGINAL PAGE
BLACK AND WHITE PHOTOGRAPH

ORIGINAL PAGE
BLACK AND WHITE PHOTOGRAPH

Figure 3. Restraint chair.

ORIGINAL PAGE IS
OF POOR QUALITY

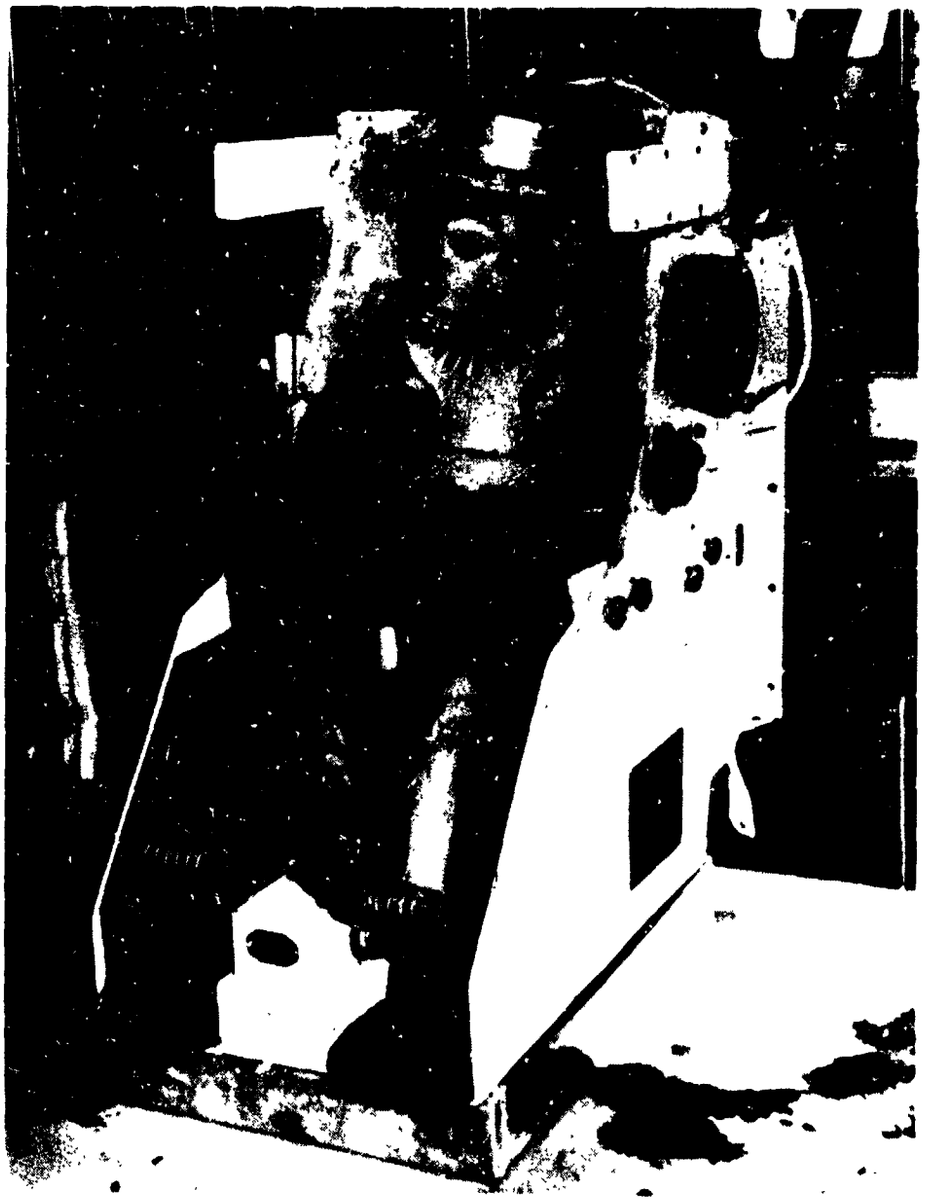

Figure 4. Monkey in BIOS restraint chair.

ORIGINAL PAGE
BLACK AND WHITE PHOTOGRAPH

Figure 5. Monkey restraint chair showing excreta orifice (arrow), lap restraint and foot psychomotor response lever.

Figure 6. Paste feeder and juice dispenser.

ORIGINAL PAGE
BLACK AND WHITE PHOTOGRAPH

ORIGINAL PAGE
BLACK AND WHITE PHOTOGRAPH

Figure 7. Rat BIOS with separator (as for Cosmos 1129).

II. U.S. FLIGHT AND GROUND-SUPPORT HARDWARE

A. HARDWARE OVERVIEW

This section defines the equipment used to support the U.S./U.S.S.R. joint experiments conducted on the Cosmos 1887 Biosatellite. It provides descriptions of flight and ground-support hardware, and outlines the hardware verification test procedures and general operating procedures.

The radiation dosimetry and spectrometry experiment on Cosmos 1887 required the design and use of passive detectors to detect heavy cosmic ray, proton, neutron and total dose radiation. Dosimeters were developed and assembled for mounting both inside and outside the spacecraft. Units outside the spacecraft were integrated into a clamshell-type protective housing (Soviet-supplied) which contained radiation experiments from many different countries (see Figure 9 in Benton Science Report K-6-24, 25, 26).

The United States also supplied a portable X-ray film processor to the Soviet Union for developing primate radiographic films taken preflight and postflight by Soviet specialists.

The Cosmos 1887 Biospecimen Program required the design and development of shipping containers for the transfer of rat samples postflight from the recovery site to Moscow and from Moscow to the United States. These biotransporters were designed to maintain and preserve biospecimens within a prescribed temperature band ranging from –70 to +23°C.

FLIGHT HARDWARE DESCRIPTION AND TEST PLAN

1. Radiation Dosimetry and Spectrometry Hardware

The following hardware was developed for the radiation dosimetry and spectrometry experiments by the U.S. investigator team with consultation provided by the Soviet joint investigator team:

K-6-24 Lexan Box Detector Assembly—7.0 cm × 7.0 cm × 4.0 cm; 233.2 g; contained orthogonal set of PNTD stacks, a set of TLDs and a nuclear emulsion stack. Dosimeters were placed inside the spacecraft.
Measurements: The heavy particle LET spectrum ($LET_{\infty} \cdot H_2O \geq 4$ keV/μm) was measured with the PNTD stacks, the total absorbed dose was measured with the TLDs, the emulsions were included for high-energy proton flux measurements.

K-6-25 Thermoluminescence Detector Assembly (2)—5.0-cm-diam cylinder × 2.0 cm thick. Total mass: 106.7 g; contained stacks of thin and thick TLDs.
Measurements: Depth doses (total absorbed dose) were measured with the TLD stacks outside the spacecraft.

K-6-26A Sealed Plastic Stacks (2)—5.0-cm-diam cylinder × 1.91 cm thick. Total mass: 91.89 g. Measurements: The heavy particle LET spectra ($LET_{\infty} \cdot H_2O \geq 4$ keV/μm) were measured as a function of shielding depth in plastic outside the spacecraft. Doses and dose equivalents were also generated for the heavy particles.

K-6-26B Outside Activation Foil Assembly (2)—5.1 cm × 5.1 cm × 1.0 cm. Total mass: 165.4 g. Measurements: ^{59}Co activation foils were used to measure neutron fluences outside the spacecraft.

K-6-26C Inside Activation Foil Assembly (1)—5.1 cm × 5.1 cm × 0.65 cm. Total mass: 145.5g. Measurements: A ^{59}Co activation foil was used to measure neutron fluences inside the spacecraft.

2. Test Plan

All dosimeter units developed for this flight were single-use, passive systems which eliminated the possibility of using them for preflight testing. The U.S. investigator conducted final assembly of the units in his University of San Francisco laboratory according to a NASA-approved assembly plan. The assembly of flight and ground-control dosimeter packages was monitored and certified by a NASA Reliability and Quality Assurance (R&QA) representative.

GROUND-SUPPORT HARDWARE DESCRIPTION AND TEST PLAN

1. Rat Biospecimen Experiments

The following ground-support equipment was designed for the transfer of rat tissue samples between the recovery site and Moscow and between Moscow and the United States. Some equipment was also required for processing of tissues in Moscow prior to final shipment to the United States.

Recovery Site to Moscow:

- A +23°C biotransporter was developed that could be powered from either 28 Vdc or rechargeable batteries. The battery-charging circuit was designed for use with either 120 or 220 Vac power. This biotransporter could maintain biospecimens at a temperature of 23 ±2°C for a minimum of 40 hours when powered by its prime and backup (rechargeable) batteries. Optional set-point temperatures of +6°C and +37°C were also available.

Moscow to United States:

The biotransporters developed for shipment of rat tissues from Moscow to the United States were constructed from insulated cases (Polyfoam Packers) that were placed inside shipping cases (Anvil) with locking caster wheels. All units were passively cooled and configured to maintain biospecimens within the specified temperature ranges for a minimum of 48 or 72 hours, depending on the application.

- The 4°C transporter contained a battery-operated heating system and phase-gel refrigerant packs (–2°C phase change temperature) to maintain biospecimens at a temperature between +2 and +10°C for a minimum of 72 hours.

- The –23°C transporter used phase-gel refrigerant packs (–23°C phase change temperature) to maintain biospecimens frozen at temperatures between –5 and –35°C for a minimum of 48 hours.

- The –70°C transporter used an insulated internal container which could hold a maximum of 160 lb of dry ice and maintain biospecimens in a frozen state for a minimum of 48 hours.

Laboratory Equipment:

A significant quantity (4000 lb) of tissue-processing equipment and supplies were prepared and shipped to Moscow to support the rat experiments. General categories included fixatives, surgical supplies, tissue culture equipment and many laboratory disposable items.

2. Primate Experiment

A portable X-ray film processor (AFP Imaging Corporation) was supplied to the Soviets for the development of X-ray films. The tabletop processor was equipped for the development of RP-type medical X-ray films in sizes from 4" × 5" (10 × 12.5 cm) to 14" × 46" (35 × 91 cm) at a rate of sixty 14" × 17" (35 × 45 cm) sheets per hour. The portable processor was checked out by the U.S. investigator in his laboratory before it was shipped to the Soviet Union. Soviet specialists developed numerous films in the months prior to the mission in an attempt to find the optimum X-ray camera intensity and exposure settings for use with this system. After extensive testing, and after evaluation of these results by the U. S. investigator, it was decided that the portable processor could not provide the clarity of processing (using the Soviet X-ray system) required for the experiment. Soviet specialists processed the radiographs by hand in Soviet laboratories.

B. BIOTRANSPORTER DEVELOPMENT

+23°C BIOTRANSPORTER

1. Development and Operation

This biotransporter was used at the recovery site and it was designed to maintain biospecimens at a temperature of 23 ±2°C for a minimum of 40 hours. The biosample container, as photographed in Figure 1a-c, had a selector switch for three discrete temperatures (6°C, 23°C and 37°C) with a temperature readout on the top of the unit. The biosample container was mounted in a metal carrying frame and powered by an 80 ampere-hour rechargeable battery mounted inside the carrying frame. A retractable power cord allowed the sample container to be removed from the carrying frame/battery assembly and to be operated remotely at a distance of 4 feet. The carrying frame was designed to fit into an insulated exterior case suitable for shipping. The exterior case also contained a battery-charging circuit and a spare 80-ampere-hour battery.

While the biotransporter was primarily a battery-operated system, it was possible to operate it from a 28 ±4-Vdc, 3-A source (for example, aircraft power). It was not possible to operate the +23°C biotransporter from AC power. The battery charger, however, was designed for operation on either 120-Vac or 220-Vac power. It could charge the backup battery while the prime battery powered the biotransporter, or vice versa.

2. Test Plan

The biotransporter was tested to verify that it would maintain an internal temperature of 23 ±2°C, over an ambient temperature range of –20°C to +29°C, when operated either with a 28-Vdc power supply or its internal batteries.

Test Procedure: The complete biotransporter was used for thermal tests and both the primary and backup batteries were used to power the biotransporter. The primary battery was charged for at least 12 hours before starting the test. A temperature recorder was placed in the bottom of the biosample container. Three sample racks were prepared containing five teflon vials, each with a thermocouple protruding into the center vial of each rack. The racks were stacked one on top of the other inside the biospecimen container. The thermocouple leads were fed out of the container and the lid closed. The biotransporter was placed into the ARC Quality Assurance (QA) environmental chamber and the thermocouple leads connected to the QA Lab's temperature recorder. For the battery-operated test, the temperature chamber was programmed to cycle at 12-hour intervals between 0°C and –20°C for a period of 36 hours with the first 12 hours of the test at 0°C. This was followed by a 6-hour period at 29 ±2°C. Temperature recorder printouts were provided at 20-minute intervals throughout the test. To test the biotransporter using 28 Vdc, the power supply was connected to the power receptacle on the shipping case with voltage level set for 28 Vdc ±4V. A 6-hour test was completed for a test chamber temperature of 0 ±2°C.

+4°C BIOTRANSPORTER

1. Development and Operation

The 4°C biotransporter was designed to maintain biospecimens at temperatures between +2°C and +10°C for a minimum of 72 hours. The design of the biotransporter was similar to the +23°C biotransporter, as photographed in Figures 1a and 1c, but contained thirty refrigerant packs (–2°C phase change temperature) placed at the bottom of an insulated inner container (Fig. 2). Dry ice was added for approximately 12 hours and then removed. A two-layer barrier consisting of sheet aluminum and polyimide foam was placed on top of the refrigerant gel packs. An aluminum sample container with thick insulation foam on the bottom was placed on top of the two-layer barrier. Twenty thermofoil strip heaters were glued to the outside walls of the aluminum box with five heaters per wall. The walls and top of the aluminum box were covered with thick polyimide insulation. A temperature probe, mounted to the top of the box, extended into the sample volume. This probe contained two temperature sensors, one to monitor internal temperature and one to provide information for the temperature control circuit. The 4°C biotransporter also contained a control panel and a rechargeable battery, but it did not include a self-contained battery-charging circuit. The battery was charged using the +23°C biotransporter's charging system.

2. Test Plan

The complete biotransporter was tested to verify that the 4°C biotransporter would hold an internal temperature within the range of +2 to +10°C, for a minimum of 72 hours, for ambient temperatures ranging from –20 to +25 ±2°C.

Test Procedure: Refrigerant packs were placed in the container with the sheet aluminum portion of the two-layer barrier resting on top. Approximately 50 lb of dry ice were added, the lid was attached and the container closed for approximately 12 hours. The dry ice and barrier were removed and the container was allowed to stand for approximately 8 hours (with the lid partially open) to allow the refrigerant packs to warm. The surface and core temperatures of the refrigerant packs were monitored, and the system judged ready for use when the surface temperature reached –5 to –10°C and the core temperature was –10 to –15°C. The two-layer barrier was then reinserted on top of the packs. Prior to insertion of the aluminum sample container, a screw mount was removed from the cover of the container and seven thermocouple leads were fed through the opening.

The thermocouple leads were connected in the following manner. Two racks of five water-filled teflon vials had a thermocouple inserted in the center vial of each rack while two racks of water-filled vials had a thermocouple inserted in the end vial of each rack. Six additional racks of water-filled vials were taped around the test racks and two thermocouples attached to the top of the rack assembly. The remaining thermocouple was attached to the temperature probe mounted on the cover of the aluminum sample container. An additional temperature sensor (Ryan TempMentor) was attached to the rack assembly and the assembly placed in the sample container. This elaborate scheme was designed to measure temperatures at several points within the sample container to ensure that all locations within the container maintained the target temperatures. The sample container was placed inside the insulated case and the lid latched. The insulated case was then placed in the exterior case with the thermocouple leads fed outside the case. The biotransporter was placed in the QA environmental chamber with another thermocouple lead attached to the outside of the exterior case, and all leads were connected to the QA Lab's temperature recorder. The heater and temperature probe cables were connected and the transporter's automatic heating circuit was activated. Testing was started when all internal temperatures were within the desired range (approximately 1 1/2 hours later).

The environmental chamber was programmed to cycle at 12-hour intervals between –20 and +25°C for a period of 72 hours, with the first 12 hours at –20°C. The readings from the internal thermocouples (six) moved into a range between +2 and +10°C and maintained that range for the duration of the 72-hour test. Temperature printouts were provided at 20-minute intervals throughout the test.

–23°C BIOTRANSPORTER

1. Development and Operation

The –23°C biotransporter was designed to maintain biospecimens at temperatures between –5 and –35°C for a minimum of 72 hours. With an assembly similar to the +4°C biotransporter (Fig 1a,c and 2), the inner insulated container of the –23°C biotransporter had 36 refrigerant packs (–23°C phase change temperature) placed in the bottom. An aluminum sample container was subsequently placed on top of the

refrigerant packs. A foam section was placed on top of the sample container before the insulated container was closed. The insulated container was then placed into an insulated shipping container.

2. Test Plan

The –23°C biotransporter was tested to verify that it would hold an internal temperature between –35 and –5°C for 72 hours with the ambient temperature fixed at 29 ±2°C.

Test Procedure: Thirty-six refrigerant packs (-23°C phase change temperature) were placed in the bottom of the inner container. The sample container was placed on top of the refrigerant packs, filled with dry ice, and the inner container closed and allowed to stand for 21 hours. The sample container and dry ice were then removed and the surface and core temperatures of the refrigerant packs were monitored with the cover to the inner container opened 1 to 3 inches. The biotransporter was ready for use when the core temperature was between –35 and –25°C, and the surface temperature was between –35 and –10°C (within 3 hours). The empty sample container was placed on top of the refrigerant packs. Two racks of air-filled teflon vials were taped, parallel to each other, to the bottom of the interior of the container. A thermocouple was placed inside the center vial of each rack and another placed inside the cover of the sample container with the leads fed to the outside of the container. A fourth thermocouple was attached to the top of the exterior case. The biotransporter was placed into the QA environmental chamber with the thermocouple leads connected to the QA Lab's temperature recorder. The temperature readings of the internal thermocouples (three) were monitored until they dropped below –5°C. The environmental chamber's temperature control was set for 29 ±2°C and the test was started. The test continued for 72 hours. Temperature printouts were provided at 20-minute intervals.

–70° C BIOTRANSPORTER (DRY ICE)

1. Development and Operation

The dry ice biotransporter was designed to maintain biospecimens in a frozen state for a minimum of 48 hours. The construction of the biotransporter differed from the –23° and +4°C biotransporters by the inner sample/dry ice container which could hold five plastic-coated, wire-mesh baskets. The baskets were placed one on top of the other. The bottom three were used for biospecimens. The top two baskets were used for dry ice. In practice, it was possible to use this biotransporter without the wire-mesh baskets to allow the maximum amount of dry ice to be added. The insulated container fit into an exterior insulated case suitable for shipping.

2. Test Plan

Because the QA lab's environmental chamber could not accommodate the fully assembled –70°C biotransporter, only the inner insulated container was used. This was deemed appropriate since use of the external shipping case would only enhance the biotransporter's performance. Three sample racks were prepared containing five teflon vials each with a thermocouple inserted through the top of the center vial of each rack. The racks were individually wrapped in several layers of bubble packing material and each was placed in a different sample basket. The sample baskets were placed into the insulated container, one on top of the other, and the thermocouple leads were routed to the outside. A wind-up temperature recorder was placed in one of the three sample baskets. The fourth and fifth racks, filled with

approximately 80 lb of dry ice, were added and the cover was closed. The container was placed in the QA environmental chamber. A thermocouple was attached to the outside of the container to record the ambient temperature. All four thermocouples were connected to the temperature recorder. After the temperatures of the internal thermocouples (three) dropped below –5°C, the environmental chamber's temperature control was set for 29 ±2°C and the chamber was started. The test was continued for 48 hours. Temperature printouts were provided at 20-minute intervals throughout the test.

ORIGINAL PAGE
BLACK AND WHITE PHOTOGRAPH

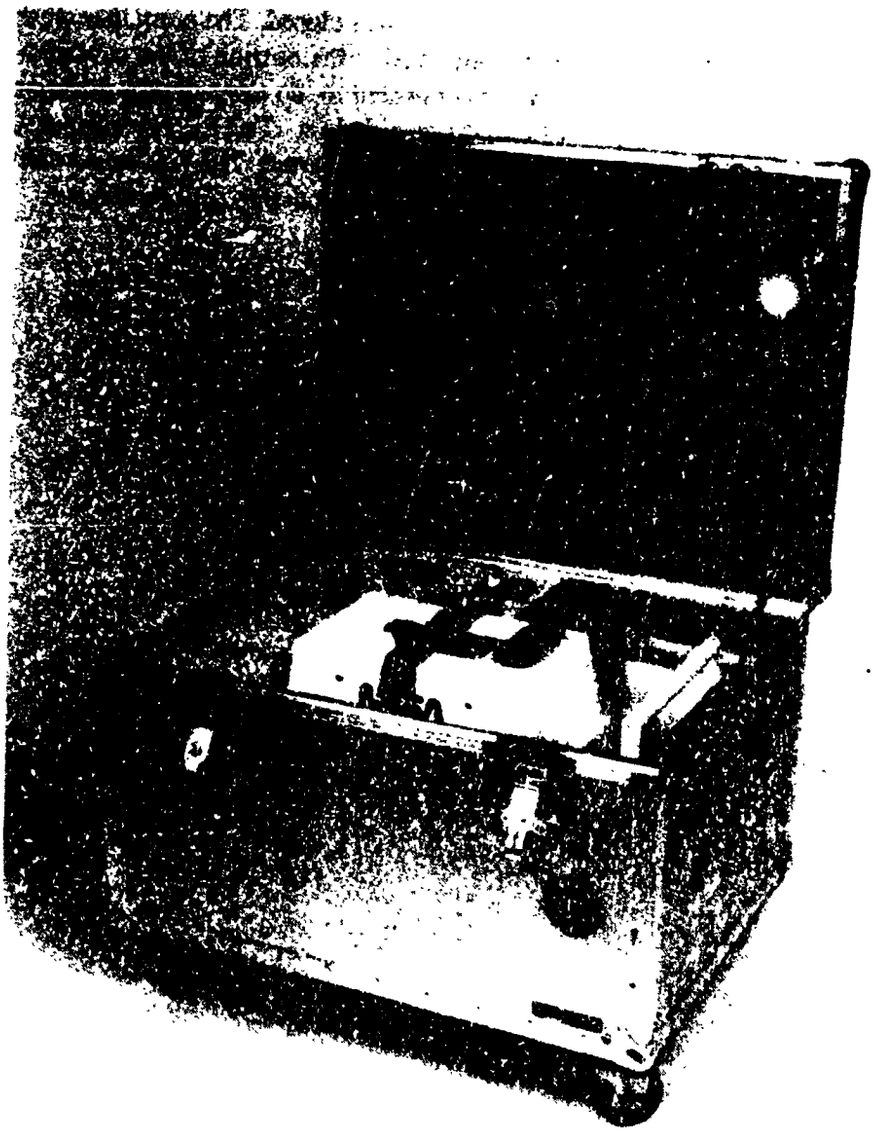

Figure 1a. Aluminum Anvil case for biotransporters.

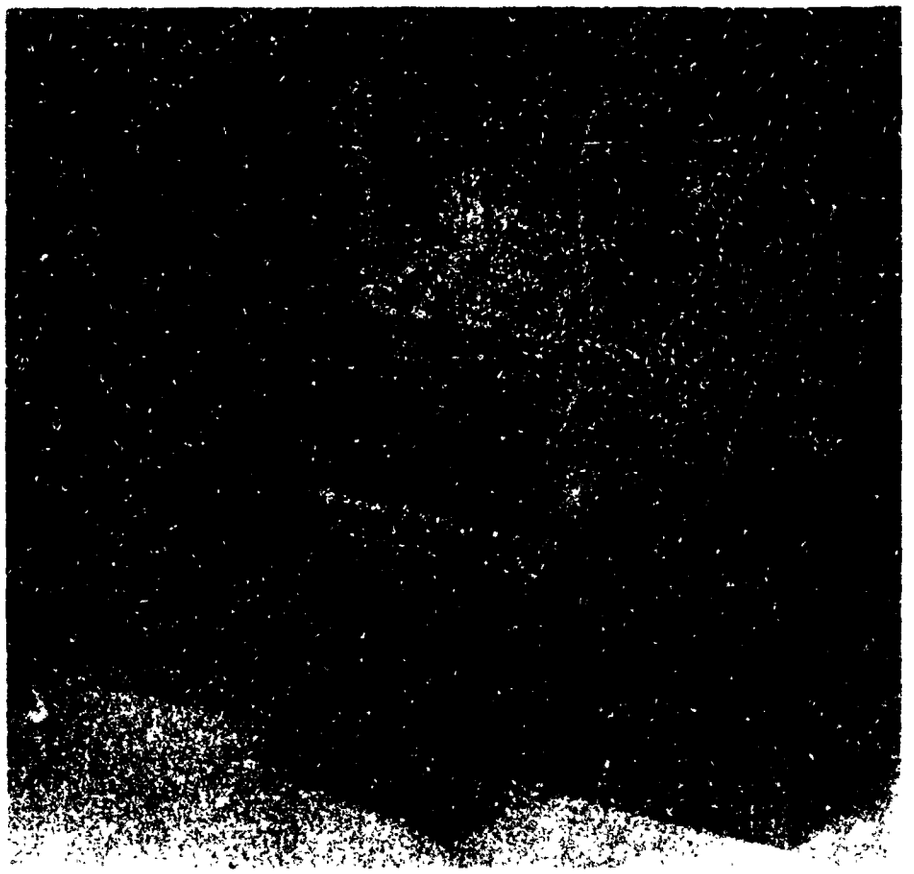

Figure 1b. Battery-operated heating unit for +23°C biotransporter.

ORIGINAL PAGE
BLACK AND WHITE PHOTOGRAPH

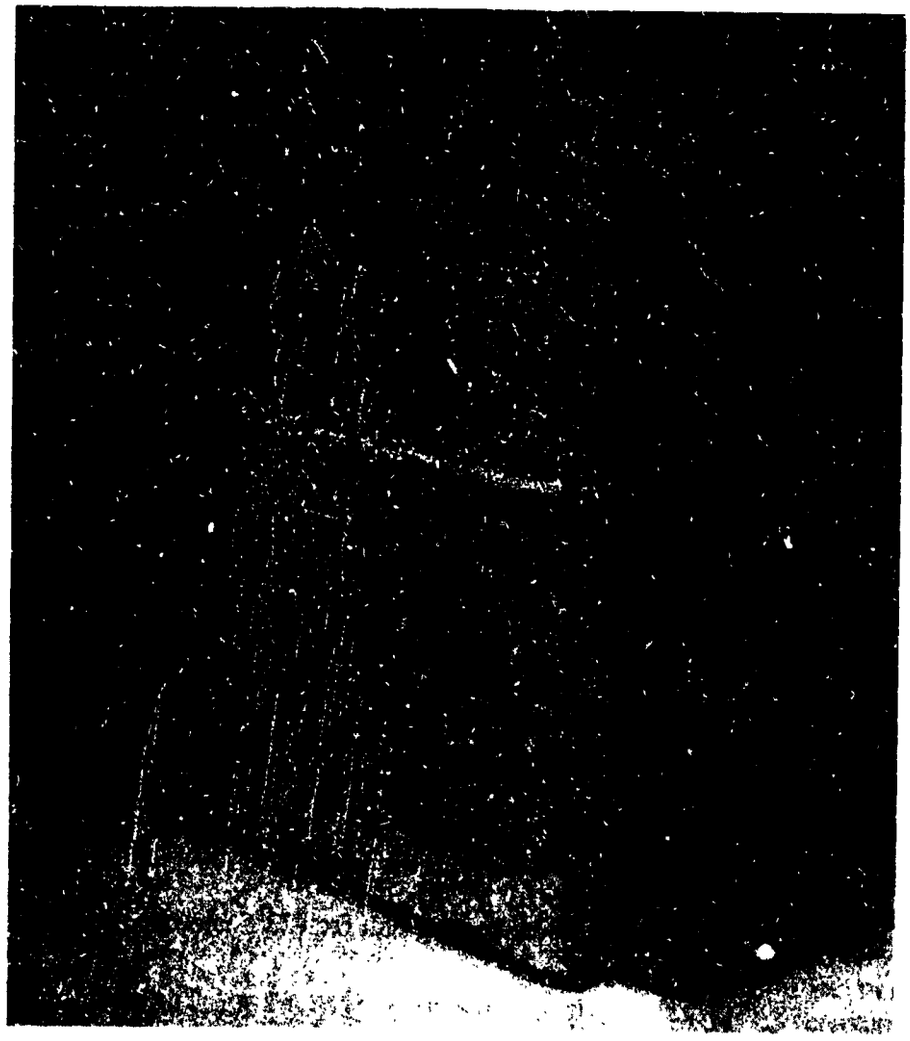

Figure 1c. Temperature chamber for biotransporter.

ORIGINAL PAGE
BLACK AND WHITE PHOTOGRAPH

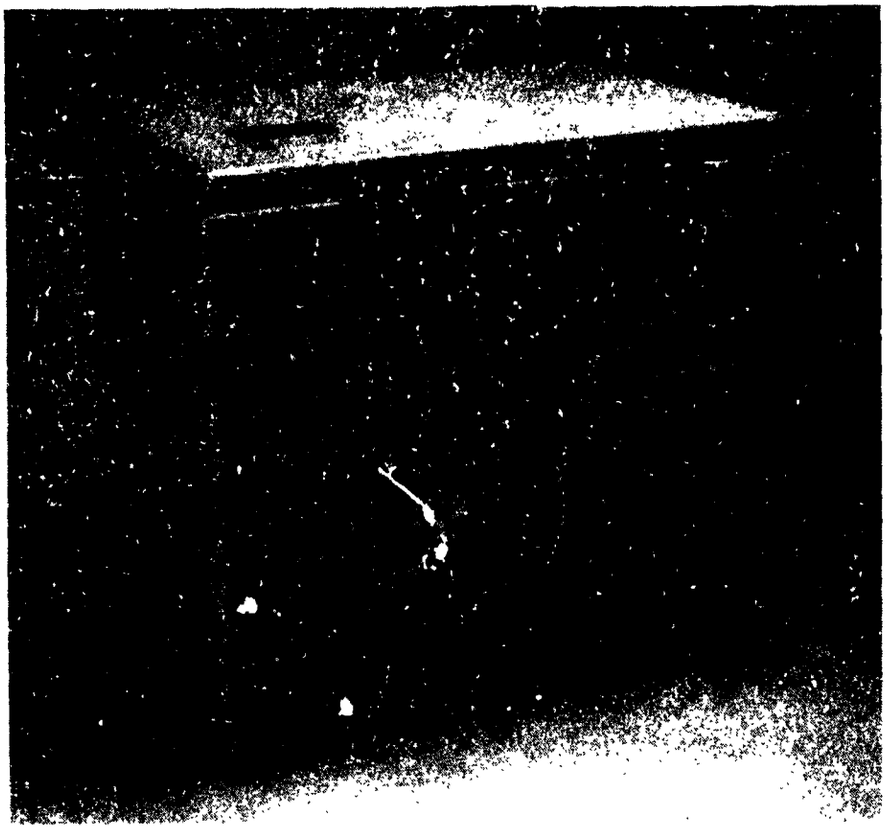

Figure 2. Polyfoam insulated container for +4, –23 and –70°C biotransporters.

ORIGINAL PAGE
BLACK AND WHITE PHOTOGRAPH

N90-26453

III. MISSION OVERVIEW AND SUMMARIES OF EXPERIMENTS

EFFECTS OF MICROGRAVITY ON RAT MUSCLE

D.A. Riley
Department of Anatomy and Cellular Biology
Medical College of Wisconsin
Milwaukee, Wisconsin 53225

It is well known that humans exposed to long term spaceflight experience undesirable progressive muscle weakness and increased fatigability. This problem has prompted the implementation of inflight exercise programs because most investigators believe that the major cause of diminished muscle performance is a combination of disuse and decreased workload. Inflight exercise has improved muscle health, but deficits have persisted, indicating that either the regimens utilized were suboptimal or there existed additional debilitating factors which were not remedied by exercise.

Clarification of this question requires an improved understanding of the cellular and molecular basis of spaceflight-induced muscle deterioration. To this end, multiple investigations have been performed on the muscles from rats orbited 5-22 days in Cosmos biosatellites and Spacelab-3 (2,4,5,8,10-14,16,18,19, 21-23,25,27,28).

The eight Cosmos 1887 investigations that follow examined the structural and biochemical changes in skeletal and cardiac muscles of rats exposed to microgravity for 12.5 days and returned to terrestrial gravity 2.3 days before tissues were collected. Even though interpretation of these results was complicated by the combination of inflight and postflight induced alterations, the consensus is that there is marked heterogeneity in both the degree and type of responses from the whole muscle level down to the molecular level. Consistent with previous reports, red (oxidative) antigravity muscles (such as soleus, adductor longus, and vastus intermedius) were more atrophic than white (glycolytic) non-antigravity muscles (extensor digitorum longus, tibialis anterior, vastus lateralis and medialis) (2,4,5,13,14,16,17, 19,23,25,27). To some extent, fiber type composition predicts the degree of muscle atrophy. The most affected muscles were composed primarily of slow oxidative fibers whereas fast oxidative glycolytic and fast glycolytic fibers predominated in the least affected muscles. However, at another level of complexity, fibers of a given type located deep in a muscle (closer to the bone) exhibited greater atrophy than fibers of the same type located superficially in the same muscle (7). More limited in occurrence than muscle atrophy was the degeneration of muscle fibers, nerves, and micro-vessels which only involved the adductor longus and soleus muscles (24). Within the adductor longus, the pathology affected the mid-belly or endplate region more extensively than the ends or myotendinous zones.

Generally speaking, muscle enzyme properties shifted from slow oxidative toward fast glycolytic, but microheterogeneity was evident. During atrophy, contractile proteins, especially slow myosin, were preferentially lost relative to cytoplasmic non-contractile proteins (1,7,28). Increased ubiquitination of contractile proteins was observed (24). This process is postulated to promote selective protein degradation (26). Within slow oxidative fibers, slow myosin was replaced by fast myosin resulting in hybrid slow/fast fibers with elevated myosin ATPase activity (1,7). The shifts in cytoplasmic enzymes were not uniform. In soleus muscles, oxidative enzymes (citrate synthase and malate, beta-hydroxyacyl CoA, and

PRECEDING PAGE BLANK NOT FILMED

succinate dehydrogenases) decreased in step with muscle atrophy so that their concentrations were minimally altered (15). In contrast, glycogenolytic enzymes (glycogen phosphorylase, glycerophosphate dehydrogenase, lactate dehydrogenase, and pyruvate kinase) were not lost and their amounts per fiber increased during atrophy. In contrast to soleus, individual muscle fibers of the tibialis anterior showed elevated oxidative enzymes in atrophic fibers whereas glycogenolytic enzymes minimally changed in concentration (15). Mitochondrial enzyme changes were not uniform across the diameter of a muscle fiber. Mitochondria and their associated enzyme activities were essentially unchanged centrally but showed a marked decrease in the peripheral subsarcolemmal population (7,24). The mechanism by which proteins are turned over selectively and enzyme levels are altered within specific regions of atrophic muscle fibers are not understood.

The absence of detectable shifts in alpha-actin and cytochrome c mRNA levels may have resulted from the postflight muscle contractile activity because messenger levels can easily be altered within two days (29). Other parameters, such as atrophy, do not change markedly in two days and therefore, more accurately reflect microgravity induced changes. Distinguishing between microgravity induced and postflight readaptation induced alterations is a primary objective for the proposed studies in which muscles are harvested immediately (within 4 to 9 hours) upon landing (Cosmos July 1989, SLS-1) or inflight (SLS-2).

The muscle atrophy associated with spaceflight is most likely due to disuse and reduced workload. The observed decrease in mature collagen cross-links, collagen concentration and DNA concentration in the patellar tendons of flight rats is consistent with lowered workload (30). However, the Achilles tendon, serving the gastrocnemius/soleus/plantaris complex, was unchanged in the same animals (3). Again, these findings illustrate the diversity of skeletal muscle tissue responses. Activity and workload can be assessed by instrumenting muscles with electromyographic electrodes and tendon tension transducers. Systematic factors may have also contributed to atrophy. The suspected lower levels of growth hormone would have had a general catabolic effect on a skeletal muscle and elevated glucocorticoids, indicated by adrenal cortex hypertrophy, would have specifically induced fast fiber atrophy (9).

Some cardiac and skeletal muscle fibers were necrotic (20,24). The motor innervation of skeletal muscle was partially degenerated (24). Microcirculatory vessels were disrupted in skeletal muscle and abnormal in cardiac muscle (20,24). Repair of necrotic muscle fibers, motor axons, and blood vessels is dependent upon the effectiveness of complex processes of regeneration. Ground-based evidence predicts that regeneration may be compromised in space because of reduced active muscle tension and exposure of the dividing stem cells to damaging cosmic radiation (3,6,13). The ability of tissues to regenerate effectively during spaceflight is important to address in future missions.

Collectively, the muscle investigations of Cosmos 1887 clearly illustrate the wide diversity of muscle tissue responses to spaceflight. Judging from the summary report of this mission, heterogeneity of responses is not unique to muscle tissue. Elucidating the mechanism underlying this heterogeneity holds the key to explaining adaptation of the organism to prolonged spaceflight.

REFERENCES

1. Baldwin, K.M. and Herrick, R.E. Effect of Zero Gravity on Myosin Isoform Expression in Rodent Skeletal Muscle. In Final Reports of U.S. Experiments Flown on the Soviet Biosatellite Cosmos 1887. (Connolly, J.P., Grindeland, R.E., and Ballard, R.W., eds). This report.

2. Baranski, S., Baranska, W., Marciniak, M., Ilyina-Kakueva, E.I. 1979. Ultrasonic ("Ultrastructual") investigations of the soleus muscle after space flight on the Biosputnik 936. Aviat. Space Environ. Med. 50:930-934.

3. Benton, E.V. Peterson, D.D., Marenny, A.M, Popov. V.I. 1978. HZE particle radiation studies aboard Kosmos 782. Health Physics. 35:643-648.

4. Castleman K.R et al. 1978. Spaceflight effects on muscle fibers: Final Reports of U.S. Experiments Flown on Soviet Satellite Cosmos 936. Rosenzweig, S.N., Souza, K.A., Eds. NASA Technical Memorandum 78526. pp. 224-289.

5. Castleman, K.R., Chui, L.A., Van Der Meulen, J.P. 1981. Automatic analysis of muscle fibers from rats subjected to spaceflight. NASA Technical Memorandum 81289. pp. 267-277.

6. Denny-Brown, D. 1951. The influence of tension and innervation on the regeneration of skeletal muscle. J. Neuropath. Exp. Neurol. 10:94-95.

7. Edgerton, V.R., Martin, T.P., Roy R.R., Marini, J.F., Leger, J.J. Metabolic and Morphological Properties of Muscle Fibers after Spaceflight. In Final Reports of U.S. Experiments Flown on the Soviet Biosatellite Cosmos 1887. (Connolly, J.P., Grindeland, R.E., and Ballard, R.W., eds). This report.

8. Gazenko, O.G., Genin, A.M. Il'in, Y.A, Portugalov, V.V., Serova, L.V., Tigranyan, R.A. 1978. Principal results of experiment with mammals onboard the Kosmos-782 biosatellite. Kosmich. Biol Aviakosmisch. Med. 6:43-49.

9. Grindeland, R.E., Popova, I., Vasques, M. Effects of Microgravity on Rat Body and Adrenal Weights and Plasma Constituents. In Final Reports of U.S. Experiments Flown on the Soviet Biosatellite Cosmos 1887. (Connolly, J.P., Grindeland, R.E., and Ballard, R.W., eds). This report.

10. Ilyin, E.A. 1983. Investigations on biosatellites of the Cosmos series. Aviat. Space Environ. Med. Suppl. I. 54:S9-S13.

11. Ilyina-Kakuyeva, E.I. 1987. Investigation of rat skeletal muscles following short-term spaceflight aboard Cosmos-1667 biosatellite. Kosmich. Biol. Aviakosmich. Med. 21:31-35.

12. Ilyina-Kakuyeva, E.I. Portugalov, V.V. 1981. Structural changes in the soleus muscle of rats flown aboard the Cosmos series of biosatellites and submitted to hypokinesia. Kosmich. Biol. Aviakosmich. Med. 15:37-40.

13. Ilyina-Kakuyeva, E.I. Portugalov, V.V. 1977. Combined effect of space flight and radiation on skeletal muscles of rats. Aviat. Space Environ. Med. 48:115-119.

14. Ilyina-Kakueva, E.I. Portugalov, V.V., Krivenkova, N.P. 1976. Space flight effects on the skeletal muscle of rats. Aviat. Space Environ. Med. 47:700-703.

15. Lowry, O.H. McDougal, D.B., Chi, M.-Y., Pusateri, M.E., Carter, J.G., Manchester, J.K. Effect of Microgravity on 1) Metabolic enzymes of Type 1 and Type 2 Muscle Fibers and on 2) Metabolic Enzymes, Neurotransmitter Amino Acids and Neurotransmitter Associated Enzymes in Motor and Somatosensory Cerebral Cortex. In Final Reports of U.S. Experiments Flown on the Soviet Biosatellite Cosmos 1887. (Connolly, J.P., Grindeland, R.E., and Ballard, R.W., eds). This report.

16. Martin, T.P. Edgerton, V.R., Grindeland, R.E. 1988. Influence of spaceflight on rat skeletal muscle. J. Appl Physiol. 65:2318-2325.

17. Musacchia, X.J., Steffen, J.M., Fell, R.D. Skeletal Muscle Atrophy in Response to 14 Days of Weightlessness. In Final Reports of U.S. Experiments Flown on the Soviet Biosatellite Cosmos 1887. (Connolly, J.P., Grindeland, R.E., and Ballard, R.W., eds). This report.

18. Oganov, V.S., Skuratova, S.A., Potapov, A.N. Shirvinskaya, K., Marusich, M. 1982. Physiological mechanisms of adaptation of rat skeletal muscles to weightlessness and similar functional requirements. The Physiologist. 23:S16-S21.

19. Oganov, V.S., Rakhmanov, A.S., Skwatova, S.A., Shirvinskaya, Magedov, V.S. 1985. Functions of skeletal muscles of rats and monkeys after 5-day spaceflight on Cosmos 1514. Proc. 2nd Int. Conf. Space Physiol., Toulouse, France.

20. Philpott, D.E., Mednieks, M.I., Papova, I.A., Serova, L.V., Kato, K. Stevenson, J., Miquel, J. Sapp, W. Morphological and Biochemical Examination of Heart Tissue.

21. Portugalov, V.V., Ilyina-Kakueva, E.I. Prolonged spaceflight and hypokinesia. Aerospace Med. 44:764-768.

22. Portugalov, V.V., Ilyina-Kakueva, E.I. Starostin, V.I., Rokhlenko, D.K., Savik, Z.F. 1971. Morphological and cytochemical studies of hypokinetic effects. Aerospace Med. 42:1041-1049.

23. Rapcsak, M., Oganov, V.S., Szoor, A., Skuratova, S.A., Szilagyi, R. 1983. Effect of weightlessness on the function of rat skeletal muscles on the biosatellite Cosmos-1129. Acta Physiol. Hung. 62:225-228.

24. Riley, D.A., Ilyina-Kekueva, E.I., Ellis, S., Bain, J.L.W., Sedlak, R.F., Slocum, G.R. Morphological, Histochemical and Biochemical Investigation of Microgravity-induced Nerve and Muscle Breakdown. In Final Reports of U.S. Experiments Flown on the Soviet Biosatellite Cosmos 1887. (Connolly, J.P., Grindeland, R.E., and Ballard, R.W., eds). This report.

25. Riley, D.A., Ellis, S., Slocum, G.R., Satyanarayana, T., Bain, J.L.W., Sedlak, F.R. 1987. Hypogravity-induced atrophy of rat soleus and extensor digitorum longus muscles. Muscle & Nerve. 10:560-568.

26. Riley, D.A., Bain, J.L.W., Ellis, S., Haas, A.L. 1988. Quantification and immunocytochemical localization of ubiquitin conjugates within rat red and white skeletal muscles. J. Histochem. Cytochem. 36:621-632.

27. Rokhlenko, K.D., Savik. Z.F. 1981. Effect of space flight factors on ultrastructure of skeletal muscles. Kosmich. Biol. Aviakosmich. Med. 1:72-77.

28. Takacs, O., Rapcsak, M. Szoor, A., Oganov, V.S., Szilagyi, T., Oganesyan, S.S., Guba, F. 1983. Effect of weightlessness on myofibrillar proteins of rat skeletal muscles with different functions in experiment of biosatellite Cosmos-1129. Acta Physiol. Hung. 62:228-233.

29. Thomason, D.B., Morrison, P.R., Booth, F.W. Messenger RNA Levels in Skeletal Muscle. In Final Reports of U.S. Experiments Flown on the Soviet Biosatellite Cosmos 1887. (Connolly, J.P., Grindeland, R.E., and Ballard, R.W., eds). This report.

30. Vailas, A.C., Zernicke, R.F., Grindeland, R.E. Biomechanical, Biochemical and Morphological Alterations of Muscle and Dense, Fibrous Connective Tissues during 14 Days of Spaceflight. In Final Reports of U.S. Experiments Flown on the Soviet Biosatellite Cosmos 1887. (Connolly, J.P., Grindeland, R.E., and Ballard, R.W., eds). This report.

N90-26454

EFFECTS OF MICROGRAVITY ON RAT BONE, CARTILAGE AND CONNECTIVE TISSUES

S. Doty
School of Oral and Dental Surgery
Columbia University
New York City, New York

INTRODUCTION

The response to hypogravity by the skeletal system was originally thought to be the result of a reduction in weight bearing. Thus a reduced rate of new bone formation in the weight-bearing bones was accepted, when found, as an obvious result of hypogravity. However, data on non-weight-bearing tissues have begun to show that other physiological changes can be expected to occur to animals during spaceflight. In this overview of the Cosmos 1887 data we will comment on these results as they pertain to individual bones or tissues because the response seems to depend on the architecture and metabolism of each tissue under study.

INVESTIGATIONS OF THE FEMUR

The femur was surgically divided into three sections: proximal, distal and central. Biochemical analysis of each section revealed that in the flight animals the central region (i.e., diaphyseal bone) showed a reduction in bone mineral and content of osteocalcin, but no change in collagen content. The collagen results were difficult to analyze because of the wide variation in animal weights and age among the three control groups. Some additional biochemical changes which were noted were a decrease in serum osteocalcin in the flight animals compared to synchronous controls. And adrenal weights were increased in the flight animals suggesting a certain level of stress existed in this group which was not present in the control groups.

Two non-chemical, non-destructive methods were used to analyze the distribution of mineral content in different regions of the femur. In one case, an x-ray microbeam with a ten micron diameter resolution was scanned across the surface of the mineralized cross-sections of femur. Absorption of these x-rays was correlated with mineral content and density relative to the area of bone being scanned. However, because of the extremely long time required to do this analysis, only one femur from the control and the flight group was studied. In the second method, an electron microbeam, generated by a scanning electron microscope, bombarded a cross-section of mineralized femur and generated backscattered electrons which were captured and analyzed. The backscattered electron image generated a density map of the specimen surface and these densities were related to the morphology of the specimen surface. There was considerable variation in these results between groups of animals and no conclusions were reached using these new methods although they offer a significant new approach for future studies.

INVESTIGATIONS OF THE TIBIA

Morphometric measurements were made on cross-sections of tibia but no differences were found in bone area, marrow area, periosteal perimeter or marrow perimeter between flight and control animals. In previous flights tetracycline was used to indicate areas of new bone formation. This matrix marker was not

PRECEDING PAGE BLANK NOT FILMED

used in Cosmos 1887 so it was not possible to distinguish areas of new bone formation from pre-flight bone surfaces. Thus possible alterations in bone formation could not be determined in this flight.

Measurements were made of the surface electrical charge of particles of bone from tibias of the flight and control rats. When uniform particles of bone move through an electrical field (this technique is similar to electrophoresis) information is obtained concerning the surface charge on these particles. Experience from earth-bound control studies suggests that when new bone formation predominates in the skeleton, the bone particles carry a greater than normal negative charge. These same measurements made on bone from the Cosmos 1887 rats indicated that there was new bone formation occurring to a greater degree in the flight animals compared to the controls. This result is contradictory to morphometric data obtained from several previous flight in which bone formation was reduced during spaceflight. The Cosmos 1887 data could be interpreted to mean that the animals were already beginning to recover due to their 55 hours on earth prior to sacrifice. However, this technique has not been applied to bones from spaceflight which were known to have reduced new bone formation so the interpretation of this data is still unclear.

Histochemistry and morphometry of the osteoblast population located along the diaphyseal endosteal surface was done to compare osteoblast function among the different groups. There was no obvious change in alkaline phosphatase activity or overall osteoblast morphology as a result of the spaceflight. This compared well with the biochemical measurements which showed no change in collagen synthesis in the femur diaphysis (1). However, the histochemical demonstration of NADPase activity in the small Golgi vesicles of the osteoblast indicated that there were more vesicles present in flight osteoblasts compared to control osteoblasts. This result could be due to a decrease in cellular energy stores needed to move the vesicles out of the cytoplasm (thus their accumulation when energy is decreased) or it could be due to an acute increase in procollagen synthesis resulting from the 55 hours at 1g prior to sacrifice.

The vascularity of the diaphyseal bone was studied by morphology and histochemistry. The flight animals showed a reduction in enzyme activity of the vascular endothelial cells, an increase in numbers of vessels per bone cross-section area, some lipid accumulation in vessels near the periosteum, and occasional degenerate osteocytes in the vicinity of these same vessels. These results strongly suggest that the vascular supply which nourished the compact bone of the tibia had been damaged either due to spaceflight conditions or to the effects of re-entry from the flight. These same observations could explain the reduction in some mechanical properties seen in the humerus following flight (2) although the vascularity of the humerus was not studied in this flight.

INVESTIGATIONS OF THE TIBIA EPIPHYSEAL PLATE

The epiphyseal growth plate has been shown to respond to the absence of gravity in the Spacelab-3 experiments. But the growth of long bones is also sensitive to other influences, especially the presence or absence of growth hormone. It has been shown by Hymer and Grindeland (3) that secretion of growth hormone from the pituitary somatotrophs is inhibited in spaceflight.

In flight animals from Cosmos 1887, the proliferative zone at the top of the growth plate was larger than in the synchronous controls, however the hypertrophic/degenerate cell zone was smaller than in the controls. The total number of cells in the growth plate was greater following flight, yet the overall area of the plate was smaller. These data are contradictory to results found in the Spacelab-3 experiment and

suggest that in Cosmos 1887 the proliferation of cartilage cells had resumed following flight due to the 55 hour delay in sacrifice following the return of the biosatellite.

In a parallel study on the tail-suspended non-weight bearing rat model of Morey-Holton there was also a decrease in plate height and decreased numbers of cells per volume of growth plate. However in these suspended animals the greatest effect was seen in the hypertrophic zone, not in the proliferative zone. So the suspended animal model and space flight produce some slightly but significantly different effects on the growth plate of the long bones.

There needs to be a continuation of work in this area to determine which effects on growth are controlled by hormonal changes, by overall change in animal physiology, or by the absence of gravity. This is apparently a complex process of growth and may be controlled by many different biochemical and biomechanical events.

INVESTIGATIONS OF THE HUMERUS

Morphomctric measurements of cross-sections of the humerus showed a decrease within flight animals compared to synchronous controls and a decrease in periosteal circumference compared to synchronous and vivarium controls. These data are different from the results with the tibia (4) in which no changes in these parameters were seen. The mechanical bending stiffness of the humerus correlated with the morphometry in that there was a decrease in the flight animals compared to synchronous controls. The elastic modulus, which is determined by the material characteristics of the bone, was unchanged due to flight and the biochemistry indicated that there was no difference in Ca, P, or hydroxyproline content of the humerus. However, these measurements were made from whole bones. It might have been interesting to compare the biochemistry of different areas of bone (proximal, distal and central diaphysis) as was done in the study by Arnaud et al (1).

An important study was done by Grindeland at NASA Ames to compare US and USSR flight experimental procedures and how these might affect experimental results. For example, the US uses Taconic-Sprague Dawley rats, on special diet, and housed as one rat per cage. The USSR experiments use Czechoslavakian-Wistar rats, maintained on a different diet, and housed as ten rats per cage. The diet ingredients are included in the Vailas, et al report (2). A comparison was made of morphometric and biomechanical measurements on the humerus and vertebrae under these various experimental conditions and the differences in results were noted in this report.

Another aspect to the Vailas report was a comparison of the effect of spaceflight on the patellar and Achilles tendons. The measurements of collagen content, collagen cross-linking, and DNA content showed a heterogeneous spaceflight response depending on the tendon function during flight.

INVESTIGATION OF BONE AND ITS COMPARISON TO DENTINE

In this study, bone mineral from the calvaria and vertebrae (L5) was compared to mineral from dentine in the mandible. The bone ash from flight bones was reduced compared to controls, however, the concentrations of Ca Mg and P (expressed as % of dry weight) were normal. The ratio of Ca/P was reduced in the flight group and the ratio of Ca/Mg was higher than the control values. This suggests that the bone was mineralizing but was failing to mature properly. To study these mineral changes in more detail, the

bone was reduced to particles below twenty microns in size and then fractionated through a series of solutions of different specific gravity. The density of the bone particles from the flight animals showed a shift to lower specific gravity fractions compared to controls, again indicating an immaturity in the process of bone mineralization. X-ray diffraction was also used for analysis of bone mineral and dentine. These data showed that there was a reduced growth in the c-axis of the bone mineral crystal from the flight animals. The mineral from dentine did not show this change, indicating normal mineral maturation in this tissue. Because of the small amount of dentine available for study, an electron microprobe was used to determine Ca/P and Ca/Mg ratios, and concentrations of Ca, P, Mg and An. These values for dentine were normal when compared to age-matched controls. Thus the flight effects on the inhibition of mineral maturation seem confined to bone.

INVESTIGATION OF THE PERIODONTAL LIGAMENT

The periodontal ligament which stretches between the tooth root and the surrounding alveolar bone, contains bone cell precursors which are responsive to signals for increasing or decreasing bone formation. These cells can be classified by their nuclear morphology into 1) a precursor cell which gives rise to 2) an osteoprogenitor, or committed cell, which gives rise to 3) the preosteoblast, which eventually forms 4) the mature bone-forming osteoblast. Previous spaceflight experiments indicated that the progenitor cell (osteoprogenitor) increased in numbers while the preosteoblasts decreased in numbers, in response to the hypogravity environment. The present Cosmos 1887 data indicated the opposite result, with an increase in the preosteoblast population by 42% over the synchronous controls, and a concomitant decrease in the osteoprogenitor cell population. It would appear that the bone cells had begun to recover from the flight effects during the 55 hour period between the return to earth and the sacrifice of the rats. The fact that matrix mineralization defects were seen in the mandibular bone (5) provides support that a bone matrix defect did occur during the flight, however, the cellular response apparently adjusted quickly to the change in the gravitational environment.

INVESTIGATIONS OF THE VERTEBRAE

The vertebral body (L6) was biomechanically and biochemically analyzed by Vailas et al (2) following Cosmos 1887. The calcium and hydroxyproline content was unchanged due to flight; however, the number of cross-linkages per collagen molecule were less in samples from flight animals compared to vivarium or synchronous controls. Mechanical testing of the whole vertebra revealed that the compression stiffness was actually reduced as a result of flight.

Studies on the vertebrae (L4) by Cann et al (6) were done by dissecting out the posterior portion from the vertebral body. This is the region, in the rat, that contains the most dense bone and is the major supportive element of the vertebra. The measurements of weight, water content, Ca, P and osteocalcin were not very conclusive when the flight group was compared to the various controls. However, the osteocalcin concentration in the posterior of vertebrae from flight animals tended to be higher than in the control groups. (This result was opposite to the finding of Arnaud et al (1) in measurements from the diaphyseal portion of the femur.) This result suggests, based on previous ground-based studies, that the bone turnover in this region was reduced.

A study of the intervertebral disc was done by Hargens et al (4) to determine if swelling pressures within the discs could explain the back pain experienced by astronauts during space travel. Direct

measurements of swelling pressure in the nucleus pulposus from lumbar vertebrae were done using a newly developed technique. However, no significant difference was found between the flight and control groups. This lack of effect was probably due to the 55-hour recovery period prior to animal sacrifice in this experiment.

CONCLUSIONS

Various effects were seen in different tissues from the rats flown on Cosmos 1887. The femur showed a reduced bone mineral content but only in the central region of the diaphysis. This same region in the tibia showed changes in the vascularity of bone as well as some osteocytic cell death. The humerus demonstrated reduced morphometric characteristics plus a decrease in mechanical stiffness. Bone mineral crystals did not mature normally as a result of flight suggesting a defect in the matrix mineralization process. Note that these changes relate directly to the matrix portion of the bone or some function of bone which slowly responds to changes in the environment. However, most cellular functions of bone are rapid responders. The stimulation of osteoblast precursor cells, the osteoblast function in collagen synthesis, a change in the proliferation rate of cells in the epiphyseal growth plate, the synthesis and secretion of osteocalcin, and the movement of water into or out of tissues, are all processes which respond rapidly to environmental change. These rapidly responding events produced results from Cosmos 1887 which were frequently quite different from previous space flight data. It was not always possible to know if these results were due to space flight or the recovery from flight during the 55-hour period between flight and animal sacrifice. On the other hand, matrix related events or permanent cellular changes (e.g., matrix mineralization or osteocyte cellular degeneration) did not have the ability or enough time during the 55 hour delay to "recover" or to return to some other state of activity. Consequently, the more slowly responding biological processes provided a better indication of past biological events and apparently retained the record of the flight effects.

If another biosatellite were to repeat the Cosmos 1887 experiments but were followed by a more rapid satellite retrieval and sacrifice of animals, the Cosmos 1887 data would gain even more in value. We could then retrospectively determine which data indicated a true "recovery" from flight and which data showed more lasting long term effects created by the hypogravity. The flight of Cosmos 1887 and the accidental delay in retrieving the animals has provided data which are very rare in studies of space biology. An appreciation of the cellular or tissue "recovery" aspects of this flight will always remain an important contribution to our scientific understanding of the effects of hypogravity on the skeletal system.

REFERENCES

1. Arnaud, S.B. et al. Distribution of Mineral and Matrix in the Femurs of Rats. In Final Reports of U.S. Experiments Flown on the Soviet Biosatellite Cosmos 1887. (Connolly, J.P., Grindeland, R.E., and Ballard, R.W., eds). This report.

2. Vailas, A. et al. Biomechanical, Biochemical and Morphological Alterations of Muscle and Dense, Fibrous Connective Tissues during 14 Days of Spaceflight. In Final Reports of U.S. Experiments Flown on the Soviet Biosatellite Cosmos 1887. (Connolly, J.P., Grindeland, R.E., and Ballard, R.W., eds). This report.

3. Grindeland et al. Growth Hormone Regulation, Synthesis and Secretion in Microgravity. In Final Reports of U.S. Experiments Flown on the Soviet Biosatellite Cosmos 1887. (Connolly, J.P., Grindeland, R.E., and Ballard, R.W., eds). This report.

4. Holton, E. et al. Gravity and Skeletal Growth. In Final Reports of U.S. Experiments Flown on the Soviet Biosatellite Cosmos 1887. (Connolly, J.P., Grindeland, R.E., and Ballard, R.W., eds). This report.

5. Simmons, D. et al. Effect of Spaceflight on Maturation of Bone Mineral in the Axial and Appendicular Skeletons and in the Mandibles of the Rat. In Final Reports of U.S. Experiments Flown on the Soviet Biosatellite Cosmos 1887. (Connolly, J.P., Grindeland, R.E., and Ballard, R.W., eds). This report.

6. Cann, C.E. et al. Trace Element Balance in Rats during Spaceflight. In Final Reports of U.S. Experiments Flown on the Soviet Biosatellite Cosmos 1887. (Connolly, J.P., Grindeland, R.E., and Ballard, R.W., eds). This report.

RESULTS FROM OTHER EXPERIMENTS

R. Grindeland
Life Sciences Division
NASA Ames Research Center
Moffett Field, California 94035

Weight-bearing tissues, such as bone and skeletal muscles, show marked atrophic responses to microgravity. However, a number of other non-weight-bearing tissues also show altered function in response to weightlessness. These changes, observed in the Cosmos 1887 rodent studies, are summarized below.

Several components of the endocrine system responded to spaceflight whereas others did not. Cardiac atrial granules, presumably containing natriuretic factor, were increased in number, but not size, in flight rats (1). Posterior pituitary gland concentrations of both vasopressin and oxytocin were decreased (2). Why posterior lobe hormones were depleted is uncertain as flight and synchronous controls were similarly fed and watered (3). Interestingly, hypothalamic concentrations of vasopressin were similar for flight and control rats (4). Flight decreased secretion of growth hormone (GH) by pituitary somatotrophs about 50% in culture or when implanted into hypophysectomized rats (4), but intracellular concentrations of GH were increased. Curiously, the hypothalami of flight animals contained decreased amounts of both growth hormone releasing factor (GRF) and growth hormone release inhibiting hormone (SRIH). The similar concentrations of vasopressin and corticotropin releasing factor in flight and control rats, suggest a somewhat specific effect of spaceflight on the hypothalamus. Pineal 5-hydroxytryptamine (5-HT) and 5 hydroxyindole acetic acid (5-HIAA) concentrations were increased after flight (5). If the increased 5-HT leads to increased melatonin secretion, it could account for the smaller testes, slight decrease in spermatogonial numbers (6), and the large decrease in plasma testosterone (3) which were found. Plasma concentrations of thyroid hormones were lower in flight rats but plasma corticosterone titers were not elevated although their adrenal glands were hypertrophied (3).

Tissues such as bone, certain muscles, and lymphocytes grow or replicate more slowly in space (7,8). Rat body weight growth, however, was not affected by microgravity on the SL-3 flight (7). Thus, it is not known how general impeded growth is. To further clarify this question the mitotic index of the jejunal mucosa was determined (9). No differences were found, indicating that either there was no effect of microgravity or the mucosa had recovered rapidly after flight. Spaceflight rats typically have livers as big, or bigger, than Earth controls. In the present flight, liver weights of both rat groups were statistically the same although the flight animals were about 15% smaller in body weight (10,11). The disproportionately large livers of flight rats were not due to sequestered blood, edema, or lipid accumulation. Histological studies revealed that the livers had increased parenchymal tissue and increased vacuolization (11). The vacuoles were thought to contain glycogen. Chemical studies verified the increased parenchymal tissue (decreased mg DNA/g liver) and markedly increased glycogen (10). If the elevated glycogen levels occurred in flight rather than after flight, it is curious that they persisted even after a 42 h fast. Hepatic microsomal protein was also decreased after flight. A study of enzymes involved in carbohydrate, fat, and protein metabolism and xenobiotic metabolism revealed an increase in HMG-CoA reductase and decreases in aniline hydroxylase and ethylmorphine N demethylase. Cytochrome P_{450} was also reduced. The aniline hydroxylase and cytochrome P_{450} results suggest that drug metabolism may be altered by spaceflight. Serum concentrations of electrolytes and proteins were unchanged in flight rats,

but cholesterol was increased. The 80% increase in HMG CoA reductase in the face of a 50% increase in serum cholesterol is paradoxical, suggesting an alteration in regulation of this enzyme.

The left ventricle of flight rats showed edema, irregular mitochondria, and loss of actin and myosin filaments (12). Glycogen and lipids were increased and the mitochondrial density decreased. Investigation of the regulatory subunits of cyclic AMP-dependent protein kinase showed no change in RI (13). A second regulatory subunit, RII, however, was decreased in particulate subcellular fractions of ventricular tissue after flight.

Immunological studies were designed to test the responsiveness of immunogenic cells of bone marrow origin to colony stimulating factor and to determine the subpopulations of immune cells obtained from the spleen and bone marrow (14). Flight rat cells showed a suppressed response to colony stimulating factor. Among the immune cells, populations of pan T cells, suppressor T cells, and cells with interleukin 2 receptors were increased in flight rats.

The concentrations of enzymes involved in energy metabolism or gamma amino butyric acid (GABA) metabolism and GABA were measured in multiple regions of the hippocampus and spinal cord (15). In various areas of the hippocampus of flight rats glutamate decarboxylase, GABA transaminase, and glutaminase were increased. In the spinal cord aminotransferase was increased whereas transaminase and glutaminase were decreased. Beta hydroxyacyl CoA dehydrogenase was decreased in dorsal horn tissue. Some of the determinations were too few in number, or the enzyme concentrations too variable, to allow statistically rigorous conclusions. Nonetheless, the data strongly suggest that space flight evokes changes in neuronal metabolism and that further studies are warranted. Daunton, et al (16) endeavored to quantify cholinergic (muscarinic) and GABA (benzodiazepine) receptors and glial fibrillary acidic protein in the frontal lobes of flight rats. The receptors and protein labelled satisfactorily but the investigators were unable to adequately localize the labels for comparison with control brains.

REFERENCES

1. Kraft, L.M. and Keil, L.C. (1989) Morphometric study of liver and atria. II: The atrial granule accumulation. In Final Reports of U.S. Experiments Flown on the Soviet Biosatellite Cosmos 1887. (Connolly, J.P., Grindeland, R.E., and Ballard, R.W., eds). This report.

2. Keil, L., Evans, J., Grindeland, R., and Krasnov, I. (1989) The effect of spaceflight on pituitary oxytocin and vasopressin content of rats. In Final Reports of U.S. Biosatellite Cosmos 1887 (Connolly, J.P., Grindeland, R.E., and Ballard, R.W., eds). This report.

3. Grindeland, R.E., Popova, I.A., Arnaud, S.B., and Vasques, M. (1990) Cosmos 1887 mission overview; Effects of microgravity on rat body and adrenal weight and plasma constituents. The FASEB Journal. Vol. 4(1);Jan.

4. Hymer, W.C., Grindeland, R., Krasnov, I., Sawchenko, P., Vale,W., Victorov, I., Motter, K., and Vasques, M. (1990) Changes in the pituitary and hypothalamus of rats flown on Cosmos 1887. In Final Reports of U.S. Biosatellite Cosmos 1887 (Connolly, J.P., Grindeland, R.E., and Ballard, R.W., eds). This report.

5. Holley, D.C., Soliman, M.R.I., Kaddis, F., and Markley, C.M. (1989) Pineal physiology in microgravity: relation to gonadal function. In Final Reports of U.S. Experiments Flown on the Soviet Biosatellite Cosmos 1887 (Connolly, J.P., Grindeland, R.E., and Ballard, R.W., eds) This report.

6. Sapp, W.J., Philpott, D.E., Williams, C.S., Kato, K., Stevenson, J., Vasques, M., and Serova, L.V. (1990) Effects of spaceflight on the spermatogonial population of rat seminiferous epithelium. The FASEB Journal. Vol. 4(1);Jan.

7. Grindeland, R.E., Fast, T., Ruder, M., Vasques, M., Lundgren. P., Scibetta, S., Tremor, J., Buckendahl, P., Keil, L., Chee, O., Reilly, T., Dalton, B., and Callahan, P. (1985) Rodent body, organ, and muscle weight responses to seven days of microgravity The Physiologist 28:375.

8. Bechler, B. and Cogoli, A. (1986) Lymphozyten and schwerkraftempfindlich. Naturwissenschaften. 73: 400-403.

9. Sawyer, H.R. and Phillips, R.W. (1990) Effects of spaceflight on the proliferation of jejunal mucosal cells The FASEB Journal. Vol. 4(1);Jan.

10. Merrill, A.H. Jr., Hoel, M., Wang, E., Mullins, R.E., Hargrove, J.L., Jones, D.P., and Popova, I.A. (1990) Altered carbohydrate, lipid, and xenobiotic metabolism by liver from rats flown on Cosmos 1887. The FASEB Journal. Vol. 4(1);Jan.

11. Kraft, L.M. (1989) Morphometric study of liver and atria. I. The liver. In Final Reports of U.S. Experiments Flown on the Soviet Biosatellite Cosmos 1887. (Connolly, J.P., Grindeland, R.E., and Ballard, R.W., eds). This report.

12. Philpott, D.E., Popova, I.A., Kato, K., Stevenson, J., Miquel, J., and Sapp, W. (1990) Morphological and biochemical examination of Cosmos 1887 rat heart tissue: Part 1 - Ultrastructure. The FASEB Journal. Vol. 4(1);Jan.

13. Mednieks, M.I., Popova, I., Kato, K., Stevenson, J. and Philpott, D.E. (1989) Cellular distribution of cyclic AMP dependent protein kinase regulatory subunits in heart muscle of rats flown on Cosmos 1887 In Final Reports of U.S. Experiments Flown on the Soviet Biosatellite Cosmos 1887. (Connolly, J.P., Grindeland, R.E., and Ballard, R.W., eds). This report.

14. Sonnenfeld, G., Mandel, A.D., Konstantinova, I.V., Taylor, G.R., Berry, W.D., Wellhausen, S.R., Lesnyak, A.T., and Fuchs, B. (1989) Cosmos 1887 immunology studies. In Final Reports of U.S. Experiments Flown on the Soviet Biosatellite Cosmos 1887. (Connolly, J.P., Grindeland, R.E., and Ballard, R.W., eds). This report.

15. Lowry, O.H., McDougal, D.B. Jr., Maggie, M-Y. C., Pusateri, M.E. Carter, J.G., and Manchester, J.K. (1989) Metabolic enzymes of the hippocampus and spinal cord. In Final Reports of U.S. Experiments Flown on the Soviet Biosatellite Cosmos 1887. (Connolly, J.P., Grindeland, R.E., and Ballard, R.W., eds). This report.

16. Daunton, N.E. and D'Amelio, F. (1989) Study of muscarinic (cholinergic) and GABA (benzodiazepine) receptors and immunocytochemical localization of neurotransmitter gamma aminobutyric acid (GABA) and glial fibrillary acidic protein (GFAP). In Final Reports of U.S. Experiments Flown on the Soviet Biosatellite Cosmos 1887. (Connolly, J.P., Grindeland, R.E., and Ballard, R.W., eds). This report.

IV. SCIENCE REPORTS

A. RAT EXPERIMENTS

N90-26455

EXPERIMENT K-6-01

DISTRIBUTION AND BIOCHEMISTRY OF MINERAL AND MATRIX IN THE FEMURS OF RATS

Principal Investigator:

S. Arnaud
NASA-Ames Research Center
SLP 239-17
Moffett Field, California 94035

Co-Investigators:

G. Mechanic
Dental Research Center
University of North Carolina
Chapel Hill, North Carolina 27514

J. Elliott
Dept of Child Dental Health
London Hospital Medical College
Turner Street
London E12AD, England

P. Buckendahl
Thimann Laboratories
University of California
Santa Cruz, California 95064

E. Katz
School of Dental Medicine
University of Connecticut Health Science
Farmington, Connecticut 06032

T. Bromage
Dept of Child Dental Health
The London Hospital Medical College
Turner Street
London E12AD, England

C. Durnova
Institute of Biomedical Problems
Moscow, USSR

A. Boyde
Dept of Anatomy and Developmental Biology
University College London
Gower Street
London WC1E 6BT, England

PRECEDING PAGE BLANK-NOT FILMED

SUMMARY

Previous analyses of the composition of mineral and matrix in the bone of young rats following space flight has revealed deficits in calcium, phosphorus, and osteocalcin, a non-collagenous protein, without an associated decrease in collagen. To characterize the location and nature of this mineralization defect in a weight bearing long bone, the femur, we attempted to relate the spatial distribution of mineral in situ in the proximal, central and distal thirds of the femoral diaphysis to the biochemical composition of bone from the same areas. Biochemical analyses revealed lower concentrations of calcium, phosphorus and osteocalcin but not collagen only in the central third of the diaphysis of the flight animals (F) compared to synchronous controls (S). Collagen concentration was reduced only in the proximal third of the diaphysis, where all 3 crosslinks, expressed as nM/mol collagen, were higher in F than S. A new technique, X-ray microtomography, with a resolution of 26 microns, was used to obtain semi quantitative data on mineral distribution in reconstructed sections of wet whole bone. To improve the resolution of the mineral density distribution, images of the surfaces of cut sections were analyzed by backscattered electrons in a scanning electron microscope (BSE). There was good agreement between the results of the two stereochemical techniques which revealed distinct patterns of mineralization in transverse and longitudinal directions of the diaphysis. The longitudinal gradient in mineral concentrations in the proximal two- thirds of the diaphysis compared well with the semi-quantitative estimates from the microtomography study in F and S. Correlation of mineral concentrations and BSE patterns added a new dimension to our knowledge of the changes in distribution of mineral most vulnerable to the environmental effects in this experiment.

Circulating parameters of skeletal metabolism revealed differences in serum calcium, osteocalcin and alkaline phosphatase, suggestive of steroid hormone excess in the flight animals. These findings, the reduced body weight and enlarged adrenal glands of the flight animals, possibly due to post flight environmental stress, preclude any interpretation of our results with reference to space flight per se. Nevertheless, the novel methodology developed for this flight experiment shows considerable promise in elucidating the biochemical nature of what appear to be regional alterations in the mineralization of long bones of animals exposed to spaceflight.

INTRODUCTION

Analyses of the morphology (1-4) and biochemical composition (5,6) of the bone of young rats following space flight reveals reduced formation of bone. Quantitatively normal amounts of collagen, reduced content of calcium, phosphorus and a non-collagenous protein associated with hydroxyapatite, indicates that the basic defect is centered in the calcification of collagen.

The collagen fibril, which comprises 90% of the organic matrix of osteoid, is the structural determinant of the mineral content of an element of bone (7,8). The fibril provides microspaces, within its structure, for most of the mineral particles of bone. Events in these spaces serve to orient mineral crystal growth such that the c-axis of a mineral crystal is parallel to the c-axis of the collagen fibril. The lateral dimensions of these mineral particles are constrained by the details of the molecular packing within a fibril.

The findings of an hypomineralized arrest line on the periosteal surface of a tibia (2) and smaller crystallites in density gradients of pulverized bone (9) of young rats in orbit on earlier Soviet and American flights suggest that newly synthesized collagen does not mineralize, and that the maturation of collagen mineralization, initiated on land, is altered in space. This indicates that the fibril structure could be somewhat compressed, perhaps by the same forces which cause the redistribution of extracellular fluids in space flight (10). To determine collagen centered effects in mineralization, it is critical first, to know the mineral concentration and its spatial orientation in hydrated bones. The mechanism of space flight effects on mineralization can then be estimated by

correlating quantitative estimates of mineral density with chemical analyses of mineral and matrix in selected regions, our ultimate goal.

The biochemical analyses of bone carried out in the laboratories of Dr. Mechanic and P. Buckendahl are documented in section I. Technology capable of mapping the distribution of mineral in rat bone to a spatial resolution of about 20 microns and providing reference data in terms of known units, i.e. grams per unit volume, required development and is described in section II by Drs. Bromage, Elliot and Boyde. Section III describes the circulating indices of skeletal metabolism in the four experimental groups of rats and other data essential to the interpretation of structural changes in bone exposed to both post flight environmental changes and space flight.

I. BIOCHEMICAL ANALYSES OF 3 REGIONS OF THE FEMORAL DIAPHYSIS

This aspect of the study was carried out to determine quantitative estimates of the essential components in bone calcification, collagen and mineral, in the three same regions in which density distribution was analyzed. We have measured the concentration of calcium and phosphorus to relate to the density distribution data. A non-collagenous protein, osteocalcin, associated with hydroxyapatite in mineralized bone was also measured (11). The function of this non-collagenous protein is not known, but its concentration in bone, determined by species specific radioimmunoassay, roughly parallels the mineral content of that bone. Collagen was assayed by the measurement of hydroxyproline, based on a value of 300 residues of hydroxyproline per molecule of collagen. The fibrils of collagen are stabilized by reducible and non-reducible intermolecular crosslinks which may also function to provide the proper distance between collagen molecules in bone for calcification (12). The two principle reducible crosslinks of bone collagen are dihydroxylysinonorleucine (DHLNL) and hydroxy- lysinonor leucine (HLNL) (13). A third non-reducible crosslink, pyridinoline, derived from DHLNL crosslinks during the normal process of ageing, is found in high concentration in non-mineralized collagen (14), and may have a role in preventing mineralization. A collagen profile quantitating these 3 crosslinks was also carried out on each third of the femoral diaphysis to relate to the mineral data and stereochemistry.

Methods and Materials

Our interest in localizing mineralization activity in the diaphysis of the femur to proximal, central and distal thirds made it necessary to pool the bone samples from each experimental group to provide enough material for chemical analysis. The proximal 10 mm of bone with the neck and greater trochanter of the femur and the most distal region of the femur are not included in the powders for chemical analysis. Determinations of collagen and crosslinks were carried out in Dr. Mechanic's laboratory where the bone was pulverized and weighed. Methods are as reported (15,16,17). The mineral and osteocalcin assays were done on a 1 mg aliquot of each pool of powders in P. Buckendahl's laboratory by previously reported methods on an EDTA extract (18). Because statistical analyses of a determination from a single pool could not be done, we selected a value two standard deviations above or below the error of the method to denote the difference in two comparison groups (i.e., exceeding 6 percent for calcium, 12 percent for phosphorus, and 10 percent for hydroxyproline and osteocalcin etc.) See Table I.

Results

The concentrations of calcium, phosphorus, and osteocalcin are listed on Table II. The differences in the mineral composition are confined to the central section of the diaphyses where concentrations in B and F are the same and lower, by about 50 percent, than either V or S. Figure 1 depicts the percent change in V, S, and F estimated from B for the minerals and osteocalcin. Concentrations in the proximal region of all 3 experimental groups and of the distal region in the vivarium, show little change. The increases in mineral and osteocalcin are in the central or

midshaft in V and S. In F, relative to B, phosphorus and osteocalcin are the same, and calcium 19 percent lower. The concentration of hydroxyproline in F is 14 percent lower than S only in the proximal region.

Comment

The data identify two regions in the diaphyses where bone of different chemical composition is generated in the experimental F group, the proximal and central diaphysis.

Proximal diaphysis

The chemical composition of the proximal section reveals lower concentrations of collagen and higher concentrations of the reducible crosslinks, DHLNL and HLNL. The increase in crosslink concentration is indicative of new collagen synthesis. The increase in pyridinoline concentration indicates poorly mineralized collagen since pyridinoline formation is reduced when collagen is mineralized. The modest reduction in total collagen reflects accelerated degradation. These results are similar to the results of collagen and crosslink analysis in the femurs of immobilized monkeys (19). See Table III.

Central diaphysis

Differences in the mineral concentration were evident only in the central portion of the diaphysis, where values in F were 19 percent lower than the basal controls, and 39 percent lower than S. Given that these measurements represent a single assay of a pool of 4 small sections of the mid-diaphysis, a qualitative interpretation is more appropriate than a quantitative one. We cannot state from the data presented whether the low concentration in mineral is the result of failure of mineral apposition or loss of mineralized bone.

Distal diaphysis

The absence of differences in the mineral and osteocalcin composition of the distal section of the femur in B and V and modest increases in both S and F suggests either an influence of diet schedule, caging, or maturity of the animals in the experimental groups for flight, as compared to the vivarium controls. The range of increased concentration of mineral and osteocalcin, unassociated with an increased concentration of hydroxyproline, were the same for all components and ranged from 19 to 25 percent in both F and S. This suggests that these compositional changes were unaffected by either flight or post flight environments.

Clear differences in the biochemistry of distal, central and proximal thirds of the diaphysis of the femur were evident from the above analysis, and require confirmation.

II. MINERAL DENSITY DISTRIBUTION OF THE FEMORAL DIAPHYSIS

A. Surface remodeling activity

Illustrated in Figure 2 is the structure and remodeling activity of the surface of the left femur of a 300 gram Czech Wistar rat. The diaphysis of this long bone is the object of this entire study. This specimen in the figure came from an animal used in a pilot study to compare effects of diet and housing at 1 G. This animal was housed in a group cage and received the same diet as the animals in the flight experiment. Scanning electron microscopy (SEM) of the surface of the whole bone was used to identify areas of resorption by the presence of resorption cavities and osteoclasts, and areas of formation by the presence of bundles of collagen associated with active osteoblasts. Active remodeling involves less than one half the periosteal surface, the remainder being in the resting phase. Surface resorption activity is extensive on the distal third, and the neck (proximal),

primarily. Evidence of active formation is confined to two areas on the medial aspect of central and proximal shaft and a third area in the greater trochanter.

The diversity of remodeling activity on the periosteal surface of this bone illustrates the wide range of metabolic activity which occurs simultaneously in a long bone during growth. Our effort is complicated by awareness that surface remodeling does not necessarily parallel the metabolic activities of the interior of the bone at the same levels or the differing rates of acquisition of matrix and mineral in the regions of growing bone. In this study, we used the basal (B) and vivarium (V) controls for estimation of changes during growth.

This surface map and scale is provided primarily for purposes of orientation to our study which details the mineral densities of the proximal, central and distal thirds of the shaft, with analyses beginning 10 mm distal to the proximal tip of the whole bone.

B. X-ray microtomographic examination of rat femurs

Methods and Materials

X-ray microtomography is a miniaturized version of the well known X- ray computer tomography (CT scanning) that is used for medical diagnosis. Methods and principals are detailed in the references (20-23). In the microscopic form used in this project, the X-ray beam was 10 microns in diameter and was formed by an aperture in front of a 100 X 100 micron source (silver target, 35 kv, 1.5 ma, 60 microns palladium filter). Sections of the cross-section of the femur are reconstructed from 240 projections, each consisting of 256 points. The X-ray absorbtion at each point was measured by counting for 5s, so the total observational time for each section was 85.3 hours. The translation of the bone across the X-ray beam was done by mounting it at the end of a pivoted rod which was moved up and down by fixed micrometer. This means that the actual pixel size in the reconstructions is only a nominal 26 microns, and will change slightly when the position of the section along the bone is changed (actually, 28.75 to 26.88 in 5 sections of the synchronous control (S) and 29.10 to 28.63 microns in the 3 sections of the flight femur (F)).

The information that is obtained in the reconstructed section of the bone is the distribution of the linear X-ray absorption coefficient (measured in cm^{-1}) for the particular wavelength of the X-rays used (silver K-alpha) for each of the nominal 26 micron pixels. At this wavelength, by far the biggest constributor to the absorption will be the mineral of bone. This mineral is similar to calcium hydroxy- apatite, Ca10(PO4)6(OH)2, and it makes up about 65 percent of the bone by weight. The linear absorption coefficient of pure hydroyapatite for silver K-alpha radiation is 15.9 cm-1. The information for the reconstruction of each section is represented by a 2-dimensional array of numbers, in this case 256 X 256 array in which each number can take one of 256 values. The digital images can be displayed in a number of different forms, including grey scale images of the whole intensity range, expanded grey scale of part of the intesity range and contour maps of constant linear absorption coefficient. Figure 3 illustrates 5 'sections' from S and 3 from F 'cut' at 4 mm intervals starting 10 mm from the tip of the proximal end of the bone at the same intensity and similar grey scales. Two sections are missing from the flight specimen because the distal end of the bone fragmented. Figure 4 illustrates a contour map of the proximal section of S and F femurs drawn at two intensity levels, 150 for interior and 230 for external outlines.

Results

The quantitative results of the microtomography study are given in Table IV. The control femur shows a decrease in mineralization from the proximal toward the distal metaphysis. The F femur shows a more rapid decrease from the first to the 3rd section, (15 vs 7.5 percent from sections 1 to 3) than S.

Comment

The results of this study involves a new technique and should be regarded as a first attempt. As far as we know, there is no detailed information about the biological variability of the mineralization along the length of the femur, among different animals of the same or different ages. The clinical characteristics of the two animals whose left femur served as the prototype for this study are given in Table V. As yet no detailed analysis of the digital images is possible because of the need for furthur work to establish the absorption coefficient values on an absolute scale, to improve the method of tissue preservation, and to repeat these studies in additional specimens. The number of specimens for each of these analyses was the most serious limitation. Chemical analyses could not be done on the same bone subjected to microtomography because of the time required, i.e. more than 80 hours per section.

C. Image analysis using backscattered electrons in a scanning electron microscope

Previous studies of mass distributions within thin slices of biological tissues have all been made using microradiography. With this technique, it was demonstrated that mineralized bone is not homogenous, and that individual zones of packets have different densities. In lamellar bone, the mineral content is lowest at the time of formation and slowly increases during a maturation process as osteons age. Primary membrane (woven) bone mineralizes rapidly, and to a level which is slightly higher than that of mature lamellar bone. The density of newly formed lamellar bone packets is 70-80% of that achieved in fully mature bone. A computerized system for the analysis of mineral densities from microradiographs has been described but no studies conducted with it have so far been published (24).

The backscattering of electrons is a process which is dependent on the atomic number of an element and hence is also proportional to density. We have previously shown that the mineral density distribution within bone can also be studied using backscattered electron (BSE) imaging in the scanning electron microscope (SEM). BSE images of flat (cut and polished or micromilled) bone surfaces resemble microradiographs: the darker an area appears, the less mineral it contains. However, these images have a much higher spatial resolution than microradiographs because BSE are collected from only a thin layer at the surface of the specimen. Since a surface is examined, tney are also not subject to false contrasts due to variations in section thickness.

Methods and materials

The BSE signal can be thresholded and pixels counted to measure the phase volumes of bone lying within given density fractions (25,26). We have used this approach to study the density distributions in femur samples from the Cosmos 1887 experiment. The amount of bone having discrete, constant density ranges was measured using an image analysis system interfaced directly to the SEM (27).

The specimens were 150 um thick transverse sections cut from the proximal, central and distal thirds of the femurs from each experimental group. The thick sections were embedded in methyl methacrylate, copolymerised with styrene to enhance the stability of the resin under electron bombardment. After hardening was complete, topography-free surfaces were prepared by careful grinding and polishing and the specimens rendered electrically conductive by sputter coating with a layer of silver.

The image analysis system was interfaced directly to the SEM. The BSE signal was digitized at each pixel during a single slow scan of the electron beam across the sample and converted to grey level histograms. The pixel data was allocated to one of eight equal-width grey level bins in RAM which spanned the range from peak black to peak white (i.e., 0-5 volts) in the BSE image. Non-bone, marrow spaces, vascular canals and osteoid were all assigned bin "zero", least dense to 1 and

most dense mineral to bin 7. The percentage area of each density level was printed after each scan and is expressed as the percentage of the total of mineralized tissue analyzed.

We selected operating conditions as a working compromise between pixel resolution and sampling density. Effective pixel size was roughly 0.2um diameter and we could resolve useful detail at 500X in a 100 mm diameter, 1000 line image. Pixels were widely spaced at the specimen, constituting a "stereological grid" sampling the surface composition at intervals. Four fields were analyzed per specimen, centered on the medial lateral, anterior and posterior cortices. We used System 80K software (Sharp MZ 80K microcomputer) interfaced to a Cambridge Stereoscan S4-10 SEM, operated at an accelerating voltage of 19.3kV. To ensure the same operating conditions for the specimens, a special carousel stage was developed for continuous analysis of specimens arranged to alternate experimental groups and levels. Drift was checked by returning to the starting field of the first specimen of the run. We were able to reproduce the image analysis data on successive runs of the same samples, but there are problems in setting up identical operating conditions on repeated occasions. Although we have attempted to set up the system against known, pure standards (e.g. polished aluminium and fluoroapatite), we have not yet found uniform, characterized materials which fall at the margins of the range of densities we wish to cover.

Results

1. The amount unmineralized tissue per field analyzed (Bin zero)

The value in the first bin of each histogram fluctuates mainly as a consequence of variations in the thickness of the cortex. The lowest value recorded (at 23%) reflects the largest amount of mineralized bone present in the field of view, i.e. the "solid bone" contains 23% of osteocyte lacunae plus blood vessel canals, plus non- mineralized osteoid. The highest values (at about 75%) reflect very thin bone which did not fill the lmm wide field of view. The amount of non mineralized tissue analyzed for each experimental group was nearly identical: for B,V,S, and F, values were 59, 55, 56, and 57% in bin 0, respectively.

2. Modal density as a function of experimental group

Average mineralized tissue analyzed was 42.25%. A histogram of the percent calcified tissue in each bin for each experimental group is illustrated in Figure 5 which shows the modal density in each bin, according to Table VI.

The density distribution of the entire diaphysis of the flight bone resembles that in the preflight B more than either of the age matched controls. The density spectrum of each group cannot be considered to be different from any other group, however, because of the large variation in the bones of each group (n=5 in B and V, 4 in S and F).

3. Modal density as a function of longitudinal position

There appears to be one type of pattern for the pair of B and V, and a second type for the pair S and F. To compare S and F, we have separated the pairs in Table VII which enumerates the percent mineral in bins < 3 and >6 in the proximal, central and distal regions.

Low density fractions are most abundant in the distal regions of the femoral shaft, as expected in growing animals. The variation in the central segment is striking, and may reflect either biological diversity or a problem with technique or both. In this central segment, the highest percentage of dense fractions are found, as might be expected in the midshaft of cortical bone.

Variation in the proximal segment in each experimental group is also apparent. The F group has half as much low dense bone as its pair, S. Percentages in bin 0 for F and S were the same, 55% and 53%. Feeding schedules and housing are the same in B and V, but differ from S and F, a possible explanation for the different longitudinal distribution of mineral during growth.

4. Histograms as a function of anatomical quadrant

Averaged results for all experimental groups and for the 3 longitudinal positions are similar with the grand mean showing the predominant density levels in the central bins, 3, 4, and 5, as follows: 6/13/20/20/19/14/5 for bins 1-7, respectively. Of interest are the higher values for the most dense bin in 3 quadrants (not lateral) of the midshaft and for the least dense bin in the distal shaft in F than S. These apparent regional density differences may account for the flatter appearance of the histogram of the whole diaphysis in figure 5 (central F, 0/0/1/8/27/36/24 and central S, 0/1/2/10/39/40/5; distal F, 23/36/28/3/0/0/0 and distal S, 6/24/44/19/2/0/0). The histograms in figure 6 show the density profile of the lateral quadrant (selected for graphic presentation because of low intra-group variation) of the 3 longitudinal sections in S and F.

Comment

The technique of BSE and SEM appears to be a powerful method to identify regional differences in mineral density distribution capable of determining the effects of space flight on calcification. However, we can draw no conclusions from any of the data acquired at this time for a number of reasons. Major problems which introduce uncertainty in the data are the fractures, possibly due to rapid freezing. Group comparisons pose problems of matching levels in bones of slightly different size in growing animals of different age. Apparent differences observed may be related to artifacts of sample preservation and other aspects of the newly developed techniques. The number of bones examined was too small to establish statistical validity of any of the observations in the regions and there is considerable variation in mineral density distribution of the specimens in each group. There is as yet no data base established for reference of space flight data to changes with age, diet, and other variables known to affect mineral density.

On the other hand, we regard this as a first successful attempt to document regional mineral gradient densities in the femoral diaphysis of the rat. The density levels in the longitudinal direction are consistent with our understanding of normal physiology, with least dense fractions predominating in the distal region and intermediate density fractions predominating in the central region of cortical bone. The dissimilarity in the high density fraction percentages in the pairs B/V and S/F may be related to different growth activities of these pairs from different habitats. Also, there are similarities in these results to those derived from density gradients of powdered cortical bone from the femur of rats 7 days in space. Simmons et al observed a trend for density profiles to shift toward the higher density fractions post flight (9). The unique and novel aspects of this study are observations of apparent regional differences in the patterns of mineral density distribution in both horizontal and longitudinal directions which we hope to confirm in experiments in future space flights.

CORRELATION OF BIOCHEMISTRY WITH IMAGE ANALYSIS

To attempt to relate the measured elements in bone to density images is a challenge because the distribution density is referenced to 100 percent of an area, and the chemical measures are referenced to a known mass, i.e. microgram, which may be distributed sparsely (low density) or in a more compact way (high density) in the same area. In spite of this we tried to relate these sets of data, by comparing the fraction or percent of mineral or unmineralized collagen of the chemical assays to the percent of high, low or soft tissue density in the 3 sections of diaphysis in F and S.

The proximal region shows half as much mineral in F in the low density bins (31 vs 63) and a smaller increment in the higher density bins than in S (6 vs 0 percent) with no change in the concentration of mineral or collagen. This could indicate less newly mineralized collagen in F, consistent with the crosslink concentrations. Only the lateral quadrant shows an increase in uncalcifed tissue (see Figure 6) in bin 0. The sum of all quadrants for bin 0 is 55 for F and 53 for S, consistent with morphologic data which fails to show increases in unmineralized osteoid in cross sections of long bones after space flight.

The central region shows the scant amount of mineral in F to be more distributed in the high density fractions compared to S. There is only 2 percent less in the low density fractions of F vs S.

The distal regions show 15 percent less mineral in the low density fractions in F compared to S.

The above suggests shows regional variation in the concentration and distribution of matrix and mineral which is consistent, and similar to the findings of Rogacheva et al after a longer flight (3). Of interest is the low concentration of mineral in the mid section where measurements of reduced breaking strength are reported (28,29).

III. CIRCULATING INDICES OF SKELETAL METABOLISM AND OTHER CLINICAL CHARACTERISTICS OF ANIMALS RATS IN COSMOS 1887 FLIGHT

Essential to the interpretation of structural changes in bone exposed to microgravity is an evaluation of the animals calcium metabolism, bone cell activity, nutritional and endocrine status at the time of the necropsy. For this purpose, the small amount of serum available for study was analyzed for a few constituents that have relevance to the bone biochemistry study.

Total serum calcium and total protein can be a reflection of hydration. Osteocalcin in serum, originates from the osteoblast and has been shown to correlate well with indices of bone formation (30). Another product of the osteoblast in blood, alkaline phosphatase, may also originate in the liver. The enzyme originating in bone is heat sensitive and can be distinguished from hepatic enzyme partly by an assay for the heat sensitive component which we used in this study (31). Serum 25-hydroxyvitamin D is the best indicator of the status of vitamin D nutrition (32), always a consideration when evaluating mineralization since low levels are associated with vitamin D deficiency bone disease. Serum levels of corticosterone were assayed to determine relationships between circulating levels of osteocalcin, known to be depressed by this steroid (33).

Results

The results are enumerated on Table VIII. Flight animals showed lower body weight, serum total calcium, and osteocalcin than S. Serum alkaline phosphatase, and adrenal weights were higher in F than in S.

Comment

The clinical data in this experiment indicate that there were two factors in addition to space flight which may have contributed to the the mineralization defects. The low body weights of F, the same as the preflight group, are indicative of either failure to gain or of weight loss during their stay in the Siberian forest. If they did not eat for two days before necropsy, the absence of a dietary source of calcium may have stimulated bone resorption. The large adrenal glands of the flight animals suggest high levels of endogenous steroids which we could not demonstrate because of the large range of variation in all groups. Excess adrenal steroids regularly cause metabolic bone disease manifested by increased bone resorption and reduced bone formation. As well, high steroid levels may be directly responsible for suppressing the formation of osteocalcin, reduced to a greater degree in this flight than the 7 day Spacelab 3 flight (55 vs 22%) (5). Of interest is the

relationship between the adrenal gland weights and the circulating level of osteocalcin as shown in Figure 7. The flight group is clearly separated from the controls, an indication of the impact of excess steroid on the activity of the osteoblast, and possibly on the changes we observed.

REFERENCES

1. Morey ER and Baylink DJ. Inhibition of bone formation during spaceflight. 201:1138-1141, 1978.

2. Turner RT, Bell NH, Duval P, Bobyn JD, Spector M, Holton EM, and Baylink DJ. Spaceflight results in formation of defective bone. Proc Soc Exptl Biol Med 174:224-228, 1983.

3. Rogacheva IV, Stupakov GP, Volozhin AI, Pavlova MN, and Polyakov AN. Rat bone tissue after flight aboard COSMOS-1129 Biosatellite. Moscow Kosmichesdaya Biologiya I Aviakosmicheskaya Meditsina 18:39-44, 1984.

4. Yagodovsl , US, Trifranidi LA, Goroklova GP. Space flight effects on skeletal bones of rats: light and electron microscopic examination. Aviat Space and Environ Med. 47:734-740, 1976.

5. Patterson-Buckendahl P, Arnaud SB, Mechanic GL, Martin RB, Grindeland RE, and Cann CE. Fragility and composition of growing rat bone after one week in spaceflight. Am. J. Physiol. 252:R240- R246, 1987.

6. Prokhonchukov AA, Desyatnichenko KS, and Tigranyan RA. Mineral phase and protein matrix of rat osseus tissue following flight aboard the Cosmos-1129 biosatellite. Space Biol and Med 16:87-92, 1982.

7. Glimcher MJ. Molecular Biology of Mineralized Tissues with Particular reference to Bone. Rev Modern Physics 31:359-393, 1956.

8. Katz EP and Li ST. The Structure and Function of Bone Collagen. J Mol Biol 80:1-15, 1973.

9. Simmons DJ, Russell JE, and Grynpas MD. Bone maturation and quality of bone material in rats flown on the space shuttle 'Spacelab-3 Mission'. Bone and Mineral 1:485-493, 1986.

10. Linnarson D, Tegner B and Eiken D. Effects of gravity on the fluid balance and distribution in man. Physiologist 28:S28-29, 1988.

11. Price PA, Otsuka AS, Poser JW, Kristaponis J and Raman N. Characterization of a gamma-carboxyglutamic acid-containing protein from bone. Proc Narl Acad Sci. USA 73:1447-1451, 1976.

12. Mechanic GL, Banes AJ, Henmi M, and Matsuo Y. Possible collagen structural control of mineralization In The Chemistry and Biology of Mineralized Tissues, Butler WT, Ed. Ebsco Media, Birmingham. pp 98-102, 1985.

13. Mechanic GL, Gallop PM, Tanzer ML. The nature of crosslinking in collagens from mineralized tissues. Biochem & Biophys Res Comm 45:644-653, 1971.

14. Banes AJ, Yamauchi M, and Mechanic GL. Non-mineralized and mineralized compartments of bone: the role of pyridinoline in nonmineralized collagen . Biochem & Biophys Res Comm. 113:975-981, 1983.

15. Yamauchi M, London RE, Guenat C, Hashimoto F, and Mechanic GL. Structure and formation of a stable histidine-based trifunctional cross-link in skin collagen. J Biol Chem 262:11428-11434, 1987.

16. Yamauchi M, Katz EP, and Mechanic GL. Intermolecular cross- linking and stereospecific molecular packing in type I collagen fibrils of the periodontal ligament. Biochemistry 25:4907-4913, 1986.

17. Mechanic GL, Katz EP, Henmi, Noyes C, and Yamauchi M. Locus of a histidine-based stable trifunctional, helix to helix collagen cross-link: stereospecific collagen structure of type I Skin Fibrils. Biochemistry 26:3500-3509, 1987.

18. Patterson-Allen PE, Brautigam CE, Grindeland RE, Asling CW, and Callahan PX. A specific radioimmunoassay for osteocalcin with advantageous species cross reactivity. Anal Biochem 120:120:1-7, 1982.

19. Mechanic GL. Personal communication.

20. Elliott JC and Dover SD. Three dimensional distribution of mineral in bone at a resolution of 15 microns determined by X-ray microtomography. Metabolic Bone Dis and Rel Res 5:219-221, 1984.

21. Elliott JC and Dover SD. X-ray microscopy using computerised axial tomography. J. Microscopy 138:329-331, 1985.

22. Bowen DK, Elliott JC, Stock SR and Dover SD. X-ray microtomography with synchotron radiation. SPIE X-ray Imaging II, 691:94-98, 1986.

23. Elliott JC, Bowen DK, Dover SD, and Davies ST. X-ray tomography of biological tissues using laboratory and synchotron sources. Biological Trace Element Res. 13:219-227, 1987.

24. Phillips HB, Owen-James S, Chandler B. Quantitative Histology of Bone: A computerized method of measuring the total mineral content of bone. Calc Tiss Res 26:85-89, 1978.

25. Boyde A. New methods for SEM bone stereology. Calc Tiss Int 33:Suppl, abst 43, 1981.

26. Boyde A, Reid SA, Howell PGT. Stereology of bone using both backscattered electron and cathodoluminescence imaging for the SEM. Beitr Elektronenmikroskop Direktabb Oberfl (Muenster) 16:419- 430, 1983.

27. Howell PGT, Reid SA. A microcomputer-based system for rapid on- line sterological analysis in SEM. Scanning 8:129-144, 1986.

28. Spengler DM, Morey ER, Carter DR,j Turner RT, and Baylink DJ. Effects of spaceflight on structural and material strength of growing one. Proc Soc Exptl Biol Med 174:224-228, 1983.

29. Dobelis MA, Saulgozis Yu. Zh., Novikov VY, Ilin YA, and Oganov VS. Effect of weightlessness and some of its models on mechanical properties of animal bones submitted to torsion. Moscow Kosmicheskaya Biologiya I Aviakosmecheskaya Meditisina 19:40-45, 1985.

30. Price PA, Parthemore JG, and Deftos LJ. A new biochemical marker for bone metabolism. J. Clin Invest. 66:878-883, 1980.

31. Posen S, Neal FC, Club JS. Heat inactivation in the study of human alkaline phosphatase. Ann Int Med 62:1234-1243, 1965.

32. Arnaud SB and Meger J. A micro-assay for 25-hydroxyvitamin D: method and interpretation In ASBMR Workshop on Calciotropic Hormone Measurements, Ed D. Bikle, Springer-Verlag, 1983, Chapter 5.

33. Patterson-Buckendahl PE, Grindeland RE, Shakes DC, Morey-Holton ER, Cann CE. Circulating osteocalcin in inversely responsive to changes in corticosterone. Am J Physiol 254:R828-833, 1988.

TABLE I. The weight of the bone powders, in milligrams, from each section of the diaphysis were comparable in each experimental group:

Group	Proximal	Central	Distal	Total/bone
B	104.6	74.2	197.4	376
V	109.6	79.2	196.2	385
S	123.5	86.5	233.5	444
F	109.8	83.8	211.5	405

TABLE II. Concentration, µg/mg, in 3 regions of femoral diaphysis.

	B	V	S	F
Calcium				
Proximal	171	150	179	173
Central	93	139	123	75 *
Distal	167	170	215	206
Phosphorus				
Proximal	89	77	95	89
Central	45	71	65	42 *
Distal	86	88	102	104
Osteocalcin				
Proximal	2.20	2.00	2.22	2.10
Central	0.88	1.79	1.48	0.77 *
Distal	1.74	1.82	2.18	2.15
Hydroxyproline				
Proximal	---	---	31.0	26.6 *
Central	---	---	22.2	22.2
Distal	---	---	28.8	28.8

*indicates a value outside error of method in F relative to S

TABLE III. Concentration of Crosslinks, nM/mol Collagen

Crosslink	S	F
Dihydroxylysinonorleucine		
Proximal	0.47	1.70 *
Central	0.81	0.75
Distal	0.77	0.66
Hydroxylysinonorleucine		
Proximal	0.13	0.46 *
Central	0.28	0.28
Distal	0.30	0.28
Pyridinoline		
Proximal	0.12	0.34 *
Central	0.15	0.13
Distal	0.24	0.28

TABLE IV: Maximum values of the linear absorption coefficent cm-1 from the control and flight femur microtomography study

Section #	S	F
1	7.20	7.63
2	6.86	7.23
3	6.76	6.46
4	6.65	
5	6.51	

TABLE V: Body and adrenal weight, serum corticosterone and indices of skeletal metabolism in two rats whose femurs were analyzed by X-ray microtomography.

	Synchronous Control #6	Flight #6	Vivarium range
Body weight, gms	345	304	295 - 345
Adrenal, mg/100 gm body weight	11.3	15.8	11 - 13
Serum total calcium, mg/dl	10.4	8.8	9.6 - 11.4
Total protein, g/dl	6.8	6.8	6.1 - 7.3
Alkaline phosphatase, IU/L	50	112	35 - 67
Osteocalcin, ng/ml	154	60	130 - 166
25-hydroxyvitamin D, ng/ml	18	19	18 - 20
Corticosterone, ug/dl	12.2	8.6	1.8 - 17.8

TABLE VI: Average modal densities or gray levels for whole diaphysis

Experimental group	#1	#2	#3	#4	#5	#6	#7
Basal	9	15	15	25	20	16	5
Vivarium	2	7	19	27	23	13	4
Synchronous Control	4	15	27	20	15	13	2
Flight	9	14	17	16	17	14	8

TABLE VII. Percent mineral in bins of low and high density

	B	V	B	V	S	F	S	F
	<3		>6		<3		>6	
Proximal	11	5	24	45	63	31	0	6
Central	12	19	41	4	3	1	45	60
Distal	79	94	0	0	87	74	0	0

TABLE VIII. Body and adrenal weights, circulating parameters of skeletal metabolism in the rats flown on the Cosmos 1887 biosatellite mission. (Mean ± SD)

	Basal	Vivarium	Synchronous	Flight
Body weight, g	316±19	342±17	349±13	303±5 *
Adrenal weight, mg/100g BW	13.5±.5	12.5±.9	12.5±.8	16.8±1.5 *
Serum total calcium, mg/dl	10.7±.6	10.5±.7	10.1±.3	9.5±.6*
Total proteins, g/dl	6.5±.2	6.8±.2 +	6.8±.6	6.6±.6
Osteocalcin, ng/ml	227±20	148±16#	166±22	74±12 *
Alkaline phosphatase, IU/L	97.4±21	53.8±12	46.4±9	70±29
25-hydroxyvitamin D, ng/ml	20±5	19±1	20±2	20±1
Corticosterone, ug/dl	11.7±5	10.1±6	10.5±6	15.6±9

* p<.05 compared to Synchronous, # p<.05 compared to basal, +n=3

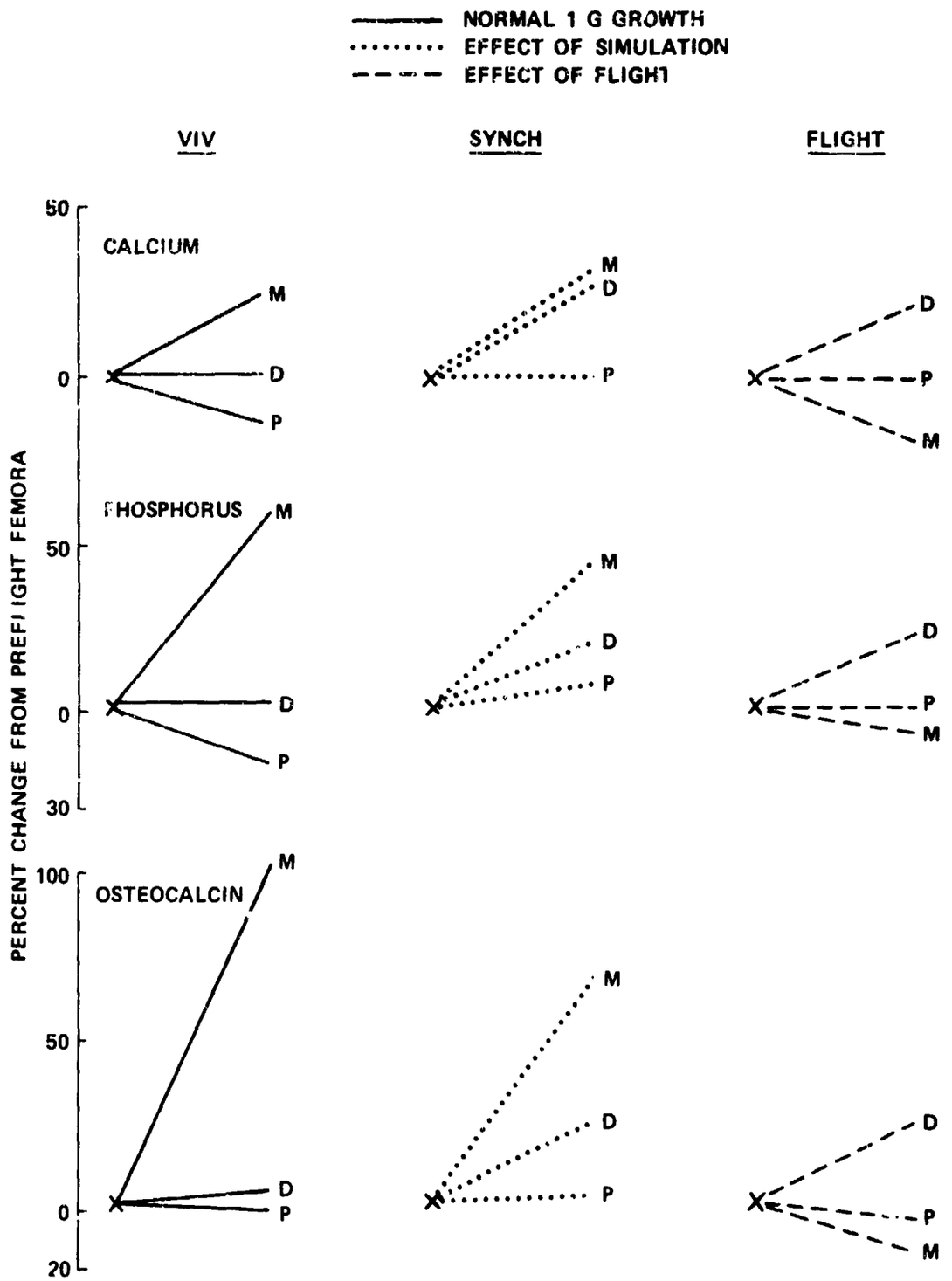

Figure 1. The percent change in the average concentration of calcium, phosphorus, and osteocalcin in the vivarium, synchronous control and flight groups in the proximal (P), central (C), and distal (D) thirds of the diaphysis of the femur, referenced to the basal control for all groups. Concentration of mineral shows increases expected with age in V and S in the mid-diaphyseal region, but not in the flight group.

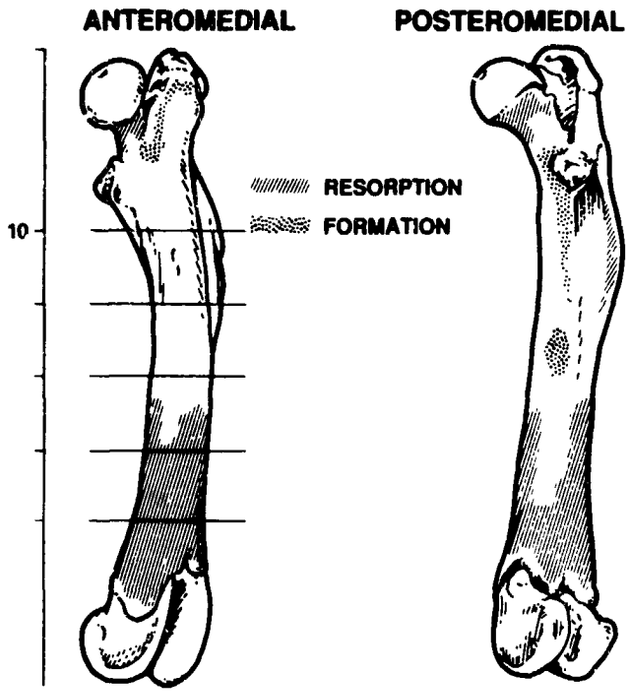

Figure 2. Line drawings from a photograph of the femur of a 300 gram Wistar Czech rat. Surface areas of resorption and formation determined by scanning electron microscopy are depicted. Areas of resorption were identified by resorption cavities and osteoclasts, and of formation by collagen bundles and active osteoblasts.

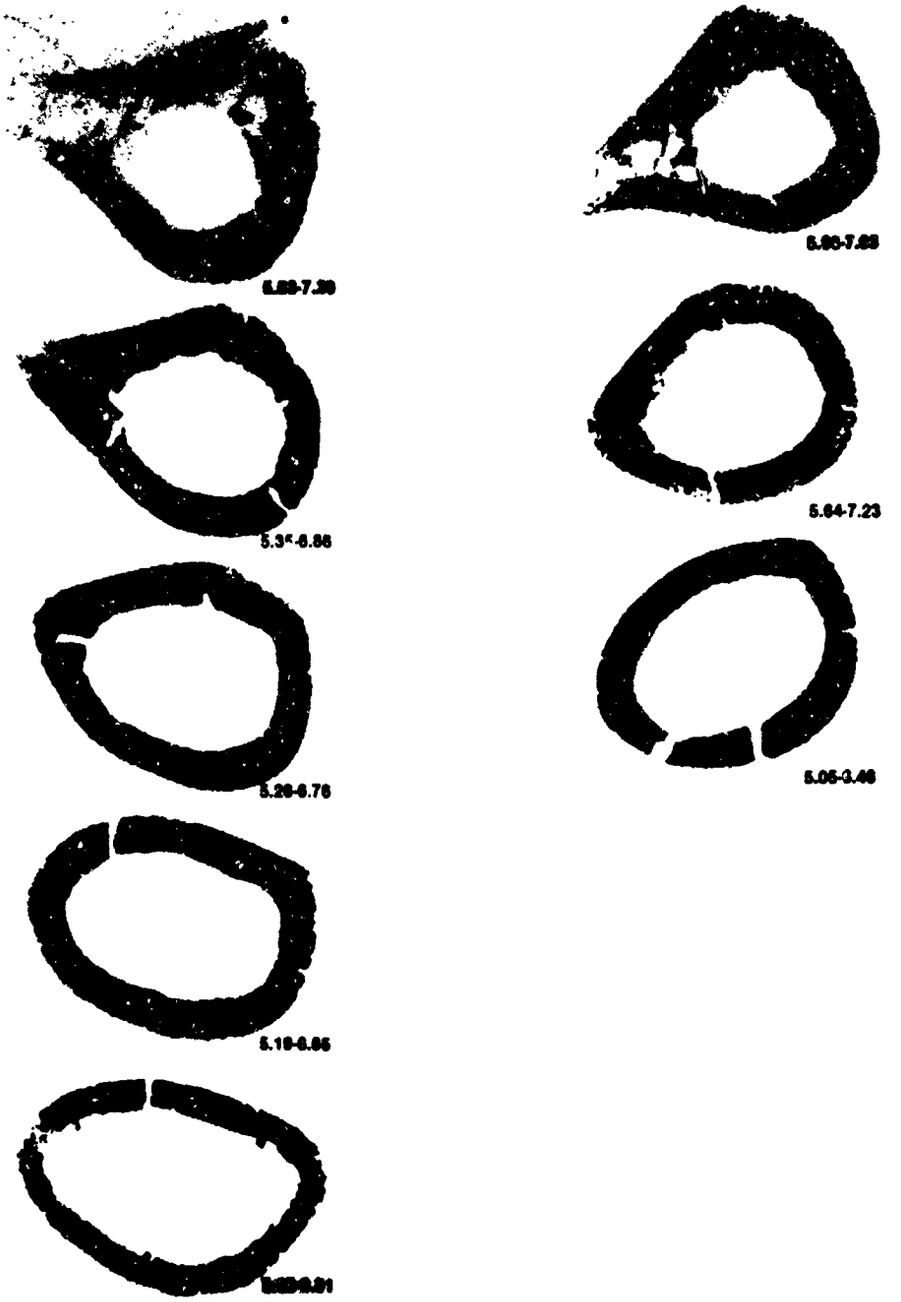

Figure 3. X-ray microtomography of 5 computer generated sections of a synchronous control femur, 4 mm apart, beginning 10 mm from the top of the bone on the left. Three 'sections' from the same locations in the diaphysis of a flight animal. See text for details of the method. Intensity range 200-250, resolution 26-28 microns.

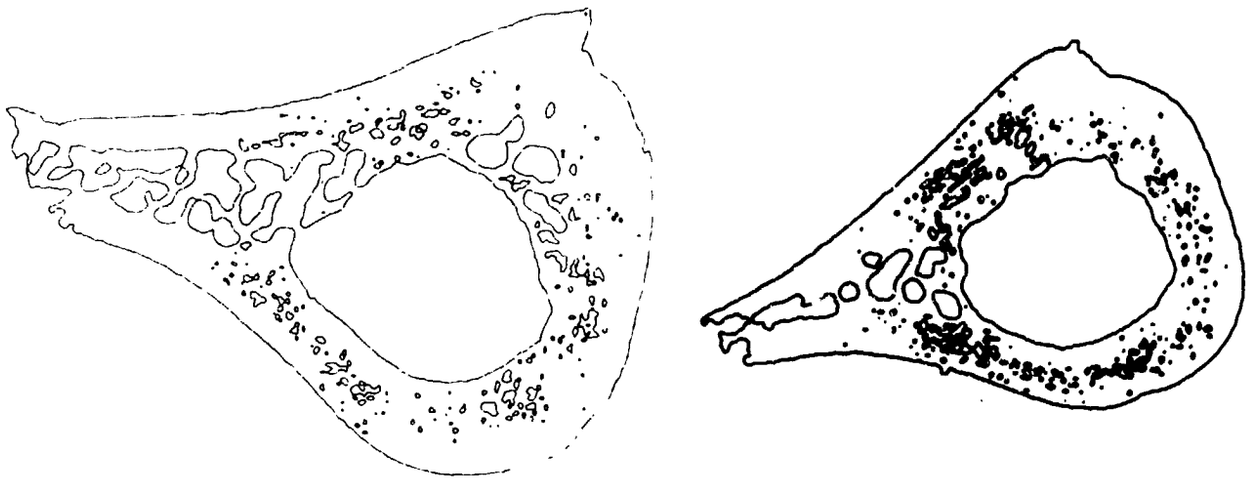

(a) SYNCHRONOUS CONTROL (b) FLIGHT FEMUR

Figure 4. Contour map drawn from x-ray microtomography sections at two levels of intensity, 150 for interior and 230 for exterior lines.

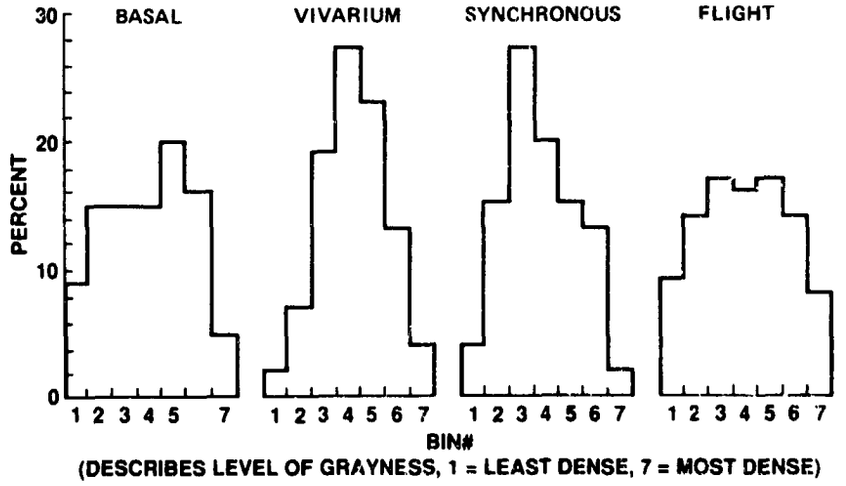

Figure 5. Histograms of the modal densities of combined proximal, central, and distal sections of the diaphysis in 4 experimental groups obtained by backscattered electrons and an image analysis system interfaced directly to a scanning electron microscope. The columns, 1-7, represent the percent of the mineralized bone fraction falling within a fixed computer-selected density range from 1 (least dense) to 7 (most dense).

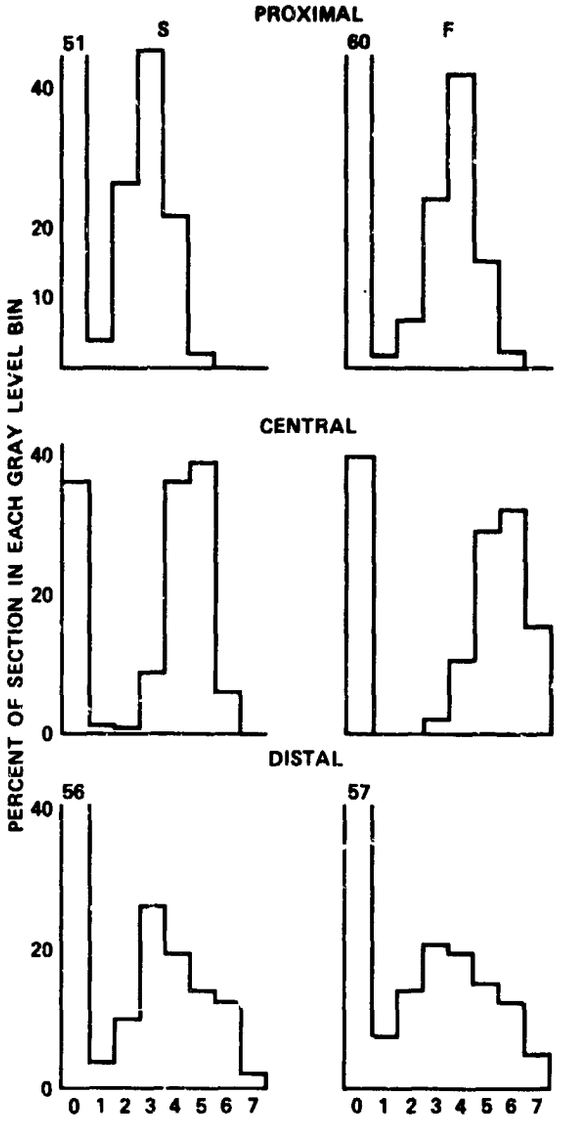

Figure 6. Histograms of the modal densities of the lateral quadrants of proximal, central, and distal sections of the femoral diaphyses of synchronous control and flight groups. Bar heights are the averages of data from 4 animals in the proximal and distal regions, and of 3 in the central region. Note bin O (non-bone and osteiod) in the proximal and bins 3 and 7 of the central regions of the flight group compared to the control.

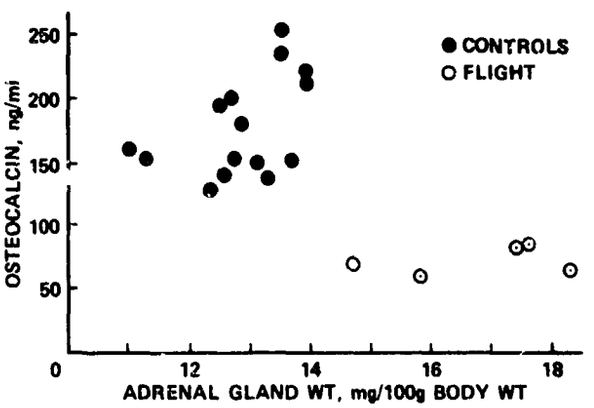

Figure 7. The concentration of serum osteocalcin, ng/ml, as a function of the weight of the adrenal gland, mg/100 g body weight, of flight and all controls.

N90-26456

EXPERIMENT K-6-02

BIOMEDICAL, BIOCHEMICAL AND MORPHOLOGICAL ALTERATIONS OF MUSCLE AND DENSE, FIBROUS CONNECTIVE TISSUES DURING 14 DAYS OF SPACEFLIGHT

Principal Investigator:

A. Vailas
University of Wisconsin
Madison, Wisconsin 53706

Co-Investigators:

R. Zernicke
University of California
Los Angeles, California 90024

R. Grindeland
NASA-Ames Research Center
Moffett Field, California 94035

A. Kaplansky
Institute of Biomedical Problems
Moscow, U3SR

INTRODUCTION

This is a final report summarizing our findings on the connective tissue response to short-term space flight (12 days). Specifically this report represents data regarding the biochemical, biomechanical and morphological characteristics of selected connective tissues (humerus, vertebral body, tendon and skeletal muscle) of growing rats.

RESULTS

Humerus Cortical Bone:

The vivarium control humeri were significantly longer than either basal controls or flight rats, but were not different in length when compared to synchronous controls (Figure 3A). Using the basal group for comparison, during the 12.5 day period, the humeral lengths increased 4.3% for vivarium controls, 1.4% for synchronous controls, and 0.04% for flight rats.

The humeral cross-sectional geometries showed significant differences among the four groups (Table 1). The synchronous and vivarium controls had greater cortical cross-sectional areas than the flight group by 20% and 13%, but only the synchronous control humeri were significantly different from the flight group (Figure 3B). The endosteal cross-sectional area was not significantly different among groups. Humeral periosteal circumferences were identical both for the basal controls in flight groups and were 6-9% less than the synchronous and vivarium controls.

The lack of middiaphysial growth in the flight humerus bones were evident in several morphological measures other than the overall periosteal circumference (Table 1 and Figure 4). In particular, the second moments of area and cortical (periosteal) diameters for the basal control and flight rats were the same, and synchronous and vivarium control humeri were typically significantly larger. The second moment area is an indicator of the amount of cortical bone and the distance that bone mass is located from the bending axis. The test bending axis (anterior-posterior) and the non-bending axis (medial-lateral), the average area moments of the vivarium and synchronous controls were significantly greater (29-30%) than those of the basal and flight humeri (Figure 4). Concomitantly, the anterior-posterior cortical diameters of the vivarium and synchronous controls were significantly larger (9%) than the basal and flight humeri (Table 1). The middiaphysial cross-sectional densities (Table 1), as well as the regional (anterior, posterior, medial and lateral) cortical thickness, however, were not significantly different among the groups.

The average flexural rigidity (bending stiffness) of flight humeri were significantly less than the vivarium (40%) and synchronous (35%) controls, but the average flexural rigidity of the flight humerus was not different from the basal control group (Figure 5A). The elastic modulus, however, showed no statistically reliable differences among the four groups (Figure 5B). Thus, the geometrical differences in the vivarium and synchronous control humeri vs. the basal control and flight humeri accounted for differences in flexural rigidity, while the elastic modulus (material characteristics) was not different among the humeri of the various groups. The flight group had a non-statistical tendency for lower loads than the vivarium controls at the proportional limit (35% less), maximum (15% less), and failure (17% less) (Table 2). The flight humeri also had a tendency to have a greater (36%) non-linear displacement than the vivarium control humeri.

Vertebral Bone:

The flight group had an average vertebral body (L6) compressional stiffness that was 39% less than vivarium, 46% less than the synchronous, and 16% less than the basal controls (Figure 8). When stiffness was normalized to a vertebral body weight, the flight group's average stiffness remained substantially lower than the vivarium (27% less), the synchronous (33% less), and the basal (7% less)

controls (Figure 8). The average initial maximum load of the flight group was 22% of the vivarium, 18% of the synchronous and 6% of the basal controls (Figure 9). However, when normalized for vertebral body weight, the initial maximum load of the flight group was 11% of the vivarium and synchronous controls, but did not differ from the basal controls. The average linear load of the flight group was 34% less than the vivarium, 25% less than the synchronous, but only 4% less than the basal controls (Figure 10). When normalized for vertebral body weight, the flight group was still only 22% of the vivarium, 70% of the synchronous, and essentially the same as the basal controls.

Average calcium (170.0 ± 8.1 μg/mg dry mass) phosphorous (122.3 ± 4.0 μg/mg dry mass) and hydroxyproline (23.0 ± 1.7 μg/mg dry mass) concentrations were not significantly different among groups. The average hydroxypyridinoline crosslink content per collagen molecule of the flight group (0.02472/moles/moles), however, was 35% less than the vivarium, 17% less than synchronous and 15% less than the basal controls.

Nutritional Effects On Bone Biomechanical Properties:

Because of differences between the rodent experiments on U.S.S.R. and U.S. space flights, the present experiment was designed to generate comparative data about the sensitivity of cortical bone (humerus) and trabecular bone (vertebral, T7) to caging environment, diet and rat strain differences. For two weeks (48-62 days), male Taconic-Sprague Dawley and Czechoslovakian-Wistar rats were maintained in flight simulation cages (1-rat/cage = U.S., 10 rats/cage = U.S.S.R.) and fed U.S.S.R. or U.S. diets. On average all rats increased (> 60%) their body mass during the two weeks, and there were no differences among humeral lengths for the different groups. Rats in U.S.S.R. cages had significantly larger total and endosteal cross-sectional areas for the humerus, and the cross-sectional areas for the T7 of Taconic rats were greater than the Czechoslovakian rats. U.S.S.R. caging affects resulted in significantly enhanced structural material properties in rat humeri, while the U.S. diet induced a significantly humeral maximum and failure loads. The bending stiffness of the Czechoslovakian rat humeri were significantly greater than the Taconic rats. Humeri from Czechoslovakian rats on the U.S. diet had significantly greater material properties in the elastic loading region than did the Taconic rats on the U.S.S.R. diet. Also, the humeral failure loads of Taconic rats on the U.S.S.R. diet were more adversely effected by U.S. cages than were the Czechoslovakian rats on the U.S.S.R. diet. The vertebral (T7), had no significant structural differences among the different groups, but material properties were influenced by all three factors; generally, the combination of factors that produced significantly greater material properties were U.S.S.R. caging, U.S.S.R. diet, and the Czechoslovakian strain of rat.

Soft Dense Fibers Connective Tissue Response:

Acute exposure to space flight did have a tendency to modify the composition in the tendon matrix. Data summarized in Table 10 showed that patellar tendons obtained from flight animals had consistently lower amounts of mature collagen crosslinks, collagen concentration and DNA concentration. Decreases in both the level of collagen maturity and concentrations of fibroblasts and structural protein would range from 8-22%. However, there were no significant trends reported in Achilles tendon obtained from flight animals. These data seems to suggest that there is a hetrogeneous response of tendon types to spaceflight in rodents. This hetrogeneity can reflect differences in load history of each tendon.

There seems to be no significant effect upon the collagen concentration in various types of skeletal muscles. Data summarized in Table 12 showed that collagen concentration was not significantly modified by space flight. However, the concentration of collagen is slightly higher in soleus muscle of flight animals as compared to basal and synchronous groups. However it should be noted that we were unable to obtain whole muscles in order to determine total collagen content. These data only reflect muscle connective tissue composition on the basis of concentration.

APPENDIX:

RAT DIET COMPOSITION

1. USSR Cosmos Diet *

Ingredients: (quantities in g)

Casein (milk)	3.0
Cornstarch	3.0
Sucrose	6.7
Sunflower seed oil	1.7
Dry Brewers yeast	1.0
Salt mixture	0.6
Water	24.0

Food Content (quantities in g)

Protein	3.06
Fats	1.79
Carbohydrates	9.61

Mineral Content (quantities in mg)

Sodium	60.900
Chlorine	15.500
Potassium	67.100
Phosphorus	86.300
Calcium	84.260
Iron	3.190
Iodine	0.070
Zinc	0.080
Copper	0.080
Cobalt	0.008
Flourine	0.130
Aluminum	0.0008
Magnesium	6.960
Sulfur	11.170
Manganese	0.900

Vitamin Content (quantities in μg)

B1	64.8
B2	62.4

B6	50.5
Pantothenic acid	240.0
Nicotinic acid	493.6
E	1380.0
A	20.0
D	6.0
Folic acid	32.0
Inosine	800.0
B15 Biotin	16.0
P-amino benzoic acid	800.0
B12	480.0
Choline	16000.0
K	16.0

* Sorbic acid 0.5% to weight of feed added as a preservative.

Quantities are for 40 g of diet, wet weight.

2. **USA Diet** (TEKLAD TD85348, values are g/kg, *fed for first week of experiment*)

Casein, High Protein	100.0
DL-Methionine	3.0
Wheat Gluten	120.0
Wheat Flour, durum 2nd clear	225.0
Corn Syrup (supplied by customer)	100.0
Sucrose	100.0
Corn Oil	40.0
Cellulose (fiber)	50.0
Mineral Mix, AIN-76 (#170915)	35.0
Calcium Carbonate, $CaCO_3$	5.0
Vitamin Mix, AIN-76A (#40077)	20.0
Choline Bitartrate	2.0

USA Diet (TEKLAD L-356, values are g/kg, *fed for second week of experiment*)

Casein, "Vitamin-Free" Test	200.0
Autolyzed Yeast Powder, Low Sodium	20.0
Liver, Desiccated (Whole Liver Substance)	20.0

Rice, White Polished (Finely ground)	582.8293
Corn Starch (Diluent for Vitamin Mix)	2.1743
Corn Oil	67.7
Non-Nutritive Fiber (Cellulose)	50.0
Calcium Carbonate, $CaCO_3$	15.0024
Potassium Phosphate, Dibasic, K_2HPO_4	11.2518
Sodium Phosphate, Dibasic, Na_2Hpo_4	10.0016
Magnesium Sulfate, $MgSO_4 \cdot 7H_2O$	3.7506
Ferric Citrate (16.7% Fe)	3.7506
Calcium Phosphate, Dibasic, $CaHPO_4$	2.7505
Sodium Chloride, NaCl	2.5004
Manganese Sulfate, $MnSO_4 \cdot H_2O$	0.6251
Cupric Sulfate, $CuSO_4$	0.192
Zinc Sulfate, $ZnSO_4 \cdot 7H_20$	0.05
Potassium Iodide, KI	0.0375
Aluminum Potassium Sulfate, $AlK(SO_4)_2 \cdot 12H_20$	0.0375
Cobalt Chloride, $CoCl_2 \cdot 6H_2O$	0.025
Sodium Borate, $Na_2B_4O_7 \cdot IOH_2O$	0.025
Asorbic Acid	2.0
Inositol	1.0
Choline Chloride	1.9934
Pyridoxine HCl	0.0202
Pyridoxamine Dihydrochloride	0.0041
Thiamin HCl	0.0606
Riboflavin	0.0303
Niacin	0.0504
Niacinamide	0.0504
Calcium Pantothenate	0.303
Biotin	0.001
Folic Acid	0.0101
p-Aminobenzoic Acid	0.0504
Vitamin B12 (0.1% trituration in mannitol)	0.2518
Dry Vitamin A Palmitate (500,000 U/g)	0.016
Vitamin D3 triturated in Vft Casein (3000 U/g)	0.3333
Mixed Tocopherals (372 U/g)	1.0214
Manadione	0.1

TABLE 1

MIDDIAPHYSIAL CROSS-SECTIONAL MORPHOLOGY OF HUMERUS

	Basal	Synchronous	Vivarium	Flight
Periosteal circumference (mm)	8.3±0.2*	9.1±0.3	8.8±0.3	8.3±0.3*
Endosteal circumference (mm)	4.1±0.3	4.4±0.6	4.4±0.3	4.2±0.3
Medial-lateral cortical diameter (mm)	2.4±0.1	2.5±0.1	2.4±0.2	2.3±0.2
Medial-lateral medullary diameter (mm)	1.2±0.1	1.2±0.2	1.2±0.1	1.2±0.2
Anterior-posterior cortical diameter (mm)	2.7±0.1†	3.0±0.2	3.0±0.1	2.8±0.3†
Anterior-posterior medullary diameter (mm)	1.3±0.1	1.4±0.2	1.5±0.2	1.3±0.1
Density (mg/mm^3)	1.58±0.24	1.79±0.48	1.74±0.07	1.76±0.11

Values are means ± S.D. for 5 rats in the basal and synchronous control groups and for 4 rats in the vivarium and flight groups.

* Synchronous group is significantly ($p \leq 0.05$) different from the basal and flight groups.
† Synchronous and vivarium groups are significantly ($p \leq 0.05$) different from the basal and flight groups.

TABLE 2

MECHANICAL CHARACTERISTICS OF HUMERUS

	Basal	Synchronous	Vivarium	Flight
Load at yield (N)	70.2±12.4	71.1±12.5	87.0±16.6	64.5±18.3
Load at maximum (N)	91.0±15.5	96.9±18.3	117.1±17.6	100.3±21.6
Energy to yield load (N•s)	13.2±4.5	11.9±5.1	17.5±6.6	12.3±6.0
Energy to maximum load (N•s)	33.3±10.4	37.2±8.2	44.3±11.6	42.0±14.2
Tensile yield stress (N/mm^2)	298±49	251±40*	346±47	329±48
Nonlinear displacement (mm)	0.20±0.05	0.25±0.04	0.21±0.01	0.29±0.06

Values are means ± S.D. for 5 rats in the basal and synchronous control groups and for 4 rats in the vivarium and flight groups.

* Synchronous group is significantly ($p \leq 0.05$) different from the vivarium group.

TABLE 3

BIOCHEMICAL CHARACTERISTICS OF HUMERUS

	Basal	Synchronous	Vivarium	Flight
Calcium (μg/mg dry mass)	297±10*	306±9	322±10	314±10
Phosphorous (μg/mg dry mass)	155±7	152±4	152±4	157±4
Hydroxyproline (μg/mg dry mass)	22.0±9*	20.0±0.7	20.0±0.9	20.0±0.9
Hydroxypyridinoline (nMoles/mg dry mass)	0.0345±0.008	0.365±0.014	0.0310±0.021	0.044±0.018
Ratio of hydroxyproline to collagen (moles/moles)	0.059±0.020	0.054±0.018	0.054±0.037	0.064±0.020

Values are means ± S.D. for 5 rats in the basal and synchronous control groups and for 4 rats in the vivarium and flight groups.

* Basal group is significantly ($p \leq 0.05$) different from all other groups.

TABLE 4

CAGE EFFECTS ON HUMERUS

	10-Rat/Cage	1-Rat/Cage
Load at proportional limit (N)	66.33±13.12	56.82±10.77*
Load at maximum (N)	82.03±16.51	76.51±15.11
Energy to proportional limit (N•s)	13.59±4.93	10.42±3.88*
Energy to maximum load (N•s)	29.93±12.75	30.25±11.71
Energy to failure load (N•s)	46.19±21.27	44.24±19.58
Flexural Rigidity (kN/mm)	10.45±2.41	10.05±2.59
Elastic Modulus (GPa)	3.59±1.34	2.64±1.40*
Tensile stress at proportional limit (MPa)	206.8±69.2	143.4±53.1*

* $p \leq 0.05$

TABLE 5

DIET EFFECTS ON HUMERUS

	USA	USSR
Load at proportional limit (N)	63.34±11.60	58.92±13.70
Load at maximum (N)	85.03±12.57	73.17±16.79*
Energy to proportional limit (Ns)	12.23±5.43	11.51±3.68
Energy to maximum load (Ns)	34.93±12.80	25.01±8.92*
Energy to failure load (Ns)	52.63±20.58	37.23±16.71*
Flexural Rigidity (kN/mm)	10.84±2.49	9.59±2.38
Elastic Modulus (GPa)	3.27±1.13	2.86±1.71
Tensile stress at proportional limit (MPa)	179.9±56.2	164.9±79.7

*$p \leq 0.05$

TABLE 6

RAT-STRAIN EFFECTS ON HUMERUS

	Taconic	Czech
Load at proportional limit (N)	61.04±13.25	61.32±12.52
Load at maximum (N)	77.17±15.76	81.05±15.93
Energy to proportional limit (Ns)	13.32±5.32	10.66±3.62
Energy to maximum load (Ns)	30.57±12.93	29.72±11.53
Energy to failure load (Ns)	48.82±23.42	42.01±16.79
Flexural Rigidity (kN/mm)	9.15±1.75	11.16±2.68*
Elastic Modulus (GPa)	2.84±1.40	3.27±1.47
Tensile stress at proportional limit (MPa)	174.4±72.5	171.0±66.1

$p \leq 0.05$

TABLE 7

CAGE EFFECTS ON RAT THORACIC VERTEBRA (T7)

	10-Rat/Cage	1-Rat/Cage
Load at proportional limit (N)	70.8±22.7	63.3±19.5
Maximum load (N)	112.8±23.7	99.2±22.8
Compressional stiffness (N/mm)	690.7±265.5	691.1±207.9
Elastic modulus (MPa)	1.89±0.66	1.81±0.58
Stress at proportional limit (MPa)	15.50±6.35	12.99±4.28
Strain energy density at maximum stress (kNmm/ml)	1.38±1.35	1.04±0.75

TABLE 8

DIET EFFECTS ON RAT THORACIC VERTEBRA (T7)

	USSR	USA
Load at proportional limit (N)	72.6±27.0	60.9±9.9
Maximum load (N)	110.5±27.9	100.8±18.4
Energy at maximum load (N•s)	48.04±30.86	41.46±20.43
Compressional stiffness (N/mm)	718.6±286 6	661.6±165.3
Elastic modulus (MPa)	1.96±0.74	1.73±0.44
Stress at proportional limit (MPa)	15.88±7 16	12.44±1.51*
Strain energy density at maximum stress (kNmm/ml)	1.43±1.35	0.96±0.67

* $p \leq 0.05$

TABLE 9

RAT-STRAIN EFFECTS ON RAT THORACIC VERTEBRA (T7)

	Taconic	**Czech**
Load at proportional limit (N)	66.01±18.66	67.90±24.01
Maximum load (N)	107.9±18.1	103.5±29.3
Compressional stiffness (N/mm)	723.4±192.3	656.5±273.2
Elastic modulus (MPa)	2.07±0.48	1.61±0.66*
Stress at proportional limit (MPa)	15.25±5.86	13.11±4.92
Strain energy density at maximum stress (kNmm/mm)	1.36±1.23	1.03±0.91

* $p \leq 0.05$

TABLE 10 COSMOS #1887 PATELLAR TENDON COMPOSITION

Group	Hydroxyproline concentration (μg/mg)	Hydroxypyridinoline collagen crosslinks (mole/mole)	DNA concentration (μg/mg)
Flight	66.23±15.01	0.0489±0.020	8.93±3.47
Basal	71.57±10.52	0.0335±0.008	9.76±5.39
Synchronous	71.43±8.45	0.0245±0.003	10.69±4.37
Vivarium	71.82±16.29	0.0625±0.042	9.53±3.31

Values represent mean and standard deviations. * denotes a statistical significant difference, $P < 0.05$ from vivarium control group. There were no significan differences, however, values associated with flight animals were consistently lower than vivarium rats (8%-22%).

TABLE 11 COSMOS #1887 ACHILLES TENDON COMPOSITION

Group	Hydroxyproline concentration (µg/mg)	Hydroxypyridinoline collagen crosslinks (mole/mole)	DNA concentration (µg/mg)
Flight	63.15±17.18	0.0328±0.018	8.39±3.14
Basal	64.74±12.55	0.0347±0.015	8.81±2.26
Synchronous	58.56±15.07	0.0256±0.008	8.93±2.76
Vivarium	58.99±9.86	0.0274±0.010	7.18±1.87

Values represent mean and standard deviation. * denotes a statistical significant difference, $P < 0.05$ from vivarium control group. There were no significant differences among the experimental group.

TABLE 12 COSMOS #1887 SKELETAL MUSCLE COLLAGEN CONCENTRATION (µg/mg)

Group	Soleus	Medial Gastroenemius	Tibialis Anterior
Flight	9.17±1.8	5.37±0.60	7.12±3.8
Basal	5.33±2.6	6.94±2.1	7.16±2.7
Synchronous	8.50±2.3	5.08±1.4	6.73±0.9
Vivarium	9.46±3.9	5.43±1.0	4.79±1.5

Values represent mean and standard deviations. * denotes a statistical significant difference, $P < 0.05$ from vivarium control group. There were no significant differences.

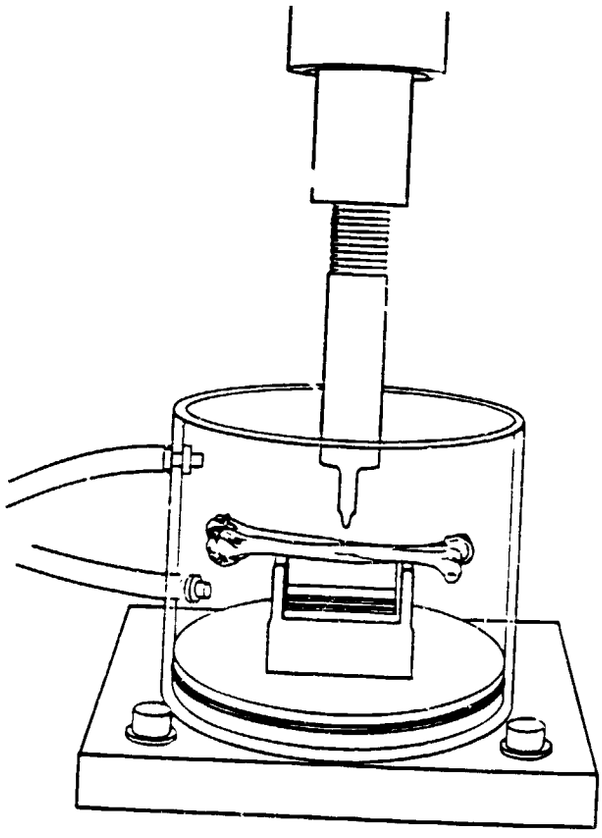

Figure 1. Apparatus used for three-point bending of the humerus.

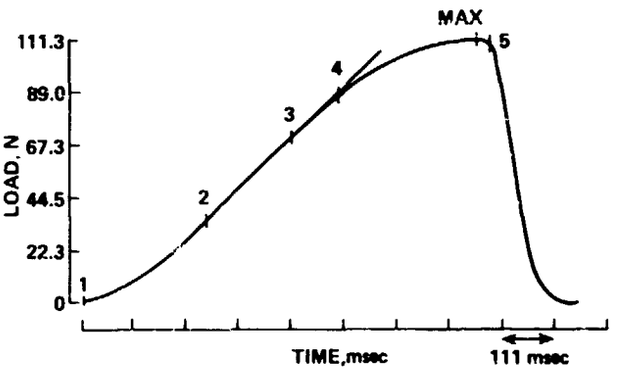

Figure 2. Exemplar load-time curve for humerus test. Point 1 indicates the application of the initial load. Points 2 and 3 are boundary marks for the linear regression line that is calculated to estimate the slope of the load-deflection curve. Point 4 is the proportional limit. MAX indicates the maximum load, and Point 5 is failure load.

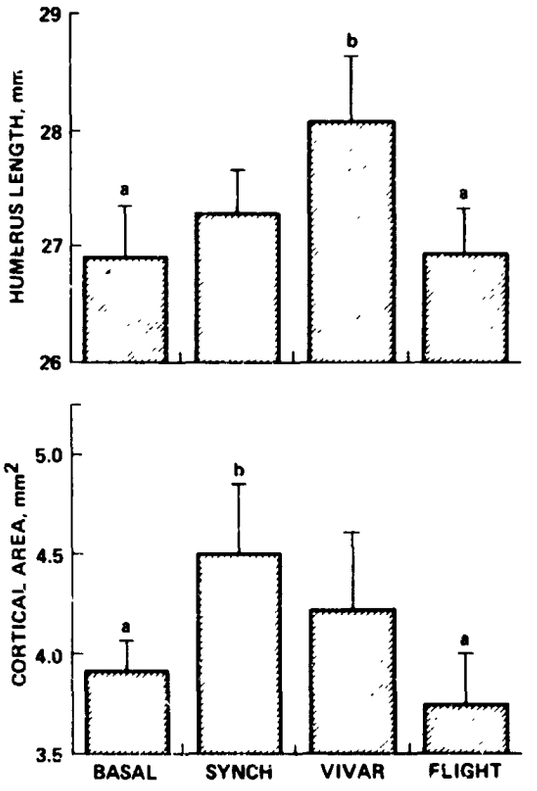

Figure 3. Humeral length (a) and middiaphysial cortical cross-sectional area (b). Mean values and SD error bars are indicated. Statistically significant ($p \leq 0.05$) relationships include the following: b > a.

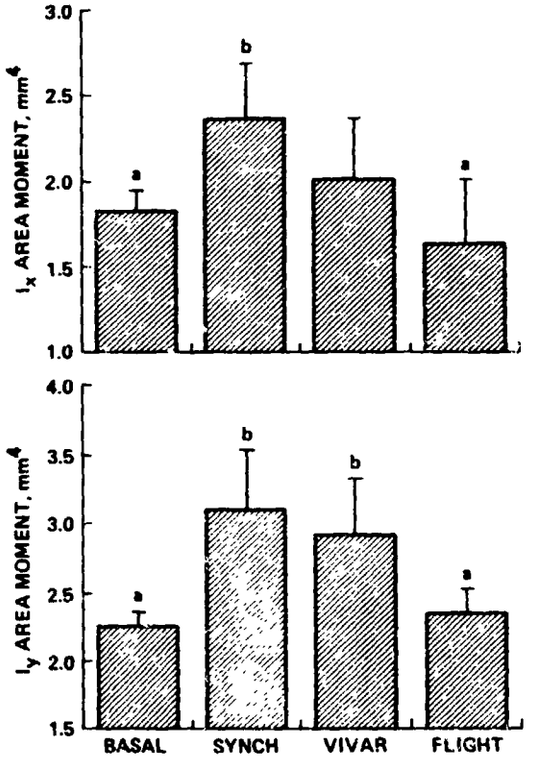

Figure 4. Humeral second moment of area with respect to anterior-posterior axis (Ix, Fig. 4a) and medial-lateral axis (Iy, Fig. 4b). Mean values and SD error bars are indicated. Statistically significant ($p \leq 0.05$) relationships include the following: b > a.

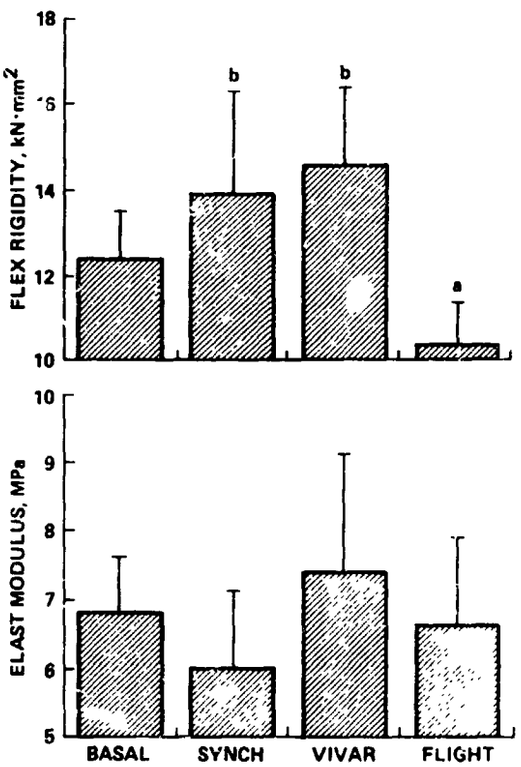

Figure 5. Humeral flexural rigidity (a) and elastic modulus (b). Mean values and SD error bars are indicated. Statistically significant ($p \leq 0.05$) relationships for flexural rigidity include the following: b > a. No statistically reliable differences were found among the elastic moduli of the groups.

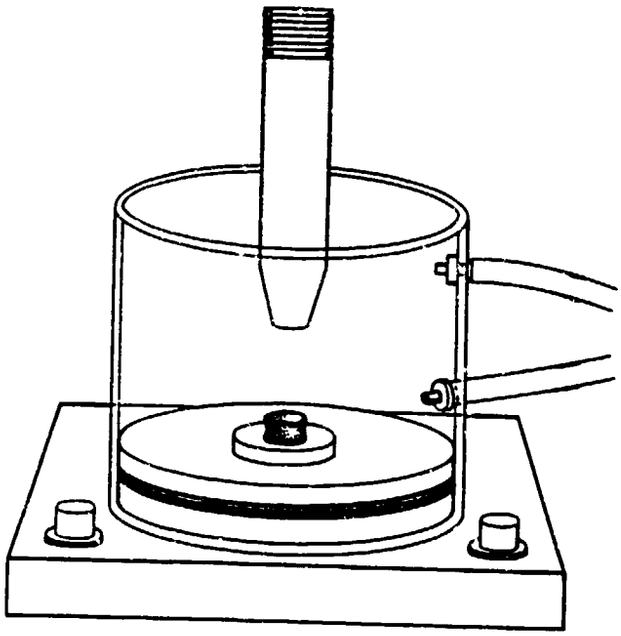

Figure 6. Set-up for the rat vertebral body compression tests. The vertebral body is shown fixed to a cylindrical stainless-steel plate while immersed in a warmed, circulating buffer solution.

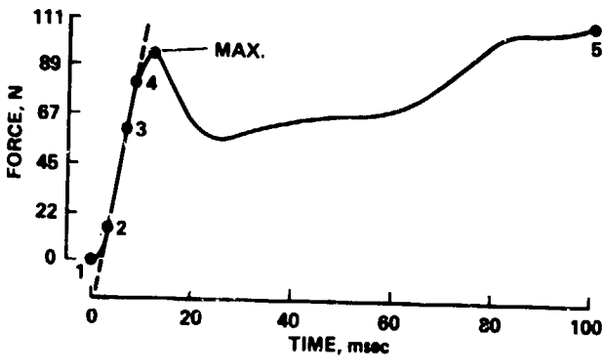

Figure 7. Exemplar load-time curve for a compression test of a rat L6 vertebral body. (1) denotes the point of initial loading, (2 and 3) are arbitrary points in the linear load region, (4) is the proportional limit, (5) is 50% strain, and MAX represents the initial-maximum load.

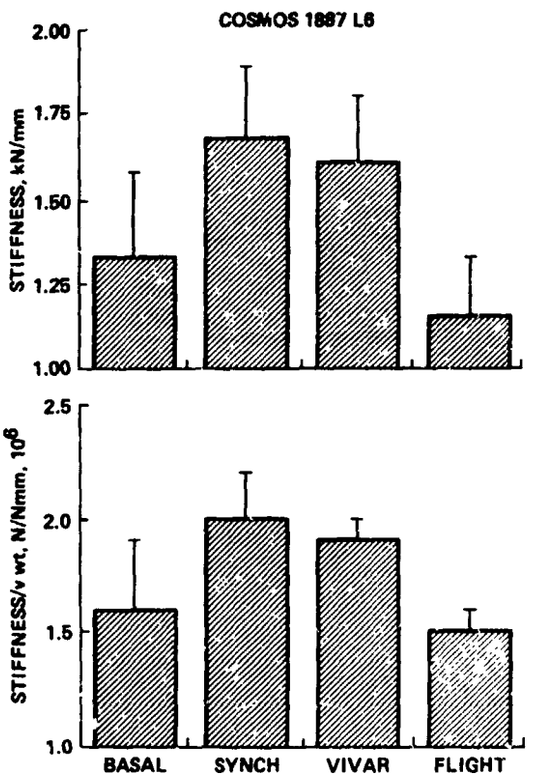

Figure 8. Compressional stiffness and normalized stiffness (per unit vertebral-body weight) for rat L6. Mean and SD values are indicated for the flight, vivarium, synchronous, and basal control groups.

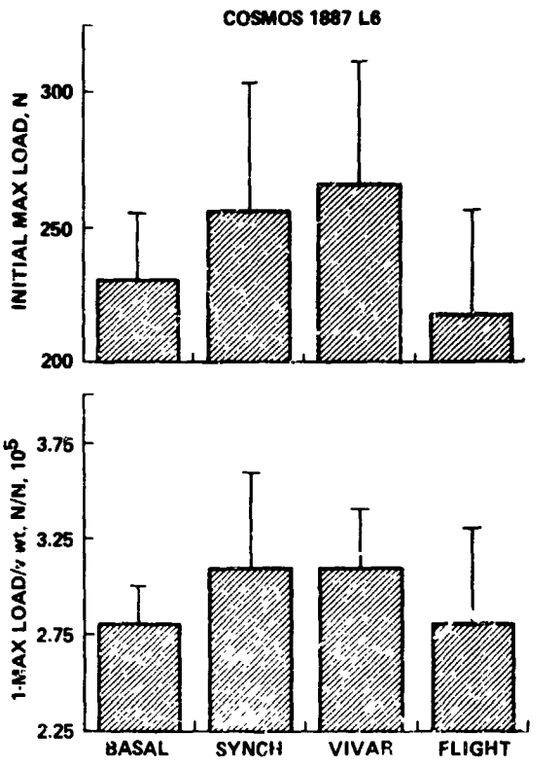

Figure 9. Initial-maximum load and normalized initial-maximum load (per unit vertebral-body weight) for rat L6. Mean and SD values are indicated for the flight, vivarium, synchronous, and basal control groups.

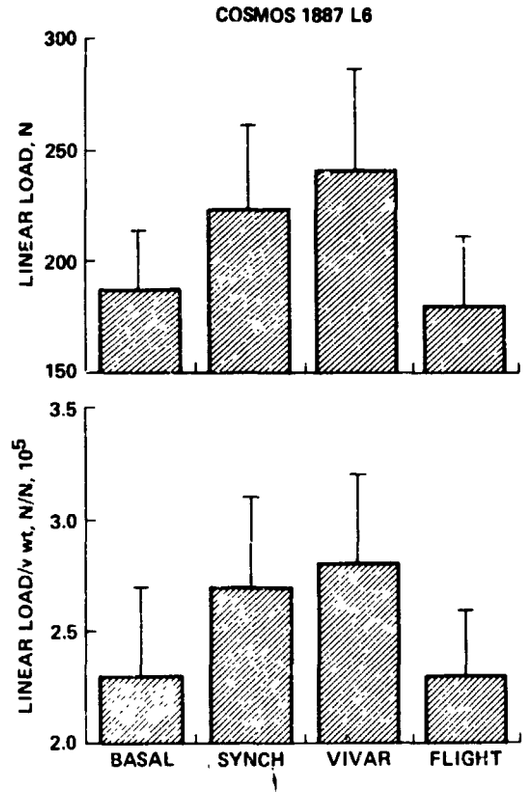

Figure 10. Linear load and normalized linear load (per unit vertebral-body weight) for rat L6. Mean and SD values are indicated for the flight, vivarium, synchronous, and basal control groups.

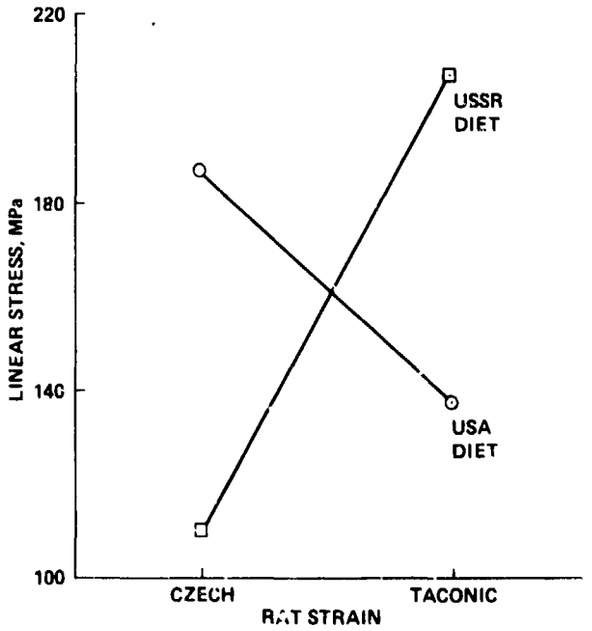

Figure 11. Humerus linear stress two-way significant interaction (diet x strain).

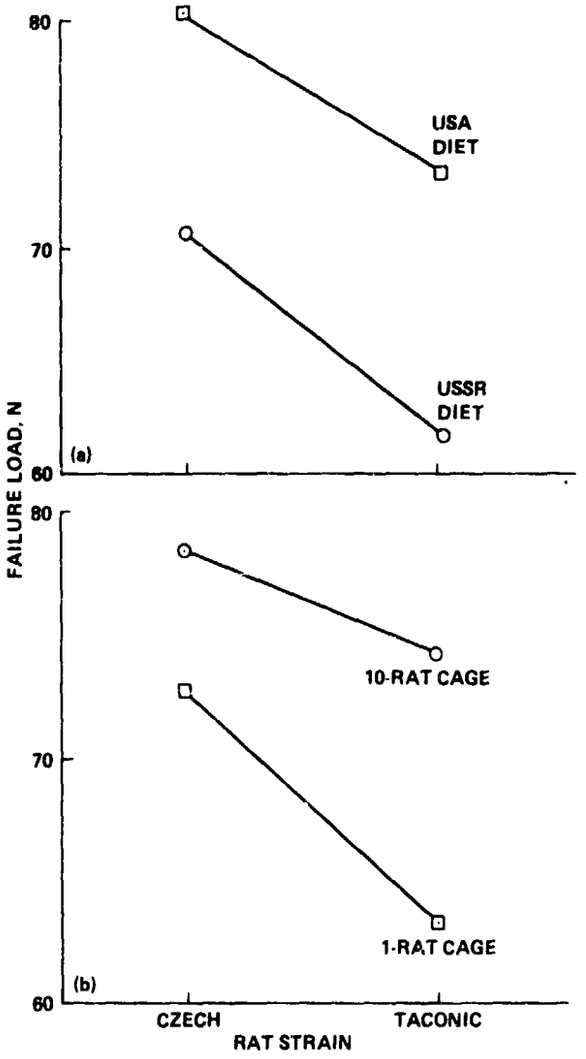

Figure 12. Humerus failure stress three-way significant interaction (diet x cage x strain). (a) illustrates diet x rat strain and (b) illustrates cage x rat strain effects.

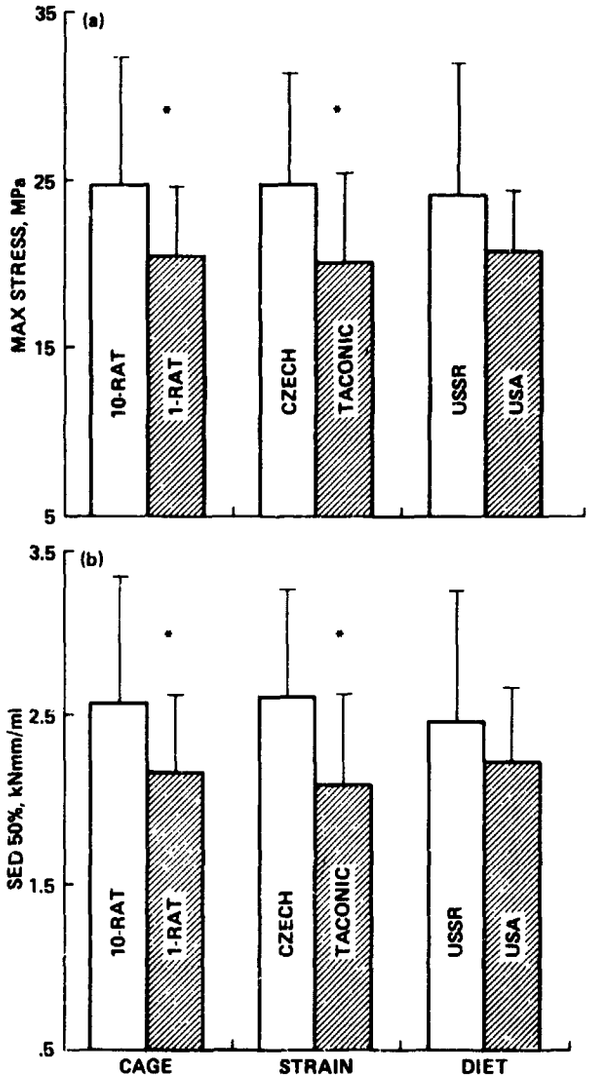

Figure 13. T7 vertebral-body differences for maximum stress (a) and strain energy density at 50% strain (b). Both the cage and rat-strain effects were statistically significant differences (*). The diet effect was not significant.

N90-26457

EXPERIMENT K-6-03

GRAVITY AND SKELETAL GROWTH

PART I: GRAVITY AND SKELETEL GROWTH

PART II: MORPHOLOGY AND HISTOCHEMISTRY OF BONE CELLS AND VASCULATURE OF THE TIBIA

PART III: NUCLEAR VOLUME ANALYSIS OF OSTEOBLAST HISTOGENESIS IN PERIODONTAL LIGAMENT CELLS

PART IV: INTERVERTEBRAL DISC SWELLING PRESSURE ASSOCIATED WITH MICROGRAVITY

Principal Investigator:

E. Holton
NASA Ames Research Center
Moffett Field, California 94035

Co-Investigators:

A. Hargens
M. Gonsalves
NASA Ames Research Center
Moffett Field, California 94035

A. Kaplansky
G. Durnova
Institute of Biomedical Problems
Moscow, USSR

D. Berretta
University of Pennslyvania
Philadelphia, Pennsylvania

S. Gott
University of California
San Diego, California 92161

S. Doty
Columbia University
New York City, New York

B. Rydevik
University of Goteborg
Goteborg, Sweden

W. Roberts
L. Garetto
Indiana University School of Dentistry
Indianapolis, Indiana 46202

EXPERIMENT K-6-03

PART I: GRAVITY AND SKELETAL GROWTH

E. Holton, D. Berretta, S. Doty, W. Roberts, and L. Garetto

SUMMARY

Bone area, bone electrophysiology, bone vascularity, osteoblast morphology, and osteoblast histogenesis were studied in rats associated with Cosmos 1887. The results suggest that the synchronous animals were the only group with a significantly larger bone area than the basal group, that the bone electrical potential was more negative in flight than in the synchronous rats, that the endosteal osteoblasts from flight rats had greater numbers of transitional Golgi vesicles but no difference in the large Golgi saccules or the alkaline phosphatase activity, that the perioteal vasculature in the shaft of flight rats often showed very dense intraluminal deposits with adjacent degenerating osteocytes as well as lipid accumulations within the lumen of the vessels and sometimes degeneration of the vascular wall (this change was not present in the metaphyseal region of flight animals), and that the progenitor cells decreased in flight rats while the preosteoblasts increased compared to controls. Many of the results suggest that the animals were beginning to recover from the effects of spaceflight during the two day interval between landing and euthanasia; flight effects, such as the vascular changes, did not appear to recover.

INTRODUCTION

Experiments flown on Soviet Cosmos biosatellites suggest that growth in tibial diameter is suppressed in the long bones of growing rats (Morey and Baylink, 1978; Wronski and Morey, 1983). Further experimentation on Cosmos and Spacelab 3 (SL3) suggests that bone strength does not increase in these animals although the bone continues to grow in length (Spengler *et al.*, 1983; Shaw *et al.*, 1988). Strength tests of the humeri of flight rats on SL3 show that the difference from ground controls might be related not only to reduced bone diameter, but also to the composition and quality of new bone formed (Patterson-Buckendahl *et al.*, 1987). Also, a higher percentage of the total bone mineral has smaller crystals (which could be more soluble) in flight rats as compared to animals that remained on earth (Simmons *et al.*, 1986). Such data suggest that matrix turnover is altered during flight which in turn decreases the amount of bone added and either this defect alters the size of bone crystals formed or the flight environment somehow impedes crystal growth independent of matrix production; the suppressed bone formation may be a major factor in the failure of bone to increase in strength. These experiments were conducted in growing rats and suggest that gravity is important to normal growth and development of the mammalian skeletal system. The objectives of the Cosmos 1887 study were to continue the investigation of the effect of spaceflight on bone in growing rats by measuring bone area, bone electrophysiology, bone vascularity, osteoblast morphology, and ostoblast histogenesis.

MATERIALS AND METHODS

Specific pathogen-free, male, Wistar rats from the Institute for Experimental Endocrinology of the Slovakian Academy of Sciences were divided into 3 groups of 10 animals/group. The flight and synchronous groups were each housed in a single cage which had 10 nozzles for paste diet and 10 lixits for water. Fourteen gram boluses of food (55g/day/nozzle) were delivered every 6 hours beginning at 0200 each day. Water was provided ad libitum. The vivarium animals were housed similarly but were fed in a single bolus each day. The flight rats were launched on September 29, 1987, at 1550 hours and landed at 0703 hours on October 12, 1987. Problems associated with

PRECEDING PAGE BLANK NOT FILMED

recovery of the craft were duplicated as closely as possible with the synchronous animals. The flight rats were killed 53.5-55.8 hours after landing; during the postflight time, they were transported from the landing site to the recovery site necessitating a 42hr fast and at least a 3 hour exposure to external temperatures ranging from -5 to -20C. Approximately 16 hrs before euthanization, the flight and synchronous rats were given 28 grams of food, and water ad libitum. The flight rats were 20 days older than the basals while the vivarium rats were 3 days older than the flight and the synchronous group was 3 days older than the vivarium group at the end of the experiment. At the end of each test period, rats were guillotined. One-half of each calvaria, 1/2 the proximal tibial metaphysis, and the tibial shaft were place in vials of 2% parformaldehyde in 0.1M cacodylate buffer, plus 0.5% glutaraldehyde, pH 7.4 at 4C for 48hr then rinsed 3 times with 0.1M cacodlylate buffer, pH 7.4 and shipped immersed in the buffer. The maxillae, with teeth, were fixed in phosphate buffered formalin, pH 7.0, stored and shipped at 4C. The thoracic vertebra was frozen and kept frozen during shipping. All samples arrived at this laboratory in excellent condition. The calvaria, maxilla, and tibial shaft were inadvertently placed in the freezer overnight causing potential freezing artifacts in these samples. The calvaria and proximal tibia were shipped at 4C by overnight mail to Dr. Doty for processing. The frozen vertebrae were shipped by overnight mail to Dr. Berretta for analysis. Dr. Roberts' samples were taken by car to San Francisco. All tissue arrived at their destination without incident.

The tibial shafts were dehydrated in ethyl ether and embedded undecalcified in polyester casting resin (Chemco, San Leandro, CA). The portion of the tibial shaft immediately proximal to the tibiofibular junction was sawed into 50 micron-thick cross sections with a Gillings-Hamco thin sectioning machine. Bone remaining in the blocks were shipped to Dr. Marc Grynpas, Toronto, Canada, (a collaborator with Dr. David Simmons) for further mineral analysis. Sections were mounted on slides and exposed to incident and polarized light.

The technique for measuring zeta potential has been described in detail (Berretta and Pollack, 1986). The vertebra were thawed, and wet ground in various solutions of NaCl using a diamond-tipped dental bur. The bone particles were homogenized for 10min and serially transferred twice for 15min of sedimentation per transfer to obtain a particle size of 5±2μm. A narrow size distribution of bone particles was desired so that light-scattering methods used in the zeta-potential measurements would yield histograms that could be interpreted as the percent of particles exhibiting a given zeta-potential value. Electrophoresis was used as the direct method of determining the zeta potential of bone particles. The bone particle velocity was measured in a fluid with a given ion concentration and pH while an electric field of known amplitude was applied. The ratio of the particle velocity to the electric field amplitude is defined as electrophoretic mobility (EPM) which, in turn, is proportional to the zeta potential. The direction of motion of the bone particles relative to the direction of the applied electric field was used to determine the polarity of the zeta potential. The PenKem System 3000 Automated Electrokinetic Analyzer (Pen Kem, Inc., Bedford Hills, NY) was used to measure EPM. In this instrument, a vertical, cylindrically focused beam of laser illumination traverses the stationary level (where net electroosmotic fluid velocity is zero) of a horizontally mounted cylindrical electrophoresis chamber 0.1 by 1.0cm. Light that is scattered 90° from the beam by the particles undergoing electrophoresis is focused through an objective onto the surface of a rotating radial grating. Pulses of light transmitted through the grating strike a photomultiplier tube whose output is analyzed. In the absence of current at the electrodes the particles in the chamber are stationary. Since the size of each particle is smaller than the width of each grating segment, the light scattered by each particle will be alternately blocked and then transmitted by the grating as the disk moves. Thus, the reference signal for the system corresponds to an output voltage from the photomultiplier tube that has a signal component at a frequency proportional to the speed of the disk. If a current is applied across the electrodes, an electric field will be produced that causes the particles in the chamber to move electrophoretically. The velocity of each particle produces a change in the tangential velocity of the image of that particle with respect to the grating. If the image of the particle is moving in the same direction as the grating, the image will cross fewer line pairs per unit time, producing a signal component for

that particle at a slightly lower frequency than the reference frequency. If the particle image moves in the opposite direction, the image will cross more line pairs per unit time and the signal will be at a higher frequency. Since there will normally be many particles in the field of view at any one time, each particle produces a signal component at a frequency shift related to its electrophoretic velocity. The mobility is thus determined by measuring the amount of the frequency shift with respect to the reference signal. This difference in frequency is proportional to the particle mobility, which is calculated directly on the basis of physical constants. When a population of particles

undergoing electrophoresis is examined, the frequency difference spectrum gives the EPM distribution of the population. A mobility histogram is then produced which shows the mobilities of various subpopulations of the bone particles studied. From this histogram, an average mobility can then be computed for the population. All solutions were prepared using distilled deionized water to which NaCl was added. The specific conductance of each sample was measured using a square wave current applied across palladium electrodes, with the resultant potential corrected for electrode polarization and joule heating. The NaCl concentrations corresponding to each conductivity value were determined from standard tables. The pH of each sample was measured automatically. Temperature was controlled by a water bath set at 20°C. The field strength used was 50±0.3V/cm. The EPM of human erythrocytes prepared using the method outlined by Seaman and Heard (Seaman and Heard, 1960) was used as a standard prior to each day's experiment. All specimens were allowed to equilibrate in their respective NaCl solutions at least 6 hr prior to testing. The average zeta potential was calculated from the average EPM using the Helmholtz-Smoluchowski equation:

$$\zeta = \frac{4\pi\mu\eta}{\varepsilon} \quad \text{or} \quad \zeta = \mu \times 12.873$$

where ζ is the zeta potential, μ the EPM, η the viscosity of the fluid, and ε the dielectric constant of the fluid

Techniques used by Dr. Doty in processing his tissues and the data are discussed in detail in Supplemental Report 1: Morphology and histochemistry of bone cells and vasculature of the tibia from Cosmos 1887. The techniques and dat from Dr. Roberts and his colleagues are discussed in detail in Supplemental Report 2: Nuclear volume analysis of osteoblast histogenesis in periodontal ligament cells of Cosmos-1887 rats.

RESULTS

The body weight of the basal group was 316+8.3(S.E.) on 9/24/87. The flight group weighed 303+2.4 on 10/14/87, while the vivarium group weighed 342+7.7 on 10/17/87 and the synchronous group weighed 349+5.8 on 10/20/87. The vivarium group gained an average of 1.13gm/day in the 23 days after the basal group was euthanitized while the synchronous group gained an average of 1.27gm/day in 26 days. The flight group lost an average of 13gm over a 20 days period compared to the basal group or -0.65gm/day. Further information on the weights of all groups before launch and following the flight period is essential to interpret the data.

Visual observations of tibial cross sections under brightfield or polarized light did not show any obvious differences between groups. Area and perimeter measurements (Table 1) showed no significant changes between any of the experimental groups. The only differences appeared in the periosteal perimeter and cross-sectional bone area at the tibiofibular junction in the basal rats as compared with the synchronous group ($p<0.05$).

The electrophysiology measurements are found in Table 2. The synchronous and vivarium control groups have very similar EPMs while the basal group is slightly less electronegative and the flight group is more electronegative than the controls. The summary histograms for the flight and synchronous groups are found in Figure 1.

DISCUSSION

Data from Cosmos 1887 are more difficult to interpret than previous missions due to unanticipated postflight problems and to the significant difference in mean body weight between the flight and the synchronous control group. Whether the weight difference reflects the six day age difference between the groups is not known. In preliminary experiments using normal, control animals, we found significant differences in bone strength in young, growing rats differing in age by only three days (approximately 235 vs 260gm). Thus, the older age of the control rats might bias some data toward significance. Also, the unanticipated postflight period (2.2-2.3 days) may have been sufficient for certain parameters to either recover or to begin recovery; distinguishing those parameters which are recovering and those which are not is extremely difficult.

The bone parameters including area and perimeter measurements at the tibiofibular junction show differences only between the synchronous and basal groups (Table 1). Data from the large rats in SL3 and previous Cosmos flights including Cosmos 782 and 1129 also showed no signficant changes in bone area between flight and synchronous controls; however, using a bone marker, a significant decrease in bone mineralization during flight was detected in these experiments. Only on Cosmos 936 was the bone area of the flight group significantly smaller than the synchronous group. Apparently the total bone area at the beginning of the flight period is much larger than the amount of bone formed in 1-3 weeks and can mask a mineralization defect unless bone markers are used.

Underlying Wolff's law on bone remodeling is the hypothesis that physical stresses applied to bone result in the formation of endogenous electrical potentials and that these potentials alter bone cell activity in a feedback manner to result in bone remodeling. Thus, any factor that can bring about a change in either sign or magnitude or both may alter these endogenous electrical potentials and change the balance between bone formation and bone resorption. The zeta potential is thought to be the surface charge at the bone-fluid interface which is related to streaming potentials. Streaming potentials are thought to occur when hydrated bone is mechanically deformed. The potentials have been determined to be of electrokinetic origin and can be quantified using the direct measurement of EPM which is proportional to the zeta potential. The electrical double layer at the bone-fluid interface within bone is different for some types of osteoporotic bone compared to normal bone and this difference can be quanitifed using zeta potentials characterized by EPM histograms (Berretta, *et al.*, 1987). The differences in the mean values of the histogram peaks may be only a manifestation of the disease or alternateively, this feature may indeed be responsible for the disease process. Systemic osteoporosis is characterized by EPM histograms with two or more peaks compared to controls which are single peaked (Berretta, *et al.*, 1987). The mean zeta potential for normal human bone in bone ECF was -3.6mV, while osteoporotic human bone was significantly less electronegative (-0.77mV). In rats, six months after castration, osteoporosis in the femur was indicated by double peaks and a significantly less negative mean EPM value. These data suggest that the more positive EPM values indicate net bone resorption; more negative values may be indicative of net bone formation.

In Cosmos 1887, the synchronous animals, which gained the most weight, had essentially normal zeta potential values (Table 2). The flight group has a more negative potential, indicating net bone formation, than all other groups. Interestingly, the potential in the flight rats is in the opposite direction of osteoporotic bone (that is, more negative rather than more positive mean EPM values). Whether the value reflects increased matrix synthesis during flight or during postflight recovery is not known. Data in this report by Roberts and coworkers suggest that osteoblastic histogenesis is

increased during the postflight period whereas a suppression of osteoblastic activity has been reported on past missions. The more negative potential in the space bone may also indicate that this bone defect may be theoretically reversible because it is of the same sign as normal bone; postmenopausal osteoporosis, which is opposite in sign to normal bone, is more difficult to return to the normal set point.

The time course and extent of bone changes during spaceflight must be understood before long duration spaceflight without compensating forces should be considered. A major concern is that adaptation to spaceflight might impair the ability to return to earth or other planets. Thus, we must understand what is happening to the mammalian skeleton during spaceflight. The Cosmos missions provide data for understanding skeletal adaptation in the growing rat to spaceflights lasting longer than one week.

ACKNOWLEDGMENTS

The authors thank the many Soviet scientists who assisted with the experiment by dissecting tissues, preparing samples, and expediting the shipment of biological specimens to this country. We also thank the NASA personnel who made this experiment possible. We are grateful for the technical assistance provided by Christopher Maese in shipping the bone specimens from our laboratory and analysing the tibial shaft specimens.

REFERENCES

1. Berretta, DA and SR Pollack. Ion concentraiton effects on the zeta potential of bone. J. Orthopaed. Res. 4:337-345, 1986.

2. Berretta, DA, SR Pollack, and ME Steinberg. Osteoporosis and the electrical double layer in bone. Transactions of the Orthopaed. Res. Soc. 12: 353, 1987. (Abstract)

3. Morey, ER and DJ Baylink. Inhibition of bone formation during space flight. Science. 201:1138-1141, 1978.

4. Patterson-Buckendahl, P, SB Arnaud, GL Mechanic, RB Martin, RE Grindeland, and CE Cann. Fragility and composition of growing rat bone after one week in spaceflight. Am. J. Physiol. 252:R240-246, 1987.

5. Seaman, GVF and DH Heard. The surface of the washed human erythrocyte as a polyanion. J. Gen. Physiol. 44:251-268, 1960.

6. Shaw, SR, AC Vailas, RE Grindeland, and RF Zernicke. Effects of a one-week spaceflight on the morphological and mechanical properties of growing bone. Am J. Physiol. 254:R78-83, 1988.

7. Simmons, DJ, JE Russell, and MD Grynpas. Bone maturation and the quality of bone mineral in rats flown on the Space Shuttle 'Spacelab-3 mission'. Bone Mineral. 1:485-493, 1986.

8. Spengler, DJ, ER Morey, DR Carter, RT Turner, and DJ Baylink. Effects of space-flight on structural and material strength of growing bone. Proc. Soc. Exptl. Biol. Med. 174:224-228, 1983.

9. Wronski, TJ and ER Morey. Effect of spaceflight on periosteal bone formation in rats. Am J. Physiol. 244:R305-309, 1983.

TABLE 1. COSMOS TIBIAL BONE PARAMETERS

	BASAL	FLIGHT	SYNCHRONOUS	VIVARIUM
Bone area	3.43±0.23	3.60±0.27	3.94±0.37*	3.75±0.34
Marrow area	0.79±0.19	0.77±0.16	0.84±0.17	0.79±0.17
Periosteal perimeter	7.93±0.20	7.97±0.29	8.38±0.29*	8.11±0.41
Marrow perimeter	3.37±0.13	3.32±0.31	3.45±0.34	3.36±0.37

Data are expressed as mean ± S.D.
* = significantly different from basal ($p<0.05$)
Area units are mm^2 while perimeter units are mm

TABLE 2. ZETA POTENTIAL MEASUREMENTS

GROUP	Mean electrophoretic mobility ($x10^{-8}$ µm-cm/V-s)	±SD	Mean zeta potential (mV)
Basal	-0.49±0.06		- 6.3
Flight	-1.20±0.04		-15.4
Synchronous	-0.56±0.35		- 7.2
Vivarium	-0.62±0.09		- 8.0

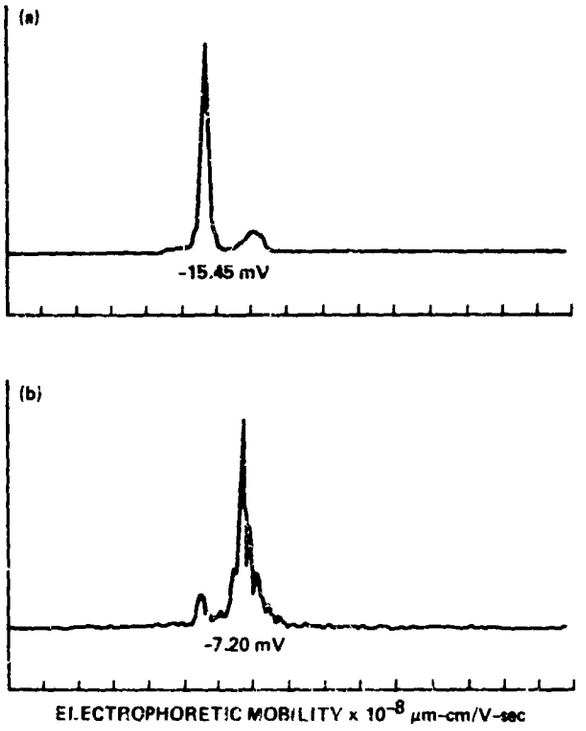

Figure 1. Summary histogram of zeta potentials. (a) Flight group; (b) synchronous group.

EXPERIMENT K-6-03

PART II: MORPHOLOGY AND HISTOCHEMISTRY OF BONE CELLS AND VASCULATURE OF THE TIBIA FROM COSMOS 1887

S.B. Doty

SUMMARY

Electron microscopy, light microscopy and enzyme histochemistry were used to study the effects of spaceflight on metaphyseal and cortical bone of the rat tibia. Cortical bone showed the most significant changes, which were reflected in changes in the endosteal osteoblast population and the vasculature near the periosteal surface. The osteoblasts demonstrated greater numbers of transitional Golgi vesicles following spaceflight, an effect possibly caused by a decreased cellular metabolic energy source. The vasculature showed accumulations of lipid and adjacent degenerated osteocytes. This result may be due to ischemia of bone or a developing fragility of the vessel walls as a result of spaceflight.

INTRODUCTION

A decrease in new bone formation during spaceflight (Morey and Baylink, 1978) occurs in weight-bearing bones and appears to be due to a reduction in new bone formation rather than increased bone resorption (Wronski and Morey, 1983). Therefore we have concentrated our studys on the bone forming cells, the osteoblasts, and more recently we have begun to investigate the vascular supply within bone matrix. It is the vascular supply which provides all the nutrients for collagen formation, including oxygen for the hydroxylation of proline to form hydroxyproline (Bornstein, 1974; Kruse and Bornstein, 1975), an important step for mature collagen fibril formation.

In a previous study of animals from Spacelab-3, the osteoblasts appeared to be slightly smaller in size following 7 days of flight (Wronski, et al, 1987). These osteoblasts were found along the endosteal surface of the diaphyseal bone and tended to have a more uniform size as compared to osteoblasts along trabeculae in the metaphyseal region of the long bones. Therefore we have concentrated much of our efforts on the cells found within the diaphyseal area of long bones following flight in Cosmos 1887.

Because the animals from spaceflight cannot undergo any experimental procedures while in space, we have applied electron and light microscopic and morphometric procedures to bone samples collected following spaceflight. We have applied histochemistry to enzyme activity along cell membranes (ie, alkaline phosphatase distribution), within various Golgi compartment (ie, NADPase and acid phosphatase) and within the lysosomal bodies (ie, acid lipid accumulation occurs in bone sites as a result of spaceflight [Jee, et al, 1983]). However lipid also accumulates in bone as a result of ischemia (Chryssanthou, 1978). Therefore we have begun to apply methods to localize lipid deposits in bone. And the relationships between vascular morphology, lipid accumulation, and osteocyte and osteoblast morphology have been studied in the weight-bearing long bones.

METHODS

These methods have been discussed in great detail previously (Doty, 1971; 1980). Tissue fixation was limited to the use of 2% paraformaldehyde plus 0.5% glutaraldehyde in 0.05M cacodylate buffer, pH 7.4, at 4°C for 18-24 hours. For histochemical purposes the tissues were decalcified in

PRECEDING PAGE BLANK NOT FILMED

Tris buffered 10% EDTA, pH 7.4, following the aldehyde fixation. Following fixation and decalcification, 50µm thick selections were obtained with a vibratome, and sections incubated in the various media for alkaline or acid phosphatase, or NADPase (Smith, 1980). Tissues were embedded in LR White resin for light microscopy or Spurrs resin for electron microscopy. Staining for lipids was carried out on frozen sections of aldehyde fixed tissues or on vibrotome sections which were subsequently embedded material was thin sectioned and observed with a JOEL 100C microscope. Morphometry was carried out on light or electron micrographs using the Zeiss Interactive Data Analaysis System (ZIDAS). This system uses a dedicated computor and a hand held light pen to quantitate structures, determine areas, etc.

RESULTS

Light microscopy of trabecular and cortical bone and the included osteoblast populations showed no obvious morphological differences as a result of spaceflight. Attempts to quantitate osteoblast size were abandoned because of the extreme variation in cell size even within control groups. Thus any potential difference was hidden within the statistical variation. Initial data does indicate that, in the endosteal diaphyseal osteoblast population, osteoblast cell numbers were decreased by about 15%. Whether the variability reflects postexperiment changes or is the normal physiological state is not known. These measurements will have to be varified by the use of many more tissue sections before the stastics can be considered reliable.

Blood vessels within normal diaphyseal bone showed a typical appearance of endothelial cells enclosing a large open lumen. The endothelium was surrounded by pericytes and some undifferentiated cells (Figure 1). In large vascular spaces the undifferentiated cells were often replaced by osteoblasts and new bone formation was evident.

In diaphyseal bone from flight animals, blood vessels near the periosteal surface often showed very dense intraluminal deposits (Figures 2 & 3). The control tissues occasionally showed a similar pattern but in these instances a packing of intact red blood cells could be seen in the lumen. The deposits within blood vessels from flight animals showed no recognizable cell structure and were not red blood cells. In addition, near these vessels, darkly staining osteocytes were found. This unusual arrangement of intraluminal deposits and adjacent degenerating osteocytes were only seen along the periosteal portion of cortical bone.

Electron microscopy indicated rather normal morphology of the bone cells in the metaphyseal regions. In the diaphysis, the endosteal osteoblasts showed considerable variation in size, but no specific morphological change. The structural aspects of these osteoblasts were normal. In the periosteal region, however, many osteocytic lacunae were found devoid of osteocytes and sometimes filled with an osmiophilic substance (Figure 4). The blood vessels in this region showed endothelial cell disruption and lipid accumulations within the lumen of the vessels (Figure 5). In some cases there was cell debris within the lumen rather than lipid deposits but the degeneration of the vascular wall was evident. It was also apparent by electron microscopy that these osteocytic and vascular changes were confined to the periosteal portion of the diaphyseal bone. These results were never found in the metaphyseal region of the long bones.

The histochemistry of the NADPase activity indicated that this enzyme was localized to the intermediate Golgi saccules of the osteoblast and to the small vesicles and granules within the Golgi complex (Figure 6). All osteoblasts contained such activity within their Golgi regardless whether they were from flight or control animals. A quantitative count of the saccules and small vesicles associated with the Golgi showed that the number of saccules containing reaction product was similar for flight and control osteoblasts. Flight animals contained reactive saccules which averaged 11.3±6.1 saccules per cell, and the vivarium controls averaged 14.4±3.4 saccules per cell which contained reaction product. However when we counted the small vesicles (the transitory or intermediate vesicles) which bud off the saccules and which also contained NADPase activity, the

flight animals averaged 17.0±6.2 vesicles compared to the control average of 10.5±2.7. These reactive vesicles were found only in the Golgi region and are not found in any other area of the cytoplasm.

The histochemistry of alkaline phosphatase activity showed that the osteoblasts contained very high enzyme content along the external surface of the cell membrane (Figure 7). On very rare occasions, activity was also found within the large Golgi saccules prior to forming a secretory granule. Alkaline phosphatase activity was quite strong in the osteoblasts of the metaphyseal region such that we could not distinguish any differences in staining between flight and control animals. However in the diaphysis there was definite decrease in alkaline phosphatase associated with the vascular channels within diaphyseal bone. The vasculature of the flight animals were definitely less reactive than the control groups. This reaction was not limited to the osteoblasts within the vascular channels since the endothelial cells of the blood vessels also contained alkaline phosphatase activity (Figure 8). Therefore at the light microscope level of observation, the alkaline phosphatase activity associated with the vascular space is a combination of reactions from endothelial cells and perivascular cells.

The alkaline phosphatase activity in the blood vessels of bone was located along the basement membrane surrounding the endothelial cells, and along adjacent cells (Figure 8). The pericytes and non-osteoblastic cells associated with the vessel were surrounded with alkaline phosphatase activity as were the osteoblasts adjacent to the vessels but aligned along the bone surface. In the flight animals, the alkaline phosphatase activity was significantly lessened compared to controls (Figures 9 & 10) around the vascular endothelium, and often appeared as an incomplete line of reaction compared to the complete reaction found in the controls.

In order to determine whether the vascular channels themselves had been affected by flight, we measured the area of these space in diaphyseal bone. The data collected shows that for flight animals, the average area of each vascular space was $762\pm157\mu^2$ whereas the same measurement in the simulated control group was $921\pm267\mu^2$. The difference was not highly significant because of the large standard deviation but does suggest that the vascular spaces were smaller within the diaphyseal bone of the flight animals. Measurements made of the numbers of vessels per area of bone also showed a difference:

Flight = 72.3±6.8 vessels per mm^2 of bone area.
Simulated controls = 49.0±8.8 vessels per mm^2 of bone area.

These results would indicate that more vascular space per area of bone existed in flight animals as compared to the simulated controls.

DISCUSSION

The decrease in new bone formation due to spaceflight has been documented (Morey and Baylink, 1978; Wronski and Morey, 1983) and most results suggest that the effect is on the bone forming cells, the osteoblasts. Bone resorption in weight-bearing bones appears to be functioning normally during hypogravity exposure (Vico, et al, 1987). Therefore the osteoblast has been the bone cell of interest for determining the effect of gravity on the skeleton. In addition, other studies have indicated that bone strength in reduced (Spengler, et al, 1983) and that a redistribution of bone crystal sizes occurs (Simmons, et al, 1986) as a result of spaceflight. So the structural integrity of the weight-bearing bone has been compromised in the hypogravity environment.

In our studies of the osteoblast cell size, the measurements were quite variable in different areas of the bone. Thus, these measurements were not usefull in this study. Similar measurements from osteoblasts flown on Spacelab-3 showed only about a 10% decrease in cell size following 8 days

of flight (Wronski, et al, 1987). These variations in size are also reflected in the alkaline phosphatase activity because the cells which are larger and more differentiated tend to have greater phosphatase activity (Doty, 1980). Therefore the large variation in cell size also produced considerable variation in alkaline phosphatase histochemistry. With careful timing of the appearance of the reaction product, it was estimated that the osteoblasts from the flight animals showed less reactivity than the various controls (data not shown) but the data were not always consistent. These observations were limited to the osteoblasts along the endosteal surface of the cortical bone.

The histochemical NADPase reaction has been used to study the activity of the intermediate saccules of the Golgi in ameloblasts (Smith, 1980). Because the Golgi saccules and the transitional vesicles were so specifically stained by the NADPase reaction, and are directly involved in collagen synthesis and secretion, we quantitated these structures in osteoblasts. The appearance of increased numbers of vesicles in cells from flight animals compared to controls was unexpected in that collagen synthesis must be altered during the reduced new bone formation induced by flight (Morey and Baylink, 1978; Wronski and Morey, 1983). However in other non-bone cell types, these vesicles have been shown to accumulate whenever the energy sources of the cell have been depleted (Saraste, et al, 1986). It is also interesting that in osteogenesis imperfecta, a collagen deficient disease of bone, we previously noted that these vesicles were present in unusually large numbers (Doty and Mathews, 1971). Thus the present data may be used to suggest that the condition of space flight creates an energy loss within the osteoblast and this could lead to reduced collagen synthesis. However, postflight readaptation complicates interpretation of these data.

The other area of bone physiology which appears greatly affected by spaceflight is the vasculature within bone matrix. In an earlier histochemistry study we showed that the blood vessels in bone contain a calcium-stimulated ATPase activity (Doty, 1985). The present study shows that there is a strong alkaline phosphatase activity as well, located between the endothelial cells and the pericytes and includes the basement membrane between the cells. However, as a result of space flight this activity was decreased. We cannot apply the calcium stimulated ATPase staining to samples from space because the enzyme is destroyed by the chemical fixation process, however it would be important to know if this activity is also reduced due to the hypogravity environment. Nevertheless these histochemical results indicate that the vessels within bone matrix contain enzyme activities which could be important in regulating ion transport between serum and bone matrix.

It was noted in this study that many of the vessels near the periosteal surface contained lipid inclusions and/or morphological signs of endothelial degeneration. Lipids can result in necrosis of bone (Jones, 1985) although the exact mechanism is unknown. Ischemia may also cause cell death and degeneration (Chryssanthou, 1978) and may occur with or without the appearance of lipid accumulation. So whether ischemia in bone and the presence of lipid are related events is not known at this time.

It was noteworthy that the vessels and osteocytes near the periosteal surface were most affected by space flight, as the periosteal surface receives less oxygenated blood than the bone next to marrow cavity (Lopez-Curto, et al, 1980).

We also noted that the vasculature cross-sections were more numerous in the compact bone from flight animals, even though the average cross sectional area per vessel was smaller than in the control bones. This smaller size could also be a factor in lipid being "trapped" within some of these vessels. And the increase in numbers of vessels may indicate a slower turnover of the whole skeleton, therefore not as much bone is produced between vessels during bone growth.

We have not determined whether a single factor is responsible for the decrease in bone formation as a result of hypogravity. But the evidence presented here would suggest that a vascular change may occur during flight which would then influence the bone forming ability of the osteoblasts in the weight-bearing bones. It is also possible however, that the vascular damage noted here could occur as an injury received to these fragile vessels during the impact and hypergravity forces of re-entry from space or during recovery following spaceflight. This possibility has not been investigated but needs to be considered for study in future space flights.

REFERENCES

1. Bornstein, P. The Biosynthesis of Collagen. Ann. Rev. Biochem. 43: 567-603, 1974.

2. Chryssanthou, C.P. Dysbaric Osteonecrosis. Clin. Orthop. Rel. Res. 130:94-106, 1978.

3. Doty, S.B. Histochemical Investigations of Secretory Activity in the Osteoblast. In: Third International Workshop on Bone Histomorpho-metry. W.S.S. Jee and A.M. Parfitt, editors; Sun Valley, Idaho, pp.201-206,1980.

4. Doty, S.B. Localization of Calcium Stimulated Adenosine Triphospha-tase Activity in Blood Vessels of the Skeleton. Physiologist. 28: S125,1985.

5. Doty, S.B. and R. Mathews. Electron Microscopy and Histochemical Studies of Osteogenesis Imperfecta. Clin. Orthop. Rel. Res. 80:191-200, 1971.

6. Jee, W.S.S., T.J. Wronski, E.R.Morey, and D.B. Kimmel. Effects of Spaceflight on Trabecular Bone in Rats. Am. J. Physiol. 244: R310-314, 1983.

7. Jones, J.P. : Rat Embolism and Osteonecrosis. Orthop. Clinics N. Am. 16:515-633, 1985.

8. Kruse, N.J. and P. Bornstein. Metabolic Requirements for Trans-cellular Movement and Secretion of Collagen. J. Biol. Chem. 250:4841-4847, 1975.

9. Lopez-Curto, J.A., J.B. Bassingthwaighte, and P.J.Kelly. Anatomy of the Microvasculature of the Tibial Diaphysis of the Adult Dog. J. Bone Jt. Surg. 62A: 1362-1369, 1980.

10. Morey, E.R. and D.J. Baylink. Inhibition of Bone Formation During Spaceflight. Science. 201:1138-1141, 1978.

11. Saraste, J., G.E. Palade, and M.G. Farquhar. Temperature-sensitive Steps in the Transport of Secretory Proteins Through the Golgi Complex in Exocrine Pancreatic Cells. Proc. Natl. Acad. Sci. 83:6425-6429, 1986.

12. Simmons, D.J., J.E. Russell, and M.D. Grynpas. Bone Maturation and the Quality of Bone Mineral in Rats Flown on the Space Shuttle "Spacelab-3 Mission". Bone Mineral. 1: 485-493, 1986.

13. Smith, C.E. : Ultrastructural Localization of Nicotinamide Adenine Dinucleotide Phosphatase (NADPase) Activity to the Intermediate Saccules of the Golgi Apparatus in Rat Incisor Ameloblasts. J. Histochem. Cytochem. 28:16-26, 1980.

14. Spengler, D.M., E.R.Morey, D.R. Carter, R.T. Turner, and D.J. Baylink. Effects of Spaceflight on Structural and Material Strength of Growing Bone. Proc.Soc.Exptl.Biol.Med. 174: 224-228, 1983.

15. Vico, L., D. Chappard, C. Alexandre, S. Palle, P. Minaire, G. Riffat, V.E. Novikov, and A.B. Bakulin. Effects of Weightlessness on Bone Mass and Osteoclast Number in Pregnant Rats after a Five Day Spaceflight (Cosmos 1514). Bone. 8:95-103, 1987.

16. Wronski, T.J. and E.R. Morey. Effect of Spaceflight on Periosteal Bone Formation in Rats. Am. J. Physiol. 224: R305-R309, 1983.

17. Wronski, T.J., E.R. Morey-Holton, S.B.Doty, A.C. Maese, and C.C. Walsh Histomorphometric Analysis of Rat Skeleton Following Space- flight. Am. J. Physiol. 252: R252-R 255, 1987.

Figure 1. An electron micrograph of a normal blood vessel within diaphyseal bone. Thin walled endothelial cells (arrows) surround an open lumen which contains two macrophages (MP). Perivascular or pericytic cells (PC) are situated between the endothelium and the bone matrix. An osteocyte (OC) is located in bone matrix adjacent to the vascular space. The bone matrix has been demineralized. Magnification = 5,600 X

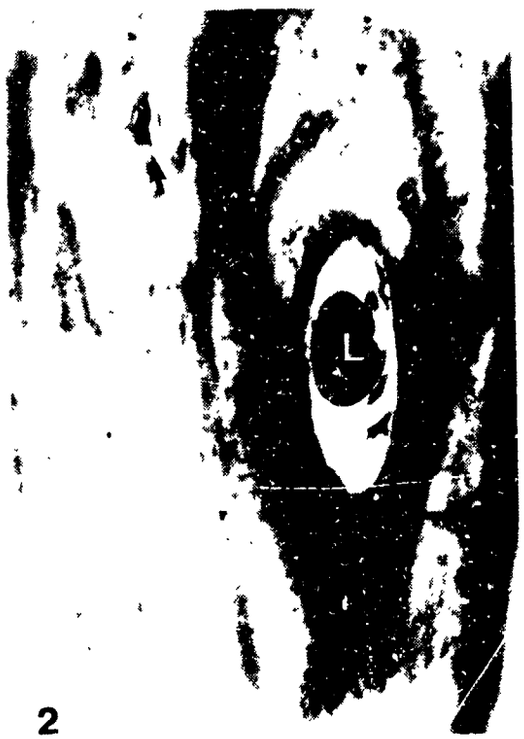

Figure 2. A light micrograph of a vascular space in bone filled with a large lipid (L) inclusion. Osteocytes are present in nearby matrix (arrows). This sample is from the diaphysis of a "flight" animal. Magnification = 1,200 X

Figure 3. A light micrograph of a normal vascular space from the tibia of a vivarium control rat. The lumen (L) of the vessel and the endothelial cells (arrows) can be seen; no lipid deposits are present. Magnification = 1,200 X

Figure 4. This electron micrograph shows a portion of the vascular space (VS) and an osteocyte (OC) from the periosteal region of a "flight" animal. Both structures are darkly stained and structurally degenerate, suggesting either a lipid accumulation or cell death. Magnification = 9,200 X

Figure 5. This electron micrograph shows the large lipid (L) inclusion which are found within the vascular spaces in diaphyseal vessels of the "flight" animals. Some structures resemble the remains of vascular endothelial cells (arrows) which have undergone degeneration. Magnification = 18,000 X

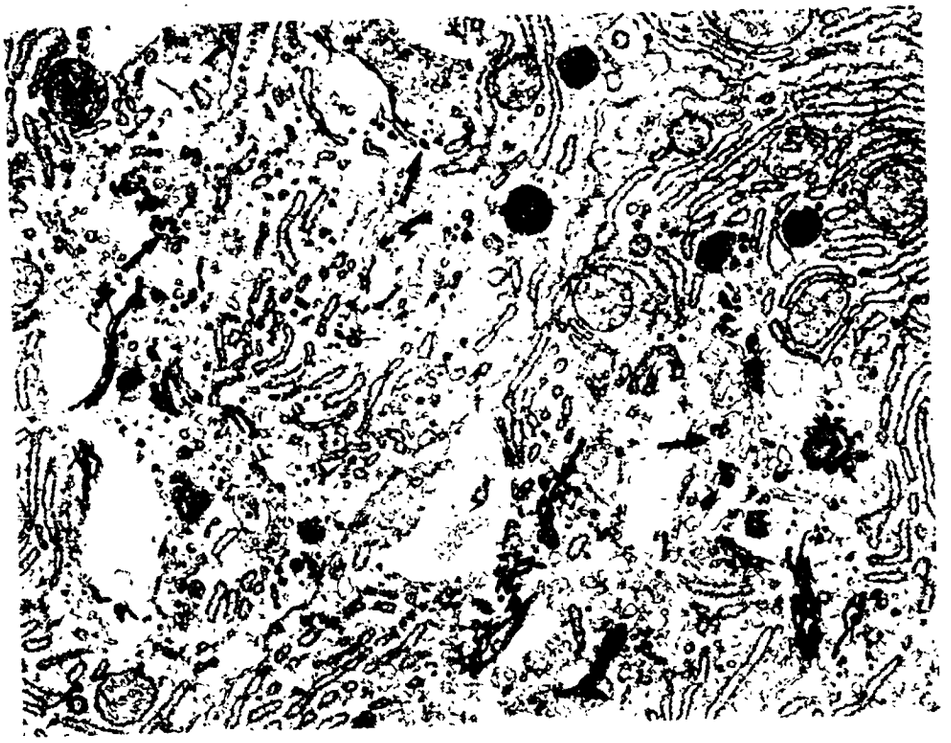

Figure 6. An electron micrograph of the Golgi region of a single osteoblast which has reacted for NADPase activity. The small transitory vesicles (arrows) were found to be more numerous in osteoblasts from "flight" animals. Magnification = 16,000 X

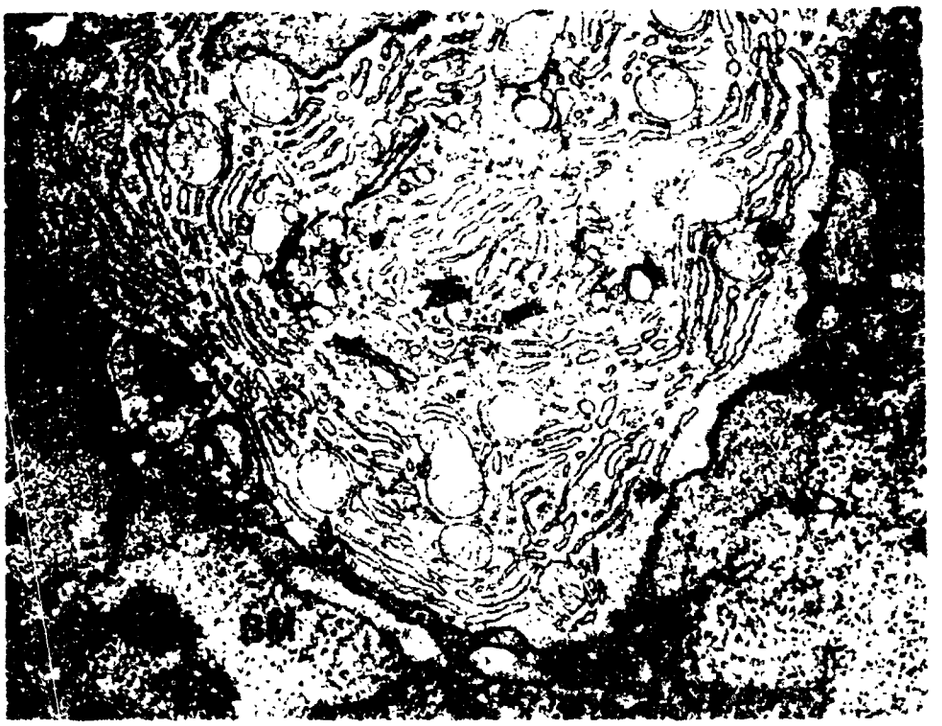

Figure 7. An electron micrograph which shows the alkaline phosphatase reaction (arrows) along the external cell membrane of a single osteoblast. Enzyme reaction can also be seen in the underlying bone matrix (BM). Magnification = 16,000 X

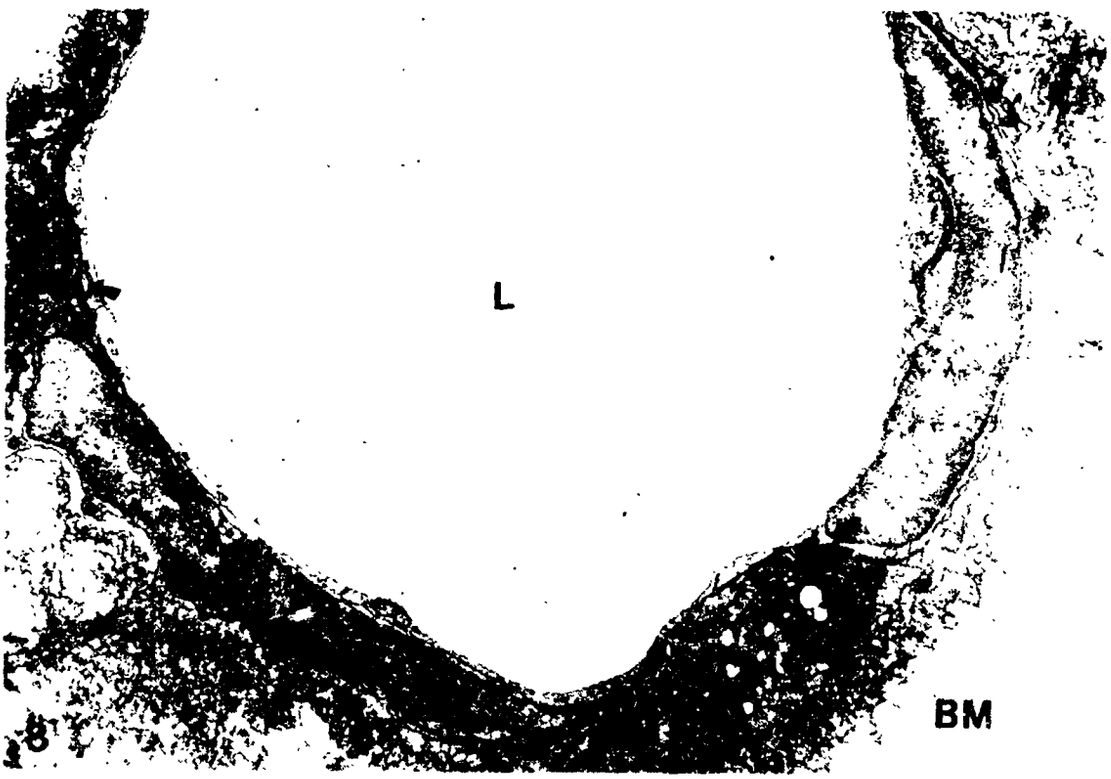

Figure 8. An electron micrograph of the alkaline phosphatase activity (arrows) distributed among the endothelial cells and pericytes of a blood vessel in bone. L = lumen of blood vessel; BM = demineralized bone matrix; Magnification = 10,000 X

Figure 9. A light micrograph showing the alkaline phosphatase reaction (arrows) among the blood vessels of normal bone. BM = bone matrix. Magnification = 700 X

Figure 10. A preparation identical to Figure 9, except the bone is from a "flight" animal. Note that the intensity of the reaction is less than the control and some areas (arrows) show a definite reduction or loss of enzyme activity. Magnification = 700 X

EXPERIMENT K-6-03

PART III: NUCLEAR VOLUME ANALYSIS OF OSTEOBLAST HISTOGENESIS IN PERIODONTAL LIGAMENT CELLS OF COSMOS 1887 RATS

L.P. Garetto, W. Eugene Roberts, and M. R. Gonsalves

SUMMARY

Periodontal ligament (**PDL**), the osteogenic interface between tooth and bone, was morphometrically analyzed in rats subjected to 12.5 days of weightlessness and a ~55h recovery period at 1 G. Compared to synchronous controls, this treatment resulted in a 40% decrease in less differentiated osteoblast progenitor cells, a 42% increase in preosteoblasts (immediate precursors to osteoblasts) and increased numbers of **PDL** fibroblast-like cells within 25μm of the bone surface. These results are consistent with a post-flight osteogenic response in **PDL** adjacent to previously resting or resorbing alveolar bone surfaces. This osteogenic response occurred despite physiological stress in the flight animals that resulted in a highly significant ($p \geq 0.001$) increase in adrenal weight. The data suggest that following spaceflight there is a strong and rapid recovery mechanism for osteoblast differentiation that is not suppressed by physiological stress.

INTRODUCTION

Bone is a mechanically sensitive tissue that is particularly responsive to gravitational factors. An understanding of changes in bone mass is important since it functions not only as a structural support, but also as a metabolic source of calcium (Morey-Holton *et al.*, 1988). Previous studies have shown that microgravity associated with spaceflight results in marked musculoskeletal changes including muscle atrophy (Riley *et al.*, 1985) and suppression of bone formation (Morey *et al.*, 1978). The reduction in bone formation appears to occur as a generalized, systemic phenomenon since both the weightbearing axial skeleton (Jee *et al.*, 1983) and non-weightbearing bones (Simmons *et al.*, 1983) are similarly affected.

At least one aspect of the suppression of bone formation during spaceflight is an inhibition of osteoblast production (Roberts *et al.*, 1981; Roberts *et al.*, 1987). The periodontal ligament (**PDL**), a well defined cell kinetic model for assessing the proliferation and differentiation of the cells associated with osteoblast histogenesis (Roberts *et al.*, 1981), was used to study the effect of microgravity on osteoblast production. Roberts and Morey (1985) have identified distinct, fibroblast-like, cellular compartments within the **PDL** that comprise progressively more differentiated osteoblast precursor cells. These compartments have been classified as 1) **A**, less-differentiated, self-perpetuating precursor cells; 2) **A'**, committed osteoprogenitors that are derived from **A** cells and are the source of preosteoblasts; 3) **C**, G_1 stage preosteoblasts; and 4) **D**, G_2 stage preosteoblasts which undergo mitosis and form mature osteoblasts as shown in Figure 1.

Previous spaceflight data has suggested that the population of the less differentiated osteoblast progenitor cells (**A+A'**) increases (Roberts *et al.*, 1981; Roberts *et al.*, 1987) while the number of preosteoblast cell types (**C+D**) is reduced (Roberts *et al.*, 1987). Recovery of osteoblast precursor differentiation following spaceflight has been sparsely investigated. Analysis of rat **PDL** from the Cosmos 1129 flight revealed that all cell populations were identical to synchronous control animals by 6 d post-flight and remained so at 29 d post-flight (Roberts *et al.*, 1981). Twelve hours following the landing of the 7 d, Space Lab-3 (**SL-3**) flight, there were no residual changes in the

 PRECEDING PAGE BLANK NOT FILMED

cell population of young rats; the only significant difference was an increase in the A+A' category of older animals. Assuming 7 d of spaceflight is sufficient to suppress osteoblast differentiation, these data suggest that 12 h of recovery at 1 G is sufficient to return the osteogenic compartments to near normal.

The present study of the **PDL** from the Cosmos 1187 flight allows evaluation of 12.5 Days of spaceflight and 55 h of recovery under somewhat stressful conditions. The data indicate that a return to normal gravity resulted in a very strong compensatory replenishment of osteogenic capacity that occurred despite post-flight physiological stresses.

METHODS

Ten male (specific pathogen free) Czechoslovakian-Wistar rats were housed in a single cage aboard the Cosmos 1887 satellite. A paste diet was provided in 14g boluses at 0200, 0800, 1400, 2000h each day through ten nozzles in the cage. Water was provided *ad lib* via ten lixits. The rats were maintained on a light cycle with the lights on from 0800-2400 h. The flight group (F; born 7/1/87) was launched on 9/29/87 and remained in space until 10/12/87. The total duration of the microgravity environment was 12.5d (Fig. 2). Rats were last fed in flight on 10/12/87 at 0200 h but due to difficulties upon re-entry were not fed again until 42 h later, which was approximately 11-13h prior to sacrifice. As a result of the re-entry problems and distant landing location in Siberia, the animals were subjected not only to disruption of their feeding schedule, but also disruption of the light cycle and a decreased capsule temperature. Furthermore, it was necessary to transport the animals for about 10h by bus, airplane and van to reach the sacrifice/dissection area. Because of these post-flight recovery problems, sacrifice (at 105d of age) was delayed a total of~53-55h following re-exposure to 1 G.

Three groups of rats were used as controls for the flight animals (Fig. 2). Ten basal controls rats were housed in similar cages and placed on a paste diet for 14d with sacrifice occurring 5d prior to the actual flight (at 85d of age). The temperature and lighting conditions were maintained similar to the inflight conditions. An equal number of animals served as vivarium controls (108d of age at sacrifice). These rats were kept in similar environmental conditions to the flight animals, but were fed all of their food at a single feeding. Finally, a synchronous control (S) group (10 rats) was maintained in flight-type cages on a paste diet. These rats were subjected to similar launch forces, vibration, lighting regimen and temperature as flight rats. After their simulated flight, the S group was deprived of food for 42h and their sacrifice was delayed for 53-55h to mimic the F group conditions. Re-entry G forces, vibration and post-flight transportation conditions were not simulated for this group. Synchronous controls were sacrificed 6d after flight animals and were 111d of age.

At sacrifice, the maxillae from five animals in each group were removed and immersed in neutral buffered formalin for 48h at 4°C. Fresh fixative was added and the samples were maintained at 4°C during shipment to the NASA Ames Research Center, Moffett Field, CA. The samples were prepared for demineralized histological sectioning in the midsagittal plane of the mesial root of the first molar. Details of the histological methods are published (Roberts *et al.*, 1987). Briefly, 3µm sections of methyl methacrylate embedded maxillary halves were stained with hematoxylin and eosin. Nuclear volume analysis of the cells in the midroot area of the **PDL** was performed as described by (Roberts *et al.*, 1982). Only **PDL** samples with a resorbing (scalloped with occasional osteoclasts) or resting (no morphological evidence of active resorption or formation) alveolar bone margin were selected for analysis. At some point during transport or storage prior to reaching the authors' laboratory, the samples appear to have been frozen, resulting in varying degrees of artifact within the tissue. Because of this, only four animals from each group could be evaluated. It was necessary to select areas within the **PDL** where cells were not morphologically disrupted. Following ocular micrometer measurement of the major (a) and minor (b) nuclear dimensions at x1000, the nuclear volume for the cells were calculated as previously described

(Roberts *et al.*, 1982) according to the formula for a prolate spheroid: Volume = $4/3\pi ab^2$. Each cell was classified as **L, A+A', B, C,** or **D** type according to the following nuclear size categories : <40, 40-79, 80-119, 120-169 and ≥170μm^3, respectively (Roberts *et al.*, 1985). Data from each category is expressed as group means ± SE. Statistical analysis of differences between groups was performed using the two-tailed Student t-test with $p \leq 0.05$ considered as statistically significant.

RESULTS

Body Weights. At sacrifice, the body weight (mean±SE) of the animals in the flight group (302.2±2.4g) was significantly less than that for vivarium (342.0±7.7g) and synchronous controls (349.0±5 g). The terminal weight of the basal controls (316.0 ± 8.3 g) was significantly lower than the synchronous controls and reached a near statistical difference from the vivarium group. The effect of the ~42h of fasting on the synchronous control and flight groups was not measured.

Cell Population Kinetics. A comparison of the **PDL** cell populations from the three control groups showed significant differences in only the **L** and **A+A'** categories (Fig. 3). The basal control rats had fewer **A+A'** cells than did both the synchronous and vivarium controls. Although the sample of **L**-type cells was small (< 10% of the population), the synchronous control group had nearly twice the number of these cells compared to any other group. Because the environment and handling of the synchronous control group most closely simulated that of the flight group, all further comparisons were made between these two groups.

Spaceflight followed by a ~55 h recovery period resulted in a 40% decrease in the **A+A'** cell population (**F**-17.75±2.53 vs. **S**-29.25±3.17; $p \leq 0.05$)and a 42% increase in the **C+D** cells (**F**-50.26±4.09 vs. **S**-31.25± 3.35; $p \leq 0.05$) compared to synchronous controls (Fig. 4). The increase in the **C+D** cell category was significant primarily because of the **D** cell population. The mean of the flight group **C** cell population tended to be higher that its corresponding control but did not reach statistical significance. The total cell density of fibroblast-like cells along the **PDL**/bone interface was also increased by 39% (**F**-0.24±0.01 vs. **S**-0.14 ±0.02 cells/100μm; $p \leq 0.05$) in the flight group compared to synchronous controls (Fig. 5). The differences in the flight group occurred despite a degree of physiological stress that was highly significant compared to synchronous controls, as indicated by the increased adrenal weights in the flight animals (Fig. 6). The adrenal weights of the flight animals were higher than that of the control group despite the reduced body weights in the flight group.

DISCUSSION

Previous spaceflight data have demonstrated that microgravity induces a block in the **A' --> C** conversion (a mechanical-stress dependent step) of osteoblast histogenesis (Roberts *et al.*, 1981). This block results in an increase in the **A+A'** cells and a decrease in the more differentiated **C+D** cells. Assuming a similar flight effect, results from the analysis of **PDL** in rats flown on Cosmos 1187 show that a recovery of preosteoblast formation occurred within ~55h following return to a 1 G environment. **L** cells are a subclassification of fibroblast-like cells with very small nuclei. This type cell is commonly seen lining inactive surfaces of trabecular bone. The significance of this population of cells in **PDL** is unknown. Unfortunately, the increase numbers of **L** cells in synchronous controls is uninterpretable at this time.

There has been little opportunity, however, to study recovery from the effects of microgravity. The length of time needed to restore osteoblast histogenesis following spaceflight is not known. Young rats flown on **SL-3** apparently recovered their ability to form preosteoblasts within 12h after returning from 7d of spaceflight. However, older rats on the same mission still exhibited a significant increase in the **A+A'** cell compartment suggesting an age related delay in recovery of

osteogenic differentiation (Roberts *et al.*, 1987). In contrast, numbers of osteoblast precursor cells in **PDL** of rats flown for 18.5d aboard Cosmos 1129 were recovered 6d after return to earth (Roberts *et al.*, 1981). In the present study, the large increase in **C+D** cells and the decrease in the **A+A'** cells at ~55h post-flight indicate that return to 1 G strongly stimulated the osteogenic activity of the **PDL** following 12.5d in space.

The strong post-flight recovery of preosteoblast differentiation (Fig. 4) is similar to the osteogenic response when **PDL** is subjected to orthodontic force (Roberts *et al.*, 1982). Placement of a 0.5mm latex elastic between the maxillary first and second molars induces a stimulation of differentiation in the osteogenic cells of the area studied in the **PDL**. Cell kinetic data following orthodontic stimulus shows a burst in differentiation of preosteoblasts (i.e. an increase in **C+D** cells) at 10h after insertion of the latex elastic. A second wave of preosteoblast formation occurs 40 h later, at approximately 50h post orthodontic stimulus (Roberts *et al.*, 1982).

With respect to the present study, it follows that the increase in the **C+D** cells seen ~55 h after spaceflight is probably the second wave of preosteoblast differentiation stimulated by return to a 1 G environ-ment. Support for this conclusion is the significant increase in cell density at the alveolar bone surface of the **PDL**. Roberts and Chase (1981) previously reported similar kinetics of cell migration toward the bone surface during osteogenic induction. The decrease in **A + A'**, and increase in **C + D** cells and increase in cell density at the bone surface suggest a strong osteogenic response in **PDL** post-flight. The strength of the osteogenic recovery following spaceflight is striking. It persists despite an array of physiological stresses endured by flight animals following return to .. Physiological stress is thought to result in a increase in the less differentiated osteoblast progenitor cells (**A+A'**) and a decrease in the more differentiated precursor cells (**C+D**; Fielder *et al.*, 1986); i.e. a pattern opposite to that presently observed.

Physiological stress was probably a contributing factor to the considerable difference in weights between the flight and synchronous control groups. A similar effect of spaceflight was seen in the data from the Cosmos 1129 flight. Flight animals sacrificed 6d following re-entry actually lost weight during this period (Wronski *et al.*, 1981) The inability of the flight rats to regain weight at the same rate as the synchronous controls may be associated with physiological stress during spaceflight, and upon return to a gravitational environment. Stresses such as the disruption of the circadian light cycle, wide fluctuations in capsule temperature and the lack of food for 42h post-flight are expected to reduce preosteoblast production. Enhanced osteoblast histogenesis under stressful conditions post-flight highlights the strength of the compensatory recovery of osteoblast histogenesis.

The three control groups had significant differences in only the **L** and **A+A'** cell categories (Fig. 3). These data are difficult to interpret because the basal control rats were about 3wk younger at sacrifice than animals in the other control groups. The synchronous control group was subjected to conditions intended to simulate the physiological stresses endured by the flight group except for the reentry G forces and post-flight transportation conditions. While not showing statistically significant changes, the differences in this group compared to the other controls was in the direction one would expect for physiologically stressed animals.

The reason for the lack of significant stress effects in cells of **PDL** from synchronous control rats (as judged by the lack of difference in adrenal weights; data not shown) is not clear. These data may mean that flight animals were exposed to a longer duration, more chronic stress, i.e. spaceflight *per se* is stressful. Considering that the flight animals were probably chronically stressed, the persistence of the post-flight osteogenic response was remarkable.

REFERENCES

1. Fielder, P.J., E.R. Morey & W.E. Roberts. Osteoblast histogenesis in periodontal ligament and tibial metaphysis during simulated weightlessness. Aviat. Space Environ. Med. 57: 1125-1130, 1986.

2. Jee, W.S.S., T.J. Wronski, E.R. Morey & D.B. Kimmel. Effects of spaceflight on trabecular bone in rats. Am.J.Physiol. 244: R310-R314, 1983.

3. Morey, E.R. & D.J. Baylink. Inhibition of bone formation during space flight. Science. 210: 1138-1141, 1978.

4. Morey-Holton, E.R. & S.B. Arnaud. Spaceflight and calcium metabolism. Physiologist. 26: S9-S12, 1988.

5. Riley, D.A., S. Ellis, G.R. Slocum, T. Satyanarayana, J.L.W. Bain & F.R. Sedlak. Morphological and biochemical changes in soleus and extensor digitorum longus muscles of rats orbited in Spacelab-3. Physiologist 28: S207-S208, 1985.

6. Roberts, W.E. & D.C. Chase. Kinetics of cell proliferation and migration associated with orthodontically-induced osteogenesis. J. Dent. Res. 60(2): 174-181, 1981.

7. Roberts, W.E., P.J. Fielder, L.M.L. Rosenoer, A.C. Maese, M.R. Gonsalves & E.R. Morey. Nuclear morphometric analysis of osteoblast precursor cells in periodontal ligament, SL-3 rats. Am. J. Physiol. 252: R247-R251, 1987.

8. Roberts, W.E. & E.R. Morey. Proliferation and differentiation sequence of osteoblast histogenesis under physiological conditions in rat periodontal ligament. 174: 105-118, 1985.

9. Roberts, W.E., P.G. Mozsary & E. Klingler. Nuclear size as a cell-kinetic marker for osteoblast differentiation. Am. J. Anat. 165: 373-384, 1982.

10. Roberts, W.E., P.G. Mozsary & E.R. Morey. Suppression of osteoblast differentiation during weightlessness. Physiologist. 24:S75-S76, 1981.

11. Simmons, D.J., J.E. Russell, F. Winter, P. Tran Van, A. Vignery, R. Baron, G.D. Rosenberg & W.V. Walker. Effect of spaceflight on the non-weight bearing bones of rat skeleton. Am. J. Physiol. 244: 319-326, 1983.

12. Wronski, T.J., E. Morey-Holton, C.E. Cann, C.D. Arnaud, D.J. Baylink, R.T.Turner, & Jee, W.S.S. (1981) in *Final Reports of U.S. Rat Experiments Flown on the Soviet Satellite Cosmos 1129* (Heinrich, M.R. & Souza, K.A., eds.), pp. 101-125, NASA Technical Memorandum 81289, Moffett Field, CA.

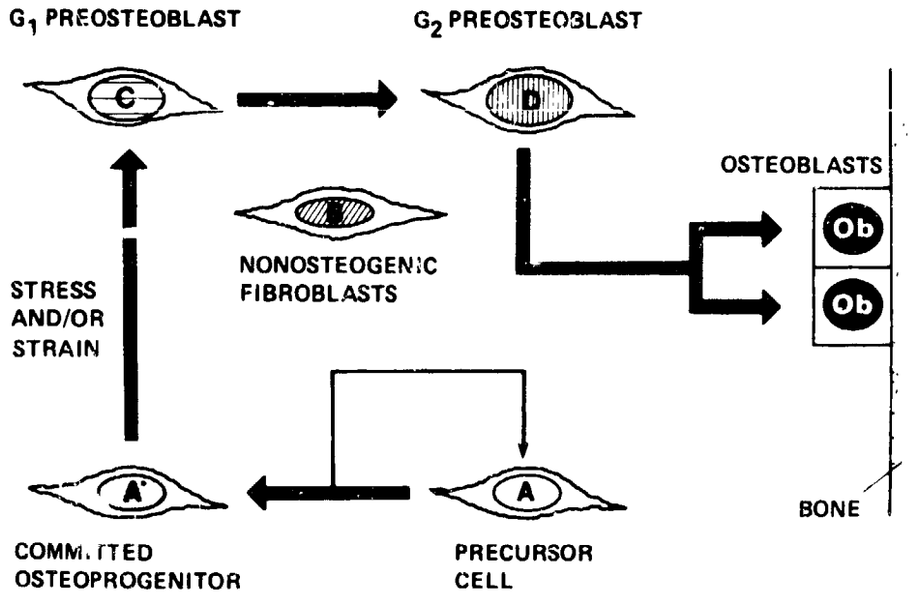

Figure 1. G_1 and G_2 stage preosteoblasts undergo mitosis and form mature osteoblasts.

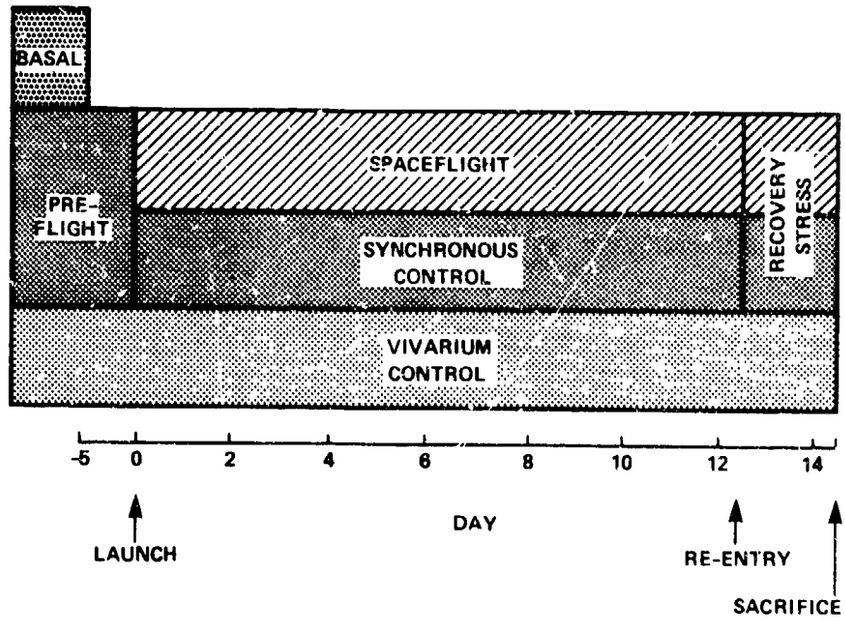

Figure 2. Diagramatic representation of flight and control groups of Cosmos 1887. The basal control group was sacrificed prior to flight. See description in Methods.

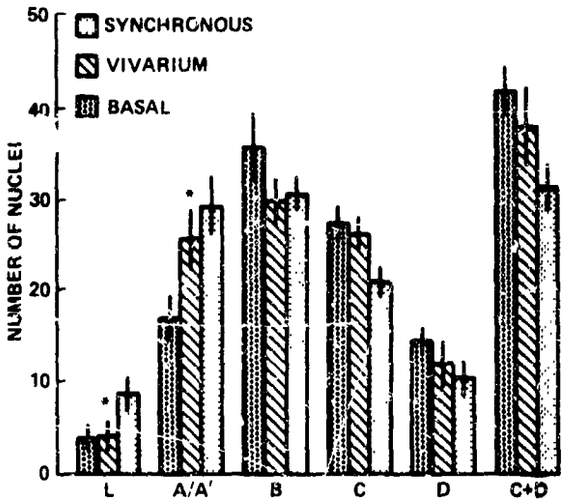

Figure 3. Comparison of control group PDL cell populations. * indicates a significant difference ($p \leq 0.05$).

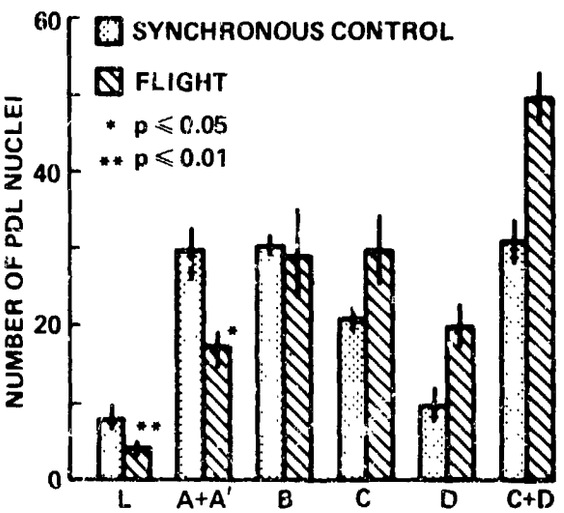

Figure 4. Comparison of synchronous control and flight PDL cell populations.

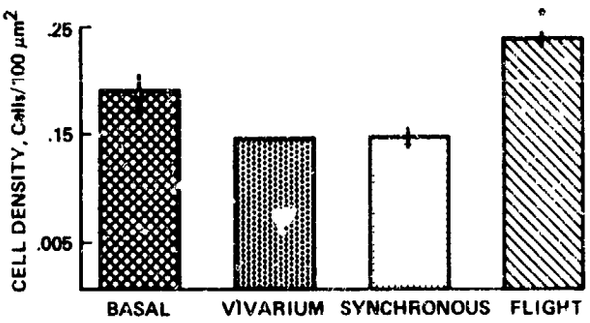

Figure 5. Comparison of the cell densities within 25 μm of the PDL/bone interface. Total nuclei were counted in this region without regard to their size classification. * indicates a difference from the synchronous control group significant at $p \leq 0.01$.

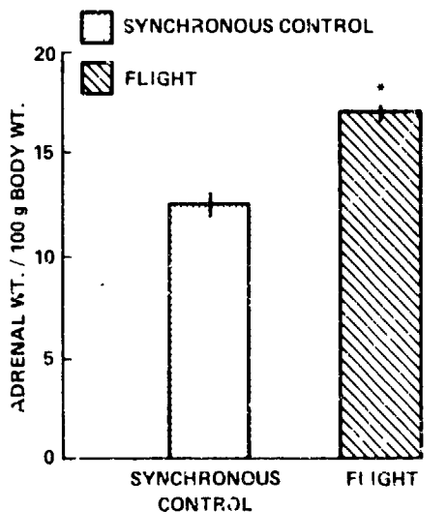

Figure 6. Comparison of adrenal weight/100 g body weight. * indicates a difference from the control group significant at $p \leq 0.001$.

EXPERIMENT K-6-03

PART V: INTERVERTEBRAL DISC SWELLING PRESSURE ASSOCIATED WITH MICROGRAVITY ON COSMOS 1887

A. R. Hargens, S.A. Gott, B. Rydevik, and G. Durnova

SUMMARY

Swelling pressures within discs from Cosmos 1887 rats exposed to 12.5 days of microgravity were compared to those in two groups of ground-based control rats. Swelling pressures were not significantly different between the three groups, probably because rats aboard Cosmos 1887 were re-exposed to normal gravity for over 50 hours prior to tissue harvesting.

INTRODUCTION

The back pain experienced by space travelers during exposure to microgravity may be caused by spinal lengthening due to swelling of their discs, and subsequent stretching of anterior and/or posterior spinal ligaments. This hypothesis may be supported by the observation that the human spine lengthens about 4-6 cm during microgravity (Thornton et al., 1977). To examine fluid movement into discs of animals exposed to actual microgravity, we compared equilibrium swelling pressure of nucleus pulposus from rats exposed to 12 days of microgravity to that of two groups of ground-based control rats. Recently, we developed a new compression-type osmometer that allows direct measurement of nucleus pulposus swelling pressure in samples as small as 5-10 mm^3 (Glover, et al., 1987) Subsequently, we determined that these swelling pressures depend on environmental conditions and species (Gott, et al., 1987, Gott, et al., 1988). Other work has documented that pooling of lumbar discs from the rat spine allows sufficient disc material for direct measurement of swelling pressure in this species (Gott, unpublished observations). Therefore, studies of Cosmos rats allowed testing of the hypothesis that microgravity causes fluid uptake and decreased swelling pressure within the intervertebral disc of flight rats as compared to ground-based, control rats.

METHODS

Isolated spines were frozen and transported to NASA-Ames Research Center. Lumbar discs were incised by scalpel and nucleus pulposus was pooled for direct measurement of equilibrium swelling pressure for each rat. Data from each group (flight group versus two groups of ground controls) were compared using paired t tests. Statistical significance was set at $p < .05$. All measurements were completed within ten days after we received the isolated spines.

RESULTS

No significant differences were found in the swelling pressures between the flight and control groups of rat nucleus pulposus. Swelling pressures ranged between 622 to 690 mmHg (Table 1).

DISCUSSION

Because of the extended period between the time that the flight rats returned to Earth and the time of death (53-56 hours), we conclude that the flight animals already were fully readapted to normal gravity in terms of fluid movement into and out of their intervertebral discs. We hope that we will

be given an opportunity to participate in tissue analysis of future Cosmos missions so that our hypothesis can be resolved definitively.

ACKNOWLEDGEMENT

We thank Dr. R. Grindeland, Dr. L. Keil, Marilyn Vasques, Mike Skidmore and Juli Evans for transporting the samples safely to us and we thank the superb Cosmos Dissection Team for their assistance.

REFERENCES

1. Glover, M.G., A.R. Hargens, S.R. Garfin, M.D. Brown and W. H. Akeson. New osmometer for rapid, equiiibrium measurement of swelling pressure of nucleus pulposus. Trans. 33rd Meeting, Orthop. Res.Soc. 12:369, 1987.

2. Gott, S.A., A.R. Hargens, and J. Hulse-Neufeld. Comparative swelling pressures of intervertebral disc nucleus pulposus. 1987 APS Fall Meeting, San Diego, CA., and Physiologist 30:121(5.9), 1987.

3. Gott, S.A., A.R. Hargens, S.R. Garfin, B.L. Rydevik and M.D. Brown. Swelling pressure of nucleus pulposus from herniated and intact human intervertebral discs. Trans.34th Meeting, Orthop.Res.Soc. 13:377, 1988.

4. Thornton, W.E., G.W. Hoffler and J.A. Rummel. Anthropometric changes and fluid shifts. In: Biomedical Results from Skylab, edited by R.S. Johnston and L.F. Dietlein (NASA SP-377),pp. 330-338, 1987.

TABLE 1

COSMOS 1887 RATS

SWELLING PRESSURES OF LUMBAR DISCS
(mm Hg ± S.E.)

Cosmos Flight Rats (N = 5)	690 ± 45
Synchronous Controls (N = 5)	675 ± 32
Vivarium Controls (N = 5)	622 ± 25

No significant difference between groups.

N90-26458

EXPERIMENT K-6-04

TRACE ELEMENT BALANCE IN RATS DURING SPACEFLIGHT

Principal Investigator:

C.E. Cann
Department of Radiology
University of California
San Francisco, California 94143

Co-Investigators:

P. Patterson-Buckendahl
Department of Radiology
University of California
San Francisco, California 94143

G. Durnova
A. Kaplansky
Institute of Biomedical Problems
Moscow, USSR

 PRECEDING PAGE BLANK NOT FILMED

INTRODUCTION

Exposure to microgravity causes alterations in the skeletal and mineral homeostatic systems. Decreased mass of bone can be explained by decreased formation, increased resorption or a combination of processes. Previous investigations have shown that in young growing rats, diaphyseal bone formation is decreased (1). Other evidence shows that bone resorption is also decreased, apparently secondary to a decrease in total body calcium turnover (3); this is evidenced systemically even in the non-weight-bearing bones of the jaw (3). In young rats exposed to only 7 days of flight, however, bone composition was not significantly affected (4). This overall slowing of bone turnover, the dynamics of calcium excretion (2) and differential effects on bone seen in flights of varying duration suggest that, at least in the younger growing rat, a variety of different metabolic processes may be affected in addition to bone formation and resorption.

Little is known about the effects of flight in an older skeleton; limited data suggest that bone resorption is increased after 5 days (5) but no data are available about other metabolic effects. The response of a more slowly-growing skeleton to microgravity may be different than that of a younger animal, similar to the different responses seen in adolescents and adult humans to immobilization (6). This experiment was designed to investigate changes occurring in skeletal and mineral homeostatis in these older rats flown for two weeks in space.

METHODS AND RESULTS

Vertebral specimens from a total of twenty rats were obtained for analysis (five each from basal control, flight, synchronous control, and vivarium control groups). In addition, a pooled excreta collection from each group and samples of the flight paste diet were received for analysis. The vertebrae (fourth lumbar) were dissected free of surrounding tissues using titanium tools to minimize possible elemental contamination. Each vertebra was weighed, then separated into four parts. The vertebral body was dissected free of the posterior elements at the base of the pedicles, then each of these components was split into two parts for analysis.[1] The results in this report include analyses to date of major constituent elements and osteocalcin.

Separated bone specimens were lyophilized to constant weight, then ground to a fine powder in a liquid-nitrogen-cooled mill. Osteocalcin content was measured in EDTA extracts of the powder using the method of Patterson-Allen et al (7) with a rat-specific osteocalcin assay. Calcium was measured using atomic absorption spectrophotometry, and phosphorus was determined using a modified Fiske-Subarow method. The results of these assays are given in Table 1. Derived quantities are given in Table 2.

DISCUSSION

The spine is composed of two types of bone. The trabecular portions of the vertebral body as well as the compact shell in this region are in direct contact with bone marrow and can be very responsive to metabolic stimuli. In contrast, the posterior elements containing many muscle attachments are primarily compact bone with a slower turnover rate. In humans and non-human primates, significant vertical loading forces exist in the spine during normal weightbearing and much of this force is transmitted through the vertebral body which makes up about half of the

[1] The original experiment design called for constituent analysis to include both major and trace elements and bone osteocalcin content. However, between design of the experiment and receipt of samples the technique to be used for trace analysis in these small samples (neutron activation analysis) became unavailable because of closure of the nuclear reactor at the University of California, Berkeley. At the present time, development and testing of new techniques sensitive enough to do this analysis are underway (using high-sensitivity x-ray fluorescence spectrometry) and will be used within the next six months to complete the sample analysis. These data will be included in a supplemental report at that time.

vertebral mass. In rats, the posterior elements take up much more of the loading forces at 1-g as well as the torsional forces due to muscle pulls, and are significantly different in their morphology than in primates, comprising about two-thirds of the total vertebral mass. Thus, we may expect that the two portions of the rat vertebra, the vertebral body and the posterior elements, will show different responses to spaceflight.

The results of the analyses from this study confirm major differences between portions of the vertebra. The posterior bone is more highly mineralized, evidenced by increased concentration (per unit weight of bone) of calcium (5%), phosphorus (6%) and osteocalcin (37%), similar to the differences seen between proximal and mid humerus in previous studies (4). The major increase in osteocalcin content indicates the presence of mature, low-turnover bone.

The differences between flight and control animals were minimal in these older, slowly-growing rats. Mass of whole vertebrae increased 6.2% in synchronous rats compared to less than 2% in flight rats over the 16 days when compared to basal controls, suggesting a decreased rate of bone growth in flight. Compared to young rats in which vertebral mass increased over 40% in 10 days in controls and 20% in flight rats (5), this may be a clear indication that even in the older skeleton bone growth will slow in microgravity. The increased osteocalcin concentration in the posterior spine of flight rats compared to all other groups suggests a higher state of maturation of this compact bone, possibly due to a slowed turnover with the removal of both dorsal-to-ventral loading as well as torsional muscle pulls in spaceflight. This is similar to the differential effects of long-term microgravity exposure seen on the vertebral body and posterior elements in cosmonauts (8), and suggests further study of the muscle-spine interaction is necessary to determine the actual effects of spaceflight and changed patterns of activity and loading on the spine.

REFERENCES

1. Morey E.R., Baylink D.J.: Inhibition of bone formation during spaceflight. Science 201:1138-1141, 1978.

2. Cann C.E., Adachi R.R.: Bone resorption and mineral excretion in rats during spaceflight. Am.J.Physio 244 (Reg. Comp. Integ.): R327-R331, 1983.

3. Simmons D.J., Russell J.E., Winter F., Tran Van P., Vignery A., Baron R., Rosenberg G.D., Walker W.V.: Effect of spaceflight on the non-weight-bearing bones of rat skeleton. Am.J. Physio 244 (Reg. Comp. Integ.): R319-R326, 1983.

4. Patterson-Buckendahl P., Arnaud S.B., Mechanic G.L., Martin R.B., Grindeland R.E., Cann C.E.: Fragility and composition of growing rat bone after one week in spaceflight. Am.J. Physiol 252 (Reg. Comp. Integ.): R240-R246, 1987.

5. Vico L., Chappard D., Alexandre C., Palle S., Minaire P., Riffat G., Grigoriev A.I., Oganov, V.S.: Effets de l'apesanteur sur le tissu osseux de rat apres un vol spatial de cinq jours (Cosmos 1514) in Proceedings, Second International Conference on Space Physiology, Toulouse, November 1985, p. 67-68.

6. Henke J.A., Thompson N.W., Kaufer H.: Immobilization hypercalcemic crisis. Arch. Surg 110:321-323, 1975.

7. Patterson-Allen P.E., Brautigam C.E., Grindeland R.E., Asling C.W., Callahan P.X.: A specific radioimmunoassay for osteocalcin with advantageous species cross-reactivity. Anal. Biochem. 120: 1-7, 1982.

8. Cann C.E., Oganov V.S., Rakhamanov A.: unpublished results.

TABLE 1. MAJOR CONSTITUENTS OF LUMBAR VERTEBRAE

	Basal	Vivarium	Synchronous	Flight
Wet Weight (mg) Whole Vertebra	189.4±6.6	207.6±5.9	201.1±4.0	193.0±7.4
Vertebral Body Wet Weight (mg)	66.1±3.1	86.3±3.1	66.0±4.1	67.3±4.1
Vertebral Body Water Content (%)	36.4±0.8	32.6±0.8	34.9±0.9	40.0±1.9[a]
Posterior Element Water Content (%)	30.8±1.2	28.4±1.6	29.9±1.0	27.2±1.9
Ca (mg/gm) Vertebral Body	203.5±4.7	220.0±4.7	217.1±2.7	213.1±0.6
Ca (mg/gm) Posterior Elements	217.3±1.2	224.8±3.3	222.9±5.0	233.7±3.4
P (mg/gm) Vertebral Body	110.3±2.1	115.3±2.1	114.2±1.4	115.0±2.1
P (mg/gm) Posterior Elements	119.4±3.8	116.9±5.3	119.7±5.3	123.5±1.0
Osteocalcin (mg/gm) Vertebral Body	1.72±0.07	2.05±0.07	1.74±0.12	1.77±0.12
Osteocalcin (mg/gm) Posterior Elements	2.42±0.01	2.46±0.07	2.42±0.07	2.61±0.08

TABLE 2. DERIVED MEASUREMENTS FROM ANALYSIS OF VERTEBRAE (MEAN±SEM)

	Basal	Vivarium	Synchronous	Flight
Vertebral Body % of Total Vertebra	35.0±1.0	41.8±2.1	32.7±1.6	35.0±2.3
Ca/Pi (Molar) Vertebral Body	1.43±0 04	1.48±0.04	1.47±0.03	1.44±0.02
Ca/Pi (Molar) Posterior Elements	1.41±0.03	1.49±0.01	1.47±0.04	1.47±0.01
OC/Ca Vertebral Body	8.53±0.53	9.34±0.54	8.02±0.49	8.32±0.55
OC/Ca Posterior Elements	11.14±0.05	10.93±0.33	10.90±0.42	11.16±0.30

N90-26459

EXPERIMENT K-6-05

THE MATURATION OF BONE AND DENTIN MATRICES IN RATS FLOWN ON COSMOS 1887

Principal Investigator:

D. Simmons
University of Texas Medical Branch
Department of Surgery
Division of Orthopedic Surgery
Galveston, Texas 77551

Co-Investigators:

M. Grynpas
University of Toronto
Mt. Sinai Hospital
Department of Pathology
Toronto, Ontario, Canada

G. Rosenberg
Indiana University- Purdue University
Department of Geology
Indianapolis, Indiana 46202

G. Durnova
Institute of Biomedical Problems
Moscow, USSR

PRECEDING PAGE BLANK NOT FILMED

SUMMARY

The chemistry, hydroxyapatite crystal size, and maturation of the bone and dentin is characterized in rats exposed to microgravity for 12.5d in a Soviet Biosatellite (Cosmos-1887). Calvarial and vertebral bone ash was subnormal, but contained a normal percent composition of Ca, P, and Mg. These tissues varied from the norm by having lower Ca/P and higher Ca/Mg ratios than any of their age-matched controls [Vivarium and Synchronous Groups]. Gradient density analyses [calvaria] indicated a strong shift to the lower sp.gr. fractions which was commensurate with impaired rates of matrix-mineral maturation. X-ray diffraction data were confirmatory. Bone hydroxyapatite crystal growth in Flight rats was preferentially altered in a way to reduce the dimension of their C-axis. Flight rat dentin was normal with respect to age-matched control Ca, P, Mg, and Zn concentrations and their Ca/P and Ca/Mg ratios. These observations affirm the concept that microgravity adversely affects the maturation of newly formed matrix and mineral moieties in bone.

INTRODUCTION

There is much concern to maintain musculo-skeletal integrity in astronauts during prolonged spaceflight. This concern translates to questions about the role of gravity in calcium-mediated physiological mechanisms. The 'side effects' of spaceflight include impaired bone modeling and remodeling, loss of [trabecular] bone mass and reduced capacity of the vertebrae and long bones to withstand certain loads. These changes are the species independent common thread of experience in space biology research (Jee et al 1983; Kazarian 1981; Roberts et al 1981; Simmons et al 1983).

Our particular interest in the skeletal status of rats flown in space focuses upon the normality of the matrix and mineral moieties deposited in the bones and teeth. Gradient density analyses have shown that the environment of space retards the maturation of newly synthesized collagen and hydroxyapatite [see Cosmos-1129 (Rosenberg et al 1984; Simmons et al 1983)] and Spacelab-3 Missions (Simmons et al 1986). A larger than the normal percent of total calcium, inorganic phosphorus and matrix hydroxyproline and osteocalcin is found in the lowest density fractions which include the most recently formed osseous and dentinal substance. Importantly, we were unable to duplicate the spaceflight density profiles in a ground based 1G model of hypokinesia--the jaws of tail-suspended rats (Simmons 1983a), and the jaws of primates whose postcranial skeleton was immobilized in plaster (Simmons et al 1984). We have since determined that the vertebral, femoral, and mandibular bone mineral in biosatellite flown rats differs from normal in having a smaller crystal size (Grynpas et al 1986; Simmons et al 1986). All of these changes indicate that the maturational deficit in spaceflight has a special gravity component.

Judgments about the effects of gravity on bone maturation are necessarily tentative since our experiences are limitted to a single "long term Mission [18 5d Cosmos-1129] and a single mid-deck Space Shuttle flight [7d Spacelab-3]. This report deals with the analyses of various weight and non-weight bearing bones and incisor dentin from rats carried on a biosatellite flight of intermediate duration--the 12.5d joint Soviet-U.S.A. Cosmos-1887 Mission. In this work, we sought to extend our observations on how microgravity affects the skeletal maturational and compositional changes.

MATERIALS AND METHODS

The study involved 12 week old male Wistar rats bred and reared at the Czechoslovakian Academy of Sciences [325 g average body weight]. The rats were segregated into 4 groups of 6 animals each.

Group	Sacrificed	Wt.at Sacrifice (g)
I Basal C	5d Preflight	325 ± 5
II Vivarium Controls	3-4d Postflight	318.6± 6
III Synchronous Co	5d Postflight	392 ± 9
IV Biosatellite	2.5d Postflight	352 ± 6

The Synchronous Controls (Group III) differed from the other Control rats (Groups I and II) by being artificially exposed to a level of noise and vibration equivalent to that experienced by the Flight rats (Group IV) during the launch, reentry, landing and recovery periods.

All animals were multiply housed (10/cage) and fed a semi-synthetic paste diet [40g/d (70% water)], identical in composition to that used on previous biosatellite flights. The diet is adequate in calories [protein= 18.2%, fat= 24.2%], carbohydrates [57.4%], minerals and calciotropic vitamins, but the feed is relatively low in zinc [0.07mg/40g= 39% of the daily requirement (Pace et al 1981)]. Drinking water was freely available. All animals were exposed to temperatures of 23 + 1C and a 16h/8h light-dark cycle. The intensity of light at the cage bottom was 4-8 lux.

The Flight rats were loaded into the biosatellite some 24h prior to launch [Sept. 29, 1987], and they were flown in space for 12.5d. The flight was terminated on October 12, 1987, and the spacecraft landed near Murni, Siberia rather than at the designated recovery site near Kustanei in Kazakhstan. Due to this unforseen occurrence, there was a 56h delay between landing, sacrifice and autopsy.

The rats were sacrificed by decapitation. The skull cap (calvarium), 5th lumbar vertebra, and a mandible from each rat was stripped of soft tissues and fixed in 100% ethyl alcohol. The mandible was transversely sectioned at the diastema to remove a 2.0mm slab for electron microprobe compositional studies. The more anterior and posterior regions of the jaw were reserved for the studies on bone maturation [bone density fractionation, chemistry].

A. Bone Maturation Studies

1. Bone Density Fractionation: Insufficiency of material limited this study to the calvarial samples.

The bone specimens were frozen in liquid nitrogen, lyophilized and pulverized in a percussion mill [Spex Freezer Mill, Metuchen, N.J.], cooled in liquid nitrogen, and sieved in a sonic sifter to isolate bone particle sizes below 20 um. The powder was then fractionated [1.7-2.3 g/ml] in a bromoform-toluene mixture by the stepwise centrifugation method of Grynpas et al (1986). In practice, 200-300 mg of sieved powder was added to a polyallomer tube containing 35ml of a 2.0g/ml density solution [calibrated with sink floats]. The tubes were capped and sonicated to obtain a homogeneous suspension of the powder, and it was centrifuged at 10,000 rpm for 30 min. The density of the supernatant was then modified to 1.9 mg/ml by the addition of toluene,

and the new solution was recentrifuged. Under the same conditions, each precipitate obtained from solutions of progressively decreasing density [at 0.1 g/ml steps] was collected. To obtain a range of mineral densities greater than 2.0 g/ml, the precipitate obtained from the initial 2.0 g/ml density solution was resuspended in a solution of density 2.3 g/ml. Successive centrifugation of precipitates at progressively decreasing densities [0.1 g/ml steps] provided the higher density fractions. The series of specific gravity [sp.gr.] fractions obtained in this way were centrifuged in 100% ethyl alcohol to remove organic solvent and they were dried in a dessicator at room temperature.

The relative contribution of each of the fractions to the original weight of the unfractionated bone powder was calculated from the mineralization profile in each sp.gr. fraction. In our hands, the reproducibility of the method was ± 2.0 % [SD].

2. X-Ray Diffraction: Samples of bone powder from the unfractionated samples were analyzed with a Rigaku microdiffractometer using Ca Ka radiation and using a highly crystalline mineral fluoroapatite as a standard. The values of B 1/2 [002] and [130], the widths at one-half the maximum height of the hydroxyapatite reflections, were measured using a step-scanning procedure with 0.4 degrees/step and 100 sec of counting. Because the instrumental broadening was small compared with sample peak breadths, the measured half-widths were corrected for instrumental broadening by subtracting the square of B[002] and B[130] for the standard [fluoroapatite] from the square of the bone value and taking the square root of the difference. D-values, which are related to the crystal size and strain in the long dimension [002] and the cross section [130] of the apatite crystal, were calculated from the corrected B[002] and B[130] value [B 1/2] using the Sherrer Equation (Simmons et al 1986):

$$D = \frac{K \lambda \text{ radian}}{B_{1/2} \cos \theta}$$

where λ is the X-ray wavelength, $B_{1/2}$ the breadth at half the height of the 002 and 130 peaks, and θ the diffraction angle. K is a constant varying with crystal habit and chosen as 0.9 for the elongated crystallites of bone. Each measurement was repeated 3-times and the results are presented as the ± standard deviation.

3. Chemical Studies: Aliquots of tissue weighing an average of 10mg were washed in a 4:1 v/v nitric: percholoric acid mixture. A blank containing only the acid mixture served as a control for the procedure. An external control was provided by including 10 mg phosphate rock [NBS Standard #120b]. The samples placed in covered Teflon beakers were slowly heated and then brought to a boil for 1.5h. The lids were then removed and the digested samples were brought to a final volume of 20 ml with double deionized water.

Calcium and magnesium analyses were performed on ashed samples. For calcium, 1:50 and Mg 1:125 lN 10Mm lanthanum chloride [250 ml 10% La from BDH in 18L distilled water] was added to 100ml of each sample. The samples were thoroughly shaken and analyzed by atomic absorption spectrophotometry [Perkin-Elmer 400]. Ca and Mg were measured thrice and the average was used for further calculations.

For inorganic phosphate, one part 10% ascorbic acid [10g/100 ml distilled water] was mixed with 6 parts 0.42% ammonium molybdate $\cdot 4H_2O$ in 1N H_2SO_4 [28.6 ml concentrated H_2SO_4 and 4.2 g ammonium molybdate$\cdot 4H_2O$ to 1000 ml distilled water], and the solution was kept on ice. 10ml ashed sample and 90 ml distilled water were plated in duplicate in Tetertek Plates. 230 ml of the acid-molybdate solution was added. The plate was covered with paraffin and incubated for 1h at 37C. The plate was then read on a Tetretek Multiskan at 620nm.

B. Electron Microprobe Investigations for Mandibular Bone and Incisor Dentin Composition

The diastemal mandibular slab was embedded in epoxy and the exposed surfaces were polished using successively finer grades of sandpaper and alumina grit. The blocks were then mounted in a MAC-5 Microprobe. Analyses for calcium, phosphorus, magnesium and zinc in bone were made on continuous traverses which passed across the mid-lateral periosteal-endosteal surfaces, the periodontal membrane, and dentine to the pulp-dentine margin using a 3.0-4.0um spot size, with measurement at 4.0um intervals. Analyses for these elements in teeth were made in a traverse which passed from the pulp-dentin border to the enamel surface (Rosenberg et al 1984; Simmons et al 1983). The quantitative analyses were Bence-Albee reductions of 10 measurements made across the bone/teeth. Zinc [Zn] was detected using a LiF crystal. P and Mg were detected using a RAP crystal, and calcium and phosphorus was detected using a PET crystal. Calcium and phosphorus were standardized on an apatite crystal, Mg on a MgO standard, and Zn on the Zn-silicate Willemite. The specimen current was 0.015 uamps. The accelerating potential was 15 kv, and each measurement was made for 10 sec without noticeable deterioration of the specimen. Background and drift were measured and subtracted from each measurement.

In this study, we report only the average composition of the tissues in terms of the ratios of Ca/P, Ca/Mg, and Ca/Zn. The analyses do not compare the compositions of the calcified matrices deposited pre-and postflight. These will be the subject of further study.

RESULTS

1. Bone Maturation Studies (Calvaria)

The sp.gr. mineralization profiles for the calvarial samples are shown in Table 1. Compared to control animals, the profile for the Flight group showed a sharp shift to the lower density fractions. The lower sp.gr. fractions [1.8-1.9] contained the larger percent sample weight, while the higher sp.gr. fractions [2.0 & 2.3] contained the smaller than normal sample weights. This shift was confirmed by the observation that the Flight rat calvaria exhibited the lowest sample ash weight and percentages of dry weight Ca, P and Mg [Table 2].

The size of the samples for the 5th lumbar vertebrae and mandibles were insufficient for gradient density evaluation. However, their chemistries were assessed [Table 2]. While calvarial and vertebral Mg levels were the lowest in the Flight rats, the overall composition of these tissues were not aberrant [ex. Ca/P & Ca/Mg] and thus the data are consonant with the results of all previous investigations (Rosenberg et al 1984; Simmons et al 1983). The results from the electron microprobe studies were very similar (see Tables 4 & 5).

2. X-ray Diffraction
The data consist of analyses from the Synchronous Control and Flight Groups. Table 3 indicates that the hydroxyapatite crystals in the mandibles and calvaria of Flight rats are comparatively much the smaller, but the change is found only in the longer C-axis.

3. Electron Microprobe Compositional Analysis-Diastemal Mandibular Bone [Table 4]:
Flight rat bones exhibited normal Ca/P and Ca/Zn ratios when compared to any of the three control groups. However, the Flight rat bones were relatively richer in Mg than the bones from the Vivarium and Synchronous Controls -- animals which were closest in age at sacrifice. Anomalously, the Ca/P ratio for the Synchronous Controls were subnormal with respect to the Basal Controls.

4. Diastemal Incisor Dentin [Table 5]:
Flight rat dentin exhibited trends which were somewhat similar to the mandibular bone. The tissue from the Flight rat and Synchronous Controls had lower Ca/P ratios than the Basal Controls [$P<0.05$]. The Ca/Zn ratios were similarly equivocal. The Flight rat dentin had significantly less Zn than the Basal Controls [$P<0.01$], but there were no differences in concentration between the Flight and the other two control groups. The Ca/Mg ratios suggested the lack of important intergroup differences in tissue Mg. There was, then, little in the way of compositional changes that could be attributed to spaceflight.

DISCUSSION

Despite the fact that it was not possible to obtain tissue samples from the Flight rats until after they had been exposed to earth's gravity for 2.5d postflight, the bones recorded effects of microgravity which were similar to those observed after shorter and longer Missions. The bone mineral (Ca, Mg, P)-matrix (hydroxyproline) gradient density distributions from a variety of weight bearing and non-weight bearing bones have always shown a delay in tissue maturation. This conclusion is based on three findings: that the bulk of bone [particles] sediments-out in the lower sp.gr. range, that the mineral hydroxyapatite crystals formed in spaceflight remain small/immature, and their low Ca/P ratio and higher than normal sulfur content reflects the protracted adolescence of the forming tissue. The higher than normal Ca/Mg ratios can be interpreted within the context of a literature that recognizes that Mg levels are always higher in immature/newly forming skeletal tissues than in temporally older regions which have mature/achieved full mineralization (Schwartz 1988). Herein, the trend to low Mg was pronounced in the Flight rat bone [vertebrae, calvaria, jaws], indicating a subnormal rate of new bone formation. There was no such trend in the rat dentin where the rate of dentinogenesis has never been demonstrated to deviate from normal-- perhaps, teleologically speaking, a metabolic concession that in space the teeth are more necessary than the weight bearing bones.

The inclusion of zinc determinations in the electron microprobe study was pursued to investigate whether the decrease in skeletal ash might have been related to low zinc nutriture. There are reasons for believing that the 30% of the rat daily Zn requirement provided by the paste diet might have direct and indirect skeletal consequences. A diet high in Ca and P and casein (18%) could interfere with intestinal zinc absorption (Allred et al 1964; Pecoud et al 1975). Indirectly, poor zinc nutriture is associated with decreased circulating levels of plasma somatomedin-C/ insulin-like

growth factor-I, as well as impaired synthesis of DNA, alkaline phosphatase, collagen, non-collagen protein, prostaglandin and mineralization (Cossack 1984). More directly, Zn stimulates differentiated bone cell function -- the ability of osteoblasts to synthesize and export collagen (Yamaguchi et al 1987). In terms of bone resorption, Zn deficiency compromises immune responsiveness and the activity of Zn-containing collagenase, effects which might be considered to interfere with the mobilization of the monocytic/macrophagic precursors of osteoclasts, macrophagic collagen resorption, and even the putative resorptive activity of osteoblasts to abet monocytic homing to calcified bone surfaces. Thus, in severe Zn deficiency, collagen turnover could be decreased (Starcher et al 1980). The fact is that our electron microprobe studies which present tissue-wide average compositions did not indicate that microgravity had an effect on the bioavailability of Zn; the Flight rat mandibular bone and incisor dentin proved to have a normal Ca/Zn ratio. It may be that the high Vitamin D content of the paste diet was adequate to overcome such potentially deleterious effects (Chang et al 1969). Yet, this conclusion may need to be modified upon reanalysis of the Ca/Zn ratios in the tissues formed before and during flight.

CONCLUSION

The present study lends additional evidence that long-term exposure to microgravity will compromize the integrity of skeletal structures. Within the context of measurements of young growing rats made during a 7d Space Shuttle Mission and two U.S.S.R. biosatellite flights of 12.5 and 18.5 days duration, the risks of spaceflight entail a decrease in the quantity of hard tissues formed, a delay in maturation of those matrices, and the resorptive loss of preexisting [preflight] trabecular bone structures. The consequences of these changes is a decrease in the biomechanical strength of the rat skeleton. While we did not have access to Cosmos 1887 Flight animals that had been permitted to recover at earth's gravity, our experience indicated that the degree of change was comparable to that observed with the 18.5d Cosmos-1129 Mission, and that the maturational defect would be reversed within a period of 7-14 days.

REFERENCES

1. Allred, J.B., Kratzer, F.N. and Porter, J.W.G.: Some factors affecting the in vitro binding of zinc by isolated soyabean protein and by a-casein. Br. J. Nutr. 18: 575, 1964.

2. Chang, J.H., Harrill, I. and Gifford, E.D.: Influence of zinc and vitamin D on bone constituents of the rat. Metabolism 28: 625, 1969.

3. Cossack, Z.T.: Somatomedin-C in zinc deficiency. Experientia 40: 498, 1984.

4. Grynpas, M.D., Patterson-Allen , P. and Simmons, D.J.: The changes in quality of mandibular bone mineral in otherwise totally immobilized Rhesus monkeys. Calcif. Tissue Int. 39: 57, 1986.

5. Jee, W.S.S., Wronski, T.J., Morey, E.R. and Kimmel, D.B.: Effect of spaceflight on trabecular bone in rats. Amer. J. Physiol. 244: R310, 1983

6. Kazarian, L.E.: Strength characteristics of rat spinal columns. Cosmos 1129. In: Hideg, J. and Gazenko, O. (eds). Advances in Physiological Sciences. Vol. 19, Gravitational Physiology, New York, Pergamon Press, 1981, p. 129.

7. Pace, N., Rahlmann, D.F., Smith, A.H., and Pitts, G.C.: Effects of the Cosmos-1129 Soviet paste diet on body composition in the growing rat. Report of the UCLA-Berkeley Environmental Physiology Laboratory [EPL-81-1], Feb. 16, 1981.

8. Pecoud, A., Donzel, P., and Schelling, J.L.: Effect of foodstuffs on the absorption of zinc sulfate. Clin. Pharmacol. Ther. 17: 459, 1975.

9. Roberts, W.E., Mozsary, P.G. and Morey, E.R.: Suppression of osteoblast differentiation during weightlessness. Physiologist 24: S75, 1981.

10. Rosenberg, G.D., Campbell, S.C. and Simmons, D.J.: The effects of spaceflight on the mineralization of rat incisor dentin. Proc. Soc. Exp. Biol. Med. 175: 429, 1984.

11. Rosenberg, G.D. and Simmons, D.J.: Electron microprobe analyses of Ca, S., Mg, and P distribution in incisors of Spacelab-3 rats. The Physiologist 28 (Suppl 1): S189, 1985.

12. Schwartz, R.: Magnesium metabolism. In: Simmons, D.J. (ed). Nutrition and Bone Development. Oxford Univ. Press, N.Y., 1988 (in press).

13. Simmons, D.J., Russell, J.E., Winter, F., Tran Van, P., Vignery, A., Baron, R., Rosenberg, G.D. and Walker, W.V.: Effect of spaceflight on the non- weight bearing bones in the rat skeleton. Amer. J. Physiol. 244: R319, 1983.

14. Simmons, D.J., Grazman, B., Russell, J.E., Walker, W.V., Bikle, D.D. and Morey, E.R.: Simulating certain aspects of hypogravity effects on bone maturation in the non-weight bearing skeleton. Aviat. Space and Environ. Med. 54: 1080, 1983a.

15. Simmons, D.J., Russell, J.E., Walker, W.V., Grazman, B., Oloff, C. and Kazarian, L.: Growth and maturation of mandibular bone in otherwise totally immobilized Rhesus monkeys. Clin. Orthop. 182: 220, 1984.

16. Simmons, D.J., Russell, J.E. and Grynpas. M.D.: Bone maturation and quality of bone mineral in rats flown on the space shuttle 'Spacelab-3 Mission'. Bone and Mineral 1: 485, 1986.

17. Starcher, B.C., Hill, C.H. and Madras, I.G.: Effect of zinc deficiency on bone collagenase and collagen turnover. J. Nutr. 110: 2095, 1980.

18. Yamaguchi, M., Oishi, H. and Suketa, Y.: Stimulatory effects of zinc on bone formation in tissue culture. Biochem. Pharmacol. 36: 4007, 1987.

TABLE 1

Mineralization Profile in Calvaria of Cosmos 1887 Rats

Percent Sample Weight

Specific Gravity Fraction	Basal Control	Vivarium Control	Synchronous Control	Flight
1.8	1.1	1.4	0.7	16.7 (>15.2-23.8)
1.9	9.7	6.0	7.7	38.2 (> 3.9- 6.3)
2.0	80.7	89.7	89.2	44.2 (< 1.8- 2.0)
2.1	6.8	2.4	1.9	0.6 (< 3.1-11.3)
2.2	0.6	0.3	0.2	0.3
2.3	1.1	0.2	0.2	0.1 (< 2.0-11.0)

Underlining indicates values which are higher or lower than those recorded by control rats. ( )= range of differences.

TABLE 2

Bone Chemistry in Cosmos-1887 Rats
(Unfractionated)

Group	Ca (1)	P (1)	Mg (1)	Ca/P	Ca/Mg(2)	Ash Wt.(3)
Calvaria						
Basal Control	23.0±0.07	10.1±0.09	0.46±0.004	1.75	50.0	54.12
Vivarium Ctrl	24.6±0.06	10.8±0.25	0.49±0.008	1.76	50.2	57.66
Synchronous Ctrl	24.3±0.15	10.5±0.15	0.4650.009	1.78	52.8	56.54
Flight	20.3±0.07	9.6±0.64	0.38±0.004	1.63	50.2	57.66
5th Lumbar Vertebra						
Basal Ctrl	20.5±0.21	9.3±0.72	0.38±0.001	1.71	53.9	48.84
Vivarium Ctrl	23.8±0.06	10.5±0.09	0.46±0.007	1.75	51.7	55.99
Synchronous Ctrl	20.3±0.14	10.2±1.21	0.46±0.041	1.53	44.1	51.65
Flight	20.7±0.01	9.3±0.17	0.37±0.001	1.72	55.9	49.13
Mandible						
Basal Control	25.4±0.07	11.5±0.09	0.48±0.004	1.71	52.9	60.52
Vivarium Ctrl	23.8±0.12	12.6±0.48	0.48±0.001	1.46	49.5	62.40
Synchronous Ctrl	26.6±0.15	12.0±0.20	0.47±0.013	1.72	56.5	63.24
Flight	28.0±0.13	12.1±0.10	0.50±0.005	1.78	56.0	65.11

(1) % of dry weight
(2) Molar ratio
(3) as % ($Ca+PO_4$)

TABLE 3

X-Ray Diffraction of Bone from Cosmos-1887 Rats

Group	$b_{1/2}$	D-002 (*)	$b_{1/2}$	D-130 (*)
Calvaria				
Synchronous Ctrl	0.68±0.01	147± 5	1.70±0.29	55±12
Flight	0.73±0.06	132±13	1.57±0.09	57± 3
5th Lumbar Vertebra				
Flight	0.77±0.01	122±2	1.78±0.19	50±6
Mandible				
Synchronous Ctrl	0.56±0.04	209±29	1.23±0.26	80±20
Flight	0.68±0.01	145± 5	1.32±0.14	71± 5

* In angstrom units

TABLE 4

Composition of Diastemal Mandibular Bone in Cosmos-1887 Rats
(Electron Microprobe Investigations)

Group	N	Ca/P	Ca/Mg	Ca/Zn
Basal Controls	5	1.439±0.049^	43.38±1.01	330.92± 46.14
Vivarium Controls	5	1.315±0.116	44.27±3.59^	290.94± 40.75
Synchronous Ctrls	5	1.300±0.023#	46.28±3.99^	358.35± 97.34
Flight	5	1.318±0.068	39.80±3.34#	337.17±124.00

Dissimilar superscripts are statistically different P<0.01.

TABLE 5

Composition of Diastemal Incisor Dentin in Cosmos 1887 Rats
(Electron Microprobe Investigations)

Group	N	Ca/P	Ca/Mg	Ca/Zn
Basal Control	5	1.331±0.117^	13.79±1.15	198.46±10.03^
Vivarium Control	5	1.130±0.102	16.03±2.17	246.83±35.63
Synchronous Ctrl	5	1.050±0.026#	16.94±2.78	179.26±39.51
Flight	5	1.085±0.050	14.30±1.74	295.42±36.23*

^ vs # = P<0.05 ^ vs * = P<0.01

N90-26460

EXPERIMENT K-6-06

MORPHOMETRIC AND EM ANALYSES OF TIBIAL EPIPHYSEAL PLATES FROM COSMOS 1887 RATS

Principal Investigator:

P.J. Duke
University of Texas Health Science Center
Dental Branch, Dental Science Institute
Houston, Texas 77225 U.S.A.

Co-Investigators:

D. Montufar-Solis
University of Texas Health Science Center
Dental Branch, Dental Science Institute
Houston, Texas 77225 U.S.A.

G. Durnova
Institute of Biomedical Problems
Moscow, USSR

SUMMARY

Light and electron microscopy studies were carried out on decalcified tibial epiphyseal plates of rats flown aboard Cosmos 1887 (12.5d flight plus 53.5h recovery). Analysis of variance showed that the proliferative zone of flight animals was significantly higher than that of synchronous controls, while the hypertrophic/calcification zone was significantly reduced. Flight animals had more cells than synchronous controls in the proliferative zone, and less in the hypertrophic/calcification region. The total number of cells, however, was significantly higher in flight animals. No differences were found for perimeter or shape factor of growth plates, but area was significantly lower in flight animals in comparison to synchronous controls. Collagen fibrils in flight animals were shorter and wider than in synchronous controls. The time required for a cell to cycle through the growth plate is 2-3 days, so most of the cells and matrix present were formed after the animals had returned to 1g, and probably represent stages of recovery from microgravity exposure, which in itself is an interesting question.

INTRODUCTION

The effect of spaceflight on bone development in growing rats has been studied using animals flown on the Soviet Cosmos series, and on Spacelab 3 (Morey-Holton and Arnaud, 1985). These studies have shown that bone formation ceases during spaceflight (Wronski and Morey, 1983), that matrix formed in flight does not mature normally, and consequently cannot mineralize normally (Simmons, et al., 1983) and that these changes are well underway after seven days of spaceflight (Russell and Simmons, 1985).

The cartilagenous epiphyses of the long bones of space rats have received less attention (only two studies have been conducted) even though some of the changes that are seen in bone --e.g. decreased length (Wronski, et al., 1981) and decreased trabecular bone mass (Je[illegible] et al., 1983) -- must originate in the epiphyseal region.

In the first study, epiphyses of rats flown aboard Cosmos 1129 (an 18.5 d flight) showed a delay in matrix vesicle production and mineralization, and lack of collagen maturation (Matthews, 1981).

In the other study, conducted in our laboratory, proximal tibial epiphyses of Spacelab 3 rats (7 d flight, 12 h recovery) were analyzed at the light and electron microscope levels using interactive image analysis and computerized planimetry, and cartilage differentiation was found to be markedly affected after only seven days of spaceflight (Duke, et al., 1985; Duke and Montufar-Solis, 1989). Heights of plates and zones of flight animals were less than those of controls, and there were fewer cells per column in the proliferative zone and the hypertrophic/calcification (H/C) zone. When both height of zones and cell number were considered, the greatest effect was on the proliferative zone. Areas of flight plates were significantly less than areas of control plates, and the shape factors of the two sets of plates were different. At the EM level, important alterations in matrix production and maturation were found (Duke and Montufar-Solis, 1989). Collagen fibers of flight animals were shorter and thinner than those of controls. Proteoglycan granules were found at higher densities (PGG/mm ^{2}) in flight animals. Areas of these granules were also measured and a significantly different pattern of zonal distribution of PGG sizes was found between the two groups (Duke and Montufar-Solis, 1989).

Some decrease in plate height on SL3 may have resulted from exposure to earth gravity during the twelve hour period between landing in California and sacrifice at Kennedy, especially since matrix organization was altered. To examine this question, a simulation of SL3 was carried out at Ames Research Center using the Holton suspended rat model (Morey, 1979). Besides testing the validity of the Holton model by allowing a direct comparison with SL3 animals, the sim also provided an

opportunity to determine what effect loading during the last 12 hours of SL3 may have had, since one group of animals was sacrificed at time of recovery (R+0) and another after an additional 12 hours of loading (R+12).

Growth plates analyzed in our laboratory showed that suspension of animals produced a significant decrease in plate height and in number of cells per column. An additional decrease was observed in both experimental and control groups during the final 12 hours of the experiment, but the differences were significant only in experimental animals. The percent reduction in plate height (17%) and cells/column (17%) were almost the same as those seen in SL3 (16% and 18%), but per zone measurements indicate different mechanisms might be involved in unloading due to spaceflight versus unloading due to suspension, since in suspended animals, the greatest effect was on the hypertrophic/calcification zone (Montufar-Solis and Duke, 1988).

These studies indicate that normal maturation and/or differentiation in the growth plate is altered under exposure to μg. From a detailed study of morphology, changes in matrix production and cellular proliferation due to exposure to μg can be elucidated, as can matrix calcification and matrix calcifiability.

The objectives of the present study were to look for differences in plate parameters (height, cell number, area, perimeter, shape factor), and cell and matrix ultrastructure, in proximal tibial epiphyseal plates of rats flown aboard the 12.5d Cosmos mission, and to compare any differences noted to those found in growth plates of SL3 and SL3-sim rats.

METHODS

Figure 1 shows a general outline of the complete experimental procedure.

Tissue Preparation

Decapitation of the animals was carried out by the Soviet team in Kazakhstan, 53.5 hours after landing of the 12.5 d flight. Using a fresh razor blade, the heads of right tibias were cut from the shaft and placed upside down on the dissecting surface. With another razor blade, the epiphysis was cut in half in the saggital plane (figure 2). The halves used in our studies were placed in screwtop Teflon vials containing cold (4 °C) fixative (2% paraformaldehyde in 0.1M cacodylate buffer with 0.5% glutaraldehyde, pH 7.4). The tissue was maintained at 4 °C for the entire 48 h fixation period. When samples arrived in Moscow, they were rinsed three times with 0.1M cacodylate buffer, and transferred into cold (4 °C) decalcifying solution (10% EDTA in 0.1M TrisHCl buffer, pH 7.4) for storage and shipment.

Samples (n=5/treatment) were received in our lab on November 4, 1987. Decalcification continued for 2 weeks with the EDTA solution being changed every other day. Following decalcification, the medial portion of the plate was embedded in Spurr for electron microscope studies, while the lateral portion was embedded in Paraplast for light microscopy (figure 2).

Light Microscopy and Image Analysis

Five micron coronal sections from the central region of the plate, alternately stained with hematoxylin and toluidine blue, were subjected to image analysis using the video input and digitizing components of the Bioquant system. Area, perimeter, and shape factor (4π area/perim ^{2}) were determined per section to obtain a mean value per animal. Following the definition of zones (figure 3) by Reinholt et al. (1984), determination of zone height and number of cells per zone were made using an ocular micrometer and magnification of 25X. Three measurements (left, middle, and right regions) were used to obtain a mean per section, and these

averaged to obtain a mean per animal. Statistical analyses were carried out using one-way ANOVA. Data was processed using the Number Cruncher Statistical Analysis System, version 3.1.

Electron Microscopy

After thick sections were taken for orientation, thin sections stained with uranyl acetate and lead citrate were examined in a Hitachi 11-E transmission electron microscope. A series of micrographs were taken in each zone, and measurements of collagen fibril length and width were made using a ZIDAS digitizing tablet. Means per section were averaged to obtain means per animal and statistical analyses were carried out using one-way ANOVA.

RESULTS

Light Microscopy

Sections of growth plates of each treatment are shown in figure 4. The difference in plate height between the basal group and the other three is due to aging of the animals. In the flight group, note the small, closely packed cells in the proliferative zone.

Results of all parameters measured in light microscopy and image analysis studies are summarized in table 1. The proliferative zone (PZ) of flight animals was significantly larger than that of synchronous controls (0.124mm vs 0.091mm) while the hypertrophic/calcification zone was significantly reduced (0.025mm vs 0.058mm-figure 5). These changes cancelled out so that the difference in total plate height (0.177mm vs 0.188mm) was not statistically significant.

The same pattern was seen in cell number per zone. Flight animals had more cells than synchronous controls in the proliferative zone (17.88 vs 12.87), and less in the H/C region (1.44 vs 3.74). The increase in cell number in the proliferative zone was so large that the decrease in the H/C zone did not compensate for it, resulting in a significantly higher number of cells in the plates of flight animals (19.31 vs 16.61-figure 6). The area of total growth plate was significantly lower in flight animals ($1mm^2$ vs $1.3mm^2$) than synchronous controls. No significant difference was observed in perimeter or shape factor between flight animals and synchronous controls.

Electron Microscopy

Pictures of collagen fibrils observed in each treatment are shown in figure 7. Collagen fibrils in flight animals were significantly wider than controls in the proliferative zone, (19.3 nm vs 14.9 nm) and also in the hypertrophic zone (18.7 nm vs 12.9 nm - figure 8). Flight animals showed a reduction in fibril length from controls in the proliferative zone, (905.5 nm vs 1212.7 nm) and in the hypertrophic zone (873.3 nm vs 943.1 nm-figure 9), but these differences are not significant due to small sample size and large variance in length measurements.

DISCUSSION

The lack of inflight animal sacrifice makes interpretation of data from flight studies difficult, especially so in the case of Cosmos 1887 where animals were at 1g for 53.5 hours prior to sacrifice (figure 10). Interpretation is also complicated by the responsiveness of growth plate to factors such as feeding time (Russell, et al., 1983), light/dark cycle (Simmons, 1974), and endocrine status (Russell, et al., 1984). Comparisons with SL3 and Holton's SL3 simulation are suspect as well, since the US flight and the simulation used a different rat strain, singly-housed animals, lower lipid food pressed into bars, and a 12-12 light/dark cycle. In spite of these

differences, several points of commonality were found between the three experiments (refer to Table 2).

Area of growth plates, measured with computerized planimetry, was less in each case, and, except for group SL3-sim/R+12, significantly less. In each case, the difference in area is probably a function of the decrease in height.

Perimeter was not significantly altered in any of the experiments, and shape factor (a function of area and perimeter^2) was significantly decreased in SL3 animals only. Since matrix organization was altered in these animals, the difference in shape factor could be due to compression effects on the growth plate during and after landing. Any such effect on the Cosmos growth plates would have been obliterated due to longer recovery time. Suspended animals, of course, are not freed from all gravitational effects during suspension and are not exposed to gravitational changes that occur during landing of spacecraft.

Examination of the data for heights of zones and number of cells leads to the speculation that during unloading (as in SL3-sim/R+0), cells and matrix accumulate in the reserve zone, and, upon reloading, receive stimuli causing them to move into the proliferative zone, thus depleting the reserve zone, as seen in SL3-sim/R+12, SL3 and Cosmos 1887.

The number of cells responding to a stimulus is dependent in part on the number of cells in the respondent population, and perhaps Cosmos 1887 had large numbers of cells in the reserve zone after 12.5d of spaceflight, which moved rapidly into the proliferation zone upon reloading. The large increase in proliferation zone is likely to be the beginning of the rebound phenomenon seen on previous Cosmos missions where tibial length of rats sacrificed 25d postflight was the same as or greater than controls (Yagodovsky et al., 1976; Holton and Baylink, 1978; Holton, et al., 1978, 1979).

This buildup and depletion in the reserve zone corresponds to the pattern seen in growth hormone production (Grindeland and Hymer, this volume). Release of growth hormone by cultured pituitary cells was found to be depressed after SL3, and somatotrophs implanted into hypophysectomized rats did not support tibial growth (Hymer, et al., 1985). Similar results were seen on the SL3-sim (Motter, et al., 1987). For Cosmos 1887, analysis of transport medium of flight cells showed increased growth hormone release, but after 6 days of culture, secretion dropped significantly (see Grindeland and Hymer, this volume).

The decrease in cell number in the H/C zone which was seen in each experimental case is likely due to lack of cell differentiation. The decreases seen in SL3 and both SL3-sim groups are less than that in Cosmos 1887, perhaps due to the latter's longer time in space. Of all the cell groups observed, the H/C zone is most likely comprised of cells that differentiate during the spaceflight period. This is so even for Cosmos 1887 with its long recovery time. The very large decrease seen here makes it likely that even after 53.5 hour of recovery, cells that proliferate postflight have yet to hypertrophy. If these proliferative cells hypertrophied and produced matrix, the height of the total plate would increase. Additional spaceflights and/or simulations are needed to answer questions regarding recovery.

Ultrastructural analyses on SL3 and Cosmos 1887 show that aggregation of collagen fibrils and of proteoglycan granules (PGG's) is altered by spaceflight. For SL3, collagen fibrils were shorter and thinner and proteoglycan granules, smaller and more numerous, than those of controls (Duke and Montufar- Solis, 1989). Measurements of PGG size and distribution in Cosmos 1887 growth plates are not yet complete, but preliminary observations indicate that PGG's of flight animals are bigger than those of synchronous controls. Changes in proteoglycan production produce concommitant changes in fibril aggregation (Duke, 1979), and it may be that the differences seen in

fibril size are secondary to differences in PGG production and/or aggregation. PGG's are also thought to be important in regulating mineralization. (Carrino, et al., 1985) and the impaired mineralization seen in flight animals may be due to defective proteoglycan production and/or processing.

A number of morphometric measurements have yet to be completed. Besides the size and density (number/unit area) of PGG's, the size, number and distribution of matrix vesicles, volumes of cells and matrix, and width of RER cisternae have not been determined, and are needed to complete the morphometric and ultrastructural picture of spaceflight effects upon rat growth plates. Additional experiments with very short recovery times, or, ideally, in-flight animal sacrifice, are needed to allow examination of effects of spaceflight uncomplicated by questions of post-flight exposure to 1g.

Nevertheless, there can be no doubt that spaceflight changes cell proliferation and differentiation, and matrix organization within the growth plate, and that these changes are reflected in decreased length and impaired mineralization of long bones.

ACKNOWLEDGMENTS

M. Campbell, R. Grindeland, V. Hubbard, E. Puente, C. Solis, C. Williams and Soviet Scientists.

REFERENCES

1. Carrino, D. A., M. Weitzhandler, and A. I. Caplan. 1985. Proteoglycans synthesized during the cartilage to bone transition. In: The Chemistry and Biology of Mineralized Tissues (W.T. Butler, ed.), pp. 197-208.

2. Duke, J. and W.A. Elmer. 1979. Effect of the brachypod mutation on early stages of chondrogenesis in mouse embryonic hind limbs: an ultrastructural analysis. Teratology 19:367-376.

3. Duke, J., L. Janer, J. Morrow, and M. Campbell. 1985. Microprobe analyses of epiphyseal plates from Spacelab 3 rats. The Physiologist 28.S217-S218.

4. Duke, J. and B. Montufar-Solis. 1989. Proteoglycan granules in growth plates of Spacelab 3 rats. In: Proceedings of the Third International Conference on the Chemistry and Biology of Mineralized Tissues. In press.

5. Holton, E. Morey and D.J. Baylink. 1978. K005: Quantitative analysis of selected bone parameters. In: Final Reports of US Experiments Flown on the Soviet Satellite Cosmos 782 (Rosenweig, S.M. and K.A. Souza, eds). (NASA TM-78525), pp. 321-351

6. Holton, E.M., R.T. Turner, and D.J. Baylink. 1979. K205: Quantitative Analysis of selected bone parameters. In: Final Report of U.S. Experiements Flown on the Soviet Satellite Cosmos 936 (Rosenweig, S.M. and K.A. Souza, eds). (NASA TM-78526), pp. 135-178.

7. Hymer, W.C., R. Grindeland, M. Farrington, T. Fast, C. Hayes, K. Motter and L. Patil. 1985. Microgravity associated changes in pituitary growth hormone (GH) cells prepared from rats flown on Spacelab 3. The Physiologist 28:S197-S198.

8. Jee, W.S.S , T.J. Wronski, E.R. Morey, and D.B. Kimmel. 1983. Effects of spaceflight on trabecular bone in rats. Am. J. Physiol. 244.(Regulatory Integrative Comp. Physiol. 13):R310-R314.

9. Matthews, J.L. 1981. Mineralization in the long bones. In: Final Reports of US Rat Experiments Flown on the Soviet Satellite Cosmos 1129, (Heinrich, M.R., and K.A. Souza, eds). NASA TM 81289, pp. 199-228.

10. Montufar-Solis, D. and J. Duke. 1988. Effect of simulated spaceflight on tibial epiphyseal plates. ASGSB Bulletin 1:34.

11. Morey-Holton, E.R. and S.B. Arnaud. 1985. Spaceflight and calcium metabolism. The Physiologist 28:S9-S12.

12. Morey, E.R. 1979. Spaceflight and bone turnover: correlation with a new model of weightlessness. Bioscience 29: 168-172

13. Motter, K., M. Vasques, C. Hayes, M. Kendall, G. Tietjen, W.C. Hymer and R. Grindeland. 1987. Effects of microgravity on rat pituitary growth hormone (GH) cell function: comparison of results of the SL-3 mission with rat "unloading" on Earth. Space Life Sciences Symposium: Three Decades of Life Science Research in Space, pp. 52-53.

14. Reinholt, F. P., A. Hjerpe, K. Jansson and B. Engfeldt. 1984. Stereological studies on the epiphyseal growth plate in low phosphate vitamin D- deficiency rickets with special reference to the distribution of matrix vesicles. Calcif. Tissue Int. 36:95-101.

15. Russell, J.E. and D.J. Simmons. 1985. Bone maturation in rats flown on the Spacelab 3 mission. The Physiologist 28:S235-S237.

16. Russell, J.E., W.U. Walker and D.J. Simmons. 1984. Adrenal/parathyroid regulation of DNA, collagen and protein synthesis in rat epiphyseal cartilage and bone. J. Endocr. 103:49-57.

17. Russell, J.E., D.J. Simmons, B. Huber and B.A. Roos. 1983. Meal timing as a Zeitgeber for skeletal deoxyribonucleic acid and collagen synthesis rhythms. Endrocrinology 113:2035-2042.

18. Simmons, D.J. 1974. Chronobiology of endochondral ossification. Chronobiologia 1:97-109.

19. Simmons, D.J., J.E. Russell, F. Winter, P. Tran Van, A. Vignery, R. Baron, G.D. Rosenberg and W.V. Walker. 1983. Effect of spaceflight on the non-weight bearing bones of the rat skeleton. Am. J. Physiol. 244 (Regulatory Integrative Comp. Physiol. 13):R319-R326.

20. Wronski, T.J. and E.R. Morey. 1983. Effect of spaceflight on periosteal bone formation in rats. Am. J. Physiol. 244(Regulatory Integrative Comp. Physiol. 13):R305-R309.

21. Wronski, T.J., E. Morey-Holton, C.E. Cann, C.D. Arnaud, D.J. Baylink, R.T. Turner, W.S.S. Jee. 1981. K305: Quantitative analysis of selected bone parameters. In: Final Reports of US Rat Experiments Flown on the Soviet Satellite Cosmos 1129, NASA TM 81289, pp. 101-125.

22. Yagodovsky, V.S., L.A. Triftanidi, and G.P. Gorokhova. 1976. Space flight effects on skeletal bones of rats (light and electron microscopic examination). Aviatio Space Environ. Med. 47:734-738.

TABLE 1. LIGHT MICROSCOPY AND IMAGE ANALYSIS RESULTS

GP Parameter	Basal (a)		Synchronous (b)		Vivarium (c)		Flight (d)	
Height/Zone (mm)								
Reserve	.053±	.002	.038±	.004a[2]	.039±	.002a[2]	.028±	.002a[1], c[2]
Proliferative	.104	.005	.091	.032	.091	.006	.124	.004a[3],b[1],c[2]
Hyper/Calcif	.112	.009	.058	.001a[1]	.064	.004a[1]	.025	.004a[1],b[1],c[1]
Total GP	.269	.010	.188	.006a[1]	.194	.007a[1]	.177	.008a[1]
Cell Number/Zone								
Proliferative	15.39	1.00	12.87	.45	2.91	.85	17.88	.57 b[1],c[1]
Hyper/Calcif	6.30	0.36	3.74	.15 a[1]	3.68	.15 a[1]	1.44	.23 a[1],b[1],c[1]
Total GP	21.69	0.95	16.61	.44 a[1]	16.60	.90 a[2]	19.31	.53 b2,c2
Area (mm^2)	1.4	0.11	1.3	.09	1.2	.07	1.0	.016a[1],b[2]
Perimeter (mm)	14.27	1.73	14.31	.55	12.76	.39b[4]	13.11	.23
Shape Factor	.095	0.011	.08	.004	.09	.003	.074	.0029c[2]

Mean ± S.E.M. for each treatment, and level of significant difference between groups. Comparisons made between all groups. Lower case letters states group to which the comparison was made, and the number next to it indicates level of significance:

1 - $p \leq .001$
2 - $p \leq .01$
3 - $p \leq .03$
4 - $p \leq .05$

TABLE 2. CHANGES OBSERVED IN COSMOS 1887, SL3, AND SL3-SIM

Parameter	SL3-SIM		SL3	CM 1887
	R+0	R+12		
Area	- 16.6*	- 11.2 %	- 9 %*	- 23 %*
Perimeter	- 5.2	+ 3.2 %	+ 1.8 %	- 8 %
Shape Factor	- 7.5%	- 7.3 %	- 12.5 %*	- 7 %
Height RZ	+ 44.5%*	- 10 %	- 11 %*	- 26 %
PZ	+ 1 %	- 7 %	- 14 %*	+ 36 %*
H/C Z	- 26 %*	- 25 %*	- 19 %*	- 57 %*
Total Growth Plate	- 12 %	- 17 %*	- 16 %*	- 6 %
Cell number PZ	- 6 %	- 16 %	- 21 %*	+39 %*
H/C Z	-			
23 %	- 20 %*	- 15 %	- 61 %*	
Total Growth Plate	- 14 %*	- 17 %*	- 18 %*	+ 16 %*

* = significantly different; $p \leq .05$
- = decrease; + = increase from correspondent controls.

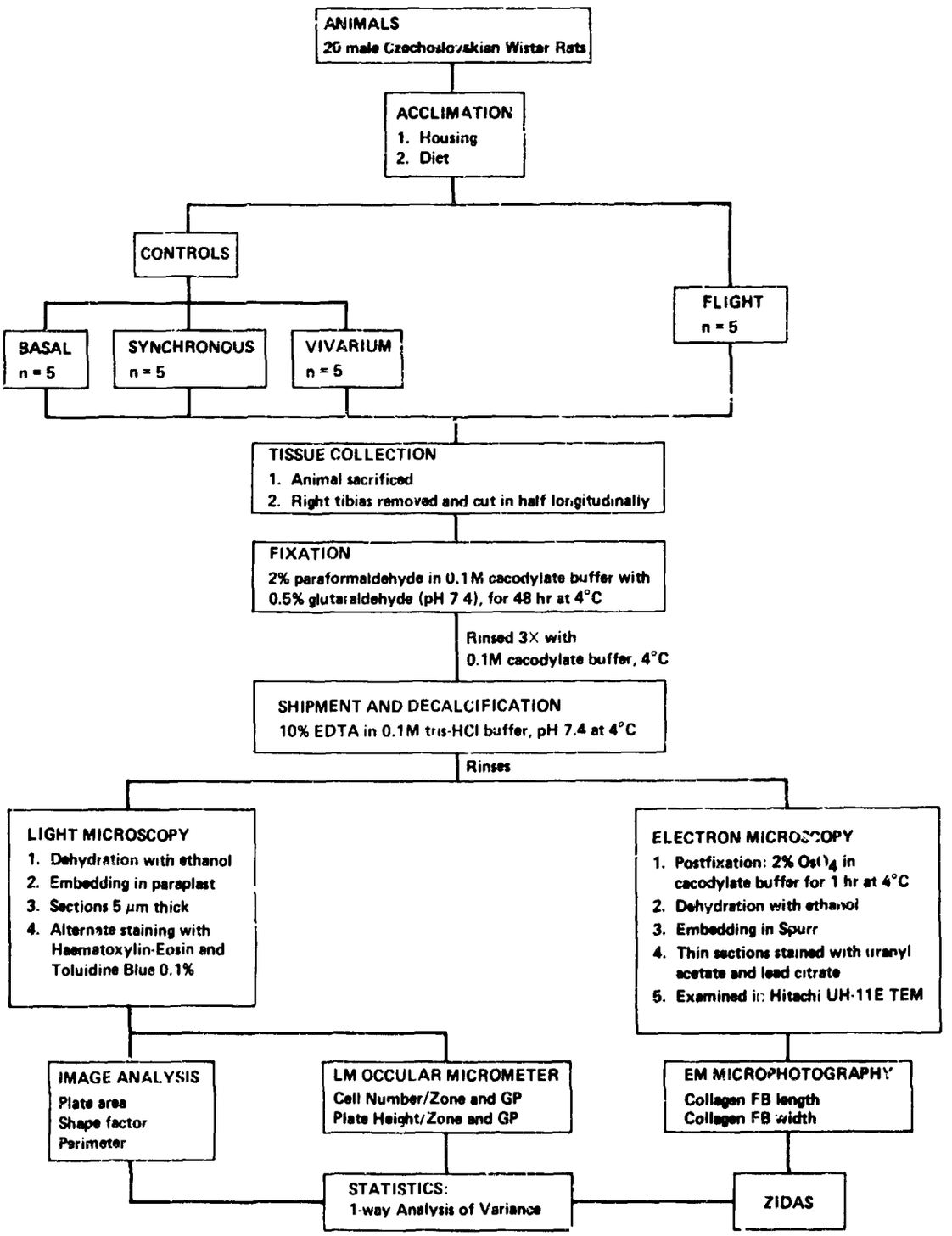

Figure 1. Flow chart of the general procedure followed in Experiment K-6-06: Morphometric and EM analyses of tibial epiphyseal plates from Cosmos 1887 rats.

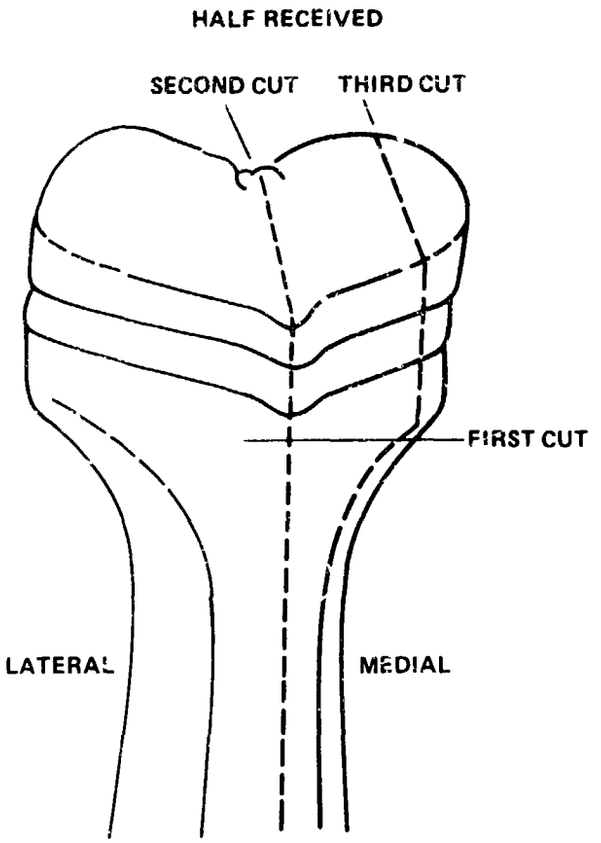

Figure 2. Dissection of right tibias.

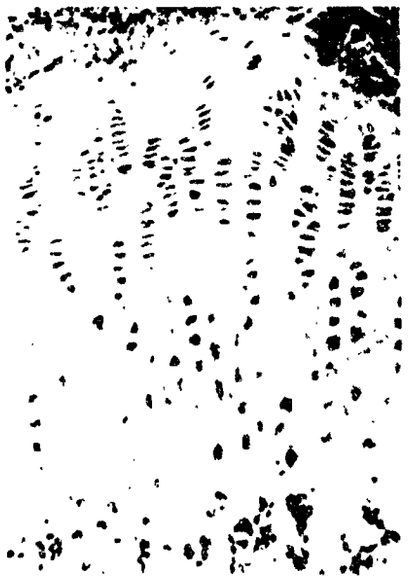

*Taken from Reinholt et al., 1984.

Resting: from upper plate border to top of first cell column.

Proliferative: ratio cell width/ height > 2.

Hypertrophic: ratio cell width/ height < 2.

Calcification: not distinguishable in decalcified sections.

Figure 3. Definitions of zones of growth plate.

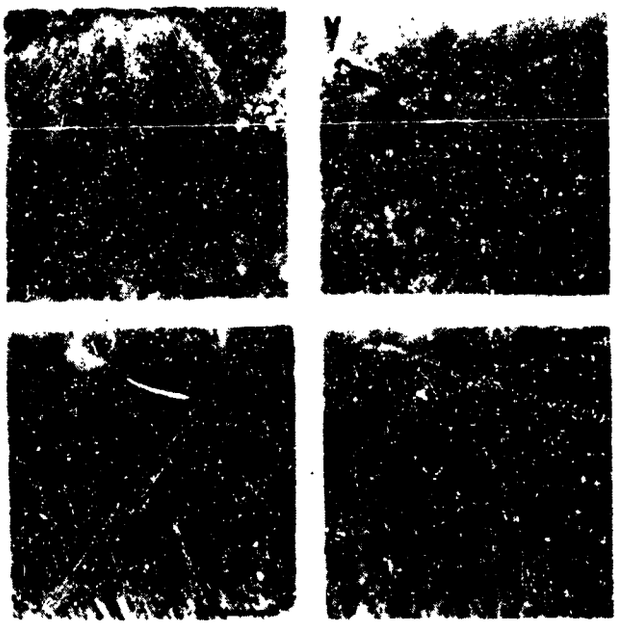

Figure 4. Representative sections of growth plates from each group.

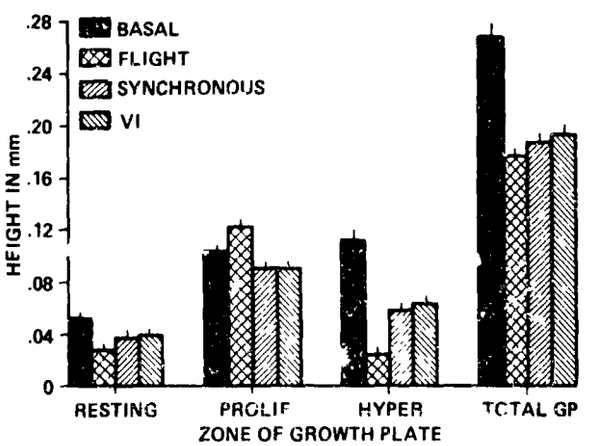

Figure 5. Mean height per zone and total growth plate. For detailed comparison between groups, refer to Table 1.

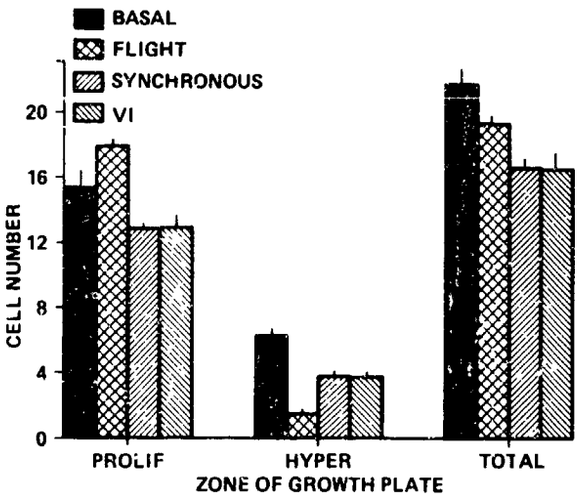

Figure 6. Mean cell number per zone and total growth plate. For detailed comparison between groups, refer to Table 1.

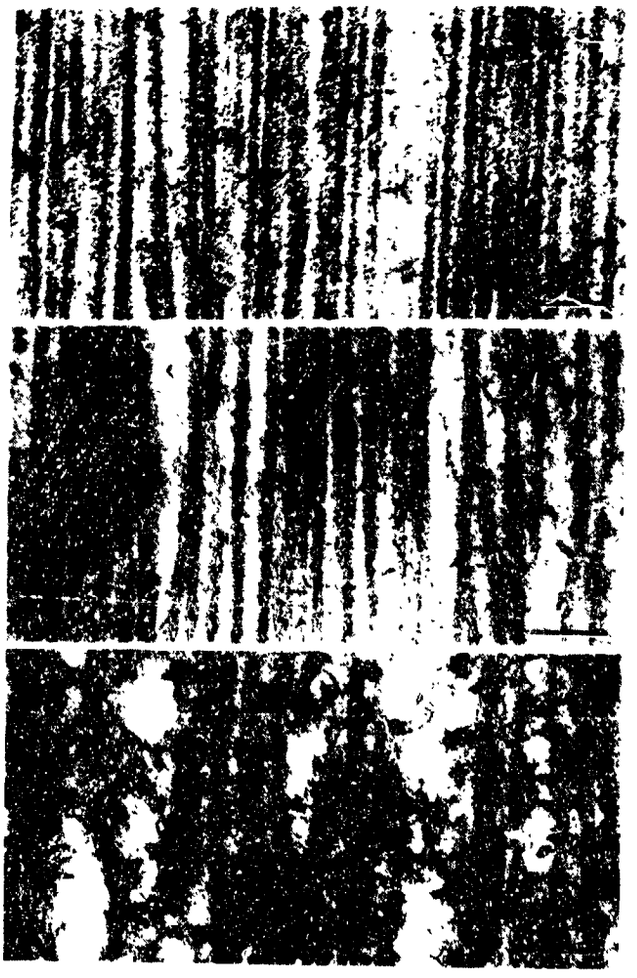

Figure 7. Representative collagen fibrils from each group.

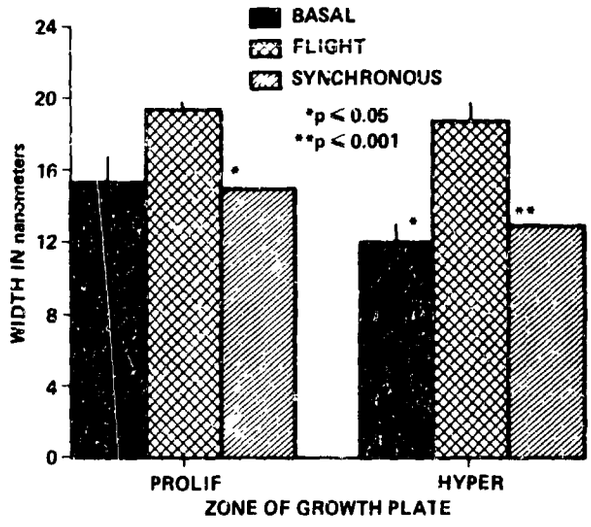

Figure 8. Mean collagen fibrial width per zone of growth plate.

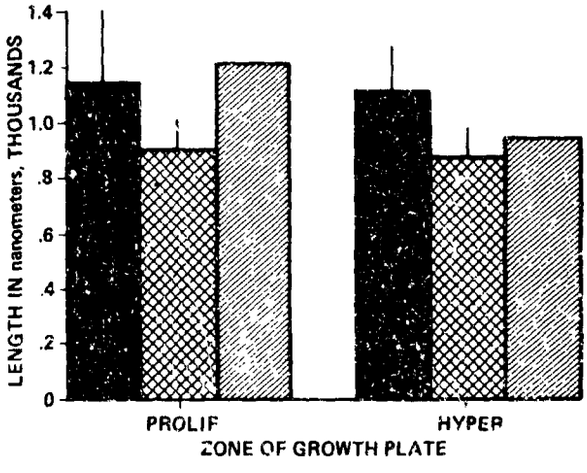

Figure 9. Mean collagen fibrial length per zone of growth plate.

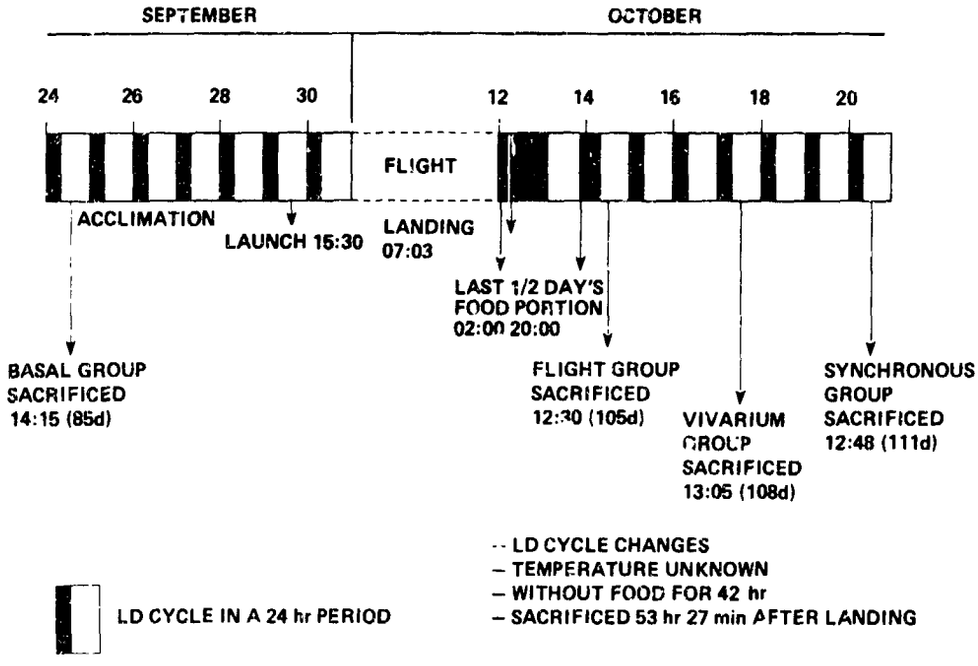

Figure 10. Time line for Cosmos 1887.

N90-26461

EXPERIMENT K-6-07

METABOLIC AND MORPHOLOGIC PROPERTIES OF MUSCLE FIBERS AFTER SPACEFLIGHT

Principal Investigator:

R. Edgerton
Department of Kinesiology
University of California
Los Angeles, California 90024-1568

Co-Investigators:

B. Miu
Thomas P. Martin
R. Roy
University of California
Los Angeles, California 90024

J. Marini
J.J. Leger
Unite' de Recherches Neurobiologique
INSERM U6
230 Bd Ste Marguerite
13009 Marseille, France

V. Oganov
E. Ilyina-Kakueva
Institute of Biomedical Problems
Moscow, USSR

INTRODUCTION

Based on previous Cosmos biosatellite and space shuttle (SL-3) flights, it is apparent that a variety of biochemical and physiological properties of rat skeletal muscle are altered following 5-22 days of exposure to microgravity (4,5,8,13,15a,18,19,20,22,23,24,29,30). Since these studies have been based primarily on the analysis of whole muscle properties and given the potential difference in the response of muscle fibers differing in alkaline adenosine triphosphatase type (ATPase) and size, the adaptation to space flight of single muscle fibers were studied. The purposes of this study were 1) to define the size and metabolic and responses of single fibers to space flight and 2) to determine the specificity of these responses to the muscle and the myosin type and size of its fibers. The present findings also permit a comparison with similar data obtained from the ground-based experimental model hindlimb suspension, which is intended to simulate the conditions of space flight (7,9,10,28). Previous studies using hindlimb suspension suggest that the magnitude of the adaptive response of fibers is dependent on the muscle and the ATPase type properties of its fibers (7,9,28). The present data suggest that some fibers acquired a higher glycolytic potential (alpha-glycerolphosphate dehydrogenase; GPD) and the rate at which they can hydrolyze ATP is increased. Further, the potential of the tricarboxylic acid cycle, as indicated by succinate dehydrogenase activity (SDH), was maintained or elevated depending on the muscle and ATPase type. These data suggest a shift in the metabolic profile of the fibers to that consistent with the fast oxidative-glycolytic profile defined by Peter et al. (2,1). Also, in the present data the degree of atrophy in the flight muscles depended more on the muscle and the region of the muscle than on fiber type as defined by ATPase staining or the immunohistochemical properties. The similarities between these data those from a previous space shuttle flight (SL-3) and those of hindlimb suspension are striking (7,9,10,28).

METHODS

Five male rats, body weight = 303.2 $\pm$ 2.4 ($\bar{X}$ + SE), flown on Cosmos 1887 for 12.5 days were studied. An additional five rats, body weight = 349.0 $\pm$ 5.8, were maintained under identical ground based conditions (cage size, temperature, lighting, and food and water availability) for the duration of the mission and acted as a synchronous control. Details of the experimental protocol related to flight conditions are described elsewhere. Ground based control rats were killed on a similar time schedule as the flight rats. From each rat, the left soleus (SOL) and the medial gastrocnemius (MG) muscles were resected, weighed. The muscle was mounted on cork and frozen in freon cooled in liquid nitrogen. All samples were maintained at -70^{o}C until analyzed. Frozen serial tissue sections (10mm thick) were cut at -20^{o}C in a cryostat. Sections were prepared for the qualitative histochemical determination of alkaline (pH 8.8) myofibrillar ATPase staining density in a population of fibers from each muscle according to the modification of Brooke and Kaiser (2) as described by Nwoye et al (17). Fiber cross-sectional areas also were determined from these ATPase-stained sections. The same fibers from serial sections were subsequently prepared for the determination of SDH and GPD activity as described by Martin et al. (16). Frozen sections of the Sol were also reacted to antibodies for slow and fast myosin. Fasicles of fibers free of tissue artifact and considered visually to be representative of the tissue section were chosen for analyses. A computer assisted image analysis system was used to quantify the reaction product based on the rate of change of optical density (OD) for each fiber. The rate of staining (OD/min) was directly proportional to the enzyme activity as reported by Martin et al. (3,16). The hardware and software components of this system have been described previously (2,4,16).

RESULTS

Cross Section Area

Mean wet muscle weights of the flight and control rats were 130.4 and 153.4g, a 15% decrease (Fig. 1). Muscle fiber cross sectional area (CSA) in the Sol was about 50% lower in flight than control rats. The percent difference in CSA in the Sol between flight and control was similar in light and dark ATPase as well as those that stained moderately with ATPase. The mean wet weights of the flight and control MG were 634.9 and 754.9g, a 16% decrease. The mean CSA of the light and dark ATPase fibers of the deep MG were 17 and 28% smaller than control while the dark ATPase fibers of the superficial MG were 15% smaller (Fig. 1). Based on the population distribution of each of the ATPase types in the Sol and MG, it is clear that a general downward shift in the CSA of the population of fiber occurred (Fig 2 and 3) as opposed to an apparent shift in any portion of the population

Succinate Dehydrogenase Activity

Mean SDH activity was unchanged for each of the ATPase categories in the Sol (Fig. 4). However examination of the population distribution for SDH activity suggests a slight shift toward higher activities in the light ATPase fiber and a slight downward shift in the dark ATPase fibers (Fig.5). To reflect the total amount of enzyme that may have changed per muscle fiber, the product of activity and CSA were calculated. These results show that the net amount of the SDH enzyme, assuming no change in specific enzyme activity, was significantly lower than control in each ATPase type of the Sol in the flight rats (Fig.4).

In the MG the mean SDH activity remained at control levels in the flight rats for each ATPase type. The population distributions also suggest that no changes occurred in SDH activity (Fig. 7). Further, there was no effect of flight on the integrated SDH activity in any ATPase type in the MG (Fig. 6).

Glycerolphosphate Dehydrogenase Activity

In the Sol, mean GPD activity was elevated significantly in the dark, but not in light or intermediate ATPase types in the flight rats (Fig.8). In control and flight rats the dark ATPase fibers of the Sol had higher GPD activity than the light ATPase fiber. Based on the population distribution it can be seen that values of near zero activity in the dark ATPase fibers were rare in the flight, but common in the control rats (Fig. 9).

In the MG there were no GPD activity changes due to flight in either of the ATPase types in either the deep or superficial regions (Fig. 10). In control rats the GPD activities of each ATPase type differed between the Sol and MG. For example, GPD of the light ATPase fiber was lower in the MG than the Sol while in the dark ATPase fiber GPD was lower in the Sol than the MG. The dark ATPase fiber of the superficial MG had the highest GPD activity of any fiber. In both control and flight rats, GPD activity had a skewed distribution with a predominence of low values in the deep MG while the population distribution was normal in the superficial MG (Fig.11). There was a strong hint of a shift toward higher GPD values in the superficial MG of flight compared to control, although the mean was not significantly different.

The integrated GPD (GPD activity x CSA) of each ATPase type in both muscles was similar in the control and flight rats (Fig. 8 and 10), suggesting no net change in the amount of this enzyme per fiber. This is quite remarkable, particularly, for the Sol given the marked atrophy that occurred in this muscle.

Enzyme Activity Ratios

In the Sol the GPD:SDH activity ratio was elevated in the dark ATPase fiber, but not in the light or intermediate ones. In control rats, the GPD;SDH ratio was higher in the light than dark ATPase fibers. In the flight rats, the dark ATPase fibers had the higher ratio, thus reflecting the large increase due to flight on this one ATPase type.

In the MG the GPD:SDH activity ratios were unaffected by flight. The magnitude of the ratios were light ATPase,deep < dark ATPase, deep < dark ATPase, superficial, with these mean ratios differing by 40-fold. The mean GPD:SDH ratios were about 10-fold higher in the MG than the Sol (Fig.12).

Immunohistochemistry and Myosin ATPase Staining

Immunohistochemical reactions were completed in the Sol of 4 control and 4 flight rats (Table 1). One antibody was used to label slow myosin and one to label fast myosin. These results were then compared with the qualitative myosin ATPase staining reaction as well as to SDH and GPD activities and finally fiber size (Table 2). Based on these antibody reactions, fibers were separated into Type I (reacted only to slow antibody), Type "IIc" (reacted to both slow and fast myosin antibodies) and IIa+b (reacted only to fast myosin antibody).Using this approach 77.9% of the Sol fibers were Type I in the control rats compared to 60.2% in flight rats (Table 1). There were 8.0% "IIc" fibers in control and 30.9% in flight rats. The remaining percent of Type II(a+b) fiber in the control was 14.0% and in the flight rats, 9.0%.

Based on myosin ATPase staining at a basic pH, 15.9% of the fibers were darkly stained in control and 20.3% in flight rats. It appears that the immunohistochemically defined "IIc" fibers in control rats were consistently categorized as darkly stained with myosin ATPase, base (Table 2). However, in the flight rats it appears that the newly occurring "IIc" fibers did not fall consistently into either the light or dark ATPase category (Table 1 and 2). There was about a 4-fold greater proportion of "IIc" fiber (8.0% vs. 30.9%) in flight than control rats while the difference in proportion of dark ATPase fibers suggested only approximately a 28% increase (15.9% vs. 20.3%). In the flight rats it appears that there was a reduction in percent type I, increase in "IIc" and reduction in percent IIa+b (Table 1).

In a select group of fibers identified as reacting to slow and fast antibodies from 2 control and 2 flight rats, a profile of other features were compared at the single fiber level so as to determine the degree to which they could be associated with other quantitative measures (Table 2). The profiles of individual IIc fibers in the two control rats (S6, n=2 and S7, n=6) more closely match the dark ATPase profile with respect to myosin ATPase stain, SDH activity, and CSA. In two flight rats (F8, n=7, and F9, n=9) the "IIc" fibers could not be clearly associated with either ATPase type and the related enzyme properties. In the flight rats it is clear that some of the "IIc" fibers were categorized as light and some dark myosin ATPase. The mean profiles of light and dark ATPase fiber in Table 2 were derived from the mean of all of the fibers analyzed for rats S7, F8 and F9.

DISCUSSION

Data from previous Cosmos flights have demonstrated that a space flight of 5-22 days results in muscular atrophy (4,5,8,13,18,19,20,22,23,29,30). The decreased muscle mass observed in the present study are consistent with these reports. While both the Sol and MG of the flight animals showed atrophy based on fiber CSA,the degree of atrophy was different among the muscles, e.g., the SOL being the more than twice as atrophic as the MG. Further, the atrophy in the super region of the MG was less than in the deep region. This differential response among muscles and muscle regions to adaptive perturbations has been a common finding in many studies (7) and is similar to the responses to hindlimb suspension (8,28). A direct comparison of the fiber size changes in the

7-day shuttle flight (SL-3) and the present 12.5 day Cosmos 1887 flight can be made since the same muscles were studied using the same procedures in the same laboratory. The overall CSA of the Sol of SL-3 rats suggested 35% atrophy compared to 45% in the present Cosmos data. Similar comparisons of the MG suggests 16% atrophy occurred in the SL-3 rats and 20% in the Cosmos 1887 rats.

In addition to the specificity of the effect of space flight on certain muscles and fiber types, there seems to have been an unequal effect of space flight on various muscle proteins. For example, the cross-sectional areas of both light and dark ATPase fibers in the flight SOL and MG were reduced while the SDH and GPD activities in these fibers remained the same or were enhanced. Identical conclusions were made from similar studies of the 7-day flight SL-3 rats (15a). A preferential loss of muscle volume (and probably contractile protein) relative to metabolic enzymes in the muscles may account for the fact that SDH and GPD activity was essentially maintained after 12.5 days of flight. If the net rate of degradation and synthesis of SDH or GPD was unchanged per fiber, or reduced by a lesser amount relative to other proteins, and assuming no change in the specific activity, enzymatic activity would be elevated proportionate to the reduction in fiber volume. Stated more simply, if the number of SDH or GPD molecules per fiber had remained the same or decreased less than fiber volume, the enzyme activity would be elevated. Based on this concept, the average light or dark ATPase fibers of the SOL may have lost about 40% of the total amount of the SDH enzyme per fiber (product of CSA and SDH activity = integrated OD) even though the SDH activity, which reflects its concentration, remained virtually the same as control levels. Using this same rationale, the low ATPase fibers in the flight MG had control levels of SDH per fiber. Similar calculations were made for GPD among the different fiber types and muscles. These results suggest no net changes in the number of GPD enzyme molecules per fiber as a result of flight. This was true for all ATPase types in the Sol and MG. The integrated enzyme activities in the present study were also similar to that observed in the SL-3 rats. In the Sol, it does appear, however that the loss of SDH per fiber was about twice as great in the Cosmos than the SL-3 rats. Obviously, an important question in considering the effects of long-term space flight is whether there is some point in time at which these proteins and the cell volume reach a homeostatic state.

The quantitative histochemical assessment of single fibers enzyme activities after a 12.5 day flight study showed that oxidative and glycolytic metabolic capacity essentially is maintained or enhanced following space flight just as has been reported in the same muscles after a 7 day flight It is interesting to note that based on qualitative visual assessments of oxidative enzymes in previous studies or rats flown on a Cosmos biosatellite, the oxidative capacity of the SOL appeared to have been reduced (13). However, the glycolytic potential of the SOL was reported to have increased (13). This latter but not the former observation has now been confirmed using quantitative analyses after two space flight studies. Also, a shift in the SOL muscle LDH isoform profile toward the predominant M-isoform has been reported in flight animals (22). These glycolytic enzyme data are consistent with the present study in that slow muscles (SOL) tend to develop characteristic of fast muscles (which also have a high relative glycolytic potential). The GPD activity data suggest that some flight muscles may have an elevated capacity to utilize carbohydrate derived carbon sources. It is of interest to note that the glycogen content of both the SOL and EDL was elevated in SL-3 flight rats relative to control (11) even though the rats had remained at 1G for about 11 hours after the 7 days at 0G.

In SL-3 rats there was an increase in the biochemically assayed myofibrillar ATPase activity of a homogenate of the flight SOL. This was consistent with the increase in the percentage of fibers that stained darkly with ATPase and the enhanced GPD activity. These two enzymes have been shown to be highly correlated and to remain so in the face of marked alterations in the properties of a muscle as occurs in chronically spinalized animals (25). The increase in myofibrillar ATPase activity measured in the homogenate of the SL-3 rat Sol and the higher proportion of dark ATPase fibers in this muscle are consistent with the report of an increase in the fast myosin light chain isozymes in the SOL of a previous Cosmos study (30). However, there are other data from a

Cosmos flight in which myosin ATPase activity in the SOL of rats was reduced (13). This latter finding appears to have been an anomaly. The conversion of light ATPase staining fibers to dark staining in SL-3 rats did not completely reflect the quantitative myofibrillar ATPase changes reported (15a).

Based on the present results, the significance of the previously reported increase in percentage of dark ATPase fibers has additional significance. For example, in the present study there was an increase in percent dark ATPase fibers using a basic pH as there was in SL-3 rats. However, this may underestimate the number of fibers that were induced to synthesize fast myosin. Based on immunohistochemical identification of slow and fast myosin types 31% of the Sol fibers contained both slow and fast myosin types. In control rats, only 8% had this property. However, in flight rats, the percentage of slow fibers based on myosin ATPase, basic pH, was overestimated when compared to the percentage that reacted positively to only a slow antibody (80% vs. 60%). It appears that about 10% of the fibers in the Sol of flight rats had begun to synthesize fast myosin, but was not reflected in an enhanced myosin ATPase staining reaction. This is as it might be expected in that the more sensitive indication of fast myosin would be expected to be immunological. Fibers that stain darkly at an acid and basic pH when staining for myosin ATPase have been call IIc fibers. In the present work when there was a immunohistochemical identification of both myosin types we have labeled them "IIc".

Although it appears that most of the nearly acquired "IIc"fibers in the Sol of the flight rats develop from light ATPase fibers (commonly called Type I), it is possible that some of the dark ATPase (Type II) fibers that normally would have reacted only to a fast myosin antibody, also reacted positive to a slow myosin antibody after flight. When comparing each of the parameters studied with respect to their ATPase type the "IIc" fibers resembled the dark ATPase fibers more than the light ATPase fibers Table 2. This was the case in comparing the SDH and GPD activities, as well as CSA.

The interrelationship between ATPase, SDH and GPD activity in the fibers of the flight muscles suggests that the metabolic profiles found in normal rats also occur in fibers following exposure to microgravity. In the SOL more fibers stained darkly with the ATPase stain in the flight than control rats. In conjunction, it appears that these same fibers maintained or increased their GPD activity while maintaining their SDH activity. As a result, a greater percentage of fibers in these muscles could be categorized as fast oxidative-glycolytic. This shift in metabolic profile apparently occurred at the expense of slow oxidative fibers.

The explanation of why muscles atrophy in space flight and why the effect of space flight differs among muscles has not been defined clearly. Based on carcass composition and the weights of various vital organs, the rats flown aboard the space shuttle mission, SL-3, were healthy and experienced minimal stress (8). It is unlikely that the changes observed in the present study can be attributed to factors associated with increased levels of glucocorticoids. However, a general loss of muscle mass is consistent with the decrease in the growth hormone observed in the pituitary gland of SL-3 rats (12). Also, the in vivo release of growth hormone from pituitary gland cells decreased in the SL-3 animals (12).

The present study demonstrates that the general capability of skeletal muscle to maintain its proteins decreases rapidly in response to space flight. The present findings suggest further that the magnitude of enzymatic and cell volumes changes in response to space flight depend on several factors including the muscle and its fiber type composition. It appears that in order to associate physiological relevance to the observed enzymatic changes, cell volume should be considered also. Although it remains unclear as to the stimulus, or lack of stimulus, that triggers the rapid changes in muscle proteins in response to space flight, ground-based models of muscle atrophy suggest that the reduction in mechanical loading of muscle may be more important than the total amount of activation over a 24-hr period (1).

REFERENCES

1. Alford, E.K., Roy, R.R., Hodgson, J.A. and Edgerton, V.R. Electromyography of rat soleus, medial gastrocnemius and tibialis anterior during hindlimb suspension. *Exp. Neurol.* 96:635-649, 1987.

2. Brooke, M.H. and K.K. Kaiser. Muscle fiber types: How many and what kind? *Arch. Neurol.* 23:369-379, 1970.

3. Castleman, K.R., L.A. Chui, T.P. Martin, and V.R. Edgerton. Quantitative muscle biopsy analysis. *Monographs in Clinical Cytology.* Basal, Karger, 1984, 101-116.

4. Castleman, K.R., L.A. Chui and J.P. Vandermeulen. Spaceflight effects on muscle fibers. IN: *Final Reports of U.S. Experiments Flown on Soviet Satellite Cosmos 936,* edited by S.N. Rosenzweig and K.A. Souza, Houston, TX:NASA, 1978, p. 274-289. (NASA Tech. Memo. 78526).

5. Chui, L.A. and K.R. Castleman. Morphometric analysis of rat muscle fibers following space flight and hypogravity. *Physiologist.* 23:S76-S78, 1980.

6. Fast, T., R. Grindeland, M. Ruder, M. Vasques, P. Lundgren, S. Scibetta, J. Tremor, P. Buckendahl, L. Keil, O. Chee, T. Reilly, B. Dalton, and P. Callahan. Rat maintenace in the animal holding facility during the flight of Spacelab 3. *Physiologist* 28:375, 1985.

7. Fitts, R.H., J.M. Metzger, D.A. Riley, and B.R. Unsworth. Models of disuse: a comparison of hindlimb suspension and immobilization.*J. Appl. Physiol.: (Respirat. Environ. Exercise Physiol.)* 60:1946-1953,1986.

8. Grindeland, R., T.Fast, M. Ruder, M. Vasques, P. Lundgren, S. Scibetta, J. Tremor, P. Buckendahl, L. Keil, O. Chee, T. Reilly, B. Dalton, and P. Callahan. Rodent body, organ, and muscle weight responses to seven days of microgravity. *Physiologist* . 28:375, 1985.

9. Hauschka, E.O., Roy, R.R. and Edgerton, V.R. Size and metabolic properties of single muscle fibers in rat soleus after hindlimb suspension. *J. Appl. Physiol.: (Respirat Environ. Exercise Physiol.)* 62:2338-2347, 1987.

10. Hauschka, E.O., Roy, R.R., and Edgerton, V. R. Periodic weight support effects on rat soleus fibers after hindlimb suspension. *J. Appl. Physiol.: (Respirat. Environ. Exercise Physiol.)* (In Press).

11. Henriksen, E.J., M.E. Tischler, S.Jacob, and P. H. Cook. Muscle protein and glycogen responses to recovery from hypogravity and unloading by tail-cast suspension. *Physiologist.* 28:376, 1985.

12. Hymer, W.C., R. Grindeland, M. Farrington, T. Fast, C. Hayes, K. Motter, and L.Patil. Microgravity associated changes in pituitary growth hormone (GH) cells prepared from rats flown on Space Lab 3: Preliminary results. *Physiologist.* 28:377, 1985.

13. Ilyina-Kakueva, E.I., V.V. Portugalov, and N.P. Krivenkova. Space flight effects on the skeletal muscles of rats. *Aviat. Space Environ. Med.* 47:700-703, 1976.

14. Jenkins, W.T. and M.M. Marshall. A modified direct phosphate assay for studying ATPases. *Anal. Biochem.* 141:155-160, 1984.

15a. Martin, T.P., V.R. Edgerton and R.E. Grindeland. Influence of spaceflight on rat skeletal muscle. *J. Appl. Physiol.* 65: 1988.

15. Lowry, O.H., N.J. Rosebrough, A.L. Farr and R.J. Randall. Protein measurements with folin phenol reagent. *J. Biol. Chem.* 193:265, 1951.

16. Martin, T.P., A.C. Vailas, J.B. Durivage, V.R. Edgerton, and K R. Castleman. Quantitative histochemical determination of muscle enzymes: Biochemical verification.*J. Histochem.Cytochem.* 10:1053-1059, 1985.

17. Nwoye, L., W.F.H.M.,Mommaerts, D.R. Simpson, K. Seraydarian, and M. Marusich. Evidence for a direct action of thyroid hormone in specifying muscle properties. *Am. J. Physiol. (Regulatory Integrative Comp. Physiol.*)11.242: R401-R408, 1982.

18. Oganov, V.S.,S.A. Skuratova,A.N. Potapov, and M.A. Shirvinskaya. Physiological mechanisms of adaptation of rat skeletal muscles to weightlessness and similar functional requirements. *Physiologist.* 23:S16-S21, 1980.

19. Oganov, V.S. and A.N. Potapou. On the mechanisms of changes in skeletal muscles in the weightless environment. *Life Sciences and Space Research XIV.* 18th Plenary Meeting of COSPAR and Symposium on Gravitational Physiology, Bulgaria, 1975.

20. Oganov, V.R., Rakhmanov, A.S., Skwatova, S.A., Shirvins-Kaya and V.S. Magedov. Functions of skeletal muscles of rats and monkeys after 5-day spaceflight (On Cosmos-1514). *Proceed 2nd Int. Conf. Space Physiol.*, Toulouse, France, 1985

21. Peter, J.B., R.J. Barnard, V.R. Edgerton, G.A.Gillespie, and K.E.Stempel. Metabolic profiles of three fiber types of skeletal muscle in guinea pigs and rabbits. *Biochem.* 11:2627-2633, 1972.

22. Portugalov,V.V. and N.V. Petrova. LDH isoenzymes of skeletal muscles of rats after space flight and hypokinesia. *Aviat. Space Environ. Med.* 47:834-838, 1976.

23. Rapcsak, M., V.S. Oganova, A. Szoor, S.A. Skuratova, T. Szilagyi, and O. Takacs. Effects of weightlessness on the function of rat skeletal muscles on the biosatellite COSMOS-1129.*Acta Physiol. Hung.* 62:225-228, 1983.

24. Riley, D.A., S. Ellis, G.R. Slocum, T. Satyanarayana, J.L.W. Bain, and F.R. Sedlak. Hypogravity-induced atrophy of rat soleus and extensor digitorum longus muscles. *Muscle Nerve.* 10:560-568, 1987.

25. Roy, R.R., Sacks, R.D., Baldwin, K.M., Short, M. and Edgerton, V.R. Interrelationships of contraction time, Vmax and myosin ATPase after spinal transection. *J. Appl. Physiol.*: (*Respirat. Environ. Exercise Physiol.)* 56:1594-1601, 1984.

26. Roy, R.R., Baldwin, K.M., Martin, T.P., Chimarusti, S.P., and Edgerton, V.R. Biochemical and physiological changes in overloaded fast-and slow-twitch ankle extensors.*J. Appl. Physiol.: (Respirat. Environ. Exercise Physiol.)* 59:639-649, 1985.

27. Roy, R.R., Hutchinson, D., Edgerton, V.R. Electromyography of rat ankle extensors and flexors during treadmill locomotion at varying speeds and grades. *Med. Sci. Sports. Ex.* 18:545, 1986.

28. Roy, R.R., Bello, M.A., Boissou, P. and Edgerton, V.R. Size and metabolic properties of fibers in rat fast twitch muscles after hindlimb suspension. *J. Appl. Physiol. : (Respirat. Environ. Exercise Physiol.)* 62:2348-2357, 1987.

29. Szilagyi T., A. Szoor, O. Takacs, M. Rapcsak, V.S. Oganov, S.A. Skuratova, S.S. Oganesyan, L.M. Murashko, and M.A. Eloyan. Study of contractile properties and composition of myofibrillar proteins of rat skeletal muscles with different functions in experiment of biosatellite Cosmos-1129. *Acta Physiol. Hung.* 62:228-233, 1983.

30. Takacs, O., M. Rapcsak, A. Szoor, V.S. Oganov., T. Szilagyi, S.S. Oganesyan, and F. Guba. Effect of weightlessness on myofibrillar proteins of rat skeletal muscles with different functions in experiment of biosatellite COSMOS-1129. *Acta Physiol. Hung.* 62:228-233, 1983.

31. Tibbits,G.F., Barnard, R.J., Baldwin, K.M., Cugalj, N. and Roberts, N.K. Influence of exercise on excitation-contraction coupling in rat myocardium. *Am. J. Physiol.* 240:H472-H480, 1981.

TABLE 1. FIBER TYPE POPULATIONS BASED ON IMMUNOHISTOCHEMISTRY AND MYOSIN ATPASE

	Immunohistochemistry				Myosin ATPase (pH 8.8)		
Animal	I	IIc	IIa+b	Total	Light	Dark	Total
S6	1326	49	257	1632	1712	397	2109
%	**81.3**	**3.0**	**15.7**		**81.2**	**18.8**	
S7	1544	152	160	1856	1612	220	1832
%	**83.2**	**8.2**	**8.6**		**88.0**	**12**	
S8	865	192	188	1245	1555	398	1953
%	**69.5**	**15.4**	**15.1**		**79.6**	**20.4**	
S9	1249	94	267	1610	1619	346	1965
%	**77.6**	**5.8**	**16.6**		**82.4**	**17.6**	
S10	-	-	-	-	1133	132	1237
%					**89.3**	**10.7**	
Mean							
%	**77.9**	**8.0**	**14.0**	**100**	**84.1**	**15.9**	**100**
F6	1065	522	160	1747	1393	307	1700
%	**61.0**	**29.9**		**9.2**	**81.9**	**18.1**	
F7	-	-	-	-	1764	494	2258
%					**78.1**	**21.9**	
F8	1050	440	157	1647	1498	382	1880
%	**63.8**	**26.7**	**9.5**		**79.7**	**20.3**	
F9	1178	542	125	1845	1223	339	1568
%	**63.8**	**29.4**	**6.8**		**78.3**	**21.7**	
F10	582	418	118	1118	1474	362	1836
%	**52.1**	**37.4**	**10.6**		**80.3**	**19.7**	
Mean							
%	**60.2**	**30.9**	**9.0**	**100**	**79.7**	**20.3**	**100**

TABLE 2: CHARACTERISTICS OF "IIC" FIBERS IDENTIFED IMMUNOHISTOCHEMICALLY

Rat	Fiber Identification	*Antibody S - F	Myosin Type	SDH (OD/Min x 10^{-4})	Area (μm^2)	GPD (OD/min x 10^{-4})
S6	38	+ +	dark	629	4067	0**
	49	+ +	dark	610	4554	1
S7	19	+ +	dark	711	4184	18
	8	+ +	light	485	3295	26
	65	+ +	interm	504	2855	16
	67	+ +	dark	559	3372	15
	55	+ +	dark	582	4592	17
	24	+ +	dark	516	3423	19
***Overall Mean Profile, S7		+ -	Light	310	5048	6.9
		- +	Dark	548	4006	5.9
F8	1	+ +	dark	428	1741	14
	12	+ +	light	330	1420	10
	26	+ +	dark	403	1519	15
	38	+ +	light	343	1457	10
	77	+ +	dark	363	1593	18
	48	+ +	dark	353	1915	11
	23	+ +	dark	468	1115	19
***Overall Mean Profile, F8		+ -	Light	258	2236	5
		- +	Dark	444	2107	19
F9	75	+ +	light	449	2088	10
	80	+ +	dark	515	2263	8
	54	+ +	dark	485	1108	28
	66	+ +	dark	393	2274	21
	77	+ +	dark	485	2418	33
	68	+ +	light	419	2387	13
	25	+ +	light	338	4283	15
	27	+ +	light	434	3223	26
	40	+ +	dark	460	1868	25
***Overall Mean Profile, F9		+ -	Light	344	2771	8
		- +	Dark	502	2170	28

*Positive reaction to slow (+) or fast (+) antibody
**GPD mean of population of fibers were also unusally low.
***Means based on ATPase type of population of S7,F8, or F9.

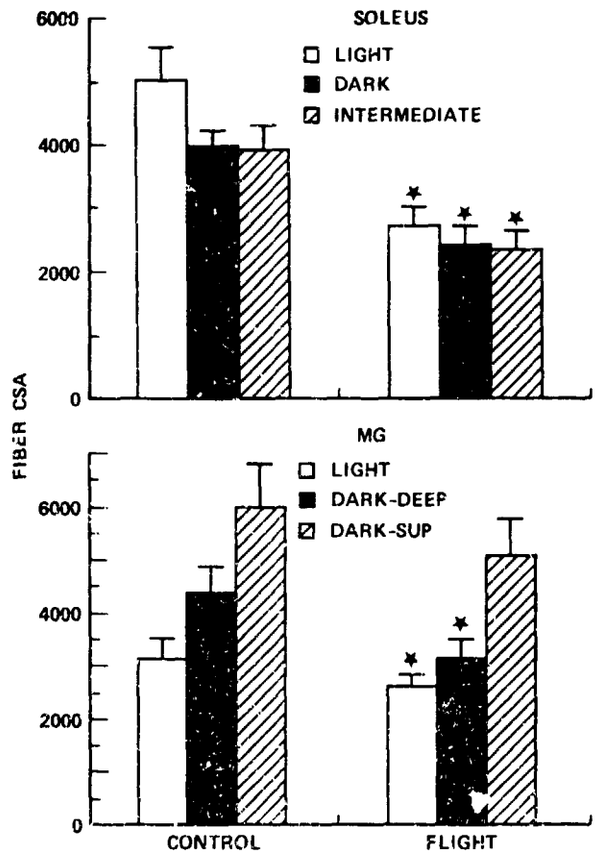

Figure 1. Mean fiber cross-sectional area (CSA, μm^2) of light, dark and intermediate ATPase fibers of the Sol and MG of control and flight rats Vertical bars are SEM. Light and dark ATPase fibers of the deep and dark fibers of the superficial region of the MG are illustrated. *, significant difference between control and flight. $p < 0.05$.

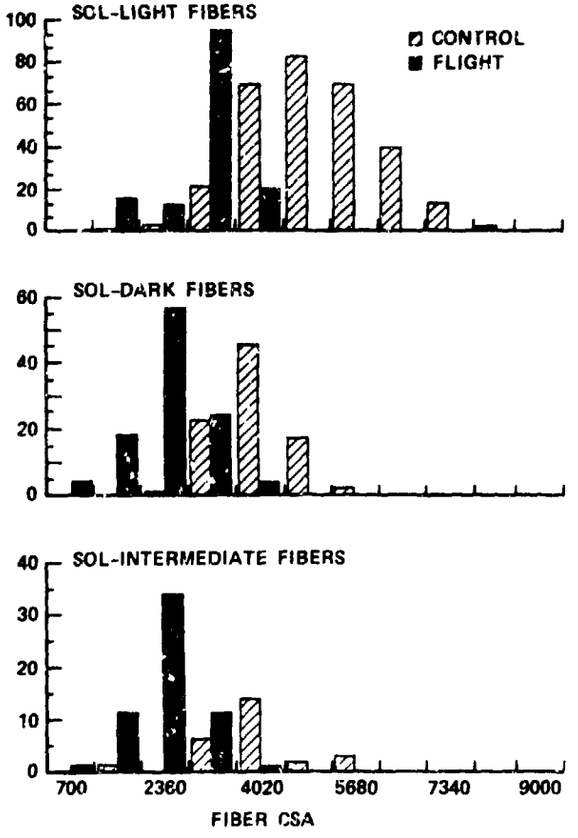

Figure 2. Frequency distributions of fiber cross-sectional area (CSA, μm^2) for light, dark and intermediate ATPase fibers of the Sol of control and flight rats.

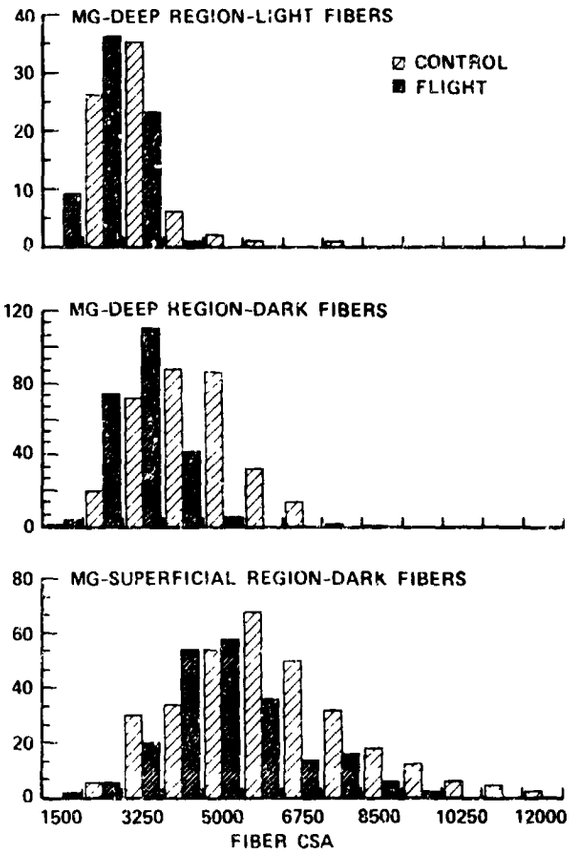

Figure 3. Frequency distributions of fiber cross-sectional area (CSA, μm^2) for light and dark ATPase fibers in the deep and dark ATPase fibers in the superficial region of MG of control and flight rats.

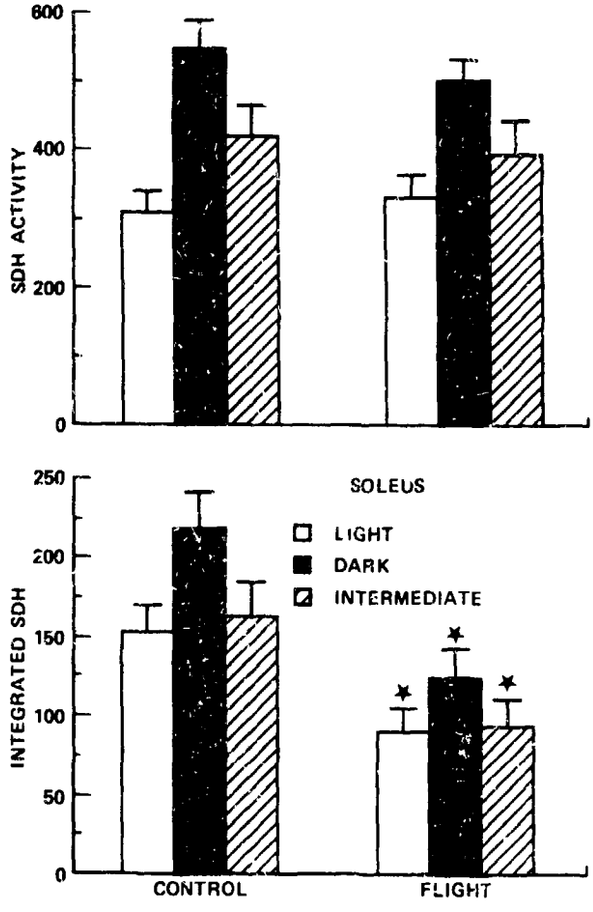

Figure 4. The mean ± SEM of SDH activity (OD/min x 10^{-4}) and integrated SDH (CSA x OD/min) for light, dark and intermediate ATPase fibers of the Sol of control and flight rats. *, $p < 0.05$.

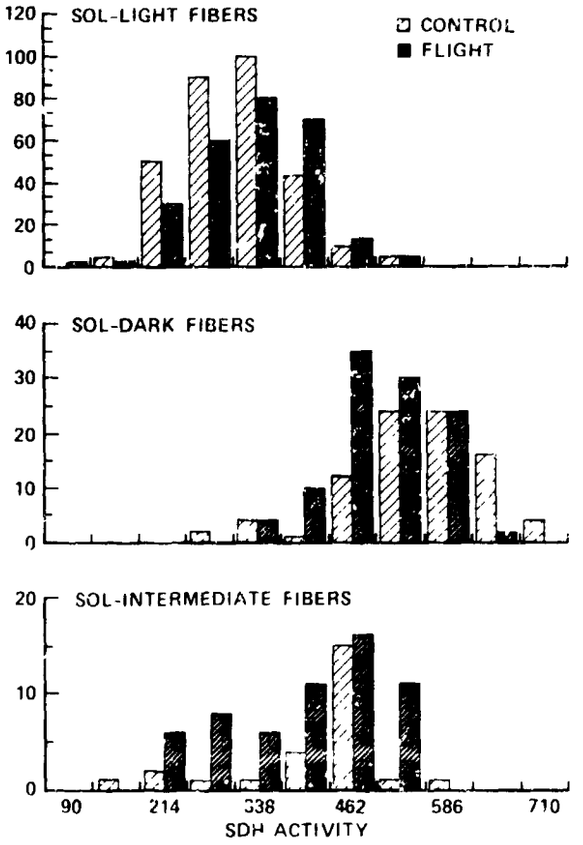

Figure 5. Freq' ency distributions of SDH activity (OD/min x 10^{-4}) for light, dark and intermediate ATPase fibers of the Sol of control and flight rats.

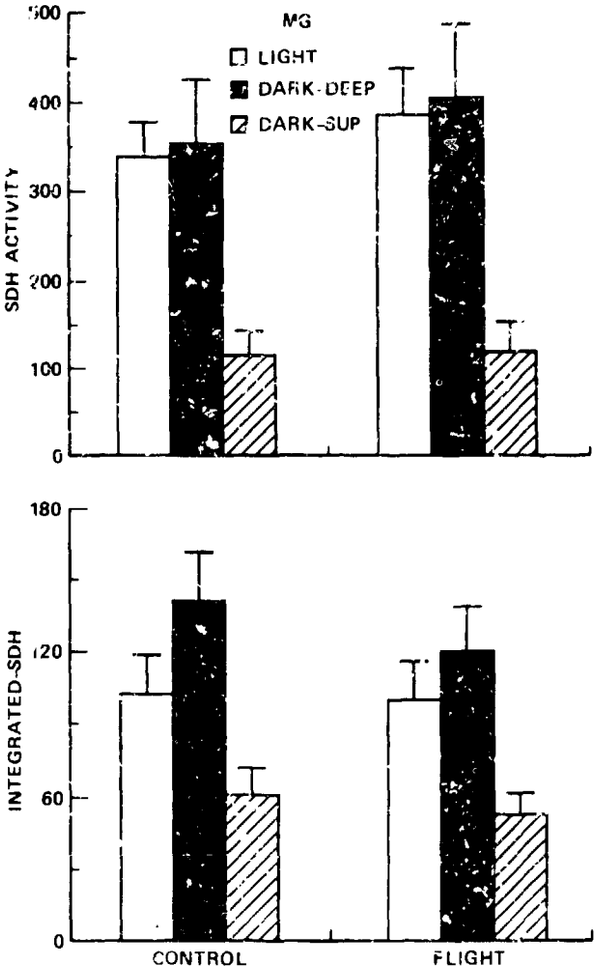

Figure 6. The mean ± SEM of SDH activity (OD/min x10^{-4}) and integrated SDH (CSA x OD/min) for light and dark ATPase fibers in the deep region and dark ATPase fibers of the superficial region of the MG of control and flight rats.

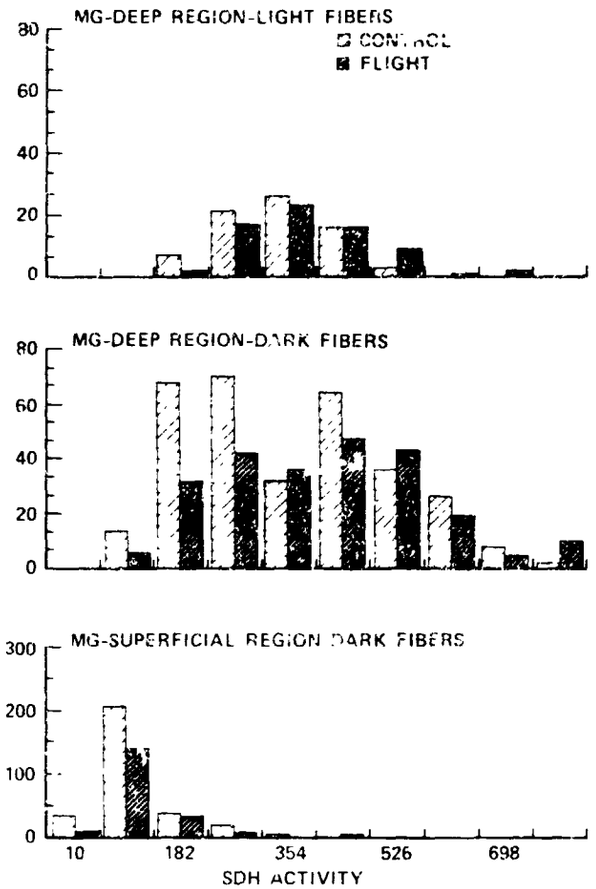

Figure 7. Frequency distributions of SDH activity (OD/min x10^{-4}) for light and dark ATPase fibers of the deep and dark ATPase fibers of the superficial MG of control and flight rats.

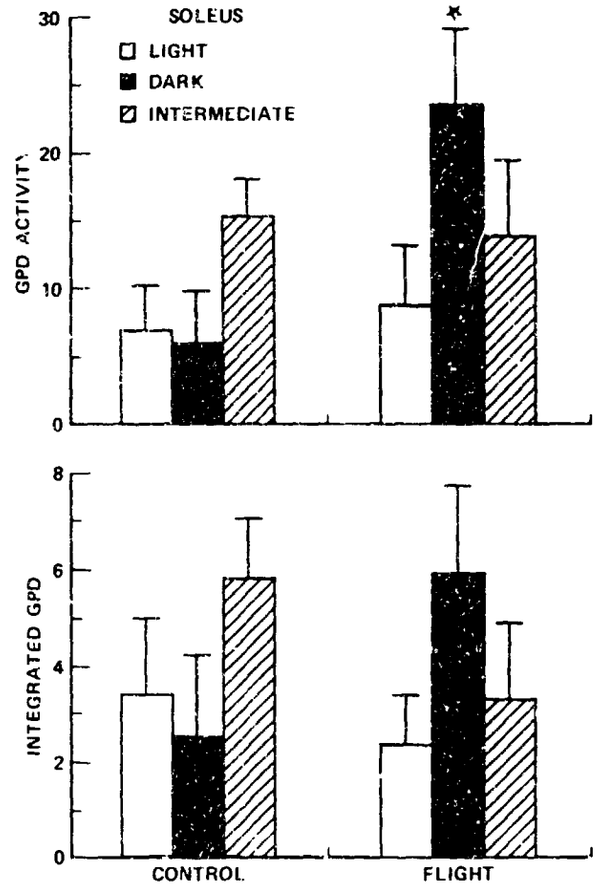

Figure 8. The mean ± SEM of GPD activity (OD/min x 10^{-4}) and integrated GPD (CSA x OD/min) for light, dark and intermediate ATPase fibers of the Sol of control and flight rats. *, $p < 0.05$.

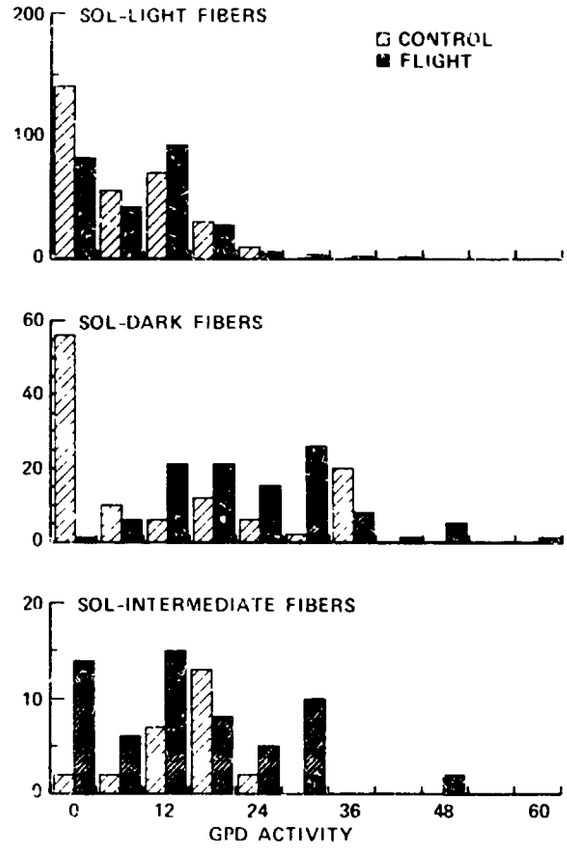

Figure 9. Frequency distributions of GPD activities (OD/min x10^{-4}) for light, dark and intermediate ATPase fibers of Sol of control and flight rats.

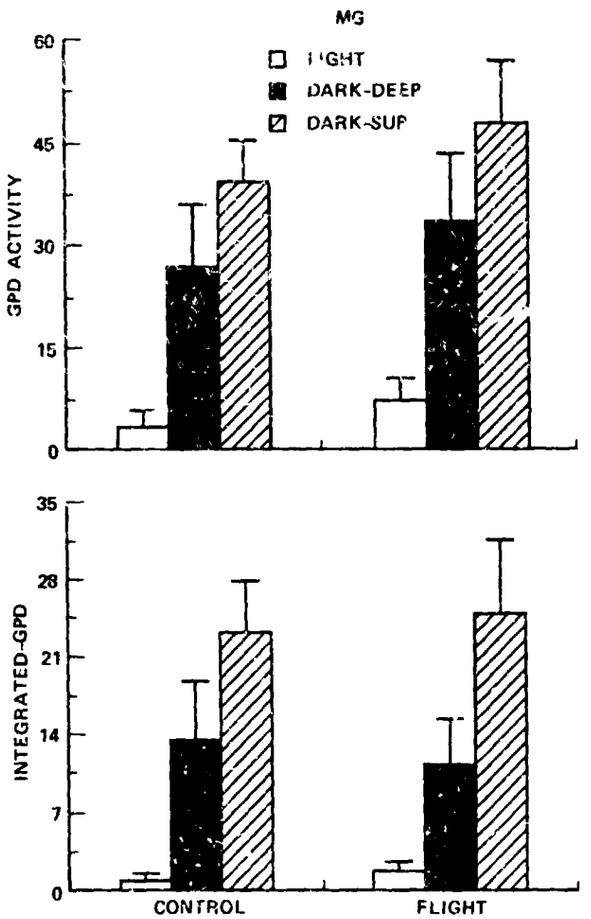

Figure 10. The mean ± SEM of GPD activity (OD/min x 10^{-4}) and integrated GPD (CSA x OD/min) for light and dark ATPase fibers of the deep and dark ATPase fibers of the superficial MG of control and flight rats.

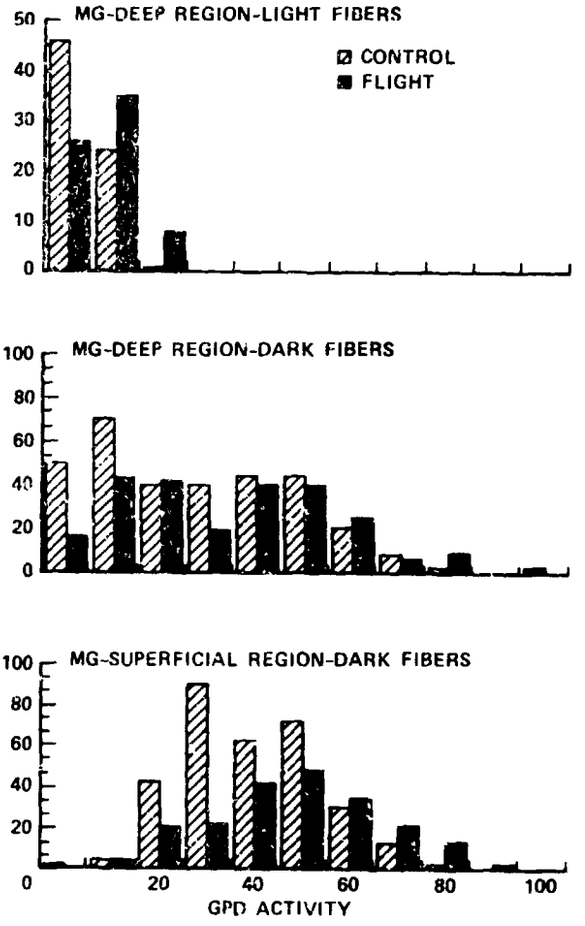

Figure 11. Frequency distributions of GPD activities (OD/min x 10^{-4}) for dark and light ATPase fibers of the deep and dark fibers of the superficial region of control and flight rats.

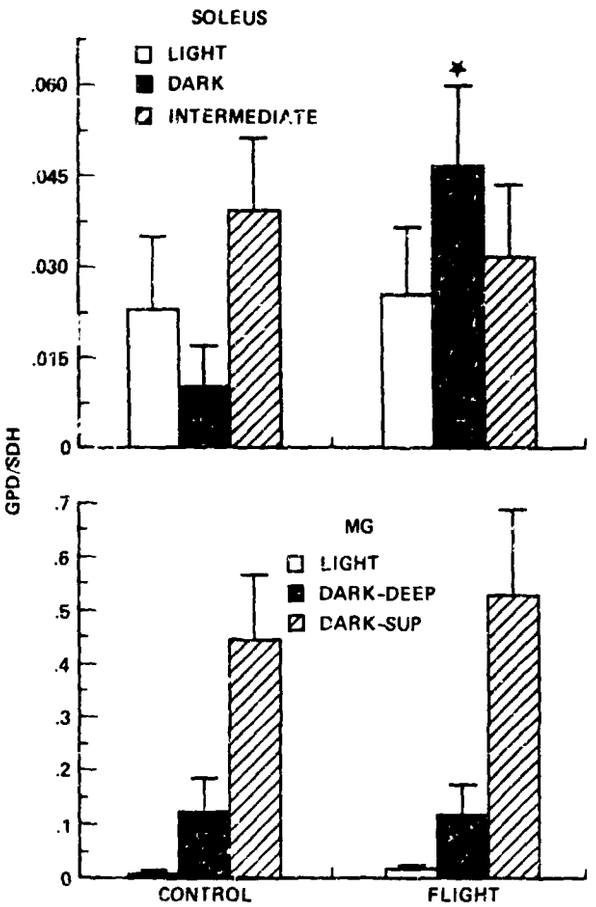

Figure 12. The mean ± SEM of GPD/SDH for light, dark and intermediate ATPase fibers of the Sol, and light and dark ATPase fibers of the deep region and dark ATPase fibers of the superficial region of the MG of control and flight rats. *, $p < 0.05$.

N90-26462

EXPERIMENT K-6-08

BIOCHEMICAL AND HISTOCHEMICAL OBSERVATIONS OF VASTUS MEDIALIS

Principal Investigator:

X. J. Musacchia
Department of Physiology & Biophysics
University of Louisville
Louisville, Kentucky 40292

Co-Investigators:

J. M. Steffen
Department of Biology
University of Louisville

R. D. Fell
Exercise Physiology Laboratory
University of Louisville

V. S. Oganov
Institute of Biomedical Problems
Moscow, USSR

PRECEDING PAGE BLANK NOT FILMED

INTRODUCTION

Muscles of the hindlimb in the rat have been used to demonstrate the effects of unloading in weightlessness and in animal models used to mimic weightlessness. This report deals with the vastus medialis (VM). Samples were obtained from rats exposed to weightlessness for 12 days in Cosmos 1887 (Experiment K-6-08, coordinated by Dr. V.S. Oganov).

The VM in the rat is chiefly composed of fast twitch fibers, comparably divided between oxidative glycolytic and glycolytic types (Ariano, et al., 1973). In many respects it is similar to the extensor digitorum longus (EDL), chiefly fast twitch fibers (97%), oxidative glycolytic and glycolytic (59 and 38%, respectively) and a few (3%) slow twitch fibers (Ariano, et al., 1973). The VM and EDL are not load bearing muscles and, in addition to morphological similarity, it is reasonable to assume that there is some functional and metabolic similarity. We obtained the VM because of its availability and it afforded us an opportunity to compare data with the EDL which has been used in both microgravity flights (Ilyina-Kakueva, et al., 1976, Oganov and Potapov, 1976, Castleman and Chui, 1978, and Steffen and Musacchia, 1986) and earthside model experiments (Musacchia, et al, 1980, and Fitts, et al, 1986).

The EDL is recognized as being relatively unaffected by exposure to weightlessness for periods of seven (SL-3) to 22 (Cosmos 605) days (Steffen and Musacchia, 1986, and Ilyina-Kakueva, et al, 1976). Also, there is limited disuse atrophy in response to unloading in earthside laboratory experiments using both tail suspension (Jaspers and Tischler, 1986) and whole body suspension (Musacchia, et al., 1980) models.

The principal objectives of the present study were to ascertain if the VM responded to 12 days of microgravity exposure. Three approaches were used: (a) a histochemical evaluation of cellular morphology (fibers and capillaries), (b) an assessment of biochemical composition (protein, RNA and DNA concentrations) and (c) an estimation of metabolic activities and capacities (oxidative and glycolytic metabolism).

MATERIALS AND METHODS

Samples of muscles were obtained from five rats exposed to weightlessness for 12 days (F), basal control rats (B), vivarium control rats (V) and synchronous control rats treated comparably to rats exposed to weightlessness (S). Muscles were frozen in liquid nitrogen and shipped on dry ice to the University of Louisville. Samples from the belly of two muscles from rats in each group were examined histochemically for morphometric characteristics as in a previous report (Musacchia, et al., 1987). Frozen sections were stained for ATPase activity, muscle fibers and capillaries were differentiated. Fiber area and density measurements were made and capillary distribution was assessed. The remaining muscle samples were lyophilized, weighed and powdered with a Wiley Mill. Aliquots were used for protein (mg/mg dry wt.) RNA and DNA concentration determinations (ug/mg dry wt) as previously described (Steffen and Musacchia, 1986), for lactate dehydrogenase (LDH) (Pesce, et al., 1964), citrate synthase (CS) activities (μ moles/min/gm) (Srere, 1969), and lipoprotein lipase (LPL) activities (nmoles FA liberated) (Lithrell and Boberg, 1978).

RESULTS AND DISCUSSION

The principal objective of this study was to ascertain if the vastus medialis responded to 12 days of microgravity exposure. The loss in muscle mass (Table 1) is greatest, -43%, when comparing F vs B, and least, -13%, when comparing F vs. V. Taken at face value these differences may be misleading, due to the variability of the muscle weight in the basal group these muscle mass losses may be exaggerated. In terms of percent water, there were no differences between the flight and

the control groups. In spite of the limited sample, we conclude that muscle mass changes in the VM are not significant.

Comparing the VM from 12 day microgravity exposed rats and the EDL from seven days of microgravity exposured rats, there appears to be much similarity. The EDL lost about 10% mass and this was reflected in a comparison with vivarium weight matched controls (Steffen and Musacchia 1986). This figure compares favorably with the present 13% loss if one compares VM from flight subjects with vivarium controls.

The muscle specimens were found to be almost completely composed of type II fast twitch fibers. In the flight rats examined, there were significant reductions in fiber area (μM^2), i.e., about 30% when compared to basal subjects (Table 2). The fiber area in vivarium controls was comparable to that in flight subjects, however the data from synchronous controls was not uniform and did not provide a basis for comparison. Fiber density measurements (cells/mm^2) were inversely related to the area measurements. The limited morphological responses in the VM are comparable to the EDL after seven days of flight (Musacchia, et al., 1987).

Protein concentrations in flight, basal and synchronous subjects were comparable (0.7 to 0.8 mg/mg dry wt) (Table 3). However, the vivarium controls exhibited higher values (0.88 ± .06 mg/mg dry wt.). RNA concentrations in flight subjects (5.5 ± .1 µg/mg dry wt) were significantly reduced below basal controls (6.0 ± .1 µg/mg dry wt). RNA concentrations in flight subjects were not different from either vivarium (5.5 ± .1 µg/mg dry wt) or synchronous (5.1 ± .6 µg/mg dry wt) controls. DNA concentrations in flight, vivarium and basal subjects were similar (13 to 14 µg/mg dry wt), however, the synchronous controls exhibited markedly higher values (16.8 ± .9 µg dry wt). The biochemical profiles suggest that changes in the VM due to weightlessness were minimal. In this respect the VM is similar to the EDL, which was examined by us following the SL-3 mission (Steffen and Musacchia 1986).

The level of LDH activity (>2100) is characteristic of fast twitch highly glycolytic (type II B) fibers (Figure 1). Conversely, the oxidative capacity (circa 10 µ moles/min/gm) as measured by CS activity was low and characteristic of fast twitch muscle (Figure 2). These results are supported by the histochemical data.

LPL measurements indicate that enzyme activity in flight rats is lower than the vivarium and basal control roups (Figure 3). This could suggest that VM from flight rats had a reduced capacity to utilize stored triglycerides for energy production. However, the lack of difference between flight and synchronous control rats indicates that the previous deduction must be considered with caution.

CONCLUSIONS

Although some of the morphological parameters suggest a small degree of atrophy in the vastus medialis, the biochemical analyses (protein, RNA and DNA) suggest that these may be minimal and functionally nonsignificant. The relatively similar CS and LDH activities of VM from F and various control groups, as well as the lack of difference in LPL activity between F and S rats, suggests that there is little or no effect on the oxidative or glycolytic function of this muscle. Since the VM is chiefly a mixed fast twitch muscle, these metabolic indices of energy production are relatively unchanged. The results of VM studies are in agreement with our previous observations of another type II fast twitch muscle, the EDL, from SL-3 rats which did not respond markedly to weightlessness and whole body suspension.

ACKNOWLEDGEMENT:

We wish to acknowledge Kenneth A. Mook, M.J. Dombrowski and N. Dugan for technical assistance, and Dr. Richard E. Grindeland, NASA-Ames Research Center for providing the muscle samples. Also, we are grateful to Drs. E. Ilyina-Kakueva and V.S. Oganov, Institute of Biomedical Problems, Moscow, for their efforts in our behalf.

REFERENCES

1. Ariano, M.A., R.B. Armstrong and V.R. Edgerton. Hindlimb Muscle Fibers Population of Five Mammals. J. Histochem and Cytochem. 21: 51-55, 1973.

2. Castleman, K.R. and L.A. Chui Cosmos 936, Experiment K-2-08, Spaceflight Effect on Muscle Fibers. In: Final Report of U.S. Experiment Flown on the Soviet Satellite Cosmos 936 Eds: Rosenzweigh, S.N. and K.A. Souza. NASA TM 78526, 1978.

3. Fitts, R.H., J.M. Metzger, D.A. Riley , and B. R. Unswroth. Models of Disuse: A Comparison of Hindlimb Suspension and Immobilization, J.Appl. Physiol. 60 (6): 1946-1953, 1986.

4. Ilyina-Kakueva, E.I., V.V. Portugalov and N.P. Krivenkova. Space Flight Effect on the Skeletal Muscle of Rats, Aviat. Space and Environ. Med. 4: (7): 700-703, 1976.

5. Jaspers, S.R. and M.E. Tischler, Atrophy and Growth Failure of Rat Hindlimb Muscles in Tail Cast Suspension. J. Appl. Physiol 57: 1472-1479, 1986.

6. Lithrell, H. and J. Boberg. Determination of Lipoprotein Lipase Activity in Human Skeletal Muscle Tissue. Biochem. Biophys. Act. 528: 58-68, 1978.

7. Musacchia, X.J., D.R. Deavers, G.A. Meininger and T.P. Davis. A Model for Hypokinesia: Effects on Muscle Atrophy in the Rat. J. Appl, Physiol: Respirat, Environ. Exercise Physiol. 48: 479-486, 1980.

8. Musacchia, X.J., J.M. Steffen, R.D. Fell and J. Dombrowski. Physiological Comparison of Rat Muscle in Body Suspension and Weightlessness. The Physiologist. 30 (#1, suppl.): S-102-S-105, 1987.

9. Oganov, V.S. and A.N. Potapov, On the Mechanisms of Change in Skeletal Muscles in the Weightless Environment. In: Life Science in Space Research. Vol. XIV, Akademie-Verlag, Berlin, 1976.

10. Pesce, A., R.H. McKay, F. Stolzenback, R.D. Cahn and N.O. Kaplan. Comparative Enzymology of LDH. J. Biol. Chem. 239: 1753-1761, 1964.

11. Srere, P.A., Citrate Synthase. Methods Enzymol. 13:3-5, 1969.

12. Steffen, J.M. and X.J. Musacchia. Effect of Hypokinesia and Hypodynamia on Protein, RNA, and DNA in Rat Hindlimb Muscles. Am.J. Physiol. 247 (Reg. Integrat. Comp., Physiol. 16): R 728-R732, 1986.

TABLE 1

RAT, VASTUS MEDIALIS AND BODY WEIGHTS

Groups	Body Wt (gm)	Muscle Wt (mg)	Muscle Wt/B Wt	%Water
Flight	303 ±2.4	334 ± 41.1	1.1 ± 0.14	73.9± 2.16
Controls				
Basal	316 ± 8.3	586 ± 85.0	1.9 ± 0.28	74.2 ± 0.64
Vivarium	342 ± 7.7	386 ± 31.0	1.1 ± 0.08	75.5 ± 0.72
Synchronous	349 ± 5.8	427 ± 19.4	1.2 ± 0.04	75.8 ± 0.26

TABLE 2

RAT, VASTUS MEDIALIS, MORPHOMETRIC MEASUREMENTS

Groups	Rat Number	Fast Twitch Fibers Cross Sec * Area (μm^2)	Fast Twitch Fibers Density** (Cells /mm^2)	Capillary *** Density (cap/mm^2)
Flight	8	3889	249	565
	10	3852	253	725
Controls				
Basal	7	5536	190	374
	8	5201	202	409
Vivarium	6	3469	239	554
	9	3940	247	634
Synchronous	7	3562	156	390
	9	3962	266	673

Type II * number of cell areas measured; 40 or more
** number of cells counted; 70 to 100
*** number of capillaries counted; 300 to 700

TABLE 3

RATS, VASTUS MEDIALIS, BIOCHEMICAL OBSERVATIONS

Groups	Protein (mg/mg Dry Wt)	RNA (µg/mg Dry Wt)	DNA (µg/mg Dry Wt)
Flight	0.70 ± 0.07	5.5 ± 0.1	14.1 ± 0.6
Controls			
Basal	0.73 ± 0.66*	6.0 ± 0.1	13.9 ± 0.4
Vivarium	0.88 ± 0.06	5.5 ± 0.1	12.9 ± 1.4
Synchronous	0.81± 0.0o	5.1 ± 0.6	16.8 ± 0.9

*Mean ± S.E. N = 5

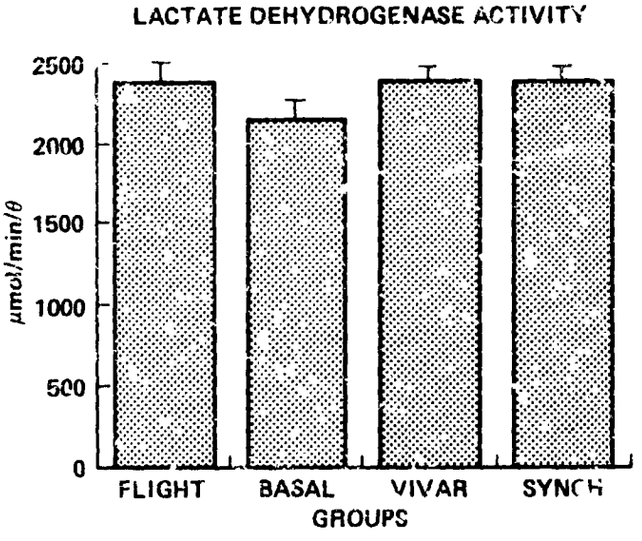

Figure 1. Lactate dehydrogenase activity of vastus medialis from rats: flight and control groups (5 in each group; mean and SEM).

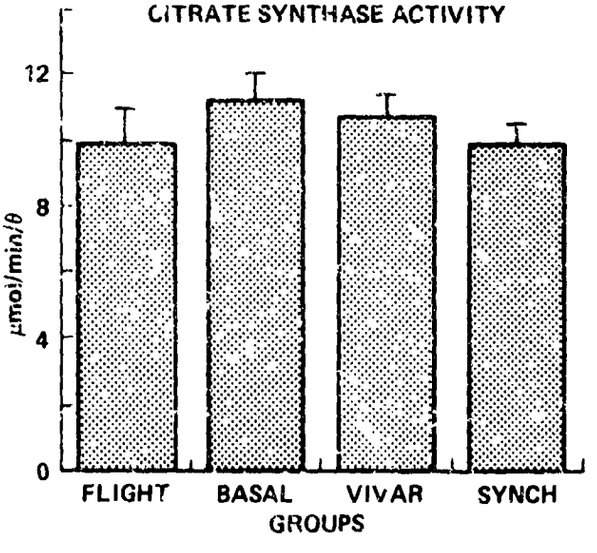

Figure 2. Citrate synthase activity of vastus medialis from rats: flight and control groups (5 in each group; mean and SEM).

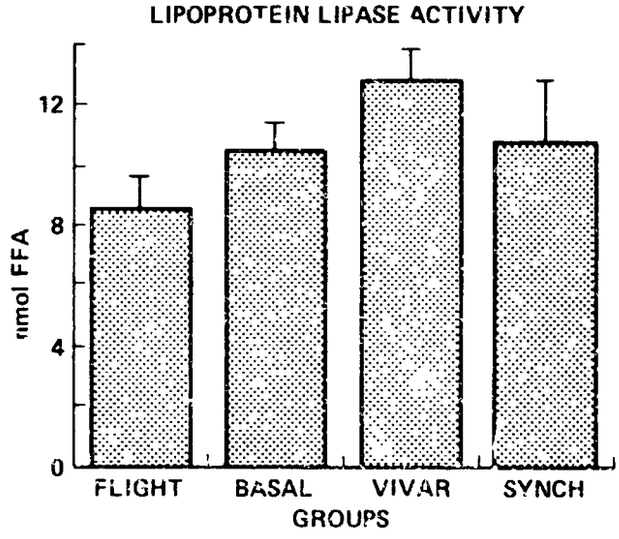

Figure 3. Lipoprotein lipase activity of vastus medialis from rats: flight and control groups (5 in each group; mean and SEM).

N90-26463

EXPERIMENT K-6-09

MORPHOLOGICAL AND BIOCHEMICAL INVESTIGATION OF MICROGRAVITY-INDUCED NERVE AND MUSCLE BREAKDOWN

PART I: INVESTIGATION OF NERVE AND MUSCLE BREAKDOWN DURING SPACEFLIGHT

PART II: BIOCHEMICAL ANALYSIS OF EDL AND PLT MUSCLES

Principal Investigator:

D.A. Riley
Department of Anatomy and Cellular Biology
Medical College of Wisconsin
Milwaukee, Wisconsin 53225

Co-Investigators:

S. Ellis
San Jose State University
San Jose, California

J. Bain, F. Sedlak, G. Slocum
Medical College of Wisconsin
Milwaukee, Wisconsin 53225

V. Oganov
Institute of Biomedical Problems
Moscow, USSR

EXPERIMENT K-6-09

PART I: INVESTIGATION OF NERVE AND MUSCLE BREAKDOWN DURING SPACEFLIGHT

D.A. Riley, J. Bain, F. Sedlak, and G. Slocum

SUMMARY

The present findings on rat hindlimb muscles suggest that skeletal muscle weakness induced by prolonged spaceflight can result from a combination of muscle fiber atrophy, muscle fiber segmental necrosis, degeneration of motor nerve terminals and destruction of microcirculatory vessels. Damage was confined to the red adductor longus (AL) and soleus muscles. The midbelly region of the AL muscle had more segmental necrosis and edema than the ends. Macrophages and neutrophils were the major mononucleated cells infiltrating and phagocytosing the cellular debris. Toluidine blue-positive mast cells were significantly decreased in Flight AL muscles compared to controls; this indicated that degranulation of mast cells contributed to tissue edema. Increased ubiquitination of disrupted myofibrils may have promoted myofilament degradation. Overall, mitochondria content and SDH activity were normal, except for a decrease in the subsarcolemmal region. The myofibrillar ATPase activity shifted toward the fast type in the Flight AL muscles. Some of the pathological changes may have occurred or been exacerbated during the 2 day postflight period of readaptation to terrestrial gravity. While simple atrophy should be reversible by exercise, restoration of pathological changes depends upon complex processes of regeneration by stem cells. Initial signs of muscle and nerve fiber regeneration were detected. Even though regeneration proceeds on Earth, the space environment may inhibit repair and cause progressive irreversible deterioration during long term missions. Muscles obtained from Flight rats sacrificed immediately (within a few hours) after landing are needed to distinguish inflight changes from postflight readaptation.

INTRODUCTION

Extended exposure of humans to microgravity produces progressive skeletal muscle weakness. The mechanism of the loss of strength must be understood in order to develop rational countermeasures. Our previous flight investigation of rats flown 1 week aboard Spacelab 3 (SL3) revealed that most of the soleus (Sol) muscle fibers exhibited simple atrophy, but up to 1% of the fibers showed segmental necrosis (Riley et al., 1987). Muscle atrophy and necrosis as well as evidence for degeneration of blood vessels and motor nerve terminals were observed previously for 3 week Cosmos Biosatellite missions (Gazenko et al., 1978; Baranski et al., 1979; Ilyina-Kakueva & Portugalov, 1981; Ilyin, 1983; Takacs et al., 1983). Disruption of motor innervation appears to occur after 1 week because neuromuscular junctions appeared normal in the SL3 Flight animals. In the present study, the sol, adductor longus (AL), plantaris (Plt), and extensor digitorum longus (EDL) muscles were examined from rats orbited 12.5 days in Cosmos 1887. These specimens allowed us to determine quantitatively that both muscle atrophy and necrosis were progressive. Furthermore, degeneration of microcirculatory vessels and motor nerve terminals were detected.

METHODS

Preparation of tissues. Selected muscles were obtained immediately following decapitation of rats from the Basal, Vivarium, Flight, and Synchronous groups. The caudal (posterior) one third of the AL and the distal third of the EDL muscles were removed by cutting with a fine scissors. Each

PRECEDING PAGE BLANK NOT FILMED

piece was separately pinned on a stretch on a flat stick. The specimens were fixed in vials for 2 to 12 hours at 20±2 deg C in 4% glutaraldehyde, 2% paraformaldehyde, buffered at pH 7.4 with 0.1 M cacodylate containing 5 mM $CaCl_2$. The vials were transferred to a refrigerator at 2 to 10 deg C for 24 or 50 hours until rinsed in the calcium containing buffer at room temperature for 3 hours. After rinsing, the specimens were removed from the sticks and postfixed for 2 to 2.5 hours in 1.3% osmium tetraoxide in the calcium- containing cacodylate buffer. The postfixed specimens were rinsed and stored in 0.1 M cacodylate buffer at 2 to 10 deg C for 3 to 6 weeks before routine dehydration in ethanols, clearing in propylene oxide and infiltration in epoxy resin. Half of each muscle was en bloc stained with uranyl acetate before initiating dehydration. Following resin polymerization at 60 and 90 deg C, semithin (0.5 μm) and ultrathin sections were cut for light and electron microscopic examination. Ultrathin sections were poststained with uranyl acetate and lead citrate before examination in a JEOL 100 CXII electron microscope.

Plt muscles and the remaining portions of the AL and EDL muscles were put individually on labeled index cards and quick frozen by immersing in liquid nitrogen. Frozen muscles were stored in liquid nitrogen until shipped at -70 deg C to the Medical College of Wisconsin. Upon arrival, portions of the frozen EDL and Plt muscles were removed by transecting with a cold razor blade to obtain specimens for assays of tripeptidyl aminopeptidase II, calcium activated protease, carbonic anhydrase III and parvalbumin by Dr. Ellis in San Jose State, California. These portions were repackaged and shipped on dry ice. The remaining specimens were stored in liquid nitrogen until frozen sectioned (10 μm) with a cryostat microtome at -25 deg C.

Tissue section staining. Serial sections were collected on glass slides and stained as follows: hematoxylin and eosin, toluidine blue, and histochemical enzyme activities of alkaline and acid myofibrillar ATPase, NADH and succinic dehydrogenase activities, alpha glycerophosphate dehydrogenase, and acid phosphatase as well as immunohistochemical localization of ubiquitin conjugates and tripeptidyl aminopeptidase (Riley & Allin, 1973; Riley et al., 1987; Haas, 1988; Riley et al., 1988a). Sections of Flight and Synchronous Sol muscles were kindly provided by Dr. Edgerton for H&E staining for assessment of atrophy and aberrant fiber content; this permitted comparison of changes in the Sol muscles of Cosmos 1887 and Spacelab 3.

Light microscopic quantitation. The percentages of aberrant fibers were determined in the H&E sections of AL, EDL, Plt and Sol muscles; aberrant fibers consisted of mononuclear cell-invaded fibers with segmental necrosis and small angular fibers with central nuclei.

Fast twitch glycolytic (FG), fast twitch glycolytic oxidative (FOG), and slow twitch oxidative (SO) were classified using the histochemical staining properties as defined previously (Riley et al., 1987). Alkaline ATPase reacted sections of AL muscles were utilized for areal measurements of SO and FOG fibers in all groups. At least 100 fibers of each type were traced on paper at a final magnification of X98.5 using a Tri Simplex projector. Fiber areas were determined by computerized planimetry of the traced images (Bioquant II). Similar areal measurements were performed on the SO, FOG, and FG fibers of the EDL and Plt muscles.

Mast cells were counted in sections of Flight and Synchronous AL muscles stained with toluidine blue. The number of cells was normalized per section, per section unit area, and per muscle fiber number.

Electron microscopic quantitation Z line length and mitochondrial content. The AL muscles of Flight rats nos. 7 and 9 showed much higher levels of fiber necrosis than Flight rats nos. 6, 8 and 10. Since it was difficult to assess atrophic changes in myofibrils and mitochondria of severely disrupted fibers, ultrastructural quantitation was performed in rats 6, 8 and 10. Two micrographs each of 7 fibers, chosen at random, were printed at 30,000 magnification. All of the Z lines totally within the micrograph were measured by the length paradigm on a computerized digitizing pad. The mean length was determined for each rat, and a grand mean was calculated for each group and

compared statistically. The concentrations of mitochondria in the subsarcolemmal region (3 μm depth), within A band and non-A band regions of the myofibrils in cross sections were determined for 10 fibers/rat by areal digitizing planimetry as described previously (Riley et al., 1987).

RESULTS

Muscle fiber type changes. In the alkaline myofibrillar ATPase reacted sections of AL muscles, the SO fibers were lightly stained, the FOG fibers were darkly stained and the intermediate fibers were moderately reactive (Figs. 1,2). The average number of intermediate fibers per section was 233±47 for Flight muscles which was significantly greater ($p<0.003$) than the number (19±17) in comparable Synchronous control sections. Since there was no difference in the average number of dark fibers in the muscles of the Flight and Synchronous groups (213±44 and 206±35, respectively) the intermediate fibers represented transformation of the lightly staining fibers to moderately staining fibers.

The percentages of fiber types was determined for the Flight and Synchronous AL, EDL, and Plt muscles (Table 1). The Flight AL muscles showed an 18% increase in intermediate fibers and a concomitant decrease in SO fibers. No changes in fiber type percentages occurred in the Flight EDL and Plt muscles.

Muscle fiber atrophy. Overall, the mean cross sectional area of Flight AL fibers was 36% less than that of the Synchronous control (Figs. 1-4). When assessed at the fiber type level, the average area of SO fibers in the ATPase sections of Flight AL muscles was significantly ($p<0.001$) less (43.8%) than that of the Synchronous controls (Table 2). The approximately 16% atrophy of the intermediate and FOG fibers in Flight AL muscles was not significantly different from values for comparable fiber types in the Synchronous controls (Table 2).

On the basis of the myofibrillar ATPase reaction three fiber types were defined in the EDL and Plt muscles. SO fibers were light, FOG fibers were dark, and FG fibers were moderate (Riley et al., 1982). The mean areas of all three fiber types were decreased in both muscles (Table 2). For the Plt, the decrease was significant for all fiber types; in the EDL, only the atrophy of the FOG fibers was significant.

Occurrence of aberrant muscle fibers. Two types of aberrant fibers were observed at the light microscopic level: small angular fibers with central nuclei (Fig. 3) and fibers exhibiting segmental necrosis with partial or total invasion by mononucleated cells (Figs. 2,4,5,6). Pronounced interstitial edema was present in the AL and Sol Flight muscles, but not in the EDL and Plt Flight muscles (Figs. 5,6). Flight AL muscles contained both types of aberrant fibers with segmental necrosis accounting for more than 80% of the aberrant fiber population. The Synchronous, Vivarium, and Basal control muscles possessed only the small angular type of aberrant fibers; this was also true for both the EDL and Plt muscles. The mean percentage of aberrant fibers was significantly increased in the Flight AL muscles compared to the control values (Table 3). There were no significant differences in aberrant fiber content between the control groups (Table 3).

The Flight Sol (n=3) exhibited significantly ($p<.001$) more (6.8±0.8%) necrotic fibers compared to only 0.9±0.1% in the Synchronous control (Fig. 6). As in the AL, greater than 80% of the damaged fibers in the Flight Sol were undergoing segmental necrosis. No necrotic fibers were present in the EDL and Plt Flight muscles. Aberrant fibers in these muscles were all angular fibers with central nuclei, and no differences in the mean percentages of aberrant fibers per muscle section was observed for either the EDL Flight (.07±.03%) and Synchronous (.07±.02%) muscles (n=3 rats) or the Plt Flight (.12±.02%) and Synchronous (.08±.02%) muscles (n=3 rats).

Toluidine blue-stained mast cells were counted in sections of Flight and Synchronous AL muscles. In both groups, degranulation was rare. The vast majority of cells were densely packed with blue

granules (Fig. 7). Flight ALs had fewer mast cells/section (4.5±1.3) than that of Synchronous muscles which contained 8.8±1.1 cells/section ($p<.05$, 1 tailed t-test). When the number of mast cells was normalized to muscle fiber number, the Flight muscles continued to show a significant ($p<.05$) decrease compared to control (4 mast cells/1000 muscle fibers versus 7 mast cells/1000 fibers, respectively).

Mononucleated cells infiltrated the necrotic regions of muscle fibers (Fig. 8). These cells were darkly reactive for acid phosphatase activity, suggesting the presence of lysosome-rich macrophages (Fig. 9).

The protease, tripeptidyl aminopeptidase (TAP), was localized immunohistochemically within Synchronous and Flight AL muscle sections, and serial ATPase sections corroborated fiber types. In the control, SO fibers were moderately immunoreactive for TAP, and the FOG fibers exhibited high reactivity (Fig. 10). Omission of the primary antiserum eliminated this immunostaining (Fig. 11). The SO fibers atrophied to a greater extent than FOG fibers in the Flight AL muscles. The FOG fibers retained high levels of TAP immunoreactivity whereas SO fiber staining ranged from below to above that of the control (Fig. 12).

The SO and FOG fibers in the Synchronous control AL muscles possessed moderate immunoreactivity for ubiquitin conjugates (Fig. 13). Specificity of the immunostaining was verified by leaving out the primary ubiquitin conjugate antibodies (Fig. 14). Immunostaining of atrophic fibers in the Flight AL muscles ranged from diminished to markedly elevated. Fibers manifesting elevated immunofluorescence, were not stained uniformly throughout the sarcoplasm (Fig. 15).

Ultrastructural properties of Flight AL and EDL muscles. The AL and EDL muscles were well preserved and free of fixation artifacts, except for swelling and extraction of mitochondria deep within the tissue block where fixation by immersion was not rapid. For the present study, comparisons of structure were made in the well fixed superficial regions. In addition, the structure of the Flight muscles was more severely affected by spaceflight in the midbelly (endplate) region than the proximal and distal ends. Therefore, comparable regions were compared for Flight and controls when assessing changes. For both the AL and EDL muscles, no detectable differences in morphology were evident between the Synchronous, Vivarium and Basal control groups.

At the ultrastructural level, muscle fiber atrophy and necrosis were evident in the Flight AL muscles (Figs. 16,17). On average, 3.8±.2% of the subsarcolemmal area (3 μm deep) was occupied by subsarcolemmal mitochondria in the Flight muscles compared to 5.5±.2% in the Synchronous controls (Figs. 18,19). This 31% decrease was significant ($p<.005$) and consistent with the observed reduction in peripheral SDH histochemical staining of Flight AL muscle fibers (not illustrated). The content of mitochondria in the A bands of the Flight AL muscles was increased 4 fold compared to the Synchronous control value (0.8±.01% versus 0.2±.04%, respectively, $p<.005$) (Figs. 20,21). A 28% increase in the mitochondrial content of the non-A band was detected (Flight 11.3±1.6% versus Synchronous 8.8±.3%), but this difference was not statistically significant (Figs. 20,21).

Atrophy of the myofibrils of AL Flight muscles was quantitated by measuring the length of the Z lines viewed in longitudinal section (Figs. 22,23). The mean length of Z lines in Flight AL (413±17 nm) was significantly ($p<.005$) less than that of the Synchronous controls (538±7 nm).

Closer to the midbelly region of the Flight AL muscles, the myofibrils were disrupted in addition to being reduced in size (Figs. 24,25). There was longitudinal streaming of the Z bands and loss of sarcomere banding (Fig. 24). In the transition zone from intact myofibrils to complete disruption, the Z bands were reduced to very short, punctate densities (Fig. 25). Other portions of the fiber

lacked thick filaments and exhibited large Z band-like densities on bundles of actin-like filaments (Fig. 25).

Muscle fiber disruption and cellular infiltration. Normal AL muscle fibers of the Synchronous controls contained well organized contractile proteins and peripheral myonuclei (Figs. 16,26). The rich vascularity of the muscle was evidenced by the numerous capillaries surrounding the fibers (Fig. 16). Distributed among the atrophic fibers of the Flight muscles were damaged fibers exhibiting segmental necrosis (Figs. 27,28). The lesions were segmental because in both directions away from the damage site the fiber was intact and exhibited simple atrophy. At the lesion, the cell membrane was violated, and the fiber was invaded by macrophages, neutrophils, occasional eosinophils, and other, as yet unidentified, mononucleated cells (Figs. 17,27,29,30).

Some necrotic fibers contained large cells, rich in ribosomes, suggestive of myoblasts initiating regeneration (Fig. 30,31). These putative regenerating myoblasts were most likely derived from activated satellite cells. In the control muscles, the satellite cells were unremarkable; they occupied a pocket between the basal lamina and muscle cell membrane (Fig. 32). They appeared dormant, possessing little cytoplasm and containing a nucleus with highly condensed chromatin. In contrast, satellite cells associated with intact fibers in the necrotic regions of Flight muscles showed signs of active growth; the cytoplasm was increased and filled with ribosomes, rough endoplasmic reticulum, and hypertrophied golgi complexes (Fig. 33). Compared to the Synchronous controls, there was a significant ($p<.05$) increase (47%) in the number of satellite cell nuclei that were euchromatic and contained enlarged nucleoli. A similar trend was found for myonuclei. There was a 39% increase in hypertrophied myonuclei which were larger, possessed less heterochromatin, and contained more extensive nucleoli than controls (Figs. 34,35).

Characterization of mononuclear cells and edema. The fixed-tissue macrophages of control AL muscles showed little phagocytic activity. The nucleus was small and condensed, the cytoplasm was sparse with few phagocytic vacuoles, and cell processes were not elaborate (Fig. 36). In contrast, macrophages in the Flight AL muscles, especially within and near damaged regions, were enlarged, exhibited profuse phagocytic activity, and numerous cell processes (Fig. 27,37). They often assumed elongated shapes suggestive of migration along and into damaged muscle fibers. The other major invading cell was the polymorphonuclear neutrophil (Baggiolini, 1980) (Fig. 38). As with macrophages, neutrophils engaged in phagocytosis (Figs. 27,30,39,40). Eosinophils, easily recognized by their oval granules, were rare, but occasionally found within necrotic fibers (Fig. 39). An ultrastructural tally of the mononucleated cells, based strictly on morphological characteristics, indicated that up to 70% were macrophages, up to 29% were neutrophils, and 1% or less were eosinophils, mast cells and unidentified cell types. Immunological cell markers are needed to classify cell types with certainty (Engel & Arahata, 1986).

The extracellular matrix showed increased electron density of a particulate and fibrillar nature in the damaged regions of Flight AL muscles. It appeared that proteins derived from the blood and fragmented muscle fibers permeated the interstitium and caused edema (Figs. 5,6,17,27,29,30,38,40). Extravasated erythrocytes implied breakdown of the microcirculatory vessels (Figs. 27,30,39,40). Disruption of the endothelial cells of capillaries, venules and small arterioles was common in the damaged regions (Fig. 41).

Neuromuscular junctions in control and flight muscles. The neuromuscular junctions of control AL muscles consisted of motor nerve terminals nestled over primary and secondary synaptic clefts of the postjunctional membrane (Fig. 42). A dense basement membrane filled the synaptic cleft, separating the motor nerve terminals and the postjunctional membrane. Nerve terminals were capped by Schwann cell processes on the side away from the muscle fiber. Numerous synaptic vesicles filled the terminals. The neuromuscular junctions on intact fibers in the AL muscles of Flight animals exhibited an equal mixture of normal and degenerating terminals (Figs. 43-46). Degenerating nerve terminals contained few synaptic vesicles, but there was an abundance of

membranous and filamentous debris (Figs. 44-46). Schwann cell processes insinuated between the severely damaged terminals and the postjunctional basement membrane. Often in the vicinity of degenerating terminals, expanses of postjunctional membrane were not contacted by nerve elements (Fig. 45). These morphological relationships are characteristic of axon degeneration and denervation of the muscle fibers (Riley, 1981). In contrast to the junctions in the Flight AL muscles, those in the Flight EDL muscle fibers were indistinguishable from controls (Fig. 47).

Inspection of the intramuscular nerve bundles revealed that the nerve degeneration involved more than the nerve terminals. The nerve bundles in the non-damaged portions of the Flight AL muscles appeared normal; they contained myelinated and nonmyelinated axons separated by perineurial bundles of collagen (Fig. 48). Nerve bundles in the damaged regions often showed clumping and diminution of the neurofilaments and microtubules within the axons (Fig. 49). More striking was the apparent extraction and dissolution of the perineurial collagen bundles, suggestive of collagenase activity (Figs. 49,50). In some disrupted nerve bundles, small clusters of naked nerve processes, abutting the schwann cell, were indicative of nerve fiber regeneration (Fig. 50).

The ultrastructure of the Flight EDL muscles was not distinguishable from the controls. The macrophages and satellite cells were in the resting states (Figs. 51,52). The microcirculatory vessels were intact. There was no interstitial edema or extravasation of erythrocytes (Fig. 53). Neutrophils were not encountered in the interstitium. The myofibrils and mitochondria of the SO, FOG and FG fibers appeared normal (Figs. 54-56). As in controls, SO fibers possessed medium-sized mitochondria nearly completely confined to the I bands (Fig. 54). The mitochondria in the FOG fibers were larger and present in both the I and A bands (Fig. 55). The FG fibers contained low numbers of small mitochondria residing mainly in the I bands (Fig. 56).

Biochemical assays. The biochemical results and discussion are described in Dr. Eliis's final report (Part II).

CONCLUSIONS

The present study demonstrates that skeletal muscle weakness associated with prolonged spaceflight is complex, resulting from more than simple muscle fiber shrinkage (atrophy). Reduction of muscle strength may result from a combination of simple muscle fiber atrophy, muscle fiber segmental necrosis, degeneration of the motor innervation, and disruption of the blood supply. The present Cosmos 1887 findings are consistent with previous spaceflight reports (Ilyina-Kakueva et al., 1976; Baranski et al., 1979; Castleman et al., 1978; 1981; Rokhlenko & Savik, 1981; Martin & Edgerton, 1985; Ilyina-Kakuyeva, 1987; Riley et al., 1987). The weightbearing antigravity muscles (AL, Sol, and Plt) atrophied more than the nonweightbearing EDL muscle. Ranking mean percentage of muscle fiber atrophy from greatest to least puts Sol 38% & AL 36% > Plt 21% > EDL 16%. This differential atrophy is partly explained by the fiber type makeup of the muscle, and differing degrees of fiber type atrophy which occurs SO > FOG > FG. The AL and Sol are mostly composed of SO fibers whereas FG and FOG predominate in the EDL. Thus, the degree of spaceflight- induced atrophy is muscle fiber type specific.

More restrictive than atrophy was the occurrence of the muscle fiber, nerve, and vascular pathologies which only involved the AL and Sol. Within the AL, the degree of pathology was not uniform throughout. The midbelly or endplate region was more extensively damaged, and the destruction was more advanced than either end of the muscle, suggesting that the initial lesions occurred in the middle and spread towards the ends. Since the muscle fibers span the entire length of the muscle, the regional susceptibility cannot be explained by muscle fiber population differences. The basis for this regional heterogeneity is unknown, but studies are continuing to identify unique characteristics that may account for the phenomenon. The greater disruption in the midbelly cannot be explained by excessive shortening of the muscle during spaceflight because

tenotomy, which permits hypershortening, generates segmental necrosis preferentially at the ends of the muscle (Baker, 1983).

Another type of regional difference in the Flight AL muscles correlated with fiber type composition. The rostral half of the AL, composed of both SO and FOG fibers, exhibited less atrophy and damage than the caudal half, predominantly SO fibers. These fiber types were defined by the histochemical myofibrillar ATPase reaction. Recent studies by Hoh and coworkers (Hoh & Hughes, 1988; Hoh et al., 1988) using isomyosin antibodies suggest that there are genetically distinct subtypes of the three basic fiber types not resolved histochemically. Furthermore, these subtypes exhibit differential atrophy following denervation. Consideration of the regional heterogeneity within a skeletal muscle will be even more important when investigating the effects of spaceflight on primates, including humans, which have larger muscles. Choice of biopsy sites could greatly affect the types and extent of changes seen.

The increased myofibrillar ATPase histochemical activity in SO fibers of AL muscles indicated that they were acquiring fast fiber properties during the 12.5 day mission. If the transformation was complete, the mitochondrial content should decrease. While subsarcolemmal mitochondrial content and peripheral SDH histochemical staining were reduced, intermyofibrillar mitochondria were unchanged or somewhat elevated. These observations are consistent with Dr. Edgerton's quantitative measurements of SDH activity of Flight Sol muscles from the same rats. Similar results were obtained previously for the Sol muscle fibers of the Spacelab-3 Flight rats (Riley et al., 1987). It appears that subsarcolemmal mitochondria are selectively reduced whereas the progressive breakdown of myofibrils maintains the relative intermyofibrillar mitochondrial concentration near normal. These findings indicate the red AL and Sol will not show increased contractile fatigability which is characteristic of FG fibers. However, the reduction of subsarcolemmal mitochondria should affect energy-requiring processes associated with the cell membrane, such as the transport of ions and metabolites.

The Sol muscle fibers of Spacelab 3 rats exhibited focal losses of myofilaments from the margins and central portions of myofibrils (Riley et al., 1987). Since the atrophy was more severe in the present mission, the focal loss of myofilaments was expected to be more pronounced. However, the focal deletions were unremarkable. Perhaps, the two-day postflight period of muscle contractile activity caused synthesis and restoration of myofilaments. The hypertrophy of myonuclei, accompanied by enlarged nucleoli and increased euchromatin, is consistent with elevated protein synthesis. Muscles harvested immediately upon landing, to minimize the early readaption to gravity, are needed to assess whether focal lysis of myofibrils is progressive.

The selective loss of contractile proteins during disuse atrophy has not been satifactorily explained (Guba et al., 1977; Riley et al., 1988a). Recently, we proposed that ubiquitination of contractile proteins enhances their susceptibility to proteolysis (Rechsteiner, 1987; Haas, 1988; Riley et al., 1988a). Ubiquitination and TAP activity were increased in the atrophic muscles of Spacelab 3 rats and those undergoing atrophy during hindlimb unloading by tail suspension (Fitts et al., 1986; Riley et al., 1986; Riley & Haas, unpublished observations). The AL muscles from the present animals were not large enough to perform biochemical measures of ubiquitin pools and TAP activity. Immunostaining for TAP did not provide a clear indication of an increase in the protease in the Cosmos 1887 muscles. However, elevated immunofluorescence staining for ubiquitin conjugates was consistent with increased ubiquitination of muscle proteins during spaceflight-induced muscle atrophy.

As striking as the marked atrophy of the AL and Sol muscle fibers of the Cosmos 1887 rats was, the extensive segmental necrosis was more dramatic, involving 2 to 5% of the fibers in 4 Flight rats (no.s 6,7,8,10) and 24% in the fifth rat (no. 9). Interestingly, for 4 of 5 rats there was a direct correlation between the percentage of damaged fibers and the degree of atrophy in the AL. Why rat no. 9 was the most severely affected by spaceflight should be better understood when the effects

on other body systems are compared at the Cosmos Final Report Symposium in Moscow. While the changes in muscles during spaceflight are expected to be predominantly influenced by a reduced workload and decreased contractile activity, extrinsic systemic factors, such as hormonal and immunological, should be considered.

Segmental lesions represent portions of the muscle fibers destroyed when the cell membrane is violated. It is necessary to perform additional studies to identify the primary cause of membrane disruption. There are a number of possible scenarios to explain some of the observations. For example, leakage of muscle cell contents could have activated and attracted macrophages as well as neutrophils into the lesioned site where they participated in phagocytosis. Many unidentified mononuclear cells were also present; since determining the identities of these cells would aid in understanding the mechanism of muscle necrosis, future experiments will employ immunomarkers as described by Engel and Arahata (1986). The milieu surrounding damaged fibers generally was edematous. Release of cell contents stimulates mast cell degranulation and the release of histamine which promotes edema by increasing vascular permeability (Schwartz & Austen, 1984). Degranulated mast cells were uncommon; however, the number of toluidine blue-positive mast cells was lower in the Flight AL muscles. Mast cells may have secreted during flight or landing and contributed to the muscle edema.

One identified cause of edema was breakdown of the endothelial cells of the microcirculatory vessels which leaked erythrocytes into the interstitium. Destruction of capillaries was reported for previous Cosmos missions and following restricted-movement hypodynamia (Portugalov et al., 1971; Portugalov & Ilyina-Kakueva, 1973; Ilyina-Kakueva et al., 1976; Roknlenko & Savik, 1981; Ilyina-Kakuyeva & Portugalov, 1981; Ilyina-Kakuyeva, 1987). It was hypothesized that during reduced muscle contractile activity there is congestion of blood flow in the muscle and loss of vascular tone. This results in ischemia and anoxia that damages the muscle cell membranes (Maki et al., 1986). The edema and endothelial necrosis was limited to the highly vascularized AL and Sol muscles. This is reasonable because these muscles function primarily on oxidative metabolism making them more susceptible to oxygen deprivation than the Plt and EDL which can compensate by anaerobic glycolysis (Maki et al., 1986). Interestingly, vascular occulsion produces muscle fiber necrosis more common in the middle of the Plt muscle, and the susceptibility of fiber types to ischemic damage is SO > FOG > FG (Maki et al., 1986). The vascular pattern was the primary factor in determing the distribution of ischemic changes. The distribution of the blood vessels in the AL muscles is one of the features being examined that may account for the higher incidence of segmental necrosis in the midbelly.

The type of muscle fiber destruction present in the Flight AL muscles is very similar to that reported for eccentric strenuous exercise (Armstrong et al., 1983; Salminen & Vihko, 1984; Ogilvie et al., 1988). Weightbearing lengthening contractions appear to disrupt the muscle fiber membrane and cause segmental necrosis within one or two days after exercising. Since the Flight rats with debilitated antigravity muscles were exposed to the increased workload of gravity for 2 days before sacrifice, it is possible that some of the pathological changes resulted from postflight "strenuous exercise". This can be assessed by analyzing muscles removed immediately upon landing. Some damage may occur during spaceflight because Sol muscles harvested 4.5 to 9 hours after landing possessed necrotic muscle fibers (Roknlenko & Savik, 1981; Ilyina-Kakuyeva, 1987). Inflight and postflight conditions may generate similar neuromuscular pathologies, as the tissue has a limited repetoire of responses to injury. Postflight stress may exacerbate the inflight changes. Regardless of when the damage occurred, it is important to recognize that pathological changes result from spaceflight and effective countermeasures to reduce this damage must be found.

Destruction of the motor innervation produces muscle weakness because denervated muscle fibers are not activated. In the Flight AL muscles, approximately 14% of the neuromuscular junctions examined had their motor nerve terminals disrupted. The nerve damage involved preterminal

axons as well. Degenerating terminals had fewer synaptic vesicles, and the axon cell membrane was violated. In the worst cases, the damaged terminals were engulfed and degraded by hypertrophied schwann cells with increased lysosomes. The morphological changes were similar to those seen following axotomy (Riley, 1981). Similar destruction of nerve terminals was reported for Cosmos 936 (Baranski et al., 1979). They postulated that reduced neural activity during spaceflight produced the terminal degeneration. A primary defect in the axon is possible because, in the present study, damaged junctions were observed on intact muscle fibers. This suggests that the nerve lesions were not secondary to destruction of the muscle fibers.

Early signs of regeneration were detected in both damaged muscle fibers and nerves. Myoblast-like cells were present in the segmental necrotic lesions cleared of cell debris. The source of these myoblasts is most likely activated satellite cells which were more prevalent in the damaged Flight AL muscles. Bischoff has demonstrated that crushed muscle fibers release a soluble factor that stimulates satellite cell mitosis (Bischoff, 1986a,b). In the present study, there was a direct correlation between the distributions of hypertrophied satellite cells and segmental necrosis. Activated satellite cells in nondamaged regions are capable of migrating into the damaged fibers (Schultz et al., 1985). Promoting muscle fiber regeneration by injecting a satellite cell mitogenic factor may facilitate repair of muscle during spaceflight.

Following distal destruction of an axon, the axon dies back to some extent and then initiates regrowth within a day or two (Riley et al., 1988b). The presence of naked fine nerve processes along the schwann cells of small intramuscular nerve bundles, in which most of the myelinated axons were missing, suggests that nerve regeneration was in progress. Functional reinnervation of the endplates should occur rapidly because the axons can follow the schwann cells back to the junctions. These results indicate that if similar nerve damage occurred in human muscles during spaceflight, there might be reinnervation and recovery of strength without the pathological process being detected unless biopsies were taken.

In the present study, the onset of regeneration of both muscle and nerve fibers was detected postflight. There is previous evidence that restoration would have resulted, if the Flight animals had been allowed to survive (Ilyina-Kakueva & Portugalov, 1977). It must be remembered, however, that human muscles and nerves generally do not regenerate as rapidly or as completely as rodent muscles. Scarring and partial denervation of human muscle may result and produce a permanent weakness.

That humans may manifest pathological changes as well as simple atrophy during spaceflight is supported indirectly by recent ultrastructural findings showing disrupted capillaries in soleus muscles following 30 days of head down bedrest (Hikida & Dudley, 1988). During long term spaceflight, simple atrophy may be reduced by exercise, but repair of necrosis of muscle fibers, motor axons, and blood vessels would be dependent upon the effectiveness of complex processes of regeneration. There is ground-based evidence to expect that regeneration may be compromised in space because of the reduction in active muscle tension and exposure of the dividing stem cells to high energy radiation (Denny-Brown, 1951; Ilyina-Kakueva & Portugalov, 1977; Benton et al., 1978; Kovalev, 1983; Gulati, 1987). These issues should be addressed in future missions.

ACKNOWLEDGMENTS

We gratefully acknowledge the dedication and expert assistance of the NASA and Soviet workers who collaborated to obtain the excellent specimens used in this study.

REFERENCES

1. Armstrong, RB, Ogilvie, RW, Schwane, JA. 1983. Eccentric exercise-induced injury to rat skeletal muscle. J. Appl. Physiol. 54:80-93.

2. Baggiolini, M. 1980. The neutrophil. Handbook of Inflammation 2: The Cell Biology of Inflammation. Weissmann, G. Ed. Elsevier/North Holland pp.163-187.

3. Baker, JH. 1983. Segmental necrosis in tenotomized muscle fibers. Muscle & Nerve 6:29-39.

4. Baranski, S, Baranska, W, Marciniak, M, Ilyina-Kakueva, EI. 1979. Ultrasonic ("Ultrastructural") investigations of the soleus muscle after space flight on the Biosputnik 936. Aviat. Space Environ. Med. 50:930-934.

5. Benton, EV, Peterson, DD, Marenny, AM, Popov, VI. 1978. HZE particle radiation studies aboard Kosmos 782. Health Physics 35:643-648.

6. Bischoff, R. 1986a. A satellite cell mitogen from crushed adult muscle. Devel. Biol. 115:140-147.

7. Bischoff, R. 1986b. Proliferation of muscle satellite cells on intact myofibers in culture. Devel. Biol. 115:129-139.

8. Castleman et al. 1978. Spaceflight effects on muscle fibers:Final Reports of U.S. Experiments Flown on Soviet Satellite Cosmos 936. Rosenzweig, SN. Souza, KA. Eds. NASA Technical Memorandum 78526 pp. 224-289.

9. Castleman, KR, Chui, LA, Van Der Meulen, JP. 1981. Automatic analysis of muscle fibers from rats subjected to spaceflight. NASA Technical Memorandum 81289 pp. 267-277.

10. Denny-Brown, D. 1951. The influence of tension and innervation on the regeneration of skeletal muscle. J. Neuropath. Exp. Neurol. 10:94-95.

11. Engel, AG, Arahata, K. 1986. Mononuclear cells in myopathies. Hum. Pathol. 17:704-721.

12. Fitts, RH, Metzger, JM, Riley, DA. 1986. Models of skeletal muscle disuse: a comparison of suspension hypokinesia and hindlimb immobilization. J. Appl. Physiol. 60:1946-1953.

13. Gazenko, OG, Genin, AM, Il'in, YA, Portugalov, VV, Serova, LV, Tigranyan, RA. 1978. Principal results of experiment with mammals onboard the Kosmos-782 biosatellite. Kosmich. Biol. Aviakosmisch. Med. 6:43-[illegible].

14. Guba, F, Meszaros, MG, Takacs, O. 1977. Degradation of myones as a consequence of disuse and denervation. Acta Biol. Med. Germ. 36:1605-1619

15. Gulati, AK. 1987. The effect of X-irradiation on skeletal muscle regeneration in the adult rat. J. Neurol. Sci. 78:111-120.

16. Haas, AL. 1988. Immunochemical probes of ubiquitin pool dynamics. Ubiquitin. Rechsteiner, M. Ed. Plenum Publ. pp.173-206.

17. Hikida, RS, Dudley, GA. 1988. Ultrastructural changes in human skeletal muscle after 30 days of bedrest. Anat. Rec. 220:44A.

18. Hoh, JFY, Hughes S. 1988. Myogenic and neurogenic regulation of myosin gene expression in cat jaw-closing muscles regenerating in fast and slow limb muscle beds. J. Muscle Res. Cell Motil. 9:59-72.

19. Hoh, JFY, Hughes, S, Hale, PT, Fitzsimons, RB. 1988. Immunocytochemical and electrophoretic analyses of changes in myosin gene expression in cat limb fast and slow muscles during postnatal development. J. Muscle Res. Cell Motil. 9:30-47.

20. Ilyin, EA. 1983. Investigations on biosatellites of the Cosmos series. Aviat. Space Environ. Med. Suppl. I 54:S9-S15.

21. Ilyina-Kakuyeva, EI. 1987. Investigation of rat skeletal muscles following short-term spaceflight aboard Cosmos-1667 biosatellite. Kosmich. Biol. Aviakosmich. Med. 21:31-35.

22. Ilyina-Kakuyeva, EI, Portugalov, VV. 1981. Structural changes in the soleus muscle of rats flown aboard the Cosmos series of biosatellites and submitted to hypokinesia. Kosmich. Biol. Aviakosmich. Med. 15:37-40.

23. Ilyina-Kakueva, EI, Portugalov, VV. 1977. Combined effect of space flight and radiation on skeletal muscles of rats. Aviat. Space Environ. Med. 48:115-119.

24. Ilyina-Kakueva, EI, Portugalov, VV, Krivenkova, NP. 1976. Space flight effects on the skeletal muscle of rats. Aviat. Space Environ. Med. 47:700-703.

25. Kovalev, EE. 1983. Radiation protection during space flight Aviat. Space Environ. Med. Suppl. 1 54:S16-S23.

26. Maki, T, Korthals, JK, Prockop, LD. 1986. Distribution of muscle changes in experimental ischemic myopathy. Muscle & Nerve 9:394-398.

27. Martin, TP, Edgerton, VR. 1985. The influence of space flight on the rat soleus. Physiologist 28:379.

28. Ogilvie, RW, Armstrong, RB, Baird, KE, Bottoms, CL. 1988. Lesions in the rat soleus muscle following eccentrically biased exercise. Amer. J. Anat. 182:335- 346.

29. Portugalov, VV, Ilyina-Kakueva, EI. Prolonged space flight and hypokinesia. Aerospace Med. 44:764-768.

30. Portugalov, VV, Ilyina-Kakueva, EI, Starostin, VI, Rokhlenko, KD, Savik, ZF. 1971. Morphological and cytochemical studies of hypokinetic effects. Aerospace Med. 42:1041-1049.

31. Rapcsak, M, Oganov, VS, Szoor, A, Skuratova, SA, Szilagyi, T. 1983. Effect of weightlessness on the function of rat skeletal muscles on the biosatellite Cosmos-1129. Acta Physiol. Hung. 62:225-228.

32. Rechsteiner, M. 1987. Ubiquitin-mediated pathways for intracellular proteolysis. Ann. Rev. Cell Biol. 3:1-30.

33. Riley, DA. 1981. Ultrastructural evidence for axon retraction during the spontaneous elimination of polyneuronal innervation of the rat soleus muscle. J. Neurocytol. 10:425-440.

34. Riley, DA, Allin, EF. 1973. The effects of inactivity, programmed stimulation, and denervation on the histochemistry of skeletal muscle fiber types. Exp Neurol. 40:391-413.

35. Riley, DA, Bain, JLW, Ellis, S, Haas, AL. 1988a. Quantification and immunocytochemical localization of ubiquitin conjugates within rat red and white skeletal muscles. J. Histochem. Cytochem. 36:621-632.

36. Riley, DA, Bain, JLW, Haas AL. 1986. Increased ubiquitin conjugation of proteins during skeletal muscle atrophy. J. Cell Biol. 103:401a

37. Riley, DA, Ellis, S, Bain, JLW. 1982. Carbonic anhydrase activity in skeletal muscle fiber types, axons, spindles, and capillaries of rat soleus and extensor digitorum longus muscles. J. Histochem. Cytochem. 30:1275-1288.

38. Riley, DA, Ellis, S, Slocum GR, Satyanarayana, T. Bain, JLW, Sedlak FR. 1987. Hypogravity-induced atrophy of rat soleus and extensor digitorum longus muscles. Muscle & Nerve 10:560-568.

39. Riley, DA, Sanger, JR, Matloub, HS, Yousif, NJ, Bain, JLW, Moore, GH. 1988b. Identifying motor and sensory myelinated axons in rabbit peripheral nerves by histochemical staining for carbonic anhydrase and cholinesterase activities. Brain Res. 453:79-88.

40. Rokhlenko, KD, Savik, ZF. 1981. Effect of space flight factors on ultrastructure of skeletal muscles. Kosmich. Biol. Aviakosmich. Med. 1:72-77.

41. Salminen, A, Vihko, V. 1984. Autophagic response to strenuous exercise in mouse skeletal muscle fibers. Virch. Arch. Cell Pathol. 45:97-106.

43. Schultz, E, Jaryszak, DL, Valliere, CR. 1985. Response of satellite cells to focal skeletal muscle injury. Muscle & Nerve 8:217-222.

44. Schwartz, LB, Austen, KF. 1984. Structure and function of the chemical mediators of mast cells. Prog. Allergy 34:271-321.

45. Takacs, O, Rapcsak M, Szoor, A, Oganov, VS, Szilagyi, T, Oganesyan, SS, Guba, F. 1983. Effect of weightlessness on myofibrillar proteins of rat skeletal muscles with different functions in experiment of biosatellite Cosmos-1129. Acta Physiol. Hung. 62:228-233.

TABLE 1

PERCENTAGES OF FIBER TYPES IN FLIGHT AND SYNCHRONOUS MUSCLES

Muscle	Percentages of fiber types Flight	Synchronous
Adductor longus		
SO	63±5*	83±1
I	19±3**	1±1
FOG	18±3	16±3
Extensor digitorum longus		
SO	5±1	5±1
FG	37±5	31±2
FOG	58±5	64±2
Plantaris		
SO	10±1	10±1
FG	21±3	24±3
FOG	69±3	66±2

SO - slow twitch oxidative
I - intermediate (putative SO fiber changing to FOG)
FG - fast twitch glycolytic
FOG - fast twitch glycolytic oxidative
* - Flight significantly different from control at $p<.01$
** - Flight different from control at $p<.001$
two tailed Student t test

TABLE 2

FIBER TYPE ATROPHY IN FLIGHT MUSCLES

Muscle	Fiber Cross-sectional Area: Flight	Synchronous	Percent Atrophy
Adductor Longus			
SO	1332±125	2370±121	43.8%**
I	1209±167	1600±148	24.5%
FOG	1854±173	2232±178	17.0%
Extensor Digitorum Longus			
SO	955±77	1157±69	17.4%
FG	2768±290	3170±162	12.7%
FOG	1323±107	1623±58	18.5%*
Plantaris			
SO	1506±67	1919±104	21.5%*
FG	3074±110	4503±333	31.7%*
FOG	1974±80	2364±111	16.5%*
Soleus			
ND	1864±115	3005±100	38.0%**

SO - slow twitch oxidative
I - intermediate (putative SO fiber transforming to FOG fiber)
FG - fast twitch glycolytic
FOG - fast twitch glycolytic
ND - fiber types not distinguishable for soleus (H&E section)
* - percentage atrophy significantly different at $p<.05$
** - percentage atrophy significantly different at $p<.001$
two tailed t-test

TABLE 3

PERCENTAGES OF ABERRANT FIBERS IN ADDUCTOR LONGUS MUSCLES

Group	Normal Fibers	Aberrant Fibers	Mean Total No. Counted	Percentage Aberrant
Flight n=4*	1200±66	45±9	1245±73	3.6±0.6%**
Synchronous n=5	1331±75	2.2±0.5	1333±75	0.17±.04%
Vivarium n=5	1226±85	2.3±0.3	1228±85	0.19±.03%
Basal n=5	1074±134	1.1±0.5	1075±134	0.09±.03%

---

* - The AL muscle of Flignt rat #9 was excluded as a statistical outlier because 24% of the fibers were damaged.

** - The percentage aberrant fibers in the Flight group is significantly different from each of the other three groups ($p < 0.001$; two tailed Student t-test)

Figure 1. An alkaline myofibrillar ATPase stained section of a normal AL muscle from a Cosmos Synchronous control rat. Most fibers are lightly reactive slow twitch oxidative fibers (SO). Darkly stained fast twitch oxidative glycolytic (FOG) fibers are also present. X250.

Figure 2. Following 12.5 days of spaceflight, the AL muscles exhibited overall a 36% fiber atrophy. While all fiber types atrophied, the SO fibers showed the greatest decrease in size. There was an increase in moderately staining fibers which indicated that SO fibers were acquiring myofibrillar ATPase properties of fast fibers. X250.

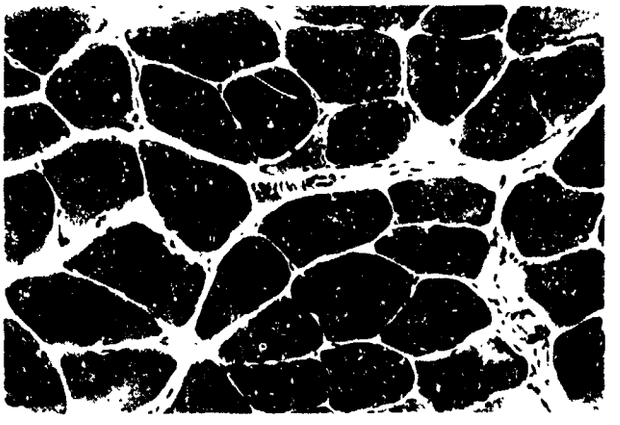

Figure 3. A hematoxylin & eosin (H&E) stained section of an AL Synchronous muscle. The fibers are large, except for the occasional (.02%) small angular fiber (arrow), suggestive of a low rate of spontaneous neurogenic atrophy in normal muscles. X175.

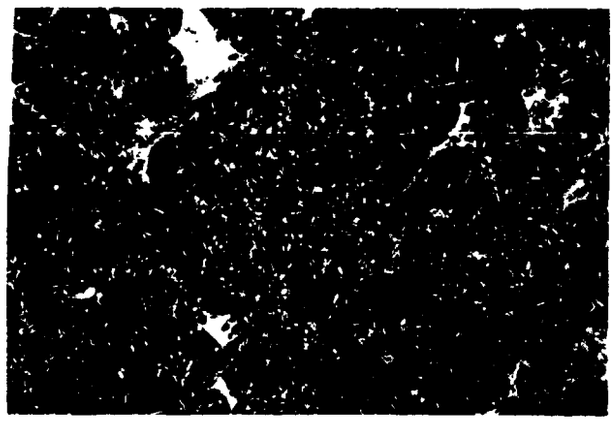

Figure 4. The muscle fibers of the Flight AL are atrophied, and, on average, 3.6% of the fibers exhibit segmental necrosis with invasion by mononucleated cells (arrows). Some lesioned fibers (double arrows) possess a central core of disruption surrounded by intact myofibrils. X175.

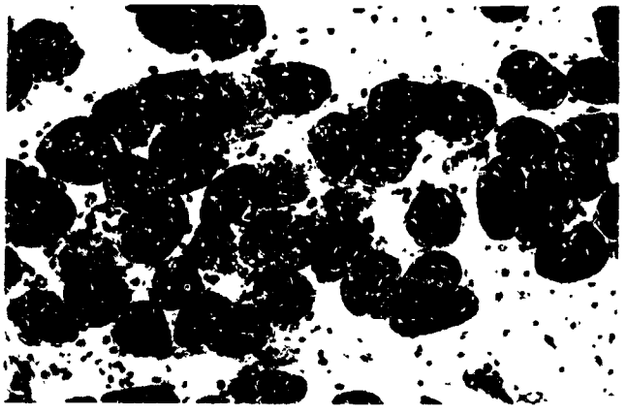

Figure 5. An H&E stained cross section of a Flight AL. The pale staining fibers are undergoing destruction. The edematous extracellular space surrounding the muscle fibers is filled with numerous mononuclear cells. X175.

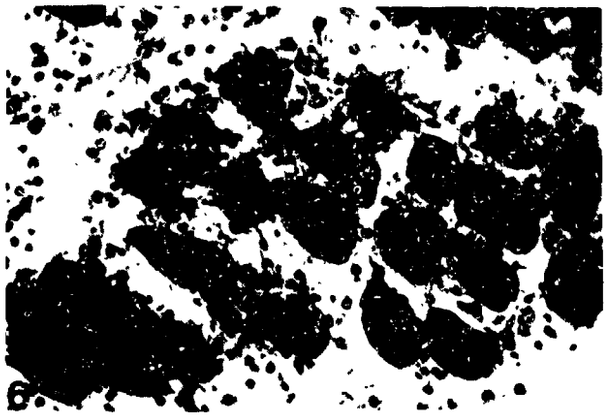

Figure 6. Extensive interstitial edema and mononuclear cell infiltration, as well as muscle fiber necrosis, is present in the Flight soleus muscles. X175.

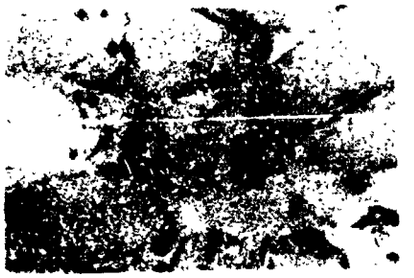

Figure 7. Toluidine blue stained section of a normal AL muscle. Two granule- laden mast cells occupy the perimysial connective tissue. X313.

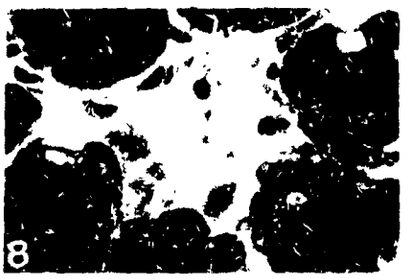

Figure 8. An H&E stained section of a Flight AL. The central necrotic fiber is devoid of myofibrils and filled with mononuclear cells. X400.

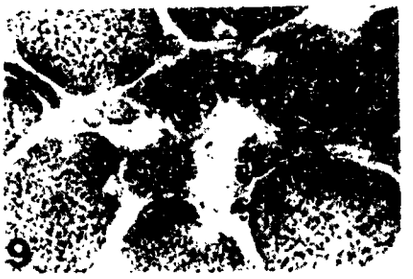

Figure 9. A section, serial to figure 8, stained by acid phosphatase histochemistry reveals that many of the invading cells are darkly reactive, suggestive of high lysosome content. X400.

Figure 10. Indirect immunofluorescence localization of tripeptidyl aminopeptidase (TAP) in a Synchronous AL muscle. The SO fibers show uniformly moderate immunoreactivity, and the six FOG fibers in this section are highly reactive. X145.

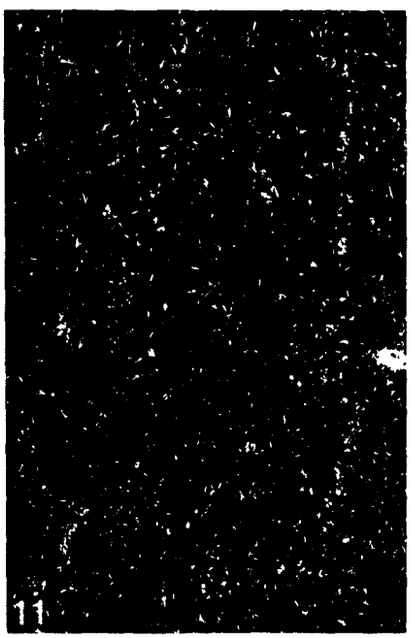

Figure 11. A section serial to that in figure 10. Omission of the primary antiserum eliminates fiber immunostaining, except for autofluorescence of mitochondria at the periphery of the fibers. X145.

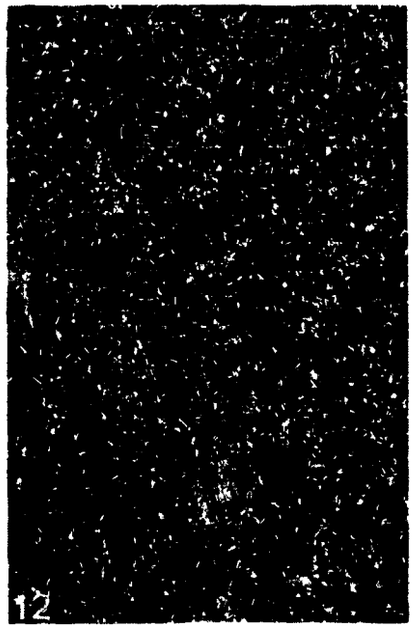

Figure 12. The less atrophic FOG fibers in an AL Flight muscle continue to manifest high levels of TAP immunoreactivity. The more atrophic SO fibers exhibit a range of reactivity from high to low levels of staining compared to the Synchronous control. X145.

Figure 13. Cross section of a Synchronous AL muscle immunostained with ubiquitin conjugate antibodies. Fibers show uniform moderate immunofluorescence. X145.

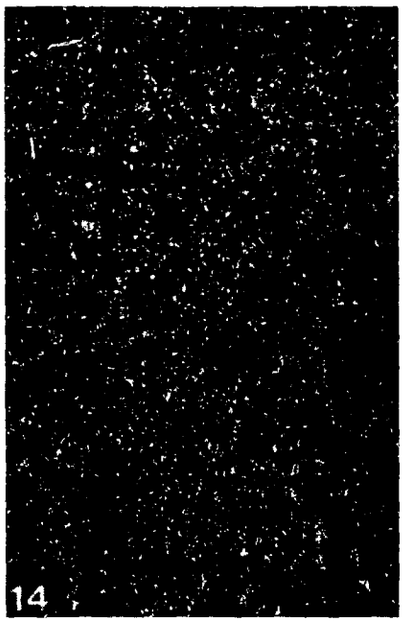

Figure 14. A section serial to that in figure 13. Elimination of the primary antiserum blocks fiber staining, supporting specificity of the antibodies for ubiquitin conjugates. Nonspecific background staining of the subsarcolemmal mitochondria remains. X145.

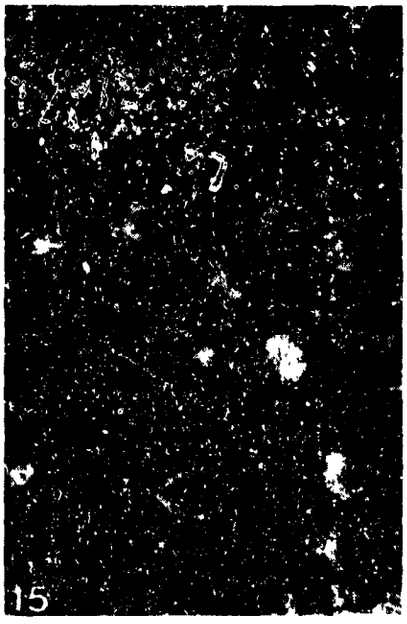

Figure 15. Ubiquitin conjugate antibody staining of atrophic fibers in an AL Flight muscle. Uneven elevated immunofluorescence staining is present in many fibers, indicating regional subcellular increases of conjugates. Other fibers possess uniform staining, ranging from above to below control levels. X145.

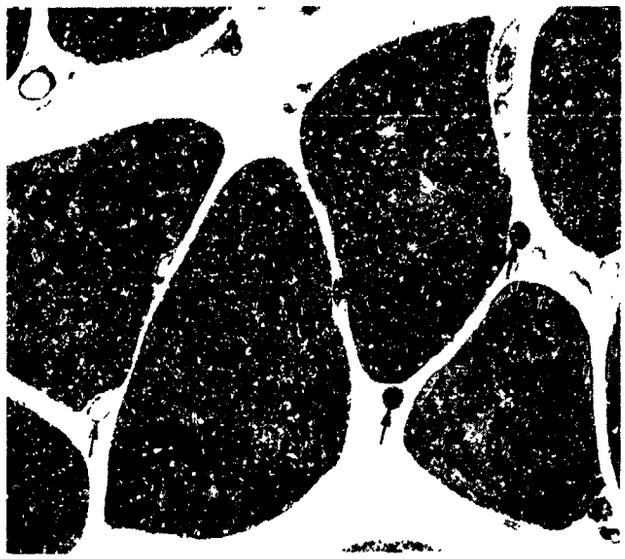

Figure 16. A low magnification electron micrograph illustrating normal muscle fibers in a Basal control AL muscle cut in cross section. Fibers contain well organized contractile proteins and peripheral myonuclei. Capillaries (arrows) occupy the surrounding endomysial connective tissue; some capillaries contain erythrocytes. X840.

Figure 17. Cross section of a Flight AL muscle showing a severely necrotic fiber among the small intact atrophic fibers. The damaged fiber exhibits invasion by macrophages and other unidentified cells. The extracellular matrix is more dense than normal. X840.

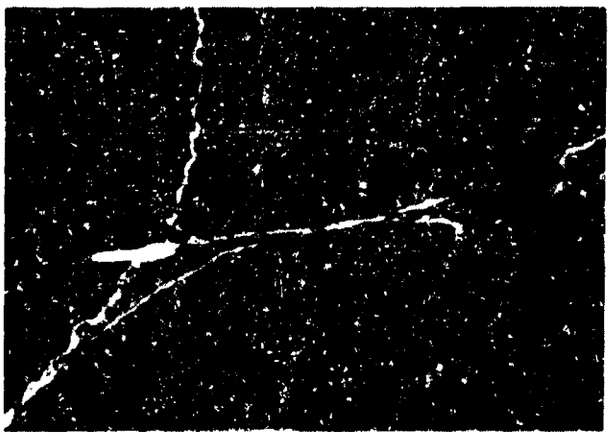

Figure 18. Prominent subsarcolemmal accumulations of mitochondria are present in Synchronous control AL fibers. X5,250.

Figure 19. In the Flight AL muscles, there is a significant reduction in the subsarcolemmal concentration of mitochondria. X5,250.

Figure 20. A cross section of a Synchronous AL muscle fiber illustrates that the majority of the mitochondria encircle the myofibrils at the I band level. Very few mitochondrial profiles are present in the A band. X15,000.

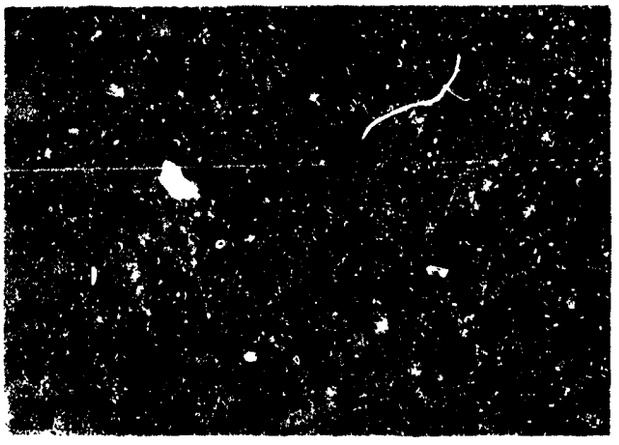

Figure 21. The atrophic Flight AL muscle fibers contain more mitochondria profiles in the A bands than controls. X15,000.

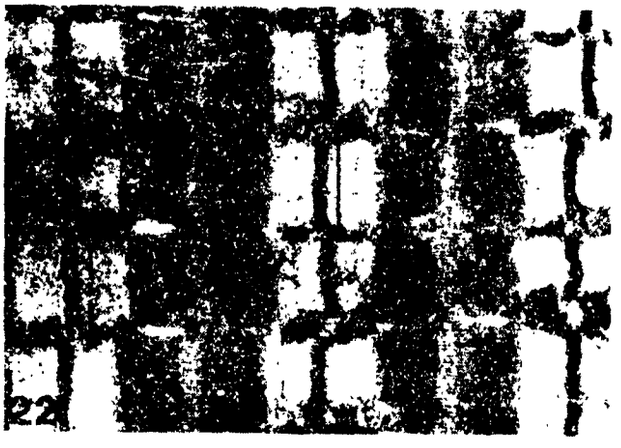

Figure 22. A longitudinal section of a Synchronous AL muscle fiber. The myofibrils are wide with long Z bands (brackets). X14,500.

Figure 23. The myofibrils decrease in diameter in the atrophic Flight AL muscle fibers. The mean Z band length is less than that of controls. X14,500.

Figure 24. Some regions of the atrophic Flight AL muscle fibers exhibit loss of sarcomere structure with longitudinal streaming of the Z bands. X6,750.

Figure 25. In regions of myofibril disorganization, the Z bands (arrows) are extremely short. Areas of this Flight AL in which myofibrils are nearly completely broken down, large Z band-like densities are present (arrowheads). X3,900.

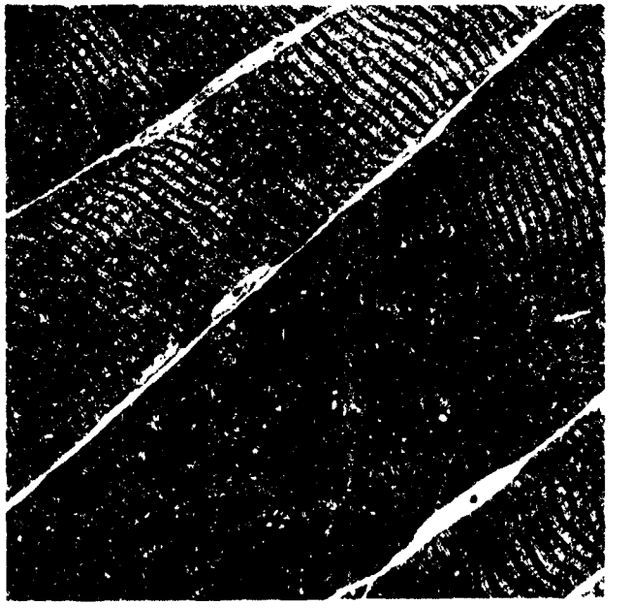

Figure 26. A longitudinal section of AL muscle fibers from a Basal control muscle demonstrating the regular cross striated pattern of the myofibrils. X840.

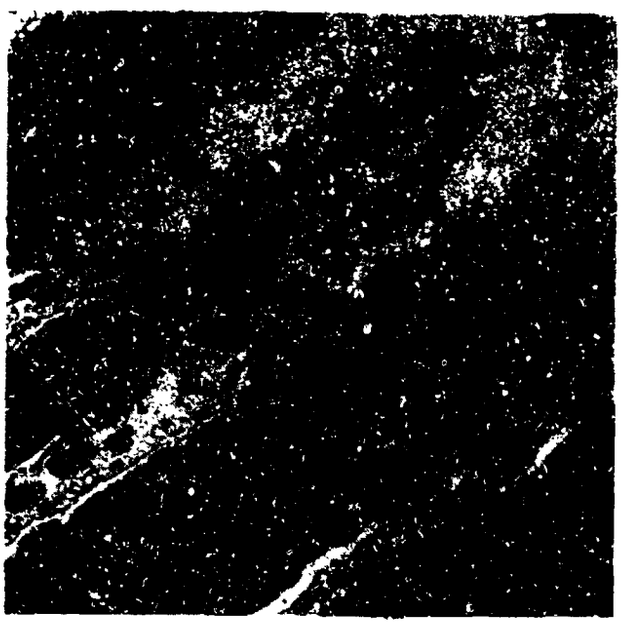

Figure 27. A longitudinal section through the segmental necrotic regions of three muscle fibers in a Flight AL muscle. The plasma cell membranes of the degenerating fibers are disrupted, the contractile proteins form amorphous masses, and fibers are invaded by macrophages (arrows), neutrophils (arrowheads) and other unidentified cell types. Escaped erythrocytes (e) are free in the connective tissue. X840.

Figure 28. A lesioned fiber in a Flight AL muscle. This fiber illustrates the transition from partially disrupted myofibrils leading to a supercontracted mass which borders the segmental necrotic region completely devoid of intact contractile elements. X840.

Figure 29. A cross section of a contraction clot in a necrotic AL Flight muscle fiber. The clot in the right half of this figure is invaded by two macrophages engulfing cellular debris. X2,900.

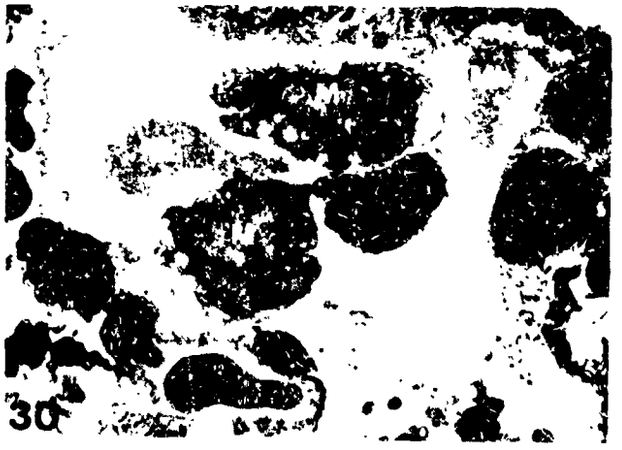

Figure 30. An advanced stage of breakdown of the contractile material within a segmental necrotic region of a Flight AL fiber viewed in cross section. The muscle fiber basal lamina surrounds two macrophages (M) and portions of two regenerating myoblasts (Mb). X2,800.

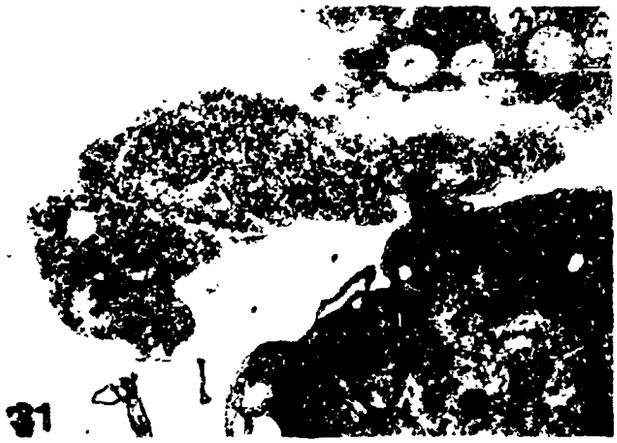

Figure 31. A higher magnification of the regenerating myoblast in figure 30 reveals the ribosome-rich cytoplasm of the growing cell. X8,400.

Figure 32. A quiescent satellite cell on a normal fiber in a Basal control AL muscle. The nucleus is heterochromatic, the nucleolus is not prominent, and the cytoplasm is sparse and contains few organelles. X8,125.

Figure 33. An activated satellite cell on an intact atrophic fiber in an AL Flight muscle. The amount of cytoplasm is greatly increased and electron lucent. There are many ribosomes, rough endoplasmic reticulum, golgi membranes and vesicles. The nucleus exhibits more euchromatin and an enlarged nucleolus indicative of elevated protein synthetic activity. X8,125.

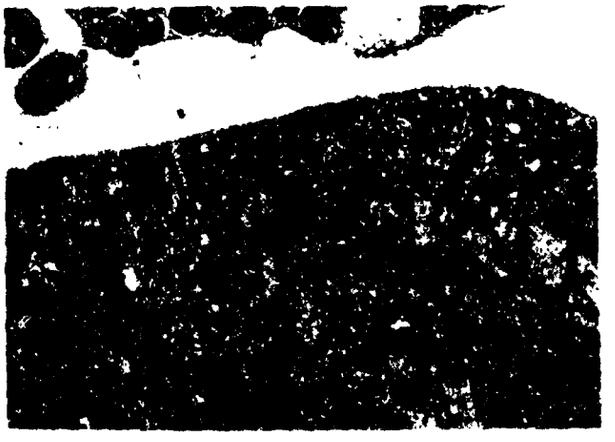

Figure 34. The edge of a Basal control AL muscle fiber. The peripheral myonucleus exhibits marginal heterochromatin and a small nucleolus. In the adjacent connective tissue, a mast cell is releasing secretory granules. Active mast cell secretion was rarely observed in control and Flight muscles. X9,750.

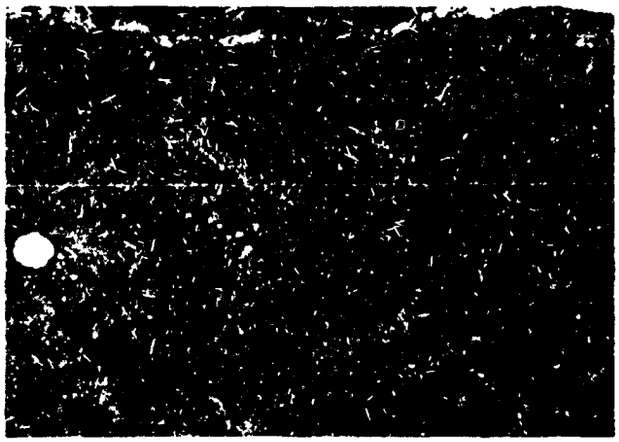

Figure 35. Approximately 40% of the myonuclei examined in the Flight AL muscle fibers showed increased euchromatin and hypertrophied nucleoli. X9,750.

Figure 36. A quiescent tissue macrophage in a Synchronous AL muscle. The nucleus is heterochromatic, the cytoplasm is dense and filled with lysosomes, and cell processes are few in number. X9,600.

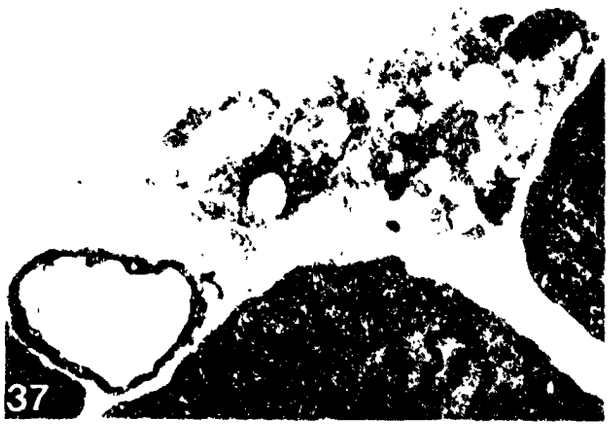

Figure 37. Activated macrophages are very common in the Flight AL muscles. They exhibit enhanced phagocytosis of extracellular material. Not visible in this section is the nucleus which is more euchromatic and contains a larger nucleolus than normal. X5,750.

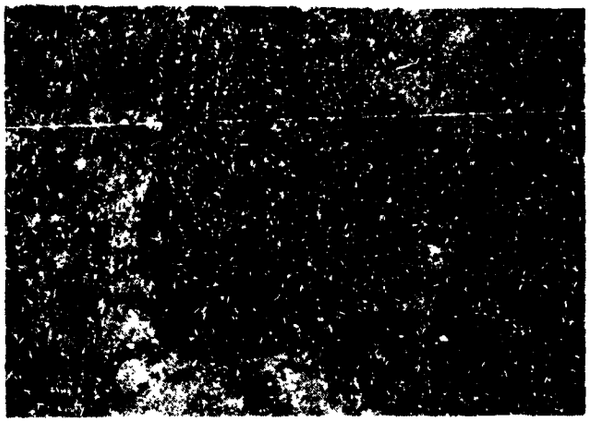

Figure 38. Invasion of Flight AL muscles by polymorphonuclear neutrophils is common in regions of muscle fiber necrosis. The neutrophil is characterized by a multilobed nucleus and dense cytoplasm. In this figure, the electron dense material surrounding the neutrophil is most likely blood serum proteins that escaped from damaged capillaries. X8,710.

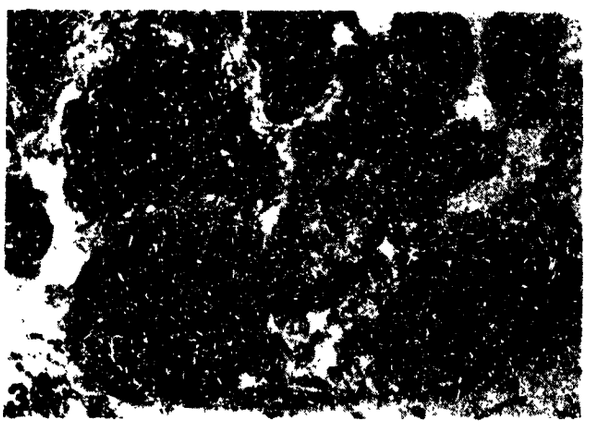

Figure 39. Flight AL muscle. Eosinophils (E) occasionally participated in the invasion of necrotic muscle fibers. A macrophage (M) with an ingested erythrocyte (R) is also present. The identities of the other mononuclear cells are uncertain. X5,625.

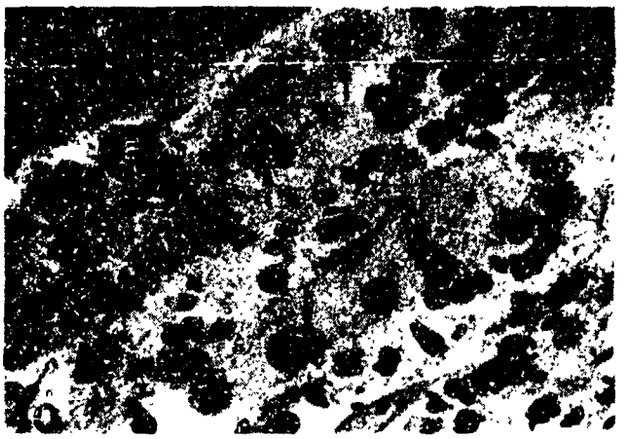

Figure 40. Extravasation of erythrocytes (E) into the connective tissue was common in the necrotic regions of Flight AL muscles. Macrophages (arrows), neutrophils (arrowheads, and other unclassified mononuclear cells fill the damaged region of the muscle. X750.

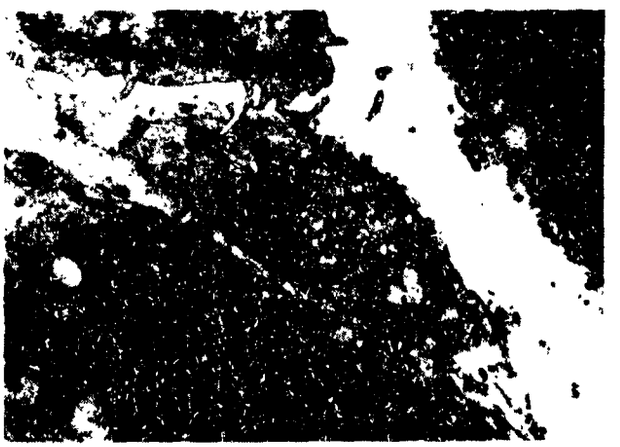

Figure 41. In the damaged regions of Flight AL muscles, many microcirculatory vessels were disrupted. A degenerating endothelial cell of a capillary is shown (D). Another endothelial cell appears intact. It is filled with pinocytotic vesicles (P). X8,375.

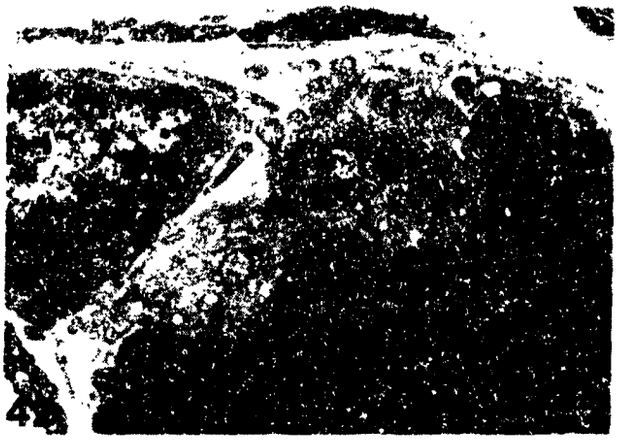

Figure 42. A normal neuromuscular junction on an AL muscle fiber in a Basal control rat. Synaptic vesicle-laden terminals are separated from the postjunctional muscle membrane by a prominent basement membrane which fills the primary and secondary synaptic clefts. X8,375.

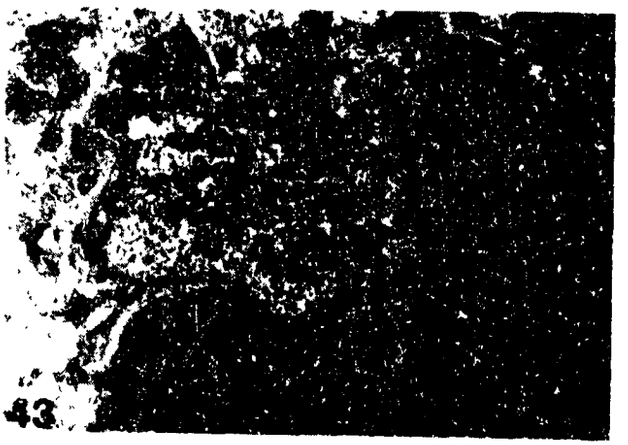

Figure 43. A normal appearing neuromuscular junction on an intact AL Flight muscle fiber. The nerve terminal is filled with synaptic vesicles. Schwann cell processes cap the side of the terminal away from the postjunctional membrane. X9,213.

Figure 44. A disrupted motor nerve terminal in a Flight AL muscle. There are fewer synaptic vesicles. Schwann cell processes partially separate the terminal and the postjunctional membrane. X9,213.

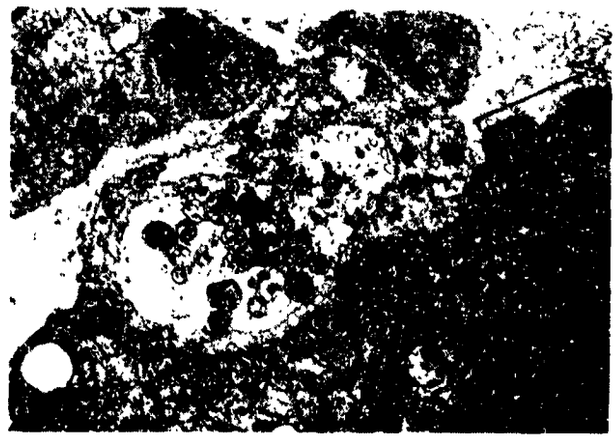

Figure 45. A more severely disrupted neuromuscular junction on an intact muscle fiber from a Flight animal. Very few synaptic vesicles are present and the axolemma appears broken. Schwann cell processes are completely interposed between the terminal and the postjunctional membrane. An adjacent area of the postjunctional membrane (bracket) is devoid of nerve elements. X9,213.

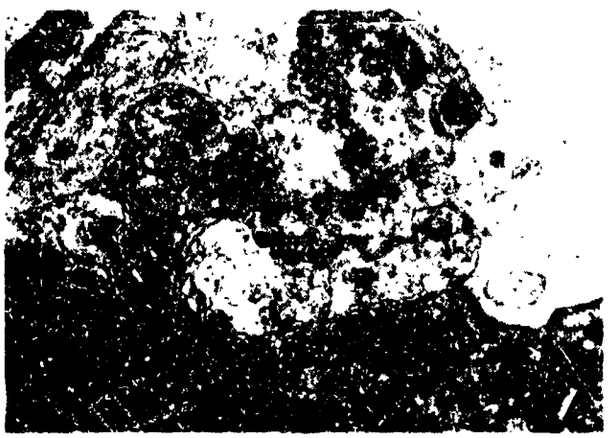

Figure 46. The nerve terminals of this degenerating neuromuscular junction in a Flight AL muscle lack synaptic vesicles and mitochondria and the axolemma is not intact. The schwann cell is hypertrophied and abuts the postjunctional membrane, presumably vacated by degenerated terminals. X9,213.

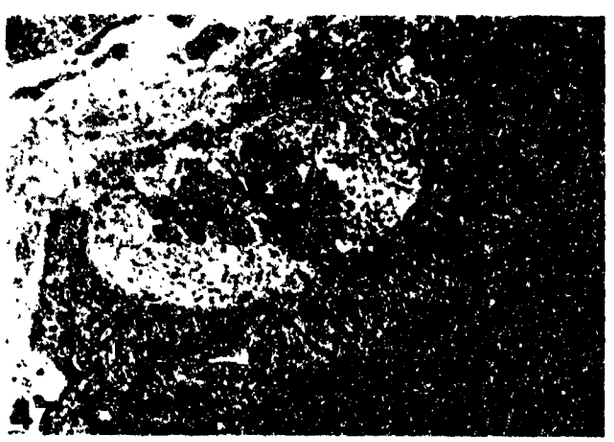

Figure 47. As illustrated here, the neuromuscular junctions of the Flight EDL muscles were normal in appearance. X13,200.

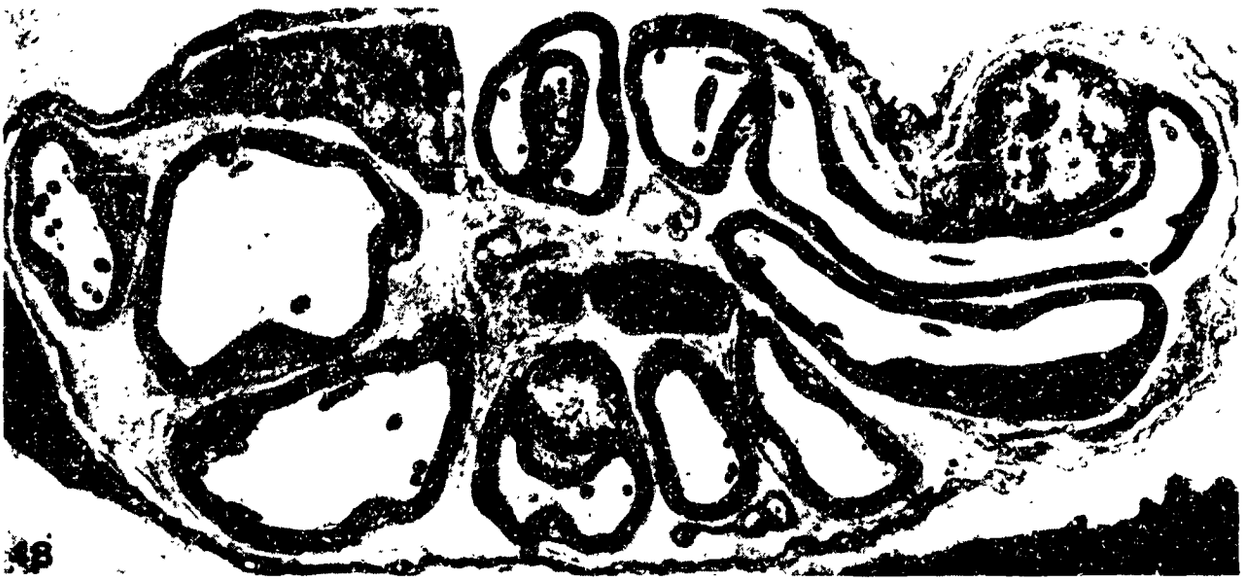

Figure 48. A large intramuscular nerve bundle in a nondamaged region of a Flight AL muscle. The nerve bundle is similar in appearance to those in control muscles. The myelinated and nonmyelinated axons have intact cell membranes. The axons contain neurofilaments, microtubules, and mitochondria. The perimysial connective tissue has prominent bundles of collagen which fill the regions between schwann cells. X6,188.

Figure 49. A portion of an intramuscular nerve bundle in a damaged region of a Flight AL muscle. The collagen bundles between schwann cells are extracted and markedly reduced in size. The neurofilaments and microtubules are clumped (arrow) and reduced in amount. Mitochondria appear swollen and disrupted. X6,188.

Figure 50. A small intramuscular nerve bundle in a necrotic region of a Flight AL muscle. A trio of fine nerve processes (arrow) contact the large central schwann cell. This suggests axon regeneration. The two myelinated axons appear normal. The perineurial collagen bundles are extracted. X6,188.

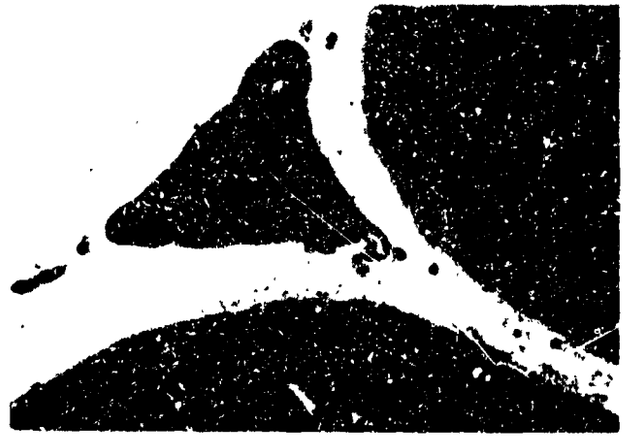

Figure 51. A resting fixed-tissue macrophage in a Flight EDL muscle. The nucleus is heterochromatic, there is little cytoplasm, and the cell has few processes. X13,000.

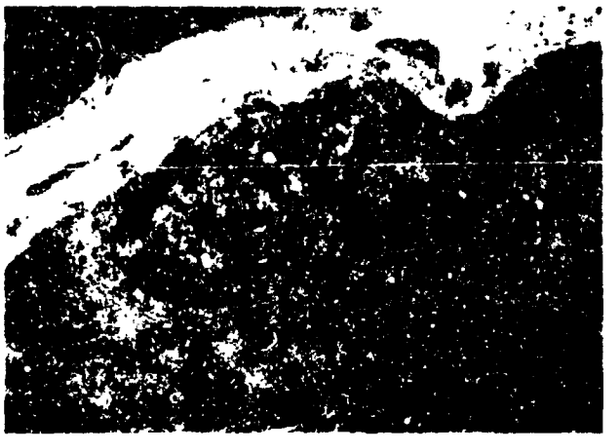

Figure 52. A quiescent satellite cell in a Flight EDL muscle. The cell has a thin rim of cytoplasm, and the nucleus is heterochromatic. X16,800.

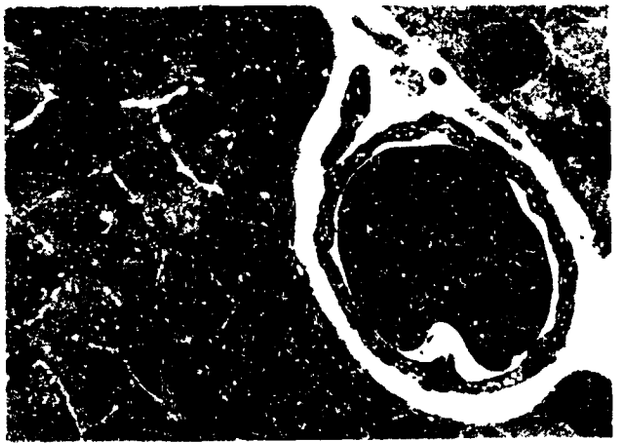

Figure 53. The capillaries in the Flight EDL muscles were not disrupted. As in control muscles, erythrocytes are often observed within the capillary lumen. X13,750.

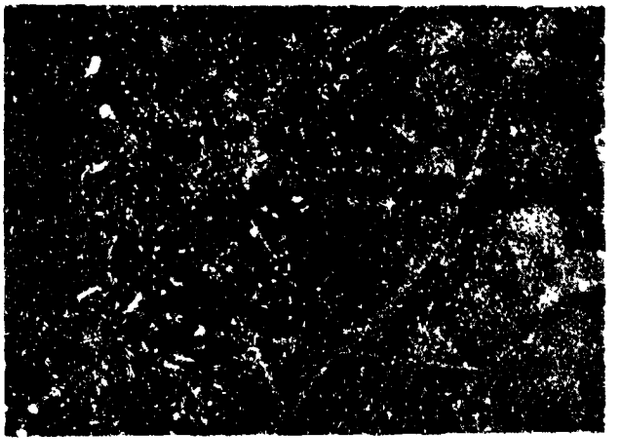

Figure 54. A cross section of an SO fiber in a Flight EDL muscle. As in normal muscles, medium-sized mitochondria surround the myofibrils at the level of the I band. X13,750.

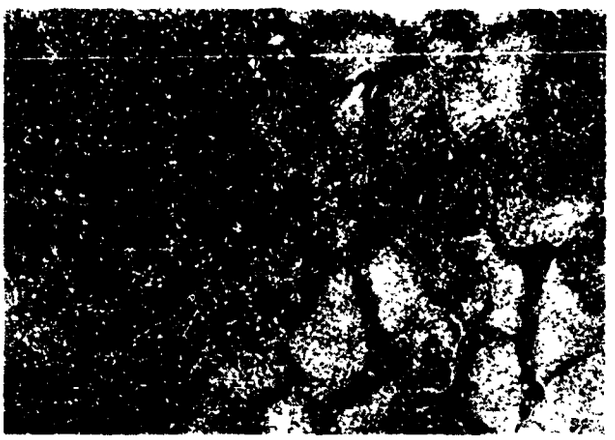

Figure 55. An FOG fiber in a Flight EDL muscle. Large mitochondria occupy the I band region and are present in the A bands. Myofibrils and membrane systems appear normal. X13,750.

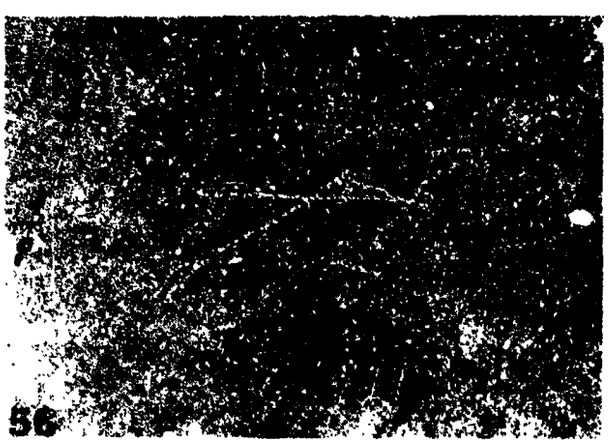

Figure 56. An FG fiber in a Flight EDL muscle. The small thin mitochondria are mostly confined to the I band region. The morphology of this fiber is indistinguishable from normal. X13,750.

EXPERIMENT K-6-09

PART II: BIOCHEMICAL ANALYSIS OF EDL AND PLT MUSCLES

S. Ellis, et al.

RESULTS

Measurements were made of two enzymes, the lysosomal tripeptidyl aminopeptidase (TAP) and the cytosolic anhydrase III (CA III), and also the calcium binding protein parvalbumin (PVA). TAP and CA III were measured as described by Riley et al (1982;1987) and PVA was measured by the electrophoretic method of Klug et al., (1983). By way of background, TAP increased 60% in the Soleus muscles after 7.5 days in the SLS-3 flight rats whereas the EDL concentrations were unchanged. Surprisingly, the PLT muscle from the Cosmos '87 rats, flown for 12.5 days, showed a 30% decrease (Table 1). The EDL did not show an increase in TAP activity.

CA III is present in highest concentrations in slow oxidative muscle fibers whereas fast fibers have very low concentrations (Riley et al., 1982), and the levels of the enzyme can be affected by a number of physiological perturbations. Although the EDL and PLT are quite gravity insensitive, it was of interest to determine the influence of space flight on the CA III levels. As can be seen from Tables I and II there was no difference in CA III content of these muscles except for the PLT of the basal group which showed a slightly slower concentration of CA III, presumably due to their younger age (90 days) (Riley et al., 1982).

Parvalbumin is highest in concentration in the fast twitch muscle and functions as a relaxing factor facilitating sequestration of calcium in the sarcoplasmic reticulum. In view of reports that unloading slows the 1/2 relaxation time, it was of interest to measure PVA for possible concentration decreases in the EDL and PLT muscles. As can be seen from Table 1, the PVA concentrations of the PLT were not significantly different in any of the groups. In the case of the EDL, only the synchronous group showed a significant reduction in PVA, whereas the basal, vivarium, and flight groups did not differ.

Thus, space flight showed significant perturbation only in the TAP concentration of the PLT, the concentrations of the CA III and the PVA being unaffected in either of the two muscles. It should be noted that these results may have been quantitatively affected by a thaw to room temperatures for approximately twenty-four hours due to a failure in the emergency back-up electrical power to our minus 80°C freezers. Simulation of the thawed condition for twenty-four hours using fresh muscles showed no reduction in TAP or CA III activities, whereas PVA was reduced by 24% in the EDL (6.8 to 5.1 µg/mg wet muscle) and unchanged in the PLT (3.9 µg/mg wet muscle), the muscles being sampled from 250g rats. These observations suggest that the thawing would not affect the conclusions or reliability to a significant degree.

REFERENCES

Riley, D.A., Ellis,S., and J. Bain. J. Histochem. Cytochem. 30: 1275 (1982).

Riley, D.A., Ellis, S., Slocum, G.R. et al. Muscle and Nerve 10: 560 (1987).

Klug, G., Reichman, H., and D. Pette. FEBS Lett. 152: 180 (1983).

PRECEDING PAGE BLANK NOT FILMED

TABLE 1

SUMMARY OF ASSAYS OF PLANTARIS MUSCLE

ACTIVITY

GROUP and RAT NO.	CA III U/mg muscle	TAP mU/mg Muscle	PVA ug/mg muscle
BASAL			
B_6	0.88	0.10	2.26
B_7	0.89	0.08	2.93
B_8	0.76	0.15	2.71
B_9	0.96	0.08	3.10
B_{10}	0.97	0.16	3.45
	0.89 ±.05 (B vs S: p <.05)	0.11±.038	2.89±0.44
VIVARIUM			
V_6	0.63	0.09	2.21
V_7	1.2	0.10	2.36
V_8	1.0	0.11	4.12
V_9	0.90	0.11	5.41
V_{10}	1.1	0.11	3.77
	0.97 ± .21	0.10 ± .01	3.57 ±1.32
SYNCHRONOUS			
S_6	0.97	0.10	2.05
S_7	1.0	0.11	2.96
S_8	1.1	0.12	3.14
S_9	1.0	0.14	2.58
S_{10}	0.95	---	3.14
	0.96 ±.058	0.12 ±.02	2.77 ±.47
FLIGHT			
F_6	1.1	0.11	2.74
F_7	1.04	0.07	2.68
F_8	0.64	0.08	3.53
F_9	1.1	0.09	4.14
F_{10}	0.97	0.04	4.09
	0.97 ±.19	0.078 ±.026	3.44 ±0.71
		(F vs S: p<.05)	

Note 1: CA III and PVA columns: Means of triplicate analysis per sample.
Note 2: p values from t statistic for two means.

TABLE 2

SUMMARY OF ASSAYS OF EDL MUSCLE

ACTIVITY

GROUP and RAT NO.	CA III U/mg muscle	TAP mU/mg muscle	PVA ug/mg muscle
BASAL			
B_6	0.11	0.24	---
B_7	0.14	0.11	2.80
B_8	0.10	0.28	3.53
B_9	0.19	0.28	3.90
B_{10}	0.13	0.40	5.06
	0.134 ±.035	0.26±.10 (F vs B: p <0.05)	3.82±.94
VIVARIUM			
V_6	0.13	0.13	---
V_7	0.18	0.32	4.24
V_8	0.21	0.14	4.89
V_9	0.12	0.38	4.20
V_{10}	0.02	0.14	5.58
	0.132 ± .073	0.22 ± .12	4.73 ±0.65
SYNCHRONOUS			
S_6	0.20	0.11	3.44
S_7	0.28	0.16	3.56
S_8	0.12	0.13	2.39
S_9	0.12	0.14	1.43
S_{10}	0.25	0.15	3.66
	.194 ±.073	0.14 ±.02	2.90 ±0.97 (S vs V, p <.05)
FLIGHT			
F_6	0.20	0.14	3.69
F_7	0.06	0.12	5.28
F_8	0.08	---	3.53
F_9	0.01	0.07	4.20
F_{10}	0.23	0.14	5.39
	0.136 ±.094	0.13 ±.03	4.42±0.87 (F vs S: p<.05)

Note 1: CA III and PVA columns: Means of triplicate analysis per sample.
Note 2: p values from t statistic for two means.

N90-26464

EXPERIMENT K-6-10

EFFECTS OF ZERO GRAVITY ON MYOFIBRIL PROTEIN CONTENT AND ISOMYOSIN DISTRIBUTION IN RODENT SKELETAL MUSCLE

Principal Investigator:

K. Baldwin
Department of Physiology and Biophysics
University of California
Irvine, California 92717

Co-Investigators:

R. Herrick
Department of Physiology and Biophysics
University of California
Irvine, California 92717

V. Oganov
Institute of Biomedical Problems
Moscow, USSR

PRECEDING PAGE BLANK NOT FILMED

SUMMARY

The purpose of this experiment was to investigate the effects of 12 days of zero gravity (0G) exposure (Cosmos 1887 Biosputnik) on the enzymatic properties, protein content, and isomyosin distribution of the myofibril fraction of the slow-twitch vastus intermedius (VI) and the fast-twitch vastus lateralis (VL) muscles of adult male rats. Measurements were obtained on three experimental groups (n=5 each group) designated as flight-group (FG), vivarium-control (VC), and synchronous-control (SC). Body weight of the FG was significantly lower than the two control groups ($p < 0.05$). Compared to the two control groups, VI weight was lower by 23% ($p < 0.10$); whereas no such reduction was observed for the VL muscle. Myofibril yields (mg protein/g of muscle) in the VI were 35% lower in the FG compared to the controls ($p < 0.05$); whereas, no such pattern was apparent for the VL muscle. When myofibril yields were expressed on a muscle basis (mg/g x muscle weight), the loss of myofibril protein was more exaggerated and suggests that myofibril protein degradation is an early event in the muscle atrophy response to 0G. Analysis of myosin isoforms indicated that slow-myosin was the primary isoform lost in the calculated degradation of total myosin. No evidence of loss of the fast isomyosins was apparent for either muscle following space flight. Myofibril ATPase activity of the VI was increased in the FG compared to controls, which is consistent with the observation of preferential slow-myosin degradation. These data suggest that muscles containing a high percent of slow-twitch fibers undergo greater degrees of myofibril protein degradation than do muscles containing predominantly fast-twitch fibers in response to a relatively short period of 0G exposure, and the primary target appears to be the slow-myosin molecule.

INTRODUCTION

Previous findings on animals exposed to either zero gravity or to conditions of simulated non weight bearing activity such as hindlimb suspension clearly show that there is marked atrophy of hindlimb muscles comprised predominantly of slow-twitch fibers (Grindeland et al, 1985; Martin and Edgerton, 1985; Thomason et al, 1987a). Furthermore, Thomason et al (1987a; 1987b) reported that hindlimb suspension of rodents induced a preferential loss of myofibril protein in the atrophying slow-twitch soleus muscle. There was little evidence of a similar response occurring in the synergistic fast-twitch plantaris muscle (Tsika et al 1987d). This suggests that the myofibril fraction may be a target of protein degradative processes primarily in muscle fibers expressing slow-myosin when there is insufficient weight bearing activity placed on the muscle. The present study was undertaken to ascertain if a similar response occurs when animals are exposed to a zero gravity environment for sufficient duration to induce atrophy. Therefore, groups of rats were exposed to zero gravity during the Cosmos 1887 12 day mission which was launched in late September, 1987. The vastus intermedius, a knee extensor comprised largely of slow-myosin (Tsika et al 1987b) and the synergistic vastus lateralis, which is comprised chiefly of the fast myosin isoforms (Tsika et al 1987b), were examined in both flight and ground control groups for the following: a) muscle mass; b) myofibril protein concentration and ATPase specific activity; and c) estimates of absolute and relative isomyosin content. We tested the general hypothesis that zero gravity would induce 1) a preferential loss of slow myosin and a corresponding increase in myofibril ATPase activity in the vastus intermedius muscle and 2) minimal changes in the vastus lateralis muscle. The results reported herein are largely in support of this hypothesis.

METHOD

Experimental Design and Rodent Groups.

The muscles used for analyses in this study were obtained from animals selected for the Cosmos 1887 Biosputnik Flight. Adult male rats (n=5 each group) of the Czechoslovakian-Wistar strain were assigned initially to one of four experimental groups designated as: 1) Flight-group (FG); 2) Synchronous-control (SC); 3 Vivarium-control (VC); and 4) Basal-control (BC). In the present

study, for simplification in reporting the data and its interpretation, comparisons are reported for only the FG, SC, and VC groups, because the muscles from these latter groups were removed and processed at approximately the same time.

The FG (n=10 total assigned for flight) was housed in a single cage equipped with individual food nozzles and water lixits for each rat. Fourteen-gram boluses of food were administered at designated times each day so that each rat received a total of 55 grams of a paste diet. Water was provided ad libitum. The flight was launched on September 29, 1987 and returned 12 1/2 days later on October 12, 1987. The rats had their last meal on the final day of the flight and were not fed again for approximately for 42 hrs, at which time they were recovered from an alternate landing site (Siberia). Although the animals were without food, they appeared to have adequate water provision, since they did not drink water when it was provided at recovery. The animals appeared healthy and were warm. It is important to note that due to the alternate site landing, there was an approximate 48 hr delay between landing and sacrificing the flight animals at the designated site in Moscow.

The synchronous-control group (SC) was maintained in flight-type cages and fed a paste diet. They were exposed to the launch G force and vibration, deprived of food for 42 hours,andexposed to the same lighting regimen and temperature (23 deg. C) as flight rats after landing. After their simulated flight, sacrifice was delayed the same period as for the flight rats. The reentry G force and post flight transportation conditions of the flight animals were not mimicked for the SC group.

The vivarium-control group (VC) was kept in the same type of cage as the flight group. They were fed the same quantity of food per day but in only one feeding, and food was withdrawn 12 hrs prior to sacrifice. Post flight conditions were not mimicked for this group.

Tissue Sampling.

At the time of sacrifice the animals were weighed, and then specific organ components were removed including the muscles of the anterior thigh. On five animals from each experimental group, the vastus intermedius (VI) and the vastus lateralis (VL) muscles were removed, cleaned free of visible fat and connective tissue, weighed, and placed in vials containing 100% glycerol. The vials were stored at liquid nitrogen temperature, and they were eventually shipped by NASA to Irvine, California on dry ice in early November, 1987, at which time the biochemical analyses were begun.

Myofibril Extraction and Myofibril ATPase.

Myofibrils were prepared by the detergent treatment technique of Solaro et al (1971), as described in detail previously (Tsika et al, 1987a). After the final washing step, the myofibrils were suspended in 150 mM KCl-20 mM Imidazole (pH 7.0) and the concentration adjusted to 6 mg/ml with the use of the biuret protein assay (Gornall et al, 1949). Myofibril yields are reported as mg/gram and mg/muscle (table 2). This procedure is quantitative for the contractile proteins, because there is little evidence of loss of myosin in the washing process, based on electrophoretic analysis of the supernatants. Aliquots of the myofibril suspension were used immediately for ATPase activity (see below) and the remainder was prepared for storage (-20 deg. C) by suspending 1 volume of myofibril suspension with 2 volumes of a buffer consisting of 75% glycerol, 25 mM sodium pyrophosphate, 1 mM EGTA, and 0.5 mM 2-mercaptoethanol (pH 8.8).

Myofibril ATPase specific activity was determined at a free calcium concentration of ~10^{-4} M with the use of an EGTA buffer system as described in detail previously (Tsika et al, 1987a). Activity was expressed as micromoles of inorganic phosphate released per milligram of myofibril protein per minute (table 2).

Electrophoresis of myofibrils.

Aliquots of myofibrils suspended in the glycerol buffer were subjected to polyacrylamide electrophoresis to separate the native myosins according to the method of Hoh et al (1976). Briefly, native polyacrylamide gel electrophoresis was performed on 6-cm-long gels that were 4% in total acrylamide, 2.5% in bis(acrylamide) (expressed as a percentage of total acrylamide), 10% glycerol, 20 mM tetrasodium pyrophosphate (pH 8.8) at 4 deg. C. The gels were run in a Pharmacia GE-2/4 apparatus with recirculation of a running buffer consisting of 20 mM sodium pyrophosphate, 0.2 mM cystein, and 10% glycerol (pH 8.8). The electrophoresis apparatus was cooled by refrigeration at 4 deg. C and additionally by immersed cooling coils connected to an external recirculation refrigeration bath. The temperature of the recirculating buffer was maintained at -1 deg. C throughout electrophoresis. Gels were prerun at 90 V (15 V/cm) maintained constant for 30 min prior to sample application. Approximately 5 micrograms of protein were electrophoresed for 20 hrs at 90 V maintained constant. Gels were stained at the end of electrophoresis for two hrs with a solution that was 0.1% Coomassie Blue R-250, 30% isopropyl alcohol, and 10% glacial acetic acid. The gels were destained by diffusion in a solution that was 20% methanol and 10% glacial acetic acid.

Myofibril samples were also used for sodium dodecyl sulfate-polyacrylamide gel electrophoresis according to the technique of Laemmli (1970) in order to estimate the relative percent of myosin heavy chain making up the myofibril protein pool. The myofibril suspensions were diluted two-fold with a buffer consisting of 100 mM Tris-HCl, 5% glycerol, 4% sodium dodecyl sulfate, 5% 2-mercaptoethanol, and 0.05% brom-phenol blue (pH 6.8) at room temperature. Purified myosin prepared from fast-twitch and slow twitch skeletal muscle were used as standards for identifying heavy chain and light chain proteins. The sample mixture was warmed to 100 deg. C for 2 min. Myofibrils were analyzed on 14% gels, which were run at room temperature in an apparatus with a central cooling reservoir through which tap water circulated. Electrophoresis was carried out at constant current (40 mA/slab gel) until the dye front reached the end of the gel. The gels were stained for 2 hrs at the end of the run using solutions as described above.

Quantitation of myosin isoforms and myosin heavy chain and light chain components.

Gel bands of the native myosins separated by pyrophosphate electrophoresis were analyzed densitometrically by directly scanning the gels at 630 nanometers using a Zeineh Soft Laser Scanning Densitometer (Biomed instruments Inc., Fullerton, Ca.) connected to an IBM PC equipped with the appropriate program for integration of peak areas. The relative proportion of myosin isoforms were obtained from the gel scan and corresponded to the percent area under the peaks of absorption of the isoform bands. Previously, we have identified five isomyosins in mixed rodent skeletal muscle in order of their decreasing ability to migrate into pyrophosphate gels as follows: fast myosins 1-3 (Fm_1, Fm_2, and Fm_3), intermediate myosin (Im), and slow-myosin (Sm) (Tsika et al, 1987b). These isomyosins have been fully characterized in terms of their light chain and heavy chain composition (Tsika et al, 1987b). In table 3, we present the distribution of these isomyosins in the vastus intermedius and vastus lateralis muscles of control and flight groups.

Myofibrils separated into denatured protein bands were also scanned on the Zeneih Densitometer in order to estimate the relative percent of myosin heavy chain making up the total myofibril protein. The assumptions and feasibility of this technique have been discussed in detail previously (Thomason et al, 1987a; Tsika et al, 1987c). With this procedure we have determined that the myosin heavy chain comprised 41$\pm$ 2 percent of the myofibril protein among all flight and control muscles analyzed. Also, there were no statistically significant differences among experimental groups (data not shown).

With the above information we were able to estimate the amount of both total myosin and the amount of individual isomyosins (mg/muscle) comprising a given muscle using the data as reported in tables 2 and 3 in combination with the following equation (1): mg myofibril protein/muscle X % myosin in myofibril pool X % isoform = estimated mg of myosin isoform/muscle. These data are reported in table 4.

Statistical analysis.

All values are expressed as the mean and standard error. Intergroup comparisons were made by using one-way analysis of variance. The significance of differences between groups was tested using a student t-test. Differences were considered significant at the 0.05 level of confidence.

RESULTS

Body and muscle weight.

Compared to control animals zero gravity induced a 21% reduction in VI muscle weight (table 1). However, this was not statistically significant due to the variability of response and the small number of observations. Little or no effect was observed for the VL muscle. In fact, muscle weights were larger for the FG as compared to the SC group. Body weight was significantly lower for the flight animals compared to the control groups. This can only be partially attributed to losses in muscle mass, because the majority of skeletal muscles in the rat are comprised of fast-twitch fibers, which do not appear to be as sensitive to zero gravity as muscles containing slow-twitch fibers.

Myofibril yields and myofibril ATPase activity.

Compared to both the VC and SC groups, zero gravity induced a significant reduction in th concentration of myofibril protein (mg/gram; $p<0.05$; table 2). The impact of this reduction is further seen when the myofibril protein data are expressed on a muscle basis (mg/g x muscle weight). In contrast, there was little evidence of an effect of zero gravity on the yield of myofibrils in the VL muscle.

Compared to the two control groups myofibril ATPase activity was significantly higher in the FG (table 2). This increase was attributed to a reduction in the relative amount of slow myosin comprising the VI of the FG, because slow-myosin has a lower ATPase specific activity than the faster isoforms. No pattern of a change in myofibril ATPase occurred for the VL muscle as a result of zero gravity exposure. However, there was poor agreement of VL ATPase activity among the SC and VC groups (table 2).

Myosin isoform distribution.

As shown in table 3, over 70% of the myosin expressed in the VI of control animals is in the Sm and Im forms. These isoforms are thought to have lower ATPase activity than the fast isoforms, which is evident by the ATPase data reported for the two muscles in table 2 . In contrast, the VL is comprised primarily of the fast isomyosin with less than 20% in either the IM or Sm form (table 3). Zero gravity induce a slight but non significant reduction in the relative content of Sm and a slight increase in the three fast isoforms in the VI muscle. In the VL muscle, there was an apparent shift suggesting a decrease in the relative content of Im and an increase in the relative content of Fm_3 isomyosin (table 3).

When the myosin content of the muscle (mg/muscle) is examined, it is apparent that there is a significant loss in the total myosin content of the VI muscle of the FG compared to the two control groups (table 4). This loss in total myosin in the VI muscle of the FG was attributed to reductions in the absolute amount of both the SM and Im isoforms. There is no evidence of a significant loss in the fast-myosins. This observation is further illustrated by the fact that there was little impact of zero gravity on the myosin isoform patterns in the VL muscle.

DISCUSSION

The most significant observation in this study is that after approximately two weeks of exposure to zero gravity there is a reduction in the capacity to maintain expression of the lower ATPase (and hence slower) isomyosins in certain skeletal muscles of rodents. Furthermore, the myofibril fraction as a total entity is a target for protein degradation processes in the absence of weight bearing activity. Analysis of the myosin content of the VI muscle indicates that the slow-myosin is the primary isoform that is degraded. This observation is consistent with previous findings on the soleus muscle of hindlimb suspended rats (Thomason et al, 1987a and 1987b), further suggesting that the absence of ground support activity is an important factor in inducing the atrophy response. Although there was a 42 hr delay in removing tissue from the flight animals upon return to normal gravitational conditions, which could have altered the magnitude of the response somewhat, we have observed previously on suspended animals that the half-life for regeneration of both the myofibril fraction and slow-myosin is approximately ten days (Thomason et al, 1987a). Thus, the delay in obtaining the tissue had a relatively small impact on reversing this response.

It is also interesting that although the vastus lateralis acts synergistically to the VI muscle, there was little evidence of either atrophy or degradation of the fast isomyosins in this fast-twitch muscle. However, it appeared that there was some loss of Im, which was balanced by an increase in Fm_3, thereby maintaining myofibril protein concentration and content in the VL muscle (table 2).

Analyses on myofibril ATPase activity suggest that there may be a net speeding of the VI muscle's contractile (force- velocity) properties following exposure to zero gravity, because there is a good relationship between myofibil ATPase activity and the shortening velocity of a given muscle (Barany 1967). This observation is consistent with the recent findings of Fitts et al (1986), which showed that the shortening velocity of the soleus. but not the superficial vastus lateralis, was increased following 14 days of hindlimb suspension.

If the above results on rodents apply to other mammalian species, including humans, it would appear that skeletal muscles expressing a large proportion of slow-twitch fibers (slow-myosin) are the chief target for the atrophy response that is associated with prolonged zero gravity exposure. Furthermore, in view of our recent findings suggesting an inability to significantly regenerate slow-myosin in large quantities in suspended rats that were subjected to low intensity treadmill running (Thomason et al, 1987b), it would appear that counter measures of sufficient duration requiring relatively high force output by those muscles sensitive to atrophy are necessary in order to maintain expression of the slow myosin and its associated myofibril proteins. Also, it is interesting that anabolic steroids, which could have an impact on maintaining muscle mass, are effective in conserving fast-twitch muscle but not slow-twitch muscle of suspended rats (Tsika et al, 1987d). Thus it would appear that mechanical stress factors, coupled with specific hormonal manipulations, may be necessary to provide sufficient counter measures to offset potential loss of all the myosin isoforms typically expressed in skeletal muscle when individuals are exposed to prolonged space flight.

ACKNOWLEDGEMENT

This research was supported by NASA Cosmos 1887-28303

REFERENCES

1. Barany, M. ATPase activity of myosin correlated with speed of muscle shortening. J. Gen. Physiol. 50: 197-213, 1967.

2. Fitts, R. H., J. M. Metzger, D. A. Riley, and E. R. Unsworth. Models of disuse: a comparison of hindlimb suspension and immobilization. J. Appl. Physiol. 60: 1946-1953, 1986.

3. Gornall, A. G., C. J. Bardawill, and M. M. David. Determination of serum proteins by means of the biuret method. J. Biol. Chem. 177: 751-756, 1949.

4. Grindeland, R., T. Fast, M. Ruder, M. Vasquez, P. Lundgren, S. Scibetta, J. Tremor, P. Buckendahl, L. Keil, O. Chee, T. Reily, B. Dalton, and P. Callahan. Rodent body, organ, and muscle weight responses to seven days of microgravity. Physiologist. 28: 375, 1985.

5. Hoh, J. F. Y., P. A. McGrath, and R. I. White. Electrophoretic analysis of multiple forms of myosin in fast-twitch and slow-twitch muscles of the chick. Biochem. J. 157: 87-95, 1976.

6. Laemmli, U. K. Cleavage of structural proteins during the assembly of the head of bacteriophage T_4. Nature. 227: 680-685, 1970.

7. Martin, T. P. and V. R. Edgerton. The influence of spaceflight on the rat soleus. Physiologist. 28: 375, 1985.

8. Solaro, R. J., D. C. Pang, and F. N. Briggs. The purification of cardiac myofibrils with triton x-100. Biochim. Biophys. Acta. 245: 259-262, 1971.

9. Thomason, D. B., R. E. Herrick, D. Surdyka, and K. M. Baldwin. Time course of soleus muscle myosin expression during hindlimb suspension and recovery. J. Appl. Physiol. 63: 130-137, 1987a.

10. Thomason, D. B., R. E. Herrick, and K. M. Baldwin. Activity influences on soleus muscle myosin during rodent hindlimb suspension. J. Appl. Physiol. 63:; 138-144, 1987b.

11. Tsika, R. W., R. E. Herrick, and K. M. Baldwin. Interaction of compensatory overload and hindlimb suspension on myosin isoform expression. J. Appl. Physiol. 62: 2180-2186, 1987a.

12. Tsika, R. W., R. E. Herrick, and K. M. Baldwin. Subunit composition of rodent isomyosins and their distribution in hindlimb skeletal muscles. J. Appl. Physiol. 63: 2101-2110, 1987b.

13. Tsika, R. W., R. E. Herrick, and K. M. Baldwin. Time course adaptations in rat skeletal isomyosins during compensatory growth and regression. J. Appl. Physiol. 63: 2111-2121, 1987c.

14. Tsika, R. W., R. E. Herrick, and K. M. Baldwin. Effect of anabolic steroids on skeletal muscle mass during hindlimb suspension. J. Appl. Physiol. 63: 2122-2127, 1987d.

TABLE 1. BODY WEIGHT (GRAMS), MUSCLE WEIGHT (MILLIGRAMS), AND MUSCLE WEIGHT/BODY WEIGHT AMONG EXPERIMENTAL GROUPS.

Group	BW	VI	VL	VI/BW	VL/BW
Flight	303 ±3	189 ±44	892 ±63	0.623 ±0.14	2.94 ±0.19
Vivarium Control	342* ±9	242 ±30	964 ±37	0.720 ±0.10	2.81 ±0.05
Synchr. Control	349* ±7	246 ±35	827* ±57	0.700 ±0.10	2.37* ±0.16

Data are reported as mean ±SEM. * P< 0.05 flight vs control
VI=vastus intermedius; VL=vastus lateralis

TABLE 2. MYOFIBRIL PROTEIN YIELDS AND MYOFIBRIL ATPASE ACTIVITY IN MUSCLES OF EXPERIMENTAL GROUPS.

Group		Vastus Intermedius	
	mg/g	mg/muscle	ATPase
Flight	71 ±7	14.1 ±4.1	415 ±72
Vivarium Control	108 ±6*	26.1 ±3.2*	334 ±17*
Synchr. Control	107 ±3*	26.1 ±2.7*	342 ±32*
		Vastus Lateralis	
	mg/g	mg/muscle	ATPase
Flight	81 ±13	62 ±16	606 ±24
Vivarium Control	79 ±17	79 ±16	734 ±55
Synchr. Control	87 ±16	74 ±17	623 ±45

Data are mean ±SEM. ATPase is expressed as nMoles/mg myofibril protein/min.

* $P < 0.05$ flight vs control group

TABLE 3. RELATIVE PERCENT OF ISOMYOSINS EXPRESSED IN VASTUS INTERMEDIUS AND VASTUS LATERALIS MUSCLES OF EXPERIMENTAL GROUPS.

Vastus Intermedius

Group	Sm	Im	Fm_3	Fm_2	Fm_1
Flight	31.0 ±4.5	34.4 ±1.5	21.8 ±0.7	8.8 ±2.9	3.9 ±1.5
Vivarium Control	37.8 ±3.3	34.5 ±2.5	17.8 ±1.7	6.8 ±0.8	3.1 ±1.0
Synchr. Control	37.0 ±5.1	37.3 ±1.2	18.8 ±3.8	4.9 ±1.9	1.9 ±0.9

Vastus Lateralis

Group	Sm	Im	Fm_3	Fm_2	Fm_1
Flight	--	8.8 ±1.1	40.8 ±1.7	32.7 ±1.2	17.3 ±0.5
Vivarium Control	--	14.8* ±0.5	32.6* ±0.6	31.8 ±0.4	20.8 ±0.7
Synchr. Control	--	16.6* ±1.7	33.5* ±1.1	31.2 ±0.9	18.8 ±0.9

Data are mean ± SEM. Sm=slow-myosin; Im= intermediate- myosin; Fm=fast-myosin

* $P < 0.05$ control vs flight

TABLE 4. ESTIMATES OF TOTAL MYOSIN AND ISOMYOSIN CONTENT EXPRESSED AS MG/MUSCLE AMONG EXPERIMENTAL GROUPS.

		Vastus Intermedius		
Group	Total	Sm	Im	Fm
Flight	6.7 ±0.3	1.8 ±0.6	2.3 ±0.8	2.6 ±0.5
Vivarium Control	12.5* ±1.3	4.6* ±0.5	4.3* ±0.6	3.7 ±0.7
Synchr. Control	10.6* ±1.2	3.8* ±0.3	3.9* ±0.4	2.9 ±0.8

		Vastus Lateralis		
Group	Total	Sm	Im	Fm
Flight	31.1 ±5	--	2.6 ±0.4	28.4 ±5
Vivarium Control	31.0 ±6	--	5.4 ±2.0	25.7 ±5.0
Synchr. Control	29.6 ±6	--	4.4 ±0.9	24.0 ±4.0

Data are mean ±SEM. Sm=slow-myosin; Im=intermediate-myosin; Fm=fast-myosin.

* P< 0.05 flight vs control

N90-26465

EXPERIMENT K-6-11

ACTIN MRNA AND CYTOCHROME C MRNA CONCENTRATIONS IN THE TRICEPS BRACHIA MUSCLE OF RATS

Principal Investigator:

F. W. Booth
University of Texas
Health Science Center at Houston
Medical School
Department of Physiology and Cell Biology
Houston, Texas 77225

Co-Investigators:

P.R. Morrison
University of Texas
Houston, Texas 77225

D.B. Thomason
University of Texas
Houston, Texas 77225

V.S. Oganov
Institute of Biomedical Problems
Moscow, USSR

 PRECEDING PAGE BLANK NOT FILMED

INTRODUCTION

It is well known that some skeletal muscles atrophy as a result of weightlessness (Steffen and Musacchia, 1986) and as a result of hindlimb suspension (Tischler et al., 1985, Thomason et al., 1987). Because the content of protein is determined by the rates of protein synthesis and degradation, a decrease in protein synthesis rate, or an increase in the protein degradation, or changes in both could produce the atrophy. Indeed, an increased protein degradation (Tischler et al., 1985) and a decreased protein synthesis (Thomason et al., 1988) have been observed in skeletal muscles of suspended hindlimbs of rats. Any decrease in protein synthesis rate could be caused by decreases in mRNA concentrations. Such decreases in the concentration and content of alpha-actin mRNA and cytochrome c mRNA have been noted in skeletal muscles of hindlimb suspended rats (Babij and Booth, 1988). From these findings we hypothesized that alpha-actin mRNA and cytochrome c mRNA would decrease in the triceps brachia muscle of Cosmos 1887 rats.

RESULTS

Forty-two hours following the landing of a 12.5-day flight on Cosmos 1887, the wet weight of the triceps brachia was significantly less (-19%) than the synchronous control group, but was not significantly different from the other two control groups (Table I). No significant differences for the ratio of triceps brachia wet weight to body weight existed between the flight group and any control group. Also no significant differences in RNA concentration and in RNA content occurred between the flight and control groups. The quantity of alpha-actin mRNA per unit of RNA was no different between the flight group and any control group. Although the quantity of cytochrome c mRNA per unit of RNA was significantly higher in the flight group than the vivarium control group, there were no differences between the flight group and either the basal control group or the vivarium control group.

DISCUSSION

It is well known that slow-twitch muscle atrophies more quickly than fast-twitch muscle, either in hindlimb suspension or in weightlessness (Steffen and Musacchia, 1986, Thomason et al., 1987). Such an observation may explain, in part, the failure to observe atrophy of the fast-twitch triceps brachia 42 hours after a 12.5-day spaceflight. It is also possible to speculate that the triceps brachia is recruited frequently in space as the rat attempts to hold on to a position in the cage or to move between two points and that this event prevented atrophy. Electromyography of rat skeletal muscles in weightlessness is necessary to document this hypothesis. The failure to replicate observations of decreases in the quantities of specific mRNAs in skeletal muscles of hindlimb-suspended rats could be due to a number of factors. First, as discussed above, the triceps brachia did not atrophy in space whereas the skeletal muscles having decreased concentrations of alpha-actin mRNA and cytochrome c mRNA were atrophied after seven days of hindlimb suspension. Second, alpha-actin mRNA concentrations could have recovered during the 42-hour period elapsing between the end of the 12.5-day flight and removal of the muscle from the rats. Rapid recovery of alpha-actin mRNA concentrations has been noted in atrophied muscle recovering from seven days of hindlimb immobilization. The concentration of alpha-actin mRNA per unit of RNA decreased 47% in fast-twitch muscle after the seventh day of limb immobilization, but returned to control values on the second day of recovery (Morrison et al., 1987b). Thus either the 42-hr recovery of skeletal muscle from weightlessness or the lack of atrophy could explain the observation of no change in alpha-actin mRNA quantities. The failure to observe a significant decrease in cytochrome c mRNA in the triceps brachia muscle is likely related either to the absence of atrophy or to a speculated absence of a decline in the electromyographic activity of the triceps brachia muscle. It is unlikely that the 42-hour recovery period following the return from weightlessness was the explanation for no change in cytochrome c mRNA in the triceps brachia muscle because cytochrome c mRNA did not recover for the first 2 days after ending seven days of limb immobilization (Morrison, et al., 1987a). Rather, it took four days of recovery for cytochrome c mRNA to increase from 60% of control to 126% of control values in fast-twitch muscle after the limb immobilization.

CONCLUSION

The triceps brachia was not atrophied after 42 hours of recovery from 12.5 days in space. Both of these factors (lack of atrophy and recovery time) likely contributed to the lack of change in RNA content and alpha-actin mRNA concentration per unit of RNA. A speculated maintenance of electromyographic activity by the triceps brachia while in space likely contributed to the absence of any change in cytochrome c mRNA in this muscle.

ACKNOWLEDGMENTS

We thank Dr. Richard Grindeland for his support and Dr. V.S. Oganov for the supply of tissue. The research was supported by NASA grant NAG 2-239.

REFERENCES

1. Babij, P and Booth, F.W.: Alpha-actin and cytochrome c mRNAs in atrophied adult rat skeletal muscle. Am. J. Physiol. Vol. 254, 1988, pp C651-C656.

2. Morrison, P.R., Montgomery, J.A., Wong, T.S., and Booth, F.W.: Cytochrome c protein-synthesis rates and mRNA contents during atrophy and recovery in skeletal muscle. Biochem. J. Vol. 241, 1987a, pp 257-263.

3. Morrison, P.R., Muller, G.W. and Booth, F.W. Actin synthesis rate and mRNA level increase during early recovery of atrophied muscle. Am. J. Physiol. Vol 253, 1987b, pp C205-C209.

4. Steffen, J.M. and M[illegible]sacchia, X.J.: Spaceflight effects on adult rat muscle protein, nucleic acids, and amino acids. Am. J. Physiol. Vol. 251, 1986, pp R1059-R1063.

5. Thomason, D.B., Herrick, R.E., Surdyka, D. and Baldwin, K.M.: Time course of soleus muscle myosin expression during hindlimb suspension and recovery. J. Appl. Physiol. Vol 63, 1987, pp 130-137.

6. Thomason, D.B., Biggs, R.B. and Booth, F.W.: Rapid protein synthesis decrease and transient protein degradation increase in atrophying soleus muscle. FASEB J. Vol. 2, 1988, p A939.

7. Tischler, M.E., Jaspers, S.R., Henricksen, E.J., and Jacob, S.: Responses of skeletal muscle to unloading - a review. The Physiologist Vol. 28, 1985, pp. S13-S15.

TABLE 1

TRICEPS BRACHIA(n=5) AMONG 4 GROUPS ANOVA, P=

	GROUP				
Measurements	Flight	Basal	Synchronous	Vivarium	Among 4 Groups ANOVA, P=
Muscle wet wt (MW) (g)	1.28±0.20	1.38±0.13	1.52±0.11*	1.51±0.15	0.063
MW/Body Weight (g/g)	0.42±0.07	0.44±0.07	0.44±0.05	0.44±0.07	0.917
RNA Concentration (mg/g muscle)	1.03±0.08	1.05±0.19	1.08±0.13	1.01±0.08	0.856
RNA Content (mg/whole muscle)	1.32±0.28	1.47±0.39	1.65±0.24	1.53±.23	0.396
ACTIN mRNA slope (DPM/µg RNA)	1686	2186	1732	1408	0.046
CYT. c mRNA slope (DPM/µg RNA)	97	97	73	74*	0.051

Values are means ± SD
* indicates P<0.05 from flight group

N90-26466

EXPERIMENT K-6-12

MORPHOMETRIC STUDIES OF ATRIAL GRANULES AND HEPATOCYTES

PART I. MORPHOMETRIC STUDY OF THE LIVER

PART II. THE ATRIAL GRANULAR ACCUMULATIONS

Principal Investigator:

L. M. Kraft
NASA Ames Research Center
Moffett Field, CA. 94035

Co-Investigators:

L.C. Keil
NASA Ames Research Center
Moffett Field, California 94035

I.A. Popova
Institute of Biomedical Problems
Moscow, USSR

EXPERIMENT K-6-12

PART I: MORPHOMETRIC STUDY OF THE LIVER

L.M. Kraft

SUMMARY

The livers of flight, F, rats from the Cosmos 1887 mission were markedly paler and heavier than those of the synchronous, S, and vivarium, V, controls. In the F group, microscopic study revealed extensive hepatocytic intracytoplasmic vacuolization which was moderate in the S and minimal in the V groups. The vacuoles were not sudanophilic and therefore were regarded as glycogenic in origin. To obtain objective data concerning the extent of the vacuolization, livers were examined by computer assisted morphometry. Measurements of profile area and perimeter of the hepatocyte nuclei and vacuoles were evaluated according to stereological principles. Results indicated that the volume density of the nuclei was less in the F group than in the S ($p = <0.0002$) and V ($p = <0.001$) groups. Mean volume of individual nuclei did not differ. Volume density of the vacuoles was greater in the F than in the V group ($p = <0.02$) while their mean diameter was less ($p = <0.05$). To ascertain the relationship between increse in liver weight of the flight animals and the results of this study, an assumption was made that the specific gravity of the vacuolar contents was similar to the other extranuclear components of the hepatocyte. On that basis, calculations showed that the elevated vacuolar volume density in the flight group did not cause the increased liver weight in those animals, but that the non-nuclear, non-vacuolar parenchymal compartment did contribute significantly. Factors that may have played a causal role in liver weight and vacuolar compartment increases are discussed.

INTRODUCTION

When participation in the Cosmos 1887 mission was first proposed, a study of hepatic mitotic index was considered as an approach to elucidating the effects of space flight on developing organs in the juvenile animal. For this purpose, however, the rats from the Cosmos 1887 mission proved to be too old (105-111 days) at the time of necropsy. Even after extensive search, no mitoses were seen in any of the liver tissues studied.

Differences among the livers were noted, however. From gross observation it was evident that those of the flight group were markedly paler than the synchronous and vivarium control livers. Subsequent microscopic examination revealed that, whereas some cytoplasmic vacuoles were present in hepatocytes of all animals, the flight group was the most severely involved. As had been recorded by the recovery team in the USSR, the livers of that group were significantly heavier than those of the control groups (Grindeland, Vasques, et al.).

The goal of the present study was to characterize the vacuoles, to obtain data with which to evaluate the gross and microscopic differences, and, if possible, to explain the increased liver weight of the flight group from microscopic morphometric findings. In addition to the use of general histologic techniques, therefore, morphometry of the hepatocyte nuclei and intracytoplasmic vacuoles was undertaken using light microscopic computer assisted image analysis.

PRECEDING PAGE BLANK NOT FILMED

METHODS

Animals and Tissues.

A portion of the liver from each of five rats of flight, synchronous control and vivarium control groups was made available. At necropsy in the Soviet Union, the caudate lobe of each liver was cut into several small portions and immersed in cold (4°C) fixative consisting of 3% glutaraldehyde in 0.1 M phosphate buffer at pH 7.4. The tissues remained in the cold until they were further processed in Moscow by the American team members who repiaced the fixative with a graded ethanol series up to a final concentration of 95%. During shipment to the United States and until histological preparations were made, the specimens remained at 4°C.

Tissue Preparation.

Because of the poor penetration by glutaraldehyde fixative after immersion, only the surface layer, about 1 mm thick, of each liver portion could be used for further processing. This well fixed layer was removed with a razor blade from most if not all of the poorly fixed core of each portion. Samples from each liver were then processed by one of the following methods:

1. for general oversight - standard dehydration through absolute ethanol to xylene, embedment in paraffin, sectioning at 4 µm, staining with hematoxylin and eosin;

2. for identification of vacuolar contents - embedment in Historesin (LKB Industries) directly from the 95% ethanol, sectioning at 4 µm, staining for neutral fat with oil red O in iso-propanol with Ehrlich's hematoxylin as counterstain, and mounting in glycerine-gelatine;

3. for morphometry of the nuclei - same as method 2., but staining only with Ehrlich's hematoxylin, and mounting in Permount;

4. for morphometry of the vacuoles - dehydration through absolute ethanol to n-butyl glycidyl ether (BGE), infiltration with BGE and a mixture of Quetol 651 (Ted Pella Inc) with hardener (nonenyl succinic anhydride [NSA]), embedment in the Quetol-NSA mixture, sectioning at 1 µm, and staining with 1% aqueous toluidine blue in 2% borax.

Morphometry and Stereology

Computer assisted morphometry was performed with the Zeiss IBAS (Kontron) image analysis system. The parameters measured were area and perimeter of the objects in question, and area of the reference fields.

Nuclei in 25 fields of view were measured in 4 µm Historesin-embedded sections stained with Ehrlich's hematoxylin. Care was taken to include representative fields from all lobular regions. These were selected at random but were included only if scanning indicated that fixation was adequate as evidenced by the appearance of the nuclei: noncrenulated, smooth perimeter (nuclear membrane); and readily identifiable nucleoli and/or structured nucleoplasm. As seen on the image monitor, the magnification was 1780x, representing an area of 7460 μm^2.

Hepatic vascular, biliary, and lymphatic systems were excluded from the measurements. The proportion of the image occupied by parenchymal cells was calculated to be about 90 per cent overall, based on the sum of the tissue areas divided by the sum of the screen areas.

Vacuoles were measured for each animal in 10 random fields of the 1 um Quetol embedded sections stained with toluidine blue. As seen on the image monitor, magnification was 4200x, and the total area of the field of view was 1194 μm^2.

From the stored measuring data, stereological parameters were calculated by area analysis (Weibel et al. 1969). Pertinent to the present study were volume density (VV), numerical density (NV), and mean diameter (DQ) of objects. The formulas for these which include a correction factor for section thickness are.

VV = 2*U*A/3*pi*(t+2/3DQ)*NA*AT (x 100 for per cent volume),
NV = NA/(t+2/3DQ)*AT,
DQ = U/pi*NA,
where AT = sum of reference areas (μm^2),

A = sum of object profile areas in AT (μm^2),
U = sum of object perimeters in AT (μm),
NA = number of objects in AT.
t = section thickness, μm.

Because of the small group size, statistical evaluation was perfonned first by scanning the data with the Mann-Whitney non-parametric U-test using all combinations of group pairings. Results were confirmed using the two-sided t test. Significance of differences from the latter test are presented in the Results and accompanying Tables.

RESULTS

General Observations.

With the exception of the intracytoplasmic vacuolization, no abnormalities could be detected in the liver portions examined. Occasional binuclear cells and somewhat enlarged nuclei (polyploid?) were seen, but their incidence was regarded as normal.

Only very rare vacuoles in all groups were sudanophilic, staining with oil red O, and therefore containing triglycerides. The vast majority of the vacuoles appeared to be empty.

Morphometry: The nuclei.

Table 1 presents the results from analysis of the volume density, numerical density, and mean diameter of the hepatocyte nuclei. Volume density was significantly lower in the F than in the control groups (F < S, p = <0.0002; F < V, p = <0.001), but S and V did not differ from each other. All groups differed from each other with regard to numerical density of the nuclear compartment: F < S, p = <0.001; F < V, p = <0.0005; and S < V, p = <0.02. No differences in mean nuclear diameter were seen in any group pairings.

Morphometry: The intracytoplasmic vacuoles.

Table 2 presents the results of the vacuolar measurements. Here a greater volume density was seen only between the F and V groups (p = <0.02). Numerical density differed among all groups: F > S, p = <0.0..., F > V, p = <0.02; and S > V, p = <0.02. Mean vacuolar diameter differed only between the F and V groups, where F > V, p = <0.05.

Additional calculations.

The data in Tables 1 and 2 were further calculated for each animal to determine the extent to which the nuclear and vacuolar compartments contributed to the increased weight of the flight animal livers.

Table 3 indicates such a possible relationship between liver weight and the nuclear and vacuolar volume densities, the estimation of which first required the assumption that the specific gravities of the vacuolar, nuclear, and residual parenchymal compartments were not significantly different, thus equating weight with volume. Second, calculations from the size of reference fields in relation to the image analyzer monitor field, indicated that the hepatic parenchymal cells comprised only about 90% of the total cell population in the regions examined. Therefore, liver weights were multiplied by 0.9 for the following calculations.

When the weight of the parenchyma (total liver weight x 0.9) (Table 3, column A) was multiplied by the combined nuclear and vacuolar volume density values (column B) and the product (column C) subtracted from the parenchymal weight (column A), the residual parenchymal weight (column D) in the flight animals remained significantly greater than that of either of the controls ($F > S$, $p = <0.0005$; $F > V$, $p = <0.0005$).

Table 4 then shows that when the mean weight of the parenchymal compartment was subtracted from the total liver weight, the mean increase in parenchymal weight of the flight animals would have been 1.258 g, about 0.133 g less than the mean total liver weight increase, 1.395 g, in the flight group. Table 4 also indicates that values of the nuclear and vacuolar compartments did not contribute significantly to that liver weight increase, but that the remaining, or residual, parenchymal cell compartment did so, the two values, 1.258 and 1.284 g being almost equal.

DISCUSSION

Conditions likely to cause a pale liver such as that seen in the flight animals are fatty change and severe glycogenic infiltration. Histologic evidence for fatty change is lacking. The tissues prepared for determination of triglycerides had been treated only with aqueous solutions, the highest concentration of ethanol used was 95%, and the temperature during processing did not exceed 25° C. Had high concentrations of triglycerides been present in the parenchymal cells, many or most vacuoles would have been stained by the oil red O. Since only rare vacuoles were stained in all groups, severe glycogenic infiltration was regarded as the most likely cause of the pale appearance of the F group livers. Supporting this conclusion is the fact that glycogen would have been dissolved in the aqueous fluids used in processing, leaving empty spaces such as those seen in the preparations. Tissue fixation in an absolute ethanol/picric acid/formaldehyde solution would have retained glycogen within the vacuoles during processing, enabling specific staining.

Regarding morphometric results, hepatocytes of the F group manifested a lower nuclear to parenchymal volume ratio than did the control (S, V) groups, indicating a greater mean distance between the nuclei of the former. The larger vacuolar volume density in the F animals might then have accounted for at least some of the increased internuclear space. When, however, the vacuolar and nuclear volumes were taken into account, the residual parenchyma in the flight animals remained statistically greater than that of either control group and therefore contributed significantly to the increase in the liver weight in that group (Table 3). If there is a fallacy in these calculations, it would lie in the assumption that has been made, that is, that the specific gravity of the various cellular components is essentially the same for all of them. Using 90% as the parenchymal proportion of the liver may be valid only for the tissue examined, for Gates, et al. (1961) found that 80% of the human liver consists of parenchymal cells. Their study, however, encompassed the entire liver. In the present case, for example, no vessels larger than 30-40 μm in diameter were

encountered, thereby enriching the specimens with parenchymal cells rather than with major vessels.

Regardless of the correctness of the assumption that has been made, there is little doubt that changes in the nuclear and vacuolar components were only minor contributors to the increased liver weight of the F animals, while the remainder of the hepatocytic cytoplasm contributed the major portion of the increase.

Among possible causes for that increase are hydropic change and/or markedly elevated intracellular glycogen in addition to that in the vacuoles. In this regard, the smaller mean diameter of the vacuoles in the flight group could have some implications as to genesis of their formation or, once they are formed, to their stability. Whether such knowledge would be helpful in determining the cause of their increased volume and numerical density will require additional investigation. Diet, feeding regimen, liver enzyme changes, hormonal effects, and "stress" have, among other factors, been studied by others, e.g. Babcock and Cardell, 1974; Cardell, 1971, in regard to liver changes, and it is well known that insulin and the glucocorticoids favor the accumulation of liver glycogen. Whether present data can be explained on the basis of such factors must await further study.

Alterations in other liver components and their contents (biliary system, lymphatic including Kupffer cells, vascular system) may also have taken place in the flight group. Although there is no evidence from the present histological preparations that would point to changes in those systems, they should be included in liver studies of future missions.

It is impossible to ascribe the present results to a particular leg of the Cosmos 1887 mission. Nevertheless, they may serve as background information on which interpretation of future flight data might be based.

CONCLUSIONS

1. The livers of flight animals on the Cosmos 1887 mission not only weighed more but also were paler in appearance than those of control groups.

2. Microscopically the principal difference between the flight animals and the controls was extensive intracytoplasmic (hepatocytic) vacuolization.

3. Based on lack of sudanophilia, which would have indicated the presence of triglycerides, the vacuoles were presumed to have contained glycogen.

4. Morphometric evaluation of nuclear volume densities in parenchymal cells demonstrated differences among the groups: $F < S$, $p = <0.0002$; $F < V$, $p = <0.001$.

5. Nuclear numerical density differed among all groups: $F < S$, $p = <0.001$; $F < V$, $p = <0.0005$; $S < V$, $p = <0.02$.

6. Mean diameter of the nuclei did not differ among the groups.

7. Volume density of the vacuoles differed only between the F and V groups: $F > V$, $p = <0.02$.

8. Numerical density of the vacuoles differed among all the groups: $F > S$, $p = <0.01$; $F > V$, $p = <0.02$; and $S > V$, $p = <0.02$.

9. Mean diameter of the vacuoles differed only between F and V groups: $F < V$, $p = <0.05$.

10. On the assumption that the specific gravity of the various parenchymal components were not significantly different from each other, calculations showed that the increased vacuolar compartment together with the nuclei did not contribute significantly to the increased liver weights in the flights, but that the residual (non-nuclear, non-vacuolar) parenchymal compartment constituted virtually all of that increase.

11. The cause of the alterations in the liver cannot be ascertained at this time, although such factors as "stress", diet, feeding regimen, hormonal and enzymatic changes, among others, need to be considered.

12. Although the results of this study cannot be ascribed to specific segments of the Cosmos 1887 mission, they may be useful as background information for future flights or ground based studies.

ACKNOWLEDGMENTS

The author is grateful to:

Dr. Kaplansky, Director of the Soviet Science Team and to his Team member, Dr. I. A. Popova, who was responsible for the preparation of the heart and liver at the dissection site in the USSR.

Dr. Richard Grindeland and Ms. Marilyn Vasques of the American Team in Moscow who performed the preliminary processing of tissues for shipment to the United States.

Ms. Rosemarie Binnard for her expertise in thin sectioning tissues needed for certain aspects of this work.

REFERENCES

1. Babcock, M. B.; and Cardell, R. R., Jr.,: Hepatic Glycogen Patterns in Fasted and Fed Rats. Am. J. Anat., vol. 140, 1974, pp. 299-320.

2. Cardell, R. R., Jr.: Action of Metabolic Hormones on the Fine Structure of Rat Liver Cells. I. Effects of Fasting on the Ultrastructure of Hepatocytes. Am. J. Anat., Vol. 131, 1971, pp. 21-54.

3. Gates, G. A., Henley, K. S., Pollard, H. M., Schmidt, E., and Schmidt, F. W.: 1961. The Cell Population of the Human Liver. J. Lab. Clin. Med., vol. 57, 1961, pp. 182-191.

4. Grindeland, R. et al. Cosmos 1887 mission.

5. Weibel, E. D., Staeubli, W., Gnaegi, H. R., and Hess, F. A.: Correlated Morphometric and Biochemical Studies on the Liver Cell. I. Morphometric Model, Stereologic Methods, and Normal Morphometric Data for Rat Liver. J. Cell Biol., vol. 42, 1969, pp. 68-91.

TABLE 1

VOLUME DENSITY AND MEAN VOLUME OF HEPATOCYTE NUCLEI

Group	Animal Number	N*	AT	VV	NV	DQ
F	06	191	1.84	0.0340	0.1026	9.147
	07	218	1.84	0.0365	0.1188	8.933
	08	208	1.85	0.0329	0.1145	8.732
	09	194	1.76	0.0344	0.1103	8.952
	10	254	1.85	0.0392	0.1413	8.580
	Mean	213.0	1.83	0.0354(a)	0.1175(b)	8.869
	SD		0.04	0.0025	0.0146	0.218
S	06	264	1.83	0.0452	0.1448	8.933
	07	300	1.80	0.0554	0.1638	9.194
	08	287	1.74	0.0525	0.1639	9.077
	09	290	1.83	0.0517	0.1565	9.187
	10	281	1.75	0.0462	0.1643	8.649
	Mean	284.4	1.79	0.0502	0.1587	9.008
	SD		0.04	0.0044	0.0084	0.227
V	06	291	1.81	0.0507	0.1611	8.960
	07	349	1.84	0.0500	0.1979	8.367
	08	305	1.83	0.0390	0.1791	7.940
	09	355	1.67	0.0612	0.2178	8.644
	10	372	1.71	0.0665	0.2200	8.847
	Mean	334.4	1.77	0.0535	0.1952	8.552
	SD		0.08	0.0011	0.0253	0.410

* N, Number of nuclear profiles measured in reference area.
AT, sum of reference areas, $\mu m^2 \times 10^{-5}$.
VV, volume density.
NV, numerical density $\times 10^3$.
DQ, mean nuclear diameter, µm.
SD, standard deviation.
F, flight group.
S, synchronous control group.
V, vivarium control group.

(a), F < S, p = <0.0002; F < V, p = <0.001.
(b), F < S, p = <0.001; F < V, p = <0.0005; S < V, p = <0.02.

TABLE 2

VOLUME DENSITY AND MEAN VOLUME OF INTRACYTOPLASMIC VACUOLES

Group	Animal Number	N*	VV	NV	DQ
F	06	845	0.0172	42.75	0.983
	07	660	0.0109	35.22	0.853
	08	864	0.0183	44.36	0.946
	09	746	0.0149	38.33	0.945
	10	770	0.0173	39.07	0.975
Mean		777	0.0157(a)	39.94(b)	0.940(c)
SD		82.0	0.0030	3.64	0.052
S	06	605	0.0098	31.71	0.896
	07	377	0.0144	18.09	1.117
	08	664	0.0160	33.16	1.015
	09	613	0.0181	29.62	1.099
	10	331	0.0073	16.95	0.952
Mean		518	0.0131	25.91	1.016
SD		152.3	0.0045	7.77	0.094
V	06	319	0.0080	15.76	1.042
	07	320	0.0129	15.36	1.117
	08	231	0.0066	11.22	1.085
	09	347	0.0122	16.63	1.121
	10	245	0.0046	12.74	0.915
Mean		292.4	0.0089	14.34	1.056
SD		51.2	0.0036	2.27	0.085

* N, number of vacuolar profiles measured in reference area.
Sum of reference areas for each animal was 1.194×10^4 μm^2.
VV, NV, DQ, SD, F, S, and V as for Table 1.

(a), F > V, p = <0.02.
(b), F > S, p = <0.01; F > V, p = <0.02; S > V, p = <0.02.
(c), F < V, p = <0.05.

TABLE 3

ESTIMATED RELATIONSHIP BETWEEN LIVER WEIGHT AND COMBINED NUCLEAR AND VACUOLAR VOLUME DENSITY

Group	Animal Number	A*	B	C	D
F	06	9.054	0.051	0.462	8.592
	07	9.216	0.048	0.442	8.774
	08	8.937	0.051	0.456	8.481
	09	8.658	0.049	0.424	8.234
	10	8.964	0.057	0.511	8.453
Mean		8.966	0.05[illegible]		8.507(a)
SD		0.204	0.003		0.198
S	06	7.506	0.055	0.413	7.093
	07	8.514	0.070	0.596	7.918
	08	7.866	0.068	0.535	7.331
	09	8.172	0.070	0.572	7.600
	10	7.830	0.054	0.423	7.407
Mean		7.978	0.063		7.470
SD		0.381	0.008		0.309
V	06	7.812	0.059	0.461	7.351
	07	8.028	0.063	0.506	7.522
	08	6.471	0.046	0.298	6.173
	09	7.308	0.074	0.541	6.767
	10	7.578	0.071	0.538	7.040
Mean		7.439	0.062		6.971
SD		0.604	0.011		0.532

* A, weight of liver parenchyma (liver weight x 0.9; see text).
B, sum of nuclear and vacuolar volume densities; from Tables 1 and 2.
C, product of A x B.
D, A - C = residual liver parenchyma; see text for discussion of rationale for these calculations.
F, S, and V as for Table 1.
SD, standard deviation.
(a), F > S, p = <0.0005, F > V, p = <0.0005.

TABLE 4

ESTIMATED CONTRIBUTION OF VACUOLES AND NUCLEI TO INCREASED LIVER WEIGHT IN FLIGHT GROUP

	F*	S	V	(S+V)/2	F-[(S+V)/2]
Liver weight at necropsy (g),	9.960	8.860	8.270	8.565	1.395(a)
Liver weight x 0.9, g	8.966	7.978	7.439	7.708	1.258(b)
Contribution from:					
Nuclei	0.317(c)	0.400	0.398	0.399	-0.081
Vacuoles	0.141	0.105	0.066	0.086	0.055
Residual parenchyma(c)	8.508	7.473	6.975	7.224	1.284(d)

---

* F, S, and V as for Table 1. All data in this Table are mean values.
(a), Difference between liver weight of flight and combined ground controls.
(b), Increase in weight of parenchymal tissue in flight group. Non-parenchymal tissue weight would be 1.395-1.258 = 0.133 g. See text for rationale.
(c), The underlined values result from multiplication of the VV of nuclei or vacuoles (Tables 1 and 2) with the respective weight of the liver parenchyma for each group, F, S, or V.
(d), This value plus the nuclear and vacuolar portions add up to 1.115 g, the value at (b).

EXPERIMENT K-6-12

PART II: THE ATRIAL GRANULAR ACCUMULATIONS

L. Kraft and L. C. Keil

SUMMARY

Atrial myocytic intracytoplasmic granular accumulations composed of storage granules that are associated with the production of atrial natriuretic factor (ANF) were studied morphometrically in rats from the Cosmos 1887 mission. Those of the flight, F, group had a significantly greater volume density (VV) than of either the synchronous, S, ($F > S$, $p = <0.01$) or vivarium, V, ($F > V$, $p = <0.0005$) control groups, while the controls did not differ from each other in this respect. Number of granular accumulations per unit reference area (NR) was also increased in the flight animals ($F > S$, $p = <0.005$; $F > V$, $p = <0.0005$). Mean volume (VQ) of the individual granulated regions did not differ among the three groups. The increased VV in the flight group was therefore due to an increase in the number of granular regions rather than to their size. No differences were seen between right and left atria in any group for either VV, NR, or VQ. Possible reasons for the increase in the granular regions in the flight animal are discussed.

INTRODUCTION

Cytoplasmic granules are found in the atrial myocytes of all mammals. They are associated with the hormone, atrial natriuretic factor (ANF), which is involved in the regulation of blood pressure and volume and in the excretion of water, sodium, and potassium (de Bold, 1986; Ackermann and Irizawa, 1984). Because electrolyte imbalance and fluid shifts have been experienced by humans (and animals?) during space flight, it seemed appropriate to examine the ANF granulated regions in the atria of rats from the Cosmos 1887 flight and to ascertain, by means of morphometric and stereological methods (Weibel, 1969), if quantitative changes occurred in the flight animals. The method to accomplish this was based on the stereological procedure that had been employed by deBold (1975) for his morphometric and physiological studies of such granulated regions.

METHODS

Animals and Tissues

Five rats from each of three groups, the flight (F), the synchronous (S) and vivarium (V) controls, were studied.

At necropsy in the USSR the heart was cut transversely at the rostral pole of the ventricles, keeping the atria intact. The entire portion containing the atria was immediately immersed in cold, 4° C, fixative consisting of 3% glutaraldehyde in 0.1 M phosphate buffer at pH 7.4. The tissues remained in the cold until they were further processed in Moscow by the American team members who replaced the fixative with a graded ethanol series up to a final concentration of 95%. During shipment to the United States and until histological preparations were made, the specimens remained at 4° C.

Tissue Preparation

Although tissue penetration by glutaraldehyde is poor after immersion fixation, the thinness of most of the atrial wall is less than 1 mm and had therefore been well fixed for analysis.

The atria from each animal were processed separately in order to evaluate any differences between the right and left. From 95% ethanol, the tissues were dehydrated in absolute ethanol and xylene, embedded in paraffin (53° C), and sectioned at 5 μm. Two sets of slides were made containing step sections taken at 50 μm intervals through the entire extent of each atrium. One set of slides was stained with hematoxylin and eosin for general oversight purposes and the other with lead hematoxylin (deBold and Bencosme, 1975; deBold, 1979) for measurement of the granular accumulations. The tartrazine counterstain prescribed for the latter stain was omitted in order to enhance discrimination by the image analysis system.

Morphometry and Stereology

Computer assisted morphometry was performed with the Zeiss IBAS (Kontron) image analysis system. The parameters measured were area and perimeter of the granular regions and area of the reference fields. One field was chosen at random in each of 10 sections of each atrium. The sections selected were separated by at least 100 μm (two steps), and the atrial regions in which the fields were measured comprised different levels of an atrium so that the entire atrium was surveyed. Thus, the total number of fields measured in this study was 300 (3 groups x 5 animals x 2 atria x 1 field x 10 sections). The magnification on the image monitor was 1780x and represented 7460 μm^2 for each image.

Despite the absence of the tartrazine counterstain, interactive discrimination of the images was not satisfactory. Therefore, to make the measurements for area and perimeter, an editing function was used to outline the granular regions projected on the image monitor, and, because the reference area of the tissue did not always fill the monitored field, the same method was used to delineate the pertinent reference regions when necessary.

From the stored values for object (granular accumulation) area, object perimeter, and reference field area, the stereology program calculated volume density (VV) and mean volume (VQ) (μm^3) of the objects. Numerical density (NR) was calculated as number of objects per unit reference field area x 10^3.

Statistical evaluation was performed using the two-sided t test with pairings among the three groups, F, S, and V.

RESULTS

Overview of the atria using the sections that had been stained with hematoxylin and eosin failed to detect any abnormalities.

Concerning the morphometric parameters, Table 1 indicates that there was no significant difference between right and left atria regardless of the group or parameter under consideration.

Table 2 presents the results for volume density, numerical density, and mean object volume for the three groups of animals, F, S, and V. The data constitute the mean of the right and left atrial measurements for each rat. Significant differences are seen only in volume density ($F > S$, $p = <0.01$; $F > V$, $p = <0.0005$) and numerical density ($F > S$, $p = <0.005$; $F > V$, $p = <0.001$). There were no differences among the groups in the size of the accumulations.

DISCUSSION

The absolute values for volume density obtained in this study differ from those in rats reported by de Bold (1978, 1979). In those studies, mean volume density (as per cent volume) of the granulated regions was as high as 3% in 6 week old rats and 4% in 10 week old rats of the same strain (Sprague Dawley, source not given). Factors which may account for this discrepancy include the sub-strain or source of the animals, various aspects of their husbandry such as the feed, feeding regimen, feed availability (food was withheld from the Cosmos rats for 22-24 hours before necropsy), general health status, age (the Cosmos animals were 15-16 weeks old), as well as other possible conditions related to the animals and/or their environment.

The method used in this study of outlining the granular region for the profile area data as opposed to the grid analysis used by de Bold could explain some of the difference as well. The precise boundary of a granular region is often indistinct and subject to some interpretation. In many instances a thin scattering of granules extends away from the main body of the accumulation. Including all of these scantily granulated regions in the measurement can lead to a large areal value and to a smaller value for the same region if they are omitted.

Regardless of the absolute values, however, if the methods of tissue preparation and the criteria for measuring the test and reference fields remain constant, results are likely to be meaningful as, in this study, they appear to be, for the differences between the flight and control groups are for the most part highly significant.

The lack of difference in the granularity between the right and left atria in the rats of the Cosmos 1887 mission is at odds with the statement of Cantin and Genest (1986) that the right contains from 2 - 2.5 times the number of granules as the left. Others do not mention whether their results refer to right, left, or both atria. Not only may different experimental conditions prevail in each study, but it must be emphasized that in this investigation granules were not counted, only their accumulated masses were measured.

The reasons for the increase in volume density of the granular regions in the flight group is not easy to explain nor is it possible to know which phase of the mission was responsible for the change, likely causes being reduced blood volume and/or body water content. The data show that the increase was due to an elevated number, rather than to an increased size, of the individual granular regions, but an exhaustive attempt at this time to interpret these findings in terms of their physiological importance would be speculative, especially because no chemical determinations of ANF were made. Nevertheless, the data might be regarded as background information for future ground based studies and space flights where biochemical determinations may be correlated with both microscopic and ultramicroscopic morphometry.

CONCLUSIONS

1. The granular regions in the atria of flight rats from the Cosmos 1887 mission and of synchronous and vivarium ground controls were studied morphometrically and evaluated using stereological principles.

2. Volume density and numerical density related to reference area were determined as was mean volume of the individual granular region.

3. No differences in those three parameters were seen between right and left atrium in any group.

4. The mean volume density of the granular regions was greater in the flight group than in the synchronous ($p = <0.01$) and vivarium control groups ($p = <0.0005$).

5. Number of granular regions in a unit reference area was greater in the flight animals than in the synchronous ($p = <0.005$) and vivarium groups ($p = <0.0005$).

6. Mean volume of the granular accumulations was not significantly different in any group pairing.

7. Increased volume density of the granular accumulations was due to increase in their numbers rather than to any increase in size.

8. By themselves the data do not explain physiological changes that may have occurred during the mission, although several factors may be reponsible for the increase in the granular accumulations in the flight animals. Reduced blood volume and/or body water content seem most likely causes. The information obtained in this study may, however, be of value to future investigations of fluid and electrolyte balance in rodents during space flight missions.

ACKNOWLEDGMENTS

The authors are grateful to:

Dr. Kaplansky, Director of the Soviet Science Team and to his Team member, Dr. I. A. Popova, who was responsible for the preparation of the heart and liver at the dissection site in the USSR.

Dr. Richard Grindeland and Ms. Marilyn Vasques of the American Team in Moscow who performed the preliminary processing of tissues for shipment to the United States.

Ms. Rosemarie Binnard for her expertise in sectioning tissues for certain aspects of this work.

REFERENCES

1. Ackermann, U.; and Irizawa, T.: Synthesis and Renal Activity of Rat Atrial Granules Depend on Extracellular Volume. Am. J. Physiol. vol. 247 (Regulatory Integrative Comp. Physiol. 16):R750-R752, 1984.

2. Cantin, M.; and Genest, J.: The Heart as an Endocrine Gland. Scientific Amer., vol. 254, 1986, pp. 76-81.

3. de Bold, A. J.: Morphometric Assessment of Granulation in Rat Atrial Cardiocytes: Effect of Age. J. Mol. Cell. Cardiol., vol. 10, 1978, pp. 717-724.

4. de Bold, A. J.: Heart Atria Granularity Effects of Changes in Water-electrolyte Balance. Proc. Soc. Exp. Biol. Med., vol. 161, 1979, pp. 508-511.

5. de Bold, A. J.: Atrial Natriuretic Factor: An Overview. Fed. Proc., vol. 45, 1986, pp. 2081-2085.

6. de Bold, A. J.; and Bencosme, S. A.: Selective Light Microscopic Demonstration of the Specific Granulation of the Rat Atrial Myocardium by Lead-Hematoxylin-Tartrazine. Stain Technol. vol. 50, 1975, pp. 203-205.

7. Weibel, E. R.: Stereological Principles for Morphometry in Electron Microscopic Cytology. Internatl. Rev. of Cytology, vol. 26, 1969, pp. 235-302.

TABLE 1

VOLUME DENSITY, NUMERICAL DENSITY, MEAN VOLUME OF RIGHT AND LEFT ATRIAL GRANULAR REG.

Parameter	Group*	Left Atrium Mean	SD	Right Atrium Mean	SD	
VV	F	1.741	0.408	1.552	0.260	ns
	S	1.271	0.164	1.211	0.256	ns
	V	1.109	0.179	1.139	0.217	ns
NR	F	1.439	0.244	1.277	0.342	ns
	S	1.033	0.641	1.044	0.220	ns
	V	0.880	0.133	0.916	0.190	ns
VQ	F	40.113	7.117	41.820	6.432	ns
	S	42.950	8.346	39.573	9.360	ns
	V	44.565	16.977	43.364	11.512	ns

* Number of animals in each group = 5.

F, flight group.
S, synchronous control group.
V, vivarium control group.
SD, standard deviation.
VV, volume density x 10^2.
NR, numerical density, number of granular regions per μm^2 x 10^3 of the reference field.
VQ, mean volume of granular accumulations, μm^3.
ns, not significant, $p = >0.05$.

TABLE 2

VOLUME DENSITY, NUMERICAL DENSITY, AND MEAN VOLUME OF GRANULAR REGIONS IN INDIVIDUAL ANIMALS

Group	Animal Number	N*	A	AT	VV	NR	VQ
F	06	178**	2059	1.455	1.416	1.224	38.636
	07	185	2498	1.421	1.764	1.309	45.712
	08	223	2557	1.444	1.769	1.551	38.189
	09	182	[illegible]51	1.445	1.496	1.259	41.783
	10	212	2599	1.456	1.787	1.456	40.662
	Mean	196	2374.8	1.444	1.646(a)	1.360(b)	40.996
	SD	20.2	247.0	0.014	0.176	0.139	3.018
S	06	160	1677	1.437	1.166	1.113	34.613
	07	131	1832	1.386	1.314	0.953	50.094
	08	156	2050	1.473	1.392	1.059	48.532
	09	132	2008	1.441	1.396	1.139	42.406
	10	138	1367	1.458	0.938	0.946	30.663
	Mean	143.4	1786.8	1.439	1.241	1.042	41.262
	SD	13.7	277.7	0.033	0.193	0.089	8.496
V	06	152	1514	1.549	0.975	1.006	31.636
	07	106	1708	1.406	1.223	0.735	58.966
	08	159	1735	1.517	1.153	1.047	34.379
	09	119	1567	1.446	1.085	0.812	46.542
	10	132	1805	1.532	1.185	0.863	48.298
	Mean	133.6	1665.8	1.490	1.124	0.893	43.965
	SD	22.1	121.2	0.061	0.098	0.131	11.117

* N, number of granular regions measured in reference area.

** All data are the means of the right and left atrial values.

A, profile area, μm^2

AT, reference area, $\mu m^2 \times 10^{-5}$.

VV, volume density $\times 10^2$.

NR, number of granular accumulations in reference area $\times 10^3$.

VQ, volume of granular accumulations, μm^3.

SD, standard deviation.

F, S, and V as in Table 1.

(a), F > S, $p = <0.01$; F > V, $p = <0.0005$.

(b), F > S, $p = <0.005$; F > V, $p = <0.001$.

N90-26467

EXPERIMENT K-6-13

MORPHOLOGICAL AND BIOCHEMICAL EXAMINATION OF HEART TISSUE

PART I: EFFECTS OF MICROGRAVITY ON THE MYOCARDIAL FINE STRUCTURE OF RATS FLOWN ON COSMOS 1887 - ULTRASTRUCTURE STUDIES

PART II: CELLULAR DISTRIBUTION OF CYCLIC AMP-DEPENDENT PROTEIN KINASE REGULATORY SUBUNITS IN HEART MUSCLE OF RATS FLOWN ON COSMOS 1887

Principal Investigator:

D.E. Philpott
NASA Ames Research Center
Moffett Field, California 94035

Co-Investigators:

K. Kato, J. Stevenson,
NASA Ames Research Center
Moffet Field, California 94035

J. Miquel
Linus Pauling Institute of Science and Medicine
Palo Alto, California 94306
University School of Medicine
Alicante, Spain

M.I. Mednieks
Department of Molecular Biology
Northwestern University Medical School
Chicago, Illinois 60611

W. Sapp
Tuskegee University
Tuskegee, Alabama 36088

I.A. Popova, L.V. Serova
Institute of Biomedical Problems
Moscow, USSR

EXPERIMENT K-6-13

PART I: EFFECTS OF MICROGRAVTIY ON THE MYOCARDIAL FINE STRUCTURE OF RATS FLOWN ON COSMOS 1887 - ULTRASTRUCTURE STUDIES

D. Philpott, I. Popova, L. Serova, K. Kato, J. Stevenson, J. Miquel, and W. Sapp

SUMMARY

The left ventricle of hearts from rats flown on the Cosmos 1887 biosatellite for 12.5 days was compared to the same tissue of synchronous and vivarium control animals maintained in a ground based laboratory. The volume density of the mitochondria in the myocardium of the space-flown animals was statistically less ($p = < 0.01$) than that of the synchronous or vivarium control rats. Exposure to microgravity resulted in a certain degree of myocardial degeneration manifested in mitochondrial changes and accumulation of myeloid bodies. Generalized myofibrillar edema was also observed.

INTRODUCTION

Vascular deconditioning, which is an important medical problem, is recognized as one of the key concerns of space flight research. This loss of physiological performance of the circulatory system is accompanied by disuse muscle atrophy triggered by the reduced functional load of the musculo-skeletal system in the microgravity environment. Animal models are often used to examine disuse atrophy because they are more amenable to the morphological and biochemical research needed to unravel the mechanisms of muscle breakdown. Using these models, we can design preventive countermeasures.

Although early Soviet space flight data suggested that rat heart was insensitive to weightlessness (Oganessyan and Eloyan, 1979), more recent studies have shown that subcellular alterations occur in the rat heart following exposure to space microgravity or on-the-ground immobilization (Baranski, 1983). An examination of rats from a 22-day flight, sacrificed 4.5-9 hrs postflight, revealed changes in capillaries and veins consisting of edema of the endothelial cytoplasm, appearance of myeloid bodies and swelling of mitochondria. In the cardiomyocytes, exposure to microgravity results in an increase in the number of lipid droplets and an increase in the amount of extramitochondrial glycogen. Philpott et al. (1985, 1987) also reported alterations in the heart following exposure to space microgravity on Space Lab-3, including a significant decrease in volume density of the mitochondria, loss of microtubules and increases in lipid droplets and glycogen.

Rat heart mass decreased 4.26% and oxygen consumption decreased from 62 mm squared to 38 mm squared/100 mg/hr after 120 days of restraint (Kovalenko et al. 1971). Electron microscopy revealed non-uniform swelling and a decrease in the number of cristae of the mitochondria and changes in their patterns of orientation (Kovalenko et al. 1970, Kovalenko et al. 1972). The endothelium of the capillaries exhibited swelling and impairment of the cell membrane structure. Mailyan et al. (1970) induced hypokinesia by exercise restriction which resulted in reduced heart function accompanied by a clear decrease in mass and changes in the ultrastructural elements on which biological oxidation processes are dependent. Shtykhno and Udovichenko (1978) showed a decrease in the number of true capillaries, appearance of nonfunctioning empty vessels, and an opening of arteriovenular shunts.

PRECEDING PAGE BLANK NOT FILMED

In another study on male rats that were restrained for 120 days electron microscopy revealed, by day 14, an increase in the number of and a decrease in the size of mitochondria (Romanov, 1976). At days 45-60, size and number of mitochondria appeared normal, but by the 120th day both size and number of mitochondria were greater than in control non-restrained animals. The reasons for these changes are unknown and further research is needed to clarify the adaptive mechanisms involved in the response of the heart tissues to altered gravity.

Stereological methods were used to study skeletal and heart muscle changes after 30 days of hypokinesia (Nepomnyashchikh et al. 1985). Forty-eight male rats were confined in cages, allowing virtually no movement. The ratio of muscle to connective tissue in the myocardia decreased (connective tissue proliferation), the relative volume of intracellular material increased (edema), and the microcirculatory bed was altered, leading to a degrading of metabolic processes. Both morphological and stereological analysis revealed myocardial atrophy. Philpott et al. (1984) demonstrated a significant decrease in volume density of mitochondria in the rat deep quadriceps (6 & 9-days suspension) and superficial quadriceps (12-days suspension) accompanied by an increase in the number of mitochondria and a decrease in the perimeter of the mitochondria.

Microtubules perform a cytoskeletal role in cells, providing for structural integrity and intracellular transport. It is believed that microtubules have an orienting function for intracellular structures in muscle, especially the myofibrils. Cartwright and Goldstein (1985) have shown that the number of microtubules in the rat heart increase for the first nine postnatal days and then decrease to a steady state. These authors have observed a specific pattern in the number of microtubules, relative to increases in the number of myofibrils in both heart and soleus muscle. This indicates that the microtubules provide an orienting function for myofibrils. The relatively stable state of the microtubules, which are observed in the adult heart, tend to support a static cytoskeletal role for microtubules in a normal functioning heart. Warren (1968) demonstrated that the breakdown of microtubules by colchicine disrupts the orderly arrangement of myofilament bundles in regenerating frog skeletal muscle. Cartwright and Goldstein (1985) believe that reduced microtubule density reflects a decreased necessity for scaffolding after well-oriented, densely packed myofilament bundles are established. Only the microtubules required for growth remain.

Male rats were flown for 7 days on Space Lab-3 and sacrificed 12 hours after recovery of the shuttle. Philpott et al. (1985) observed a decrease in microtubules in rat heart tissue. This would suggest a decreased need for scaffolding as hearts have been shown to lose mass under simulated weightlessness. An increase in number of microtubules in response to stress-induced hypertrophy has been shown by Samuel et al. (1983), and these microtubules temporarily reorganize into bundled arrays. Little is known about the assembly and breakdown of heart microtubules. In rats flown on Space Lab-3, ultrastructural changes include an increase in glycogen and small lipid droplets, and a decrease in cytoskeletal tubules compared to controls.

The present study expands our previous research in which male Wistar rats were flown on Space Lab-3 (SL-3) for seven days (Philpott et al., 1985). In agreement with the earlier research, we have found that exposure to microgravity results in a number of myocardial changes including, myofibrillar edema, loss of cytoskeletal tubules, mitochondrial disorganization and accumulation of glycogen and lipid.

MATERIALS AND METHODS

All of the animals were male rats of the Czechoslovakian-Wistar strain, weighing about 325g at launch time. The biosatellite Cosmos 1887 flight lasted 12.5 days, and landed in Siberia. The rats were transported by bus, airplane and van to the laboratory in Moscow, and were sacrificed two days after recovery. Tissue was obtained from five space flown rats for the study of the effects of microgravity on the myocardium. Ten rats of the same age and sex served as controls. Of these, five animals were kept under normal laboratory conditions ("vivarium controls") and five were

maintained under the same conditions as the space- flown rats with the exception of no microgravity ("synchronous controls"). The hearts were removed as quickly as possible after sacrifice and immersed in cold saline (Fig. 1) to slow the metabolic rate during dissection (Kato, et al., 1987). The left ventricles were removed and cut into four parts. Two of the pieces were placed into cold Triple Fix (Philpott, et al., 1980); the remaining two pieces were frozen in liquid nitrogen and later transferred to dry ice for transportation to Ames Research Center. All tissues were placed in screw top teflon tubes to facilitate handling and transportation. Upon arrival in the United States, the tissue in Triple Fix was immersed in 1% osmic acid plus 1% $K_3Fe(CN)_6$ for one hour (McDonald, 1983), dehydrated with ascending concentrations of acetone, infiltrated with epon araldite, embedded, sectioned and stained for electron microscopy. A minimum of 100 electron micrographs from each animal were taken in a Philips-300 transmission electron microscope. Volume density of the mitochondria was determined by point counting, as described by Weibel (1969), using 8x10 micrographs at a magnification of 27,500X.

RESULTS AND DISCUSSION

The mean animal weights at recovery were: Flight = 303.2gm (S.E. 2.4), Synchronous = 349.0gm (S.E. 5.8), and Vivarium = 342.0gm (S.E. 7.7). Point counting on random micrographs to determine the volume density of mitochondria, revealed a significant decrease in volume density in the flight-animal tissue, compared to the controls. Some of the myofibrils in the flight samples exhibited degeneration of the mitochondria and formation of myeloid bodies. Generalized edema was present in the myofibrils showing degeneration. There was some increase in glycogen and lipid in the myocardium of Cosmos 1887 flown rats but not as markedly as in animals exposed to microgravity in the Shuttle Spacelab (SL-3) or subjected to immobilization-suspension.

Previous research suggests that microgravity leads to degenerative structural changes and biochemical adaptations involving storage of lipid and glycogen. In this study, the accumulation of these substances was not as evident as in previous space flights, which may be due to difficulties during recovery resulting in a 42 hour fasting period prior to sacrifice. Glycogen increase is seen in Fig. 2 and Fig. 3 where some increase in lipids is also observed.

Structural changes seen in the Cosmos flown rats include some loss of microtubules and fibrillar edema that may be linked to tissue breakdown, with a concomitant increase in osmotic pressure and fluid entry into the cells. Intermittent areas of missing protofibril (actin, myosin filaments) were observed in cross sections of flight tissue which is indicative of muscle degradation (Fig. 4). Another structural change seen is mitochondrial breakdown, which occurs both in space flown and immobilized animals. (Fig. 5). A number of fibers in the flight tissue exhibited super contraction (Fig. 3). While preparative technique can contribute to this, the super contraction was not evident in the controls. It is possible that mitochondrial breakdown is releasing calcium which may contribute to the contracted state. These changes can be compared to the vivarium and synchronous control tissues (Figs. 6, 7). Point counting of the mitochondria in the left ventricle resulted in a mean of 39.9 for the vivarium, 38.9 synchronous and 32.5 for the flight tissue. The t-test shows a significant difference between the flight and both the vivarium and synchronous controls of < 0.01, but no significant difference between the vivarium and synchronous controls (Fig. 8). It is clear that the volume density of the mitochondria in the flight group was reduced by a significant amount.

Since the sympathetic nervous system exerts a trophic influence on the biosynthesis of myofibrils and mitochondria (Joseph and Engel, 1980), a decreased sympathetic activity, under conditions of microgravity or immobilization, could play a key role in mitochondrial degeneration. Mitochondrial damage could also result from changes in intracellular oxygen tension. According to Fedorov and Shurova (1973), immobilized rabbits show capillary alterations which might impair the delivery of oxygen and nutrients to the myocardial cells. This would decrease the ATP

synthesis in all or some of the mitochondrial populations, and since ATP is needed for mitochondrial maintenance and replication, the end result would be unrepaired mitochondrial loss (Tzagoloff, 1982). Capillary alterations were also seen in the flight tissues (Fig. 9) in the form of numerous endothelial invaginations projecting into the lumen of the capillaries.

The above hypothesis is supported by the fact that alterations in the supply of oxygen and nutrients to the organelles result in fine structural and biochemical changes in the mitochondria of ischemic or anoxic myocardium (DeGasperis et al., 1970; Delatglesia and Lumb, 1972; Ferrans and Roberts, 1971; Rouslin et al., 1980; Taylor and Shaikh, 1984). Both sympathetic and oxygen-mediated mechanisms may underly the organelle changes since the decline in sympathetic nervous activity may also influence mitochondria through its effect on myocardial blood perfusion (Popovic, 1981).

The present data support the view that an optimum work load imposed on the heart, i.e. moderate physical exercise at normal Earth gravity, is essential for preservation of mitochondrial structure and function (Miquel et al., 1980; Miquel 1982). At present, our understanding of the causes and basic mechanisms of cardiovascular deconditioning is inadequate. Changes/lesions have been observed in the cardiovascular tissue. This may provide information which will be of relevance and importance for the well-being of individuals involved in prolonged space flight under conditions of microgravity and /or significantly restricted or diminished physical activity.

ACKNOWLEDGMENTS

We wish to thank Michael Penn for his contribution in preparing statistical material at Ames Research Center for this manuscript.

REFERENCES:

1. Baranski S., Subcellular investigation of the influence of real and modulated weightlessness upon performance and regeneration processes in muscular tissues. The Physiologist 26:41, 1983.

2. DeGasperis, C., A. Miani, and R. Donatelli. Ultrastructural changes in human myocardium associated with ischemic arrest. J. Mol. Cell. Cardiol. 1:169, 1970.

3. Delatglesia, F. A. and G. Lumb. Ultrastructural and circulatory alterations of myocardium in experimental coronary artery narrowing. Lab. Invest. 27:17, 1972.

4. Fedorov, I. V. and I. F. Shurova. Content of protein and nucleic acids in the tissue of animals during hypokinesia. Kosmicheskaya Biologiya I Meditsina. 7:17, 1973.

5. Ferrans, V. J. and W.C. Roberts. Myocardial ultrastructure in acute and chronic hypoxia. Cardiol. 56:144, 1971.

6. Joseph, J.J. and B. T. Engel. Nervous control of the heart and cardiovascular system. Aging. 12:101, 1980.

7. Kato, K., A. Baloun, and D.E. Philpott. Effect of supergravity on the areas of lipid droplets and mitochondria in the heart left ventricle. J. Ultrastruc. Res. 69:350, 1979.

8. Kato, K., D. Philpott and J. Stevenson. A simple method to improve heart fixation with ice water. J. Elect. Micros. Tech. 7:(2), 133, 1987.

9. Kovalenko, Ye. A., V. L. Popkov and Yu. I. Kondrat'yev. Pathological Physiology. 6: 3-8, 1979.

10. Kovalenko, Ye. A., V. L. Popkov and E. S. Mailyan. Kosmicheskaya Biologiya I Meditsina. 4: 3-8, 1971.

11. Kovalenko, Ye. A., Yu. S. Galushko and I. A. Nitochkina. Space Biol. and Aerospace Med. 1: 125-129, 1972.

12. Mailyan, E. S., L. I. Grinberg and Ye. A. Kovalenko. Adaptatsiva K Myshechnoy Deyatel'nosti I Gipokinezii. Novosibirsk, 111- 113, 1970.

13. McDonald, K. OsFeCN-uranium staining improves microfilament preservation and membrane visualization in a variety of cell types. J. Ultrastructural Res. 86: 107-118, 1984.

14. Miquel, J., A. C. Economos, J. Fleming, and J. E. Johnson, Jr. Mitochondrial role in cell aging. Exp. Gerontol. 15: 575, 1980.

15. Miquel, J. Comparison between the weightlessness syndrome and aging. In: Space Gerontology (J. Miquel and A. C. Economos, Eds.), NASA, Washington, D.C., 1982.

16. Nepomnyashchikh, L. M., L. V. Kolesnikova, G. I. Nepomnyashchikh. Myocardial tissue organization in rats under hypokinesia (a stereological investigatiion), Arkhiv Anatomii, Gistologii I Embrologii. 88:(1)57-62, 1985.

17. Oganessyan, S. S., and M. A. Eloyan. Cathepsin activity of skeletal muscle and myocardial myofibrils after exposure to weightlessness and accelerations. Kosmicheskaya Biologiya I Aviakosmicheskaya Meditsina 45, 38, 1979.

18. Philpott, D.E., R. Corbett, C. Turnbill, S. Black, D. Dayhoff, J. McGourty, R. Lee, G. Harrison and L. Sovick. Retinal changes in rats flown on Cosmos 936: A cosmic-ray experiment. Aviat. Space and Environ. Med. 51:556, 1980.

19. Philpott, D. E., J. Miquel, M. Wilke and M. Ornelas. Stereological changes in skeletal mitochondria during disuse atrophy. International Cell Biol. Special Issue. 509, 1984.

20. Philpott, D. E., A. Fine, K. Kato, R. Egnor, L. Cheng and M. Mednieks. Microgravity changes in heart structure and cyclic AMP metabolism. Suppl. to The Physiologist 28:(6),S209, 1985.

21. Philpott, D. E., K. Kato and M. Mednieks. Ultrastructure and cyclic AMP mediated changes in heart muscle under altered gravity conditions. J. Mol. Cell Cardiol. 19:(IV), S61, 1987.

22. Romanov, V. S. Quantitative evaluation of ultrastructural changes in rat myocardium during prolonged hypokinesia. Space Biol and Aerospace Med. 10, 74, 1976.

23. Rouslin, W., J. MacGee, A. R. Wessellman, R. J. Adams and S. Gupte. Mitochondrial cholesterol in myocardial ischemia. J. Mol. Cell Cardiol. 12:1475, 1980.

24. Samuel, J. L. The microtubule network of cardiac myocytes during adaptive growth. J. Mol. Cell Cardiol. 15:(4) 38, 1983.

25. Shtykhno, Yu. M. and V. I. Udovichenko. Vest. Akad. Med. Nauk SSSR. 2: 68-71, 1978.

26. Taylor, I. M. and N. A. Shaikh. Ultrastructure changes of ischemic injury due to coronary artery occlusion in the porcine heart. J. Mol. Cell. Cardiol. 16: 79, 1984.

27. Tzagoloff, A. Mitochondria. Plenum Press, New York, 244, 1982.

28. Warren, R. H. The effect of colchicine on myogenesis in vivo in Rana pipiens and Rhodnius prolixus hemiptera. J. Cell. Biol. 39: 544-555, 1968.

29. Weibel, E.R. Stereological principles for morphometry in electron microscopy cytology. Int. Rev. Cytol. 26: 235, 1969.

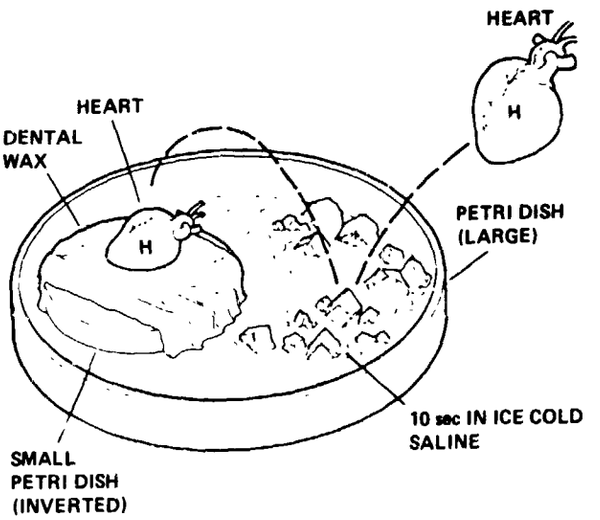

Fig. 1. Diagram of heart tissue preparation showing how the heart is quickly cooled after sacrifice, in order to decrease metabolism-linked autophagic breakdown prior to fixation.

Fig. 2. Abundant glycogen deposits (arrows) in the myocardium of a space-flown rat. 27,500X.

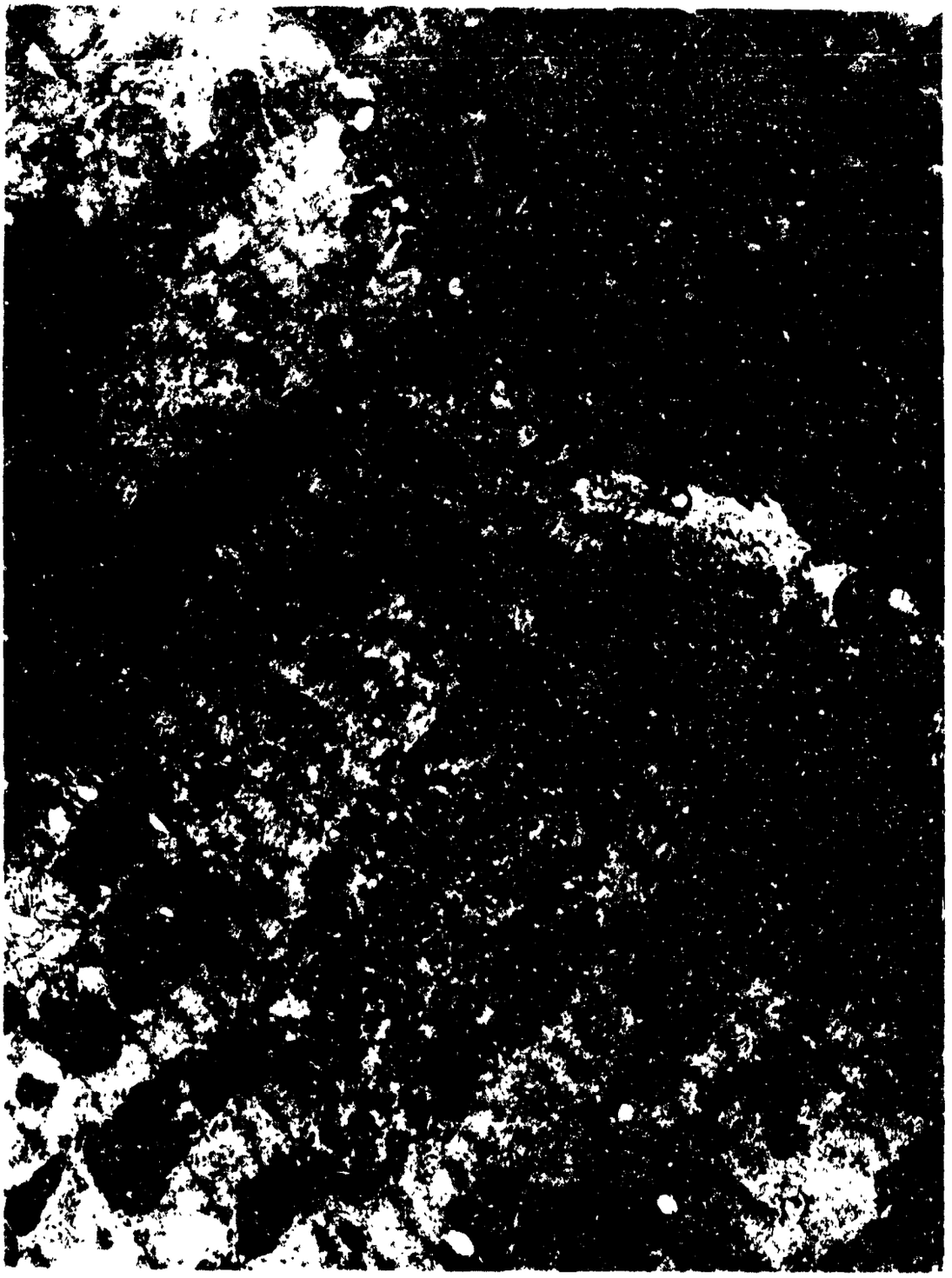

Fig. 3. A super contracted fiber connecting to a normal fiber was seen in the flight tissue. Note the lighter staining mitochondria in the super contracted fiber, increased glycogen and swollen mitochondria (arrow). 19,500X.

Fig. 4. Filaments are occasionally missing (arrows) in cross sections of the left ventricle of a flight rat. 130,000X.

Fig. 5. Evidence of mitochondrial alteration (arrow) in the left ventricle of a space-flown animal. 127,500X.

Fig. 6. Vivarium control left ventricle tissue. Note excellent preservation. 27,500X.

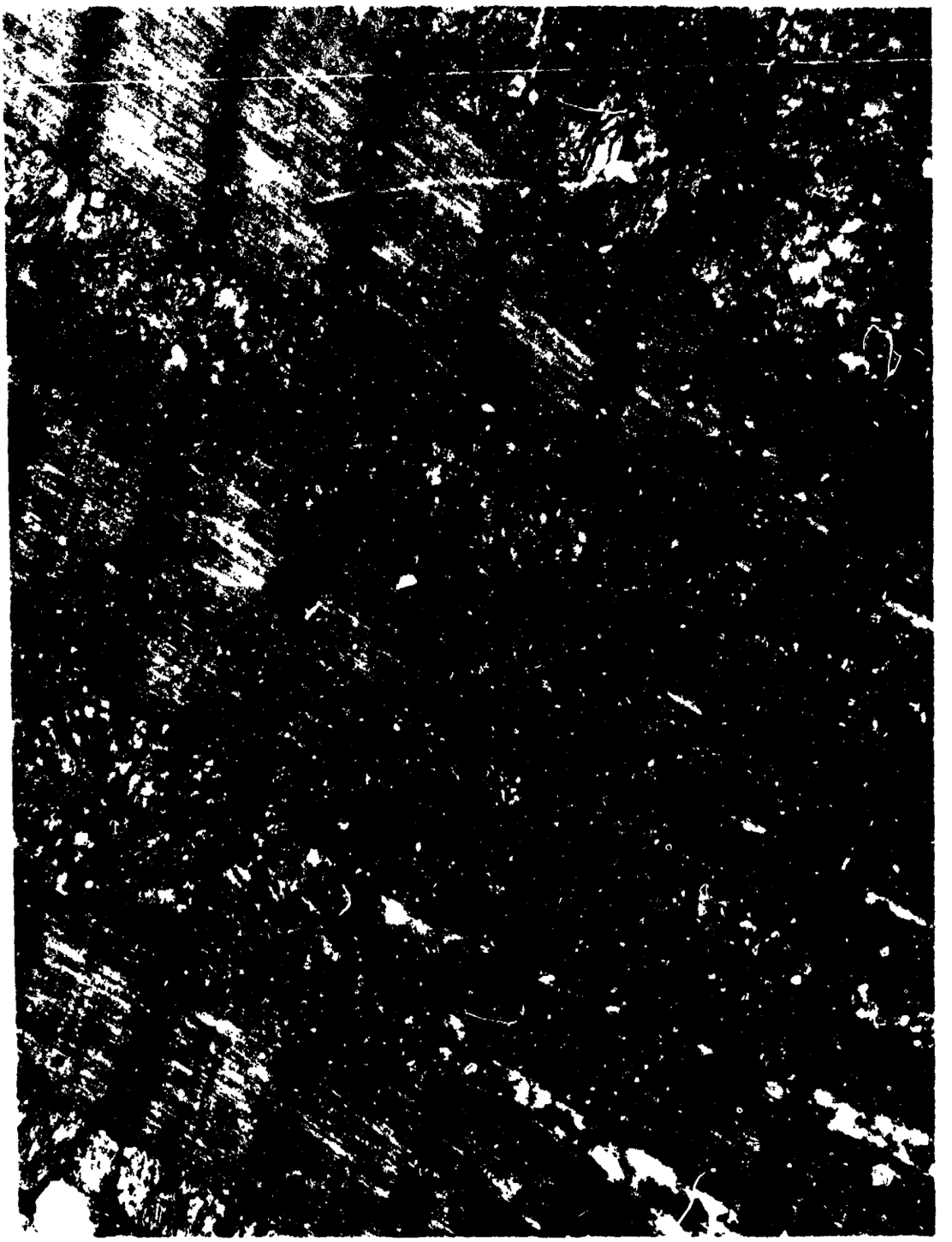

Fig. 7. S[illegible]chronous control left ventricle. Note similarity to vivarium control. 27,500X.

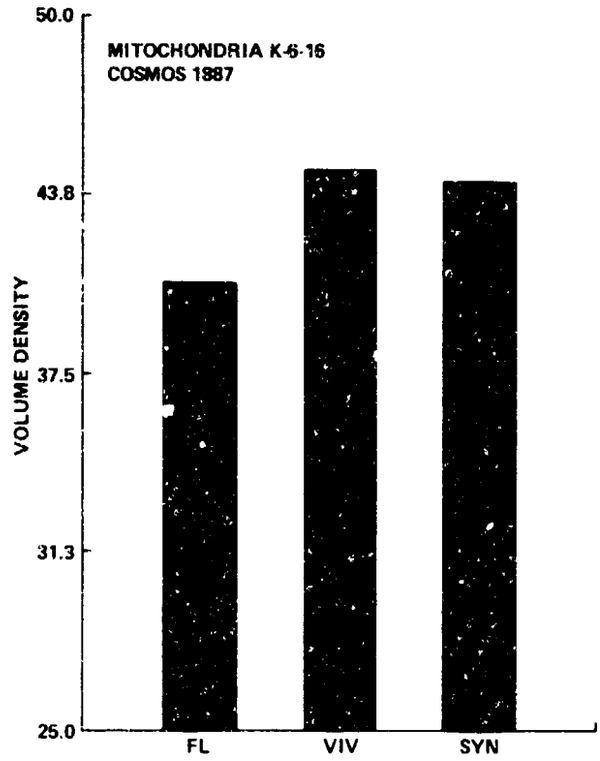

Fig. 8. Volume density of mitochondria in the myocardium of rats flown in the Cosmos 1887 biosatellite.

Fig. 9. Ultrastructural alterations seen in the left ventricle of a flight rat. Note the endothelial projections in the lumen of the capillary. 141,000X.

EXPERIMENT K-6-13

PART II: CELLULAR DISTRIBUTION OF CYCLIC AMP-DEPENDENT PROTEIN KINASE REGULATORY SUBUNITS IN HEART MUSCLE OF RATS FLOWN ON COSMOS 1887

M. Mednieks

SUMMARY

In this study, the cellular compartmentalization and biochemical localization of regulatory (R) subunits of cyclic AMP-dependent protein kinase (cAPK) of ventricular heart tissue from rats obtained from the COSMOS 1887 were determined. Photoaffinity labeling with a [^{32}P]-8-azido analog of cyclic AMP, electrophoretic separation of the proteins was followed by autoradiographic identification of the subcellular fraction in which the labeled R subunits are localized. Similarly, antibodies to R subunits were prepared and employed in an immunogold electron microscopic procedure to directly visualize cellular compartmentalization of the cAPK R subunits. Our results show that protein banding patterns in both the cytoplasmic fraction and in a fraction enriched in chromatin-bound proteins showed some individual variability in tissues of different animals, but exhibited no changes that can be attributed to the flight. Examination of cellular localization of the isotopically labeled R subunits of cAPK isotypes showed no change in the distribution of RI in either the soluble or particulate fractions whereas the presence of RII in the particulate subcellular fraction as well as in the regions of nuclear chromatin was greatly decreased in tissues from rats in the flight group when compared to controls. Identical results were obtained in comparable tissues obtained from the U.S. Space Lab 3 (SL-3) mission. These findings indicate that a major catecholamine hormone regulated mechanism in cardiac tissue is altered during some aspect of space travel.

INTRODUCTION

Samples were obtained from the Cosmos 1887 flight and tested with respect to cellular compartmentalization and biochemical localization of cyclic AMP-dependent protein kinase (cAPK). Results were compared to the findings of similar analyses performed using materials obtained from the U.S. Space Lab 3 (SL-3) mission.

The study was undertaken in order to gain insight into the mechanistic aspects of cardiac changes that both animals and humans undergo as a consequence of space travel (1,2). Cardiac hypertrophy and cephalad fluid shifts have been observed after several days of actual or simulated weightlessness and raise concerns regarding the functioning of the heart and circulatory system during and after travel in space (3,4,5).

A number of physiologic changes, attributed to space travel conditions in experimental animals and in humans, can be the consequence of increased circulating levels of catecholamine hormones. On a cellular level such responses are of two types and have been studied in other tissues (6,1). The immediate effects, which are generally transient in nature and the later or delayed effects which appear to be longer lasting, involve gene regulation and have longer or unknown recovery periods. The second type of reaction is of considerable practical concern and is addressed in this study.

A series of events occur as a consequence of stimulation of cardiac muscle tissue by catecholamine hormones: receptor binding at the cells' surface is followed by activation of adenylate cyclase in the plasma membrane resulting in increased cyclic AMP production, activation of cAPK, and is

PRECEDING PAGE BLANK NOT FILMED

played out as the intracellular signal processing which is a function of the activity and distribution of cAPK.

The two basic steps in intracellular protein phosphorylation which are mediated by cAMP are: a) holoenzyme dissociation and b) regulatory (R) and catalytic (C) subunit activity:

$$R_2{}^*C_2 \xrightarrow{+\,cAMP} 2R^*cAMP + 2\,C$$

where R*C is the catalytically inactive holozyme, R*cAMP represents regulatory subunits, with binding sites occupied. Two isotypes (I and II) of cAPK have been found which have identical C subunits, but differing R subunits, RI and RII (8,9).

An advantage in this experimental design is the specificity of the cAPK R subunits: they are the only known eukaryotic cAMP-receptor or cAMP-binding proteins (10). Labeled R subunits serve as radioactive probes to search for cytosolic or nuclear cellular localization of cAPK. Antibodies generated to R subunits served as independent means of immunocytochemical localization.

The fundamental finding of this study is the apparent decrease of nuclear cAPK RII. This is consistent with previous results using tissues from rats flown on SL-3.

MATERIALS AND METHODS

The initial experiments were carried out at NASA, Ames, Moffett Field, but were repeated and concluded at Northwestern University in Chicago. While the methods employed were identical, aliquots of the samples used, equipment, solutions and individuals carrying out the procedures varied. This repetition was undertaken to ensure that the results were reproducible.

Tissue Homogenization and Cell Fractionation

Heart (left ventricle) tissue pieces were weighed and a 0.05M Tris, pH 7.5 buffer containing 0.06M EDTA, 0.005M $MgCl_2$ and 0.001M benzamidine and phenyl methyl sulfonyl flouride (PSMF) was added to make a 15% (w/v) homogenate. The tissue pieces were disrupted using a Polytron probe at the number 5 setting with two 30 second bursts. These and all subsequent operations using the tissue homogenates were carried out at 4 °C. The homogenates were centrifuged at 10 kG for 30 minutes and the supernatant solution was removed and saved and subsequently designated the soluble fraction. The particulate fraction was suspended in the same volume as the original homogenate in 0.30M KCl containing the homogenization buffer. The samples were mixed using a Vortex mixer at the maximum setting, allowed to stand for 30 minutes, mixed again and centrifuged at 10kG for 30 minutes. The supernatant of this centrifugation was saved and is referred to as the particulate fraction extract. The tissue fractionation steps are shown schematically as follows:

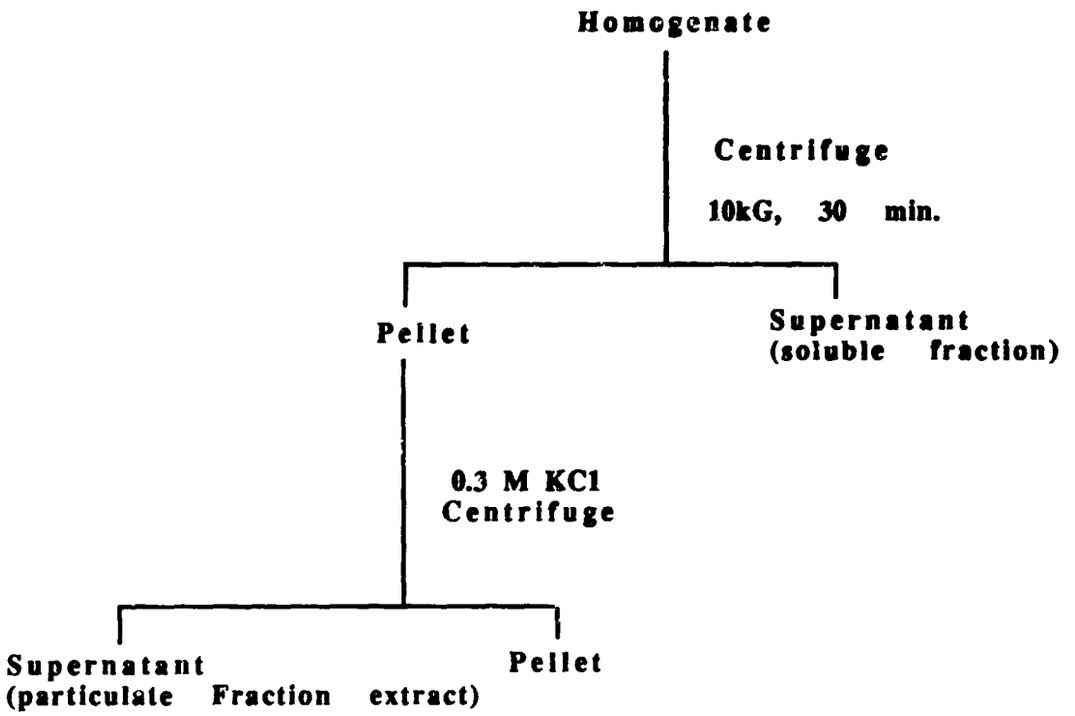

Heart muscle tissue samples from each individual animal were homogenized separately, and all analyses were carried out on these samples. Some individual variability could be observed, so that if tissues were pooled and only groups, i.e., control, simulated and flight were analyzed, the individual differences of one animal might seriously alter the average value of the whole group.

Photoaffinity Labeling.

Photoaffinity labeling was carried out using a method modified from Hoyer et al (8). as described previously (11). Duplicate aliquots containing 50 µg total protein were taken from the homogenate, the soluble fraction and the particulate fraction extract and incubated with 5 µCi each of [^{32}P] -8-azido cyclic AMP ([^{32}P]-8-N3-cAMP) in an equal volume of buffer containing 0.25M KCl, 0.002M Tris, pH 7.6, 0.001M EDTA for 30 minutes at 4 ^{o}C, in the dark. Photolysis was carried out using a mineralite UV lamp at a wavelength of 250 nm at a distance of 5 cm. The samples were then treated with activated charcoal and centrifuged.

Total incorporation of the labeled analog was measured by taking duplicate aliquots of samples representing 0.1 mg tissue adding trichloroacetic acid to the concentration of 5% and allowed to form a precipitate overnight in the cold. The precipitates were collected. solublized and duplicate aliquots were counted using a liquid scintillation counter.

Electrophoresis and Autoradiography.

Sodium dodecyl sulfate polyacrylamide gel electrophoresis (SDS-PAGE) was carried out using a mini-gel apparatus (Hoffer Instruments). Standard procedures, described before (14), were employed in preparing the electrophoresis separations. The proteins were then electrophoretically transferred to nitrocellulose by Western blotting. Autoradiography was carried out by exposing either dried gels or Western blots to X-ray film to detect the radioactively labeled protein bands. Colored standards (Amersham Rainbow markers) were used to determine relative mobilities of standard proteins and to identify the radioactively labeled R subunits.

Electron microscopic immunnogold labeling.

Polyclonal antibody reactive with cAPK RI was used for postembedding cytochemical immunogold labeling of rat heart and testis tissues from the Cosmos flight. The serum was an early positive bleeding and has not been affinity purified. The serum was used only to test for normal intracellular RI distribution. Animal handling was in accordance with NIH guidelines. Procedures for immunolabeling were modified from those of Roth and his associates and from Bendayan and have been described before (19). Dilutions of antibody were 1:200 and 1:400 The higher dilution was used to test specificity by antigen inhibition. All quantitative procedures were subjected to standard statistical analysis and all effects on the tissue of flight animals were compared to those of vivarium and simulation controls.

RESULTS

Protein Concentration and Banding Patterns

Rat heart ventricle tissue pieces were disrupted and a soluble fraction and an extract of the particulate fractions were prepared. Tissues from each individual animal were homogenized separately and were subsequently analyzed on an individual basis. The reason for this procedure is that either subtle differences between experimental and control groups might be missed by examining a single combined sample or conversely, a single tissue piece with extremes in variability may impart a disproportionately great effect. When individual samples are examined may well be explained by some special condition in one animal (since log-on data from COSMOS are available, e.g., Flight Animal #10 had a significant weight loss, compared to controls, and showed an atypical banding pattern [Figure 3, lane 8]). Additionally, as further flight data become available, accumulating a collection of banding patterns may yield statistically significant information as to possible differences or consistencies, and may become important if heart muscle changes undergoes during space flight.

Electrophoretic separation under denaturing conditions was carried out to examine the protein banding patterns of the flight animal tissues and to compare them to the simulated series and to various controls. Qualitatively, the protein banding patterns were alike for all groups. Densitometric analyses revealed individual differences from animal to animal, but no consistently observed differences between the flight animal tissues when compared to either the tissues of the rats from simulation experiments or to the control group (Fig. 1).

Weight per volume samples (tissue weight in mg/vol buffer to make a 15% homogenate) were prepared and homogenized. Protein concentrations of the soluble fraction and of the extracted particulate fraction were determined by colorimetric measurements and by densitometric analysis of the individual banding patterns (Table I and Figure 1). Table I shows that protein concentrations were the same in the majority of samples (within experimental error) so that only minor adjustments in volume had to be made in pipetting assay solutions of identical concentration with respect to total protein content. Similarly, representative densitometry patterns are shown in Fig. 1 (control A, and simulation B) where the same protein concentration is apparent as the number of peaks, and as the sum of the total area of the peaks. The individual peak heights did vary from animal to animal. No consistent pattern, however, could be correlated with the flight or with either of the control groups.

The protein banding patterns of the soluble fractions of the tissue extracts differ significantly from the banding patterns of the particulate fraction extracts. No differences, however, were observed between control, simulated or flight animal cell fractions (Fig.1A, 2A, and 3A and in densitometry in Fig. 1). Individual differences between minor bands and some major bands were seen mainly in the soluble fraction banding patterns, but no correlation could be made with either flight or

simulation conditions. Similar observations were previously made in studying cAMP-binding protein distribution on the heart muscle of rats after chronic stimulation with isoproterenol (in press).

Affinity labeling with Azido Cyclic AMP

The binding of an isotopically labeled azido analog of cyclic AMP to its receptor protein (cAPK R subunits) was determined by performing the binding assay, measuring the total incorporation into protein, followed by electrophoretic separation of RI and RII and determining their relative photoaffinity labeling. Fig. 3. shows photoaffinity labeling of the soluble fraction of 4 control and 4 flight animal heart muscle tissues. There is no difference between the groups in total binding of the cAMP analog. Similarly, (not shown) when flight, simulation, and control group labeling is compared, no consistent difference is shown. The R subunit in cytosol is predominantly of the type I isozyme and is indicated in Fig. 3 and verified in the distribution of gold particles bound to antiserum reactive with rat liver RI (Fig. 5A and B). Some azido-labeled RII was observed and it is not clear whether an entry in the photoaffinity label of RII from flight animals in the soluble fraction is present. Extensive analyses of several concentrations and incubation times have to be carried out to ascertain this. At present, the conclusion is that no differences are found in the affinity label (of RI) in the soluble fractions of heart tissues when comparing flight and control samples.

Significant differences in photoaffinity labeling, however, are consistently found in the particulate fraction extracts: less azido cAMP is bound to flight than to control animal RII (Fig. 4 A and B). Banding patterns (Fig 4A) and an autoradiogram (Fig. 4B) are shown side by side to demonstrate first, that equal amounts of protein were photoaffinity labeled and applied to each lane of the electrophoresis gel and second to demonstrate the unequivocal specificity of cyclic AMP binding to R subunits. It should be noted that while the banding pattern exhibits no difference between flight and control tissues, the autoradiogram shows a substantially reduced binding to RII (Fig. 4B, lanes 6-9). Note also that both control and flight tissue samples show a faster moving autoradiographic label, presumeably a proteolytic degradation product.

Photoaffinity labeling with 8-N_3 cAMP of soluble cell fractions and the particulate fraction extracts was undertaken to determine the cellular distribution of cAPK R subunits and to compare the compartmental distribution between flight tissues and controls. Total 8-N_3 cAMP bound to proteins is shown in Fig. 2, as counts per minute per mg protein. Generally the cytoplasmic fraction proteins are more extensively (3 to 4 fold) labeled than the particulate fraction proteins. In the soluble fraction no significant difference was observed between flight and controls (first three points shown in Fig. 2). In the particulate fraction extract, the flight heart muscle showed a significant increase in bound 8-N_3 cAMP, when compared to vivarium control. Similarly, the synchronous control showed an increase of total 8-N3 cAMP binding in the particulate fraction.

Comparison of banding patterns and cyclic AMP-binding properties between soluble and particulate cell fractions of the synchronous controls is shown in Fig. 3. Electrophoretic protein banding patterns are shown in Fig. 3A and differ between the soluble and particulate cell fractions (lanes 1-4 and 6-10, respectively). The banding patterns of the soluble or particulate fractions are not different from those of either the vivarium controls or the flight animals (not shown). This is consistent with our earlier observations. The autoradiographic results, (Fig. 3B) on the other hand, show marked differences of R subunit type and distribution. The soluble fraction contains both RI and RII, although RII should be less that RI (10-15). The particulate fraction contains more RII than RI which is also consistent with previous observations. The particulate fraction contains largely RII. In sample 6, very little RII can be seen and may be due to variation between individual animals. When compared to controls, however, the extent of labeling is significantly more than in flight animals. Thus the electrophoretic and autoradiographic determination of R

subunit presence and distribution does not represent all the label that is incorporated, since the flight particulate fraction contains markedly diminished or absent R's in the cell fractions of animals from the Cosmos flight (fig. 4B). The banding patterns of the particulate samples are shown in Fig. 4A (lanes 2-5 are controls, lanes 6-9 are flight). Lane 1 is a control sample of heart tissue taken from a laboratory rat taken at the time of the experiment to test labeling specificity by adding cold cyclic AMP. Lane 6 is a color standard to show relative mobilities. The autoradiogram of the Western blot is shown in Fig. 4B. The soluble fraction contains mainly RI and a faster moving component and no differences are seen between flight and control animal samples of heart tissue extracts, Fig. 4C. As stated previously, the R subunits in the particulate fraction are mainly RII with some RI present and occasionally a faster moving fragment is seen. These fragments are probably products of proteolysis. This might also explain the increase of total counts in the synchronous simulation samples, indicating that more label per total protein may be present due to increase in the protein degradation, but not necessarily due to increased/decreased amounts of intact RII.

DISCUSSION

A major mechanism of cellular regulation is the cyclic interconversion of enzymes between the phospho- and dephosphoforms. Phosphorylation is the most common molecular regulatory mechanism - more than other covalent modification. Desensitization of the Beta receptor (adenylase cyclase system) results from continued stimulation by catecholamine hormones. This is an adaptive mechanism which may ultimately be expressed in decreased cAPK subunit synthesis and agonist-induced desensitization of the b-adrenergic receptor-linked adenylate cyclase Pharmacological Reviews and the corresponding intracellular signal processing events have been.thoroughly reviewed (Harden, T.K. Pharmacological Reviews, 35:5-28, 1983 and references therein).

Many hormones act on responsive cells by activating second messenger pathways. Of these the cyclic AMP (and the calcium) pathways change cellular activity through specific protein kinase. By phosphorylating cytoplasmic and nuclear proteins this kinase coordinates cellular activity. Biosynthesis of specific proteins is known to be modulated in heart muscle as well as in other cell types. It has now been shown that transcriptional regulation requires a cAMP response element (CRE) which is conserved in cAMP responsive genes. Phosphorylation of CRE-binding proteins may be the mechanism of gene activation in hormonally regulated cells. Consequently the relative cellular disposition of cyclic AMP-dependent protein kinase may be an index of such events in heart muscle. The results of this study appear to be related to these phenomena and should be further investigated from the molecular biology standpoint.

CONCLUSIONS

The basic signal processing of b-adrenergic stimulation is via the adenylate cyclase system via cyclic AMP-mediated intracellular events. Indices of these events are measures of cyclic AMP-dependent protein kinase activity and distribution. While catalytic activity measurements are difficult in frozen tissues, the photoaffinity labeling of cAPK R subunits can be reliably carried and used to determine relative amounts and cellular distribution of these proteins. This method of labeling cAPK R subunits using both a photoaffinity and an immunological probe was applied to heart muscle tissue of rats from the Cosmos 1887 flight.

Rat heart ventricular tissue fractionation and R subunit labeling revealed a normal (compared to control) distribution of R subunits in the soluble cell fractions and a decrease in R subunits in the particulate cell fractions. Interpretation of these data must necessarily be conservative. First, the findings are observational, based on single (individual flight) observations. Second, no precise controls are available to compare results between flights (e.g., SL-3 to Cosmos 1887).

Changes due to gravitational effects on the heart muscle under space conditions are apparent in experimental animals. These changes are occasionally observed on a morphologic basis and can be quantitated using biochemical and immunocytochemical methods.

ACKNOWLEDGEMENTS

This study was in part carried out in the Space Physiology Branch, Life Sciences Division, NASA, Ames Research Center, Moffett Field, CA, and was completed in the Laboratory of Prof. R.A. Jungmann (NIH Grant #GM 23895), Department of Molecular Biology, Northwestern University Medical School, Chicago, IL. The expert technical assistance of Mrs. Katharine Kato, Ms. Joann Stevenson and Mr. Michael Penn is acknowledged. The contributions of Mr. Penn for maintaining computer files and statistical analysis of the data are gratefully acknowledged, as is the assistance of Mr. Monte Swarup (NIH/NCI, Laboratory of Tumor Immunology, Cellular Biochemistry Section) for computer analysis and graphing the protein data.

We thank Dr. Joanna Kwast-Welfeld for her gift of the antiserum. The completion of this study was in part due to the generous support, encouragement and advice given by Dr. A.R. Hand (NIH, NIDR).

REFERENCES

1. Bendayan, M. and Zollinger, M. Ultrastructural localization of antigenic sites on osmium-fixed tissues applying the protein A-gold technique. J. Histochem. Cytochem. 31:101-109 (1983).

2. Benovic, J.L., Pike, L.J., Cerione, R.A., Staniszewski, C., Yoshimasa, T., Codina, J., Caron, M.G. and Lefkowitz, R.J. Phosphorylation of the mammalian beta- adrenergic receptor by cyclic AMP-dependent protein kinase. J. Biol. Chem. 260:7094-7101 (1985).

3. Bhalla, R.C., Gupta, R.C. and Sharoa, R.V. Distribution and properties of cAMP-dependent protein kinase isozymes in the myocardium of spontaneously hypertensive rat. J. Mol. Cell Cardiol. 14:33-39 (1982).

4. Blomquist, G., Mitchell, J.H. and Saltin, B. Effects of bed rest on the transport system in hypogravic and hypodynamic environments. (R.H. Murray and M. McCally,eds.) NASA SP-269, Washington, DC (1969).

5. Bonder-Petersen, F., Suzuki, Y., Saduoto, T. and Christensen, N.J. Cardiovascular effects of simulated zero gravity in humans. Acta Astronautica 10:657-661 (1983).

6. Bungo, M.W. and Johnson, P.C. Cardiovascular examination and observations of deconditioning during the space shuttle orbital flight test program. Aviat. Space Env. Med. 54:1001-1002 (1983).

7. Greengard, P. Phosphorylated proteins as physiological effectors. Science 199:146-152 (1978).

8. Hover, P., Owens, J. and Haley, B. Use of nucleotide photoaffinity probes to elucidate molecular mechanisms of nucleotide-regulated phenomena. Ann. N.Y. Acad. Sci. 346:280-301 (1980).

9. Karapu, V.Y. and Ferents, A.I. Effects of hypokinesia and physical loading on cardiac myocyte ultrastructure. Arkhiv Anatomia, Gistologii I Embriologii (NASA TM-76179 28-37 (1979)).

10. Keely, S.L., Corbin, J.D. and Park, C.R. Regulation of adenosine 3',5'-monophosphate-dependent protein kinase. J. Biol. Chem. 250:4832-4840 (1975).

11. Kranias, E.G., Garvey, J.L., Srivastave, R.D. and Solaro, R.J. Phosphorylation and functional modification of sarcoplasmic reticulum and myofibrils in isolated rabbit hearts stimulated with isoprenaline. Biochem. J. 266:113-121 (1985).

12. Kvetansky, R. and Tigranayan, R.A. Epinephrine and norepinephrine concentrations in rat cardiac ventricles and atria after flight abroad Cosmos-1120 biosatellite. Kosmicheskaya Biologiya I Aviakosmicheskaya Meditsina 16:(4) 87-89 (1982).

13. Lindeman, J.P. and Watanabe, A.M. Phosphorylation of phospholamban in intact myocardium. Role of Ca+-calmodulin-dependent mechanisms. J. Biol. Chem. 260:4516-4525 (1985).

14. Lohmann, S.M., DeCamilli, P., Eining, I. and Walter, U. High-affinity binding of the regulatory subunit (RII) of cyclic AMP-dependent protein kinase to microtubule-associated and other cellular proteins. Proc. Natl. Acad. Sci. USA 81:6723-6727 (1984).

15. Lohmann, S.M. and Walter, U. Regulation of the cellular and subcellular concentrations and distribution of cyclic nucleotide-dependent protein kinases. Adv. Cyc. Nuc. Prot. Phos. Res. 18:63-117 (1984).

16. Mednieks, M.I. and Hand, A.R. Cyclic AMP-dependent protein kinase in stimulated rat parotid gland cells: compartmental shifts after in vitro treatment with isoproterenol. Eur. J. Cell Biol. 28:264-271 (1982).

17. Mednieks. M.I. and Hand, A.R. Nuclear cAMP-dependent protein kinase in rat parotid acinar cells. Exp. Cell Res. 149:45-55 (1983).

18. Mednieks, M.I. and Hand, A.R. Salivary gland ultrastructure and cyclic AMP-dependent protein kinase reactions in Space Lab-3 rats. Am. J. Physiol. (Reg. Int. Comp. Physiol., 21) 252:R233-239 (1987).

19. Mednieks, M.I., Jungmann, R.A. and Hand, A.R. Immunogold localization of the type II regulatory subunit of cyclic AMP-dependent protein kinase. J. Histochem. Cytochem. 37:339-346 (1986).

20. Mednieks, M.I., Fine, A.S., Oyama, J. and Philpott, D.E. Cardiac muscle ultrastructure and cyclic AMP reactions to altered gravity conditions. Am. J. Physiol. (Reg. Int. Comp. Physiol., 21) 252·R227-232 (1987).

21. Mednieks, M.I., Jungmann, R.A. and Hand, A.R. Ultrastructural immunocytochemical localization of cyclic AMP-dependent protein kinase subunits in rat parotid acinar cells. Eur. J. Cell Biol. 44:308-317 (1987).

22. Musacchia, X.J., Deavers, D.R., Meninger, G.A. and Davis, T.P. A model for hypokinesia effects on muscle atrophy in the rat. J. Appl. Physiol.Respirat. Environ. Physiol. 48:479-486 (1980).

23. Philpott, D.E., Fine, A., Kato, K., Egnor, R., Cheng, L. and Mednieks, M. Microgravity changes in heart structure and cyclic-AMP metabolism. The Physiologist 28:S209-210 (1985).

24. Popovic, V. Antiorthostatic hypokinesia and circulation in the rat. The Physiologist 24:15-16 (1981).

25. Sandler, H. Cardiovascular responses to weightlessness and prolonged bed rest. In: A Critical Review of the U.S. and International Research on Effect of Bed Rest on Major Body Systems. (Nicogossian, A.E. and Lewis, C.S. eds.). Washington, DC, NASA, 3-80 (1982).

TABLE I

Protein Concentration of Homogenates of Rat Heart Tissue

Protein concentration mg/ml

Sample number	Control	Simulated	Flight
1	0.65	0.65	0.67
2	0.74	0.78	0.65
3	0.74	0.75	0.68
4	0.88	0.86	0.61*
5	0.85	0.87	0.45*

Standard error calculation showed that values marked with a star (*) differ significantly from the average values of controls.

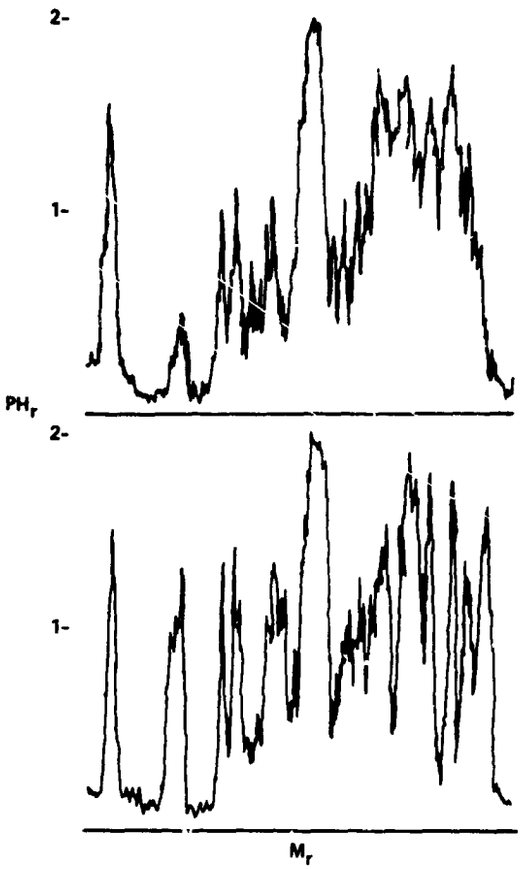

Fig. 1. Protein banding patterns of rat heart tissue fractions resolved on SDS-PAGE. The soluble fractions of a control and flight (panel A and B, respectively) are representative and contain 15-20 major bands. The axes are: relative peak height (Pr) on the ordinate and relation mobility (Mr) on the abscissa.

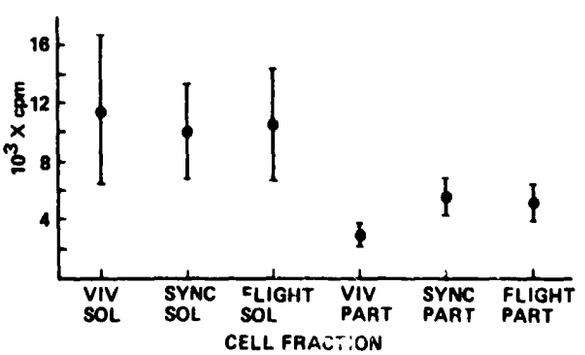

Fig. 2. Incorporation of 8-N3 cAMP into total cell fraction protein. Photoaffinity labeling was carried out as described in Methods and the proteins were precipitated with trichloroacetic acid. Total incorporation as cpm per mg proteins are shown in the three experimental groups (control-viv; synchronous control-sync and flight) of both soluble and particulate (sol, part) cell fractions.

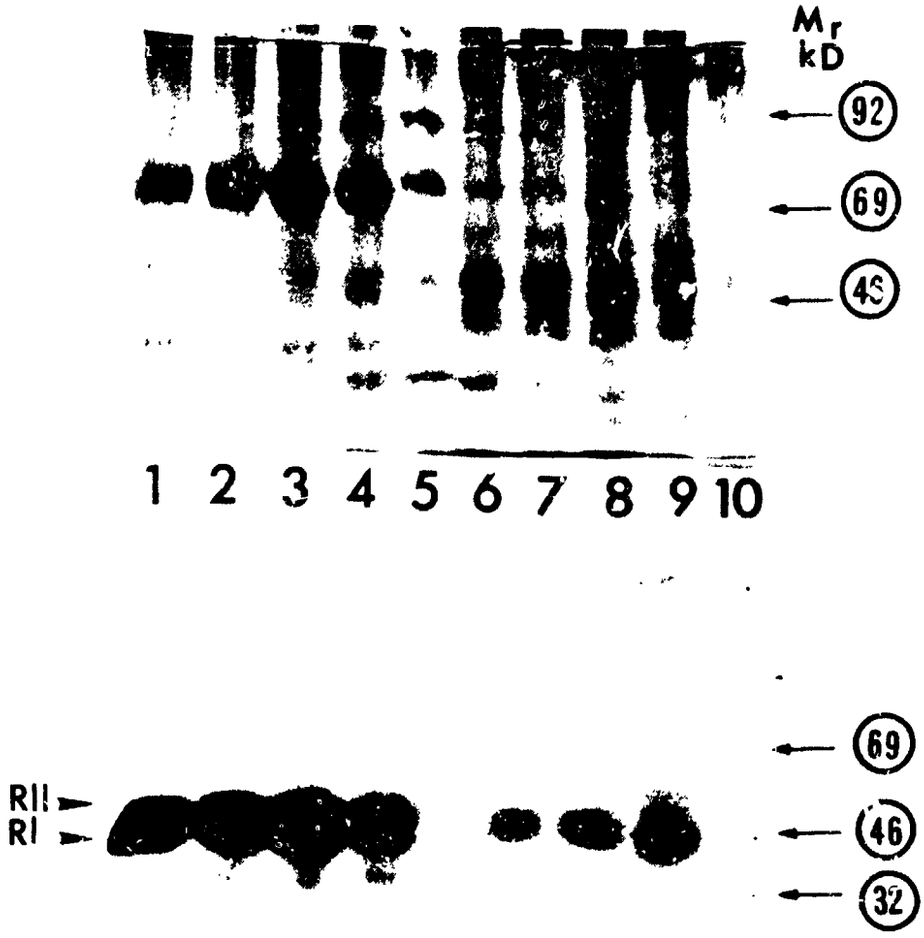

Fig. 3. Comparison of banding patterns and R subunit distribution between soluble and particulate fractions of the flight group heart muscle cell fractions. Fig. 3-A, protein banding patterns of soluble (lanes 1-4) and particulate (lanes 6-10) cell fractions. Lane 5 contains standard protein markers from which relative mobilities, shown on the right ordinate have been calculated. Fig. 3-B, autoradiogram of western-blotted, electrophoretically separated protein shown in Fig. 3-A. Lanes 1-4 soluble heart muscle cell fraction R subunit distribution. Lanes 6-9 corresponding particulate fraction, lane 10 the sample was treated in the presence of cold cyclic AMP to demonstrate specific reduction in labeling.

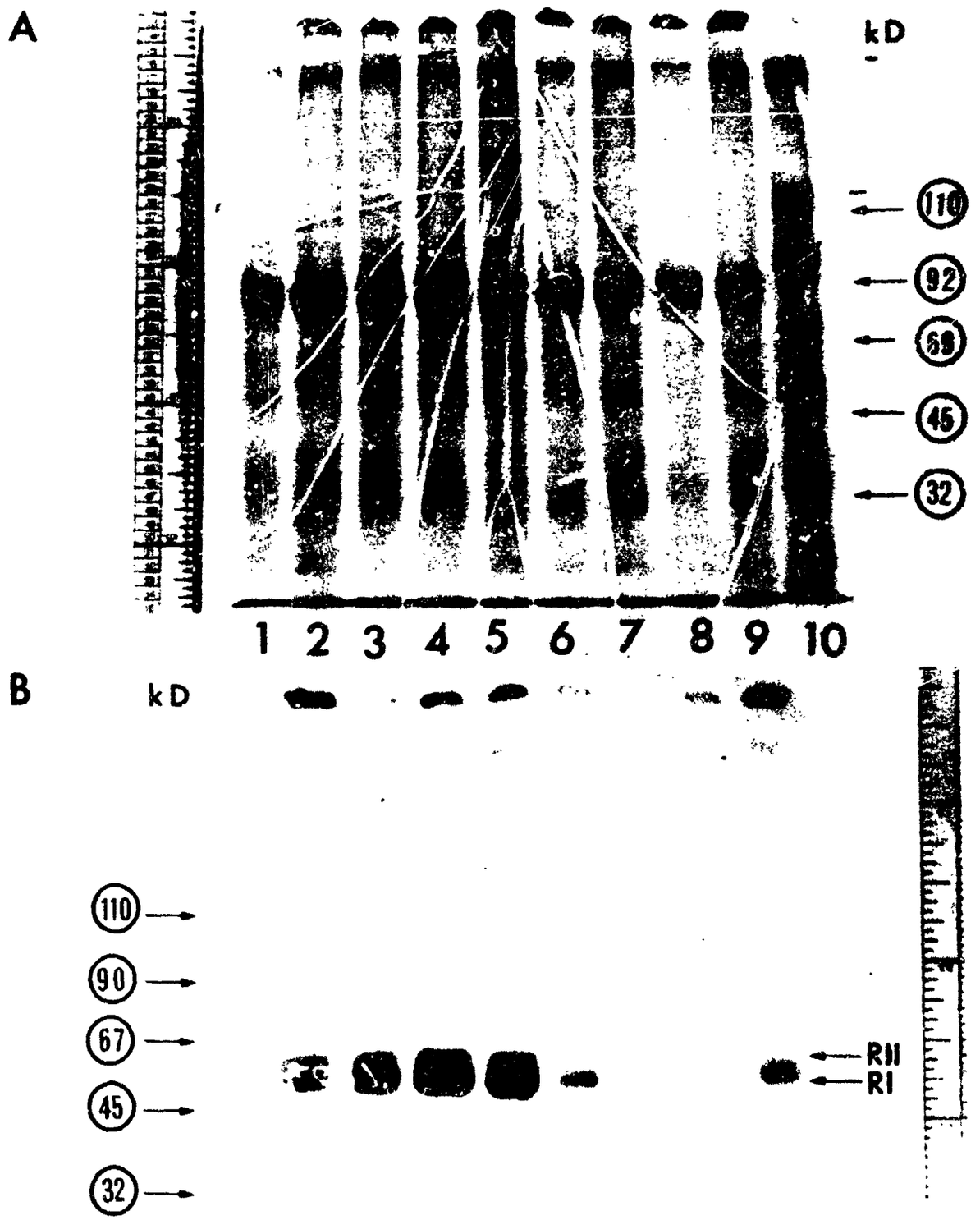

Fig. 4. Autoradiogram of particulate cell fraction of rat heart cells. Fig. 4-A, banding patterns, and Fig. 4-B, autoradiogram. Lane 1, cold competition control; lanes 2-5, controls; lanes 6-9, flight; lane 10, protein standards.

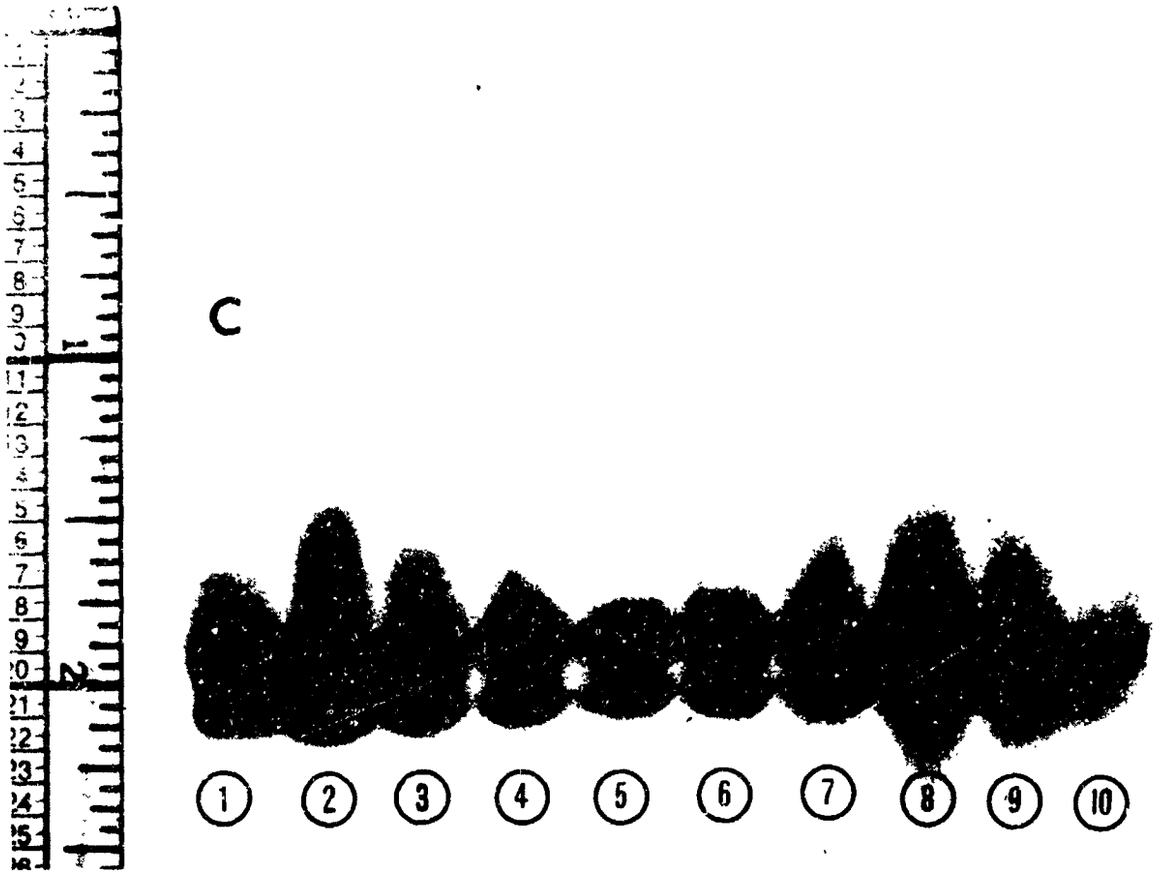

Fig. 4. Concluded. Fig. 4-C, autoradiogram of photoaffinity labeled soluable fractions of control and flight group heart muscle. Lanes 2-5, control; lanes 6-9, flight; lane 1, NIH control; lane 10, preincubated with cold cyclic AMP.

Fig. 5. Distribution of anti-RI antibody in cardiomyocytes showing e. ctron microscopic immunogold labeling. Fig. 5-A, cross section of a blood vessel, contains a red blood cell and adjacent cardiomyocyte with gold particles (x42,500). Figs. 5-B and 5-C, heart tissue showing a comparison of flight and control animal cells (x27,500).

N90-26468

EXPERIMENT K-6-14

HEPATIC FUNCTION IN RATS AFTER SPACEFLIGHT

Principal Investigator:

A. Merrill, Jr.
Department of Biochemistry
Emory University School of Medicine
Atlanta, Georgia 30322

Co-Investigators:

M. Hoel, E. Wang, D. Jones, J. Hargrove, R. Mullins
Departments of Biology, Pathology, and
Anatomy and Cell Biology
Emory University School of Medicine
Atlanta, Georgia 30322

I. Popova
Institute of Biomedical Problems
Moscow, USSR

PRECEDING PAGE BLANK NOT FILMED

SUMMARY

To determine the possible biochemical consequences of prolonged weightlessness on liver function, tissue samples from rats that had flown aboard Cosmos 1887 were analyzed for hepatic protein, glycogen and lipids as well as the activities of a number of key enzymes involved in metabolism of these compounds and xenobiotics. Among the parameters measured, the major differences were elevations in the hepatic glycogen content and HMG-CoA reductase activities of the rats flown on Cosmos 1887, and a decrease in the amount of microsomal cytochrome P_{450} and the activity of aniline hydroxylase, a cytochrome P_{450}-dependent enzyme. Decreases in these two indices of the microsomal mixed-function oxidase system indicate that spaceflight may compromise the ability of liver to metabolize drugs and toxins. The higher HMG-CoA reductase correlated with elevated levels of serum cholesterol. Other changes included somewhat higher blood glucose, creatinine, SGOT, and much greater alkaline phosphatase and BUN. These results generally support the earlier observation of changes in these parameters (Merrill et al., Am. J. Physiol. 252:R22-R226, 1987). The importance of these alterations in liver function is not known; however, they have the potential to complicate long-term spaceflight.

INTRODUCTION

The experience of weightlessness during spaceflight and the stresses associated with lift-off and reentry cause a number of physiological changes in astronauts and experimental animals. These include changes in fluid distribution, electrolyte balance, bone strength and growth, nitrogen balance, and lean body mass, inter alia (1-10). Many of these changes appear to be due to the lack of exercise that occurs in a weightless environment, but whether others represent the influence of long-term stress or other factors remains at issue.

Among the changes that have been observed during and after spaceflight are elevated adrenal steroid secretion and altered concentrations of various lipids and carbohydrates in blood and other tissues. Changes in hepatic concentrations of glycogen, lipids, and enzymes involved in metabolism of these compounds occurred during or after spaceflight in the Cosmos biosatellites (1-3,5,6,11). Secretion of a number of hormones that affect enzyme systems in liver may be altered by space flight; these include adrenal steroids, insulin, and growth hormone (3,8).

Since liver is an important site of nutrient and xenobiotic metabolism, further study of the effects of spaceflight on this organ appeared warranted. The inclusion of experimental animals aboard Spacelab 3 allowed us to conduct analyses of some of the key hepatic enzymes of cholesterol, glycerolipid, and sphingolipid biosynthesis (10) as well as quantiation of glycogen, protein, and lipids. These analyses revealed significantly lower activities for some but not all of the enzymes tested, suggesting that spaceflight can cause specific perturbations in liver function.

Based on these previous findings, we propose that several aspects of hepatic function are altered by spaceflight. In particular, these include key enzymes of cholesterol and sphingolipid biosynthesis and drug metabolism (e.g., cytochrome P_{450}). Described in this report are additional data from analyses of liver and serum samples from rats flown on Cosmos 1887 that support this hypothesis.

MATERIALS AND METHODS

Each group contained five male rats of Czechoslovakia-Wistar origin. They weighed between 300 and 400 g and were fed 55 g/day of a paste diet, and given water ad libitum. The animals were flown for 14 days and maintained on a regular cycle of 16 h of light/8 h of dark. The animals were killed between 53 and 56 hours after landing and the livers were immediately frozen and stored at

-80°. Additional information about the history of the animals and parameters such as the organ weights will be provided by the other participants of this study (e.g., Dr. Richard E. Grindeland, NASA).

Tissue preparation. The liver samples were thawed, homogenized, and centrifuged following fairly standard protocols to yield a microsomal fraction and a high-speed (cytosolic) fraction as described previously (10). We have found this procedure to recover microsomes in approximately 78% yield with little contamination with markers of other subfractions (12). Aliquots of the original homogenate, microsomes, and cytosol were stored at -80° until use. Individual aliquots were used for each assay to minimize losses of activity during freeze/thaw.

Serum analyses. The serum analyses were conducted using a COBAS Bio-centrifugal Analyzer calibrated with certified clininal standards.

Protein analyses. Total protein was assayed using a modification of the method of Lowry et al. (13) with bovine serum albumin as the standard.

Glycogen analyses. Liver glycogen was quantitated using the method of Johnson and Fusaro (14) and rabbit liver glycogen (Sigma Type III) as the standard.

Lipid analyses. The lipids were extracted as described before (10) using essentially the method of Bligh and Dyer (15) and analyzed for triglycerides and cholesterol using the COBAS Analyzer. Phospholipids were quantitated by assaying the amount of organic-solvent soluble phosphate, and the total sphingolipids were estimated by analysis of the sphingosine content after acid hydrolysis (16). Free sphingosine was quantitated by high-performance liquid chromatography (17).

Enzyme assays. Most of the enzyme assays were conducted as described previously (10). Fatty acyl-CoA synthetase was assayed with [^{3}H]palmitic acid as the substrate (18), and HMG-CoA reductase was assayed as described by Shapiro et al. (19), except that the [^{14}C]-HMG-CoA concentration was 25 μM. Serine palmitoyltransferase was assayed using [^{3}H]serine (12,21) and glycerol 3-phosphate acyltransferase using [^{3}H]glycerol 3-phosphate (21). Cytochrome P_{450} was measured spectrophotometrically (22), and aniline hydroxylase was determined as described by Gram et al. (23,24).

Tyrosine aminotransferase (25) and glutathione S-transferase (26) were assayed as described; cystathionase was measured by its ability to produce hydrogen sulfide from cysteine, using assay method III of Stipanuk and Beck (27). Alkaline phosphatase was analyzed as part of the COBAS centrifugal analyzer.

DNA measurement. DNA was quantitated by the method of Fiszer-Szafarz et al. (28) using calf thymus DNA as the standard.

Statistical methods Except where otherwise noted, the data are given as the means ± the standard deviation for n=5 in each group.

RESULTS

General effects of spaceflight on liver. The rats flown on Cosmos 1887 had slighly lower body weights than either the synchronous or vivarium controls; however, the liver weights were similar (Table 1). The groups were also similar in amounts of total liver protein, cytosolic protein, triglycerides, cholesterol and sphingolipids; however, the flight group was somewhat lower in microsomal protein (but only on a per g of liver basis) and total phospholipids. Liver DNA was

lowest for the flight rats (ca. 28% lower than the synchronous controls). The major differences were seen in liver glycogen, which was much lower for the vivarium rats and highest for the flight animals (2-fold higher than the synchronous controls). There appeared to be an inverse relationship between the amounts of DNA and glycogen, which indicates that a partial explanation for the lower cell number per g of tissue is loading of the liver with glycogen.

Liver enzymes of rats after spaceflight. All of the cytosolic enzymes examined exhibited similar activities among the three groups. Even tyrosine aminotransferase, which is highly sensitive to changes in the hormonal status the animal, was not altered significantly (Table 2). Liver alkaline phosphatase, which is primarily a plasma membrane enzyme, appeared slightly higher for the synchronous controls (58.0 $\pm$ 13.7 units/g of liver) than for the flight group (48.8 $\pm$ 3.8 units/g of liver), but the differences were not statistically significant.

Much larger differences were seen in microsomal enzymes (Table 3), without a single trend (i.e., some activities increased while others decreased); hence, the rats that had undergone spaceflight underwent selective changes in microsomal enzymes. HMG-CoA reductase was over 2- fold higher for the flight rats versus both vivarium and synchronous controls (Table 3), and this correlated with the higher serum cholesterol (Fig. 1). Serine palmitoyltransferase and fatty acyl-CoA synthetase were also elevated (by 41% and 58%, respectively), but only on a per g of liver basis.

Cytochrome P_{450} was slightly lower in the flight group (14%), and this persisted when the data were compared on per g of liver (38%) and per 100 g of body weight (21%) bases. Aniline hydroxylase, a member of the microsomal mixed-function oxidase system that utilizes cytochrome P_{450}, was also lower in the flight group (Table 3). Altogether, the similar depressions in cytochrome P_{450} and aniline hydroxylase (Fig. 2) indicate that the xenobiotic metabolizing system is somewhat depressed in the animals that underwent spaceflight.

Effects of spaceflight on serum components. As a broader indicator of the overall biochemical status of these animals, a standard profile of serum components was obtained (Table 3). Total protein, albumin, glucose, bilirubin, Ca^{2+}, K^{+}, and phosphate were virtually identical for the flight group and the synchronous controls.

Markers of muscle and tissue protein trauma (BUN, Creatine, AST, alkaline phosphatase, and lactate dehydrogenase) were consistently elevated in the flight groups (BUN was 144% higher than the synchronous controls). Furthermore, the flight animals were hyperlipidemic, with significant elevations in serum cholesterol (67%) and to a lesser extent triglycerides (16%).

DISCUSSION

Because there was a two day period between the landing of Cosmos 1887 and the removal of the livers for these biochemical analyses, the results of this study are more likely to reflect the combination of spaceflight and the responses of the rats during a post-flight recovery period than to changes due to spaceflight alone. Activities that change with a short half-time, therefore, may easily readjust during or after landing, whereas parameters that require several days to change will remain near the values attained during spaceflight. Nonetheless, many of the findings of this study agreed closely with previous biochemical analyses that were conducted with a shorter lag time.

The most significant results obtained from this analysis of liver function after spaceflight include the findings that glycogen content was elevated in the flight group, that these animals were hyperlipidemic (and had elevations in the initial enzymes of cholesterol and sphingolipid biosynthesis), and that cytochrome P_{450} values were lower than for the synchronous control group.

The major difference from the previous studies (1,10) was in the increase in HMG-CoA reductase activity, which was lower in rats from Spacelab 3. It is clear from these analyses of flight rats that there are specific and unexplained changes in the activities of the initial enzymes of cholesterol and sphingolipid biosynthesis. This finding may be important, since these lipids are primarily involved in cell surface phenomena, such as the functioning of enzymes and receptors, cell-to-cell communication, cell-to-surface antigenicity, and some aspects of nerve impulse transmission. Cholesterol and sphingomyelin are both found in lipoproteins, and these changes may relate as much to the levels of circulating lipids as to those in liver.

Serum cholesterol has been reported to decrease during both Apollo and Skylab missions (4,8). However, plasma cholesterol was higher for the rats on Spacelab 3 (29) and this Cosmos flight, which might indicate that lipoprotein cholesterol was removed from circulation more slowly for these animals. Additional experiments are needed to explain these discrepancies.

The large difference in hepatic glycogen content between flight and control groups confirms the earlier observation with Spacelab 3. Smaller increases in glycogen content have been observed after other missions, as well as significantly decreased activity of glycogen phosphorylase (1,2); and increased glycogen was noted also in heart and skeletal muscle. Since the animals had eaten little during the previous hours, the differences observed may relate to reduced glycogen breakdown in the flight group (however, the synchronous group were fed according to the same schedule). Since hepatic glycogenolysis and gluconeogenesis are critical in maintaining normal blood sugar levels, it is important to determine whether these processes were altered during weightlessness; blood glucose was the same (or slightly elevated) in the flight group at the time of sampling, as has been seen previously (10).

The indication that cytochrome P_{450} was lower in liver from the flight group confirmed the earlier finding with Spacelab 3. This enzyme protein is involved in the metabolism of steroid hormones and a variety of xenobiotics, including antibiotics and other drugs; hence, decreases might reduce the activity of such systems. This was demonstrated in the lower activity of aniline hydroxylase in the flight group. Although these differences were small, the fact that they were seen in two indices of the microsomal mixed function oxidase system lends credence to their validity. The implications of this effect of spaceflight on the body's ability to metabolize drugs have not been explored; however, it could limit the ability of an animal to detoxify various drugs and other compounds, and diminish the potency of drugs that act after bioactivation by the cytochrome P_{450} system.

We conclude that spaceflight significantly alters liver function in a number of ways. Changes in glycogen and lipid metabolism are probably consequences of weightlessness, and drug metabolism may also be altered. Because the liver functions to regulate supply, distribution, and deposition of numerous compounds that are either required by other organs or that can be toxic to them, the bearings of these findings on long-term adaptation to weightlessness should be evaluated in future work. In the future it will be essential to obtain samples taken in flight or shortly after landing to permit valid measurements of these parameters.

ACKNOWLEDGMENTS

This work was supported by the National Aeronautics and Space Administration. We thank Dr. R. E. Grindeland for helpful discussions during these studies.

REFERENCES

1. Abraham, S., C. Y. Lin, H. P. Klein, C. Volkmann, R. A. Tigranyan, and E. Vetrova. Studies of specific hepatic enzymes involved in the conversion of carbohydrates to lipids in rats exposed to prolonged spaceflight aboard Cosmos 1129. Physiologist 23 (6) Suppl.: S55-S58, 1980.

2. Abraham, S., C. Y. Lin, C. M. Volkmann, and H. P. Klein. Biochemical changes in rat liver after 18.5 days of spaceflight. Proc. Soc. Exp. Biol. Med. 172: 334-339, 1983.

3.Ahlers, I., E. Misurova, M. Praslicka , and R. A. Tigranyan. Biochemical changes in rats flown on board the Cosmos 690 biosatellite. Life Sci. Space Res. 14: 185-188, 1976.

4. Alexander, W. C., C. S. Leach, and C. L. Fischer. Clinical biochemistry. In: Biomedical Results of Apollo, edited by R. S. Johnston, L. F. Dietlein, and C. A. Berry. Washington, DC: U.S. Govt. Printing Office, 1975, p. 185-196.

5. Belitskaya, R. A. Carbohydrate and lipid content of rat liver tissue following a 22-day spaceflight. Space Biol. Aerospace Med. 4: 97-99, 1977.

6. Belitskaya, R. A. Changes in amount and composition of phospholipids in rat skeletal muscle microsomal fra[illegible]nder the influence of a flight aboard the Kosmos-690 biosatellite. Space Biol. Aeros[illegible]led. 1: 23-28, 1979.

7. Gazenko, O. G., A. M. Genin, E. A. Ilyin, L. V. Oganov, and L. V. Serova. Adaptation to weightlessness and its physiological mechanisms (results of animal experiments aboard biosatellites). Physiologist 23 (6) Suppl.: 511-515, 1980.

8. Leach, C. S., and P. C. Rambaut. Biochemical responses of the Skylab crewmen: an overview. In: Biomedical Results from Skylab, edited by R. S. Johnston and L. F. Dietlein. Washington, D.C.: US Govt. Printing Office, 1977, p. 204-216.

9. Nemeth, S., L. Macho, M. Paikovic, N. Skottova, and R. Tigranyan. Metabolic changes in rats subjected to spaceflight for 18.5 days in the biosatellite Cosmos 936. Adv. Space Res. 1: 219-224, 1981.

10. Merrill, A. H., Jr., Wand, E., Jones, D. P., and Hargrove, J. L. Hepatic function in rats after spaceflight: effects on lipids, glycogen, and enzymes. Amer. J. Physiol. 252, R222-R226, 1987.

11. Yakovleva, V. I. About dynamic changes of the lipid content in the rat liver during bioflight in "Cosmos-605" and "Cosmos-782". Arch. Anat. Histol. Embryol. 10: 39-44, 1977.

12. Williams, R. D., E. Wang, and A. H. Merrill, Jr. Enzymology of long-chain base synthesis by liver: characterization of serine palmitoyltransferase in rat liver microsomes. Arch. Biochem. Biophys. 228: 282-291, 1984.

13. Bensadoun, A., and D. Weinstein. Assay of proteins in the presence of interfering materials. Anal. Biochem. 70: 241-250, 1976.

14. Johnson J. A., and Fusaro, R. M. Use of purified amyloglucosidase for the specific determination of total carbohydrate content of rat liver homogenate in a single step. Anal. Biochem. 98, 47-52, 1979

15. Bligh, E. A., and W. J. Dyer. A rapid method of total lipid extraction and purification. Can. J. Biochem. 37: 911-917, 1959.

16. Gaver, R., and C. C. Sweeley. Methods for methanolysis of sphingolipids and direct determination of long-chain bases by gas chromatography. J. Am. Oil Chem. Soc. 42: 294-298, 1965.

17. Merrill, A. H., Jr., Wand, E., Mullins, R. E., Jamison, W. C. L., Nimkar, S., and Liotta, D. C. Quantitation of free sphingosine in liver by high-performance liquid chromatography. Anal. Biochem. 171, 373-381.

18. Tanaka, T., K. Hosaka, M. Hoshimaru, and S. Numa. Purification and properties of long-chain acyl-coenzyme A synthetase from rat liver. Eur. J. Biochem. 98: 165-172, 1979.

19. Shapiro, D. J., J. L. Nordstrom, J. J. Mitschelen, V. W. Rodwell, and R. T. Schimke. Microassay for 3-hydroxy-3-methylglutaryl-CoA reductase in rat liver and in L-cell fibroblasts. Biochim. Biophys. Acta 370: 369-377, 1974.

20. Merrill, A. H., JR., D. W. Nixon, and R. D. Williams. Activities of serine palmitoyltransferase (3-ketosphinganine synthase) in microsomes from different rat tissues. J. Lipid Res. 26: 617- 622, 1985.

21. Schlossman, D. M., and Bell, R. M. Microsomal sn-glycerol 3- phosphate and dihydroxyacetone phosphate acyltransferase activities from liver and other tissues. Arch. Biochem. Biophys. 182, 732-742, 1977.

22. Omura, T., and R. Sato. The carbon monoxide binding pigment of liver microsomes. I. Evidence for its hemoprotein nature. J. Biol. Chem. 239: 2370-2378, 1964.

23. Gram, T. E., Guarino, A. M., Schroeder, D. H., and Gillette, J. R. Changes in certain kinetic properties of hepatic microsomal aniline hydroxylase and ethylmorphine demethylase associated with postnatal development and maturation in male rats. Biochem J. 113, 681-685, 1969.

24. Guarino, A. M., Gram, T. E., Gigon, P. L., Greene, F. E., and Gillette, J. R. Changes in Michaelis and spectral constants for aniline in hepatic microsomes from phenobarbital-treated rats. Mol. Pharmacol. 5, 131-136, 1969.

25. Granner, D. K., and G. M. Tomkins. Tyrosine aminotransferase (rat liver). Methods Enzymol. 17B: 633-637, 1970.

26. Habig, W. H., M. J. Pabst, and W. B. Jakoby. Glutathione S- transferases. J. Biol. Chem. 249: 7130-7139, 1974.

27. Stipanuk, M. H., and P. W. Beck. Characterization of the enzymic capacity for cysteine desulphydration in liver and kidney of the rat. Biochem. J. 206: 267-277, 1982.

28. Fiszer-Szafarz, B., Szafarz, D., and De Murillo, A. G. A general, fast, and sensitive micromethod for DNA determination: Application to rat and mouse liver, rat hepatoma, human leukocytes, chicken fibroblasts, and yeast cells. Anal. Biochem. 110, 165-170, 1981.

29. Fast, T. N., R. Grindeland, M. Ruder, M. Vasques, P. Lundgren, S. Scibetta, J. Tremor, P. Buckendahl, L. Keil, O. Chee, T. Reily, B. Dalton, and P. Callahan. Rat maintenance in the research animal holding facility during the flight of Space Lab 3. Physiologist 28 (6) Suppl.: S187-S188, 1985.

TABLE 1.

Liver Protein, Glycogen, and Lipid Analyses

	Vivarium	Synchronous	Flight
		(Mean ± SD)	
Body weight (g)	342 ± 17.2	349.0 ± 13.0	303.2 ± 5.4
Liver weight (g)	8.27 ± 0.67	8.86 ± 0.42	9.96 ± 3.16
Liver DNA (mg/g liver)	5.11 ± 0.36	3.84 ± 0.83	2.75 ± 0.73
(mg/liver)	42.3 ± 3.4	34.0 ± 7.4	27.4 ± 8.7
(mg/100 g B.W.)	12.4 ± 1.0	9.7 ± 2.1	9.0 ± 2.9
Liver protein			
(mg/g liver)	213 ± 9	215 ± 15	228 ± 19
(g/liver)	1.76 ± 0.14	1.90 ± 0.1	2.27 ± 0.72
(mg/100 g B.W.)	0.51 ± 0.04	0.54 ± 0.03	0.75 ± 0.23
Microsomal protein			
(mg/g liver)	2.8 ± 0.2	3.3 ± 0.3	2.4 ± 0.7
(mg/100 g B.W.)	6.8 ± 0.5	8.4 ± 0.7	7.8 ± 2.2
Cytosolic protein			
(mg/g liver)	112 ± 11	110 ± 6	116 ± 15
Glycogen (mg/g liver)	5.0 ± 1.0	11.5 ± 2.9	20.7 ± 4.6
Total phospholipids			
(μmol/g liver)	32.8 ± 2.3	35.8 ± 1.9	28.6 ± 2.0
Triglycerides			
(mg/g liver)	143 ± 11	151 ± 11	155 ± 19
Cholesterol (mg/g)	7.03 ± 0.63	5.75 ± 1.46	4.69 ± 0.90
Total sphingolipids			
(μmol/g liver)	0.60 ± 0.04	0.58 ± 0.02	0.62 ± 0.06
Free sphingosine			
(nmol/g liver)	4.31 ± 0.80	2.99 ± 0.43	2.93 ± 0.21

TABLE 2.

Activities of selected cytosolic liver enzymes

	Vivarium	Synchronous	Flight
		(Mean ± SD)	
Cytosolic enzymes			
Tyrosine aminotransferase			
(µmol/min/mg protein)	8.29 ± 1.63	6.49 ± 2.18	6.69 ± 2.01
(mmol/min/g liver)	0.93 ± 0.18	0.71 ± 0.24	0.78 ± 0.23
Glutathione S-transferase			
(nmol/min/mg protein)	173 ± 10	191 ± 24	153 ± 24
µmol/min/g liver)	19.4 ± 1.1	21.0 ± 2.6	18.9 ± 2.8
Cystathionase			
(nmol/min/mg protein)	3.20 ± 0.46	3.56 ± 0.69	3.21 ± 0.64
(µmol/min/g liver)	0.36 ± 0.05	0.39 ± 0.08	0.37 ± 0.07
Cystathionine ß-synthase			
(nmol/min/mg protein)	3.27 ± 0.16	2.99 ± 0.82	3.29 ± 0.40
(µmol/min/g liver)	0.37 ± 0.02	0.33 ± 0.09	0.38 ± 0.05

TABLE 3.

Activities of selected microsomal enzymes of rat liver

	Vivarium	Synchronous	Flight
		(Mean ± SD)	
Cytochrome P-450			
(nmol/mg)	0.58 ± 0.15	0.77 ± 0.12	0.66 ± 0.11
(nmol/g liver)	1.62 ± 0.4	2.54 ± 0.4	1.58 ± 0.26
(nmol/100 g B.W.)	3.91 ± 1.01	6.48 ± 1.01	5.15 ± 0.86
Aniline hydroxylase			
(units/mg)	0.048 ± 0.008	0.050 ± 0 008	0.041 ± 0.008
(units/g liver)	0.134 ± 0.022	0.165 ± 0.026	0.098 ± 0.019
(units/100 g B.W.)	0.039 ± 0.006	0.047 ± 0.007	0.032 ± 0.006
Fatty acyl-CoA synthetase			
(nmol/min/mg protein)	34.4 ± 6.6	31.6 ± 3.5	49.9 ± 2.9
(nmol/min/g liver)	96.3 ± 18.5	104 ± 12	119 ± 7
Glycerol 3-phosphate acyltransferase			
(nmol/min/mg protein)	1.23 ± 0.18	1.32 ± 0.04	1.65 ± 0.39
(nmol/min/g liver)	3.44 ± 0.50	4.36 ± 0.13	3.96 ± 0.94
HMG-CoA reductase(μ/mg)	3.7 ± 1.1	4.7 ± 2.6	11.3 ± 4.5
(μ/g liver)	10.4 ± 3.1	15.5 ± 8.6	27.1 ± 10.8
(μ/100 g B.W.)	25.1 ± 7.5	39.5 ± 5.1	88 ± 35
Serine palmitoyltransferase			
(μ/mg)	26.9 ± 2.2	14.5 ± 2.6	20.5 ± 2.0
(μ/g liver)	75.3 ± 6.2	47.9 ± 8.6	49.2 ± 4.8

TABLE 4.
Serum Analyses

	Basal	Vivarium	Synchronous	Flight
		(Mean ± SD, n=5)		
Albumin (g/dL)	5.24 ± 0.17	5.12 ± 0.18	4.96 ± 0.22	4.92 ± 0.27
Total Protein (g/dL)	6.48 ± 0.11	6.60 ± 0.24	6.40 ± 0.24	6.40 ± 0.40
Glucose (mg/dL)	160 ± 6.6	112 ± 18	124 ± 3.8	154 ± 17.2
Total Bili (mg/dL)	0.4 ± 0	0.32 ± 0.11	0.4 ± 0	0.4 ± 0
BUN (mg/dL)	16.8 ± 2.3	17.6 ± 1.7	13.6 ± 1.7	33.2 ± 7.8
Creat mg/dL)	0.52 ± 0.11	0.46 ± 0.23	0.60 ± 0.14	0.84 ± 0.09
AST (SGOT) U/L)	179 ± 66	163 ± 47	193 ± 19	284 ± 70
Alk P'ase U/L)	323 ± 104	105 ± 17	153 ± 16	235 ± 41
LDH U/L)	866 ± 313	694 ± 276	762 ± 96	877 ± 77
Calcium (mg/dL)	10.9 ± 0.1	10.7 ± 0.2	10.1 ± 0.3	9.9 ± 0.4
Phosphate (mg/dL)	7.48 ± 0.41	7.0 ± 0.42	5.96 ± 0.36	6.60 ± 0.40
K (meQ/L)	6.08 ± 0.86	6.16 ± 0.17	5.36 ± 0.09	5.64 ± 0.26
Cholesterol (mg/dL)	62.4 ± 3.6	70.8 ± 12.0	86.0 ± 7.3	128 ± 21
Trig (mg/dL)	182 ± 50	84.8 ± 8.9	122 ± 15	142 ± 34

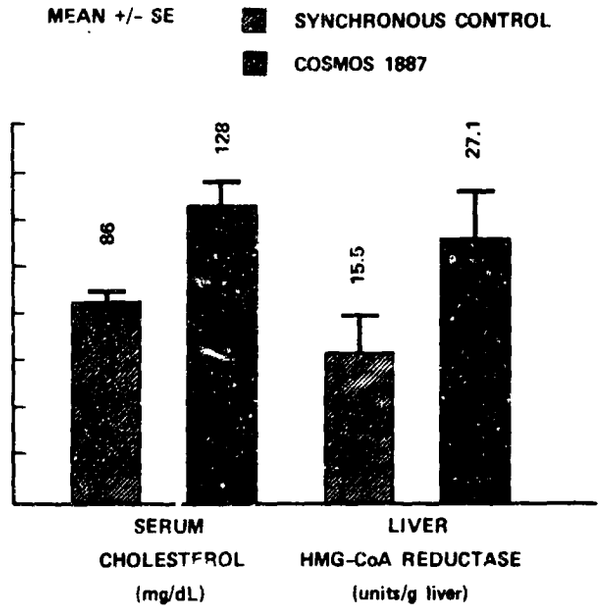

Figure 1. Comparison of serum cholesterol and liver HMG-CoA reductase activities of rats flown on Cosmos 1887 and synchronous controls. The actual amounts or units of activity are shown above the bars.

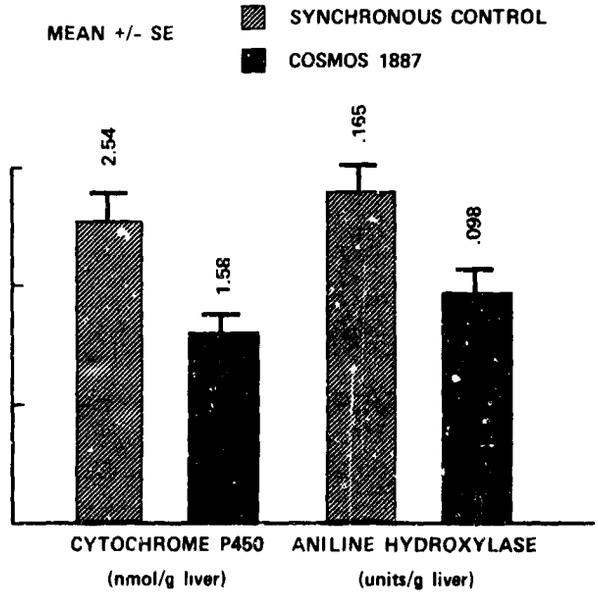

Figure 2. Comparison of microsomal cytochrome P_{450} and aniline hydroxylase activities of rats flown on Cosmos 1887 and synchronous controls. The actual amounts or units of activity are shown above the bars.

N90-26469

EXPERIMENT K-6-16

MORPHOLOGICAL EXAMINATION OF RAT TESTES

THE EFFECT OF COSMOS 1887 FLIGHT ON SPERMATOGONIAL POPULATION AND TESTOSTERONE LEVEL IN RAT TESTES

Principal Investigator:

D.E. Philpott
NASA Ames Research Center
Moffett Field, California 94035

Co-Investigators:

K. Kato, J. Stevenson, M. Vasques
NASA Ames Research Center
Moffett Field, California 94035

W. Sapp, C. Williams
Tuskegee University
Tuskegee, Alabama 36088

I.A. Popova
L.V. Serova
Institute of Biomedical Problems
Moscow, USSR

 PRECEDING PAGE BLANK NOT FILMED

SUMMARY

Testes from rats flown on Cosmos 1887 for twelve and a half days were compared to basal control, synchronous control and vivarium maintained rats. When the mean weights of flight testes, normalized for weight/100 gms, were compared to the vivarium controls they were 6.7% lighter. Although the flight testes were lighter than the synchronous, the difference is not significant. Counts of spermatogonial cells from 5 animals in each group revealed a 4% decrease in flight compared to vivarium controls. In both cases the t-Test significance was <0.02. The serum testosterone levels of all animals (flight, synchronous and vivarium) were significantly below the basal controls.

INTRODUCTION

The flight of Cosmos 1887 Biosputnik provided an opportunity to investigate the effects of a 12.5 day space flight. The testes have been shown to be affected by space flight, immobilization, irradiation and increased gravity. Two male dogs were flown on Cosmos 110 for 22 days (Fedorova, 1967). Fedorova reported an increase of 30 to 70% atypical spermatozoa consisting of tail curling and the absence of a tail. Seventy- five days after the flight, the abnormalities had decreased to their high normal range of 30%. Mating of these dogs after this period of time produced normal offspring. Rat flight testes from SL-3 showed a 7.5% decrease in stage six spermatogonia and an average weight difference of 7.1% when compared to controls (Philpott et al., 1986). In earlier studies of rats flown aboard Cosmos 690 (Plakhuta-Plakutina, 1977) and Cosmos 605 (Portugalov et al., 1976), no specific changes in the testes, directly attributed to flight, were reported.

Cannon (1914) first developed the idea that organisms react to unfavorable conditions with highly integrated metabolic activities. Selye (1950) summarized the manifestations of physiological response to nonspecific stress indicating that atrophy of the gonads always occurred. Many papers have been written on the effects of social interaction, crowding, peck order and confinement. Flickinger (1961, 1966) showed delayed testicular development in subordinant roosters influenced by group numbers, social rank and social status. Christian and Davis (1964) and Christian et al. (1965) reported that increasing population size in mice resulted in adrenal hypertrophy, inhibition of reproductive maturation and loss of reproductive function in adults. Sex organ weights also declined. Huygens et al. (1939) observed transient atrophy of the testes when dogs were confined. A decrease in testicular weight and total body weight occurred in rats and mice spun on a centrifuge at 2 X g for 8-9 weeks (Crockett, unpublished, 1969).

Immobilization, applied for a short or long period, is considered a form of physiological stress, and induces a decrease in plasma testosterone levels (Charpenet et al., 1981; Armario and Castellanos, 1984; Collu et al., 1984). While most reports indicate no change in the morphology of differentiating germ cells as a result of immobilization (McGrady and Chakraborty, 1983), a "striking" arrest of spermatogenesis in a primate has been reported (Zemjanis et al., 1970).

The sensitivity of the testes to radiation is well known and well studied. The details of spermatogonial effects of irradiation in mice and rats (Huckins, 1978; Van Alphen et al., 1988; Cunningham and Huckins, 1978; Cattanach and Crocker, 1979; Hugon and Borgers, 1966; Lu et al., 1980; Oakberg and Clark, 1961; Oakberg, 1962; Whithers et al., 1974) and primates (Zemjanis et al., 1970) have been the subject of studies utilizing X-irradiation and gamma irradiation. Our team has reported the results of cosmic (HZE) type irradiation on spermatogonial cell counts (Philpott et al., 1981, 1983a, 1983b, 1985a, 1985b). Alpen and Powers-Risius (1981) have quantitated HZE effects using testes weight loss. The Alpen and Philpott papers have reported an increase in RBE (radiobiological effect) after HZE irradiation. Philpott et al. (1983) have shown that doses of less than 0.5 rads can be detected using an assay method that concentrates on cell

numbers in spermatogonial stage six (Huckins, 1978). This sensitive response makes the testes a possible candidate as a biological dosimeter.

METHOD

The left and right testes from five rats flown on Cosmos 1887 provided material for weight determination, testosterone assay and spermatogonial cell loss quantification. Another fifteen animals were maintained on the ground, i.e., five synchronous controls, five vivarium controls and five sacrificed at the time of flight to provide material for basal control. The flight lasted twelve and a half days and landed in Siberia. The animals were transported by bus, airplane and van to the animal facility. Sacrifice occurred two days after the rats returned from space. The testes were removed, weighed, immediately slit open and immersed in cold Triple Fix (Philpott et al., 1980). The specimens were kept at four degrees C, shipped to Ames and refrigerated until time for processing. Samples were treated with 1% osmic acid for one hour, dehydrated in ascending concentrations of acetone, infiltrated with Epon-Araldite and polymerized at 60 degrees C for 48 hours. Six blocks were produced from each testis. Two-micron cross sections of the blocks were cut on a Porter-Blum ultramicrotome and mounted on glass slides. The sections were stained with Toluidine Blue. Alternate sections containing maturation stage six were used to count the surviving spermatogonia (Figure 1). Testosterone measurements were made on the rat plasma samples using Coat-A-Count kits from Diagnostic Products, Inc.

RESULTS

The mean weights for the testes were: flight 1.19 gm, synchronous 1.34 gm, and vivarium 1.44 gm. The average weight difference of the Cosmos flown rat testes was 6.7% as compared to vivarium controls when normalized for weight/100 grams. This difference is significant. However, the difference between the flight and synchronous control animals is not significant. Basal control weights were not available.

Counts of surviving spermatogonia (Table 1) per tubule cross section indicated an average of 38.79 spermatogonia for flight animals, 40.20 for the synchronous controls and 43.75 for the vivarium controls. The decreases of spermatogonia in flight tissues is a significant number as compared to the synchronous control ($P<0.02$, 1 tail; $P<0.005$, 2 tail) and vivarium control ($P<0.0002$, 1 tail; $P<0.005$, 2 tail). Rats flown on SL-3 experienced a similar decrease in number of spermatogonia (Figure 2). Preliminary counts of Sertoli cells per tubule cross section indicate no significant difference ($P>0.05$) when vivarium control animals are compared to either synchronous controls or to flight animals. This consistency in Sertoli cell numbers per tubule cross section demonstrates their stability under the adverse conditions of space flight and indicates that the minor volumetric changes in tubular epithelium due to spermatogonial cell loss do not affect the relative numbers per tubule cross section. Spermatogonial cell loss can be quantitated per number of Sertoli cells or per tubule cross section. Changes in spermatogonial cell populations are indicative of actual cell loss and are not significantly influenced by volumetric changes in the tubules (Fig. 3,a,b,c,d).

Serum testosterone (Table 2) was measured for flight animals, basal, vivarium, and synchronous controls. When means were compared between the basal controls and all other experiments, the differences were significant at the <0.001 level for flight, at the <0.05 level for synchronous control, and at the <0.01 level for the vivarium control. The mean for the flight testosterone level was lower than the mean for synchronous or vivarium controls but not significant when a t-Test was applied. These results are somewhat similar to those from rats flown on SL-3 (Figure 4).

DISCUSSION

While it is general knowledge that the testes are very sensitive to certain environmental factors including stress and irradiation, not all reports agree on the extent and nature of morphologic

changes in the seminiferous epithelia (McGrady and Chakraborty, 1983). Basically, most reports indicate that stress will decrease testosterone levels (Charpenet et al., Armario and Castellanos, 1981; Collu et al., 1984) but does not cause any morphological changes in the seminiferous tubules (McGrady and Chakraborty, 1983). Interestingly, in human beings, stress may cause either an increase or decrease in serum testosterone depending upon whether the stress is perceived as a threat to dominance/control (increased testosterone) or as a loss of control (decreased testosterone) (Collu et al., 1984). On the other hand, irradiation, depending on the dosage, can result in the depletion of all spermatogonial cells except a few of the stem cells (Philpott et al., 1983; Van Alphen et al., 1988). At the same time testosterone levels do not seem to be affected either in the serum or intratesticular tissue by irradiation (Cunningham and Huckins, 1978).

Previous space flight investigations prior to SL-3 have not reported changes in seminiferous epithelium while simulated conditions, at least in some investigators' labs, result in changes (Portugalov et al., 1976). Data obtained from rats flown on Cosmos 1887 indicated significantly reduced numbers of spermatogonia when compared to both synchronous control animals and vivarium control animals. Differences in cytological populations were significant (11% decrease compared to vivarium, 4% decrease compared to synchronous) and were generally similar to results obtained from rats flown on SL-3 (Philpott et al., 1986; Sapp et al., 1988). Our assay procedure provides excellent quality specimens and sections thin enough to provide morphological differentiation of each spermatogonial cell class, and precise quantitation.

Rats in the synchronous control group were exposed to all environmental parameters, except micro-G, and the increased G- forces of lift-off and landing, encountered in the Cosmos 1887 space flight. Vivarium controls were exposed only to similar temperature, feeding and lighting conditions. Our data indicate a significant difference in spermatogonial population when these two control groups are compared. This difference may be caused by the stresses encountered under simulated space flight conditions, or to as yet unexplained responses. A similar decrease in spermatogonia was seen in rats subjected to suspension in the simulated SL-3 flight (Figure 2).

We postulate that the decrease (4%) in spermatogonia observed in rats actually flown on Cosmos 1887 when compared to synchronous controls is due to space flight conditions not adequately duplicated in the ground based synchronous experiment. One possible factor is radiation. Dosimetry reports from Cosmos 1887 indicate a dose factor of 0.313 rad at the dosimeter location within the space craft. Dosimeters were not located proximal to the animals, therefore the exact dosage received in that area is not known. Low radiation levels do not produce gross changes in morphology; however, spermatogonia near the first meiotic division are reduced in number. This is not unexpected and many investigations, including our own, substantiate these results (Philpott et al., 1983). We have shown with X-rays and with HZE particles the extreme sensitivity and predictable response of the testicular epithelium to irradiation. The loss of cells not accounted for except by space travel could have resulted from radiation, especially since any particles penetrating the space craft would have been galactic and of similar energy to Iron. Our previous experiments (Figures 5, 6) indicate that irradiation with HZE particles of Iron at the 0.5 rad level caused significant decreases in spermatogonia in mice (Philpott et al., 1985b) and these changes could be detected down to the 0.1 rad exposure level (unpublished).

Previous work in our laboratory led us to conclude that the testicular seminiferous epithelium is a good model for radiation sensitivity studies. It has been shown to be very susceptible to radiation damage in general. It is composed of cellular populations which vary in individual radiosensitivities and is indicated by the multiple slopes seen in spermatogonial survival curves (Philpott et al., 1983b). These characteristics of the testicular epithelium provide an accurate means for biological dosimetric assessment of radiation exposure.

Data collected from this flight (Cosmos 1887) as well as from the earlier SL-3 flight indicate that the biological effects of space flight are multifaceted. Impact on the morphophysiology of the

testes through a number of different pathways, i.e. decreases in serum testosterone and testes weight loss, is observed in the animals described in this report. Stress related gonadal dysfunction and possible galactic radiation exposure, along with other possible factors, apparently contribute to the significant decrease in spermatogonial cell numbers observed in rats flown in space. Various changes in the environment can alter testicular integrity. The site of action of these various environmental impacts and the mechanisms by which they interfere with both spermatogenesis and steroidogenesis need further investigation. These important investigations should be repeated with longer flights and a shorter time span between recovery and specimen preparation. When it becomes possible, fixation in flight will remove any doubt about the effect recovery may have.

REFERENCES

1. Alpen, E.L. and P. Powers-Risius. The relative biological effect of high-Z, high-LET charged particles for spermatogonial killing. Radiat. Res. 88:132-143, 1981.

2. Armario, A., and J. M. Casstellanos. A comparison of corticoadrenal and gonadal responses to acute immobilization stress in rats and mice. Physiology and Behavior. 32:517-519, 1984.

3. Cannon, W. B. The emergency function of the adrenal medulla in pain and the major emotions. Am. J. Physiol. 33: 356, 1914.

4. Cattanach, B.M. and A.J.M. Crocker. Translocation yield from mouse spermatogonial stem cells following unequal-sized x-ray fractionations. Evidence of radiation induced loss of heterogeneity. Mut. Res. 60:73-82. 1979.

5. Charpenet, G., Y. Tache, M. G. Forest, G. Haour, J. M. Saez, M. Bernier, J. R. Ducharme and R. Collu. Effects of chronic intermittent immobilization stress on rat testicular androgenic function. Endrocrinology. 109:1254-1258, 1981.

6. Christian, J.J. and D. E. Davis. Endocrines, behavior and population. Science, 146: 1550, 1964.

7. Christian, J. J., J.A. Loyd and D. E. Davis. The role of endocrines in the self-regulation of mammalian populations. Recent Progr. Hormone Res., 21: 501, 1965.

8. Collu, R., W. Gibb and J. R. Ducharme. Effects of stress on the gonadal function. J. Endrocrinol. Invest. 7:529537, 1984.

9. Cunningham, G. R., and C. Huckins. Serum FSH, LH, and Testosterone in ^{60}Co Gamma-irradiated male rats. Rad. Res. 76: 331-338, 1978.

10. Fedorova, N. L. Spermatogenesis of the dogs Ugolyok and Veterok after their flight on board the Satellite Kosmos 110. Kosmicheskaya Biol. Med. 1: 28, 1967. Space Biol. Med. 1: 28, 1967.

11. Flickinger, G. L.,. Effect of grouping on adrenals and gonads of chickens. Gen. Comp. Endrocrinol., 1: 332, 1961.

12. Flickinger, G. L., Response of the testes to social interaction among grouped chickens. Gen. Comp. Endocrinol., 6: 89, 1966.

13. Huckins, C. The morphology and kinetics of spermatogonial degeneration in normal adult rats: An analysis using a simplified classification of the germinal epithelium. Anat. Rec. 190:905-926, 1978.

14. Huckins, C. and E.F.Oakberg. Morphological and quantitative analysis of spermatogonia in mouse testes using whole mounted seminiferous tubules. II. The irradiated testes. Anat. Rec. 192:529-542. 1978.

15. Hugon, J. and V.M. Borgers. Ultrastructural and cytochemical changes in spermatogonia and sertoli cells of whole body irradiated mice. Anat. Rec. 155:15-32. 1966.

16. Huygins, C. M., H. Masins, L. Eichelberger and J. D. Wharton. Qualitative studies of prostatic secretion. I. J. Exptl. Med. 7: 543, 1939.

17. Lu, C., M.L. Meistrich, H.D. Thames. Survival of mouse testicular stem cells after gamma or neutron irradiation. Radiat. Res. 81:402-415. 1980.

18. McGrady, A. V. and J. Chakraborty. Effects of stress on the reproductive system of male rats and mice. Arch. Andrology 10: (2),95-101, 1983.

19. Oakberg. E.F. and E. Clark. Effect of dose and dose rate on radiation damage to mouse spermatogonia and oocytes as measured by cell survival. J. of Cell and Compar Phys, 58, Suppl. 1:173-182. 1961.

20. Oakberg, E.F. The effect of low radiation doses on spermatogonia and oocytes of the mouse. In: Strahlenwirkung und Milieu, Verlag Urban and Schwarzenberg, Munchen, 103-111. 19962.

21. Philpott, D. E., R. Corbett, C. Turnbill, S. Black, D. Dayhoff, J. McGourty, R. Lee, G. Harrison and L. Sovick. Retinal changes in rats flown on Cosmos 936: A cosmic-ray experiment. Avia. Space and Environ Med. 51: 556, 1980.

22. Philpott, D. E., W. Sapp, C. Williams, J. Stevenson and S. Black. The responses of testis cells to low dose x-irradiation. Elect. Microscope Soc. Am. 39:542-543, 1981.

23. Philpott, D.E., W. Sapp, C. Williams, J. Stevenson, R. Corbett, and S. Black. The response of a mixed cell population in mouse testes to X-ray and HZE irradiation. Proc Electron Micro. Soc., 41:674, 1983a.

24. Philpott, D. E., W. Sapp, C. Williams, J. Stevenson, R. Corbett and S. Black. Response of the seminiferous epithelium of the mouse exposed to low dose high energy (HZE) and electromagnetic radiation. Scan Elect. Micros., III:1345, 1983b.

25. Philpott, D.E., W. Sapp, C. Williams, J. Stevenson, S. Black and R. Corbett. Reduction of the spermatogonial population in rat testes flown on Space Lab-3. Supp. to The Physiol. 28:(6), S211, 1985a.

26. Philpott, D.E., W. Sapp, C. Williams, J. Stevenson, S. Black and R. Corbett. Long term effects of iron particles (HZE) irradiation on mouse spermatogonia. Proc. Elect. Microscope Soc. 43: 1985b.

27. Philpott, D.E., W. Sapp, C. Williams, T. Fast, J. Stevenson and S. Black. Reduction of spermatogonia and testosterone in rat testes flown on Space Lab-3. Proc. Elect. Microscope Soc. 44: 248, 1986.

28. Plakhuta-Plakutina, Galina I. State of spermatogenesis in rats flown aboard the biosatellite Cosmos-690. Avia. Space and Envir. Med. Jan. 12-15, 1977.

29. Portugalov, V. V., E. A. Savina, A. S. Kaplansky, V. I. Yakov leva, G. I. Plakhuta-Plakutina, A. S. Pankova, P. I. Katunyan, M. G. Shubich and S. A. Buvailo. Effect of space flight factors on the mammal: Experimental-morphological study. Avia. Space and Envir. Med. Aug. 813-816, 1976.

30. Sapp, W., D. E. Philpott, C. S. Williams, K. Kato, J. Stevenson and L. V. Serova. Preliminary report of a comparative study of seminiferous tubular epithelium from rats flown on Cosmos 1887 and SL-3. Proc. Elec. Soc. Am. 46:276, 1988.

31. Selye, H., "Stress." Acta Inc. Med. Publ., Montreal, 1950.

32. Van Alphen, A.A.A., H. J. G. Van De Kant and D. G. De Rooij. Depletion of the spermatogonia from the seminiferous epithelium of the Rhesus monkey after X-irradiation. Rad. Res. 113:473-486, 1988.

33. Whithers, H.R., N. Hunter, H.T. Barkley Jr., B.O. Reid. Radiation survival and regeneration characteristics of spermatogenic stem cells of mouse testis. Radiat. Res. 57:88-103. 1974.

34. Zemjanis, R., Gondows, B., Adey, W. R., and Crokett, A.T.K. Testicular degeneration in Macaca nemistrina induced by immobilization. Fertility Sterility 21: 335, 1970.

TABLE 1. TOTAL SURVIVING SPERMATOGONIA PER STAGE 6 SEMINIFEROUS TUBULE PROFILE[A]

Treatment Group Data	Individual Animals[B]	Mean +/- SEM[C]	SL-3[D]
Flight	37.90 +/- 0.15 38.77 +/- 0.12 39.36 +/- 0.15 39.08 +/- 0.12 38.83 +/- 0.13	38.79 +/- 0.06**	39.75 +/- 0.14
Synchronous	40.44 +/- 0.10 41.13 +/- 0.15 39.08 +/- 0.19 40.00 +/- 0.12 40.35 +/- 0.12	40.20 +/- 0.06*	N/A
Vivarium	43.15 +/- 0.17 44.36 +/- 0.13 43.58 +/- 0.16 43.55 +/- 0.20 44.12 +/- 0.17	43.75 +/- 0.07	42.71 +/- 0.17

[A] Tubules identified according to Huckins (Anat. Rec. 190:905, 1978), cross section only.
[B] 200 tubules counted per animal; mean +/- Standard Error.
[C] 5 animals per treatment; total = 1000 tubules counted.
[D] SL-3 data shown here for comparison, see Philpott et al., EMSA 44:248, 1986). Mean +/- Standard Error, 200 tubules scored.

* Significantly different from vivarium control, P<0.001.
** Significantly different from vivarium control, P<0.0005.

TABLE 2. SERUM TESTOSTERONE (Cosmos-1887) ng/ml

Animal	Flight	Basal	Vivarium	Synchronous
6	0.18	4.50	2.50	0.62
7	0.18	4.20	1.20	3.50
8	0.62	3.40	0.43	0.85
9	0.10	2.40	0.43	1.85
10	0.62	2.00	0.24	0.77
Mean	0.34	3.30	0.97	1.52
SD	0.26	1.09	0.93	1.21
SE	0.12	0.49	0.42	0.54

	t	p
Basal vs Flight	5.91	<0.001
Basal vs Syn	2.45	< 0.05
Basal vs Viv	3.64	< 0.01
Flight vs Syn	2.13	N S
Flight vs Viv	1.46	N S
Syn vs Viv	0.80	N S

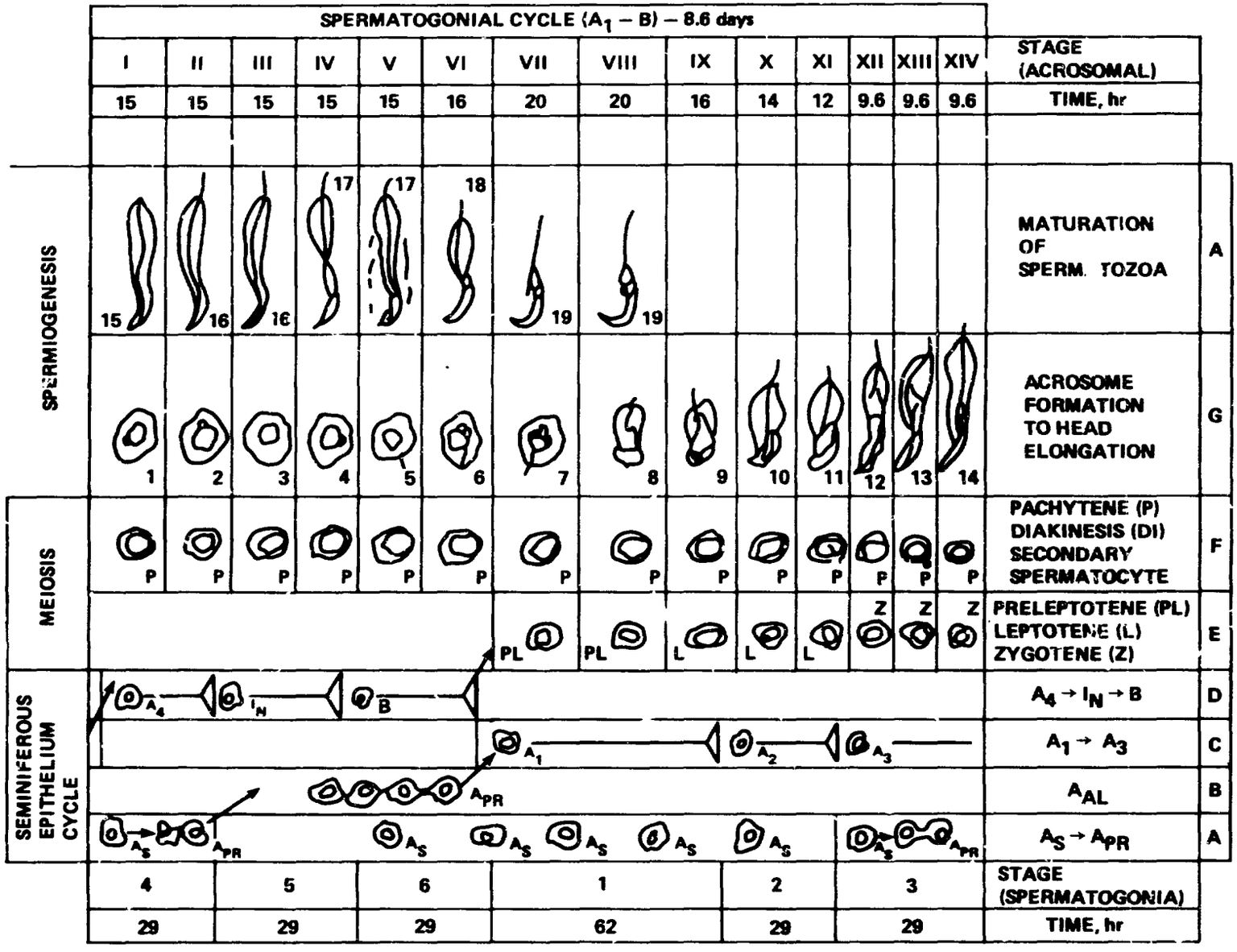

Figure 1. Schematic, showing how mature sperm develop after division of the stem cells. The spermatogonial population is counted in stage six.

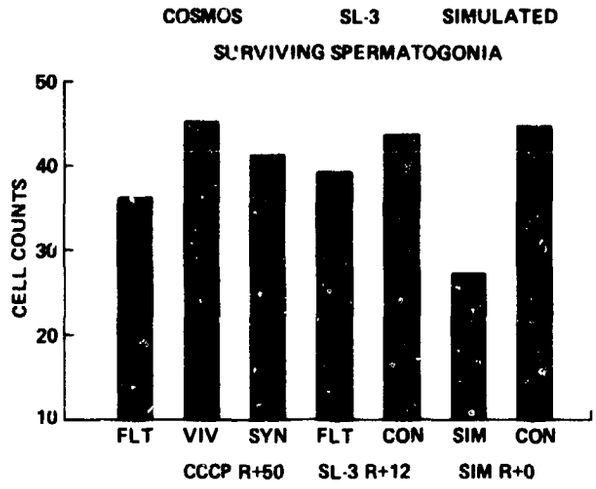

Figure 2. Preliminary comparison of volume density counts from Cosmos 1887, SL-3 and a 7 day suspension study (R + 0).

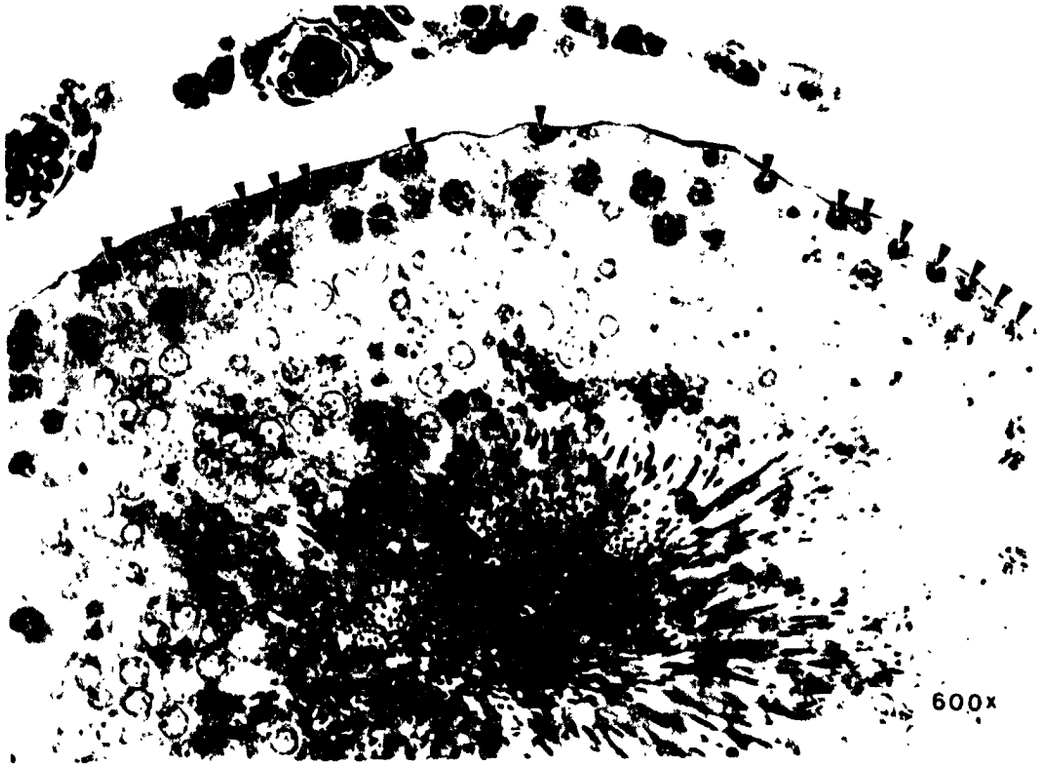

Figure 3 (a) Vivarium control. Arrows indicate spermatogonia, 600X.

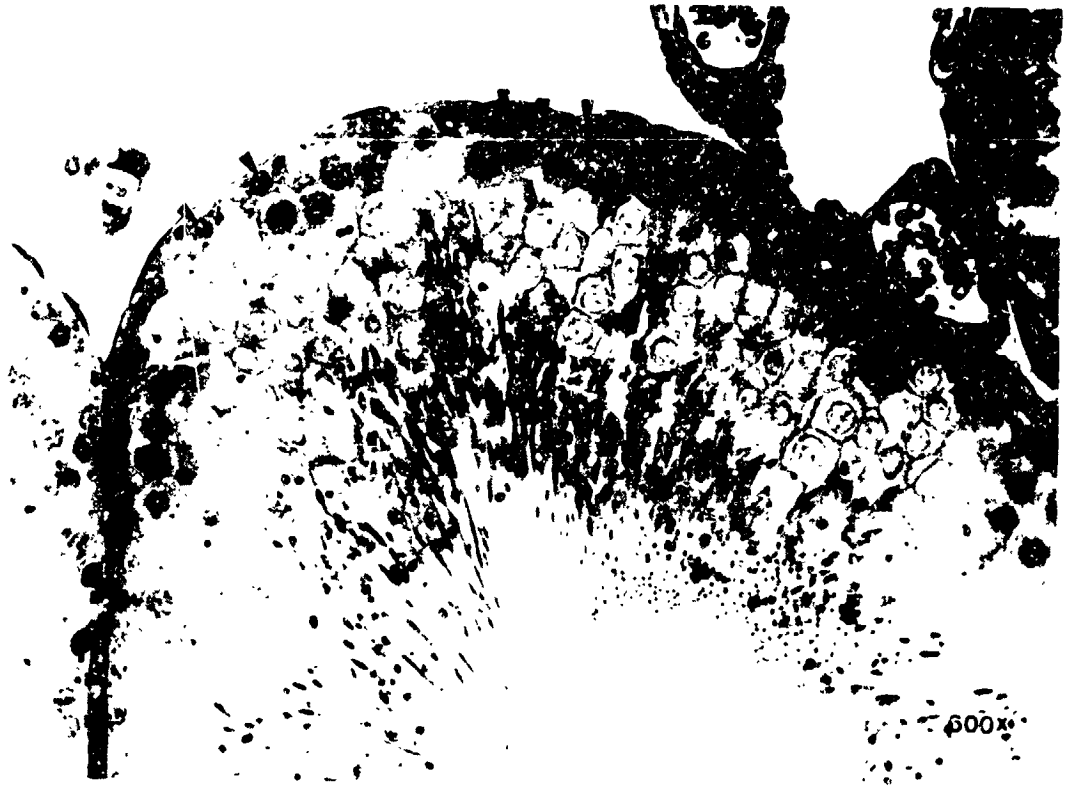

Figure 3 Continued. (b) Synchronous control. Arrows indicate spermatogonia, 600X.

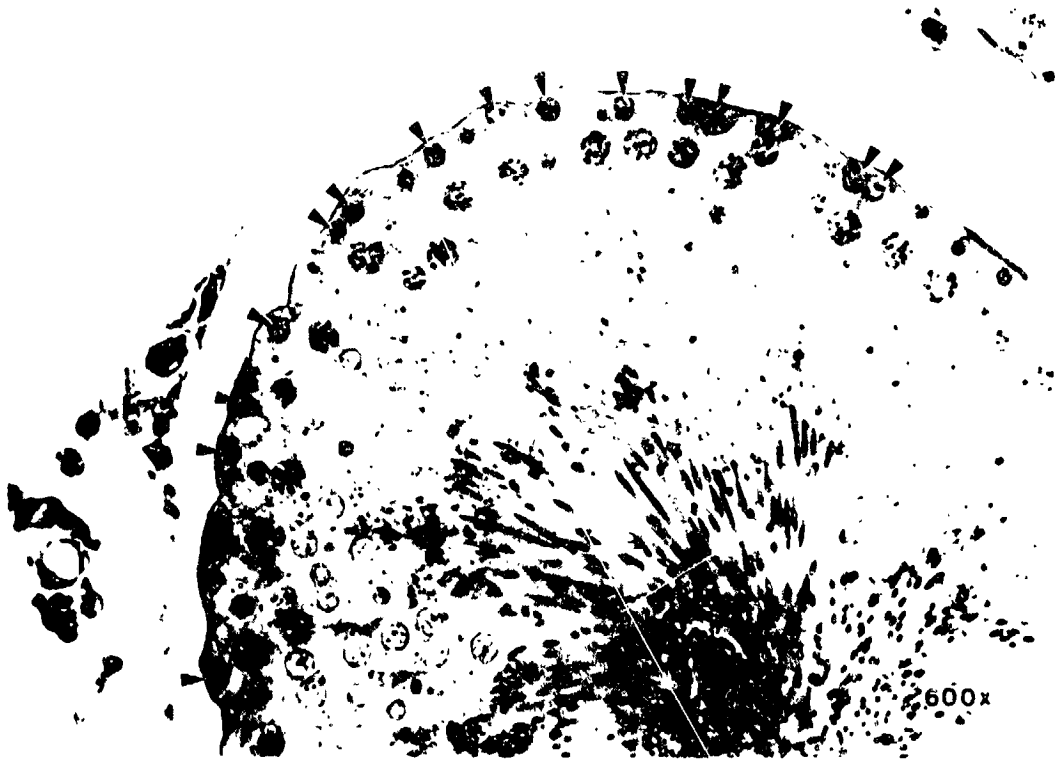

Figure 3 Continued. (c) Cosmos 1887 flight. Arrows indicate spermatogonia, 600X.

Figure 3 Concluded. (d) Cosmos 1887 flight. Abnormal tubule profiles noted in one animal. Testes weight in this animal was two-thirds of the other flight, 600X.

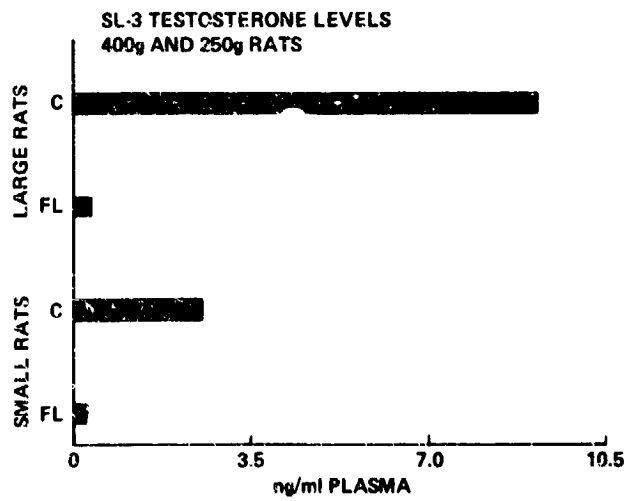

Figure 4. SL-3 testosterone levels.

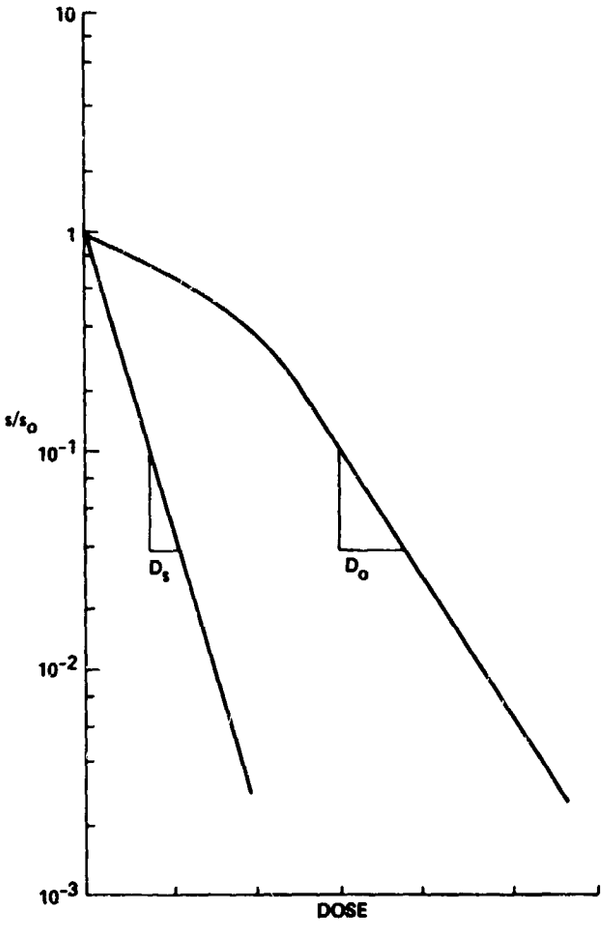

Figure 5. Representative dose response curves for spermatogonial survival after X-rays (curved line) and high energy particles (HZE) (straight line). The curved line plotted from the response to X-rays demonstrates that repair is taking place in the low dose range. The straight line (HZE particles) signifies no repair. Note that the curves show response at very low doses.

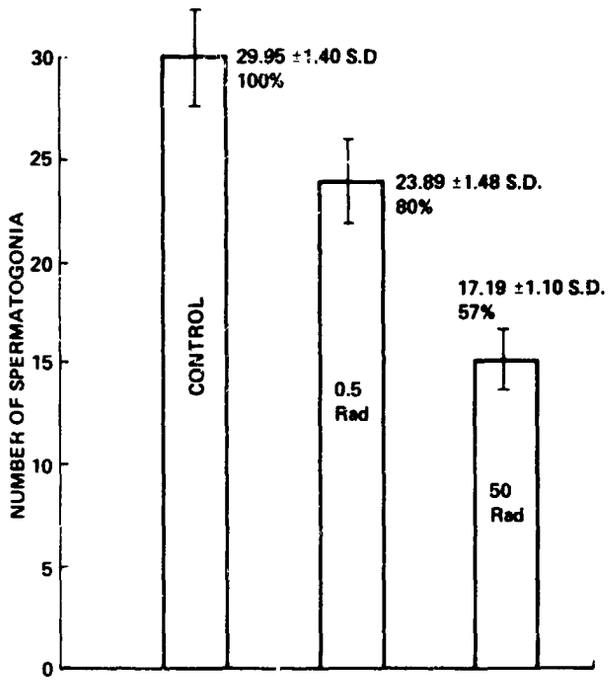

Figure 6. Spermatogonial cell counts six months after 0.5r and 50r of iron particles. Note how long suppression of counts remains after HZE irradiation.

N90-26470

EXPERIMENT K-6-17

STRUCTURAL CHANGES AND CELL TURNOVER IN THE RAT'S SMALL INTESTINE INDUCED BY SPACEFLIGHT

Principal Investigator:

R.W. Phillips
College of Veterinary Medicine and Biomedical Sciences
Colorado State University
Fort Collins, Colorado 80523

Co-Investigators:

H. R. Sawyer
Colorado State University
Fort Collins, Colorado 80523

K.V. Smirnov
Institute of Biomedical Problems
Moscow, USSR

INTRODUCTION

The purpose of this project was to test the hypothesis that the generalized, whole body decrease in synthetic activity associated with microgravity conditions of space flight as evidenced by negative nitrogen balance and muscle atrophy (Nicogossian and Parker, 1982; Oganov, 1981), as well as inhibited lymphocyte proliferation (Bechler and Cogoli, 1986), would be evident in cells characterized by a rapid rate of turnover. As a model we chose to study the turnover of mucosal cells lining the jejunum of the small intestine, since these cells are among the most rapidly proliferating in the body. Under normal conditions, epithelial cells that line the small intestine are continually produced in the crypts of Lieberkuhn. These cells migrate out of the crypts onto intestinal villi, are progressively "pushed up" the villus as new crypt cells are formed, and ultimately reach the tip of villi where they are then desquamated. In rats, the entire process, from initial proliferation in crypts to desquamation, takes approximately 2 days (Cairnie et al., 1965; Lipkin, 1973). In this study, we determined the mitotic index for mucosal cells lining the proximal, middle, and distal regions of the jejunum in rats from three treatment groups (synchronous control, vivarium control and flight), and measured the depth of the crypts of Lieberkuhn and the length of villi present in each of the three jejunal regions sampled.

MATERIALS AND METHODS

Tissue Samples

Tissue samples (1 cm in length) representing the proximal, middle and distal regions of the jejunum from each of 5 rats from the synchronous, vivarium and flight groups were processed and shipped to Colorado State University per pre- and post-flight protocols described for Cosmos 1887 Experiment K-6-17. Briefly, jejunal regions of interest were removed and flushed with 1 to 2 ml of physiological saline. Immediately thereafter each sample was flushed with 2 ml of a solution of 4% glutaraldehyde-0.1M cacodylate (pH 7.4) containing 5% sucrose and placed into 25 ml screw-top vials containing approximately 20 mls of the same fixative. After 6 - 24 hr of fixation, the samples were rinsed 3 times in 0.1 M cacodylate buffer and shipped to Colorado State University. Upon arrival, each sample was cut into 4 equal segments, post-fixed in 1% osmium tetroxide for 90 min, washed in cacodylate buffer, dehydrated in a graded series of ethanols and embedded in Polybed 812.

Mitotic Index

Sections 1 μm-thick were cut from each of the four segments from each of the three jejunal regions per animal and stained with toluidine blue. To accurately determine the mitotic index for each region, at least 2000 cells per region per animal were examined. Since mitosis is restricted to the crypts of Lieberkuhn (Lipkin, 1973), cells outside the crypts proper were not considered in determining mitotic indices. Prior to evaluation all slides were coded so that the technician reading the slides did not know the region or treatment group being examined.

Villus Length and Crypt Depth

To determine villus length and crypt depth at least 25 villi and crypts were measured per region per animal. Measurements were obtained using a computerized image analysis system coupled to a bright field microscope equipped with a 40X objective and a video camera. Special care was taken to ensure that measurements were taken only on villi and crypts that had been cut in cross-section.

Statistics

All data were statistically analyzed by analysis of variance and differences between means were detected using the Student-Newman-Keuls procedure.

RESULTS

Data obtained regarding the mitotic indices for the three jejunal regions in each treatment group (i.e., synchronous, vivarium and flight) are summarized in Table 1. In the vivarium group the number of mitotic figures was consistently lower in the middle and distal jejunal regions when compared to the same regions in the synchronous control and flight groups. In the proximal jejunum the flight group had more mitotic figures than either of the control groups. There was no significant variation in the mitotic indices among the three different anatomical regions examined in the animals included in the vivarium and flight groups. In contrast, animals in the synchronous control group had more mitotic figures in the middle jejunum region.

When the data were analyzed by jejunal region among treatment groups several differences were noted (Table 1). The number of mitotic figures observed in the proximal jejunum of the flight animals was higher compared to either the synchronous or vivarium animals. Conversely, in the middle and distal jejunum, both the synchronous controls and flight animals had an increased number of mitotic figures compared to vivarium.

As summarized in Table 2, the height of jejunal villi in flight animals was not significantly different from that observed in animals included in the synchronous and vivarium groups. Although there was a progressive and significant decrease in the height of villi from the proximal to distal region of the jejunum in both the flight and synchronous animals, no significant differences were detected among the jejunal regions examined in animals included in the vivarium group. This was due to the high degree of variability in measurements obtained for the respective jejunal regions in the vivarium group.

Irrespective of treatment group, the depth of crypts tended to be greater in the proximal jejunal region than in the middle or distal regions (Table 3). However, statistically significant differences were detected only in the flight and synchronous groups. With respect to region by treatment interactions, the only marked difference was that the crypt depth in the proximal jejunal region in the flight animals was less than that measured in the synchronous animals.

DISCUSSION

Although some statistical differences were noted in number of mitotic figures among treatment groups and jejunal regions examined, no clear pattern of change was evident when flight animals were compared to both synchronous and vivarium control groups. This is not surprising given the length of time from return to earth, and ultimate recovery and tissue collection (i.e. approximately 50 hours). Since the average life-span of intestinal epithelial cells in rats is slightly less than 2 days (Cairnie et al., 1965; Lipkin, 1973), very few, if any, of the cells present in the small intestine at the time of recovery would have been generated during flight.

Since no consistent differences were detected in the mitotic index of jejunal mucosal cells in the flight group compared to the synchronous and vivarium control groups, it is not surprising that no consistent differences were detected in the length of villi or crypt depths. Although some regional differences in villus height and crypt depth were noted, such differences appear to be normal and cannot be attributed to treatment effects.

SUMMARY AND CONCLUSIONS

The mitotic indices, villus heights and crypt depths were determined in each of three jejunal regions (proximal, middle and distal) for five animals each in the flight, vivarium and synchronous groups. Because of the rapid turnover of intestinal mucosal cells, and due to the delay in recovering the flight animals, it is not known if cell turnover is affected by microgravity conditions associated with space flight. However, since there were no consistent differences between animals in the flight group and

those in the synchronous and vivarium control groups, it appears that any effects of microgravity on the turnover of jejunal mucosal cells are short-lived and rapidly return to normal. The data obtained in this study will be valuable as a comparative reference when similar tissues are collected during or more immediately after return from microgravity conditions. Thus, this study represents an initial step in determining the effects of microgravity on the proliferation and turnover of intestinal mucosal cells.

REFERENCES

1. Bechler, B. and A. Cogoli. 1986. Lymphozyten sind schwerkraftempfindlich. Naturwissenschaften 73:400403.

2. Cairnie, A.B., L.F. Lamerton and G.G. Steele. 1965. Cell proliferation studies in the intestinal epithelium of the rat. I. Determination of the kinetic parameters. Exp. Cell Res. 39:528-538.

3. Lipkin, M. 1973. Proliferation and differentiation of gastrointestinal cells. Physiol. Rev. 53:891-915.

4. Nicogossian, A.E. and J.F. Parker, Jr. 1982. Space physiology and medicine. NASA SP-447. Washington, D.C. National Aeronautics and Space Administration. 324 p

5. Oganov, V.S. 1981. Results of biosatellite studies of gravity-dependent changes in the musculo-skeletal system of mammals. Physiologist 24 (Suppl.):S55-S58.

TABLE 1. MITOTIC INDEX FOR JEJUNAL MUCOSA CELLS

TREATMENT GROUPS (N=5 ANIMALS/GROUP)

REGIONS	SYNCHRONOUS	VIVARIUM	FLIGHT
PROXIMAL	$2.9 \pm .2^{A,a}$	$2.8 \pm .2^{a}$	$3.7 \pm .2^{b}$
MIDDLE	$3.9 \pm .3^{B,a}$	$2.7 \pm .1^{b}$	$3.4 \pm .1^{a}$
DISTAL	$3.3 \pm .4^{A,a}$	$2.7 \pm .3^{b}$	$3.2 \pm .2^{a}$

*Means (± SEM) with different lower case letter superscripts within rows are different ($p < .05$).

**Means (± SEM) with different with upper case letter superscripts within columns are different ($p < .05$).

TABLE 2. LENGTH (μm) OF JEJUNAL VILLI

TREATMENT GROUPS (N=5 ANIMALS/GROUP)

REGIONS	SYNCHRONOUS	VIVARIUM	FLIGHT
PROXIMAL	557 ± 24^{A}	556 ± 89	600 ± 29^{A}
MIDDLE	486 ± 8^{B}	510 ± 40	497 ± 23^{B}
DISTAL	296 ± 9^{C}	376 ± 78	317 ± 17^{C}

*Means (±SEM) with different upper case letter superscripts within columns are different ($P < .05$).

TABLE 3. JEJUNAL CRYPT DEPTHS (μm)

TREATMENT GROUPS (N=5 ANIMALS/GROUP)

REGIONS	SYNCHRONOUS	VIVARIUM	FLIGHT
PROXIMAL	$176 \pm 8^{A,a}$	160 ± 8^{b}	$148 \pm 3^{A,b}$
MIDDLE	139 ± 6^{B}	137 ± 4	128 ± 2^{B}
DISTAL	120 ± 3^{B}	141 ± 10	123 ± 4^{B}

*Means (±SEM) with different lower case letter superscripts within rows are different ($P < .05$).

**Means (±SEM) with different upper case letter superscripts within columns are different ($P < .05$).

N90-26471

EXPERIMENT K-6-18

STUDY OF MUSCARINIC AND GABA (BENZODIAZEPINE) RECEPTORS IN THE SENSORY-MOTOR CORTEX, HIPPOCAMPUS AND SPINAL CORD

Principal Investigator:

N. Daunton
NASA Ames Research Center
Moffett Field, Califonria 94035

Co-Investigators:

F. D'Amelio
NASA Ames Research Center
Moffett Field, California 94035

I. Krasnov
Institute of Biomedical Problems
Moscow, USSR

PRECEDING PAGE BLANK NOT FILMED

INTRODUCTION

Frontal lobe samples of rat brains flown aboard Cosmos 1887 were processed for the study of muscarinic (cholinergic) and GABA (benzodiazepine) receptors and for immunocytochemical localization of the neurotransmitter gamma-aminobutyric acid (GABA) and glial fibrillary acidic protein (GFAP).

MATERIAL AND METHODS

Receptor binding studies

a) Tissue preparation

Brain fragments were placed in a microtome chuck in a cryostat kept at -15 deg. C and surrounded with phosphate buffer 0.1M. Sections were cut at 20 µm, placed on gelatinized slides and thawed by warming the back of the slides with palm of hand. The slides were then transferred to slide boxes and kept at 0 deg. C for at least two hours to allow them to dry.

b) Radioligand binding experiment

The slides were incubated with ^{3}H-ligand, followed by washes. To allow for the determination of specific binding a slide was incubated with a displacing amount of drug ("blank" slide). The incubation mixture consisted of 40 ml buffer, 5 ml ^{3}H-ligand, and 5 ml buffer (for total binding) or drug (for "blank"). The concentrations of ^{3}H-ligand and drug are given below since they vary according to the receptor to be studied.

The incubation procedure was performed in Coplin jars (50 ml capacity) and the washes in staining trays (250 ml capacity) with slides transferred in glass racks. After the last wash the slides were dipped in distilled water and then air dried. They were subsequently stored in a slide box with dessicant at 4 deg. C for 24 hours prior to autoradiographic exposure.

Receptor localization studies were as follows:

(1) Muscarinic (cholinergic)

Incubation: 1nM [^{3}H]-1-quinuclidinyl benzilate ([^{3}H]-QNB) for 2 hours, room temperature.

Blank: 1 µM atrophine

Washes: two 5-minute washes in ice cold buffer.

Buffer: phosphate buffer saline (PBS) at pH 7.4

Exposure: 1 month at 4 deg. C (see below for details)

(2) GABA (benzodiazepine)

Incubation: 1nM [^{3}H]-flunitrazepam for 40 minutes in ice cold buffer

Blank: 1 µM clonazepam

Washes: 10 minutes in ice cold buffer.

Buffer: 0.17M Tris, pH 7.4

Exposure: 1 month at 4 deg. C (see below for details)

c) Autoradiography

The dried labelled slides were arranged on a thin sheet of cardboard and fixed to the surface with double-stick paper. They were placed in x-ray cassette, tritium sensitive film (^{3}H-Ultrafilm LKB, Gaithersburg, M.D.) was placed over slides (emulsion side facing slides) and the cassette closed. This procedure was done in total darkness.

After the period of exposure the film was developed with Kodak D-19 developer under sodium safe-light for 5 minutes at 20 deg. C and fixed with full strength rapid fix.

Immunocytochemistry of gamma-aminobutyric acid (GABA) and glial fibrillary acidic protein (GFAP).

1. GABA

a) Tissue preparation

Tissue sections slide-mounted adjacent to those used for receptor binding studies were fixed for two hours in 5% glutaraldehyde in 0.1M phosphate buffer at 4 deg. C. After fixation the slides were thoroughly rinsed in cold phosphate buffer saline (PBS).

b) Immunocytochemical procedure

The ABC method was used. The slides were incubated as follows:

(1) 2% normal goat serum in PBS for one hour, room temperature

(2) GABA antiserum conjugated to bovine serum albumin (Immunonuclear Corp.) diluted 1/4000 in PBS, overnight at 4 deg. C.

(3) Biotinylated goat anti-rabbit IgG (Vector Labs.) for one hour, room temperature

(4) Vectastain reagent (Vector Labs.) for one hour, room temperature.

(5) Reaction at room temperature, with 25 mg. diaminobenzidine tetrahydrochloride in 50 ml tris buffer saline (TBS)+5 µl 30% hydrogen peroxide 5-15 minutes, to develop reaction product.

(6) Final rinse of the sections in TBS, two changes x 10 minutes, room temperature.

Between steps the sections were rinsed with cold PBS, three changes x 10 minutes.

Some sections were dehydrated and mounted and others were counterstained with Cresyl violet, dehydrated and mounted. Omission of the primary antibody was employed as control.

2. GFAP

a) Tissue preparation

The slide-mounted sections wer fixed for 15 minutes in 4% paraformaldehyde in 0.1M phosphate buffer. After fixation the slides were rinsed in cold PBS for 30 minutes.

b) Immunocytochemical procedure.

The peroxidase-antiperoxidase (PAP) method was employed. Incubation proceeded as follows:

(1) 10% normal swine serum in PBS, 30 minutes, room temperature.

(2) GFAP antiserum (Dr. Lawrence Eng, Veterans Administration, Palo Alto) diluted 1/100 in PBS, one hour, room temperature.

(3) Swine anti-rabbit IgG diluted 1/100 in PBS, 30 minutes, room temperature.

(4) PAP diluted 1/200 in PBS, 30 minutes, room temperature.

(5) Sections reacted with 12.5 mg diaminobenzidine tetrahydrochloride in 50 ml tris buffer saline (TBS) + 5µl 30% hydrogen peroxide, 5-15 minutes.

(6) Rinse of the sections in TBS, two changes x 10 minutes, room temperature.

Between steps the slides were rinsed with cold PBS, three changes x 10 minutes.

The sections were subsequently counterstained with hematoxiline for 2 minutes, dehydrated and mounted. Normal rabbit serum was employed as control instead of the primary antibody.

RESULTS

Although radioactive labeling of both muscarinic cholinergic and GABA (benzodiazepine) receptors proved to be successful with the techniques employed, distinct receptor localization of individual laminae of the frontal neocortex was not possible since the sampling of the area was different in the various groups of animals (Fig.1). In spite of efforts made for proper orientation and regional identification of laminae it was found that a densitometric (quantitation of autoradiograms) analysis of the tissue did not contribute to the final interpretation of the effects of weightlessness on these receptors.

As to the immunocytochemical studies the use of both markers, GFAP and GABA antiserum, confirmed the suitability of the techniques (Fig.2) for use in frozen material. However, similar problems to those encountered in the receptor studies prevented an adequate interpretation of the effects of micro-G exposure on the localization and distribution of GABA and GFAP.

This study did, however, confirm the feasibility of investigating neurotransmitters and their receptors in future space flight experiments.

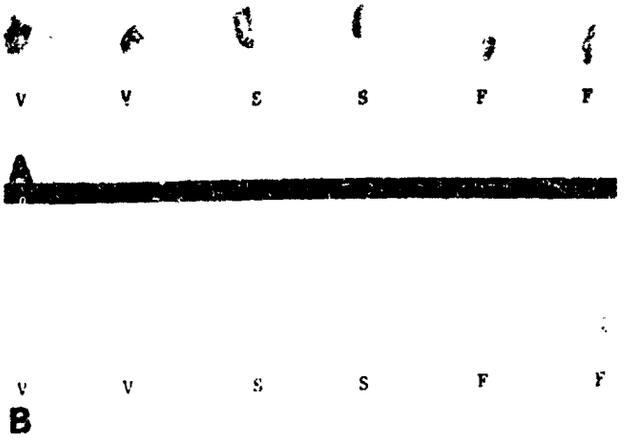

Figure 1: Autoradiograms for muscarinic cholinergic ([^{3}H]-QNB) (A) and GABA (benzodiazepine) (B) receptors of frontal cerebral cortex. Notice the difference in size and orientation of samples. V, vivarium; S, synchronous, F, flight.

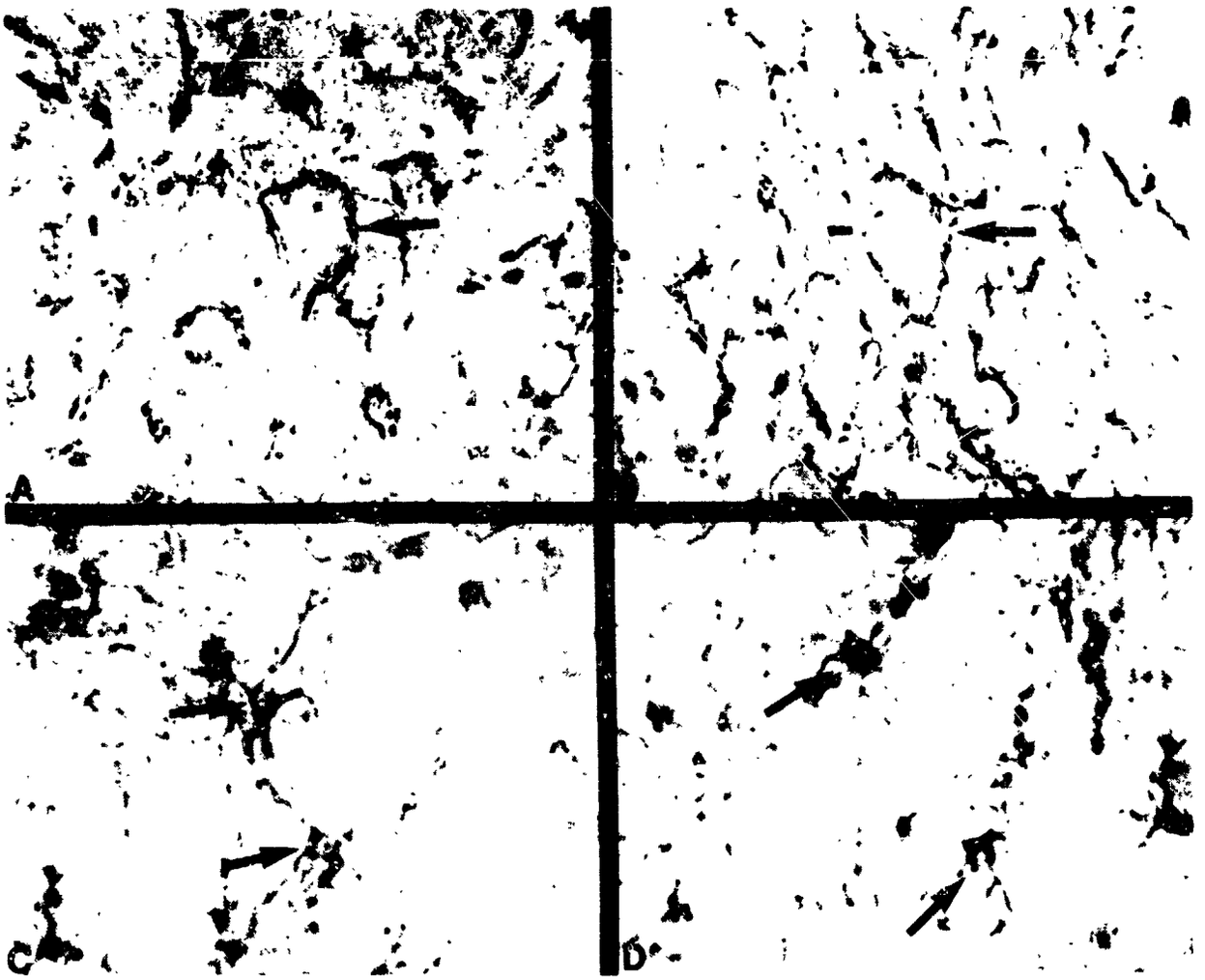

Figure 2: In (A) and (B) GABAergic boutons are seen surrounding pyramidal cells (arrows). The tissue shows some artifactual modifications due to the freezing process. (A), fligh. animal; (B), synchronous control. In (C) and (D) GFAP immunoreactive astrocytes (arrows) are seen in the boundaries between white and grey matter of the frontal cerebral cortex. (C), flight animal; (B), vivarium control.

N90-26172

EXPERIMENT K-6-19

PINEAL PHYSIOLOGY IN MICROGRAVITY: RELATION TO RAT GONADAL FUNCTION

Principal Investigator:

D. Holley
Department of Biological Sciences
San Jose State University
San Jose, California 95192

Co-Investigators:

M.R.I. Soliman
College of Pharmacy and Pharmaceutical Sciences
Florida A & M University
Tallahassee, Florida 32307

F. Kaddis
College of Pharmacy and Pharmaceutical Sciences
Florida A & M University
Tallahassee, Florida 32307

C. Markley
Department of Biological Sciences
San Jose State University
San Jose, California 95192

I. Krasnov
Institute of Biomedical Problems
Moscow, USSR

INTRODUCTION

Relative to other endocrine organs, research on the physiology of the pineal has been a rather recent endeavor, and discoveries relative to pineal physiology have proceeded rather slowly. Considerable advances in this area have occurred over the past two decades and many textbooks are now espousing it as a true endocrine gland (Hadley, 1988). It is now known that the pineal organ can interact with many endocrine and nonendocrine tissues in a regulatory fashion. It is well established that an antigonadal hormone of pineal origin (most likely the indoleamine melatonin) is involved in the photoperiodic regulation of reproduction in seasonally breeding mammalian species, and some nonseasonal breeding species (possibly also humans). Recent reviews implicate the pineal in the functioning of other organs and systems besides those involved in reproduction including: temperature regulation, thyroid, growth hormone, adrenal glucocorticoid synthesis, behavior (arousal/depression), circadian system (activity/rest), and skin pigmentation (in lower animals). Several excellent journal reviews and books on pineal physiology have appeared over the past ten years (see Reiter, 1981a; Reiter, 1981b; Vollrath, 1981; Reiter, 1982; Binkley, 1983; Axelrod, et al. 1983; Preslock, 1984; Reiter, 1984; Brown and Wainwright, 1985; O'Brien and Klein, 1986). In view of the fact that the pineal is an important link to the environment (Reiter, 1986), it is conceivable that exposure to microgravity and spaceflight might alter the function of this gland and, in turn, affect various physiological functions including the circadian timing system and reproduction.

Primary control of pineal function is mediated by the photoenvironment. Light impinging upon the retina influences the pineal via the following pathway: retino-hypothalamic tract, suprachiasmatic nuclei, median forebrain bundle, superior cervical ganglia, sympathetic efferents. Adrenergic receptor activation results in stimulation of N-Acetyltransferase (NAT) activity with resulting production of melatonin from the precursor serotonin (5- hydroxytryptamine, 5-HT). Indeed, the serotonin concentration of the pineal gland exceeds that of any other organ and is fifty times that of any other brain area (Quay, 1963). Melatonin is probably the most important pineal secretory product in terms of distant regulatory responses (e.g. antigonadal effects). However, several other non-indole hormones are reputed to be synthesized there, (e.g., arginine vasotocin, oxytocin, arginine vasopressin, an alpha-MSH like peptide, GnRh, TRH, renin, and angiotensin I). The pineal melatonin content fluctuates with a pronounced circadian rhythm (amplitude of about 20-plus orders of magnitude) and it is rapidly inhibited when the animal is exposed to light. Wurtman and Ozaki (1978) suggested that the availability of serotonin may be involved in regulating the synthesis of melatonin in the pineal. Chan and Ebadi (1980) provided evidence that under certain experimental conditions serotonin may inhibit the activity of NAT, a key enzyme in the synthesis of melatonin. Serotonin also exhibits circadian rhythmicity (amplitude of approximately 2-3 orders of magnitude) and this rhythm persists even in blinded weanling rats. Given its key role in the regulation of melatonin synthesis, its high concentration, and that its levels may persist longer than the more rapidly changing melatonin, we felt that serotonin might give a more accurate assessment of the effects of microgravity on pineal function following recovery of the animals from the flight. We also measured 5- hydroxyindole acetic acid (5-HIAA), a major metabolite of serotonin, hoping that we might be able to assess an effect on serotonin metabolism (turnover).

One of the most interesting concomitants to spaceflight and exposure to microgravity has been the disturbing alteration in calcium metabolism and resulting skeletal effects. It was recognized as early as 1685 (cited in Kitay and Altschule, 1954) that the pineal of humans calcified with age. However, little can be found in the literature relating calcification and pineal function. Given the link between exposure to microgravity and perturbation of calcium metabolism and the fact that the pineal is apparently one of the only "soft tissues" to calcify, we examined pineal calcium content following the spaceflight.

MATERIALS AND METHODS

Cosmos 1887 animal groups

a) Flight animals.

Pineals were obtained from 5 (#6-#10) of the 10 male rats (Czechoslovakian- Wistar, origin Institute of Endocrinology, Brattislava, Czechoslovakia) that were flown aboard the Soviet Biosatellite Cosmos 1887. The flight launched 9/29/87 at 15:50 and landed 10/12/87 at 07:03 (Moscow time). The orbital inclination was 62.8 degrees and the apogee and perigee were 406 and 224 kilometers, respectively. Fourteen gram boluses of food (total 55 g/ rat/ day) were provided at 02:00, 08:00, 14:00, and 20:00 hrs. each day. Water was provided ad libitum. The air pressure in the cage was 760 mmHg, the humidity averaged 58%, and the ambient temperature was 22-23 degrees C. Lights were on from 08:00-24:00, and off from 24:00-08:00. Light intensity was 4-8 lux at the cage floor and was provided by an incandescent lamp placed over each feeder. Due to problems related to the recovery of the biosatellite once it had landed, the final sacrifice and dissection occurred on the morning of 10/14/87, approximately 49 hours after the re-entry landing. The animals were last fed in flight at 02:00 hrs. on 10/12/87, and were not fed again until in the animal quarters at the recovery/dissection site at 20:00 hrs on 10/13/87 when they received a half day portion of food (28 g/ each).They were, therefore, without food for approximately 42 hours. Given the logistics of the recovery and the fact that the lights were turned on in the satellite at 05:00 hrs. on 10/12/87 in preparation for the landing, the light cycle was not constant. From data provided regarding the post flight recovery it is apparent that the animals experienced about a 3-5 hour phase advance and were subjected to a 36 hour day (20 hours darkness : 16 hours light) upon landing.

b) Basal control animals.

They were put into flight-type cages and had a flight (paste) diet for 14 days before sacrifice on 09/24/87. Temperature, humidity, and lighting were similar to in-flight conditions.

c) Synchronous control animals.

These rats were maintained in flight-type cages on a flight (paste) diet. They were exposed to the launch G forces and vibration, deprived of food for 42 hrs. and exposed to the same lighting regimen and temperature as flight rats after landing. After their "simulated flight" sacrifice was delayed the same period as for flight rats. The re-entry G force and post flight transportation conditions of the flight animals were not mimicked for the synchronous controls.

d) Vivarium control animals.

These animals were kept in cages of the same size as the flight cages with environmental conditions similar to those in flight. They were fed the same quantity of food per day (55 g) but in only one feeding. On the night prior to sacrifice, food was withdrawn from these animals at 20:00 hrs. Post flight conditions (e.g. temperature) were not mimicked for this group.

Sample collection and initial tissue extraction step.

Upon dissection the pineals were immediately placed in prechilled cryovials (10 x 55 mm), placed into liquid nitrogen for quick-freeze, and shipped to Moscow in a liquid nitrogen biotransporter. The samples were shipped to the U.S.A. and stored until analysis at -70 degrees C. Trunk blood was collected immediately following decapitation into heparinized tubes and centrifuged at 4 degrees C. Plasma (1.5 ml) was rapidly frozen in liquid nitrogen and shipped to the U.S.A. in a

biotransporter. In the U.S.A. this volume was thawed and aliquoted (100 µl) for distribution to various investigators.

The pineal glands were thawed at room temperature, weighed, and homogenized in 200 µl of perchloric acid. 100 µl of the crude homogenate was frozen and saved for the calcium analysis. The remaining aliquots (100 µl) were immediately used for the HPLC analysis of 5-HT and 5-HIAA.

HPLC analysis of pineal serotonin, 5-HIAA, and plasma.

Aliquots (100 µl) of the crude pineal homogenate were centrifuged using Centrex brand microfilters (0.45 um pore size, Schleicher and Schuell, Inc., Keene, New Hampshire, U.S.A.). Homovanillyl alcohol was added to the homogenates to act as an internal standard at a final concentration of 10^{-6}M. Serotonin and 5-HIAA were analyzed in the filtered homogenates by HPLC using a modification of the method of Medfford and Barchas (1980). The filtered homogenates were injected into a u-Bondapack brand C-18 reverse phase column of a high pressure liquid chromatograph (Bioanalytical Systems, Inc.). The mobile phase consisting of 0.1 M sodium acetate, 0.1 M citric acid and 25% v/v methanol (pH 4.1) was run through the column at a flow rate of 1.0 ml/min. The various peaks were detected using an electrochemical detector (Bioanalytical Systems, Inc.) mounted with a glassy carbon working electrode and Ag/AgCl reference electrode set at an oxidation potential of 0.85 V and sensitivity of 10 nAmps/V. Peaks were integrated and analyzed using a Bioanalytical Systems, Inc. workstation mini-computer.

For analysis of plasma 20 µl of 1.0 M perchloric acid was added to 100 µl of plasma. The mixture was filtered using micro-filter centrifuge tubes (Centrex brand, see above). The filtrate (20 µl) was injected onto the HPLC column as above.

Radioimmunoassay of pineal melatonin content.

The melatonin content of the pineal homogenates (75 µl aliquots) were determined by radioimmunoassay using "ultraspecific" melatonin antiserum and a procedure provided by Dr. G. Brown (CIDtech Research, Inc., Ontario, Canada) using ^{3}H-melatonin (Amersham Corp., Arlington Heights, IL, U.S.A.). The melatonin for standard was obtained from Sigma Chemical Co., St. Louis, MO, U.S.A. (cat, #M5250). The assay performance characteristics in our laboratory were: sensitivity (defined as three standard deviations from the counts for the zero reference standard tube), 5 pg/ml; interassay coefficient of variation, 11.5%; and intraassay coefficient of variation, 6.27%.

Atomic absorption analysis of pineal calcium content.

Total calcium content of the pineal homogenates was determined by atomic absorption spectrophotometry using an electrothermal atomizer equipped with a carbon rod. Aliquots (5 µl) of the homogenates were diluted with ultra-pure water (7 mohm resistance, Multi-Q Water System, Millipore, Corp., Bedford, MA, U.S.A.). Volume added was 200 or 250 µl to achieve absorbance values in the range 0.1-0.5 absorbance units. Calcium reference standard was obtained from VWR, Inc., San Francisco, CA, U.S.A. (cat. #EM-CX0082-1). Assay sensitivity was approximately 4 pg/µl.

Statistical analysis.

Given the experimental design, the groups were analyzed by one-way analysis of variance (ANOVA). If the ANOVA indicated a between group difference ($p < 0.05$), then the data were

further analyzed by one or more of the following statistical tests: Duncan's Multiple Range Test, Newman-Keul's Multiple Comparison Test, or Fisher's Least Significant Difference Test. In certain instances, Student's t-test for nonpaired samples was applied. The 95% confidence limit was considered significant in all tests.

RESULTS

The results of this study are summarized in Tables 1-3 and Figures 1-6.

A) Organ weights.

The data (Table 1) indicate that the flight rats were significantly smaller than the vivarium and synchronous control animals ($p < 0.01$). Due to this difference, testes and adrenal weights were normalized to percent of the body weight for group comparisons. Though the average testes weight of the flight group was less than the other two groups ($p < 0.01$ vs. vivarium), when normalized to percent body weight the differences were not significant. The pineal weights among the groups were also not significantly different. Adrenals of the flight group, however, were significantly enlarged when compared to the vivarium, synchronous and basal controls ($p < 0.001$), even for the normalized data. The adrenal enlargement is consistent with chronic exposure to one or more environmental stressors. It should be noted, however, that at time of sacrifice there was no statistical difference in the plasma corticosterone concentrations: Flight = 15.06±9.31 S.D.; Synchronous = 10.92±5.05; Vivarium = 22.10±13.67; Basal = 26.20±11.30 (data courtesy of Dr. R. Grindeland and Marilyn Vasques, NASA-Ames Research Center).

B) Pineal gland analysis.

Pineal melatonin content was determined for individual glands and the values normalized and reported as pg/milligram pineal tissue (see Table 2). There were no significant differences among the three test groups as determined by one-way analysis of variance. The results are summarized in Figure 1.

Serotonin (5-HT) and 5-HIAA content were also determined for individual glands and the values normalized and reported as ng/milligram pineal tissue (see Table 2). Results from two of the animals (F-9 and S-6), however, were considerably different from other values within their respective groups. Accordingly, if these values are included in a one-way analysis of variance, then there are no significant differences among the group means (see Figures 3 and 5). However, if the two values are removed from the analysis, then both flight group serotonin (5-HT) and 5-HIAA are significantly greater than controls (see Figures 4 and 6).

Table 2 summarizes the pineal calcium determinations. Two of the samples that had extremely high calcium concentrations were assumed to be contaminated, and were excluded from the analysis (V-6 and S-10). One-way analysis of variance indicated no statistical differences among the groups.

C) Plasma serotonin (5-HT), 5-HIAA and testosterone concentrations.

Table 3 indicates that the plasma testosterone concentration of the flight animals was lower than all the other groups. The difference, however, was significant only for the basal controls vs. the flight, vivarium and synchronous groups ($p < 0.01$). Note the difference between the flight versus basal group was highly significant ($p < 0.001$).

The plasma concentration of 5-HIAA in all groups was below the detectable sensitivity of the HPLC machine used in the analysis of the samples which indicates the plasma concentrations were less than 2.0 ng/ml.

Table 3 summarizes the plasma serotonin (5-HT) data. Three samples were lost in the extraction/ultrafiltration processing and were not included in the analysis (F-10, V-7, and S-7). Subsequent analysis revealed that the flight group had relatively lower plasma concentrations of 5-HT. The difference was not significant when subjected to one-way analysis of variance. However, the flight group was significantly different from the basal group when analyzed by Duncan's Range test, Fisher's LSD test and Student's t-test ($p < 0.05$). It should also be noted that the synchronous control group differed from the basal control group ($p < 0.05$, Fisher's LSD Test).

DISCUSSION

Considerable evidence supports the existence of a pineal humoral factor or factors (most likely melatonin) that can influence the hypothalamic-pituitary gonadal axis in many vertebrate species (Vollrath, 1981) including the rat (Binkley, 1983). If indeed the pineal is a major "link to the environment" (Reiter, 1986) it is, therefore, possible that gonadal function of rats flown in space might be altered via a mechanism that includes involvement of the pineal.

Several pieces of evidence indicate that gonadal function of the rats aboard the Cosmos 1887 spaceflight may have been compromised. Though the testes weights of the flight animals were lower than the synchronous and vivarium controls ($p < 0.01$), the body weights of the flight animals were also lower than the other groups (Table 1). When the testes weights were normalized as % body weight, the testes weight difference was not born-out. Plasma testosterone concentration, however, was lowest in the flight animals and was significantly lower than the basal control group ($p < 0.001$). Microscopic examination of the testes also revealed that there were 4% fewer spermatogonial cells in the flight group versus the vivarium control group ($p < 0.02$, data provided by Dr. D. Philpott).

It is known that light has a dramatic and rather immediate inhibitory effect upon rat pineal N-acetylserotonin and pineal melatonin levels (Binkley, 1983). As a result we felt that to assess pineal function we would have to measure parameters that were less labile. Green, et.al. (1977) indicated that potent stressors (e.g. electroconvulsive shocks) could alter serotonin turnover for up to 6 days post exposure. Since serotonin is an important precursor to melatonin we felt that its measurement and relative inertia with respect to relative changes in concentration might be used as an indirect indicator of melatonin synthesis. To do this, however, we felt measurement of 5-HIAA, a major serotonin metabolite, would be necessary as an indication of serotonin turnover.

As suspected, the pineal melatonin levels were very low at time of sacrifice (Table 2 and Figures 1 and 2). Given that the rats were sacrificed about 2 hours after lights on, and that the major circadian drop in circulating melatonin is locked to the time of lights on (Binkley, 1983), it is not surprising that the pineal melatonin content was low in all groups. Given the limited amount of plasma available to us for the analysis of 5-HT and 5-HIAA (100 µl), and given the low pineal melatonin levels, we did not measure the plasma melatonin concentration.

Figures 4 and 6 represent the 5-HT and 5-HIAA data after elimination of two statistical outliers. Note that exposure to the space environment resulted in a significant increase ($p < 0.05$) in the pineal levels of these substances. The pineal gland content profile was not reflected in the blood, however. Table 3 indicates that the flight and synchronous groups had low levels of 5-HT compared to the basal group ($p < 0.05$) and that all groups had undetectable levels of 5-HIAA. It is known that the plasma 5-HT levels may reflect peripheral secretion and may not be an accurate indicator of central serotonergic mechanisms. The results indicate that exposure to the space environment had an effect on the level of 5-HT and its turn-over as indicated by concomitant increase in 5-HIAA. This would be consistent with increased melatonin secretion during the spaceflight which may have been involved in the antigonadal activity noted.

It has been suggested that melatonin may be a hormone of "stress" given its increased secretion during conditions such as insulin-induced hypoglycemia (Wurtman and Moskowitz, 1977). Yet the melatonin circadian rhythm is 180 degrees out of phase with the corticosterone circadian rhythm and there is evidence for a direct inhibitory role of the pineal and melatonin on adrenal glucocorticoid synthesis (Ogle and Kitay, 1978). The adrenal hypertrophy in the flight animals would indicate a chronic stress response. However, at time of sacrifice the corticosterone levels were not statistically different among the groups. Either the conditions resulting in corticosterone secretion had dissipated by the time of sacrifice or the secretory response may have been inhibited (normal circadian nadir, or some other inhibitory factor or factors). The light cycle alterations (3-5 hour phase advance, and the 36 hour day (20 hours dark:16 hours light) imposed prior to sacrifice further complicate the interpretation of the data. Also, fasting is known to induce a hormonal secretory pattern similar to application of an environmental stressor (there was an approximately 4[illegible] hour fast during the recovery and sacrifice).

The pineal of humans and some other mammalian species contain multi-layered hydroxyapatite concentrations called corpora arenacea, or brain sand. Although the degree of radiologically detectable calcification of the human pineal gland appears to increase with age, there is no indication that increased calcification is related to loss of cellular activity. Histological and biochemical studies have shown that the appearance of the pinealocyte cell type, pineal serotonin content and HIOMT enzyme activity do not change with age (Giarman, 1960; Rodin and Overall, 1967; Smith, et al. 1977; Wurtman, 1964). Lukaszyk and Reiter (1975), suggest that the deposition of calcium may be related to polypeptide secretion by the pineal gland, and may serve as an index of previous glandular activity rather than degeneration. We found no statistical difference in the total pineal calcium content among our test groups. Though two values assayed extremely high, we felt that these were due to exogenous calcium contamination and were not included in the final analysis.

In summary, we conclude that the spaceflight resulted in a stress response as indicated by adrenal hypertrophy, that gonadal function was compromised, and that the pineal may be linked as part of the mechanism of the responses noted.

REFERENCES

1. Binkley, S.A. Circadian rhythms of pineal function in rats. Endocrine Reviews 4: 255-270, 1983.

2. Bosin, T.R. Serotonin metabolism. In: W.B. Essman (ed.) Serotonin Metabolism in Health and Disease, S.P. Medical and Scientific Books, New York, pp. 181- 300, 1978.

3. Brown, G.M. and Wainright, S.D. (eds.) Advances in the Biosciences, Volume 53, The Pineal Gland: Endocrine Aspects, Pergamon Press, Elmsford, New York, 367 pp., 1985.

4. Chan, A. and Ebadi, M. The kinetics of norepinephrine-induced stimulation of serotonin-N-acetyltransferase in bovine pineal glands. Neuroendocrinol 31: 244- 251, 1980.

5. Giarman, N.J., Freedman, D.X. and Picard-Ami, L. Serotonin content of the pineal glands of man and monkeys. Nature (London) 186: 480, 1960.

6. Green, A.R., Heal, D.J., and Grahame-Smith, D.G. Further observations on the effect of repeated electroconvulsive shocks on the behavioral responses of rats produced by increases in the functional activity of brain 5-hydroxytryptamine and dopamine. Psychopharmacology 52: 195-200, 1977.

7. Hadley, M.E. Endocrinology, 2nd ed., Prentice Hall, Englewood Cliffs, New Jersey, 549 pp., 1988.

8. Kitay, J.I. and Altschule, M.D. The Pineal Gland: A Review of the Physiologic Literature, Harvard University Press, Cambridge, Mass., 280 pp., 1954.

9. Lukaszyk, A. and Reiter, R.J. Histophysiological evidence for the secretion of polypeptides by the pineal gland. Am. J. Anat. 143: 451, 1975.

10. Mefford, I.N. and Barchas, J.D. Determination of tryptophan and metabolites in rat brain and pineal tissue by reverse phase high performance liquid chromatography with electrochemical detection. J. Chrom. 181: 187-193, 1980.

11. O'Brien, P.J. and Klein, D.C. (eds.) Pineal and Retinal Relationships, Academic Press, Florida, 442 pp., 1986.

12. Ogle, T.F. and Kitay, J.I. In vitro effects of melatonin and serotonin on adrenal steroidogenesis. Proc. Soc. Exptl. Biol. Med. 157: 103-105, 1978.

13. Preslock, J.P. The pineal gland: basic implications and clinical correlations. Endocrine Reviews 5: 282-308, 1984.

14. Quay, W.B. Circadian rhythms in rat pineal serotonin and its modification by estrous cycle and photoperiods. Gen. Comp. Endocrinol. 3: 473-479, 1963.

15. Reiter, R.J. (ed.) Comprehensive Endocrinology: The Pineal Gland, Raven Press, New York, 1984.

16. Reiter, R.J. (ed.) The Pineal Gland, Volume I, Anatomy and Biochemistry, CRC Press, Boca Raton, Florida, 320 pp., 1981.

17. Reiter, R.J. (ed.) The Pineal Gland, Volume II, Reproductive Effects, CRC Press, Boca Raton, Florida, 227 pp., 1981.

18. Reiter, R.J. (ed.) The Pineal Gland, Volume III, Extra-Reproductive Effects, CRC Press, Boca Raton, Florida, 240 pp., 1982.

19. Reiter, R.J. The pineal gland: an important link to the environment. NIPS 1: 202-205, 1986.

20. Rodin, A.E. and Overall, J. Statistical relationships of weight of the human pineal to age and malignancy. Cancer 20: 1203, 1967.

21. Smith, J.A., Padwick, D., Mee, T., Minneman, K.P. and Bird, E.D. Synchronous nyctohemeral rhythms in human blood melatonin and in human post-mortem pineal enzyme. Clin. Endocrinol. 6: 219, 1977.

22. Vollrath, L. The Pineal Organ, Springer-Verlag, New York, 665 pp., 1981.

23. Wurtman, R.J., Axelrod, J., and Barchas, J.D. Age and enzyme activity in the human pineal. J. Clin. Endocrinol. 24: 299, 1964.

24. Wurtman, R.J. and Moskowitz, M.A. The pineal organ. New Engl. J. Med. 296: 1329-1333, 1383-1386, 1977.

25. Wurtman, R.J. and Ozacki, Y. Physiological control of melatonin synthesis and secretion: Mechanisms generating rhythms in melatonin, methoxytryptophol and arginine vasotocin levels and effects on the pineal of endogenous catecholamines, the estrous cycle and environmental lighting. J. of Neural Transmission 13: 59-70, 1978.

TABLE 1. BODY WEIGHT, TESTES WEIGHT, AND PINEAL WEIGHT OF ANIMALS ON COSMOS 1887.

Group-Subj.#	Body Wt.(g)	Pineal Wt.(mg)	Testes wt.(g)	Testes Wt.(%B.W.)	Adrenal Wt.(g)	Adrenal Wt.(%B.W.)
F-6	304	1.51	1.24	0.41	48	15.8
F-7	306	1.90	1.25	0.41	54	17.7
F-8	296	1.38	0.85	0.29	54	18.2
F-9	300	2.47	1.30	0.43	44	14.7
F-10	310	1.45	1.32	0.43	54	17.5
X	303.2[a,b]	1.74	1.19[a]	0.39	50.8	16.78[d,e,f]
S.D.	5.40	0.45	0.19	0.06	4.60	1.47
S.E.M.	2.42	0.20	0.09	0.03	2.06	0.66
V-6	350	1.62	1.35	0.39	43	12.3
V-7	355	1.92	1.57	0.44	47	13.2
V-8	315	1.84	1.42	0.45	40	12.7
V-9	355	2.11	1.45	0.41	39	11.0
V-10	335	2.24	1.40	0.42	44	13.1
X	342.0	1.95	1.44	0.42	42.6	12.66
S.D.	17.13	0.24	0.08	0.02	3.21	0.89
S.E.M.	7.68	0.11	0.04	0.01	1.44	0.40
S-6	345	1.86	1.30	0.38	39	11.3
S-7	365	1.75	1.42	0.39	45	12.3
S-8	355	2.00	1.35	0.38	45	12.7
S-9	350	2.15	1.30	0.37	44	12.6
S-10	330	2.42	1.35	0.41	45	13.6
X	349.0	2.04	1.34	0.39	43.6	12.50
S.D.	12.94	0.26	0.05	0.02	2.61	0.93
S.E.M.	5.79	0.11	0.02	0.01	1.17	0.37
B-6	320				43	13.4
B-7	310				43	13.9
B-8	310				43	13.9
B-9	295				40	13.6
B-10	345				44	12.8
X	316.0[b,c]				42.6	13.52
S.D.	18.5.				1.52	0.46
S.E.M.	8.28				0.68	0.20

F = flight group
S = synchronous control group
V = vivarium control group
B = basal control group
Wt. = weight
B.W. = body weight

a = versus V, $p < 0.01$
b = versus S, $p < 0.01$
c = versus V, $p < 0.05$
d = versus V, $p < 0.001$
e = versus S, $p < 0.001$
f = versus B, $p < 0.001$

TABLE 2. PINEAL CONTENT OF RATS FLOWN ABOARD COSMOS 1887: MELATONIN (Mel), SEROTONIN (5-HT), 5-HYDROXYINDOLEACETIC ACID (5-HIAA), and CALCIUM (Ca).

Group-subj.#	Mel (pg/gl)	Mel (pg/mgt)	5-HT (ng/gl)	5-HT (ng/mgt)	5-HIAA (ng/gl)	5-HIAA (ng/mgt)	Ca (ug/gl)	Ca (ug/mgt)
F-6	121.9	80.8	23.103	15.300	19.306	12.785	1.02	0.68
F-7	112.9	59.4	20.228	10.646	14.740	7.759	0.95	0.50
F-8	37.6	27.1	24.302	17.610	17.404	12.612	1.12	0.81
F-9	28.2	11.4	8.594*	13.479*	6.989*	2.830*	1.09	0.44
F-10	37.5	25.9	15.669	10.806	12.893	8.892	0.42	0.30
X	67.62	40.92	20.83*a	13.59*a,b	15.09	10.51*a,b	0.92	0.55
S.D.	45.71	28.37	3.84	3.44	2.84	2.57	0.29	0.20
S.E.M.	20.44	12.69	1.92	1.72	1.42	1.28	0.13	0.09
V-6	50.3	31.0	20.810	12.846	11.912	7.353	ex	ex
V-7	57.8	30.1	12.715	6.622	7.693	4.007	2.76	1.44
V-8	92.3	50.3	14.956	8.128	17.079	9.282	1.37	0.74
V-9	176.7	83.8	15.368	7.283	9.032	4.281	0.92	0.44
V-10	12.4	5.5	18.299	8.169	11.664	5.207	0.93	0.42
X	77.9	40.1	16.43	8.61	11.48	6.03	2.06	0.53
S.D.	62.10	29.13	3.15	2.45	3.60	2.25	0.20	0.18
S.E.M.	27.77	13.03	1.41	1.10	1.61	1.00	0.12	0.10
S-6	87.8	47.2	27.878*	14.988*	54.805*	29.465*	0.99	0.53
S-7	144.0	82.3	13.419	7.668	15.361	8.778	0.98	0.56
S-8	31.2	15.2	11.169	5.845	4.358	2.179	0.90	0.45
S-9	90.8	41.8	13.390	6.228	10.080	4.688	0.97	0.45
S-10	65.7	27.1	10.875	4.493	6.617	2.734	ex	ex
X	83.9	42.72	12.15*	6.06*	9.10*	4.60*	0.96	0.50
S.D.	41.18	25.44	1.31	1.31	4.79	2.99	0.04	0.06
S.E.M.	18.42	11.38	0.65	0.65	2.40	1.50	0.02	0.02

F = flight group
S = synchronous control group
V = vivarium control group
Mel = melatonin
5-HT = serotonin
5HIAA = 5-Hydroxyindoleacetic acid
Ca = calcium
/gl = /whole pineal gland
/mgt = /milligram pineal tissue
ex = sample contaminated
a = versus S,p <0.01
b = versus V,p <0.05
* = means calculated without questionable values, see results

C5

TABLE 3. CONCENTRATION OF PLASMA SEROTONIN (5-HT), and TESTOSTERONE* OF RATS

Group-subj.#	5-HT (ng/mL)	Testosterone* (ng/mL)
F-6	11.87	0.18
F-7	7.88	0.18
F-8	17.21	0.62
F-9	7.89	0.10
F-10	N.D.	0.62
X	11.21[d]	0.34[a]
S.D.	4.42	0.26
S.E.M.	2.21	0.11
V-6	108.29	2.50
V-7	N.D.	1.20
V-8	28.06	0.43
V-9	38.14	0.48
V-10	14.99	0.24
X	47.37	0.97
S.D.	41.70	0.93
S.E.M.	20.85	0.42
S-6	20.72	0.62
S-7	N.D.	3.50
S-8	11.77	0.85
S-9	11.35	1.85
S-10	34.55	0.77
X	19.60[d]	1.52
S.D.	10.87	1.21
S.E.M.	5.43	0.54
B-6	30.05	4.50
B-7	47.88	4.20
B-8	44.87	3.40
B-9	73.50	2.40
B-10	123.99	2.00
X	64.06	3.30[b,c]
S.D.	36.97	1.09
S.E.M.	16.53	0.49

F = flight group
S = synchronous control group
V = vivarium control group
B = basal control group
N.D. = not determined

a = versus B, $p < 0.001$
b = versus S, $p < 0.01$
c = versus V, $p < 0.01$
d = versus B, $p < 0.05$
* = determined by RIA, data provided by Dr. R. Grindeland and M. Vasques, NASA-Ames

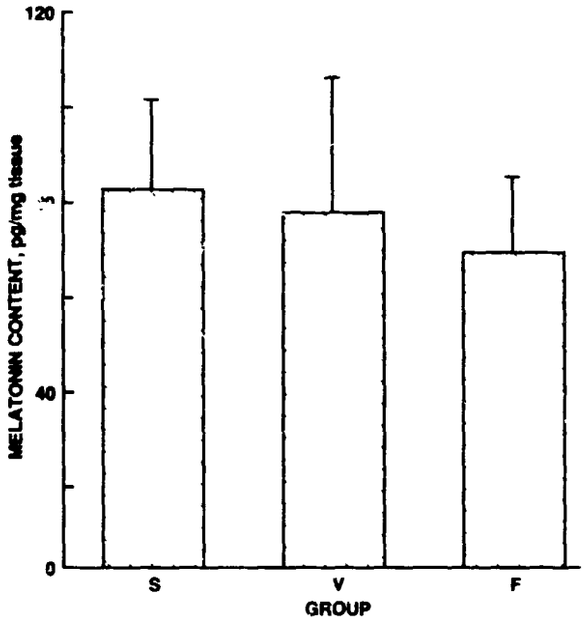

Figure 1. Pineal melatonin content (pg/gland) synchronous control group (S), vivarium control group (V), and flight animals aboard Cosmos 1887 (F). Values are means ± S.E.M., N = 5/group.

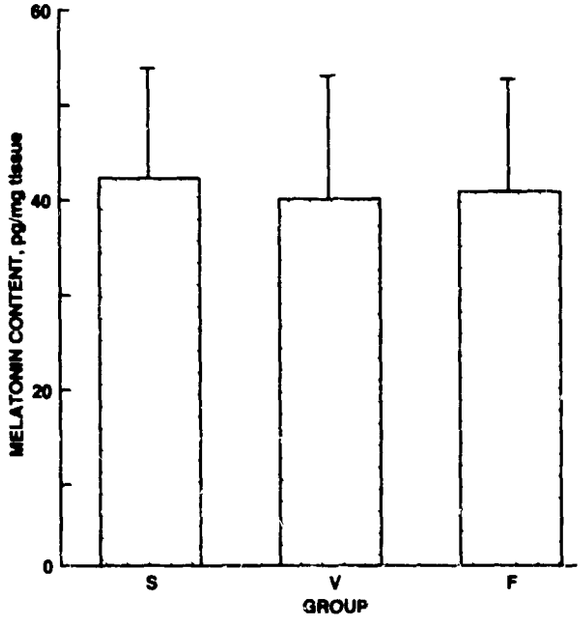

Figure 2. Pineal melatonin content (pg/mg tissue) synchronous control group (S), vivarium control group (V), and flight animals aboard Cosmos 1887 (F). Values are means ± S.E.M., N = 5/group.

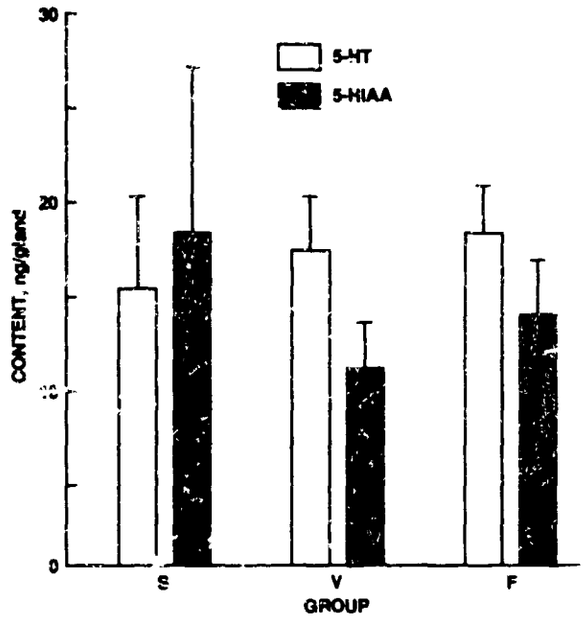

Figure 3. Pineal serotonin (5-HT) and 5-hydroxyindoleacetic acid (5-HIAA) expressed as ng/gland in synchronous control group (S), vivarium control group (V), and flight animals aboard Cosmos 1887 (F). Values are means ± S.E.M., N = 5/group.

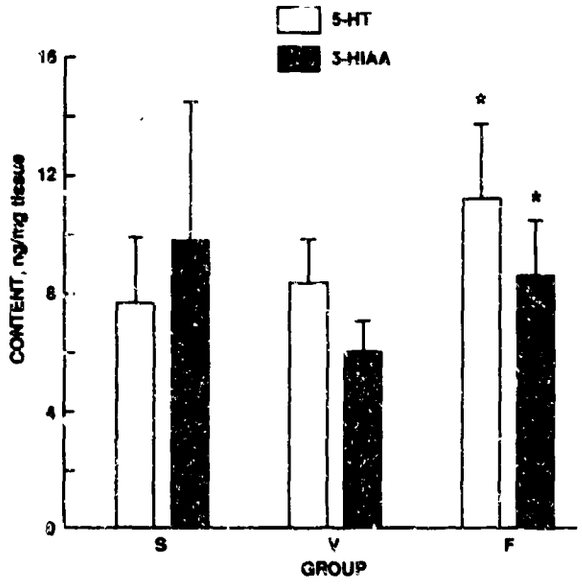

Figure 4. Pineal serotonin (5-HT) and 5-hydroxyindoleacetic acid (5-HIAA) expressed as ng/mg tissue, in synchronous control group (S), vivarium control group (V), and flight animals aboard Cosmos 1887 (F). Values are means ± S.E.M., N = 5/group.

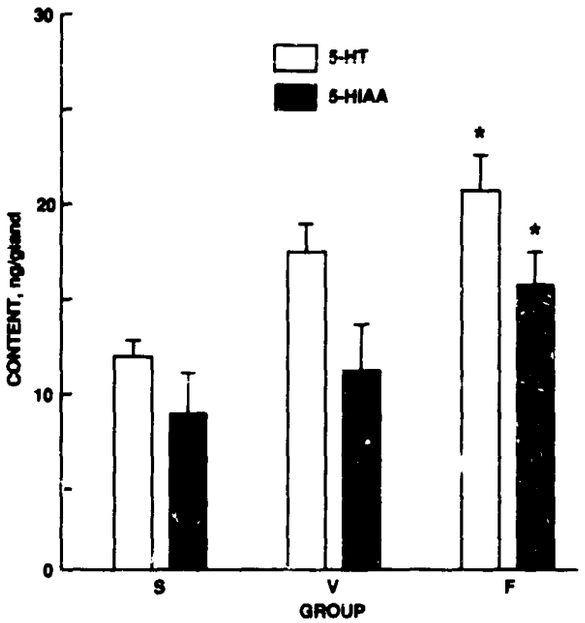

Figure 5. Pineal serotonin (5-HT) and 5-hydroxyindoleacetic acid (5-HIAA) expressed as ng/gland in synchronous control group (S), vivarium control group (V), and flight animals aboard Cosmos 1887 (F). Samples F-9 and S-6 were excluded from the analysis (see results section). Values are means ± S.E.M., N = 5 for V group, N = 4 for F and S groups. * = significantly different versus control, $p < 0.05$.

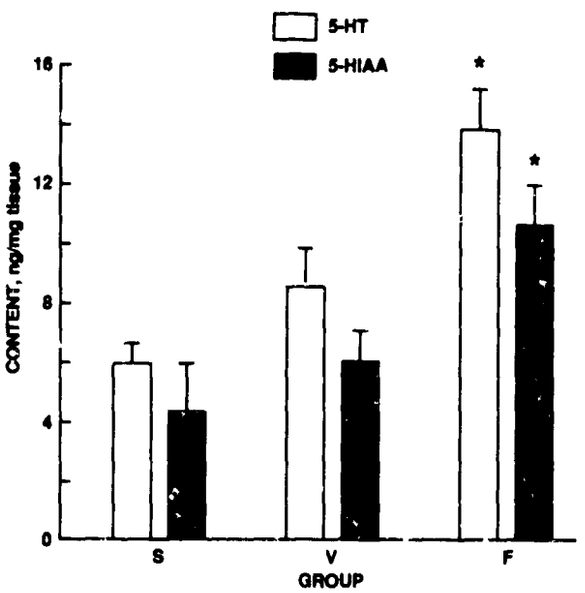

Figure 6. Pineal serotonin (5-HT) and 5-hydroxyindoleacetic acid (5-HIAA) expressed as ng/mg tissue, in synchronous control group (S), vivarium control group (V), and flight animals aboard Cosmos 1887 (F). Samples F-9 and S-6 were excluded from the analysis (see results section). Values are means ± S.E.M., N = 5 for V group, N = 4 for F and S groups. * = significantly different versus control, $p < 0.05$.

N90-26473

EXPERIMENT K-6-20

THE EFFECT OF SPACEFLIGHT ON PITUITARY OXYTOCIN AND VASOPRESSIN CONTENT OF RATS

Principal Investigator:

L. Keil
NASA Ames Research Center
Moffett Field, California 94035

Co-Investigators:

J. Evans
NASA Ames Research Center

R. Grindeland
NASA Ames Research Center

I. Krasnov
Institute of Biomedical Problems
Moscow, USSR

PRECEDING PAGE BLANK NOT FILMED

SUMMARY

Pituitary levels of oxytocin (OT) and vasopressin (AVP) were measured in rats exposed to 12.5 days of spaceflight (FLT) as well as ground-based controls, one group synchronously maintained in flight-type cages with similar feeding schedules (SYN), and one group in vivarium cages (VIV). Flight rats had significantly less ($p< 0.05$) pituitary OT and AVP (1.10 ± 0.04 and 1.69 ± 0.07 µg, n=5) than either the SYN (1.50 ± 0.08 and 2.11 ± 0.04 µg, n=5) or VIV (1.54 ± 0.03 and 2.10 ± 0.09 µg, n=5) control groups, respectively. Because the FLT group mean body weight was significantly less ($p< 0.05$) than either control group, the pituitary hormone content was also calculated on the basis of posterior pituitary protein content (µg hormone/mg protein). When calculated in this manner pituitary OT in the FLT rats (5.09 ± 0.15 µg/mg protein) was significantly less ($p <0.05$) than SYN (7.66 ± 0.39 µg/mg protein) or VIV controls (8.11 ± 0.64 µg/mg protein). Pituitary AVP was also less in the FLT animals (7.80 ± 0.13 µg/mg protein) compared to either SYN (9.84 ± 0.51, $p< 0.05$) or VIV controls (11.01 ± 0.76, $p< 0.05$). The reduced levels of pituitary OT and AVP may have resulted from increased hormone secretion resulting from the combined effects of water deprivation and the stress of the novel microgravity environment.

INTRODUCTION

Disturbances in fluid and electrolyte balance have been noted in humans exposed to spaceflight (Leach and Rambaut, 1977). This was shown by a loss of plasma volume and increased excretion of sodium and potassium during flight (Leach and Rambaut, 1977). Upon return to earth these imbalances are quickly corrected with rehydration and increased renin-angiotensin-aldosterone activity (Leach and Rambaut, 1975). Similar postflight fluid-electrolyte and hormone responses have been observed in rats that were exposed to microgravity (Gazenko, et al., 1984). Microscopic examination of the hypothalamus and posterior pituitary gland of flight rats exposed to spaceflight shows changes indicative of increased activity e.g. increased hormone synthesis and secretion (Savina, et al., 1976). The purpose of this investigation was to measure levels of pituitary oxytocin (OT) and vasopressin (AVP) as possible indicators of changes in fluid-electrolyte balance during spaceflight.

METHODS

Animals

Male, specific pathogen free Czechoslovakian-Wister rats were divided into three groups of 10 animals each. Each group was housed in a single cage equipped with 10 paste food dispensers and 10 water lixits. All animals were fed a special paste diet before flight (Grindeland, et al). The flight group (FLT) was selected and transported, with a second group that was designated the synchronous control group (SYN), to the launch site. The third group remained in Moscow and served as the vivarium controls (VIV). The SYN animals were exposed to centrifugation and vibration to simulate the increased gravity associated with launch. The SYN animals were fed on the same schedule as the FLT rats. The VIV rats received an equalivant amount of paste diet each day, but it was dispensed in a single bolus at a fixed time each day. Water was available to all animals ad lib except during reentry and recovery. Five rats from each group were available for posterior pituitary measurements of OT and AVP. Further details concerning the care and treatment of the flight and control animals during flight and recovery are presented elsewhere (in this issue (Grindeland, et al).

Collection of Pituitaries

The animals were sacrificed at various times after recovery (Grindeland, et al.). Immediately after decapitation, the skull was opened and the brain was carefully removed to expose the anterior and posterior pituitary. The posterior pituitary along with the intermediate lobe was teased free from the anterior lobe, placed on a small square of aluminum foil, and frozen by immersion in liquid nitrogen. The foil containing the pituitary was placed in a small cyrovial and reimmersed in liquid nitrogen. The vials were transported and maintained on dry ice until they were thawed immediately prior to homogenization. The pituitaries were thawed individually and homogenized in 1 ml of 0.1 N HCl. An aliquot of the homogenate was diluted 1:200,000 in 0.05M phosphate assay buffer for radioimmunoassay of OT and AVP (Keil, et al., 1984; Keil and Severs, 1977). To eliminate interassay variability aliquots from all three groups (FLT, SYN, and VIV) were measured within the same OT or AVP radioimmunoassay. After the hormone levels were determined, protein concentrations were measured in aliquots from each homogenate (Pierce BCA. protein assay , Pierce Chemical Co.). Hormone concentrations were then calculated as a function of total protein for each posterior pituitary homogenate. Statistical comparisons were made among the various groups with a one-way ANOVA and the Newman-Keul range statistic as well as the nonparametric Mann-Whitney U test.

RESULTS

The assay results are expressed as micrograms of hormone per pituitary (Fig. 1) and as micrograms of hormone per mg protein. (Fig. 2). The latter calculation was made to provide a more valid comparison of FLT data with controls because the average weight of the FLT animals was significantly less than either control group. The body weights (g ± SE) of the rats at the time of sacrifice were: FLT. 303 ± 2; SYN. 349 ± 6; and VIV. 342 ± 8.

Both neural lobe hormones levels were significantly reduced in the FLT animals when compared to either set of controls by either parametric or nonparametric tests. Oxytocin was 31% lower, 1.10 ± 0.04 µg/pituitary ($p<0.05$) in the FLT group compared to 1.60 ± 0.08 the SYN rats, and 29% lower, 1.54 ± 0.03 µg/pituitary ($p<0.05$) in the VIV controls (Fig. 1). Pituitary AVP in the FLT animals (1.69 ± 0.07 µg/pituitary) was 20% lower ($p<0.05$) than either of the control groups, 2.11 ± 0.04 SYN and 2.10 ± 0.09 VIV (Fig 1.). Because the FLT animals weighed less than either set of controls, the pituitary hormone content was calculated on the basis of protein content (µg hormone/mg protein) in posterior pituitary homogenate. The results are shown in Figure 2.

When expressed in terms of pituitary protein content, the results still indicate a significant reduction in pituitary OT and AVP compared to either control group by both parametric and nonparametric tests (Fig. 2). Pituitary OT in the FLT group was 33.6% lower (5.09 ± 0.15 µg/mg protein) compared to 7.66 ± 0.39 for the SYN controls ($p<0.05$) and 37.3 % lower (8.11 ± 0.64) than in VIV controls ($p< 0.05$). Pituitary AVP was 20.7% lower (7.80 ± 0.13 µg/mg protein) in the FLT group compared to that in SYN controls (9.83 ± 0.51, $p<0.05$) controls and 29.2% lower (11.01 ± 0.76) than that in the VIV controls ($p<0.05$).

DISCUSSION

Postflight investigations of both humans and animals have indicated that fluid-electrolyte balance is altered by exposure to microgravity (Leach and Rambaut, 1977; Gazenko, et al., 1984). Post-flight reductions in sodium excretion and urine volume, and increases in plasma renin activity are indications that changes in fluid-electrolyte homeostasis occurred during flight (Leach and Rambaut, 1975). In humans, the headward fluid shift observed during flight is thought to be the stimulus for the plasma volume reduction and other adjustments in fluid-electrolyte metabolism. Rats and other horizontal animals may not experience this headward fluid shift, and if such a shift did take place, it may be proportionally less than that of humans because of the difference in

hydrostatic columns. However, results from rat postflight experiments are similar to those of humans, e.g. sodium and water excretion reduced and water consumption increased (Gazenko, et al., 1984). These postflight results demonstrate that changes in fluid-electrolyte balance have taken place during flight. Whether the same physiological mechanisms are responsible for these changes in rodents remain to be determined.

In the present study, FLT rats had significantly less pituitary OT and AVP than either group of ground-based controls. Decreased content may be attributed, in part, to the difference in size between the flight and control groups. The mean body weight of the FLT rats was 40 to 50 g less than that of either control group. A reduction in body size indicates that the FLT animals did not maintain the same growth rate as that of the controls, and this would result in decreased pituitary size and hormone content. Since the SYN controls consumed the same amount of food as the FLT rats, the decrease in growth of this group cannot be attributed to reduced food intake.

In an effort to compensate for the difference in body weight between the groups, hormone content was calculated on the basis of pituitary protein content (Fig. 2). In this case, AVP content of the FLT rats was 20.7 and 29.2% lower than either SYN or VIV control groups, respectively. This indicates that the FLT animals may have been dehydrated. Synchronous controls had access to water on the same schedule as the FLT animals; however, the pituitary OT and AVP content of the SYN rats was sigificantly greater than that of the FLT group. This suggests that the FLT rats had water available, but for some reason did not drink or, alternatively, the SYN group had water available for a longer period of time or drank more than the FLT animals.

Pituitary OT was also significantly lower in FLT rats (Figs. 1 & 2). Dehydration reduces pituitary OT as well as AVP (Summy-Long, et al., 1984). In addition, data from recent papers indicate that OT secretion, at least in rats, is increased by stress (Gibbs, 1986a). Oxytocin facilitates the action of Corticotrophin Releasing Factor (CRF) on the anterior pituitary to stimulate the release of Adrenocorticotrophic hormone (ACTH) (Gibbs, 1986b). Gibbs (1986a) also points out that OT may be released in response to "neurogenic" stress, whereas AVP, which also has been shown to increase CRF activity, is released in response to "physical" stress. Perhaps some of the decrease in pituitary OT may be attributed to the chronic neurogenic stress the animals experienced during flight in their effort to adapt to microgravity. This OT response to stress may be unique to rats because a similar response has not been observed in humans (Legros, et al., 1987).

In rats, administration of nausea-producing agents such as lithium chloride and apomorphine results in learned taste aversion as well as a relatively specific release of OT rather than AVP (Verbalis, et al., 1986). Increased plasma levels of the gut hormone, cholecystokinin (CCK), are also associated with taste aversion and nausea (Verbalis, et al., 1986). This hormone appears to be a specific stimulus for the secretion of OT, in rats (Carter and Lightman, 1987). Interestingly, lesions of the area postrema, a circumventricular organ associated with nausea and the emetic response, signifcantly reduced OT secretion in response to CCK injection (Carter and Lightman, 1987). If the rats experienced motion sickness during flight, it is possible that this condition, along with stress and dehydration, would contribute to increased OT secretion and depletion of pituitary OT stores.

In summary, the results indicate that the FLT animals were dehydrated and this led to a significant reduction in both pituitary OT and AVP. Results also show that pituitary OT was reduced to a greater extent than AVP, and perhaps this decrease was in response to increased stress or motion sickness encountered during flight and/or recovery.

REFERENCES

1. Leach, C.S. and Rambaut, P.C. (1977) Biochemical responses of the Skylab crewmen: An overview, In: Biomedical Results from Skylab, Washington, DC, NASA SP-377, pp. 204-216.

2. Leach, C.S. and Rambaut, P.C. (1975) Endocrine response in long duration manned spaceflight. Acta Astronautiae. 2, 115-127.

3. Gazenko, O.G., Natochen, Y.V., Ilyin, Y.A., Ilyushko, N.A., Kondratiev, Y.I, Lavrova, Y.A., and Shakhmatova, Y.I., Fluid-electrolyte metabolism and renal function of the white rats in experiments aboard Cosmos biosatellites, Aviat. Space Environ. Med., 55:695-69

4. Savina, E.A., Pankova, A.S., Alekseyev, E.I., and Podymov, V.K., Morph manifestations of functional changes in the hypothalamic-pituitary neurosecretor kidneys of rats after spaceflight, Aviat., Space and Eviron. Med.;47(8): 853-855.

5. Grindeland, R.E., Popova, I.A., and Vasques, M.F., Cosmos 1887 mission overview; effects of microgravity on rat body and adrenal weights and plasma constituents. FASEB J., Submitted for publication.

6. Keil, L.C., Rosella-Dampman, L.M., Emmert, S., Chee, O. and Summy-Long, J.Y., Enkephalin inhibition of angiotensin-stimulated release of oxytocin and vasopressin, Brain Res., 297: 329-336, 1984.

6. Keil, L.C., Rosella-Dampman, L.M., Emmert, S., Chee, O., and Summy-Long, J.Y. (1984) Enkephalin inhibition of angiotensin-stimulated release of oxytocin and vasopressin. Brain Res. 297, 329-336.

7. Keil, L.C. and Severs, W.B., Reduction in plasma vasopressin levels of dehydrated rats following acute stress, Endocrinology 100: 30-38, 1977.

8. Summy-Long, J.Y., Miller, D.S., Rosella-Dampman, L.M., Hartman, R.D.and Emmert, S.E., A functional role for opioid peptides in the differential secretion of vasopressin and oxytocin, Brain Res. 309: 362-366, 1984.

9. Gibbs, D.M., Vasopressin and oxytocin: Hypothalamic modulators of the stress response: A review, Psychoneuroendocrinology 11: 131-140, 1986a.

10. Gibbs, D.M., Stress-specific modulation of ACTH secretion by oxytocin, Neuroendocrinology 42: 456-458, 1986b.

11. Legros, J.J., Chiodera, P., Geenen, V. and von Frenckell, R., Confirmation of the inhibitory influence of exogenous oxytocin on cortisol and ACTH in man: evidence of reproductivity, Acta Endocrinologica (Copenh) 114: 345-349, 1987.

12. Verbalis, J.G., McCann, M.J., McHale, C.M., Stricker, E.M., Oxytocin secretion in response to cholecystokinin and food: differentiation of nausea from satiety, Science ;Vol. 22, June 1986.

13. Carter, D.A. and Lightman, S.L., A role for the area postrema in mediating cholecystokinin-stimulated oxytocin secretion, Brain Res., 435: 327-330, 1987.

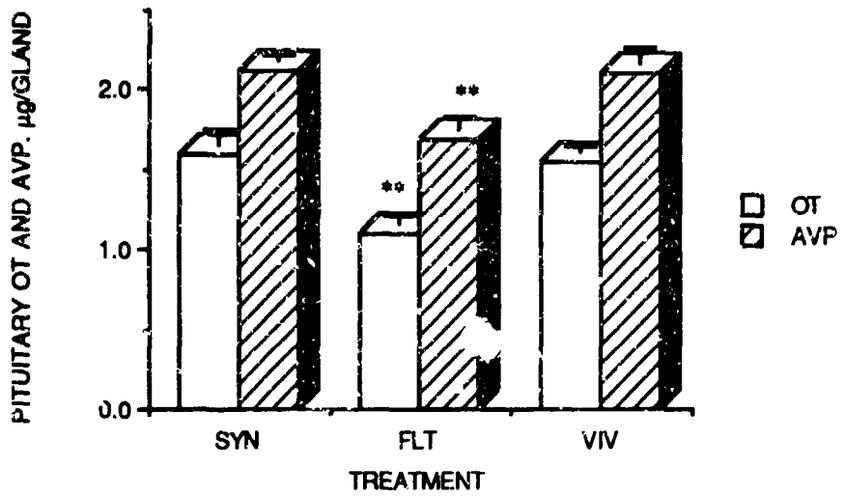

Figure 1. Pituitary oxytocin (OT) and vasopressin (AVP) content expressed as µg per posterior lobe. **p<0.05 for comparison of Flight (FLT) to either Synchronous (SYN) or Vivarium (VIV) control by both the ANOVA or Mann-Whitney U tests. Values are means ± SE.

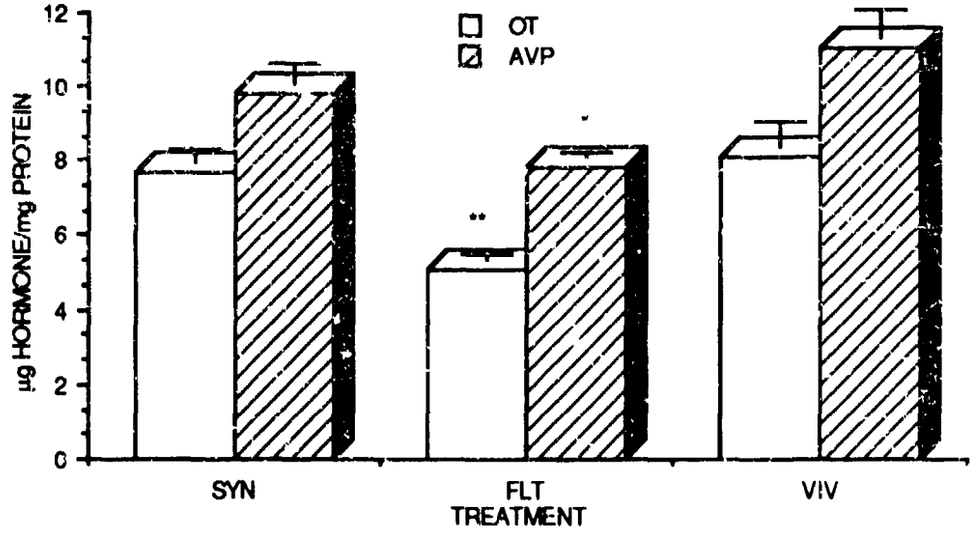

Figure 2. Oxytocin (OT) and vasopressin (AVP) content expressed as micrograms of hormone per mg of protein in the posterior pituitary extract. ** p<0.05 for comparison of Flight to either Syncronous or Vivarium control by both the ANOVA or Mann-Whitney U tests. Values are means ± SE.

N90-26474

EXPERIMENT K-6-21

EFFECT OF MICROGRAVITY ON 1) METABOLIC ENZYMES OF TYPE I AND TYPE 2 MUSCLE FIBERS AND ON 2) METABOLIC ENZYMES, NEUROTRANSMITTER AMINO ACIDS, AND NEUROTRANSMITTER ASSOCIATED ENZYMES IN MOTOR AND SOMATOSENSORY CEREBRAL CORTEX

PART I: METABOLIC ENZYMES OF INDIVIDUAL MUSCLE FIBERS

PART II: METABOLIC ENZYMES OF HIPPOCAMPUS AND SPINAL CORD

Principal Investigator:

O. Lowry
Washington University School of Medicine
St. Louis, Missouri

Co-Investigators:

D. McDougal, Jr.
Patti M. Nemeth
Maggie, M.-Y. Chi,
M. Pusateri
J. Carter,
J. Manchester
Beverly Norris
Washington University School of Medicine
St. Louis, Missouri

I. Krasnov
Institute of Biomedical Problems
Moscow, USSR

EXPERIMENT K-6-21

PART I: METABOLIC ENZYMES OF INDIVIDUAL MUSCLE FIBERS

INTRODUCTION

The individual fibers of any individual muscle vary greatly in enzyme composition, a fact which is obscured when enzyme levels of a whole muscle are measured. The purpose of this study was therefore to assess the changes due to weightless on the enzyme patterns composed by the individual fibers within the flight muscles.

METHODS

Small portions of soleus (slow-twitch) and tibialis anterior (TA, fast-twitch) muscles were freeze-dried at -35 deg. C. Portions of individual fibers, 2-3 mm long, were dissected free, weighed, and stored separately under vacuum at -70 deg. C. Studies were made on 64 soleus and 164 tibialis fibers from 2 synchronous and 2 flight animals. Each fiber was analyzed in duplicate for 2 to 8 different enzymes, and the size (µg/mm) determined. This involved more than 2300 quantitative measurements.

The work was expedited by a preliminary study which showed that most of the enzymes of interest can be extracted and stored without loss at -70 deg. C in a special glycerol-KC1-detergent medium. Each dry sample, weighing about 0.5 µg (0.5 to 1 mm long), was added to 5 µ1 of this special medium under mineral oil. After incubation for 2 hours at room temperature, the samples were transferred to a -70 deg. C freezer. Since each assay required only 0.1 to 0.2 µ1 of extract (equivalent to 10 to 20 ng of dry fiber), the single 5 µ1 extract was sufficient for duplicate assays of a large number of different enzymes.

RESULTS

The enzymes which were measured fall into two groups, four which are usually most active in slow-twitch and fast-twitch-oxidative fibers: hexokinase, and three enzymes of oxidative metabolism, citrate synthase, malate dehydrogenase (MDH), and ß-hydroxyacyl CoA dehydrogenase, and four enzymes which are most active in fast-twitch-glycolytic fibers: glycogen phosphorylase, glycerol phosphate dehydrogenase, pyruvate kinase, and lactate dehydrogenase (LDH).

Control Activities:

In the synchronous muscles the average for three of the four enzymes of the oxidative, hexokinase group were 45 to 50% higher in soleus than in TA muscles (Fig. 1, Table 1). Citrate synthase was the exception in having similar activities in the two muscles. In contrast, in the synchronous animals the fast-twitch-glycolytic group of enzymes were 7- to 12-fold higher in TA than soleus muscles (Fig. 1, Table 2). Average fiber size was almost the same for both types of muscle.

The enzyme variability among the fibers of each muscle type are of some interest. Figure 2 shows that the coefficient of variation (CV) differs markedly among the different enzymes, and between the two muscle types. In the synchronous muscles, all of the CV's were much higher (64% to 900%) for slow-twitch enzymes of TA than for those of soleus muscles, whereas the reverse was true for fast-twitch-glycolytic enzymes. (Analytical errors were in the order of 5% and were, therefore, almost negligible relative to these large C.V.'s). Note the greater variability in TA for ß-hydroxyacyl CoA dehydrogenase (a key enzyme of fatty acid oxidation) than for the two members of the citrate cycle. Variations in fiber size were the same for both muscles.

PRECEDING PAGE BLANK NOT FILMED

Effects of Weightlessness on Average Values:

Since data are available, with one exception, from only two synchronous and two flight muscles, some caution must be observed in interpreting small average differences. However, examination of individual fiber patterns is helpful in this regard.

Tables 1 and 2 and Figures 3-6 compare average enzyme activity and fiber size for each synchronous and flight muscle studied. The average size (weight per unit length) was about 35% lower in flight than in synchronous muscles of both types. All of the enzyme activities are based on dry weight. Therefore the absolute enzyme content of the fibers from flight muscles are on the average 35% lower than would appear from these data. This will be discussed later.

In soleus muscle, the only conclusive enzyme change with flight was in hexokinase which increased an average of 137% on the dry weight basis (Table 1, Figure 3). The three enzymes of oxidative metabolism were clearly unchanged. The agreement between muscles is close and standard errors are small. The four enzymes of glycolysis and glycogenolysis were on average increased 20 to 50%, but the mean differences and standard errors in this case were so large as to make any conclusion about significance uncertain (Table 2, Figure 4).

In TA muscles, hexokinase increased about the same percentage as in soleus, but in addition all the enzymes of oxidative metabolism were increased about 60% (Table 1, Figure 5). The change in MDH is most convincing, whereas the standard errors for the other two enzymes are too large to be sure the differences are meaningful. The glycolytic-glycogenolytic enzymes in TA, in contrast to the soleus muscles, were all somewhat lower (12% to 25%) in the flight muscles. If the data for the two synchronous and the two flight muscles are each pooled, the differences due to flight are statistically significant for phosphorylase ($P<0.05$), for glycerol phosphate dehydrogenase ($P<0.01$), and for LDH ($P<0.001$), but not for pyruvate kinase.

Effect of Weightlessness on Individual Fiber Enzymes:

Figure 7 compares the variability of the 8 enzymes in the control and flight TA muscles. A striking difference is the 3- to 4-fold larger C.V.'s for the glycogenolytic enzymes in the flight muscles, with much smaller effects of flight, if any, in regard to variability among the oxidative enzyme group. In the case of the soleus fibers, the C.V.'s were little changed by flight from the control values shown in Figure 2.

The basis for this increase in glycolytic C.V.'s is illustrated by the example shown in Figure 8. This figure records individual values for LDH and MDH plotted against each other in 60 TA fibers, 30 from a synchronous muscle and 30 from a flight muscle. All but one of the synchronous fibers occupied a domain with a narrow range of LDH values and a wide range of MDH values. In contrast, about half of the flight fibers had moved out of the control domain by a decrease in LDH, and in some cases by a modest increase in MDH. Note that half of the control fibers, but only one flight fiber had an MDH value less than 8 mol kg^{-1} h^{-1}. The enzyme patterns for the other flight and control TA muscles were very similar to these. These LDH-MDH patterns are those expected for a change from a population consisting predominantly of fast-glycolytic fibers, in the control TA, to a mixture of fast-oxidative, fast-glycolytic, and a few slow-twitch fibers in the flight muscle.

Also entered in Figure 8 are data for 6 control and 6 flight soleus muscle fibers from the same two animals. These all fall in a single relatively small area with moderate MDH levels and very low LDH.

Figure 9 is a similar plot against each other of two enzymes of oxidative metabolism, citrate synthase and ß-hydroxyacyl CoA dehydrogenase. The data from the two TA controls and the two TA flight muscles have been pooled, since they appeared to occupy the same domain. Note the striking degree

of correlation between the two enzymes. The only obvious difference between flight and control is that 5 of the 12 fibers have been raised out of the control domain. The patterns of these enzymes for the other flight and control TA muscles were quite similar.

Included in Figure 9 is the joint domain of 32 soleus fibers, 16 each from a flight and a control muscle. These were similarly distributed over the area outlined. Individual values have been omitted to avoid confusion.

Figure 10 plots single fiber values against each other for two fast-twitch enzymes, phosphorylase and pyruvate kinase, from one control and one flight TA muscle. Of the 12 flight fibers, 3 were raised somewhat above the control domain whereas 5 fell far below it. Similar results were observed for the other control and flight TA muscle. Apparently weightlessness can extend the range of these fast-twitch enzymes in both directions, although the biggest trend is downward.

In soleus muscle, single fiber plots of phosphorylase against pyruvate kinase also show a close correlation between the two enzymes, but at much lower absolute levels (Figure 11). Although the effect of flight was to systematically increase pyruvate kinase, only 2 of 10 fibers showed a large move away from the control zone, and results for the other flight soleus muscle did not show a major increase in the range for either enzyme.

A plot of pyruvate kinase against glycerol-P dehydrogenase in TA fibers (Figure 12) is very similar to that of pyruvate kinase against phosphorylase for the same fibers shown in Figure 9. Figure 12 is presented because data have also been obtained for these two enzymes in fibers that were typed by the myofibrillar ATPase staining reaction. Frozen cross sections were made from one synchronous and one flight TA muscle. Alternate sections were stained for ATPase, or freeze-dried for quantitative enzyme assay. The stained sections were used as a guide for selection of fibers for these assays. Although type IIB fibers predominated in the synchronous muscle, and IIA fibers predominated in the flight muscle, it was possible to select an adequate number of fibers of both types from both muscles, and in addition in the flight muscle a few type I fibers were found and analyzed (Table 3).

The results indicate that the flight fibers in Figure 12 with low values for both enzymes are type IIA, with an occasional type I fiber, and the remainder are type IIB.

Absolute Changes in Enzyme Content With Weightlessness:

As mentioned above, the data so far presented are all based on dry weight, but the flight muscle fibers consistently lost about a third of their dry weight per unit length. Since fiber length can hardly change except with skeletal growth (and synchronous animals served as controls), basing enzyme contents on fiber length should provide a valid measure of the absolute changes in amount of enzyme. Figures 13 and 14 compare average levels of enzymes in soleus and TA muscles, respectively, when calculated on either a dry weight or fiber length basis. In soleus muscle, (Figure 13), the dry weight basis seems to indicate that flight caused a very large increase in hexokinase, with the other seven enzymes either unchanged or increased. In contrast, on a fiber length basis, it is apparent that although hexokinase increased in absolute terms, the increase was no more than 50%, and that six of the other enzymes decreased by 10 to 40%. Similarly in TA muscle (Figure 14), on a dry weight basis, hexokinase and the three enzymes of oxidative metabolism appeared to increase with flight by 60 to 95%, with the glycolytic, glycogenolytic enzymes falling by at most 25%, whereas in absolute terms (fiber length basis) oxidative enzymes were almost unchanged, hexokinase increased, but only by 25%, and phosphorylase and the glycolytic enzymes decreased about 50%.

CONCLUSION

In spite of the limitation in numbers of muscles examined, it is apparent that 1) the size of individual fibers (i.e. their dry weight) was reduced about a third, 2) that this loss in dry mass was accompanied

by changes in the eight enzymes studied, and 3) that these changes were different for the two muscles, and different for the two enzyme groups. In the soleus muscle the absolute amounts of the three enzymes of oxidative metabolism decreased about in proportion to the dry weight loss, so that their concentration in the atrophic fibers was almost unchanged. In contrast, there was little loss among the four enzymes of glycogenolysis - glycolysis so that their concentrations were substantially increased in the atrophic fibers. In the TA muscle, these seven enzymes were affected in just the opposite direction. There appeared to be no absolute loss among the oxidative enzymes, whereas the glycogenolytic enzymes were reduced by nearly half, so that the concentrations of the first metabolic group were increased within the atrophic fibers and the concentrations of the second group were only marginally decreased.

The behavior of hexokinase was exceptional in that it did not decrease in absolute terms in either type of muscle and probably increased as much as 50% in soleus. Thus, their was a large increase in concentration of this enzyme in the atrophied fibers of both muscles.

Another clear-cut finding was the large increase in the range of activities of the glycolytic enzymes among individual fibers of TA muscles. This was due to the emergence of TA fibers with activities for enzymes of this group extending down to levels as low as those found in control soleus muscles. It would be interesting to know if this represents a transition stage, and whether with prolonged weightlessness most of the fibers would be transformed into a low glycogenolytic type.

TABLE 1.

SIZE AND LEVELS OF FOUR ENZYMES CHARACTERISTIC OF SLOW TWITCH MUSCLES IN INDIVIDUAL FIBERS FROM SOLEUS AND ANTERIOR TIBIALIS MUSCLES

	Size	Hexokinase	Citrate synthase	MDH	BOAC
	μg/mm	mol h^{-1}	kg^{-1} (dry) at 20°C		
SOLEUS					
S7	0.84(16) ±0.05	0.468(16) ±0.026	4.47(16) ±0.25	17.7(6) ±1.7	9.4(16) ±0.2
S9	0.92(16) ±0.06	0.507(16) ±0.028		19.7(6) ±1.4	11.5(16) ±0.3
F7	0.61(16) ±0.03	1.38(16) ±0.07	5.04(16) ±0.33	20.6(16) ±0.9	9.2(16) ±0.2
F9	0.50(16) ±0.02	0.93(16) ±0.03		19.9(6) ±1.3	11.4(16) ±0.3
TIB. ANT					
S8	1.04(32) ±0.05	0.212(20) ±0.020	4.71(12) ±0.77	8.5(32) ±0.8	5.2(6) ±2.0
S9	0.91(32) ±0.05	0.295(20) ±0.020	6.42(12) ±1.06	10.4(32) ±1.2	7.1(6) ±2.0
F8	0.55(30) ±0.02	0.472(20) ±0.038	7.81(12) ±1.13	16.1(30) ±1.2	8.9(6) ±2.5
F9	0.67(32) ±0.03	0.526(20) ±0.04	9.54(12) ±1.55	17.3(32) ±1.0	11.9(6) ±3.9

Standard errors are shown for the numbers of fibers in parentheses. Abbreviations: MDH, malate deyhdrogenase; BOAC, ß-hydroxyacyl CoA dehydrogenase; S, synchronous; F, flight.

TABLE 2.

LEVELS OF FOUR ENZYMES CHARACTERISTIC OF FAST-TWICH MUSCLES

	Phosphorylase	Glycerol-P dehydrogenase	Pyruvate kinase	Lactate dehydrogenase
	Mol h^{-1} kg^{-1} (dry) at 20°C			
SOLEUS				
S7	0.60(10) ±0.13	0.47(16) ±0.05	7.72(16) ±0.43	24.0(16) ±1.1
S9	1.04(10) ±0.23		10.1(10) ±1.5	23.0(16) ±1.6
F7	0.70(10) ±0.12	0.62(16) ±0.07	10.3(16) ±0.56	29.4(16) ±0.9
F9	1.46(10) ±0.38		16.2(10) ±2.9	28.0(16) ±2.0
TIB. ANT				
S8	5.39(12) ±0.27	6.13(20) ±0.18	60.0(12) ±2.1	132(25) ±2
S9	7.03(12) ±0.44	5.49(20) ±0.21	64.1(20) ±1.9	136(32) ±3
F8	3.97(12) ±0.59	5.04(18) ±0.40	55.9(12) ±6.8	116(30) ±7
F9	5.30(12) ±0.93	4.13(19) ±0.47	53.9(20) ±5.7	103(32) ±6

Standard errors are shown for the number of fibers in parentheses.

TABLE 3

GLYCEROL PHOSPHATE DEHYDROGENASE (GOPDH) AND PYRUVATE KINASE IN INDIVIDUAL ANTERIOR TIBIALIS MUSCLE FIBERS TYPED ON THE BASIS OF MYOFIBRILLAR ATPASE STAINING

	Type	IIB	IIA	I
GOPDH		Mol kg $^{-1}$ (dry) h $^{-1}$		
Synchronous	S6	6.61(11) ±0.51	2.39(9) ±0.61	
Flight	F6	4.43(10) ±0.71	1.93(4) ±0.88	0.84(4) ±0.03
Pyruvate kinase	S6	38.8(11) ±1.8	14.3(9) ±1.3	
	F6	40.7(10) ±2.2	19.7(4) ±2.6	8.34(4) ±0.48

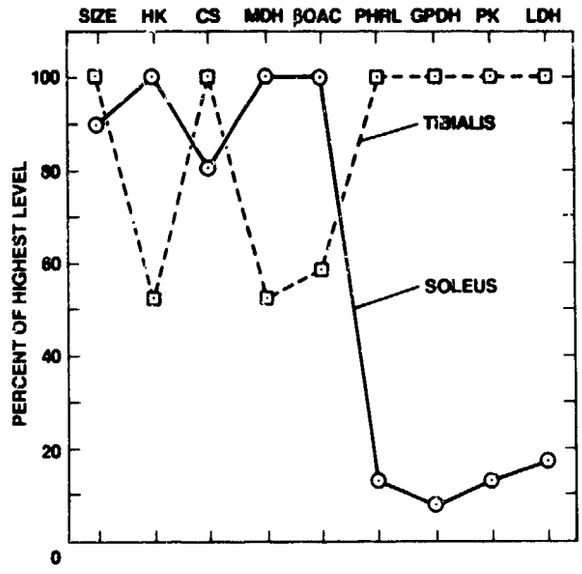

Figure 1: Comparison of average size and enzyme levels in the fibers of two synchronous soleus muscles(S7 and S9) and two synchronous TA muscles (S8 and S9). Abbreviations are HK, hexokinase; CS, citrate synthase; MDH, malate dehydrogenase; BOAC, β-hydroxyacyl CoA dehydrogenase; PHRL, glycogen phosphorylase; GPDH, glycerophosphate dehydrogenase; PK, pyruvate kinase; LDH lactate dehydrogenase.

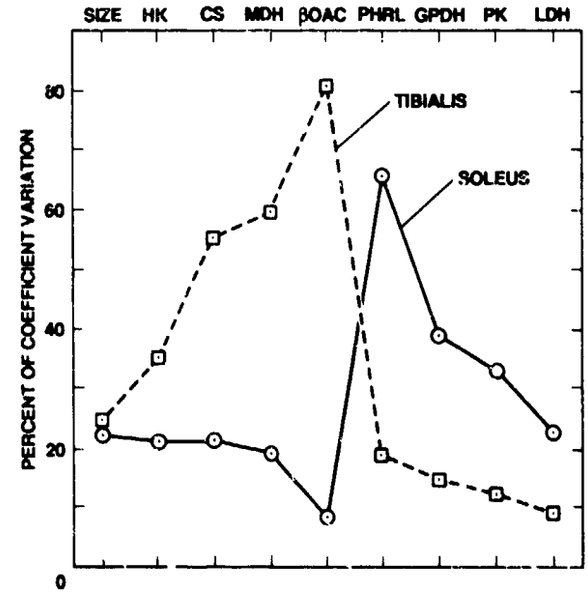

Figure 2: Average coefficient of variation for the same synchronous fibers and enzymes represented in Figure 1.

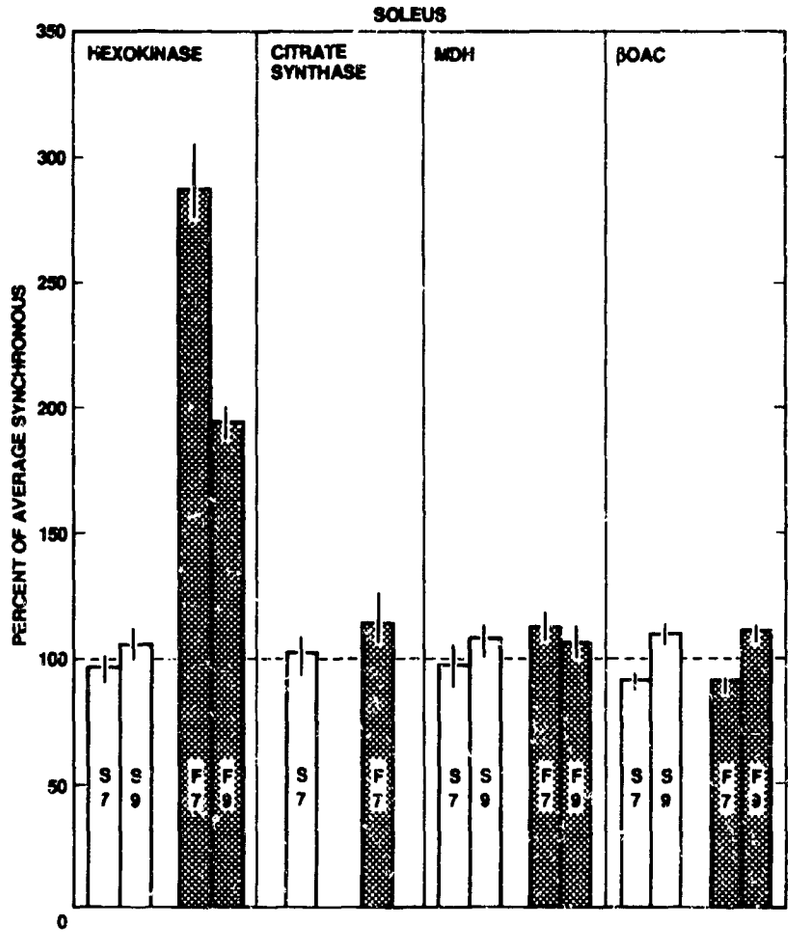

Figure 3: Comparison of synchronous and flight soleus muscle fibers in regard to levels, on a dry weight basis, of hexokinase and three enzymes of oxidative metabolism. Abbreviations as in Fig. 1.

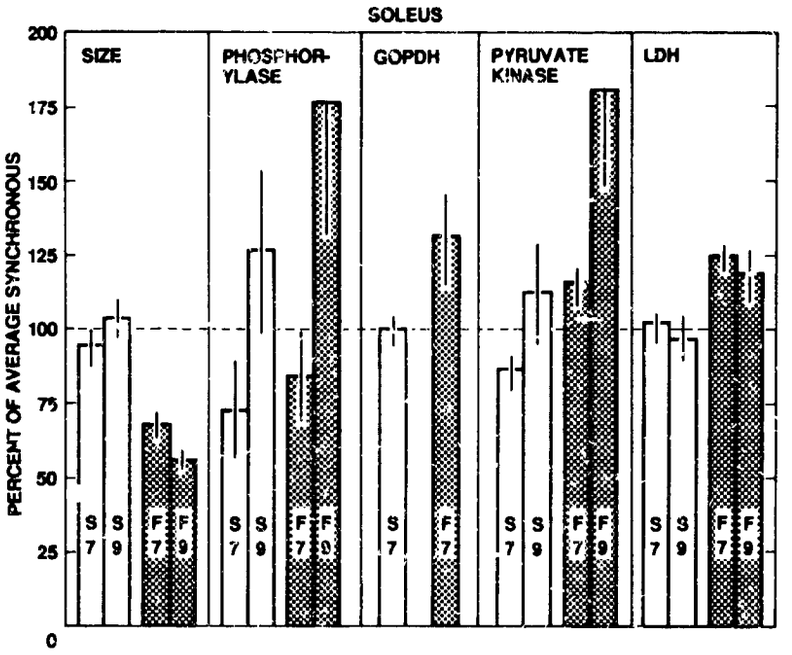

Figure 4: Comparison of synchronous and flight soleus muscle fibers in regard to size (dry weight per unit length) and the levels on a dry weight basis for four enzymes of glycolysis and glycogenolysis. Abbreviations as in Fig. 1.

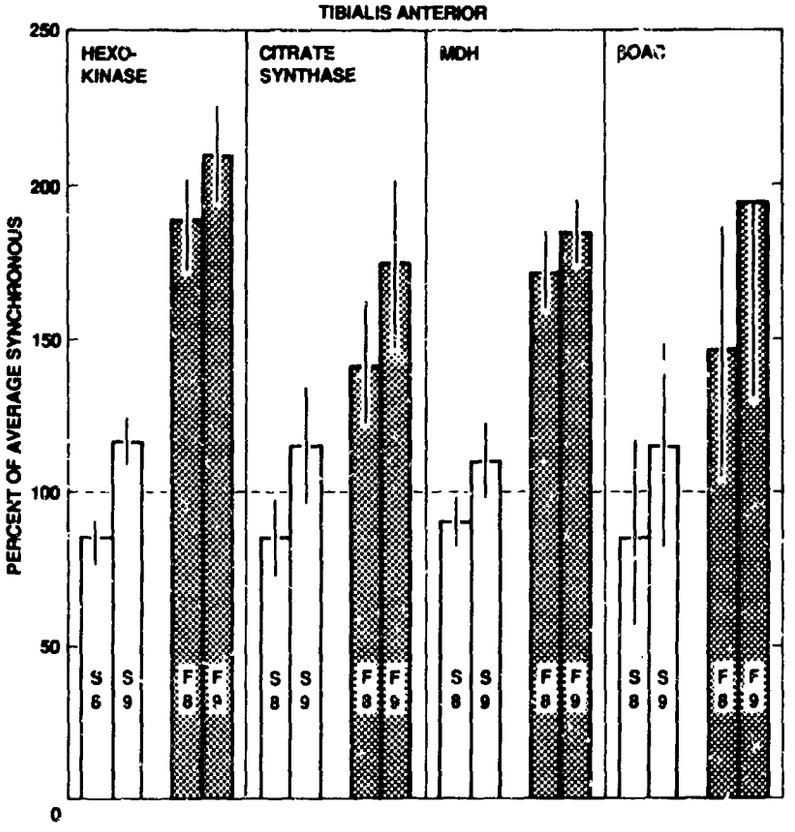

Figure 5: Comparison of synchronous and flight TA fibers in regard to levels, on a dry weight basis, of hexokinase and three enzymes of oxidative metabolism. Abbreviations as in Fig. 1.

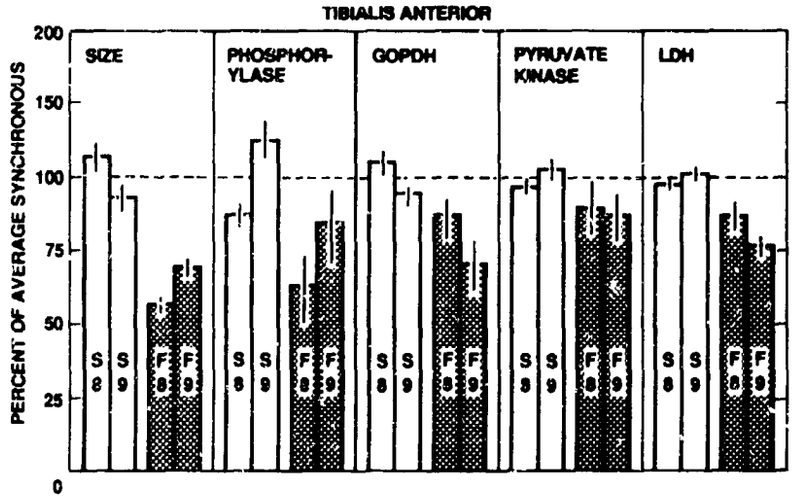

Figure 6: Comparison of synchronous and flight TA fibers in regard to size (dry weight per unit length) and the levels on a dry weight basis for four enzymes of glycolysis and glycogenolysis. Abbreviations as in Fig. 1.

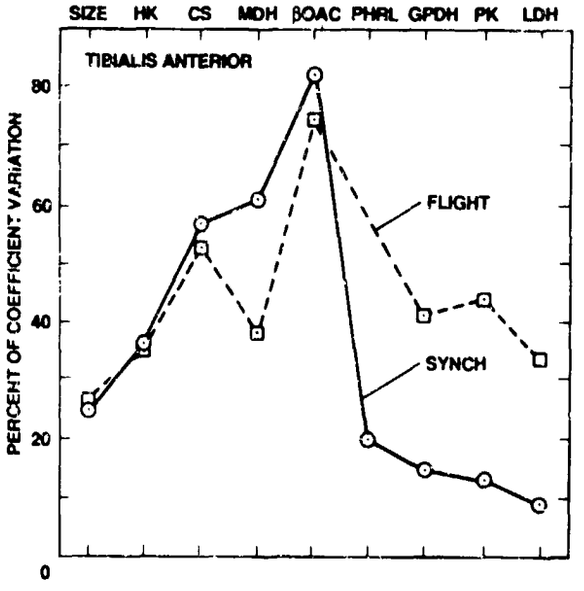

Figure 7: Average coefficients of variation for size, and the levels of eight enzymes of individual fibers from the two flight and two synchronous TA muscles of Figures 5 and 6.

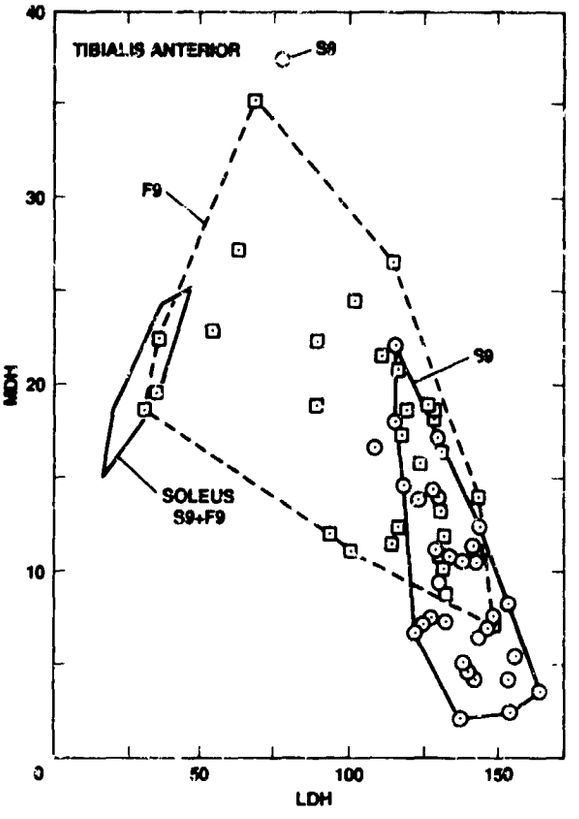

Figure 8: Malate dehydrogenase (MDH) and lactate dehydrogenase (LDH), mol h^{-1} kg^{-1} (dry wt.), plotted against each other for individual fibers from TA muscles S9 and F9. The domain occupied by 6 soleus S9 and 6 soleus F9 fibers is also indicated but without showing the individual values. Activities are mol h^{-1} kg^{-1} (dry wt.).

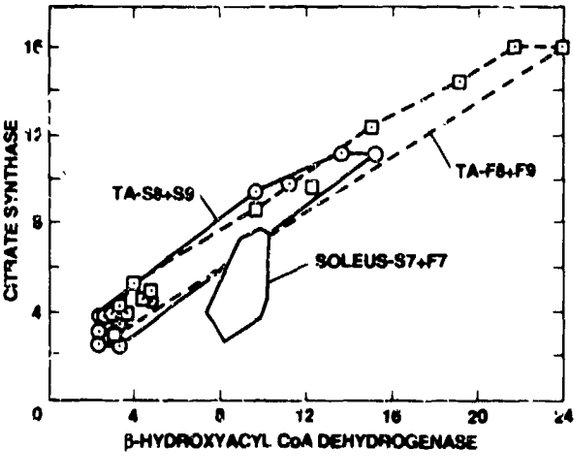

Figure 9: Citrate synthase and ß-hydroxyacyl CoA dehydrogeanse, mol h^{-1} kg^{-1} (dry wt.), plotted against each other for individual fibers from TA muscles S8, S9, F8 and F9. Six fibers were analyzed from each muscle; the flight fibers are indicated by x, the synchronous fibers by 0. Also indicated is the domain without showing individual values for 16 S7 and 16 F7 soleus fibers.

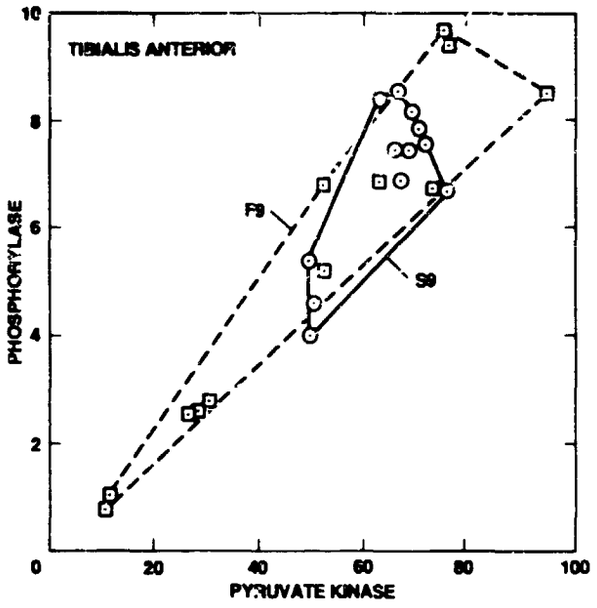

Figure 10: Phosphorylase and pyruvate kinase, mol h^{-1} kg^{-1} (dry wt.), plotted against each other for TA fibers.

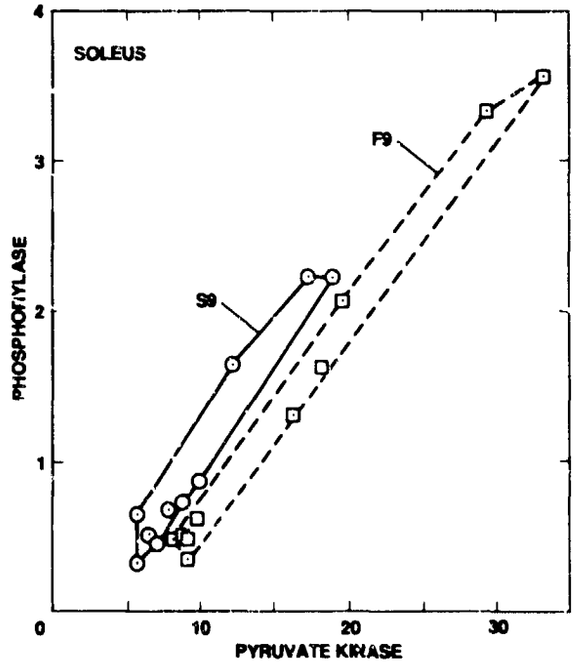

Figure 11: A plot similar to Figure 10 for 10 S9 and 10 F9 soleus fibers.

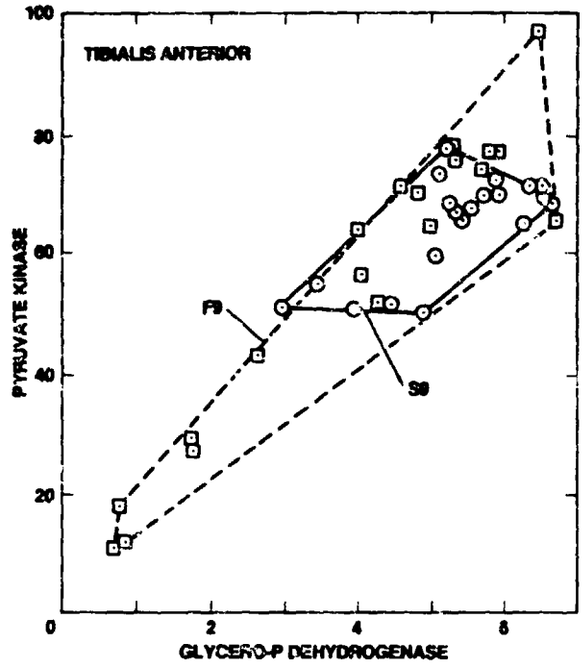

Figure 12: Pyruvate kinase and glycerophosphate dehydrogenase (GOPDH), mol h^{-1} kg^{-1} (dry wt.), plotted against each other for 20 S9 and 19 F9 TA fibers.

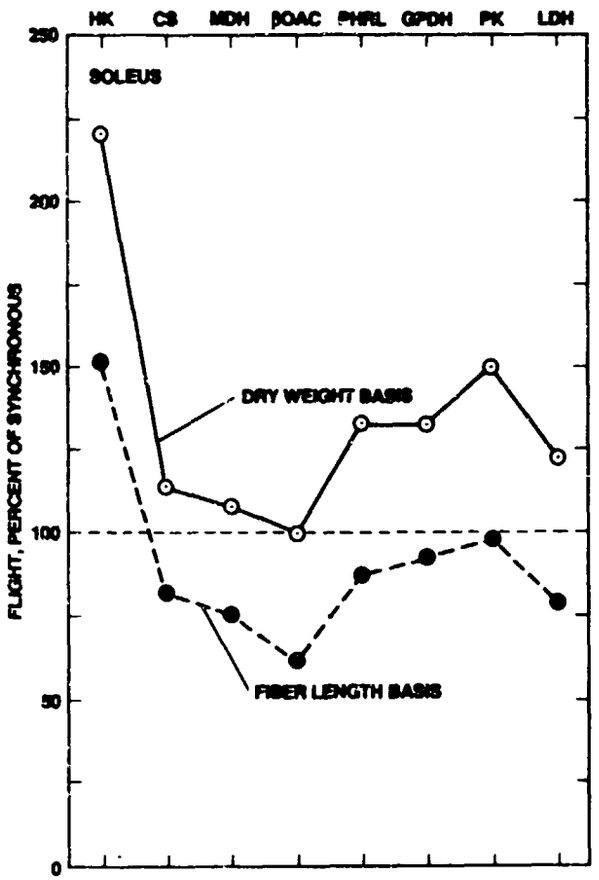

Figure 13: Average enzyme levels for soleus fibers from the two synchronous and two flight animals compared on the basis of dry weight and on the basis of fiber length.

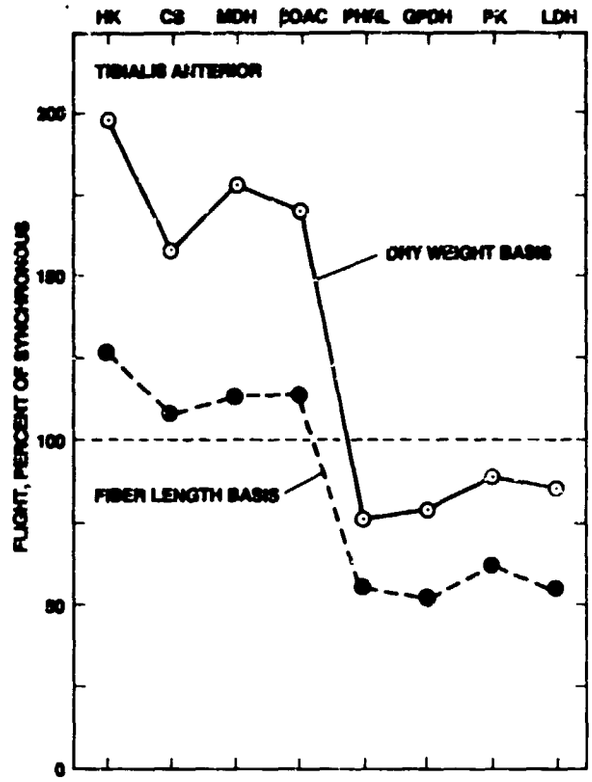

Figure 14: Average enzyme levels for TA muscles from the two synchronous and two flight animals compared on the basis of dry weight and on the basis of fiber length.

EXPERIMENT K-6-21

PART II: METABOLIC ENZYMES OF HIPPOCAMPUS AND SPINAL CORD

INTRODUCTION

The question of possible enzyme changes due to exposure to microgravity is much more complicated in the case of the central nervous system than it is for skeletal muscle. The brain is enormously complex. Valid comparisons must be made between exactly the same regions of control and flight brains, otherwise natural differences will confuse the issue.

METHODS

We have measured 9 different enzymes in 6 regions of the hippocampus and 4 and 5 enzymes in 5 regions of the spinal cord (a total of almost 500 quantitative measurements) and found differences that may be meaningful in three enzymes in a few areas of flight brains. However, statistical proof (either way) will require substantially more data. Probably, the present results should be regarded as a guide to future and more definitive studies.

Wherever possible, the assays for a number of enzymes were made in duplicate with aliquots from an extract of a single, relatively large, tissue sample, made with a medium similar to that described for muscle (Part I). For Table 1, the dry tissue samples weighed about 0.2 µg and were dispersed in 5 µl of extraction medium. The assays were made with 0.2 µgl aliquots of these extracts, each equivalent to about 8 ng of dry tissue. This methodology was not possible or practical in all cases. Glutaminase, for example, is difficult to stabilize in extracts, and enzymes of low activity are easier to measure accurately with samples added directly into the assay reagent.

RESULTS

The six enzymes of the hippocampus shown in Figure 4 of Part I were in most cases remarkably similar in flight and control (vivarium) brains. ß-hydroxyacyl CoA dehydrogenase was 35% lower in the molecular layer of CA1 of the flight brain, and should be reinvestigated, however, the other two enzymes of oxidative metabolism in this region were within 10% of the control.

GABA and two enzymes of GABA metabolism were measured in the hippocampus of two vivarium and two flight animals (Tables 2 and 3). The GABA levels are probably not definitive, since they are known to be sensitive to post mortem increase. The glutamate decarboxylase activities were quite variable, nevertheless it probably should not be ignored that the levels for the flight samples from all of the hippocampal regions were on average 30% higher than for the controls. This result is strengthened by the data for GABA transaminase: in each of the six hippocampal areas assayed the average activity for the two flight animals was higher (by 8% to 35%) than the average of the two vivarium controls. The overall average difference was plus 16%.

Another positive result for hippocampus concerns glutaminase. In CA1, average values for the three regions assayed were 25% to 59% higher in the flight than the control tissues (Table 2). In fascia dentata (Table 3), the differences were much smaller (+2% to +10%) and probably have little meaning.

The spinal cord data are limited to one (synchronous) control and one flight animal. The higher aspartate aminotransterase values for the pyramidal tract and outer dorsal horn for the flight specimens would be worth further investigation. The same is true for the lower glutaminase levels in the dorsal column and pyramidal tract of the flight animal and the higher level in the outer dorsal horn. All three differences are statistically significant ($P<0.01$), but they only concern single animals.

PRECEDING PAGE BLANK NOT FILMED

CONCLUSION

To reiterate, these somewhat fragmentary results suggest that future, more extensive, studies of this type with selected and carefully matched brain areas, should be quite rewarding.

TABLE 1

SIX ENZYMES IN SIX REGIONS OF THE HIPPOCAMPUS

	Hexokinase		G6PDH		Citrate Synthase		MDH		BOAC	
CA1	V10	F8	V10	F8	V10	F8	V10	F8	V10	F8
Pyramidalis	3.4	4.1	0.051	0.052	6.9	6.0	8.4	10.0	0.51	
0.59	8.8	8.4								
Radiata	6.6	6.3	0.056	0.058	9.4	7.7	9.9	8.1	0.52	
0.49	9.7	9.2								
Molecularis	5.7	5.7	0.057	0.061	10.1	9.4	10.5	10.3	1.05	
0.68	10.4	8.2								
Area dentata										
Molecularis	6.2	6.0	0.060	0.055	10.9	9.8	13.3	11.3	1.00	
.095	12.1	11.1								
Granularis	3.9	4.4	0.057	0.055		8.0	9.3	9.9	0.76	
0.74	10.4	11.3								
Hilus	6.0	5.7	0.053	0.047	8.1	7.1	8.3	9.1	0.62	
0.62	9.2	8.2								

Activities are moi h^{-1} kg^{-1} (dry wt.) at 20°. Abbreviations are: G6PDH, glucose 6-phosphate dehydrogenase; MDH, malate dehydrogenase; ßOAC, ß-hydroxyacyl CoA dehydrogenase; amino-T, aminotransferase.

TABLE 2

GLUTAMINASE, GABA AND TWO ENZYMES OF GABA METABOLISM IN FOUR LAYERS OF CA1 OF THE HIPPOCAMPUS

		GABA	GAD	GABA trans	Glutaminase
		mmol kg^{-1}	mmol h^{-1} kg^{-1} (dry)		
Pyramidalis	V9	11±3	59±2	471±5	2390±200
	V10	17±3	53±1	441±34	1670±60
	F8	39±7	63±8	529±36	3230±290
	F9	24±2	56±4	483±12	3240±220
Radiatum	V9	30±2	12±2	265±16	4810±120
	V10	12±1	27±0.3	259±15	4020±260
	F8	21±3	38±1	290±18	5600±80
	F9	22±1	28±1	277±13	5620±240
Lacunosum	V9	27±5	16±1		
	V10	13±1	28±2		
	F8	39±6	49±5		
	F9	19±2	29±2		
Molecularis	V9	27±5	34±2	394±20	3700±100
	V10	26±2	48±4	210±10	3960±230
	F8	25±8	52±4	269±6	4580±180
	F9	20±2	49±5	421±21	5270±240

Abbreviations: V, vivarium; F, flight; GAD, glutamate decarboxylase; trans; transaminase. GAD activity was measured at 38°C, the activities for the other two enzymes were measured at 20°C. Standard errors are shown for usualy 3 samples.

TABLE 3

GLUTAMINASE, GABA AND TWO ENZYMES OF GABA METABOLISM IN THREE REGIONS BY FASCIA DENTATA

		GABA	GAD	GABA trans	Glutaminase
		$mmol^{-1}$	$mmol\ h^{-1}\ kg^{-1}$ (dry)		
Granular	V9	27±4	59±1	436±31	2500±80
	V10	36±2	42±1	384±16	1820±150
	F8	22±1	41±4	442±5	2210±100
	F9	28±2	55±13	491±8	2540±330
Molecular	V9	19±1	50±6	289±43	5240±330
	V10	23±2	30±2	320±7	4350±330
	F8	25±1	81±8	386±18	4880±410
	F9	29±1	48±2	437±19	5250±550
Hylus	V9	21±2	30±3	364±38	4980±210
	V10	26±1	29±1	284±11	3070±310
	F8	19±1	30±2	356±12	4140±210
	F9	23±2	22±2	398±13	4050±270

TABLE 4

FIVE ENZYMES IN FIVE REGIONS OF THE SPINAL CORD AT ABOUT T11

		Hexo-kinase	G6PDH	Citrate synthase	Aspart amino-T	Glutam-inase
		mol h^{-1} kg^{-1} (dry), 20°C				
Dorsal Col.	S4	0.10	0.262	0.94	3.28	0.366±0.023 (8)
	F3	0.19	0.256	0.88	3.36	0.276±0.018 (11)
Pyram tract	S4	1.34	0.237	4.45	8.5	0.819±0.066 (4)
	F3	1.37	0.261	4.61	11.3	0.612±0.037 (4)
Rexed I-III	S4	3.52	0.263	6.66	12.7	2.06±0.11 (14)
	F4	3.28	0.285	6.29	16.6	2.57±0.13 (12)
Rexed IV-V	S4	3.54	0.228	6.61	16.4	
	F3	3.40	0.276	7.31	16.8	
Rexed VII	S4	3.32	0.254	6.21	15.1	
	F3	3.92	0.253	9.52	15.4	

Data for the first four enzymes are from duplicate assays made with 0.05 or 0.1 µl aliquots from an extract of about 0.5 µg of dry tissue made with 2 µl glycerol-detergent medium. The glutaminase assays were made with individual samples of about 25 ng dry weight.

N90-26475

EXPERIMENT K-6-22

GROWTH HORMONE REGULATION, SYNTHESIS AND SECRETION IN MICROGRAVITY

PART I: SOMATOTROPH PHYSIOLOGY

PART II: IMMUNOHISTOCHEMICAL ANALYSIS OF HYPOTHALAMIC HORMONES

PART III: PLASMA ANALYSIS

Principal Investigator:

R. Grindeland
NASA-Ames Research Center
Moffett Field, California 94035

Co-Investigators:

W. Vale
Salk Institute
LaJolla, California

W. Hymer
Pennsylvania State University
University Park, Pennsylvania

P. Sawchenko
Salk Institute
LaJolla, California

M. Vasques
NASA-Ames Research Center
Moffett Field, California 94035

I. Krasnov
A. Kaplansky
I. Popova
Institute of Biomedical Problems
Moscow, USSR

I. Victorov
Brain Research Institute
Moscow, USSR

EXPERIMENT K-6-22

PART I: SOMATOTROPH PHYSIOLOGY

R. Grindeland, W. Hymer, I. Krasnov, I. Victorov, and A. Kaplansky

INTRODUCTION

Muscle atrophy, decreased bone growth and calcium loss occur as a result of long term spaceflight. Since pituitary growth hormone (GH) controls the activity of both muscle and bone, effects of spaceflight on GH cell function have received some attention. For example, in the Space Lab 3 (SL-3) mission of 1985, pituitary glands from rats flown in space for 7 days were enzymatically dissociated into single cell suspensions upon return of the animals to Earth (1). Several structure-function tests were applied to these GH cells to determine if flight had affected their capacity to synthesize and release hormone. Although the percentage of GH cells from the 200 gm rats was not affected, the hormone content per somatotroph was greater in flight cells than in the ground based control cells. In culture, GH cells from the flight animals released about 30% less hormone. Furthermore, when implanted into the cerebral ventricles of hypophysectomized rats, GH cells from the flight group released about 50% less hormone into the recipient host than similarly treated control cells. Taken together, these results suggested that GH cells from the flight animals had experienced a partial shutdown in hormone secretion. Finally, HPLC fractionation of culture media showed that a high molecular weight GH variant, rich in bioactivity, was much less prevalent in the experimental group.

The impact of spaceflight on GH cell function was also addressed in the flight of STS-8 (1983) in which rat pituitary cells were flown in sealed tubes maintained at 37°C in a middeck locker. Upon return to Earth, GH secretion from flight cells was reduced about 20 fold compared to controls. The idea that microgravity specifically and directly affected GH secretion was supported by the finding that prolactin (PRL) release from other cell types in these same suspensions was unaffected by flight (2). Thus results from both space exper- iments offered evidence that GH cell function was attenuated in microgravity.

The Cosmos 1887 mission offered an opportunity to repeat the SL-3 experiment. The design of this new study was dictated by the following considerations: 1) five pituitary glands were available for study, 2) ~2 x 10^6 cells could be prepared from each gland and 3) a number of structure-function tests, each requiring different numbers of cells, were possible. Some of these same considerations arose in the design of the earlier SL-3 experiment. In that study, a decision was made to combine all of the glands from the flight animals prior to tissue dissociation. This strategy was flawed because it precluded statistical comparison of the differences actually found in GH cell function between flight and ground-based controls. Accordingly, a decision was made to modify the experimental design of the 1887 flight so that the GH release from cells of the five individual glands of the flight animals could be compared in a statistically meaningful way with hormone release from cells of the five glands of the ground control animals. Listed in Table 1 are the procedures used to test GH cell structure/ function and the approximate numbers of cells required for each test. In order to accomplish these experimental goals, some cells from each gland were cultured individually while the remaining cells from each gland were then pooled with the others from the same treatment groups for subsequent morphological analyses and transplantation study.

In summary, the overall objective of the 1887 mission was to determine if the results of the SL-3 experiment were repeatable. Additionally, we hoped to be able to extend the earlier findings in

PRECEDING PAGE BLANK NOT FILMED

light of the longer duration of flight. Finally, the design of the 1887 experiment was modified to permit statistical analysis of the GH secretion data.

METHOD

1. Tissue Transportation.

Four experiments were done, each involving pituitary glands from 5 animals. These experiments, identified as using glands from flight rats (F-Cos), synchronous controls (S-Cos) or 2 sets of vivarium controls (V-1 Cos and V-2 Cos), were done separately at 2-3 day intervals. Glands from the F-Cos animals were shipped to Moscow from the nominal recovery site in individual teflon vials containing 22 ml of S-MEM + 0.1% BSA + 25mM HEPES (pH 7.4) + 0.2% $NaHCO_3$ + Gentamycin Sulfate (10 µg/ml) + Penicillin (100 U/ml) /Streptomycin (100 µg/ml) (PS) at 37±1°C. The time between tissue removal and arrival in Moscow was 30 hrs. Identical intervals were used for all groups. The cell free transport medium from each vial was frozen and kept at -20C until analysis for GH.

2. Pituitary gland dissociation.

Each gland was minced with a sterile razor blade into n1 mms pieces and dissociated into single cell suspensions in a solution containing 1 ml of S-MEM + 0.3% crude Trypsin (Difco 1:250) + 0.3% BSA + 20 µg DNase (Type I, Sigma) + PS according to the method of Wilfinger, et al. (3). Modifications included hand agitation over 2-3 twenty minute periods with intervening washes. Cells were liberated from the tissue pieces by trituration with a siliconized Pasteur pipette fifty times after each wash step. After each trituration step the remaining tissue pieces were re-exposed to fresh enzyme solution. In all cases complete tissue dissociation occurred after 1 hr. Cells from each gland were numbered consecutively (i.e., rat 1 - 5). There is no relationship between cells from rat #1 in the F-Cos group and rat #1 in the S or V-Cos series. Cell counts and viabilities from each gland were estimated by hemocytometry using phase contrast microscopy (4).

3. Distribution of cells from individual glands

a. Cell blots. Cells (5 x 10^3/blot) from each of the 5 pituitary glands were cultured in humidified dishes on the surface of a 2x2 cm piece of Immobilon membrane in DMEM + 0.025% BSA + 25 mM HEPES for 2 hrs. at 37°C in 95% air:5% CO_2. After this time the media were removed and the paper processed for GH and prolactin (PRL) immunostaining exactly as described previously (5). Specific polyclonal antisera (cross reactivity < 0.3%) to these hormones were used at dilutions of 1:60,000 for GH and 1:80,000 for PRL. Quantitation of secretion from individual cells was accomplished by image analysis using rGH RP-2 or rPRL RP-3 (NIADDK) as reference standards.

b. Intracellular hormone. Cells ($2x10^5$) were incubated overnight at 4°C in 500 ul of 0.01 N $NaHCO_3$ (n=3/gland). After centrifugation (1400 xg, 4°C, 30 min) the supernatant fraction containing extracted hormone was flash frozen and kept at -20°C until analysis. The 1400 xg pellet was sonicated (40% of maximum power for 5 sec.) in 250 ul of $NaHCO_3$ and incubated overnight at 4°C. The amount of GH in the re-extracted pellet accounted for 15% of the total recovered hormone.

c. Cell culture. Cells ($5x10^4$) in 250 ul of either DMEM + 5% calf serum and antibiotics or chemically defined medium [DMEM + 0.2% $NaHCO_3$ + 25 mM HEPES + Insulin 6.25 µg/ml, Transferrin 6.25 µg/ml, Selenium 6.25 ng/ml, BSA 1.25 mg/ml, Linoleic acid 5.4 µg/ml + 0.5 nM $MnCl_2.4H_2O$, 0.5 nM $(NH_4)_6MO_7O_{24}.4H_2O$, 0.25 nM $NiSO_4.6H_2O$, 15.0 nM H_2SeO_3, 250.0 nM $Na_2SIO_3.9H_2O$, 0.25 nM $SnCl_2$, 2.5 nM $Na_3VO_4.4H_2O$, 50.0 nM $CdSO_4$ + Aprotinin 1 TIU/ml + T_3, $1x10^{-7}$ M + Gentamycin sulfate (10 µg/ml) + Penicillin (100 U/ml)/Streptomycin (100 µg/ml)] were cultured in 96 well plates for 3 days in a humidified atmosphere of 5% CO_2:95% air at 37°C.

There were 4 wells/treatment group. After 3 days media were removed from the wells, centrifuged to pellet any non-adherent cells and the supernatant fraction frozen for subsequent hormone analysis. Fresh medium (150 ml) was added to each well. Another aliquot of fresh medium (100 ml) was added to each microfuge tube (no visible cell pellets) and subsequently transferred back to the appropriate well for an additional 3 day culture period. After another 3 days the culture medium harvesting procedure was repeated. GH remaining in the cells after 6 days was measured in $NaHCO_3$ extracts prepared as described previously.

d. Hormone Assays. GH levels in cell extracts and culture media were determined by enzyme immunoassay exactly as described previously (6). In some cases (see text), the biological activity of the GH in the sample was measured using the tibial line assay of Greenspan (7).

e. HPLC. Serum free culture media from 3 and 6 day samples (S-COS, F-CCS) were chromatographed (0.5/ml/min) by gel permeation high performance liquid chromatography (300 SW Protein Pak column; Waters) using 0.1 M phosphate, pH 6.5 in 0.3 M NaCl and 10% 1-propanol buffer system. Fractions were dialyzed against 0.04 M Tris buffer, pH 7.5, lyophilized and reconstituted in PBS prior to immunoassay.

4. Distribution of cells after pooling.

After the cells from each of the 5 animals were used as described in step 3, the remainder were pooled for morphological and implantation studies.

a. Hollow fiber implantation. Cells ($2x10^5$) were loaded into 10 mm long XM-50 Amicon hollow fibers exactly as described previously (8). In the F-Cos experiment, 10 fibers were loaded with medium (1.5 ml S-MEM + 0.1% BSA) and 10 fibers were loaded with cells in the same medium. Each of these fibers was implanted into the lateral cerebral ventricle of a 100 gm male hypophysectomized rat. This experiment was repeated for the S-Cos series. In each case the time between hypophysectomy and hollow fiber implantation was 7 days. Animals were housed in individual filter top cages at 23-24°C. Animals were killed 10 days post implantation and tibia prepared for staining and measurement of the epiphyseal cartilage plate width. Hollow fiber placement was verified by visual inspection of brain slices. Selected organs and muscles of the recipients were weighed at this time.

b. Morphological analyses. Flow cytometric immunofluorescence was done exactly as described previously (9). Basically this procedure involved fixation of cells in suspension ($2x10^5$), permeabilization of cell membranes with Triton X-100, incubation in antiserum to rat GH (1:10,000) overnight, incubation in FITC conjugated second antibody, counterstained with propidium iodide, and analyzed on an Epics V flow cytometer. Immunocytochemistry on cells ($5x10^4$) attached to poly-L-lysine coated coverslips was done using the diaminobenzidene procedure described previously (9).

RESULTS.

Validation of procedures for tissue handling: preflight experiments.

Since the time that elapsed between removal of the pituitary glands at the landing site and arrival in Moscow was expected to be ~24 hrs., preliminary experiments were done at Penn State University to determine the effects of 1) medium composition and 2) temperature on subsequent GH cell function in vitro. In these experiments glands were stored at either 4°C or room temperature in Spinners minimum essential medium (S-MEM) containing 0.1% bovine serum albumin (BSA) or 5% calf serum (CS) buffered with 25 mM HEPES (pH 7.4) and fortified with antibiotics.

In each of two experiments we examined the effects of 26 hr. pituitary gland storage on 1) subsequent cell recovery (after trypsinization); 2) the percentage of GH cells; 3) GH cell size and cytoplasmic granularity; 4) GH release into the storage medium; and 5) GH release from somatotrophs over a 3 day culture period. In each experiment the tests of the GH cells after 26 hrs (experimental) were compared with that of GH cells prepared from glands obtained immediately after sacrifice (control).

The data (Table A1) established that storage of the glands in the simpler BSA medium at room temperature yielded the same number of somatotrophs as the more complex serum-containing medium. They also showed storage at room temperature in BSA gave satisfactory results. The data in Table A2 established that less GH was released from glands stored at room temperature than at 4°C.

The flow cytometer was used to study the effect of storage on GH staining intensity was well as cell size. These parameters were especially important to the 1887 mission since it is possible with this instrument to objectively categorize and study 20,000 cells in a few minutes. The data in Table A3 showed that the level of specific GH staining intensity in somatotrophs from stored glands was not significantly different from cells of non-stored glands. However, storage reduced the forward angle light scatter (FALS) peak. Since this scatter signal is related to cell size, the data established that GH cells of the stored glands were smaller than controls. It is not possible, however, to make definitive statements about the magnitude of the size change-only that it occurred. Finally, the effect of gland storage on GH secretory capacity is offered in Table A4. In both experiments GH release was reduced 31%. Since the absolute levels of released hormone were about the same for all treatment groups, we conclude that secretory rates were not drastically affected by previous storage conditions.

The preflight data in Tables A1-A4 established the feasibility of storing intact pituitary tissue for 26 hrs. prior to enzymatic dissociation to obtain GH cells. On the basis of these preflight data the decision was made to store glands from the 1887 Cosmos mission in S-MEM + 0.1% BSA at room temperature.

The various tests that were applied to pituitary cells from the Cosmos mission (Table 1) covered a time sequence that spanned a few minutes to 7 days. The results of these studies are presented in that same sequence.

RESULTS FROM THE COSMOS 1887 FLIGHT - GROWTH HORMONE

GH released into storage medium.

The concentration and total amount of immunoactive growth hormone (iGH) and bioactive growth hormone (bGH) released into the 30 hr. storage medium (i.e. the time that elapsed from animal kill to pituitary gland dissociation) in both flight (F-Cos) and synchronous control (S-Cos) groups are given in Table 2. While there was a 25% increase in iGH levels released from glands of the F-Cos group relative to the S-Cos group ($p < .05$) there was a 60% decrease in bBH levels released from the flight group ($p < .001$).

GH cell morphology

The yield of cells from individual pituitary glands in the F-Cos group averaged 1.98±0.2/gland. Cell yields from glands in the S-Cos and two vivarium (V-1 Cos and V-2 Cos) were not significantly different. Cell viability, measured by the phase contrast microscope refractility method (4), averaged 93±0.7% in the F-Cos group. Cell viabilities in the other groups were not different.

The percentages of GH cells prepared from glands in the different groups, based on counts of 50,000 cells/treatment group, was not different (Table 3). However, the staining intensity of the GH cells (as measured by the marker index (see legend to Table 3) in the F-Cos group was 2x greater than that of

cells in the S-Cos group. The increased intensity of specific cytoplasmic GH fluorescence is also documented by the morphological appearance of cells shown in Fig.1. These results suggest, but do not prove, that there was more GH/cell in the flight group. GH cells in the F-Cos group tended to be larger, as evidenced by the magnitude of their FALS signal. However the PLS signal, known to reflect cytoplasmic granularity (4), was not different between GH cells in any of the 4 treatment groups.

An example of the appearance of GH cells bound to poly-L-lysine coated slides and stained by the immunoperoxidase method is shown in Fig. 2 (top). These cells have intense dark reaction product (GH) in their cytoplasm. One hundred such cells, selected at random from both the F-Cos and S-Cos groups, were studied by image analysis to determine the area percentage of the cell occupied by specific GH reaction product Fig. 2 (bottom). A majority of the cells in the S-Cos group had 20-40% of their area occupied by GH; this number was 60-80% in the case of F-Cos cells (Fig. 3). Thus specific hormone staining of cells both in suspension (Fig. 1, Table 3) and attached to glass (Fig. 3) showed changes in intracellular patterns of GH in the flight group.

GH cell culture (short term)

The cell blot assay (5) permits quantification of hormone secretion from individual pituitary cells. Shown in Fig. 4 are zones of hormone secretion around GH cells from the F-Cos and S-Cos groups incubated on Immobilon membrane for 2 hrs. at 37°C. These images indicate that considerable variability exists in secretion from individual cells. The average amounts of iGH secreted from 35 single cells selected at random from each of the 5 animals in both treatment groups are shown in Fig. 4. Also shown in this figure are the combined secretion data from all of the cells in the F-Cos and S-Cos groups. The increased iGH release from the F-Cos cells relative to that from the S-Cos cells was statistically significant ($p < 0.05$).

GH cell culture (long term): Immunoactive GH

The issue of in vitro GH secretion from cells of individual flight animals was considered crucial to the overall experimental design and data interpretation. Levels of iGH release from cells of individual animals were surprisingly consistent within any given treatment group (Fig. 5). These data also revealed: 1) that levels of secreted iGH were, in the case of serumless medium, ~70% of those in serum-containing medium; 2) that, relative to the first 3 day culture period, levels of hormone released from cells in the S-Cos group were 2-3x greater during the second 3 day culture period and 3) that flight cells did not show the same corresponding increase in iGH release during the second 3 day culture period. When the data from the cell cultures from individual glands were combined according to treatment group, no significant differences in iGH secretion between flight and synchronous control cells were found in the initial culture period (Fig. 6 Top). However, iGH release from the S-Cos cells was significantly ($p < .05$) greater than that from the flight cells during the second culture period. This difference was found in both serum and serum-free cultures. Shown in Table 4 are results of two independant immuncassays done several months apart. They show that the data obtained in assay #1 was repeatable.

Representative examples of the appearance of cells from both F-Cos and S-Cos groups cultured in serum and serumless media are shown in Fig. 7A and 7B. Cell clumping and fibroblast growth were dominant features of the serum-containing cultures. These features were much less frequent in serumless cultures. There were no obvious differences in either the appearance or growth characteristics between the F-Cos and S-Cos cells in culture.

The results of the 2 vivarium control cell culture experiments, in comparison to the F-Cos and S-Cos cells, are also shown in Fig. 6 (Bottom). In general, iGH release from cells in the 2 vivarium experiments was greater than iGH secretion from either F-Cos or S-Cos cells during the initial culture period. However, this difference was not maintained in the second culture period.

GH cell culture (long term): bioactive GH

The sensitivity of the tibial line bioassay precluded analyses of individual culture wells. Furthermore, since 50-75% of the 250µl in each culture well was used for immunoassay and HPLC analyses we decided that the best way to obtain estimates of secreted bGH was to pool all of the remaining samples within the flight, synchronous, or vivarium groups. That is to say, for example, serum containing and chemically defined media from 3 and 6 day cultures of cells from the F-Cos groups were all combined. This strategy generated four tubes (F-Cos, S-Cos, V-1, V-2), each containing 4.0-4.5 ml. One ml was injected into a hypophysectomized rat (n=4/group) according to the method of Greenspan. The data in Table 5 clearly show that the levels of bGH released from the F-Cos cells in vitro were below the sensitivity of the assay, where as those from the other three groups were sufficient to increase tibial plate width.

Intracellular iGH

The data in Table 6 offer information relative to the intracellular contents of iGH before and after culture. They also show the capacity of the cells to synthesize iGH in culture. In general the results indicate that the flight cells, relative to S-Cos cells, 1) initially contained the same amount of iGH; 2) contained less iGH at the end of culture and 3) synthesized less iGH in culture. Levels of bGH in these samples could not be measured due to insufficient sample volume.

GH release from transplanted cells using hollow fiber methodology (8).

Over a 10 day period, hypophysectomized rats implanted with pituitary cells from the S-Cos group secreted 0.21 µg bGH as estimated by tibial line responses of the host (Table 7). Rats implanted with the same number of cells from the F-Cos group secreted significantly less GH in vivo ($p < 0.05$).

The weights of various organs and muscles of animals receiving cell implants are compared with their corresponding control groups in Fig. 8. Rats implanted with cells from the S-Cos group tended to have greater thymus and testes weights than their controls. Rats implanted with cells from the F-Cos group also showed increases in thymus weight. In addition, livers and muscles of the F-Cos cell receipients tended to be heavier than controls. Except for the livers, these differences were not statistically significant.

HPLC fractionation of serumless culture medium from S-Cos and F-Cos cells.

The percentage distributions of GH in different molecular weight fractions obtained by HPLC size exclusion chromatography are given in Table 8 and a typical protein elution profile shown in Fig. 9. In both the 3 and 6 day culture medium samples, most of the hormone was recovered in a fraction (18-62 kD) that would be expected to contain monomeric GH (22 kD). These distributions were remarkably similar between F-Cos and S-Cos samples. A greater percentage of high molecular weight GH was detected in the 3 day than the 6 day cultures.

RESULTS FROM THE COSMOS 1887 FLIGHT - PROLACTIN

PRL released into storage medium

The concentration of immunoactive prolactin (iPRL) released into the 30 hr. storage medium was not significantly different between F-COS (351±63 ng/ml) and S-COS (307±45 ng/ml) samples.

PRL cell morphology

The percentages of PRL cells prepared from glands in the different groups, each based on counts of 25,000 cells, was ~15% higher in the F-COS group (Table 9). This increased percentage is considered significant. PRL cells in flight group showed slightly less intense PRL immunofluorescence staining than those from S-COS, a result which is probably of marginal significance. Since the FALS channels are on linear scales, the size differences between F-COS and S-COS cells again appears marginal. On the other hand, the increased PLS peak channel in the F-COS group (Table 9) indicates that the cytoplasmic "granularity" of PRL flight cells is greater.

PRL cell culture (short term)

The cell blot assay (5) permits quantification of hormone secretion from individual pituitary cells. Shown in Fig. 10 are zones of hormone secretion around PRL cells incubated on immobilon membrane for 2 hrs. at 37°C. These images are representative of many, and document that considerable variation exists between cells. The average amounts of iPRL secreted from 35 single cells selected at random from each of 5 animals in both treatment groups are shown in Fig. 10. The solid bars in panels E and F depict the magnitude of the average amount of PRL secreted from the 5 rats in F-COS and S-COS groups. On average, the increased release of iPRL from F-COS cells relative to S-COS cells was statistically significant.

PRL cell culture (long term)

Levels of PRL released from pituitary cells of individual rats tended to be surprisingly consistent within any given treatment groups (Fig. 11). These data also showed that about 5x more PRL was released from cells cultured in serum containing vs chemically defined media and that the levels of secreted hormone were always significantly higher in the S-COS groups (Fig. 12).

Intracellular PRL

The levels of intracellular PRL in F-COS, S-COS and V-COS groups before and after culture were not significantly different (Table 10). Furthermore, cells cultured in serum-containing media contained n3 times more hormone at the end of 6 days than counterparts cultured in chemically defined medium.

DISCUSSION

The objectives of the 1887 mission were a) to determine if the results of the SL-3 pituitary gland experiment (1) were repeatable and b) to determine what effect a longer mission would have on the rat pituitary gland GH "system". In the 1887 experiment two issues were considered especially important. First, it was recognized that cells prepared from individual rat pituitary glands should be considered separately so that the data from the 5 glands could be analyzed in a statistically meaningful way. Second, results of the SL-3 flight involving the hollow fiber implant and HPLC GH-variant experiments suggested that the biological activity of the hormone had been negatively affected by flight. The results of the 1887 experiment documented the wisdom of addressing both issues in the protocol. Thus, the reduction in secretory capacity of flight cells during subsequent extended cell culture on Earth was documented statistically (Fig. 6) and thereby established the validity of the SL-3 result. The results of both flight experiments thus support the contention that there is a secretory lesion in pituitary GH cells of flight animals.

The issue of the biological (vs immunological) activity of the GH molecule, as it might be affected by flight, is complicated. Certainly this interesting problem is not well understood on Earth. The large discrepancy between activities of GH measured by bioassay vs immunoassay was first described by Ellis and Grindeland in 1974 (10). Since then progress has been slow and hampered by lack of

availability of sensitive GH bioassays. In this context, it is relevant that the GH cell hollow fiber implant method (8) and 3T3 cell assay (11) are established GH bioassays in the literature. Indeed, both were used in the SL-3 experiment and together indicated that release of a high molecular weight GH variant, rich in 3T3 bioactivity, was compromised as a result of spaceflight (1). It would have been desirable to perform 3T3 assays on 1887 samples; unfortunately this assay lost reliability in the years following the SL-3 flight. Thus we were forced to rely solely on the tibial line bioassay whenever possible in the 1887 tests.

Perhaps the most interesting finding to emerge from all of the 1887 pituitary data was the marked and consistent inhibition in release of bGH from the flight cells. The magnitude of this suppression was always greater than that measured by GH immunoassay. Sometimes the responses were completely non-parallel. In one instance, for example, release of iGH was significantly elevated in F-COS samples while the release of bGH was significantly depressed (Table 2).

The relationship between timing of the post-flight tests (SL-3 and 1887) and the secretory responses is depicted in Fig 13. In sum, these data indicate the importance of measuring bGH since the most dramatic differences between flight and control cells were found using GH bioassay.

What is the relationship between bioactive GH and the pituitary gland GH "system"? Several years ago it was shown that two subpopulations of GH cells in the rat pituitary could be separated on the basis of differences in density (12). Type I cells were lightly granulated and less dense (1.06-1.07 g/cm^3) than type II cells (>1.07 g/cm^3) which were laden with secretion granules. Later we found that the biological/immunological activity ratio of the GH released from type II cells in culture was consistently 4-5x, whereas that from band I cells was <1 (13).

More recently, other experiments support the hypothesis that high molecular weight S-S aggregates of the monomeric GH molecule, released specifically from type II cells, could represent the bioactive form of the GH molecule (14). Given these data, we would speculate that microgravity specifically affects type II somatotrophs in their ability to release bGH. Clearly, however, the suppression is not 100%! The mechanism of suppression is unknown, but both flight experiments offer important clues. First, when GH cells from flight animals are transplanted to a GRF-rich site (i.e. ventricles of the hypophysectomized rat), they do not respond as well to peptide stimulation. This may reflect a post flight receptor defect in a specific GH cell subpopulation that does not readily recover. Second, image analysis of F-COS GH cells showed that the hormone occupied more cytoplasmic area. A "relaxation" of the network supporting the secretory granules might lead to the result obtained in Fig. 3. Whether such data could be interpreted to reflect a microgravity effect on microtubules in somatotrophs is attractive, but of course highly speculative at this stage. Third, increased immunofluorescent staining of GH cells in the flight group (Fig. 1) could reflect a flight induced change in packaging of the GH molecules within the secretory granule. We speculate that looser packing in the crystal structure of the granule might account for a) less S-S bridging between molecules (thereby increasing sites for antibody recognition) and therefore b) less bioactivity of the GH molecules liberated from the secretory granules on secretion from the cell.

Given the obvious dissimilarities in the experimental conditions between the two missions (animal strain, diet, duration of spaceflight, interval between return to Earth and preparation of pituitary cells), it is remarkable that the results between the two experiments are as similar as they are. For convenience, these are summarized and compared in Table 11.

Prior to the 1887 flight, relatively little was known about the effect of microgravity on rat PRL cell function on return to Earth. Although no data were collected concerning in vitro PRL secretion from cells of the SL-3 flight rats, flow cytometric immunofluorescence studies on these cells had

shown that microgravity exposure for 7 days had little, if any, effect on PRL cell number (1). This was clearly not the case in the 1887 experiment since the percentage of PRL cells was significantly increased (Table 9) and PRL secretion in vitro was significantly decreased (Fig. 12). Although these responses in some ways parallel those obtained with GH cells, there are more ways in which they do not. Thus, comparison of the effects of flight on GH vs PRL cells clearly indicate that cell number and secretion responses are very different. Of course the mechanisms underlying such changes are unknown. However, it is tempting to speculate that these may be unique microgravity-induced effect(s) within each pituitary cell class.

It is worth noting that stress is a well-known stimulus for PRL release. Since PRL levels in the 30 hr. storage medium were not different between F-COS and S-COS cells, it is tempting to conclude that the flight animals were not unduly stressed.

One of the more striking differences between pituitary cells of the SL-3 vs the 1887 rats was the marked discrepancy between percentages of GH and PRL cells. Since different rat strains and diets were used in these two experiments, it is probable that disparate GH/PRL cell ratios resulted. Previous studies in our laboratory document the plasticity of PRL cells in terms of cell division. We speculate that the increased percentages in PRL cells in the F-COS pituitaries reflects the cumulative effects of altered environment, diet, and rat strain. It would be interesting to see if cell division rates in PRL cells are indeed different in microgravity.

The primary objective of both missions was a clear definition of the effect of spaceflight on the GH cell system. There can no longer be any reasonable doubt that this system is affected in microgravity. One explanation for the reason(s) underlying the better known effects of spaceflight on organisms, viz. changes in bone, muscle and immune systems may very well rest with such changes in bGH. In spite of the fact that rats in the Cosmos 1887 flight were on Earth for two days after flight, our data show that the GH system had still not recovered from the effects of flight. Many questions remain. One of the more important concerns the GRF responsiveness of somatotrophs after flight. This will be tested in an upcoming experiment.

ACKNOWLEDGEMENTS

The outstanding support of the staffs of the Institute of Biomedical Problems, Brain Research Institute, and the Institute of Psychiatry in performance of these studies is gratefully acknowledged.

REFERENCES

1. Grindeland, R., W. C. Hymer, M. Farrington, T. Fast, C. Hayes, K. Motter, L. Patil and M. Vasques. Changes in pituitary growth hormone cells prepared from rats flown on Spacelab 3. Am. J. Physiol. 252:209-215, 1987.

2. Hymer, W. C., R. Grindeland, C. Hayes, J. W. Lanhan, and D. Morrison. Life Sciences, Biotechnology, and Microgravity. Aerospace Century XXI, Vol. 64, Advances in the Astronautical Sciences, Univelt, Inc. San Diego, CA 1987, pp. 1333-1345.

3. Wilfinger, W. W., W. J. Larson, T. R. Downs, and D. L. Wilbur. An in vitro model for studies of intracellular communication in cultured rat anterior pituitary cells (Abstract) Tissue Cell 16:483, 1984.

4. Hatfield, J. Michael and W. C. Hymer. Flow cytometric analysis and sorting of live male rat anterior pituitary cell types by forward angle and perpendicular light scatter. Endocrinology 119:6, pp 2670-2682, 1986.

5. Kendall, M. E. and W. C. Hymer. Cell Blotting: A new approach to quantify hormone secretion from individual rat pituitary cells. Endocrinology. 121:6, 2260-2262, 1987.

6. Farrington, M. A. and W. C. Hymer. An enzyme immunoassay for rat growth hormone: Applications to the study of growth hormone variants. Life Sciences, Vol. 40:2479-2488, 1987.

7. Greenspan, F. S., C. H. Li, M. E. Simpson, and H. M. Evans. Bioassay of hypophyseal growth hormone: the tibial test. Endocrinology 45:455-463, 1949.

8. Hymer, W. C., D. Wilbur, R. Page, E. Hibbard, R. Kelsey, and J. M. Hatfield. Pituitary hollow fiber units in vivo and in vitro. Neuroendocrinology 32:339-349, 1981.

9. Hatfield, M. and W. C. Hymer. Flow cytometric immunofluorescence of rat anterior pituitary cells. Cytometry 6:137-142, 1985.

10. Ellis, S., and R. E. Grindeland. Dichotomy between bioassayable and immunoassayable growth hormone. In Advance in Human Growth Hormone Research, edited by S. Raiti, Washington, D.C.: USA Govt. Printing Office, 1974, pp. 409-433 [DHEW (NIH) 74-612].

11. Nixon, T. and H. Green. Contribution of growth hormone to the adipogenic activity of serum. Endocrinology 114:527-532, 1984.

12. Snyder, G., W. C. Hymer, and J. Snyder. Functional heterogeneity in somatotrophs isolated from the rat anterior pituitary. Endocrinology 101:3, pp. 788-799, 1977.

13. Grindeland, R.E., W.C. Hymer, P. Lundgren, and C. Edwards. Differential secretion of bioassayable growth hormone by two types of rat somatotrophs. The Physiologist 25:262, 1982.

14. Farrington, M. and W. C. Hymer. Characterization of high molecular weight aggregates of rat GH. Abstract for the 70th annual meeting of the Endocrine society, New Orleans, LA, June 1988.

APPENDIX

TABLE A1

EFFECT OF STORAGE CONDITIONS (26 HRS) ON CELL YIELD AND SOMATOTROPH PERCENTAGE

TREATMENT	CELLS RECOVERED/GLAND ($x10^6$)	% CELL RECOVERY	% SOMATOTROP
EXP # 1			
CONTROL (NO STORAGE)	3.6±0.3++	-	27.6±3.6
EXPERIMENTAL (26 HRS)			
MEM + 0.1% BSA - RT+++	2.1±0.1	58	33.9±2.7
MEM + 0.1% BSA - 4°C	2.5±0.2	70	31.4±1.6
√MEM + 5% CS -RT	1.4±0.2	40	16.1±4.5
√MEM + 5% CS - 4°C	2.5±0.3	71	32.5±3.3
EXP # 2			
CONTROL (NO STORAGE)	2.6	-	30.7
EXPERIMENTAL (26 HRS)			
MEM+0.1% BSA - RT	2.6±0.3	100	34.1±1.1

Based on 20,000 counts/individual sample using flow cytometric immunofluorescence

++ ±SEM. Data collected from 4 individual dissociations/ treatment group

+++ RT = room temperature

CS = calf serum

TABLE A2

iGH RELEASED INTO 26 HR STORAGE MEDIUM

TREATMENT	µg GH IN 26 HR STORAGE MEDIUM	ng GH IN STORAGE MEDIUM/1000 GH CELLS/DAY+
MEM+0.1%BSA - RT	23.1±2.2++	33.2±3.2
MEM+0.1%BSA - 4°C	36.1±2.1	46.2±2.7
√MEM+5%CS - RT	21.6±2.7	95.1±12.0
√MEM+5%CS - 4°C	28.8±2.9	35.3±3.5

++ n=4/group. GH levels measured by enzyme immunoassay.

+ Data based on somatotr[illegible]ecovered from each sample.

TABLE A3

CHARACTERISTICS OF GH CELLS AS DETERMINED BY FLOW CYTOMETRY

TREATMENT	PEAK CHANNEL NUMBER FLUORESCENCE+	PEAK CHANNEL NUMBE FALS++
EXP # 1		
CONTROL (NO STORAGE)	25.5±1.5	50.3±7.4
EXPERIMENTAL (26 HRS)		
MEM+0.1%BSA-RT	24.3±0.3	42.3±1.1
MEM+0.1%BSA-4°C	24.8±0.9	41.0±0.7
√MEM+5%CS-RT	27.0±1.2	40.5±1.9
√MEM+5%CS-4°C	25.0±0.7	40.0±0.4
EXP # 2		
CONTROL (NO STORAGE)	26	63
EXPERIMENTAL (26 HRS)		
MEM+0.1%BSA-RT	23.5±0.7	48.8±4.8

+ Value represents intensity of GH-FITC signal at fluorescent peak. Scaling = log. Intensity of signal is proportional to GH content.

++ Value represents forward angle light scatter channel # at peak. Scaling = linear. Magnitude of signal is related to cell size.

TABLE A4

GH RELEASED FROM CELLS IN CULTURE+

TREATMENT	µg iGH IN 3 DAY CULTURE MEDIUM	ng GH/1000GH CELLS SEEDED	ng GH/1000 GH CELLS/ DAY
EXP # 1			
CONTROL (NO STORAGE)	1.25±0.04	68.2±2.4	22.7±0.8
EXPERIMENTAL (26 HRS)			
MEM+0.1%BSA - RT	1.10±0.05	48.9±2.1	16.3±0.7
MEM+0.1%BSA - 4°C	1.01±0.08	48.4±3.1	16.1±1.0
∂MEM+5%CS-RT	1.02±0.08	95.5±7.2	31.8±2.4
∂MEM+5%CS-4°C	1.00±0.13	46.1±5.8	15.4±1.9
EXP # 2			
CONTROL (NO STORAGE)	1.75±0.13	85.4±6.2	28.5±2.1
EXPERIMENTAL (26HRS)			
MEM+0.1%BSA-RT	1.37±0.06	60.1±2.5	20.0±0.8

+ 66,000 cells/well in 250LL _MEM+5%calf serum. Each dissociation sample was seeded into triplicate wells. Thus, culture data shown in this table are averages from 12 determinations/treatment group.

TABLE 1

TEST PROCEDURES AND CELL REQUIREMENTS
FOR 1887 MISSION

PURPOSE	PROCEDURE	APPROXIMATE NUMBER CELLS REQUIRED
Determine % GH and PRL Cells	Flow Cytometry	6×10^5
Image analysis of GH staining	Immunocytochemistry	2×10^5
Determine intracellular GH content	Extraction	6×10^5
Determine GH secretion in vitro (serum and serumless media)	Cell Culture-immunoassay/bioassay	5×10^4/well (8 wells)
Determine GH secretion from individual cells	Cell blotting	6×10^3/blot (5 blots/rat)
Determine GH secretion in vivo	Cell transplantation into hypophysectomized rats	4×10^6
Characterize GH variants secreted in vitro	HPLC	----

TABLE 2

Levels of Immunoactive and Bioactive GH Released into Transport Medium During 30 hrs. Between Time of Pituitary Removal and Tissue Dissociation in Moscow

	iGH			bGH	
SAMPLE	µg/ml	TOTAL µg IN VIAL		µg/ml	TOTAL µg IN VIAL
F-COS	1.95±0.10+	42.9±2.2	F-COS	1.13±010+	24.9±2.2
S-COS	1.55±0.19	34.1±4.2	S-COS	2.88±0.12	61.6±2.6

436

+ Values represent averages of hormone released from each of 5 glands into 5 individual vials. iGH, F vs S $p < 0.05$; bGH, F vs S $p < 0.001$

TABLE 3

FLOW CYTOMETRIC ANALYSES OF PITUITARY GH CELLS OBTAINED FROM RATS FLOWN ON COSMOS 1887

PARAMETER	F-COS	S-COS	V-1 COS	V-2 COS
GH				
1). % GH CELLS[1]	26.6	22.9	23.4	24.3
2). BRIGHTNESS FACTOR[2]	24.5X	13.1X	9.2X	___[3]
3). PEAK CHANNEL-FALS[4]	181	151	169	147
4). PEAK CHANNEL-PLS[5]	145	145	147	143

[1] Based on counts of 50,000 - 60,000 cells

[2] Relative to unstained cells; based on marker index; i.e., fluorescence intensity converted to voltage. Ratio of stained to unstained cells = marker index.

[3] Could not be determined accurately since different filter gates were used.

[4] FALS = forward angle light scatter. Peak channel is related to cell size.

[5] PLS = perpendicular light scatter. Peak channel proportional to internal structure ("Granularity").

TABLE 4

Reassay of Selected Samples Obtained from Serum-Containing Cultures

Sample*	Days In Culture	Assay #1** ng iGH released/1000 GH	Assay #2 cells seede
F-COS	3	62±5	77±5
S-COS	3	57±4	55±8
V-1 COS	3	85±8	79±7
V-2 COS	3	96±5	86±5
F-COS	6	73±10	80±9
S-COS	6	143±7	135±9
V-1 COS	6	102±7	88±7
V-2 COS	6	151±7	128±·

* From calf-serum cultures only.

** These data are also plotted in Fig. 6.

TABLE 5

bGH Released in vitro From Pituitary Cells
Prepared From Rats Flown on Cosmos 1887

GROUP	bGH (ug/ml culture media)
F-COS	0
S-COS	2.34 (2.03-2.63)+
V-1	1.94 (1.79-2.06)
V-2	1.44 (1.40-1.57)

+ 95% confidence intervals. See text for description of assay conditions.

TABLE 6

INTRACELLULAR iGH AT THE BEGINNING AND END OF CULTURE

GROUP	INTRACELLULAR iGH AT START OF CULTURE (ng iGH/10^3 GH CELLS)*	INTRACELLULAR iGH AT END OF CULTURE (ng iGH/10^3 GH CELLS)*		iGH SYNTHESIS+ (ng iGH/10^3CELLS)	
		CALF SERUM	DEFINED MEDIUM	CALF SERUM	DEFINED MEDIUM
F-COS++	40±17 (4)	8.6±0.8 (3)	11.9±3 (5)	104	65
S-COS	61±17 (5)	22±2 (5)	13.5±2 (5)	161	78
V-1 COS	133±19 (5)	24±1 (5)	36±4 (5)	77	24
V-2 COS	102±15 (5)	42±2 (5)	23±3 (5)	186	75

+ (GH in culture media + GH in cells at end of culture) - intracellular GH at start of culture.

++F-COS = Flight; S-COS = synchronous control; V-1 COS = 1st vivarium exeriment; V-2 COS = 2nd vivarium experiment

* Expressed on the basis of the numbers of GH cells seeded (determined by flow cytometric immunofluorescence, see Table 3)

TABLE 7

GROWTH HORMONE SECRETION FROM CELLS OF S-COS AND F-COS RATS IMPLANTED INTO CEREBRAL VENTRICLES OF HYPOPHYSECTOMIZED RATS*

TREATMENT GROUPS	TIBIAL WIDTH (μ)	μg bGH+ SECRETED FROM IMPLANT
S-COS EMPTY FIBER	155±0.5 (11	0
S-COS CELL FIBER	177±1.3 (7)	0.22±0.03
F-COS EMPTY FIBER	155±0.3 (10)	0
F-COS CELL FIBER	164±0.6 (10)	0.10±0.01#

* Each hypophysectomized rat was implanted with a hollow fiber containing $2x10^5$cells. Animals were killed 10 days post implantation and fiber placement was verified by visual inspection of sliced brain tissue. Animal receiving fibers which did not come in contact with a ventricular surface were considered unsuccessful and are excluded. The number of rats receiving successful implants are shown in ( ).

+ Estimated from responses of other hypophysectomized rats receiving 4 daily injections of bovine GH standard.

# $p < .05$

TABLE 8

HPLC FRACTIONATION AND GH ASSAY OF 3 AND 6 DAY, SERUMLESS CULTURE MEDIUM FROM F-COS AND S-COS CELLS.

SAMPLE	% OF RECOVERED iGH IN FRACTION		
	FR. 1	FR. 2	FR. 3
F-COS (3 DAY)	8.5	84.5	7.0
S-COS (3 DAY)	11.5	80.8	7.9
F-COS (6 DAY)	2.2	91.4	7.4
S-COS (6 DAY)	2.6	93.8	3.6

+ Fr. 1 = void volume (n62K); Fr. 2 = 18-62K; Fr. 3 = low molecular weight
GH recoveries after HPLC, dialysis, lyophylization and
reconstitution ranged from 21-63%. Results represent average of 2
independant immunoassays for 3 day samples; one for 6 day samples.

TABLE 9

FLOW CYTOMETRIC ANALYSES OF PITUITARY PRL CELLS OBTAINED FROM RATS FLOWN ON COSMOS 1887

PARAMETER	F-COS	S-COS	V-COS
PRL			
1). % GH CELLS[1]	46.7	31.8	35.7
2). BRIGHTNESS FACTOR[2]	4.1X	5.2X	6.3X
3). PEAK CHANNEL-FALS[3]	92	64	108
4). PEAK CHANNEL-PLS[4]	40	24	32

1 Based on counts of 50,000 - 60,000 cells

2 Could not be determined accurately since different filter gates were used.

3 FALS = forward angle light scatter. Peak channel is related to cell size.

4 PLS = perpendicular light scatter. Peak channel proportional to internal structure ("Granularity").

TABLE 10

INTRACELLULAR PRL AT THE BEGINNING AND END OF CULTURE

GROUP	INTRACELLULAR PRL AT START OF CULTURE (ng PRL/10s PRL CELLS)*	INTRACELLULAR PRL AT END OF CULTURE (ng PRL/10s PRL CELLS)*	
		CALF SERUM	DEFINED MEDIUM
F-COS	0.22±0.05	4.6±0.6	1.4±0.3
S-COS	0.24±0.02	4.9±0.4	1.4±0.3
V-COS	0.26±0.06	7.6±0.7	2.2±0.2

* Expressed on the basis of the numbers of GH cells seeded (determined by flow cytometric immunofluorescence)

TABLE 11

COMPARISON OF GH CELL RESULT BETWEEN
THE COSMOS 1887 AND SL-3 MISSIONS

TEST	COSMOS FLIGHT/CONTROL	SL-3* FLIGHT/CONTI
1) iGH released into storage medium before cell preparation	↑1.25	ND[1]
bGH released into storage medium before cell preparaton	↓0.39	ND
2) % GH cells	→1.0	→1.0
3) GH fluorescence staining	↑2.0	↑1.16
4) GH cell size (FALS)	↑1.2	↑1.05
5) GH cell cytoplasmic "Granularity"	→1.0	ND[2]
6) Short term (2 hr.) GH secretion assay (cell blot)	↑1.19	ND[3]
7) 6 day cell culture (iGH)		
3 day medium (CS)	↑1.10	↓0.44
3 day medium (DM)	↑1.24	↓0.83
Next 3 day medium (CS)	↓0.51	↓0.77
Next 3 day medium (DM)	↓0.57	ND[2]
8) 3 & 6 day cell culture medium (bGH)	↓<0.01	ND
9) iGH synthesis in 6 day culture		
(CS)	↓0.64	↓0.39
(DM)	↓0.83	ND[2]
10) Tibial line response after hollow fiber transplantation (in vivo culture; bGH).	↓0.43	↓0.60

* Small rats (200 gm)
↑ = increase; ↓ = decrease
→ = no change.
ND = not done
1 Storage of pituitary tissue not required in this experiment.
2 Insufficient sample for analysis
3 Technique not developed at the time of experiment.

Fig. 1. Photomicrographs of F-Cos and S-Cos cells stained for specific GH immunofluorescence (green). Top panel, F-Cos cells showing red nuclear fluorescence due to propidium iodide. These cells, incubated with monkey non-immune serum, do not show cytoplasmic staining. Middle panel, S-Cos cells. Bottom panel, F-Cos cells. Note obvious brighter green fluorescence in F-Cos cells.

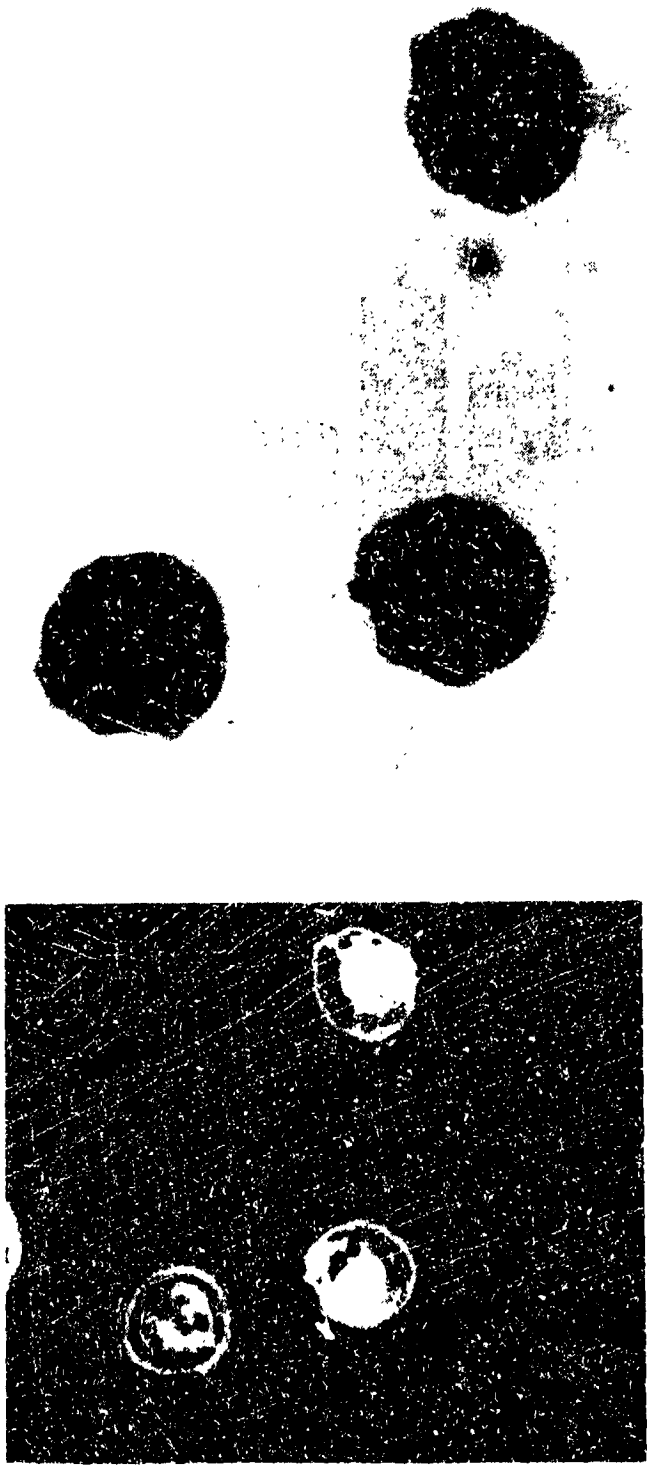

Fig. 2 (top). GH cells immunocytochemically stained for GH. The dark reaction product represents GH. Fig. 2 (bottom). Image analysis of same cells as in top figure. This represents a computerized video enhancement image whereby the GH staining in red is color thresholded in a different gray level than the yellow nuclear area. This procedure was done on 100 cells in each group to yield the information shown in Fig. 3.

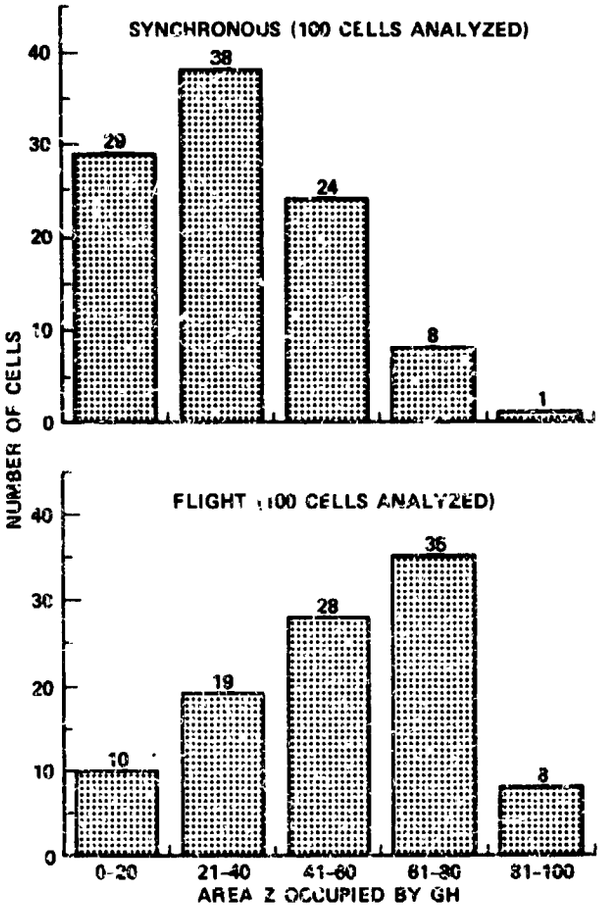

Fig. 3. Image analysis of 100 cells in both F-Cos and S-Cos groups done according to procedure shown in Fig. 2.

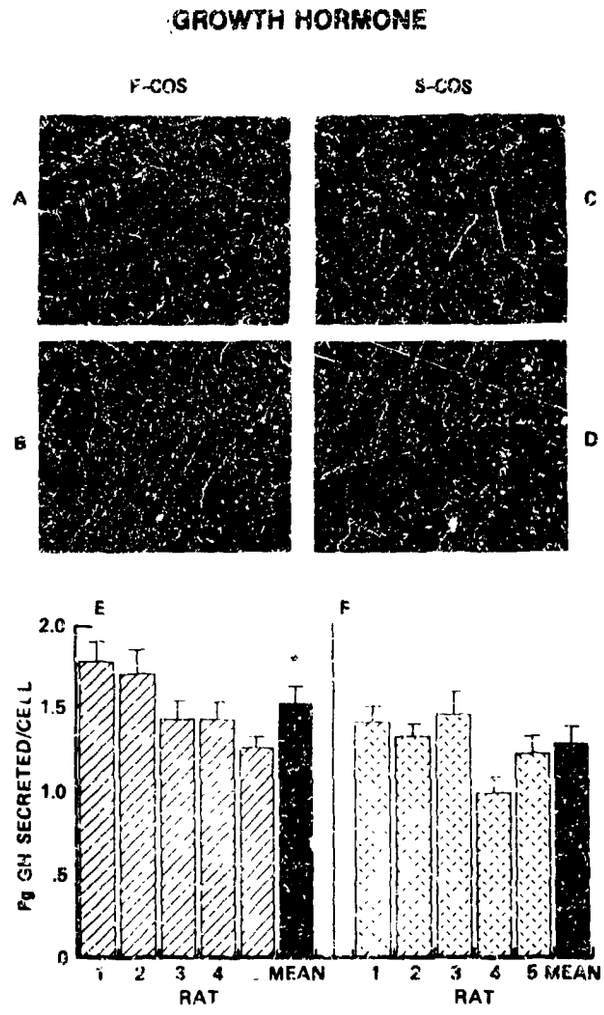

Fig. 4. Top: GH cell blot images produced by individual cells from S-Cos and F-Cos groups. Panel A: F-Cos cell blot. Panel B: video enhanced image of same F-Cos cells ( ). Panel C: S-Cos cell blot. Panel D: video enhanced image of same S-Cos cells. Panel E and F: quantitation of GH released from 35 cells/rat/group. The mean GH secretion of all cells (175) in each group is shown in black bar. * F-Cos secretion, $p < 0.05$ vs. S-Cos cells.

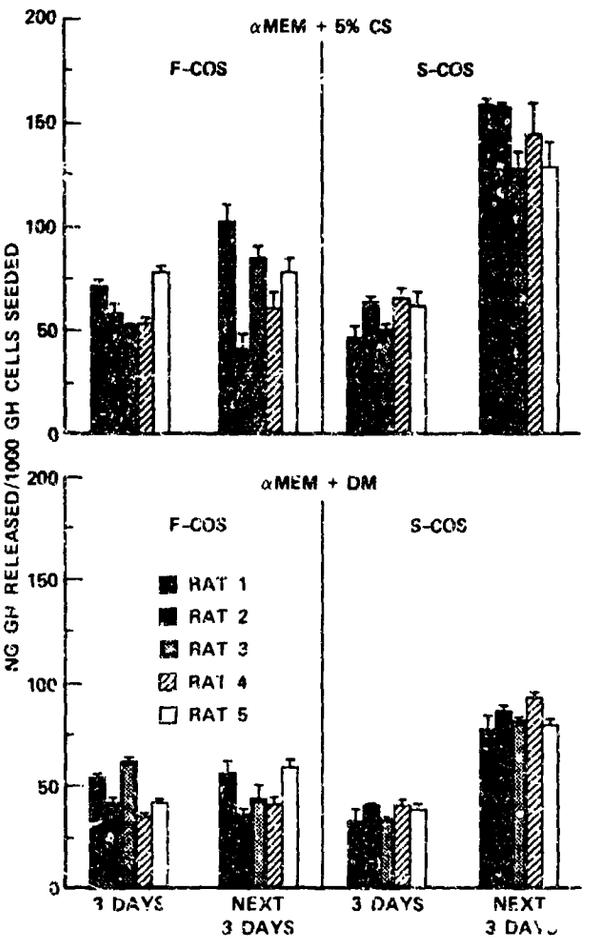

Fig. 5. Top Panels: GH released from pituitary cells of individual rats in both F-Cos and S-Cos groups. Serum containing medium. Error bars represent sem's of GH from 4 culture wells. Bottom Panels: GH released from pituitary cells of individual rats in both F-Cos and S-Cos groups. Serumless medium.

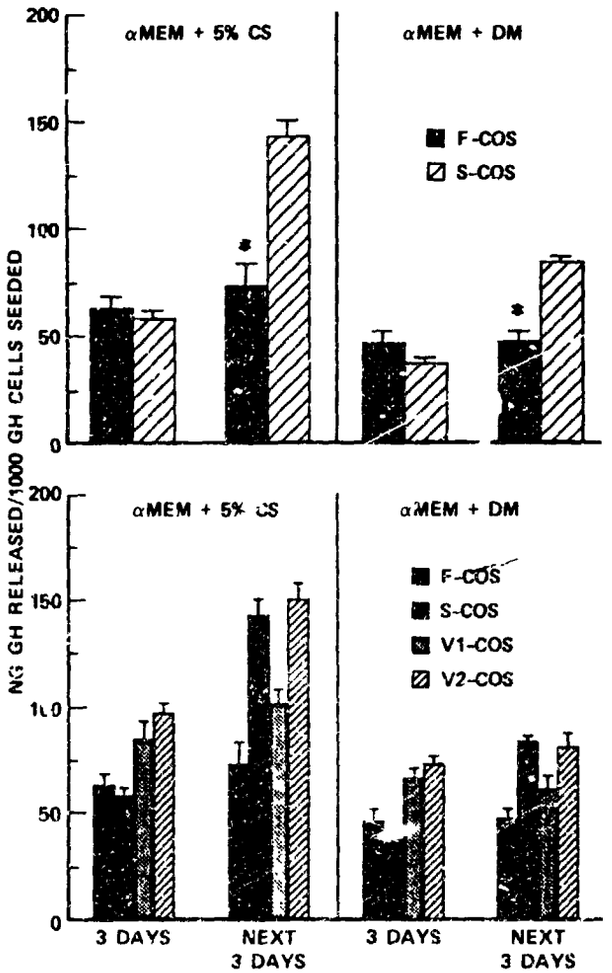

Fig. 6. Top Panels: Combined GH secretion data from cells of individual rats (Fig. 5). Bottom panels: Comparison of GH secretion from combined cells of [illegible] treatment groups.

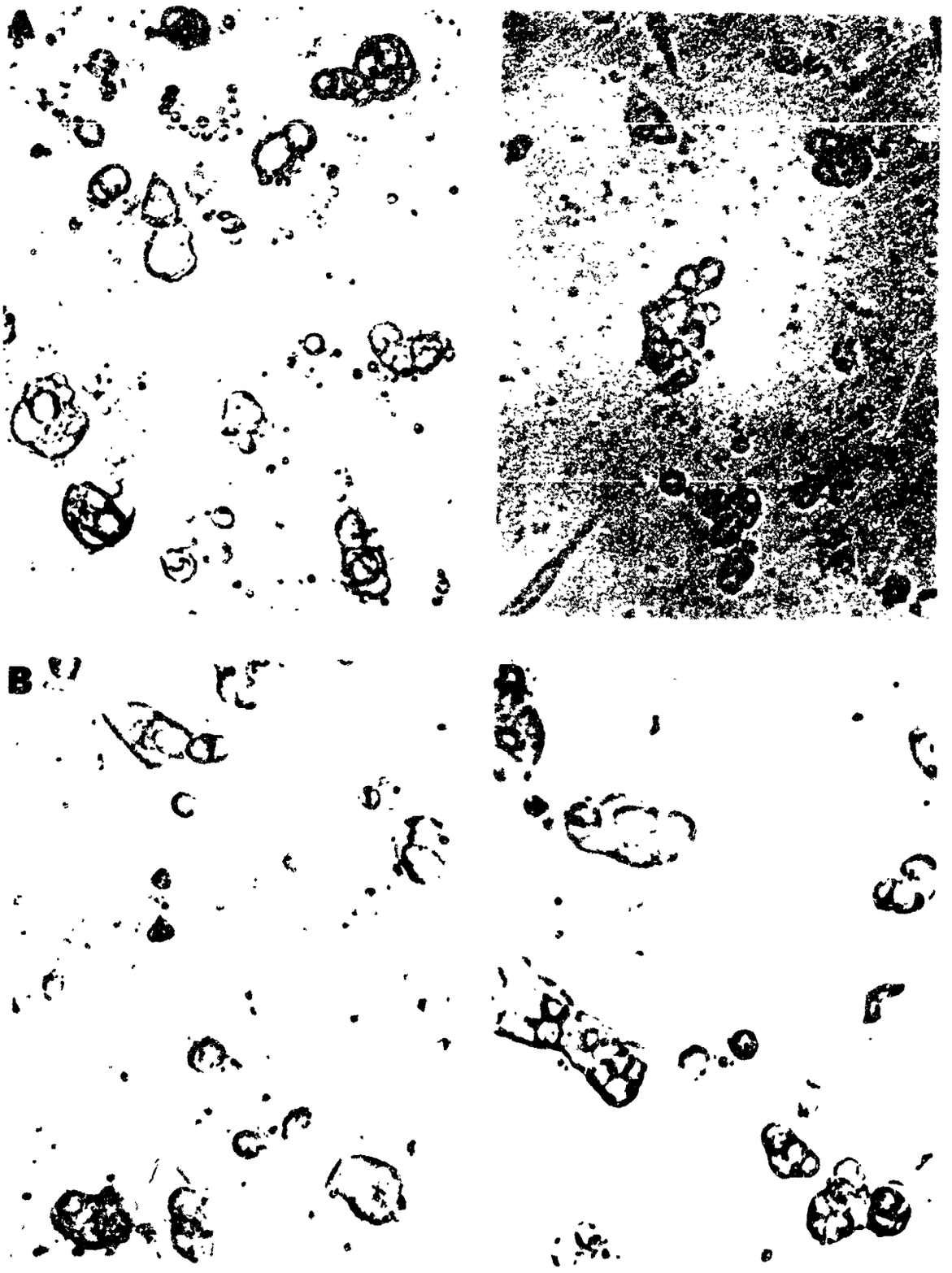

Fig. 7A. Photomicrographs of pituitary cells from S-Cos and F-Cos animals in culture for 3 and 6 days in serum containing medium. A) S-Cos, 3 day; B) S-Cos, 6 day; C) F-Cos, 3 day; D) F-Cos, 6 day.

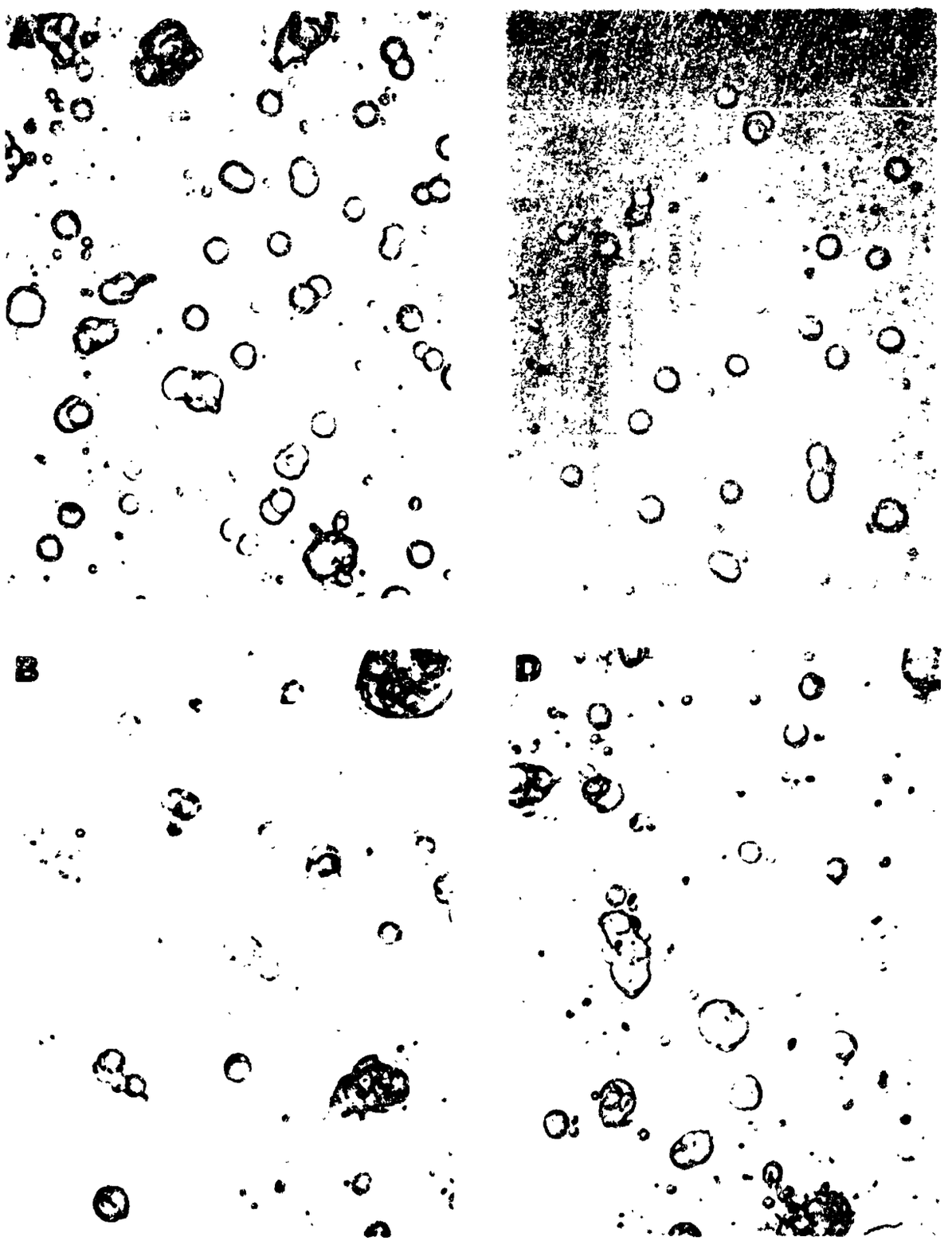

Fig. 7B. Photomicrographs of pituitary cells from S-Cos and F-Cos animals in culture for 3 and 6 days in serum free medium. A) S-Cos, 3 day; B) S-Cos, 6 day; C) F-Cos, 3 day; D) F-Cos, 6 day.

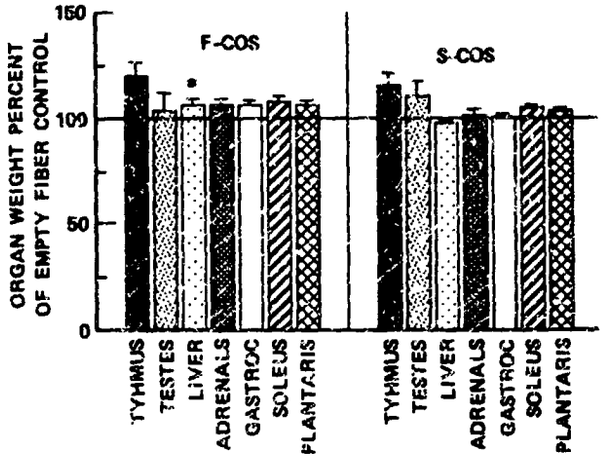

Fig. 8. Organ weights of hollow fiber implant recipients expressed as a percentage of the empty fiber controls. Actual organ weights of animals receiving empty hollow fibers shown in table.

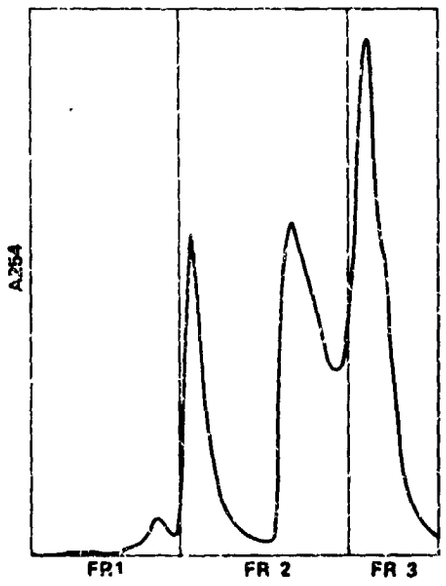

Fig. 9. Optical density profile (A254 nm) of proteins contained in 3 day culture medium from F-Cos cells. The GH contents contained in fractions 1-3 are shown in table 4.

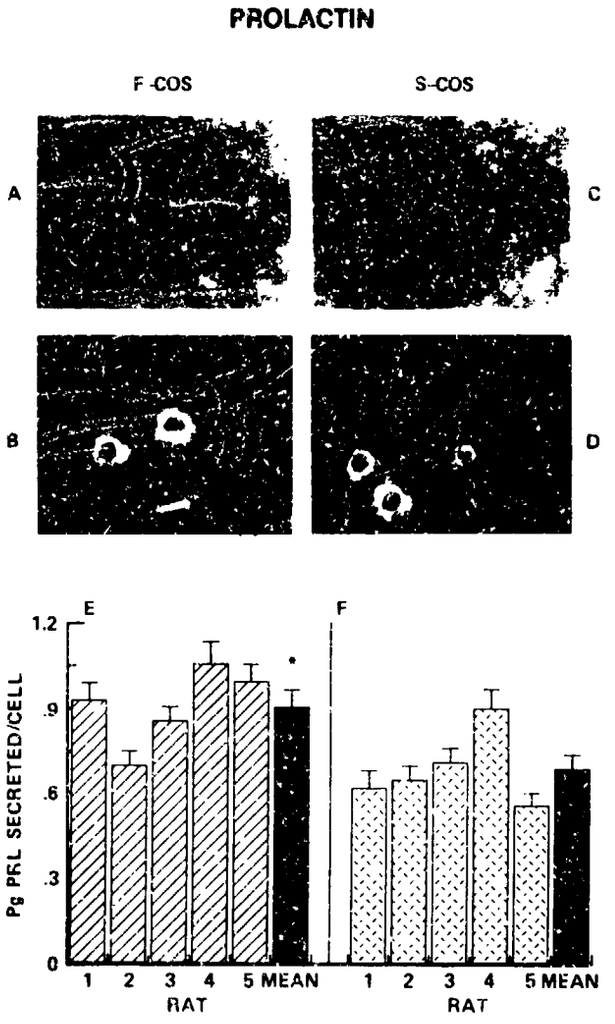

Fig. 10. Top: PRL cell blot images produced by individual cells from S-Cos and F-Cos groups. Panel A: F-Cos cell blot. Panel B: video enhanced image of same F-Cos cells ( ). Panel C: S-Cos cell blot. Panel D: video enhanced image of same S-Cos cells. Panel E and F: quantitation of PRL released from 35 cells/rat/group. The mean PRL secretion of all cells (175) in each group is shown in black bar. * F-Cos secretion, $p < 0.05$ vs. S-Cos cells.

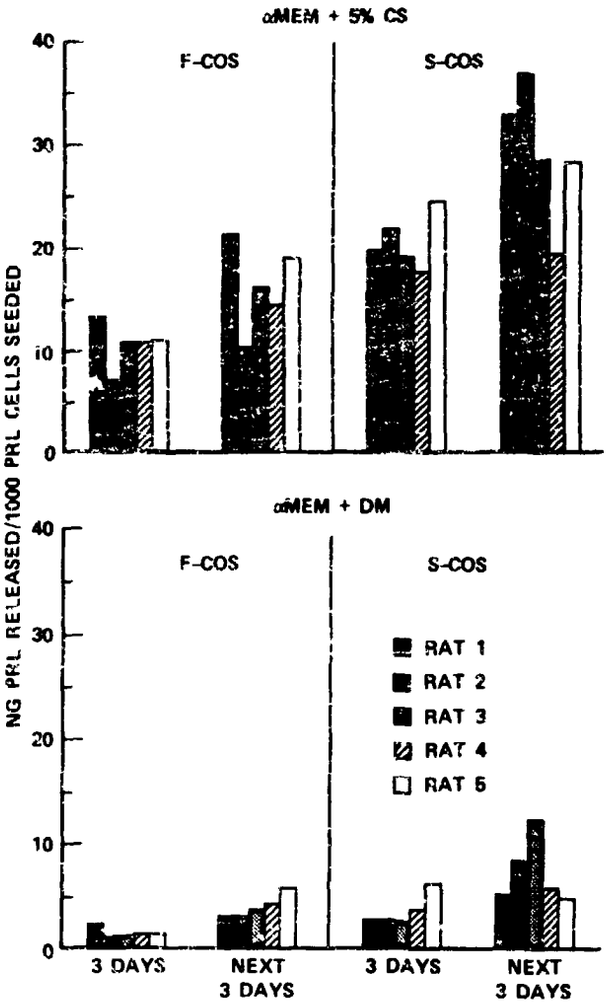

Fig. 11. Top Panels: PRL released from pituitary cells of individual rats in both F-Cos and S-Cos groups. Serum containing medium. Bottom Panels: PRL released from pituitary cells of individual rats in both F-Cos and S-Cos groups. Serumless medium.

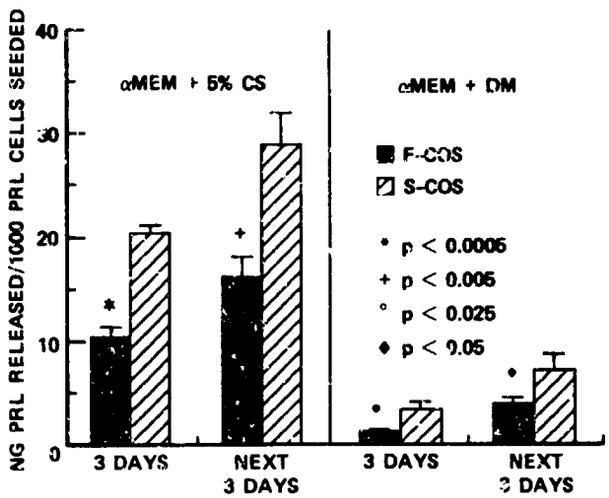

Fig. 12. Combined PRL secretion data from cells of individual rats (Fig. 11).

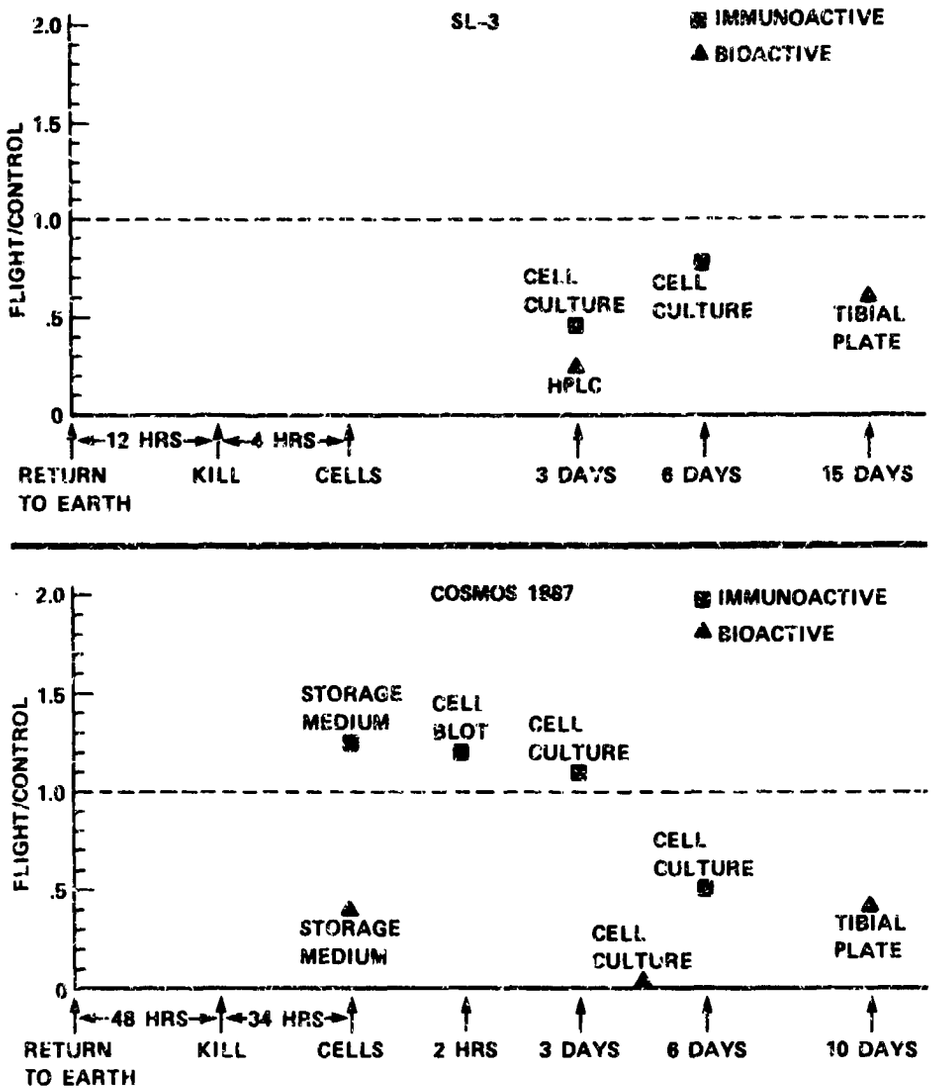

Fig. 13. Effect of spaceflight on subsequent release of bioactive and immunoactive GH release in vivo and in vitro: Comparison of the SL-3 and 1887 experiments.

EXPERIMENT K-6-22

PART II: IMMUNOHISTOCHEMICAL ANALYSIS OF HYPOTHALAMIC HORMONES

W. Vale, P. Sawchenko, and I. Krasnov

SUMMARY

It was originally anticipated that blocks of hypothalamic tissue would be prepared for radioimmunoassay of hypophysiotropic hormones mediating somatic growth (growth hormone-releasing factor, somatostatin), and stress-related corticotropin secretion (corticotropin-releasing factor). Each of these peptides is expressed in hypothalamic neurons that project directly to the hypophyseal portal vasculature for delivery to the anterior lobe of the pituitary. Even within the hypothalamus, however, each is also rather broadly distributed in cell bodies and/or axons that bear no ostensible relationship to their hypophysiotropic functions. Because of this, it was decided to attempt to employ immunohistochemical methods in an attempt to better localize any effects of flight on these neuropeptide systems.

MATERIALS AND METHODS

Blocks of fresh-frozen hypothalamic tissue were stored upon receipt at -70 deg. C. The fixation protocol employed was based on preliminary studies in which we attempted to maximize antigenicity and morphologic preservation in fresh frozen samples. The tissue was transferred for 30 minutes to a -20 deg. C freezer and then for 10 minutes to a refrigerator at 4 deg. C. The blocks were fixed for 6 hours in ice cold 4% paraformaldehyde in 0.1 M phosphate buffer, and then overnight at 4 deg. C in the same fixative containing 10% sucrose. The following day, the blocks were frozen in dry ice and five 1-in-5 series of 20 μm thick sections were cut on a sliding microtome. Sections were rinsed (2 x 10 minutes) in 0.05 M phosphate-buffered saline (PBS) and stored at -20 deg. C in cryoprotectant (30% ethylene glycol, 15% sucrose in 0.05 M phosphate buffer) until staining.

A conventional indirect immunofluorescence method (Gerfen and Sawchenko, 1984) was used for staining. Complete series of sections through the hypothalamus of each member of the flight and synchronous control groups were incubated in primary antisera raised in rabbits against rat hypothalamic growth hormone-releasing factor (GRF; serum G75 of Sawchenko, et al., 1985), somatostatin-28 (SS-28; serum S309 of Benoit, et al., 1982; see also Sawchenko, et al., 1988), rat corticotropin-releasing factor (CRF; serum C70; see Sawchenko, 1987) and arginine vasopressin (AVP; Vandesande and Dierickx, 1975; see Sawchenko, et al., 1984). Details of the characterization of these sera for immunohistochemical studies may be found in these references. All primary antisera were localized with an affinity purified, fluorescein-conjugated, goat anti-rabbit IgG (Tago, Inc., Burlingame, California).

RESULTS

Positive staining patterns, consistent with their acknowledged distributions, were obtained for each of the four peptides examined. Despite the fact that the immersion fixation protocol employed permitted localization, staining was less robust and, in the case of the median eminence, less discretely localized, than that obtainable in perfusion-fixed rats of comparable age.

Somatostatin-28. SS-28-immunoreactive (IR) cell bodies were found consistently in members of both groups in the anterior periventricular nucleus of the hypothalamus, the acknowledged primary source of hypophysiotropic SS-IR pathways. Correspondingly, immunoreactive fibers were seen in the

external lamina of the median eminence, though resolution of these was poor (Figure 1). Other acknowledged SS-IR terminal fields, for example in the ventromedial and paraventricular nuclei of the hypothalamus were moderately well-stained. Comparison of the staining patterns between the two groups showed the flight animals to be consistently less robust. This was manifest primarily in the forms of a lesser number of immunostained cell bodies in the anterior periventricular region, and a lesser intensity of staining of fibers in each of the regions enumerated above (see Figures 1 and 2).

Growth Hormone-Releasing Factor. GRF-IR appeared as a relatively diffuse band spanning the external lamina of the median eminence, and as isolated, and more discretely stained, fibers in hypothalamic regions (e.g., dorsomedial, paraventricular, anterior periventricular nuclei) shown previously to receive GRF-IR inputs (Sawchenko, et al., 1985). Perikaryal staining, which normally requires pretreatment with colchicine, was not observed. As was the case with SS-IR, staining for GRF-IR in the median eminence appeared consistently less intense in the flight animals, relative to synchronous controls (Figure 1).

Arginine Vasopressin. (AVP-IR was present in both groups in cell bodies of the paraventricular, supraoptic and suprachiasmatic nuclei, and in the hypothalamo-hypophyseal tract, coursing through the hypothalamus and the internal lamina of the median eminence. No consistent differences in staining between the two groups were encountered for this antigen. Perikaryal staining for AVP-IR in rats of both groups was somewhat unusual and worthy of comment. Staining in both magnocellular neurosecretory cell bodies was weak and granular in appearance, while staining of dendritic processes was robust. By contrast, staining of cells in the suprachiasmatic nuclei was unremarkable. No Herring Body-like swellings, which might be indicative of acute dehydration, were observed on magnocellular AVP-IR fibers.

Corticotropin-Releasing Factor. As was the case for GRF, staining for CRF-IR was weak and limited the median eminence and isolated intrahypothalamic fibers. No consistent differences in staining of either fiber type between groups was evident.

DISCUSSION

In summary, we observed consistently lesser staining intensities for both SS-28- and GRF-IR in flight, relative to synchronous control groups, and no such alterations in staining for CRF or AVP. AVP-IR in magnocellular neurosecretory perikarya appeared unusually weak in members of both groups. The fact that staining for both of the principles involved most directly in the central regulation of growth hormone secretion appeared to be affected at least somewhat selectively may be viewed as suggesting a specific neuroendocrine dysfunction within the central nervous system, some caution is warranted. The sub-optimal fixation protocol, and the (presumably associated) diffuse staining of fibers and terminals in the median eminence, must temper any interpretation of the data. Moreover, the fact that one of the ostensibly unaffected principles, AVP, is normally expressed at concentrations in hypothalamic perikarya that saturate our detection system, would lead one to question the capacity of this methodology to resolve subtle differences. Finally, the fact that both the stimulatory and inhibitory principles appeared driven in the same direction is perplexing. This could represent a compensatory or counterregulatory response of one system to a perturbation in the other. The present findings provide no insight into this issue.

REFERENCES

1. Benoit, R., Line, N., Alford, B., and Guillemin, R. (1982). Seven peptides derived from pro-somatostatin in rat brain. Biochem. Biophys. Res. Commun., 107:944-950.

2. Gerfen, C.R., and Sawchenko, P.E. (1984). An anterograde neuroanatomical tracing method that shows the detailed morphology of neurons, their axons and terminals: Immunohistochemical localization of an axonally transported plant lectin, Phaseolus vulgaris - leucoagglutinin. Brain Res., 290:219-238.

3. Sawchenko, P.E. (1987). Evidence for differential regulation of CRF- and vasopressin-immunoreactivities in parvocellular neurosecretory and autonomic-related projections of the paraventricular nucleus. Brain Res. 437:253-263.

4. Sawchenko, P.E., Benoit, R., and Brown, M.R. (1988). Somatostatin 28-immunoreactive inputs to the paraventricular nucleus: Origin from non-aminergic neurons in the nucleus of the solitary tract. J. Chem. Neuroanat. 1:81-94.

5. Sawchenko, P.E., Swanson, L.W., Rivier, J. and Vale, W.W. (1985). The distribution of growth hormone-releasing factor (GRF) -immunoreactivity in the central nervous system of the rat: An immunohistochemical study using antisera directed against rat hypothalamic GRF. J. Comp. Neurol., 237:100-115.

6. Sawchenko, P.E., Swanson, L.W., and Vale, W.W. (1984). Corticotropin-releasing factor: Co-expression within distinct subsets of oxytocin-, vasopressin-, and neurotensin-immunoreactive neurons in the hypothalamus of the male rat. J. Neurosci., 4:1118-1129.

7. Vandesande, F., Dierickx, K., and DeMey, J. (1975). Identification of separate vasopressin-neurophysin II and oxytocin-neurophysin I containing nerve terminals in the external region of the bovine median eminence. Cell Tiss. Res., 158:509-516.

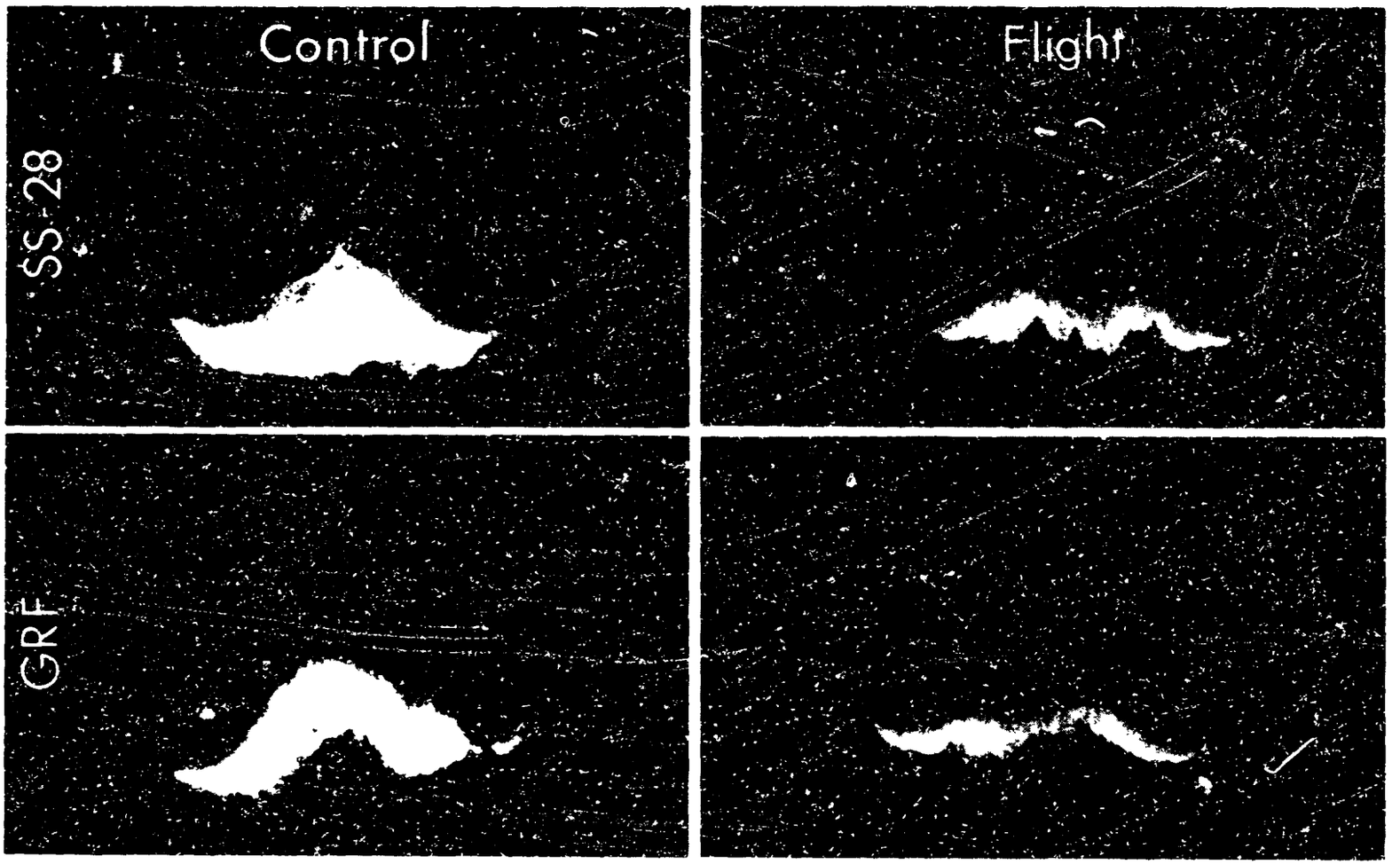

Figure 1. Fluorescence photomicrographs of frontal sections through the medial basal hypothalamus of representative rats from the synchronous control and flight groups, stained immunohistochemically for SS-28 (top) or GRF. For both peptides, staining seen in the external lamina of the median eminence was less intense in the flight group. The third ventricle appears near the center of each micrograph. All micrographs X 75.

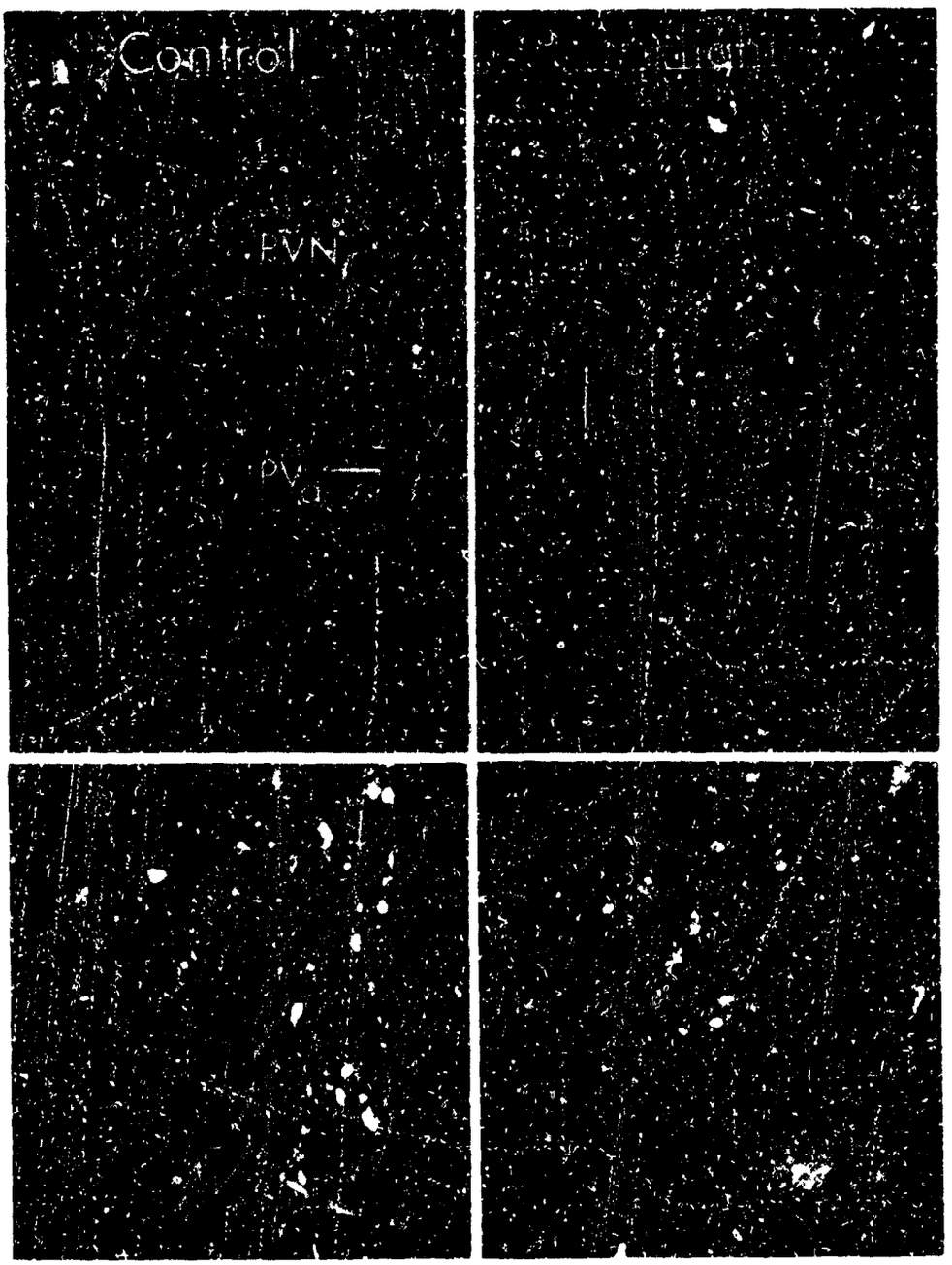

Figure 2. Fluorescence photomicrographs of frontal sections through the anterior hypothalamus to show SS-28-IR perikarya and fibers in representative animals from the flight and synchronous control groups. In the anterior periventricular nucleus (PV_a) fewer, and less intensely stained perikarya are seen in the section from the flight animal. Top two micrographs X 50. The bottom panel shows a higher magnification (X 150) view through the paraventricular nucleus (PVN). Note the pronounced difference in the number of stained fibers.

EXPERIMENT K-6-22

PART III: PLASMA ANALYSIS

R. Grindeland, I. Popova, and M. Vasques

INTRODUCTION

Plasma hormone and biochemical analyses were performed either in our laboratory or by a clinical laboratory. Results of these tests were made available to all U.S. investigators to facilitate their evaluation of animal physiological status and interpretation of their data. Specific measurements are discussed in the context of the relevant experiments. For example, phosphorus, calcium, and alkaline phosphatese values are considered with bone studies, plasma proteins and albumin concentrations are discussed with the liver enzyme studies, and testosterone titers are discussed with the testes and pineal gland investigations.

PROCEDURES

Trunk blood was collected after decapitation into tubes containing 50 ml ammonium heparin. Blood biochemical measurements were determined in automated analysis (SMAC) by Veterinary Reference Laboratory, San Leandro, CA. Plasma immunoactive growth hormone was determined in- house by an adaptation of the radioimmunoassay of Schalch and Reichlin (1). Interassay variation was 6% and intraassay variation 3.8%. Rat growth hormone standard (3 USP U/μg) and antisera, raised in monkeys, were produced in-house. The prolaction radioimmunoassay procedure was also an adaptation of the growth hormone RIA method(2). Rat prolactin (29U/μg) and rabbit antisera were produced in our laboratory. Inter and intra assay variation were 4% and 2% respectively. Testosterone and corticosterone were assayed using immunoassay kits. The testosterone kit was obtained from Diagnostic Products Corp., Los Angeles, CA and the Corticosterone kit from Radioassay Laboratories, Inc., Carson, CA. Sensitivities for these assays are 0.05-0.01 ng/ml of the possible circulating steriods in the male rat. The corticosterone antibody cross reacts with cortisol less than 0.2%; all other steriods cross react less than 0.1%. The testosterone antibody cross reacts with two other androgenic steriods as follows: androstendione-3%; 5-alpha androstan-3 beta, 17 beta-diol-0.5%, and 5- androsten3-beta; 17-beta diol-0.7%. All other physiological steriods cross react less than 0.1%.

RESULTS AND DISCUSSION

Plasma glucose was significantly elevated in Flight (F) compared to Synchronous Control (S) rats, (Table 1). These two groups, fed a half day's portion of food some 20 hours before sacrifice, were most probably fasted. F glucose concentrations were higher than Vivarium Controls (V) but the same as Basal Controls (B) levels. The fasting state of V and B rats is uncertain, so the significance of the glucose levels in the later group is open to question. The elevated glucose levels in F rats, similar to that observed in Space Laboratory 3 animals post flight (3), are not attributable to elevated corticosterone or growth hormone titers (see under hormones). Elevated catecholamine titers, especially in response to reentry, are a plausible explanation. However, the markedly increased liver glycogen (K6-14) is consistent with an inflight elevation of plasma glucose. The increased plasma glucose concentration appears to be a response to microgravity but the mechanism remains unclear.

Plasma calcium was lower in F than in V or B rats, but not different from S rats, suggesting a dietary regimen or caging effect (Table 1). In contrast, phosphorus concentrations were higher in F than S

PRECEDING PAGE BLANK NOT FILMED

animals, similar to those of V rats and less than those of B animals. Alkaline phosphatase values were 50% higher in the F animals than the S controls, consistant with changes in bone and mineral metabolism discussed elsewhere. The alkaline phosphatase levels in B rats were 2-4 times those of other groups, perhaps reflecting a more rapid bone turnover. The large standard error, however, suggests extensive variability in the B rats.

Plasma sodium concentrations were similar for all groups of rats. Potassium concentrations of F rats were similar to those of S and V animals but less than B controls. The reasons for the higher levels in B rats is not apparent.

Total protein and albumin concentrations were similar for all groups, suggesting no effect of weightlessness. If hemoconcentration occurred in F rats any decrease in protein could be obscured by the loss of plasma volume. The elevated blood urea nitrogen suggests that protein catabolism has been increased in F rats. Moreover, the apparently constant plasma protein concentrations, increased liver weights, and increased creatine levels of F rats suggest that the protein being catabolized is from skeletal muscle.

Plasma immunoreactive growth hormone measurements were statistically similar for all groups of rats (Table 3). Two groups (B,F) each contained one rat with a high value, raising the means and increasing the standard errors appreciably. Deletion of these values brought the means to similar levels, and reduced the standard error, but did not change the statistical significance between groups. Analogous results were observed in Space Laboratory 3 rats (4). However, secretion of bioassayable GH (part 1 of this report; 3) was markedly decreased after flight.

Prolactin concentrations, which ranged from 2.5 to 7 ng/ml, did not differ significantly between any of the groups. ($p>0.05$)

Corticosterone levels did not differ between F and S groups. The S rats, however, had significantly lower levels than either B or V groups, being about one-half as much. The concentrations found in S and F rats were similar to those in flight and control groups on SL-3 (4). The values are all higher than 3-5 µg/dl found in our laboratory for rats which have been handled extensively. It is of interest that adrenals of F rats were hypertrophied but their corticosterone secretion was virtually identical to that of S animals. The data suggest that either there was no lasting effects of weightlessness on adrenal cortical function or that post flight handling obscured any small difference.

Flight rats had decreased levels of testosterone compared to S controls, but similar concentrations to V rats. B rats had higher testosterone concentrations than any other group for unknown reasons. Space Laboratory-3 F rats also had lower testosterone than S controls, but levels similar to those of B and V rats (4). Data from the two flights suggest that the caging of F and S rats may have evoked an increase in testosterone which was supressed in F rats by microgravity and/or reentry. It is not clear whether the decreased testosterone concentrations reflect decreased gonadotropin secretion or decreased Leydig cell function.

REFERENCES

1. Schalch, D.S. and S. Reichlin. Plasma growth hormone concentrations in the rat determined by radioimmunoassay-Influence of sex, pregnancy, lactation, and anasthesia, hypophysectomy and extra sellar piyuitary transplants. Endocrinology 79: 275-280, 1966.

2. Ellis, S. R.E. Crindeland, J.M. Nuenke, and P.X. Callahan. Purification and properties of rat prolactin. Endocrinology 88: 886, 1936.

3. Grindeland, R., W.C. Hymer, M. Farrington, T. Fast, C. Hayes, K. Motter, L. Patil, and M. Vasques. Changes in pituitary growth hormone cells prepared from rats flown on Spacelab 3. American Journal of Physiology 252:R209-R215, 1987.

4. Vasques, M., R.E. Grindeland, M. Martinelli and R. Furlanetto. Effects of 7 days of microgravity on plasma hormone levels. Proceedings of the Fall Meeting of American Physiology Society-International Union of Physiological Sciences, Montreal, 1988.

TABLE 1

BLOOD BIOCHEMISTRY

GROUP	PHOSPHORUS (mg/dl)	CALCIUM (mg/dl)	SODIUM (mg/dl)	POTASSIUM (meq/l)
Flight				
Mean	6.5[1,3]	9.6 [2,3]	142.0	5.08[3]
S.E.	0.17	0.28	2.37	0.21
Synchronous				
Mean	5.8[2,3]	10.1[2]	142.8	4.8[2,3]
S.E.	0.15	0.15	1.02	0.12
Vivarium				
Mean	6.6[3]	10.5	145.2	5.6
S.E.	0.18	0.12	2.42	0.07
Basal				
Mean	7.2	10.4	142.0	5.7
S.E.	0.14	0.07	0.63	0.19

SUPERSCRIPT KEY
$p < 0.05$

1 differs from synchronous.
2 differs from vivarium.
3 differs from basal.

TABLE 1, CONTINUED

BLOOD BIOCHEMISTRY

GROUP	CREATINE (mg/dl)	ALKALINE PHOS (iu/l)	GLUCOSE (mg/dl)	TOTAL PROTEIN (gm/dl)	ALBUMIN (gm/dl)	BUN (mg/dl)
Flight						
Mean	0.60[1,2,3]	236[1,2,3]	155[1,2]	5.64	3.56	33 [1,2,3]
S.E.	0.00	20	8	0.20	0.12	2.6
Synchronous						
Mean	0.40	154[2,3]	126[3]	5.64	3.48	12[2,3]
S.E.	0.06	9	2	0.15	0.08	0.6
Vivarium						
Mean	0.48	108[3]	112[3]	5.52	3.56	16[3]
S.E	0.05	9	7	0.08	0.08	0.4
Basal						
Mean	0.44	418	156	5.36	3.56	15
S.E	0.04	72	2.64	0.04	0.04	1.0

SUPERSCRIPT KEY

$p < 0.05$

1 differs from synchronous.
2 differs from vivarium.
3 differs from basal.

TABLE 2

PLASMA HORMONE CONCENTRATIONS

BASAL	SYNCHRONOUS	FLIGHT	VIVARIUM
IMMUNOREACTIVE GROWTH HORMONE (ng/ml)			
25.4±8.8 (5)* 16.9±2.3 (4)	18.2±3.1 (5)	34.8±18.8 (5)* 16.0±1.4 (4)	13.5±1.0 (5)
No significant differences between groups ($p > 0.05$) * high value included			
PROLACTIN (ng/ml)			
6.7±1.8	2.7±0.5	5.9±1.9	2.6±1.8
No significant differences between groups ($p > 0.05$)			
CORTICOSTERONE (ng/ml)			
26.2±5.1	13.0±1.1	15.1±4.2	27.1±4.5
Synchronous values are significantly lower than Basal or Vivarium ($p < 0.05$)			
PLASMA TESTOSTERONE (mug/ml)			
3.3±0.49	1.52±0.54	0.34±0.12	0.97±0.42
Basal values are significantly greater than for all other groups; Flight values are lower than Synchronous ($p < 0.05$)			

N90-26476

EXPERIMENT K-6-23

EFFECT OF SPACEFLIGHT ON LEVELS AND FUNCTION OF IMMUNE CELLS

Principal Investigator:

A.D. Mandel
NASA Ames Research Center
Moffett Field, California 94035

Co-Investigators:

G. Sonnenfeld
W. Berry
Department of Microbiology and Immunololgy
University of Louisville School of Medicine
Louisville, Kentucky

G. Taylor
NASA Johnson Space Center
Houston, Texas

S. R. Wellhausen
Division of Nephrology
University of Louisville School of Medicine
Louisville, Kentucky

I. Konstantinova
A. Lesnyak
Institute of Biomedical Problems
Moscow, USSR

B. Fuchs
Institute of Human Morphology
Moscow, USSR

SUMMARY

Two different immunology experiments were performed on samples received from rats flown on Cosmos 1887. In the first experiment, rat bone marrow cells were examined in Moscow for their response to colony stimulating factor-M. In the second experiment, rat spleen and bone marrow cells were stained in Moscow with a variety of antibodies directed against cell surface antigenic markers. These cells were preserved and shipped to the United States where they were subjected to analysis on a flow cytometer. The results of the studies indicate that bone marrow cells from flown rats showed a decreased response to colony stimulating factor than did bone marrow cells from control rats. There was a higher percentage of spleen cells from flown rats staining positively for pan-T-cell, suppressor-T-cell and innate interleukin-2 receptor antigens than from control animals. In addition, a higher percentage of cells that appeared to be part of the myelogenous population of bone marrow cells from flown rats stained positively for surface immunoglobulin than did equivalent cells from control rats.

INTRODUCTION

Many alterations in immune responses after space flight (Barone and Caren, 1984; Cogoli, 1981 and 1984, Durnova et al., 1976; Gould et al., 1987a; Konstantinova et al., 1985; Lesnyak and Tashputalov, 1981; Talas et al., 1983 and 1984; Taylor et al., 1983 and 1986) or antiorthostatic suspension (Caren et al., 1980; Gould and Sonnenfeld, 1987b; Rose et al., 1984; Sonnenfeld et al., 1982) have been reported. These changes have ranged from alterations in lymphoid organ size (Durnova et al., 1976) to alterations in lymphocyte activities (Cogoli et al., 1981 and 1984) to alterations in interferon production (Talas et al., 1983 and 1984; Gould et al., 1987a). The full range of these changes and the significance of these changes with regard to resistance to infection has not been established.

The purpose of the immunology studies flown on Cosmos 1987 was to begin a systematic attempt to define the range of immunological parameters affected by space flight. Two different areas were chosen for study. The first involved a determination of the effect of space flight on the ability of cells to respond to an external immunological stimulus. For this purpose, bone marrow cells from flown rats were exposed to colony stimulating factor-monocyte/macrophage (CSF-M). CSF-M is an important regulator of the differentiation of bone marrow cells of the monocyte/macrophage lineage, and an alteration in the ability of cells to respond to CSF-M could result in altered immune function (Waheed and Shadduck, 1979). The cells were observed for their responses to CSF-M.

The second set of studies involved a determination of the effect of space flight on the expression of cell surface markers of spleen cells and bone marrow cells. These markers represent various immunologically important cell populations, and an alteration in the percentage of cells expressing the markers could result in an alteration of immunological function (Barone and Caren, 1984; Jackson and Warner, 1986). The markers that were tested included T-cell markers, B-cell markers, natural killer cells markers, and interleukin-2 receptors. The studies were carried out by staining the cell populations with fluorescein-labelled antibodies directed against the appropriate antigens. The stained cell populations were then analyzed utilizing a flow cytometer, and compared with stained cell populations from control rats for changes in percentages of cells expressing the markers.

MATERIALS AND METHODS

Ten male specific pathogen free rats of Czechoslovakian-Wistar origin (Institute of Endocrinology, Bratislava, Czechoslovakia) were flown on the Cosmos 1887 Biosputnik flight for 12 and on-half days. Flight, housing, feeding and recovery conditions were as described in the Mission

Description section of this technical report. Tissue from rats number 6-10 were used in our project. After sacrifice of the rats, bone marrow cells were extruded with a needle and syringe from the left femur of the rats using RPMI-1640 medium (MA Bioproducts, Walkersville, MD) supplemented with 10% fetal bovine serum, antibiotics, glutamine and 2-mercaptoethanol. One quarter of the spleen of each of the five rats was dissociated into individual cells and placed into supplemented RPMI-1640 medium. All of the sample were placed into transporter vials, held and 4 °C and transported to Moscow. Samples reached the laboratory and analytical work began 30-32 hrs after removal of the tissue from the rats.

Control and vivarium rats were treated as described in the Mission Description section of this technical report. Tissues were removed and treated as described for the flight tissue.

Upon arrival at the laboratory in Moscow, the cells were centrifuged and washed. Cells were washed in phosphate buffered saline, and counted in an haemocytomer using trypan blue dye for determination of viability. For colony stimulating factor, 10^5 bone marrow cells were suspended in 1 ml of McCoy's 5A medium (MA Bioproducts, Walkersville, MD) supplemented with 10% fetal bovine serum and antibiotics and containing 0.3% agar (Shadduck and Nagabhushanam, 1971). Included in the medium was 0.1 ml of colony stimulating factor-M (a gift of Dr. Robert N. Moore, University of Tennessee). The experiment was carried out in duplicate. The suspended cells were then placed in 35 mm tissue culture dishes and then incubated in a 37 °C incubator with 5% CO_2 (Shadduck and Nagabhushanam, 1971). After the appropriate incubation period (5-6 days), 5-10 microscope fields on each slide were evaluated for the number of colonies (aggregates of 50 cells or more) formed.

For the cell surface antigenic markers, the following procedure was carried out (Jackson and Warner, 1986). Approximately 1 x 10^5 bone marrow or spleen cells were placed in a microcentrifuge tube. The cells were resuspended in FTA buffer (7.65 g sodium chloride, 1.27 g disodium phosphate, 0.10 g monosodium phosphate, and 0.21 g monopotassium phosphate brought to 1 liter volume with distilled water at pH 7.4), and centrifuged for 1.5 min at 1,000 x g. Supernatants were removed and cells were resuspended. 5 µl of the appropriate antibody was added to the cells. All antibodies were obtained from Accurate Chemical and Scientific, Westbury, NY, except for anti-asialo GM-1 (obtained from WAKO Fine Chemicals, Dallas TX) and anti-rabbit IgG (Sigma Chemical, St. Louis, MO). The cells were allowed to incubate at 4 °C for 25 min. The antibodies used were as follows:

1. Anti-asialo GM-1 (anti-natural killer cells)
2. 0X-39 (anti-interleukin-2 receptor)
3. OX-1 (anti-pan-leukocyte marker)
4. W3/25 (anti-helper T-cell)
5. OX-8 (anti-suppressor T-cell)
6. OX-12 (anti-rat IgG Fab')
7. W3/13 (anti-pan T cell)
8. OX-4 (anti-polymorphic Ia)
9. Anti-rabbit IgG
10. No antibody added.

All antibodies were fluorescein tagged except for anti-asialo GM-1 and 0X-39. For these two antibodies the following special additional procedure was carried out. Cells stained with these antibodies were resuspended in 1 ml of FTA buffer and centrifuged for 1.5 min at 1,000 x g. The cells were resuspended in residual buffer and 5 ul of a second, fluorescein-conjugated anti-antibody and 25 µl of fetal bovine serum were added. The second antibody for anti-asialo GM-1 was anti-rabbit IgG and for OX-39 was anti-mouse IgG. Incubation for these samples was at 4 °C for 25 min.

At this point, the following procedure was carried out for all cells stained with all of the antibodies. One ml of lysing solution (8.26 g ammonium chloride, 1.00 g potassium bicarbonate, 37 mg of tetrasodium EDTA, brought to 1 l with distilled water at pH 7.4) was added to each sample and the cells were allowed to incubate at room temperature for 6 min to lyse erythrocytes. The cells were then centrifuged at 1,000 x g for 1.5 min, and then resuspended in 1 ml of FTA buffer. Cells were then centrifuged again and fixed by resuspending in 0.5 ml of 1% paraformaldehyde. The cells were then placed at 4 °C and transported to the United States. The cells were analyzed for fluorescence, an indicator of presence of the antigen, using an autofluorograph IIs interfaced with a 2151 Data Handler computer system (Ortho Diagnostics, Westwood, MA). For this analysis, lymphocytes and myelogenous cells (neutrophils and monocytes) were first differentiated by forward vs. right angle scatter. The green, that is, fluorescein, fluorescence of each "gated" population was then plotted on a 1,000 channel histogram from which the percentage of positive-stained cells was determined. The lower threshold for this determination was set to exclude 95-98% of the cells in tube #10 to which no antibody had been added. The individual background from tube #10 for each rat was subtracted from each of the stained populations.

RESULTS

Effect of spaceflight on the response of bone marrow cells to CSF-M.

Due to insufficient cells and CSF-M, experiments with CSF-M were carried out in duplicate only on flight and synchronous control rats. On flight samples, the results were read after 6 days of incubation. On synchronous control samples, the results were read after 5 days of incubation due to concern for dehydration of the cultures. The results of the assays show a sizeable reduction in the number of colonies from cells from flown rats exposed to CSF-M compared to cells from synchronous control rats exposed to CSF-M (Table 1).

Effect of spaceflight on the percentage of cells expressing cell surface markers.

For spleen cells, profound changes in the percentage of lymphocytes expressing various cell surface antigenic markers were observed. The results are summarized in Table 2. These results indicate that there appears to be a higher percentage of cells expressing pan T-cell antigens (W3/13), suppressor T-cell antigens (0X-8), and expressing endogenous interleukin-2 receptor markers (OX-39) (Table 2). No other changes in the percentage of spleen cells expressing a marker were observed. Measurable numbers of myelogenous cells were not detected in any of the specimens.

Because of a shortage of bone marrow cells, these cells were stained only with anti-pan leukocyte (OX-1) and anti-rat IgG fab' (OX-12). Lymphocytes and myelogenous cells were analyzed differentially as described in Materials and Methods. For the lymphoid cells, there was an equivalent increase in the percentage of cells expressing pan-leukocyte markers and IgG in both flight and synchronous control cells (Table 3). For the myelogenous cells, there was also an increase in cells expressing pan-leukocyte marker in both flight and sychronous control cells; however, there was a large increase in the percentage of cells from flight animals expressing surface IgG compared to both synchronous and vivarium control cells (Table 3).

DISCUSSION

The results of this study suggest that several of the immunological markers examined were affected profoundly by spaceflight. This is in agreement with earlier studies that indicated that other immunological parameters could be affected by spaceflight (Barone and Caren, 1984, Konstantinova et al., 1985; Taylor et al., 1983 and 1986).

In this case, it appears that the ability of bone marrow cells to respond to CSF-M was impaired after spaceflight. This could have yielded impaired production of monocytes, which could result in compromised ability to present antigens and to phagocytose potential pathogens.

In addition, there appears to be an increase in the percentage of T-cells, and suppressor T-cells in particular, in the spleens of flown rats. This increase in suppressor cells which extends previous observations, could, in part, account for immunosuppression observed after spaceflight (Konstantinova et al., 1985; Taylor et al, 1983 and 1986).

Another finding of interest is the increase in the percentage of cells with receptors for interleukin-2. Since the spleen cells were not stimulated with mitogens to increase expression of interleukin-2 receptors, these are representative of endogenous receptors on resting T cells. The increase in interleukin-2 receptors could indicate an increased immune activity, possibly induced by flight conditions, that is held in check by the increased number of suppressor cells.

Also, increases in percentages in T cells were observed in lymphoid bone marrow cells from flown and synchronous control rats compared to vivarium control rats. Since the increases were similar in both flown and synchronous control rats, it is likely that conditions of handling were responsible for the changes. The situation with expression of surface IgG on bone marrow cells is different. For the lymphoid population, an equivalent increase occurs in cells from both flown and synchronous control rats; however, for the myelogenous population, there is a large increase in cells bearing surface IgG from the flown rats only. This could indicate that spaceflight may induce a non-specific blastogenesis of the bone marrow cells that is down-regulated by increased suppressor T-cell activity.

Two unexpected results were also observed. First was the staining of spleen cells with anti-rabbit-IgG. This occurred on spleen cells from all flight and control rats. We would have not expected this to occur, and the handling, storage and shipment required could have contributed to this unusual result. Second, the percentage of spleen cells from rats in both synchronous and vivarium groups staining with anti-suppressor T-cell was higher than expected. However, since a much higher proportion of spleen cells from the flight animals stained with anti-suppressor T-cell than from either control group, we feel it is valid to conclude that spaceflight resulted in increased levels of suppressor T-cells.

CONCLUSIONS

The current study presents additional data to indicate that spaceflight, even of a relatively short duration, affects certain parameters of the immune system. Through this study, we have been able to demonstrate some specific cell populations that appear to be affected by spaceflight. These results suggest possible future directions for research in this area.

It is recognized that a number of factors associated with this flight should be considered in assessing its significance. Several areas will require further research. First, the current study was very small using only five animals.The study needs to be repeated to confirm the data and to allow a thorough statistical analysis. Second, due to limitations in the number of cells available, all desirable parameters, particularly with regard to monoclonal antibody fluorescein staining of bone marrow cells, could not be carried out. Monoclonal antibody staining of lymph node and thymus cell, if possible, might yield additional useful information. It would be desirable to expand the study to allow that additional work. Third, the functional significance of the immunological changes observed needs to be established. Fourth, a determination of the role of various factors in spaceflight, for example stress, microgravity, etc., in inducing immunological changes remains to be carried out.

Finally, the technical difficulties that resulted in a two-day delay in sacrifice and tissue sampling needs to be taken into account. This two-day maintenance of the flown animals at normal gravity could have affected the outcome of this study.

In any case, the results of the current study suggest that several profound alterations in parameters that play important roles in regulation of immune responses occur as a result of spaceflight. This is an interesting finding that supports previous findings, and the results suggest the experiments warrant repetition and expansion.

ACKNOWLEDGEMENTS

The authors wish to thank Dr. A.S. Kaplansky and the Soviet Cosmos recovery and dissection teams. Without their heroic efforts, these studies could not have been carried out. In addition, we would like to thank Igor Krasnov, Galina Tverskaya, Marilyn Vasques, Richard Grindeland, and James Connolly, without whose planning and support successful completion of these studies would have been impossible. We also express our gratitude to the Academician and staff of the Institute of Biomedical Problems and the Institute of Human Morphology, Academy of Medical Sciences of the U.S.S.R., for their help and for the use of their laboratories. This work could not have been accomplished without them. We would also like to thank Mr. M. Tanner for his help with the flow cytometric analysis. This study was funded in part by NASA grant NAG9-234 and by funds from the NASA Cosmos 1887 Parts Program.

REFERENCES

1. Barone, R.B.; and Caren, L.D.: The immune system: effects of hypergravity and hypogravity. Aviat. Space Environ. Med., vol. 55, 1984, pp.1063-1068.

2. Caren, L.B.; Mandel, A.D.; and Nunes, J.A.: Effect of simulated weightlessness on the immune system in rats. Aviat. Space Environ. Med., vol. 51, 1980, pp. 251-256.

3. Cogoli, A.: Hematological and immunological changes during space flight. Acta Astronautica, vol. 8, 1981, pp. 995-1002.

4. Cogoli, A.; Tschopp, P.; and Fuchs-Bislin, P.: Cell sensitivity to gravity. Science, vol. 225, 1984, pp. 228-230.

5. Dumova, G.N.; Kaplansky, A.S.; and Portugalov, V.V.: Effect of a 22-day space flight on lymphoid organs of rats. Aviat. Space Environ. Med., vol.47, 1976, pp. 588-591.

6. Gould, C.L.; Lyte, M.; Williams, J.A.; Mandel, A.D.; and Sonnenfeld, G.: Inhibited interferon-gamma but normal interleukin-3 production from rats flown on the space shuttle. Aviat. Space Environ. Med., vol. 58, 1987a, pp. 983-986.

7. Gould, C.L.; and Sonnenfeld, G.: Enhancement of viral pathogenesis in mice maintained in an antiorthostatic suspension model - coordination with effects on interferon production. J. Biol. Regulators Homeostatic Agents, vol. 1, 1987b, pp. 33-36.

8. Jackson, A.L.; and Warner, N.L. Preparation, staining and analysis by flow cytometry of peripheral blood leukocytes. In: Manual of Clinical Laboratory Immunology, 3 ed., N.K. Rose, H. Friedman, and J.L. Fahey, eds., American Society for Microbiology, Washington, D.C., 1986, pp. 226-235.

9. Konstantinova, I.V.; Antropova, E.N.; Rykova, M.P.; Guseva, O.A.; Lesnyak, A.T.; Vorotnikova, I.E., and Vasilyeva, E.F. Cell-mediated and humoral immunity in cosmonauts exposed to space flight factors. Vestnik Akad. Med. Nauk CCCP, No. 8, 1985, pp. 51-58.

10. Lesnyak, A.T ; and Tashputalov, R.Y.U.: Effects of space flight on lymphocyte transformation in Cosmonauts' peripheral blood. Komich. Biol., vol. 1, 1981, pp. 32-34.

11. Rose, A.; Steffen, J.M.; Musacchia, X.J.; Mandel, A.D., and Sonnenfeld, G.: Effect of antiorthostatic suspension on interferon-alpha/beta production by the mouse. Proc. Soc. Exp. Biol. Med., vol. 177, 1984, pp. 253-256.

12. Shadduck, R.K.; and Nagabhushanam, N.G.: Granulocyte colony stimulating factor I. Response to acute granulocytopenia. Blood, vol. 38, 1971, pp. 14-22.

13 Sonnenfeld, G.; Morey, E.R.; Williams, J.A.; and Mandel, A.D. Effect of a simulated weightlessness model on the production of rat interferon. J. Interferon Res., vol. 2, 1982, pp. 467-470.

14. Talas, M.; Batkai, L.; Stoger, I.; Nagy, K.; Hiros, L.; Konstantinova, I.; Rykova,M.; Mozgovaya, I.; Guseva, O.; and Kohzarinov, V.: Results of space experiment program "interferon" I. Production of interferon in vitro by human leukocytes aboard space laboratory Salyut-6 ("Interferon-I") and influence of space flight on lymphocyte function of Cosmonauts ("Interferon-III"). Acta Microbiol. Hungarica, vol. 30, 1983, pp. 53-61.

15. Talas, M.; Batkai, L.; Stoger, I.; Nagy, K.; Hiros, L.; Konstantinova, I.; Rykova, M.; Mozgovaya, I.; Guseva, O.; and Kozharinov, V.: Results of space experiment program "Interferon." Acta Astronautica, vol. 11, 1984, pp. 379-386.

16. Taylor, G.R.; and Dardano, J.R.: Human cellular immune responsiveness following space flight. Aviat. Space Environ. Med., vol. 54 supp. 1, 1983, pp. 555-559.

17. Taylor, G.R.; Neal, L.S.; and Dardano, J.R.: Immunological analysis of U.S. Space Shuttle crewmembers. Aviat. Space Environ. Med., vol. 57, 1986, pp. 213-217.

18. Waheed, A.; and Shadduck, R.K. Purification and properties of L cell derived colony stimulating factor. J. Lab. Clin. Med., vol. 94, 1979, pp. 180-194.

TABLE 1

EFFECT OF SPACEFLIGHT ON THE RESPONSE OF BONE MARROW CELLS TO CSF-M

Rat Number	Number of Cells in 5 Microscope Fields	
	Flight Rats	Synchronous Control Rats
6	2, 1*	15, 10
7	1, 0	1, 5
8	2, 1	14, 10
9	2. 1	4, 9
10	1, 3	5, 5

* Results are of two replicate cultures for each rat.

TABLE 2

EFFECT OF SPACEFLIGHT ON THE PERCENTAGE OF SPLEEN CELLS EXPRESSING CELL SURFACE MARKERS

Rat#	BKG*	GM-1	OX-39	W3/25	OX-8	OX-12	W3/13	OX-4	Rbt Ig
Flight Animals									
6	2.2	66.2	75.5	38.7	62.5	35.6	56.3	34.5	88.3
7	2.2§	53.9	94.6	55.4	95.1	26.2	91.2	69.6	94.1
8	2.2	43.1	93.6	35.4	85.8	45.0	77.3	75.0	95.9
9	2.3	47.1	91.8	39.1	75.6	29.5	51.2	43.0	92.7
10	1.2	89.9	96.2	46.9	96.2	43.8	57.5	68.7	94.4
Vivarium Control Animals									
6	2.7	39.0	50.0	39.0	51.0	30.1	41.8	36.1	20.6
7	3.3	60.7	85.2	31.0	53.3	34.7	32.0	38.3	58.3
8	1.6	46.7	82.0	32.3	47.9	42.1	43.7	49.0	75.2
9	2.1	70.7	64.1	35.6	48.0	33.1	36.5	39.9	77.9
10	2.5	57.8	61.4	32.5	59.9	42.5	43.1	34.8	89.2
Synchronous Control Animals									
6	2.3	39.6	74.9	33.9	40.3	43.7	42.1	50.1	72.4
7	2.0	44.6	69.7	-†	39.5	44.0	30.6	49.4	42.9
8	2.0	59.6	84.7	35.0	57.2	39.3	49.5	45.0	30.9
9	2.9	51.3	63.5	32.0	49.2	34.4	33.6	38.1	76.1
10	2.6	43.8	76.3	37.1	38.5	41.8	38.5	43.5	26.4

*Abbreviations used: BKG = Background (unstained no-antibody control); GM-1 = anti-natural killer cells; OX-39 = anti-interleukin-2 receptor; OX-1 = anti-pan-leukocyte marker; W3/25 = anti-helper T-cell; OX-8 = anti-suppressor T-cell; OX-12 = anti-rat IgG Fab'; W3/13 = anti-pan T cell; OX-4 = anti-poylmorphic Ia; Rbt Ig = anti-rabbit IgG.

§Insufficient cells in control sample, control used from rat number 6

†Apparently no antibody applied

C6

TABLE 3

EFFECT OF SPACEFLIGHT ON THE PERCENTAGE OF BONE MARROW CELLS EXPRESSING CELL SURFACE MARKERS

Rat #	No Antibody (Background)		Anti-pan Leukocyte		Anti-rat IgG Fab	
	Lymph*	Myelog	Lymph	Myelog	Lymph	Myelog
Flight Animals						
6			63.2	97.2	37.5	55.6
7			52.9	95.7	58.9	28.7
8			30.8	92.0	26.2	19.2
9			57.5	96.1	62.9	32.8
10			59.7	96.5	41.0	21.0
Vivarium Control Animals						
6	4.1	1.6	23.4	69.4	24.9	4.9
7	0.4	1.4	17.9	72.6	13.5	7.4
8	1.3	2.4	17.9	74.1	11.5	5.2
9	1.5	2.3	17.1	79.3	13.0	6.3
10	0.2	1.7	14.3	72.1	9.4	3.7
Synchronous Control Animals						
6			40.0	94.2	28.0	8.3
7			60.2	90.9	59.7	17.4
8			48.4	96.8	28.3	8.1
9			40.2	77.2	21.9	9.9
10			44.3	88.7	43.6	13.6

*Abbreviations used: lymph = lymphocytic cell population; myelog = myelogenous cell population

Due to insufficient cells available, the no antibody control was carried out only on vivarium controls. All other values are calculated from those background values.

ORIGINAL PAGE IS
OF POOR QUALITY

N90-26477

EXPERIMENT K-6-24, K-6-25, K-6-26

RADIATION DOSIMETRY AND SPECTROMETRY

Principal Investigator:

E.V. Benton
Physics Research Laboratory
University of San Francisco
San Francisco, California

Co-Investigators:

A. Frank,
E.R. Benton
University of San Francisco
San Francisco, California

V. Dudkin
A. Marennyi
Institute of Biomedical Problems
Moscow, USSR

PRECEDING PAGE BLANK NOT FILMED

SUMMARY

Radiation experiments flown by the University of San Francisco on the Cosmos 1887 spacecraft were designed to measure the depth dependence of both total dose and heavy particle flux, dose and dose equivalent, down to very thin shielding. Three experiments were flown and were located both inside and outside the Cosmos 1887 spacecraft. Tissue absorbed dose rates of 264 to 0.028 rad d^{-1} under shielding of 0.013 to 3.4 g/cm^2 of ^{7}LiF were found outside the spacecraft and 0.025 rad d^{-1} inside. Heavy particle fluxes of 3.43 to 1.03 x 10^{-3} cm $^{-2}s^{-1}sr^{-1}$ under shielding of 0.195 to 1.33 g/cm^2 plastic were found outside the spacecraft and 4.25 x 10^{-4} cm $^{-2}s^{-1}sr^{-1}$ inside ($LET_{\infty}H_2O \geq 4$ keV/μm). The corresponding heavy particle dose equivalent rates outside the spacecraft were 30.8 to 19.8 mrem d^{-1} and 11.4 mrem d^{-1} inside. The large dose and particle fluxes found at small shielding thicknesses emphasize the importance of these and future measurements at low shielding, for predicting radiation effects on space materials and experiments where shielding is minimal and on astronauts during EVA.

The Cosmos 1887 mission contained a variety of international radiobiological investigations to which the measurements apply. The high inclination orbit (62°) of this mission provided a radiation environment which is seldom available to U.S. investigators. The radiation measurements will be compared with those of other research groups and also with those perf .med on the Shuttle, and will be used to refine computer models employed to calculate radiation exposures on other spacecraft, including the Space Station.

INTRODUCTION

The Soviet Cosmos 1887 biosatellite mission was host to a wide variety of space biology and radiation experiments performed by several research groups. Included were three sets of radiation dosimetry and spectrometry experiments flown by the University of San Francisco (USF). Experiments employed passive detectors for heavy cosmic ray, proton, neutron and total dose measurements. The radiation environment both inside and outside the spacecraft was monitored, with particular emphasis on shielding depth dependence and including very small shielding thicknesses.

The Cosmos 1887 experiments follow from previous USF participations in the Cosmos series (on mission Nos. 782, 936 and 1129 /Peterson, et al., 1978; Benton, et al., 1978a; Benton, et al., 1978b; Benton, et al., 1981; Kovalev, et al., 1981/) as well as a wide range of U .S. space flights, including the Gemini, Apollo, Skylab, Apollo-Soyuz and Space Shuttle missions /Benton, et al., 1977a; Benton, et al., 1977b; Benton and Henke, 1983; Benton, 1984; Benton, et al., 1985; Benton, 1986; Benton and Parnell, 1987. In addition to providing radiation measurements specific to the mission and its experiments, the acquired data adds to the long-term project of mapping radiation intensities in near-Earth orbit and in providing measured comparisons for the radiation modeling codes. The Cosmos 1887 mission also offered the opportunity to intercompare measurements with other research groups and in this way compare measurements of some quantities (i.e. dose, LET) using different techniques.

EXPERIMENTS

The three Cosmos 1887 experiments are discussed individually below.

Experiment K-6-24

The objective of this experiment was to measure the radiation environment inside the spacecraft. We were able to obtain only a very approximate idea of the shielding, but useful comparisons of dose rates and LET spectra can be made with experiments positioned on the outside of the spacecraft as well as with measurements made on previous spaceflights. The detectors used were plastic nuclear track detectors (PNTDs), nuclear emulsions and thermoluminescent detectors (TLDs).

Five PNTD stacks were used to measure the heavy-particle, high LET spectra, a nuclear emulsion stack was included to measure the energetic proton spectrum, and TLDs (TLD-700) were used to measure the total dose. The components were placed in a Lexan polycarbonate plastic box (7 cm x 7 cm x 3.95 cm), with the five PNTD stacks (one thick center stack plus four thin side stacks) arranged in an orthogonal array to compensate for the angular response of PNTDs. The PNTDs used were special, high-sensitivity CR-39, developed in

this laboratory, plus several sheets of Tuffak polycarbonate detector. The physical dimensions of the detectors and their configuration in the Lexan box are shown in Figures 1 - 4.

Experiment K-6-25

The objective here was to measure the depth dose under very thin shielding on the outside of the spacecraft and to determine what fraction of the dose was due to low energy electrons versus heavy charged particles. This required that the shielding of the outermost detectors be no more than a few mg/cm^2 and that the detectors themselves also be very thin (because of the short ranges of the particles). The maximum depth in the TLD stacks was 3.4 g/cm^2. Although computer codes exist for calculating doses encountered in LEO both from protons and electrons, there have been only a few instances where a direct comparison (under very thin shielding) has been possible between experiment and theoretical prediction.

Two identical flight units (F1 and F2) each containing three stacks of TLDs were used. F1 and F2 consisted of aluminum cylinders of 5 cm diameter and 1.99 cm thickness with cylindrical holes to accommodate TLD stacks. In two stacks (Nos. 1 and 2), thin (9.14 x 10^{-3} cm) TLDs were placed at the tops, and thicker (0.889 mm) TLDs at the bottoms. In the third stack only the thicker (0.889 mm) TLDs were used. An aluminized double-window of Kapton plastic totaling 15 μm served to hold in the TLD stacks and to protect them from direct sunlight, heat and vibration. Each aluminized surface had an optical density of 3. In addition to the three USF stacks, a center hole was placed in the cylinders and left open for use by the Soviets. The detector unit configuration is shown in Figure 5.

In the stacks with only the thicker TLDs (No. 3) there were sixteen ^{7}LiF TLDs, with separators of 15 μm-thick polycarbonate film between the detectors for protection against vibration and movement. Strips of stiff 0.015 cm-thick paper were inserted along all four sides and the bottoms of the stacks to hold the TLDs in vertical alignment and give further protection against mechanical effects.

In the stacks with thin TLDs (Nos. 2 and 3) there were 30 thin chips at the top, and 12 thicker chips underneath. All TLDs were ^{7}LiF and were separated by 15 μm-thick polycarbonate film, as above. Paper was placed beneath each stack but could not be inserted along the sides of the stacks because of the fragility of the thin TLDs. The K-6-25 units were mounted on the outside of the spacecraft, with the No. 2 flight cylinder being partially shielded by the spacecraft auxiliary battery power unit which is also externally mounted.

Experiment K-6-26

Part A:

The objective here was to measure the low energy, heavy particle (excluding electrons) LET spectra under essentially zero shielding (outside the spacecraft) and as a function of depth. Although there have been some previous measurements of LET spectra under such conditions, the orbital dependence and the effects of solar cycle on the low energy charged particle component are still not well understood.

The hardware consisted of two hermetically sealed flight units containing PNTD stacks and with aluminized Kapton double-windows, as in Experiment K-6-25. The PNTD stacks were 3 cm in diameter and 1.4 cm thick and included sets of CR-39, Tuffak polycarbonate and Cronar polyester detectors. The physical configurations of the units and PNTD stacks are shown in Figures 6 and 7.

Parts B and C:

Here the intent was to obtain some information on the neutron energy spectra. Part B detectors were located on the outside of the spacecraft and Part C on the inside.

Part B of the experiment consisted of two flight units containing ^{59}Co activation foils and PNTD films. An aluminum frame with aluminized Kapton double-windows was placed above the detectors but the sides of the units were open to vacuum. The PNTDs used were Tuffak polycarbonate and Cronar polyester. The purpose of the PNTDs in this experiment was for an intercomparison between those open to vacuum and those

hermetically sealed. Due to space limitations, CR-39 was not included. The configuration of the units is shown in Figure 8.

Part C consisted of a single ^{59}Co activation foil. This foil was placed inside the spacecraft near Experiment K-6-24.

The selection of available isotopes with suitable activation cross sections and decay product half-lives for spaceflights of a few days places severe limitations on this method. Cross sections exist for the measurement of both low energy (thermal plus resonance) and high energy (>10 MeV) neutrons, with some proton contribution, with the activations forming ^{60}Co and ^{58}Co. However, readout requires a very sensitive, low background spectrometer.

Detector Exposure:

Cosmos 1887 was launched on September 29, 1987, re-entry was on October 12, 1987, for a flight duration of 12.634 days. Orbit inclination was 62.8°, while apogee/perigee were 406 km/224 km.

The K-6-25 and K-6-26 A and B units were mounted on the outside of the spacecraft, inside flat, lidded containers (see Figure 9). The container lids were open during takeoff and while in orbit, but were closed before re-entry.

The flight and ground-control units were returned to our laboratory on October 24, 1987, in generally good condition, although the K-6-26 B units were blemished. Unit B-F1 had a residue of some material beaded on the surface which had apparently become hot. When disassembled, the PNTDs inside unit B-F1 appeared warped, as though they had become hot. Unit B-F2 had the upper of the two aluminized windows mostly torn off. The ^{59}Co activation foils were unaffected by the above.

The paper strip temperature indicators in the K-6-26 A units gave maximum temperature readings between 40.6°C and 46°C (unit A-F1) and between 77°C and 88°C (Unit A-F2). The duration of the high temperature excursions is not known.

Processing and Readout:

Plastic Nuclear Track Detectors (PNTDs):

The CR-39, the polycarbonate and the polyester PNTDs were given standard processing in 6.25N NaOH solution at 50°C. The bulk etch, B, (single surface thickness) of each of the films was measured. Preliminary scanning showed that the track densities on the polycarbonate and polyester detectors were very low (<1 cm^{-2}) while the CR-39 track densities were much higher (~400-2000 cm^{-2}). Pairs of CR-39 films were reassembled in their flight configurations. The scanning took place on the two interior surfaces of the pairs. This enabled the particles to be separated into short range (SR): matching tracks appearing on only the two interior surfaces, and long range, galactic cosmic rays (GCR): matching tracks appearing on all four surfaces of the pair of films. The major and minor axes of the eliptical surface openings of tracks were measured. The axial measurements, together with the "B" of the samples and the calibrated LET response function of the CR-39 material, were then used to generate particle LET spectra.

Thermoluminescent Dosimeters (TLDS):

The TLDs were read out using a Harshaw Model 4000 TLD Reader. A 30-sec read cycle and 10°C/sec temperature ramp were employed. The total glow peak distributions were recorded by data transfer to a microcomputer, which makes possible glow peak deconvolution. This was accomplished with the Harshaw Data File Management System microcomputer software.

TLDS from the flight and ground control units and ^{137}Cs source standard irradiations were read out together. This allowed the proper background subtractions and conversion of TLD signal to absorbed dose.

^{59}Co Activation Foils:

For relatively short spaceflights of a few days there are four reactions to consider in the use of ^{59}Co activation foils. These are ^{59}Co(n,g) ^{60}Co, ^{59}Co (n,2n)^{58} Co, ^{59}Co(p,np) ^{58}Co, and ^{59}Co(n,p) ^{59}Fe. The (n,g) reaction has cross sections of 37.4 barns for thermal neutrons and a resonance integral of 77 barns for 132 eV. The 5.27 y half-life of ^{60} Co is, however, much longer than optimum. The (n,2n) reaction cross section has a maximum of about 800 mb between 17 and 20 MeV, but the 71.3 d half-life of ^{58} Co is much closer to optimum. The (p,np) reaction also yields ^{58} Co so there is a possibility of a mixed contribution from protons and neutrons. The proton ranges in a thick ^{59}Co foil will also complicate this analysis. The (n,p) reaction cross section is about 750 mb in the 14 MeV region. The ^{59}Fe half-life is 45 d, which is favorable.

It was planned that the ^{59}Co foils would be read out using a high sensitivity, very low background gamma ray spectrometer at the Manned Spaceflight Center near Huntsville. Unfortunately, the crystal of the spectrometer broke during the initial part of this procedure. The foils were transferred to a second facility having a spectrometer but this instrument had less favorable ratios of sensitivity to background. The counting results were negative in that the differences between the sample counts and the background were not statistically significant.

Nuclear Photographic Emulsions:

Nuclear emulsions have been processed and are still undergoing analysis.

RESULTS

Experiment K-6-24

The TLDs yielded a flight dose of 313 ± 13 mrads. This is compared below with the doses measured outside the spacecraft.

The CR-39 PNTDs yielded the integral particle LET flux spectra plotted in Figure 10, where the total (TOT) is the sum of GCR and SR spectra. The long-range (four-surface) tracks are due to GCRs and their projectile fragments, with the protons not included. The registration range of protons in this type of CR-39 is not sufficiently high to produce tracks on all four surfaces when the thickness of foils equals ~650 μm. The short range tracks therefore include all primary and secondary stopping protons and all higher Z stopping particles with a range ≤1300 μm in CR-39. The latter are mainly secondary particles produced from target nuclei within the PNTDs which have undergone interactions with energetic primaries (mainly protons).

Experiment K-6-25

Absorbed dose measurements in the TLD stacks from the F1 and F2 units are plotted in Figures 11, 12, and 13. The doses from the two stacks containing thin TLDs in each flight unit are plotted together in Figures 11 and 12. In the range of 0 to 1 g/cm^2 shielding thickness, the slope in the depth dose rate distribution is very steep and does rate may decline by ~4 orders of magnitude. The rate of change is greatest at the outer surface, where the very short range particles are absorbed. The doses from the thick TLD stacks in both of the flight units are plotted in Figure 13.

In Figures 11 and 12, curves have been fitted to the maximum doses at the tops of the stacks, to the doses from the thicker TLDs at the bottoms of the stacks, and to the lowest of the intermediate TLD doses. Most of the thinner TLD doses scatter above the curves. This is because the thinner TLD chips were not in precise vertical alignment. The small mass of these chips, together with springiness and electrostatic effects in the polycarbonate plastic separator films, caused horizontal displacements of the chips as they were stacked. The fragility of the thinner chips did not permit forcing them into alignment with inserts along the sides.

The magnitudes of the positive deviations in the measured absorbed doses are explained by the strong attenuation of the radiation entering through the tops of the stacks, while the radiation passing through the circular openings, but to the sides of the stacks, is less attenuated. Thus a small portion of a TLD chip extending out could contribute more to the total TLD signal than the much larger portion of the chip which lay within the stack boundary.

The thicker TLD chips (0.889 mm) at the bottoms of these stacks, and those within the stacks composed only of the thicker chips, were in a good alignment and do not show much scattering of data. The lower doses through which the curves were drawn represent those TLDs which were well-shielded from above. The curves give the best representations of the true depth-dose profiles. The depth-dose profiles measured only with the thicker TLDs show that the dose averaging of thick TLDS at low shielding thicknesses produces inaccurate results. There is also dose averaging for the thinner TLDs and, if thinner than 90 μm detectors were available, the maximum measured dose would have been higher.

Measured dose rates as a function of depth are also shown in Table 1, along with the K-6-24 data. In measuring dose versus depth in the TLD stacks, the polycarbonate plastic separator films were converted to equivalent ^{7}LiF thickness on the basis of the ranges of 10 MeV protons in the two materials (1 μm polycarbonate = 0.54 μm ^{7}LiF). It was observed that the dose rates at the bottoms of the TLD stacks (3.4 g/cm^2) located outside the spacecraft approached those found in the interior of the spacecraft.

The doses measured by the thicker TLDs (the No. 3 stacks) are seen to be higher than for the smaller type (No. 1 and 2 stacks), even above 1 g/cm^2 depth where dose averaging is not a problem. This occurs because of the larger horizontal dimensions of the TLDs in the No. 3 stacks (0.635 cm x 0.635 cm versus 0.318 cm x 0.318 cm). Larger diameter holes in the aluminum were necessary to accommodate the No. 3 stacks, which decreased the total 4π shielding around the stacks. The large holes are also slightly closer to the sides of the aluminum cylinders and to the center hole.

Experiment K-6-26

Part A:

To date, only the CR-39 detectors have undergone analysis. In the assembly of the two PNTD flight stacks, CR-39 pairs were alternated with the other films. Most of the thickness of the stacks consisted of CR-39. In the flight No. 1 stack the first CR-39 sheet had 0.0444 g/cm^2 of plastic above it. In the flight No. 2 stack the first CR-39 sheet had only the Kapton plastic double-window above it (0.00216 g/cm^2). When samples were processed, the upper surface of this least-shielded CR-39 film pitted very badly, showing that it must have been damaged by heat or by the high dose of low energy electrons. This layer could not be analyzed so the least-shielded detector layer was lost.

Integral LET flux spectra measured at four progressive depths in the F1 PNTD stack are plotted in Figures 14, 15, 16 and 17. The mass thicknesses of plastic shielding varied from 0.195 to 1.33 g/cm^2. The spectra are plotted for Total, GCR and SR as discussed previously. The SR and Total particle fluxes are variable. The GCR fluxes decrease, then increase again with increasing shielding depth. The decrease in the SR flux with depth is apparently due to a progressive stopping of primary short range particles, mainly protons, with depth. Most of the difference in the SR LET spectra is in the low LET region (<20 keV/μm), which supports the theory that low energy protons are the cause. If substantial numbers of primary particles with $Z \geq 2$ were stopping they would add to the GCR (four-surface tracks) spectra at the smaller depths. The increase in the GCR flux with depth is less easy to explain. This may be due to a slowing down of energetic primary particles, with a net increase in registered particles from the lighter nuclei which were initially outside the sensitive LET range of the CR-39. Another possibility is that energetic secondary alpha particles are produced with ranges greater than 1300 μm in CR-39. This would require energies ≥ 50 MeV. Secondaries of this type would increase the numbers of four-surface tracks with increasing depth until equilibrium between production and stopping was reached.

The LET spectra measured outside the spacecraft can be compared with that measured inside (K-6-24, Figure 10). The LET integral flux for the more heavily shielded inside detector is less than the outside fluxes for both the GCR and SR spectra. However, the GCR spectrum is lower over the full LET range

while the SR spectrum is lower only in the lower LET region. The SR spectrum inside the spacecraft is approximately equal to or greater than the outside spectra at LETs above 20 keV/μm. The effect of shielding on the PNTDs inside the spacecraft is therefore a continuation of the effect seen in the external stack where the SR spectrum is concerned.

The primary proton region in the SR spectra appears to lie below LETs of 20 keV/μm when, in fact, the maximum LETs for protons are 94.3 keV/μm (at 0.1 MeV). There are fundamental reasons for this. The LET region of 5-20 keV/μm corresponds to proton energies of 9-1.5 MeV and ranges in CR-39 plastic of 806-37 μm. LETs above 20 keV/μm correspond to proton ranges the section of a stopping proton track with LET >50 keV/μm is only about 4.5 μm in length R-39 detectors were processed, about 39 μm thickness of material was etched from each su ETs which are measured are the range-weighted average LET values within the etched laye track detection condition which was imposed in scanning the samples, that the particle be detec o adjacent surfaces, means that the particles needed a minimum range of about 85 μm in order to be counted. Since primary particles entering the tops of the PNTD stacks passed progressively through the Nos. 1, 2, 3, and 4 surfaces of each CR-39 pair, since the track parameters for the LET determinations were measured in the No. 2 surfaces, and since the corresponding tracks in the No. 3 surfaces were required for confirmation, then the sections of these tracks which determined the LETs were distant from the stopping points by a distance ≥ 45μm (this includes the 7 μm equivalent thickness of a polycarbonate separator foil between the two CR-39 films). This would yield a maximum LET of 17.4 keV/μm for measurements of these proton tracks. Given the LET resolution of CR-39 in this region, for isotropic particles (~10%), this is in reasonable agreement with the measurements. It should be noted that protons traveling in the opposite direction (up from the bottoms of the PNTD stacks) could yield higher measured LETs (up to ~35 keV/μm).

With regard to the 87 μm particle range cutoff mentioned above (the effective range cutoff for isotropic particles is greater), it should also be noted that the shorter range particles which intersect the detector surfaces are lost to the analysis and to the LET spectra. This will include a small fraction of the stopping primary particles (~6%) and perhaps a substantial fraction of secondary particles.

The integral fluxes, dose rates and dose equivalent rates for Total, GCR and SR particles and for six CR-39 detectors are given in Table 2. The steep decline in SR flux with depth in shielding is shown but it can also be seen that the dose rate and dose equivalent rate do not decrease as rapidly as flux, showing that the major difference is at the lower LETs. It is also interesting to note that the GCR flux is relatively high for the least shielded detector, drops substantially for the next least shielded, then builds up through the remainder of external stack No. 1. This suggests that the primary particles included a component with sufficient range and charge ($Z \geq 2$) to form four-surface tracks, but which was substantially absorbed in <0.4 g/cm^2 of plastic. Because the GCR fluxes were less than the SR, the statistical reliability of the GCR data is also less and this conclusion is tentative. However, in comparing the spectra, the least shielded GCR spectrum is somewhat higher than the others in the region of 100-200 keV/μm.

DISCUSSION

Results for Cosmos 1887 and a summary of data for three previous Cosmos flights are shown in Table 3. The differences in the heavy particle fluxes due to the more sensitive PNTDs used on Cosmos 1887 are quite large. The TLD doses inside the spacecraft are comparable for the different flights.

Total tissue absorbed dose rates on Cosmos 1887 varied from 264 to 0.028 rad d^{-1} under shielding of 0.013 to 3.4 g/cm^2 of ^{7}LiF outside the spacecraft and 0.025 ± 0.001 rad d^{-1} inside the spacecraft. The measurements of high LET particles ($LET_{\infty}H_2O \geq 4$ keV/μm^{-1}) show particle fluxes up to 3.43 x 10^{-3}cm^{-2}s^{-1}sr^{-1} outside the spacecraft and 4.25 x 10^{-4}cm^{-2}s^{-1}sr^{-1} inside. High LET dose rates and dose equivalent rates up to 5.25 mrad d^{-1} and 30.8 mrem d^{-1} were obtained outside the spacecraft, and rates of 1.27 mrad d^{-1} and 11.4 mrem d^{-1} were found inside. Because of damage to the least shielded CR-39 PNTD, the maximum levels of high LET particles were not obtained.

The LET spectrum from the K-6-26 A Flight No. 1 PNTD stack, layers 11 and 12, is shown as "crosses" in Figure 18 and compared with data from previous flights (Benton and Parnell, 1988). The minimum shielding of the detector was 0.436 g/cm^2 of plastic. The spectrum compares well with Soviet results from

Cosmos 782 and 936 and, in the higher LET region, Cosmos 1129. (These three flights all had similar orbits). The shielding of the electronic LET spectrometer used only by the Soviets on Cosmos 782, and presumably for the same type on 936, was only about 1 g/cm^2, while the shielding of their nuclear emulsions used on Cosmos 1129 was about 20 g/cm^2. This would account for the smaller fluxes seen on Cosmos 1129 for LET <20 keV/μm, which is in agreement with the effect of shielding reported in this paper.

An aspect of the K-6-25 experiment which needs to be improved for future measurements is in the vertical alignment of stacks of "thin" TLDs. The scatter in the measurements of TLDs intermediate in the stacks, reported above, resulted from individual misalignments of the square TLDs within the larger, circular holes which contained them. The fragile TLDs were inserted one at a time into the holes with vacuum tweezers, and clearance room at the corners was necessary. Square containing holes of close tolerance would correct the alignment problem but a method of manufacturing this configuration and of placing the TLDs without breakage must be devised. There are other advantages to using square holes. Without air gaps around the TLDs the shielding becomes more comparable to that of a uniform slab, especially for short range particles. A more accurate measure of depth dose for this geometry would then be possible.

In comparing the depth dose measurements with calculations (alt. 300 km, incl. 62°) of depth dose in an infinite slab-geometry, including e$^-$, p, GCR and bremsstrahlung (Watts, 1988), the experiment shows a factor of ~44 decrease in the first 0.1 g/cm^2 ^{7}LiF while the calculations show a decrease by a factor of 28.5 in the first 0.1 g/cm^2 Al. However, the true 0 g/cm^2 dose could not be measured because of the presence of the 15 μm-thick plastic windows and the fact that there was dose averaging across the TLDs. For the dose ratio between the calculated average of 0.002-0.026 g/cm^2 and 0.1 g/cm^2 Al, which is a better comparison to the experiment, the difference is a factor of 5.9. Thus the experiment gives a much steeper decline in dose over the first 0.1 g/cm^2 of shielding than does the calculation. It should be noted that the problem of misalignment of the thin TLD chips, discussed above, would give a lesser decline in the measured depth dose, so this cannot explain the difference.

The calculations show that the short range electron component is more than 99% attenuated at 0.5 g/cm^2 Al. The maximum proton plus GCR dose is less than 0.1% of the maximum electron dose but is more penetrating, so that at depths greater than 2 g/cm^2 Al the dose is dominated by protons. Between 0.5 and 3.4 g/cm^2 ^{7}LiF the measured dose decreased by ~90%, while between the same thicknesses of Al the calculated total dose decreases by ~99%. This difference may be due to the deviation of the experiment from infinite slab geometry. As stated above, close square holes for the TLD stacks would improve the modeling but there is also a component of the experimental dose which came obliquely through the sides of the 5 cm diameter Al TLD holder. Doses measured at the greater depths may have been enhanced by a factor of two or more, relative to an infinite slab geometry. Another difference with calculation derives from the difference in mass thickness between the TLD stacks and the surrounding aluminum. At 3.4 g/cm^2 in the TLDs, the aluminum walls were 4.6 g/cm^2 in depth. This reduces the measured dose by a few percent compared to a uniform slab.

The calculated dose averaged between 0.002 and 0.026 g/cm^2 was about 100 rads d^{-1}, which is somewhat below the maximum measured dose range (264 and 161 rad d^{-1} in F1 and F2). The altitude used in the calculation (300 km) is only approximate, and this will influence the comparison.

ACKNOWLEDGEMENTS

This work was supported by NASA Grant No. NCC2-521 (NASA-Ames Research Center) and NASA Grant No. NAG9-235 (NASA-Johnson Space Center, Houston). The authors would also like to thank Jim Connolly and Larry Chambers of NASA for their help.

REFERENCES

1. Benton, E.V., Peterson, D.D., Bailey, J.V. and Parnell, T.A. (1977a), High-LET particle exposure of Skylab astronauts. Health Phys. 32, pp. 15-20.

2. Benton, E.V., Henke, R.P. and Peterson, D.D. (1977b), Plastic nuclear track detector measurements of high-LET particle radiation on Apollo, Skylab, and ASTP space missions. Nucl. Track Det. 1, pp. 27-32.

3. Benton, E.V., Cassou, R.M., Frank, A.L., Henke, R.P. and Peterson, D.D. (1978a), Experiment K-206: Space radiation dosimetry on board Cosmos 936 -- U.S. portion of Experiment K-206, in : Final Reports of U.S. Experiments Flown on the Soviet Satellite Cosmos 936. (Rosenzweig, S.N. and Souza K.A., eds.), NASA TM 78526.

4. Benton, E.V., Peterson, D.D., Marenny, A.M. and Popov, V.I. (1978b), HZE particle radiation studies aboard Cosmos 782 Health Phys. 35, pp. 643-648.

5. Benton, E.V., Henke, R.P., Frank, A.L., Johnson, C.S., Cassou, R.M., Tran, M.T. and Etter, E. (1981), Experiment K-309: Space radiation dosimetry aboard Cosmos 1129: U.S. portion of Experiment K-309, in : Final Reports of U.S. Plant and Radiation Experiments Flown on the Soviet Satellite Cosmos 1129. (Heinrich, M.R. and Souza, K.A., eds.), NASA TM 81288.

6. Benton, E.V., and Henke, R.P. (1983), Radiation exposures during spaceflight and their measurement. Adv. Space Res. 3, No. 8 pp. 171-185.

7. Benton, E.V. (1984). Summary of current radiation dosimetry results on manned spacecraft. Adv. Space Res. 4, pp. 153-160.

8. Benton, E.V., Frank, A.L., Parnell, T.A., Watts, J.W., Jr. and Gregory, J.C. (1985). Radiation environment of Spacelab-1, American Inst. of Aeronautics and Astronautics conference, AIAA Shuttle Environment and Operations II, Houston, TX Nov. 13-15.

9. Benton, E.V., (1986), Summary of radiation dosimetry results on U.S. and Soviet manned spacecraft. Adv. Space Res., 6, No. 11, pp. 315-328.

10. Benton, E.V., and Parnell, T.A. (1987), Space radiation dosimetry on U.S. and Soviet manned missions, NATO Advanced Study Institute, "Terrestrial Space Radiation and its Biological Effects," Corfu, Greece: 11-25 Oct.

11. Kovalev, E.E., Benton, E.V. and Marenny, A.M. (1981), Measurement of LET spectra aboard Cosmos 936 biological satellite. Rad Prot. J., 1, pp. 169-173.

12. Peterson, D.D., Benton, E.V. and Tran, M. (1978), K-103: HZE particle dosimetry, in : Final Reports of U.S. Experiments Flown on the Soviet Satellite Cosmos 782. (eds., Rosenzweig, S.N. and Souza, K.A.), NASA TM 78525.

13. Watts, J.W., Jr. (1988) Marshall Spaceflight Center, Huntsville, AL, private communication.

Table 1

TLD DOSE RATES AS A FUNCTION OF DEPTH

Detector	TLD Stacks	Depth in ^7LiF (g/cm^2) +$2.16 \times 10^{-3} g/cm^2$ Plastic*	Tissue Absorbed Dose-Rate (rad/day)
K-6-25 F1	1+2	0.012	264
K-6-25 F2	1+2	0.012	161
K-6-25 F1	1+2	0.1	5.3
K-6-25 F2	1+2	0.1	4.4
K-6-25 F1	1+2	0.5	0.40
K-6-25 F2	1+2	0.5	0.29
K-6-25 F1	1+2	1.0	0.13
K-6-25 F2	1+2	1.0	0.076
K-6-25 F1	3	1.0	0.17
K-6-25 F2	3	1.0	0.13
K-6-25 F1	1+2	2.0	0.049
K-6-25 F2	1+2	2.0	0.038
K-6-25 F1	3	2.0	0.060
K-6-25 F2	3	2.0	0.046
K-6-25 F1	1+2	3.4	0.038
K-6-25 F2	1+2	3.4	0.028
K-6-25 F1	3	3.4	0.040
K-6-25 F2	3	3.4	0.032
K-6-24		Inside Spacecraft	0.0248 +/-0.0010

*Kapton

Table 2

PNTD RESULTS FROM COSMOS 1887

Experiment	Stack	Min. Shielding in plastic (g/cm^2)	Spectrum type	Flux ($cm^{-2}s^{-1}sr^{-1}$) x 10^{-4}	Dose (mrad d^{-1})	Dose equiv. rate (mrem d^{-1})
K-6-25	1-a	0.195	TOT	34.3	5.25	30.8
			GCR	2.50	1.20	16.0
			SR	31.8	4.05	14.8
	-b	0.436	TOT	20.0	3.65	22.5
			GCR	1.53	0.74	8.5
			SR	18.5	2.91	14.0
	-c	0.762	TOT	13.2	2.79	20.1
			GCR	2.24	1.10	12.6
			SR	10.9	1.69	7.5
	-d	1.33	TOT	10.3	2.50	19.8
			GCR	2.79	1.18	13.7
			SR	7.47	1.32	6.1
	2-a	0.319	TOT	21.3	3.52	19.9
			GCR	1.81	0.83	9.5
			SR	19.5	2.69	10.4
K-6-24	--- Inside Spacecraft		TOT	4.25	1.27	11.4
			GCR	1.38	0.63	7.1
			SR	2.87	0.64	4.3

*LET_{∞} $H_2O \geq 4$ keV μm^{-1}

Table 3

RADIATION MEASUREMENTS ON JOINT US/USSR COSMOS FLIGHTS

FLIGHT NO.	782	936	1129	1887
Launch Date	Nov. 1975	Aug. 1977	Sept. 1979	Sept. 1987
Duration (d)	19.50	18.30	18.56	12.63
Inclination (^{o})	62.8	62.8	62.8	62.8
Altitude (km Apogee/Perigee	405/226	419/224	394/226	406/224
HEAVY PARTICLES Flux Inside ($cm^{-2}s^{-1}sr^{-1}$)	$8.7\pm1.4\times10^{-6}$*	$5.1\pm1.0\times10^{-6}\Delta$	$6.1\pm0.1\times10^{-7}\nabla$	$4.25\pm0.24\times10^{-4}$ †
Flux Outside ($cm^{-2}s^{-1}sr^{-1}$)			$1.21\pm0.02\times10^{-6}\nabla$	$3.43\pm0.22\times10^{-3}$ †
Dose Equivalent Rate Inside (mrem d^{-1})				11.4±0.7
Outside (mrem d^{-1})				30.8±2.0
TLD DOSE RATE Inside (mrad d^{-1})		25.6±1.3	18.0±3.6 ††	24.8±1.0
Outside (max.) (mrad d^{-1})				$2.64\pm0.28\times10^{5}$
NEUTRONS Thermal Flux (cm^{-2} d^{-1})		$1.9\pm0.4\times10^{4}$	$2.7\pm0.5\times10^{4}$	
Resonance Flux (cm^{-2} d^{-1})		$6.5\pm3.2\times10^{4}$	$7.5\pm3.8\times10^{4}$	
High Energy Flux (cm^{-2} d^{-1})		$1.1\pm$ -$\times10^{5}$	$1.1\pm$-$\times10^{5}$	
Thermal Dose (mrem d^{-1})		0.020±0.004	0.028±0.006	
Resonance Dose (mrem d^{-1})		0.32±0.16	0.40±0.20	
High Energy Dose (mrem d^{-1})		6.8± ?	6.8± ?	

*LET_{∞}•H2O ≥ 105 keVμm^{-1}; .100 µm range. ΔLET_{∞}•H_2O ≥ 106 keV μm^{-1}; .180 µm range.

∇Different processing; results not comparable to other flights.

†LET_{∞}• H_2O ≥ 4 keV μm^{-1}; >100 µm range. ††Detectors irradiated during return transportation.

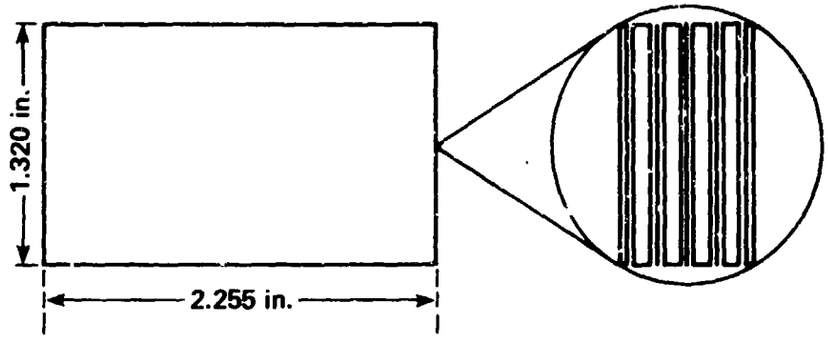

(a) SIZE OF X AND Y DETECTORS
(16 X CR-39; 8 X LEXAN)

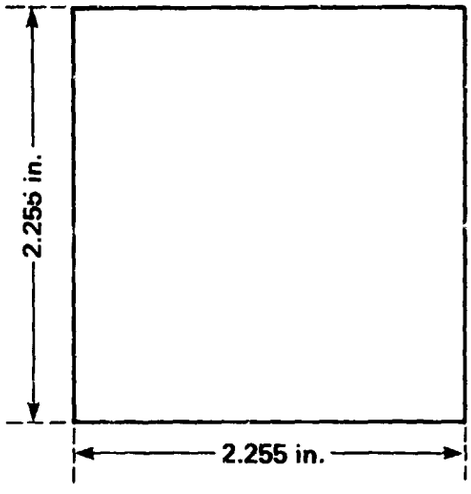

(b) SIZE OF Z DETECTOR (39 X CR-39; 4 X TUFFAK)
THE TOTAL THICKNESS OF THIS STACK IS 1.000 in.
THE COMPONENTS OF THE STACK ARE:
LEXAN (250 μm)
CR-39 (625 μm)
SEPARATED BY PC FOILS (8 μm)
·
· (39 PAIRS)
·
TUFFAK (4 X 254 μm)
LEXAN (250 μm)

Figure 1: A sketch of the PNTD stacks in Experiment K-6-24.

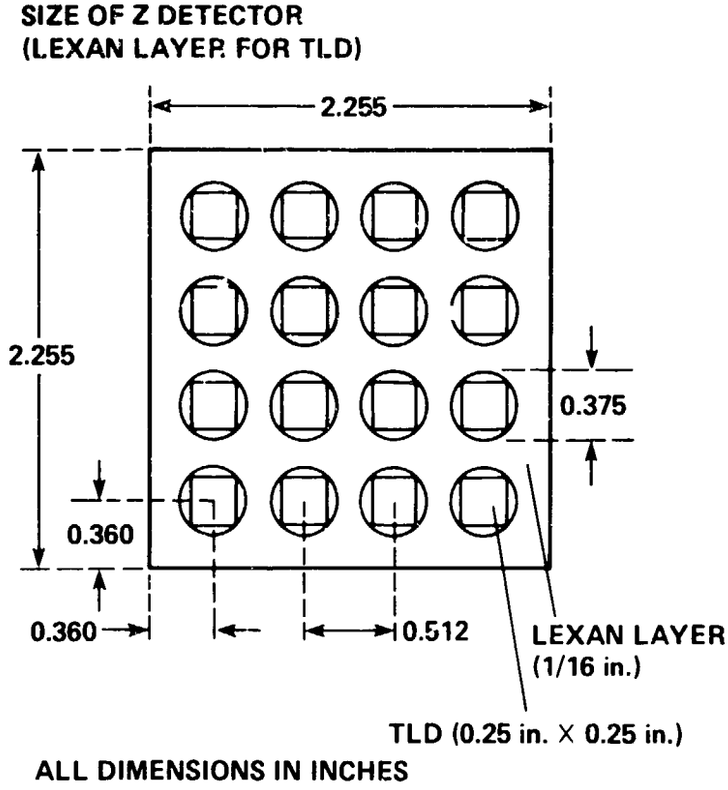

Figure 2: A sketch of the TLD array in Experiment K-6-24.

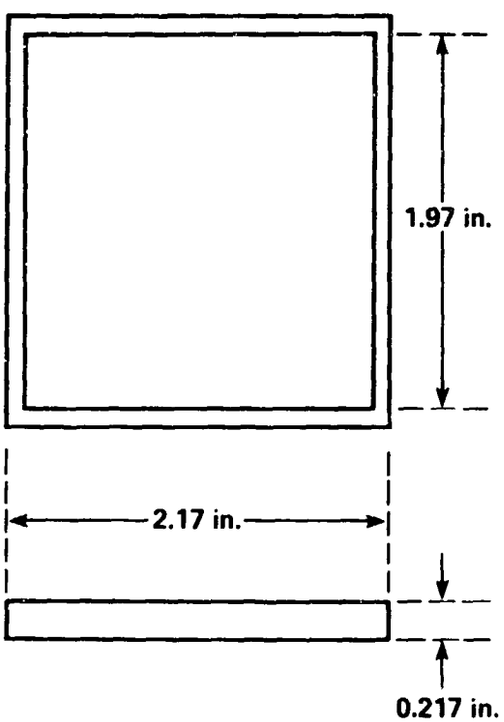

Figure 3: A sketch of the nuclear emulsion package in Experiment K-6-24.

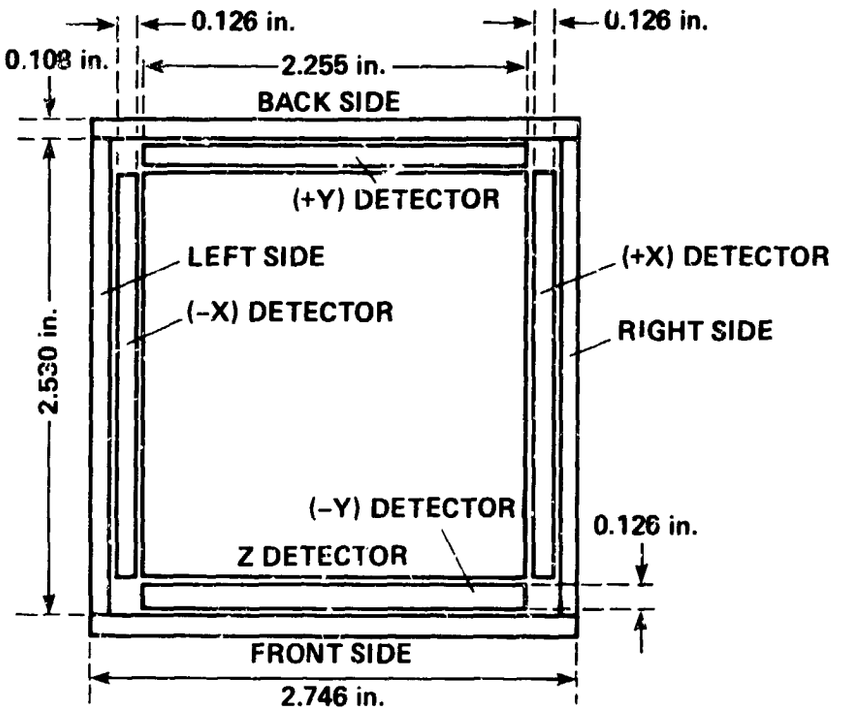

(a) TOP VIEW (SIDES ARE LEXAN 0.108 in. THICK)

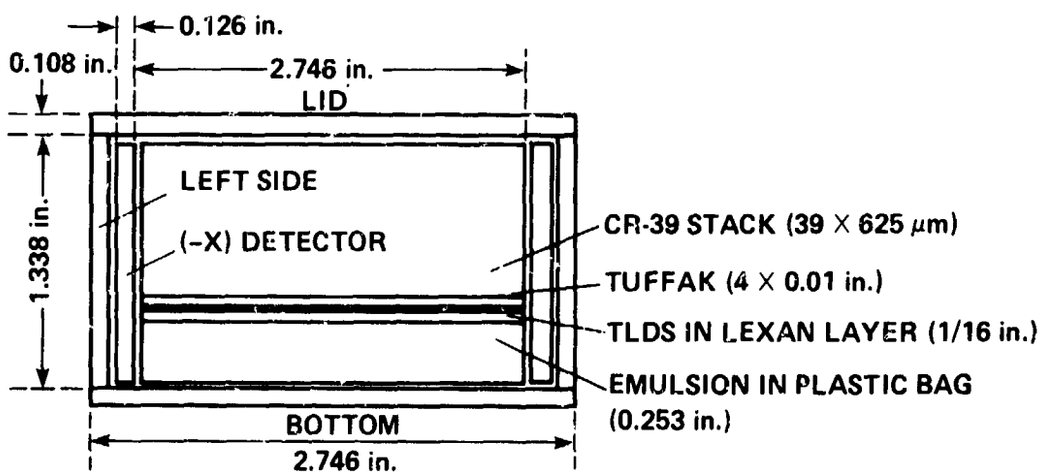

(b) SIDE VIEW

KOSMOS 87

(a) TOP VIEW OF THE OPEN LEXAN BOX

(b) SIDE VIEW INCL. Z DETECTOR STACK ALL DIMENSIONS IN INCHES

Figure 4: A sketch of the detector array in Experiment K-6-24.

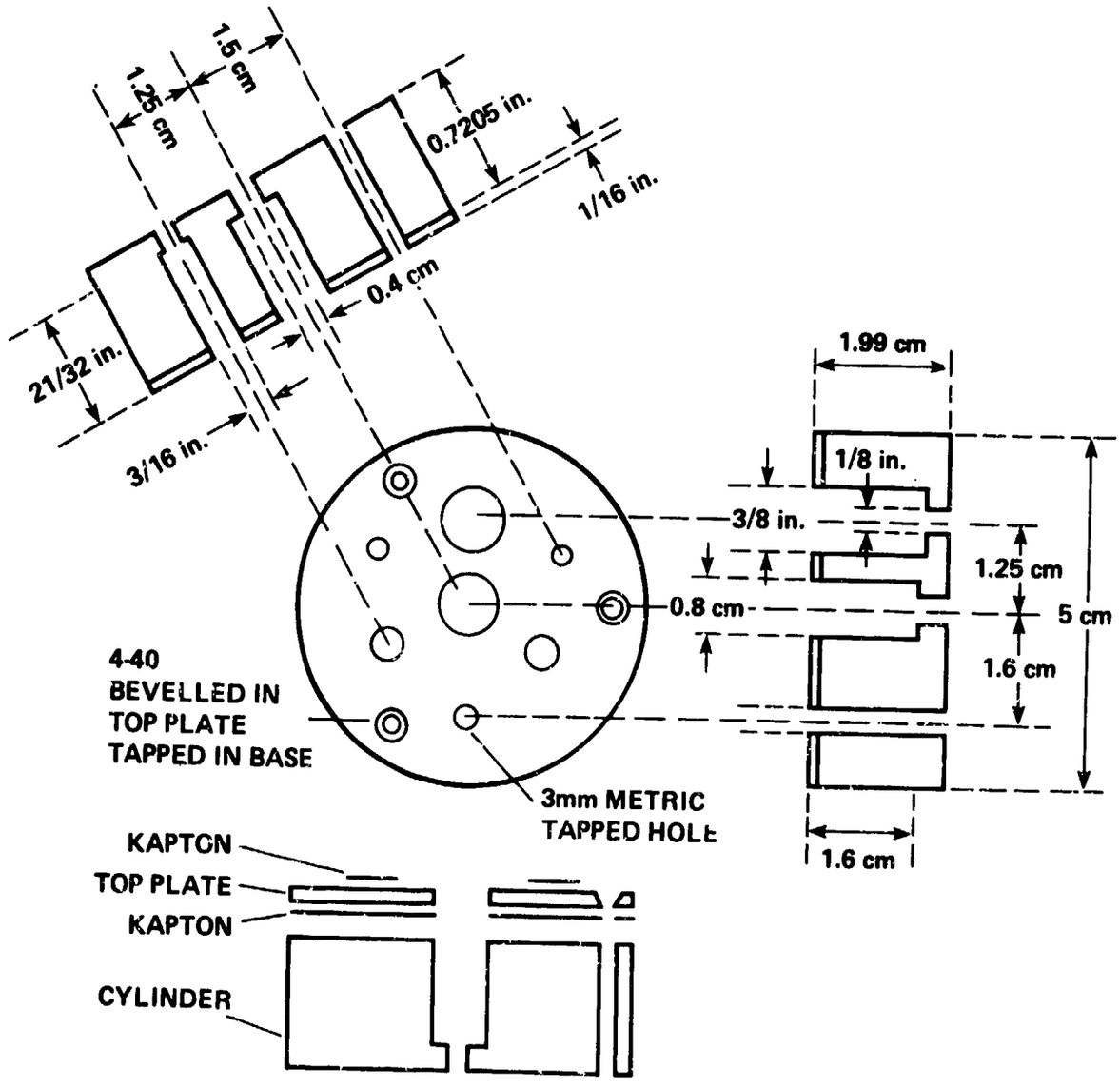

Figure 5: A sketch of the aluminum TLD stack container in Experiment K-6-25.

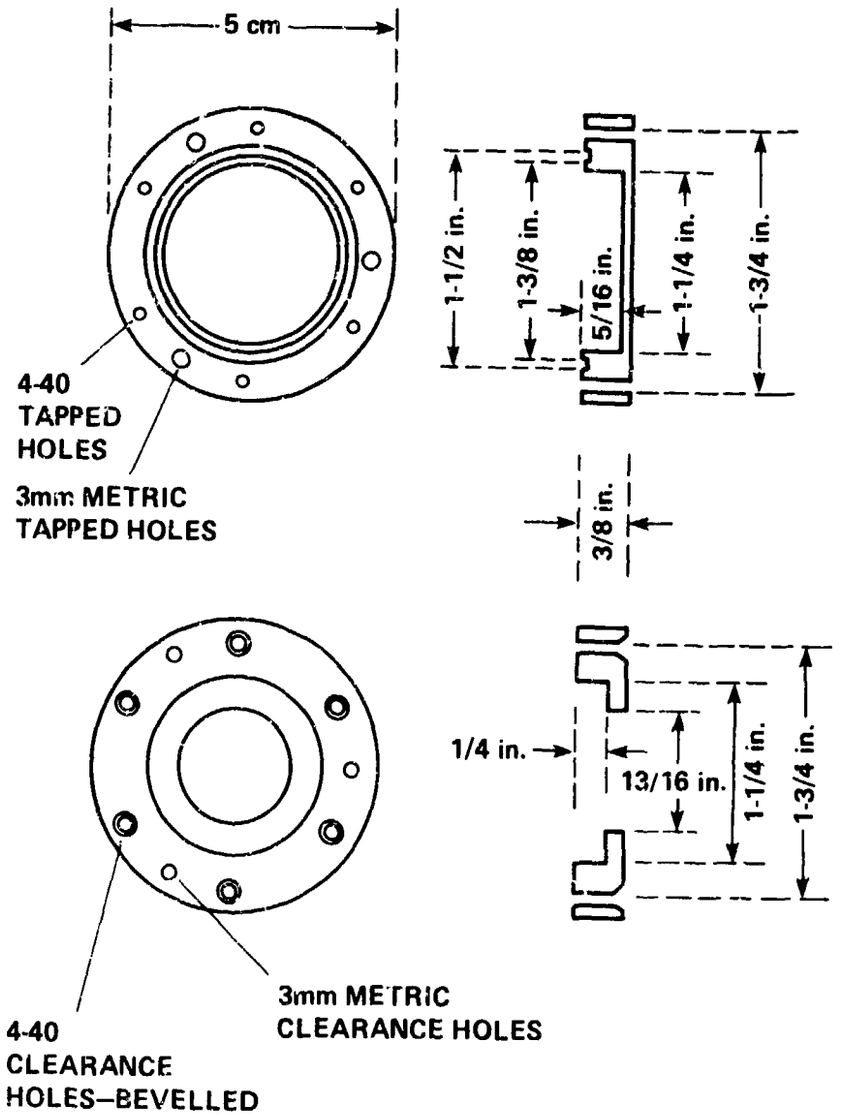

Figure 6: A sketch of the aluminum, sealed container for PNTD stacks in Experiment K-6-26 A.

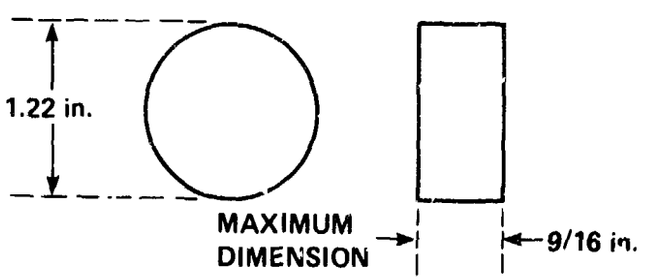

Figure 7: Dimensions of plastic nuclear track detector stacks in Experiment K-6-26 A.

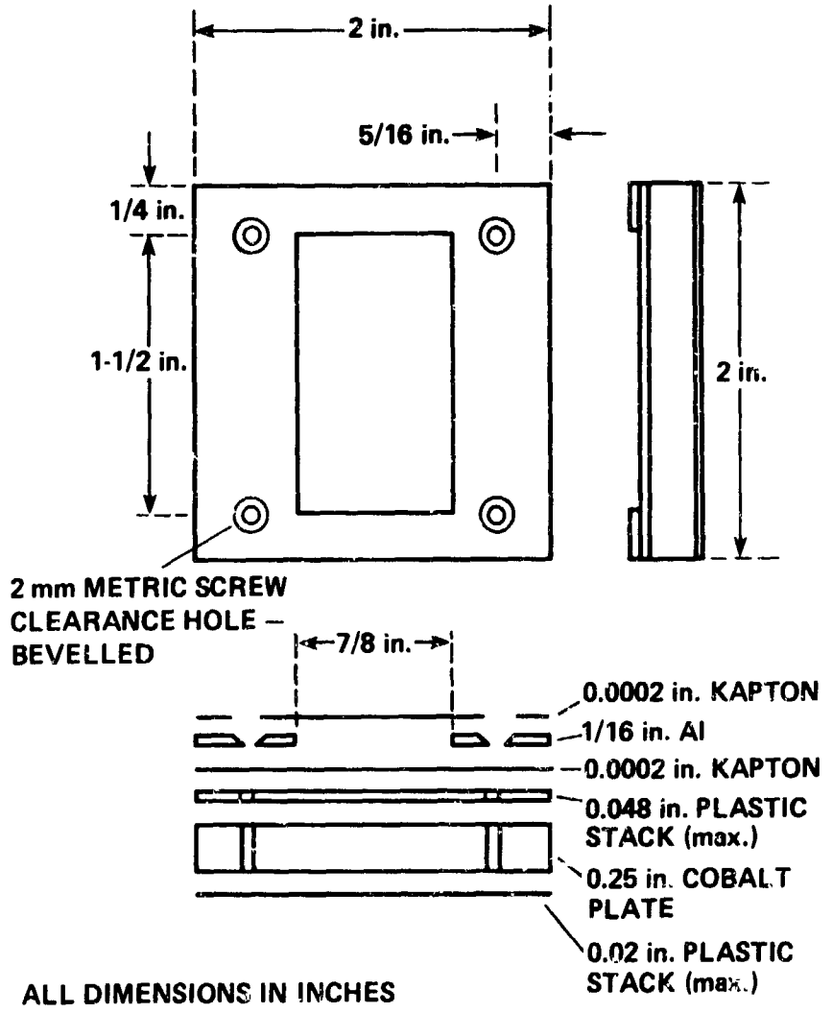

Figure 8: A sketch of the detector array in Experiment K-6-26 B.

ORIGINAL PAGE
BLACK AND WHITE PHOTOGRAPH

Figure 9: "Clam Shell" detector container flown on Cosmos 1887 showing effects of high temperature on several detector stacks.

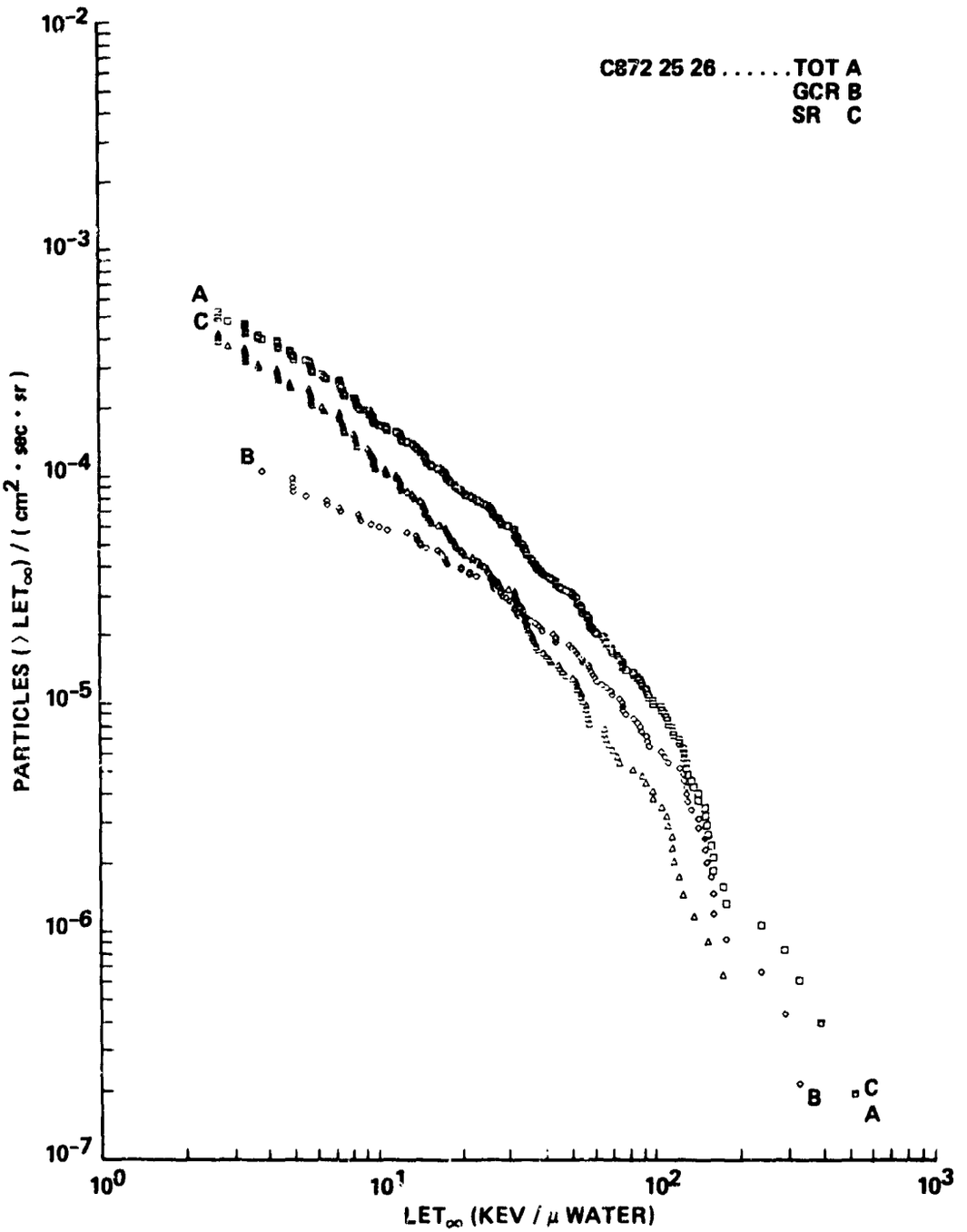

Figure 10: Integral LET flux spectra for Experiment K-6-24 (inside spacecraft). Average of three orthogonal detectors.

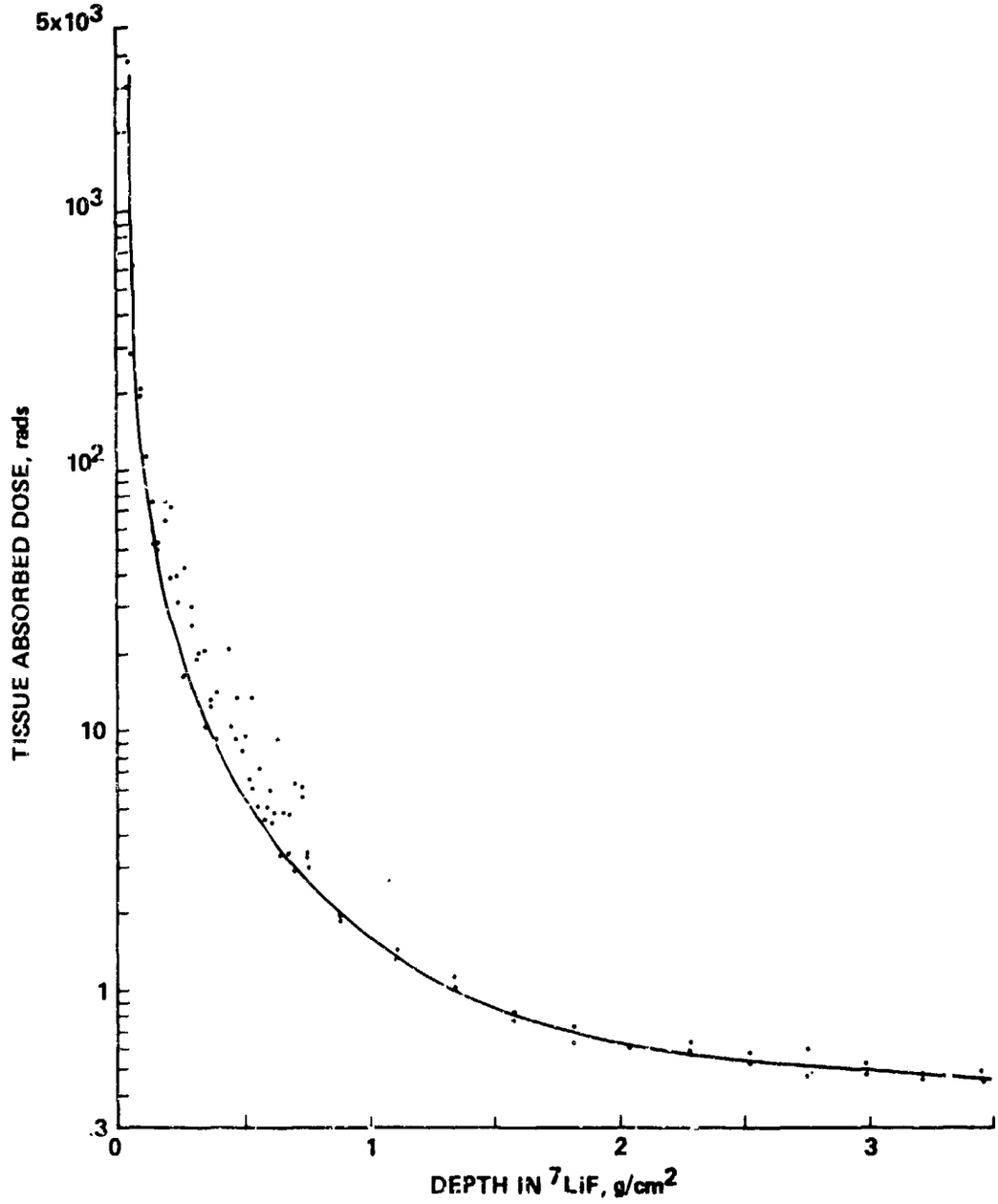

Figure 11: A plot of the depth-dose measurements for TLD stacks 1 and 2 from Experiment K-6-25 F1. Above the ^{7}LiF stacks were double windows of Kapton plastic totaling 15 μm (2.16×10^{-3} g/cm^2).

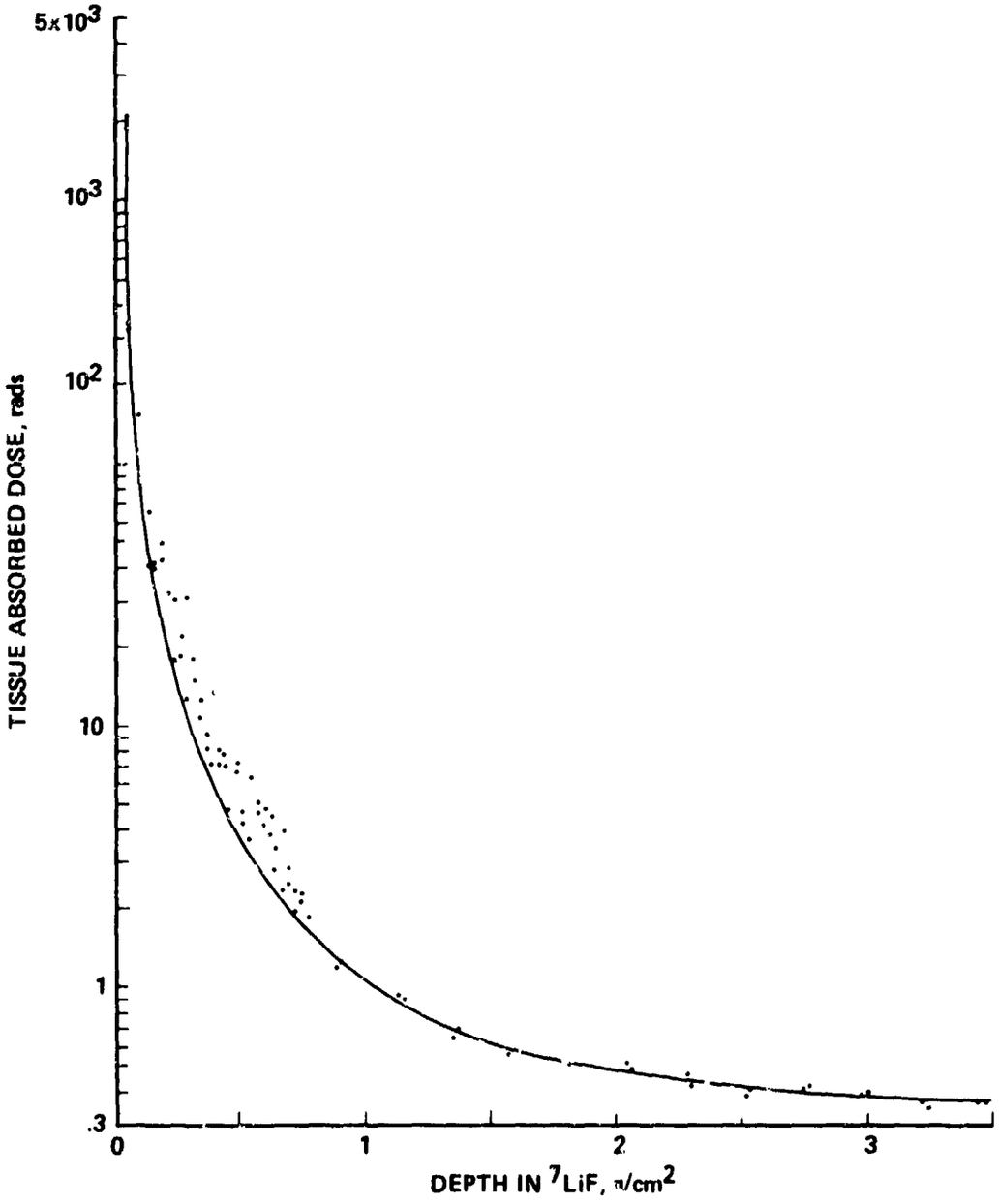

Figure 12: A plot of the depth-dose measurements for TLD stacks 1 and 2 from Experiment K-6-25 F2. Above the ^{7}LiF stacks were double windows of Kapton plastic totaling 15 μm (2.16×10^{-3} g/cm^2).

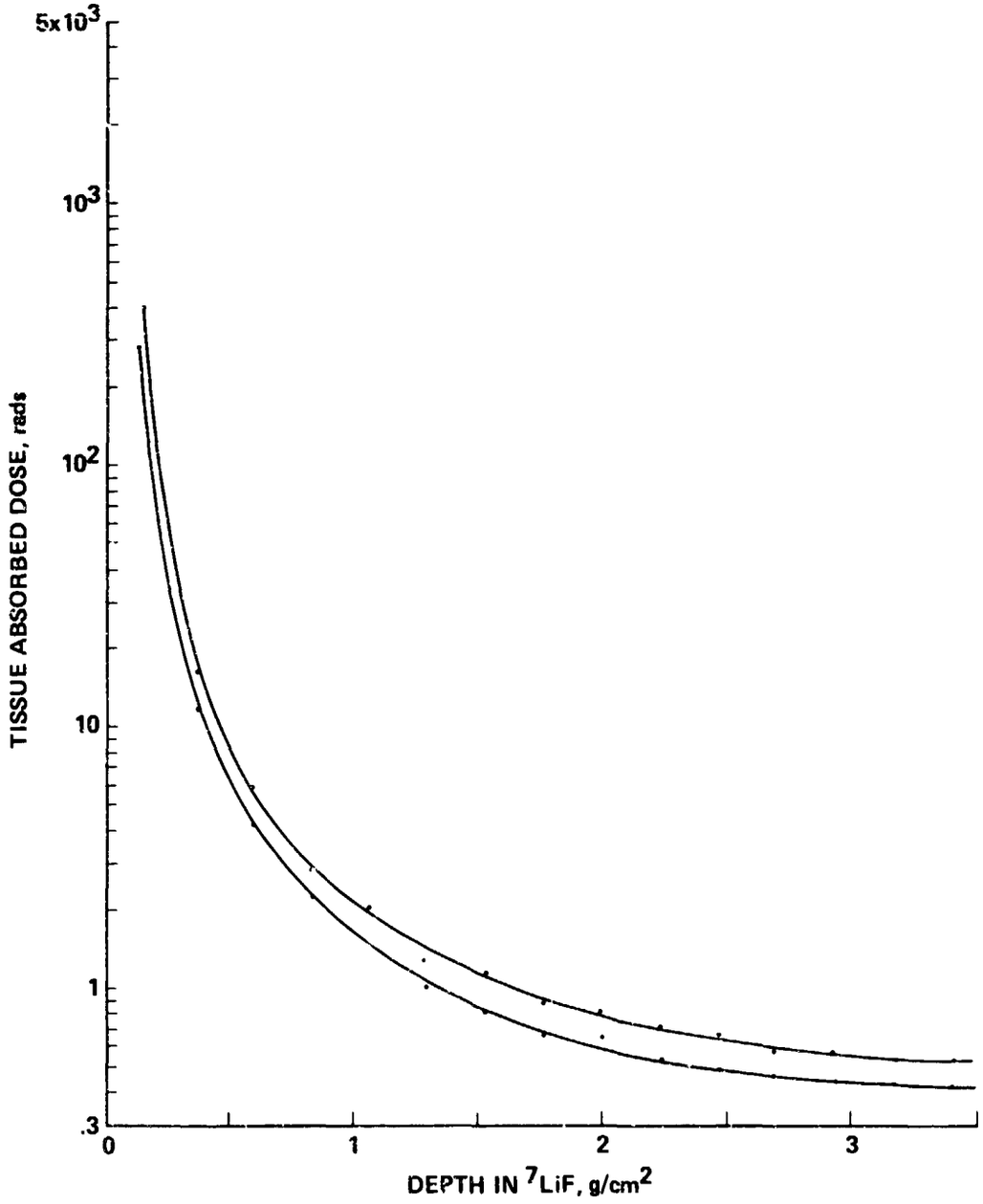

Figure 13: Plots of the depth-dose measurements for TLD stacks 3 from Experiments K-6-25 F1 and F2. Above the ^{7}LiF stacks were double windows of Kapton plastic totaling 15 μm (2.16×10^{-3} g/cm^2).

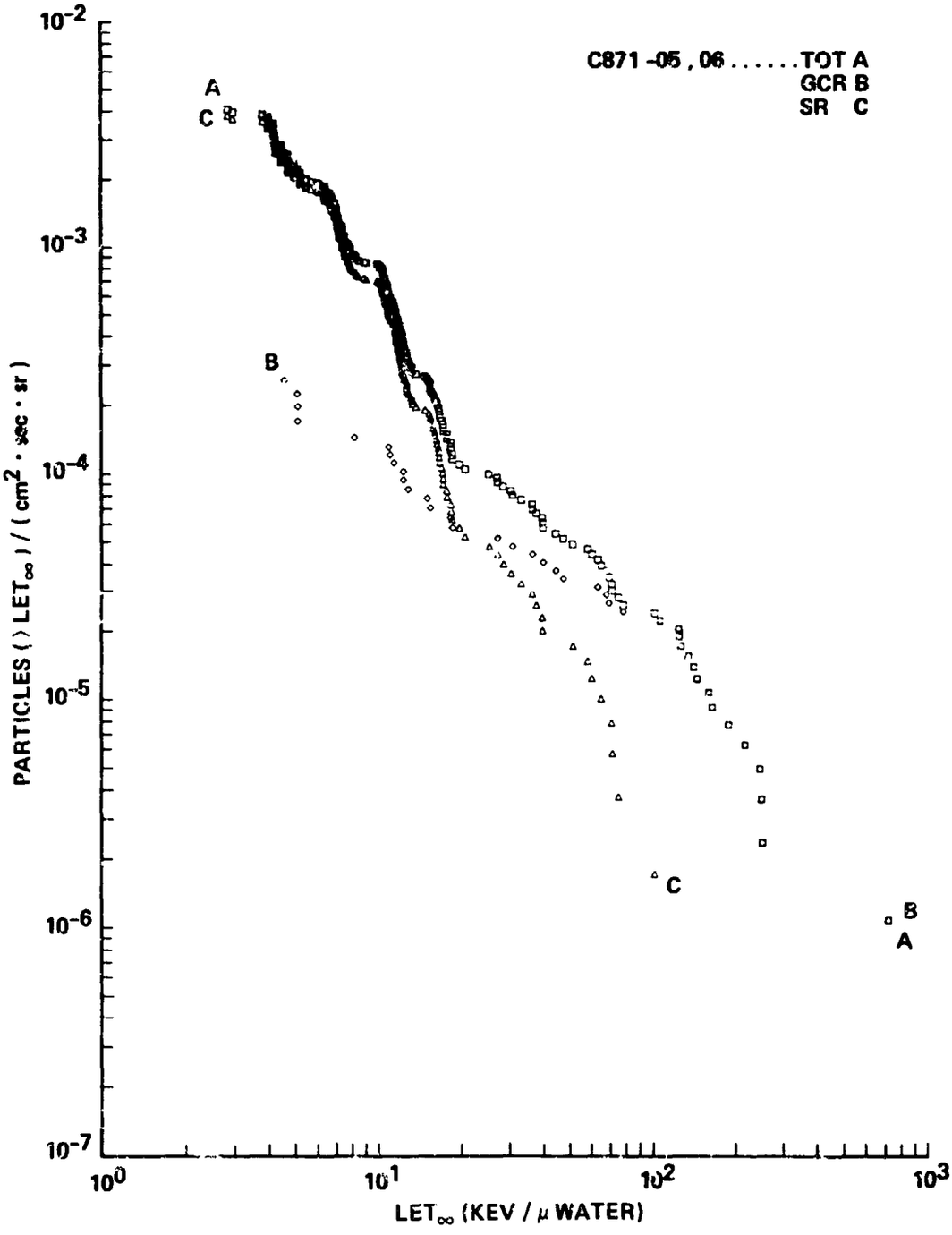

Figure 14: Integral LET flux spectra for Experiment K-6-26 A, PNTD stack F1 (outside the spacecraft). Shielding was 0.195 g/cm^2 of plastic.

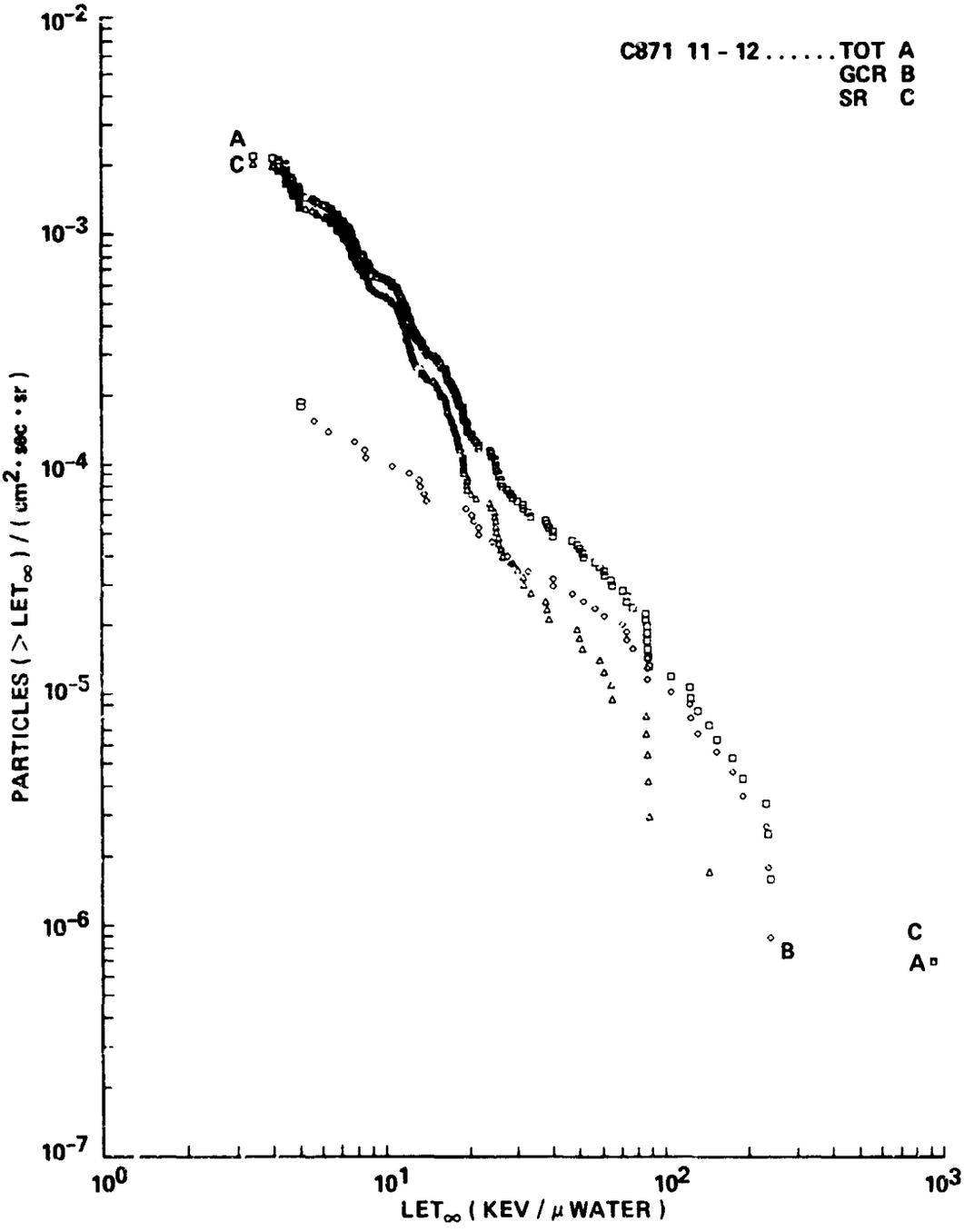

Figure 15: Integral LET flux spectra for Experiment K-6-26 A, PNTD stack F1 (outside the spacecraft). Shielding was 0.436 g/cm^2 of plastic.

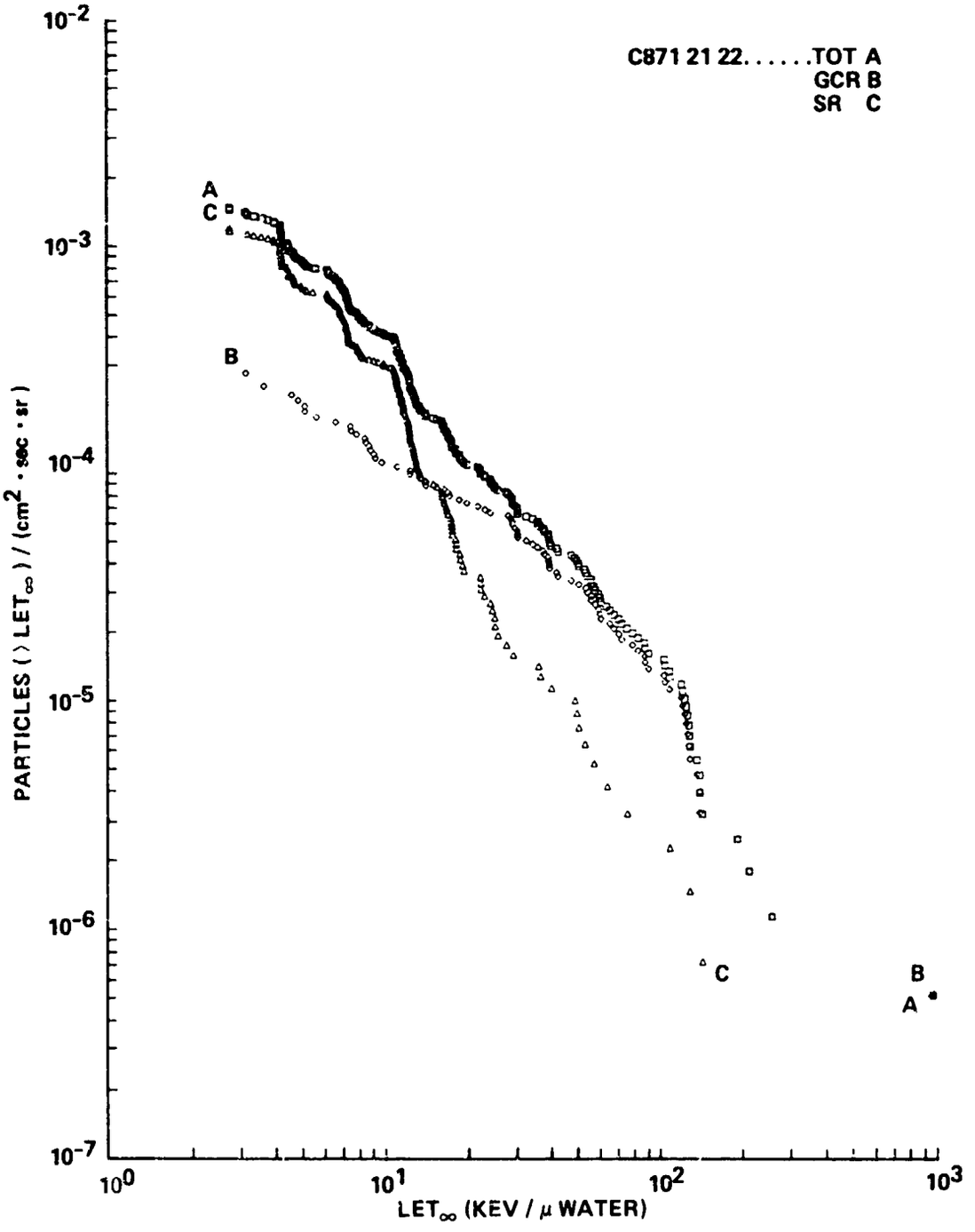

Figure 16: Integral LET flux spectra for Experiment K-6-26 A, PNTD stack F1 (outside the spacecraft). Shielding was 0.762 g/cm^2 of plastic.

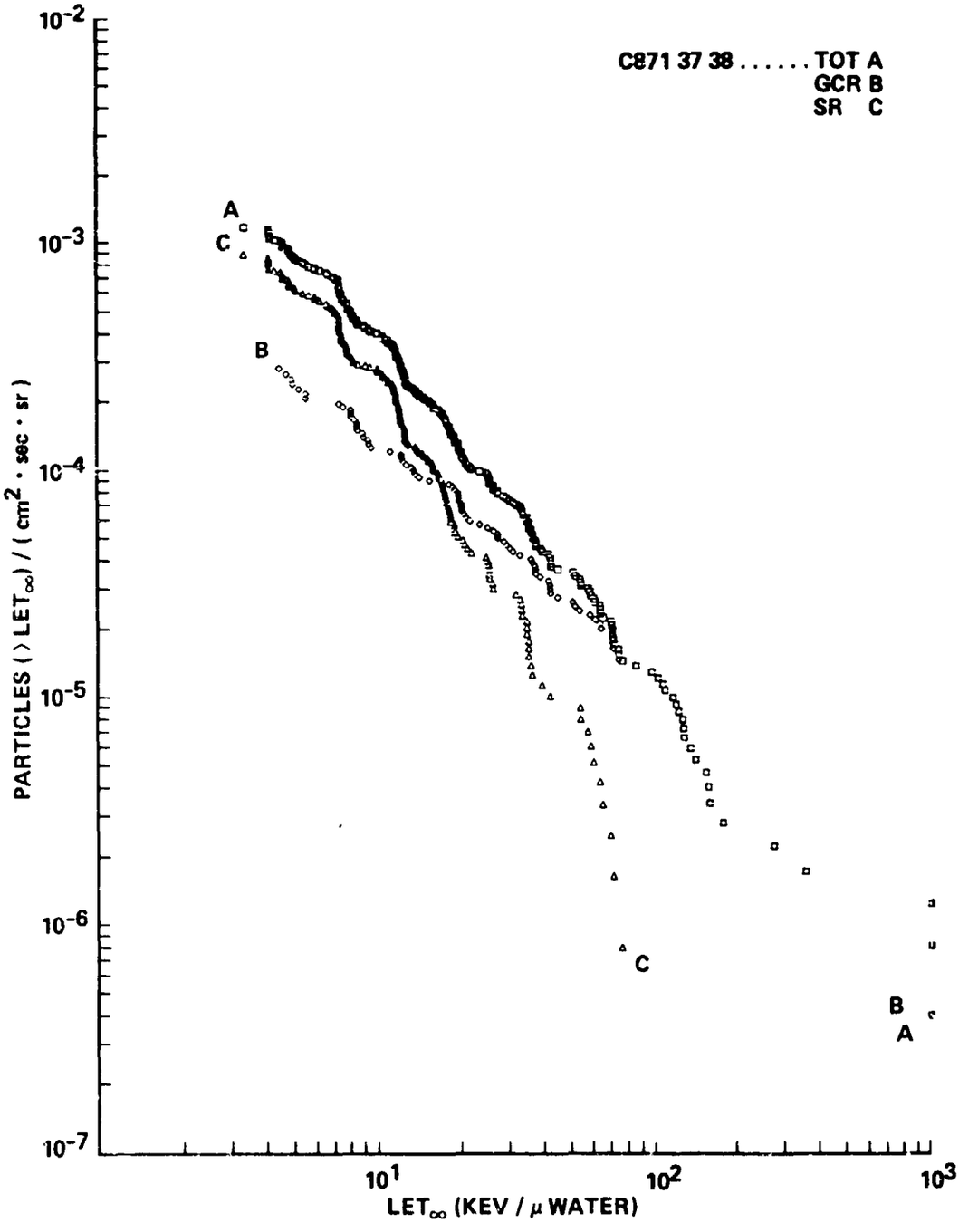

Figure 17: Integral LET flux spectra for Experiment K-6-26 A, PNTD stack F1 (outside the spacecraft). Shielding was 1.33 g/cm^2 of plastic.

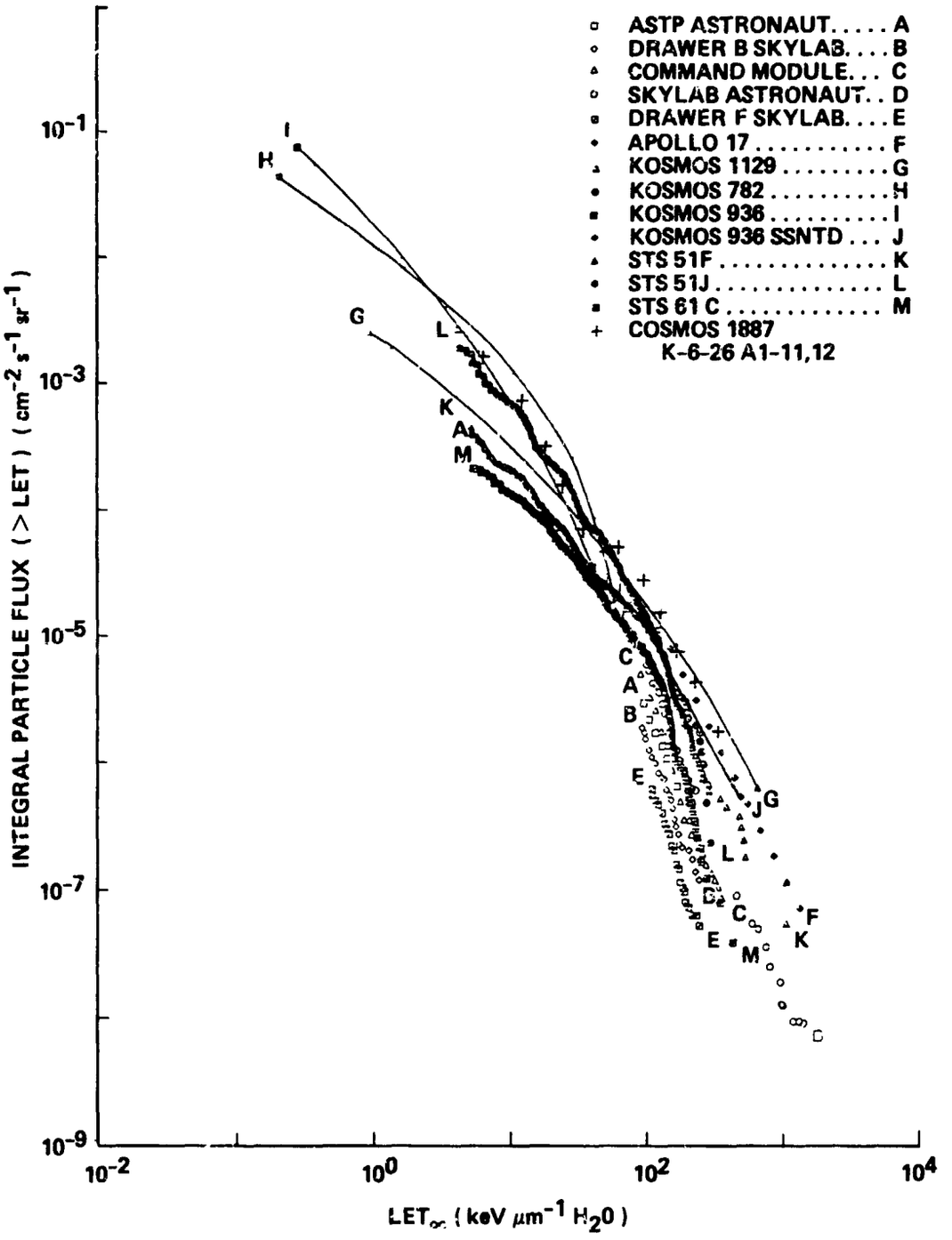

Figure 18: Integral LET spectra showing number of particles as a function of LET_∞ in water for various U.S. and Soviet flights. Not data for Cosmos 1887 (crosses). /Fenton and Parnell, 1988./

N90-26478

EXPERIMENT K-6-27

ANALYSIS OF RADIOGRAPHS AND BIOSAMPLES FROM PRIMATE STUDIES

Principal Investigator:

C. Cann
Department of Radiology
University of California
San Francisco, CA 94143 U.S.A.

Co-Investigators:

A. Rakhmanov
V. Karolkov
Institute of Biomedical Problems
Moscow, U.S.S.R.

PRECEDING PAGE BLANK NOT FILMED

SUMMARY

Serial high-contrast radiographs were obtained of both arms and the right leg of two flight and four control monkeys for the period L-60 to S+16. Longitudinal growth of the tibia, radius and ulna was linear over this period in the control monkeys. In the flight monkey for whom the feeder malfunctioned, there were significant decreases in growth of the long bones. There were also hypermineralized growth arrest lines produced in the distal radial and ulnar metaphyses following resumption of growth. In the other flight monkey, there was a suggestion of decreased long bone growth during flight and immediate postflight periods, but this recovered by the end of the postflight control experiment. There was also an increase in intracortical resorption, indicative of skeletal activation. No major changes in cortical thickness or other parameters were noted, but modification of the techniques to obtain very high quality radiographs in further studies should allow subtle changes in these processes to be quantified.

INTRODUCTION

Previous studies of primate skeletal changes on Cosmos 1514 indicated that a short (5-day) spaceflight may activate the skeleton of juvenile primates causing an increase in bone resorption as indicated by intracortical resorption on high-contrast skeletal radiographs. However, in these early studies no preflight radiographs were available for comparison, so no quantitative changes due to the flight could be determined. The present experiment was designed to study serially the growth and development of the juvenile primate peripheral skeleton and to determine if a 2-week period of spaceflight affected this development. This design was chosen because in the juvenile primate (3-5 kg) the skeleton is still undergoing rapid development at this stage, with longitudinal growth at the unfused metaphyseal-epiphyseal junctions and periosteal and endosteal architectural modeling, providing the possibility to detect an effect of microgravity by a change in the normal rate of growth and modeling. Both quantitative and qualitative parameters were assessed from radiographs of the arms and legs of the monkeys, and will be used in conjunction with single photon absorptiometry of the same limbs obtained by U.S.S.R. investigators to understand the effect of spaceflight on skeletal development.

This investigation included a significant amount of preflight testing and development of optimal radiographic techniques in the U.S.S.R., and serial radiographs of flight candidate, flight, and control monkeys from a period 60 days prior to launch to 2 weeks after the postflight control ("synchronous") experiment.

METHODS AND RESULTS

Technique Development Studies

During the 1 year prior to the launch of Cosmos 1887, U.S. and U.S.S.R. investigators collaborated on a development effort to determine optimal equipment and methods for obtaining high quality radiographs in the primate laboratory in Moscow. In Cosmos 1514, the U.S. had supplied a portable x-ray unit, x-ray film and intensifying screens, and a container to transport the exposed film back to the U.S. for automatic development and analysis. Subsequent to these studies, the institute acquired an x-ray unit of its own and access to x-ray development facilities, and both sides agreed to work to determine if these facilities could be used to obtain the radiographs needed for this study.

In February, 1987, the U.S. and U.S.S.R. investigators inspected the x-ray unit at the institute to determine its characteristics, but because it had not yet been installed it was difficult to determine operating parameters. In addition, the U.S. side suggested that it could supply a portable automatic x-ray processor to be used at the institute for development of the x-rays instead of having to take them to the clinic facilities. Prior studies in Cosmos 1514 had used an x-ray unit with a fixed kilovoltage of 65 kVp, and a primary test was to determine if the U.S.S.R. unit could be used at lower kVp (eg 50-

55 kVp) to improve contrast in the bone radiographs. In addition, the U.S.S.R. unit had variable filtration which might be used to optimize contrast. Initial tests determined that the unit at the institute could be used optimally at 75 kVp, not much different from the point of view of bone-soft tissue contrast than the 65 kVp used previously. However, there were problems with the use of the automatic processor sent to Moscow by the U.S., so it was decided to do one of two procedures: 1) develop the films at the clinic in Moscow, or 2) return the films to the U.S. for processing. The final decision was made to develop the films in Moscow.

Pre and Postflight Radiographs

Radiographs were done on 8 monkeys. Monkeys 1-6 (two flight monkeys and 4 controls) had radiographs taken at L-60, L-30, R + 16, R + 37 and S + 16. The other two controls did not have the last set of x-rays. Films were taken at 75 kVp, 25 mAs, and a focus-film distance of 100 cm, using Kodak Min-R film and a Kodak Min-R Intensifying screen. Four x-rays were taken of each monkey (arms and legs) at each time point in the posterior-anterior (lateral-medial) projection. Films were developed at the clinic in Moscow.

The U.S. received the developed radiographs in February, 1988 when the U.S. specialists visited Moscow. Films of the left and right arms and the right leg were received. The planned analysis of the left leg could not be done because those developed films were reserved by U.S.S.R. investigators for analysis of the EMG implants done in that leg for the muscle studies. A number of films (especially those taken at L-30) were lost in the development process and were unavailable for analysis. In addition, even though aluminum step wedges were included in the exposure of the films, the wide variability in film density precludes any quantitative analysis of bone density. It appears that this variability is due to the development process. Most of the films were of good quality, with a few either overexposed or slightly underexposed, but it is fairly easy to compensate for these exposure differences by viewing with a variable intensity light source. Several films were slightly blurred, due to slight motion of the monkey during the exposure, and in a few cases an arm or leg was rotated slightly in one exposure of the series, so the projected bone was in a different orientation.

The analysis of the radiographs has been done with two approaches, one quantitative and the other qualitative or semi-quantitative. The primary quantitative measurements are bone length and the combined cortical thickness of the bones at 25% and 50% of the length from the distal metaphysis (radius, ulna) or proximal metaphysis (tibia). These data are given in Table 1. The change in length and cortical thickness as a function of time is shown in figures 1-9. In the table and figures, monkey 1 is Drema, monkey 2 is Erosha, and monkeys 3-6 are control animals. The length is measured from metaphysis to metaphysis in each of the bones, so is indicative of growth of the shaft of the long bones. The change in thickness of the cortex at the midshaft can be due to normal periosteal expansion (about 0.2 - 0.4 mm in these animals) as well as a change due to erosion of the endosteal surface as an effect of spaceflight. At the sites closer to the metaphyses (the 25% sites in the table), the periosteal and endosteal surfaces are still undergoing modeling, and this process may be perturbed by flight.

Figures 1a-1c show the cumulative change in length (i.e. growth) from the baseline x-ray at L-60 through the end of the postflight control experiment. For the control monkeys, all three bones are growing at a linear rate, 0.041 ± 0.017, 0.045 ± 0.020, 0,51 ± 0.019 mm/day for the tibia, radiUS and ulna, respectively (mean ± SD). For flight monkey 1 (Drema), longitudinal growth was similar in tibia and radius, with a suggestion that ulnar growth might have been slowed by flight but then increased again so that by the end of the experiment it had reached the same level as the controls. The missing film at L-30 would have been valuable in confirming this. For monkey 2 (Erosha), there was a significant decrease in growth of both tibia and ulna. Toward the end of the postflight period, the rate of growth was the same as in the control monkeys, but the bones remained shorter than would have been expected. Again, the film at L-30 would have allowed quantification of the actual deficit in growth during this period.

Figures 2a-2f show the change in cortical thickness due to the normal modeling process. In the control monkeys, periosteal expansion at the midshaft is 0.2 - 0.4 mm over the experimental period, and the flight monkeys are not different. In general, there is a slight thinning of the cortices as the bones grow and expand, but the changes are quite small. Monkey 2 again shows a distinctly different pattern, especially in the tibia.

Qualitative evaluation of the radiographs included stage of metaphyseal closure, mineralization of the tibial tuberosity, intracortical resorption and endosteal resorption. In the 4 control monkeys, no significant qualitative changes were noted over the experimental period. The tibial tuberosity started to mineralize in monkeys 5 and 6 before L-60 and continued during the experiment. In monkey 4 it was unmineralized at the start, but partially mineralized by S+16; in monkey 3 it was not mineralized at all. In the flight animals, monkey 1 showed continuing mineralization like 5 and 6, while in monkey 2, like monkey 3, it was not mineralized. Other qualitative characteristics included an apparent widening of the fibula medullary canal at the proximal region and increased intracortical resorption in the proximal tibia in monkey 1; this resorption was evident at R+16, still evident at R+37, but starting to resolve at S+16. Monkey 2 did not receive the paste food for most of the flight, and there was a clear response of the skeleton. The radius and ulna each have a clear hypermineralized cement line in the distal metaphysis at R+37 and more clearly at S+16, but which was not evident at R+16. Apparently the deprivation of food slowed down longitudinal growth of the radius and ulna, and when growth started again a hypermineralized junction resulted. This growth arrest line was not evident in the tibial metaphysis, but may have been more subtle at this site.

DISCUSSION

Growth and modeling of the juvenile primate skeleton can be affected by many factors. The monkeys used in these experiments were at a stage in skeletal development where longitudinal bone growth was linear over the 5 month period of the study. Normal modeling at the periosteum and endosteum led to variable cortical thickness changes over the study period, not necessarily the same at each site examined. Metaphyseal closure was not evident in any of the monkeys. Consequently, it would be expected that the stage of mineralization of the cortical bone would be relatively uniform during the experiment. No attempt was made to quantify cortical density from the radiographs obtained, but single photon absorptiometry (SPA) measurements made by U.S.S.R. investigators can be normalized by the periosteal diameter measured on the radiographs to eliminate the variable of bone size from their interpretation of the SPA results.

The initial results from Cosmos 1514 indicated the need for serial radiographs during the preflight, immediate postflight, and control experiment periods to quantify the effects of spaceflight on the dynamics of bone growth. In this experiment, radiographs were obtained at L-60, L-30, R+16, R+37 and S+16 days relative to launch; most films from L-30 were lost due to technical error, and the other films had a wide variation in radiographic density presumably because of variation in the development process. Even with these technical difficulties, the data were sufficient to quantify changes in bone growth. In the one monkey who did not receive paste food for most of the flight, the effect was clear. In the other flight monkey, ulnar growth was apparently slowed but rebounded in the postflight period. The data also show the time delay in skeletal responses, so that even later films (for example, S+37) might provide more information in future studies. The suggestion of intracortical resorption evidenced in monkey 1 at R+16 and R+37 and refilling of these cavities by S+16 supports the initial results of Cosmos 1514, increased activation of the skeleton by spaceflight. However, because radiographic contrast was limited in the current studies, this effect could not be quantified nor could the existence of more subtle changes in other animals be confirmed or denied. A primary focus of further radiographic studies should be reevaluation of the techniques used to obtain films, with an effort to utilize state-of-the-art equipment (for example, microfocus x-ray sources and fine grain film) and careful animal handling and positioning procedures to optimize image quality. This would provide significant improvements in the quality of both quantitative and qualitative analyses, allowing much more subtle effects of spaceflight to be quantified with a high degree of confidence.

Table 1. Quantitative Analysis of Radiographs

		Tibia (R)			Radius (R+L)			Ulna (R+L)		
		Length[a]	CCT(50)[b]	CCT(25)[c]	Length	CCT(50)	CCT(25)	Length	CCT(50)	CCT(25)
#1	1L-60	12.35	5.60	5.50	11.58	4.10	3.45	13.05	4.05	3.25
	R+16	12.75	4.40	4.70	11.90	3.85	3.85	13.40	3.50	3.15
	R+37	12.85	4.20	5.20	12.05	3.85	3.80	13.60	3.65	3.10
	S+16	12.90	4.50	11.60	12.25	3.95	2.90	13.75	3.80	3.15
#2	L-60	11.10	5.10	5.00	9.85	4.25	3.70	11.05	4.50	3.15
	R+16	11.35	4.60	4.30	10.20	4.40	3.40	11.40	4.20	3.00
	R+37	11.45	4.50	3.30	10.30	4.10	3.45	11.48	4.05	3.00
	S+16	11.60	4.30	3.20	10.50	4.35	3.55	11.68	4.10	3.25
#3	L-60	12.25	4.10	3.30	10.88	4.40	4.70	12.28	3.60	3.35
	R+16	12.70	3.80	3.70	11.45	4.00	4.50	12.82	3.25	3.20
	R+37	12.85	4.20	3.90	11.48	3.70	4.30	12.86	3.05	3.10
	S+16	13.05	4.20	4.20	11.72	4.25	4.95f	13.18	3.30	3.05
#4	L-60	11.85	5.70	6.20	10.95	5.05	4.85	12.02	4.30	3.65
	R+16	12.15	5.00	5.30	11.20	4.65	4.15e	12.38	3.95	3.80
	R+37	12.15	5.30	5.20	11.30	4.50	4.50	12.40	4.10	3.60
	S+16	12.25	5.50	5.70	11.42	4.25	4.20e	12.52	4.10	3.80
#5	L-60	11.80	5.50	6.70	11.15	4.35	3.65	12.30	4.25	3.55
	R+16	12.15	5.50	6.50	11.28	4.25	3.35	12.62	3.45	3.15
	R+37	12.25	5.30	6.80	11.38	4.20	3.35	12.78	3.45	3.35
	S+16	12.15	4.50	6.30e	11.48	4.05	3.35	12.78	3.50	3.30
#6	L-60	11.85	6.00	4.00	10.55	4.45	3.80	11.82	3.80	2.85
	R+16	12.20	5.20	3.80	11.07	4.15	4.15	12.40	3.55	2.80
	R+37	12.35	5.40	5.00	11.22	4.30	4.05	12.62	3.50	2.95
	S+16	12.60	5.40	5.00	11.45	4.50	4.35	12.80	3.70	2.80

[a] Length in cm

[b] CCT-combined cortical thickness at midshaft, mm

[c] CCT-combined cortical thickness, 25% of length from distal (radius, ulna) or proximal (tibia) metaphysis, mm

[e] Slightly different projection due to rotation

[f] Focal change in endosteal bone at measured site

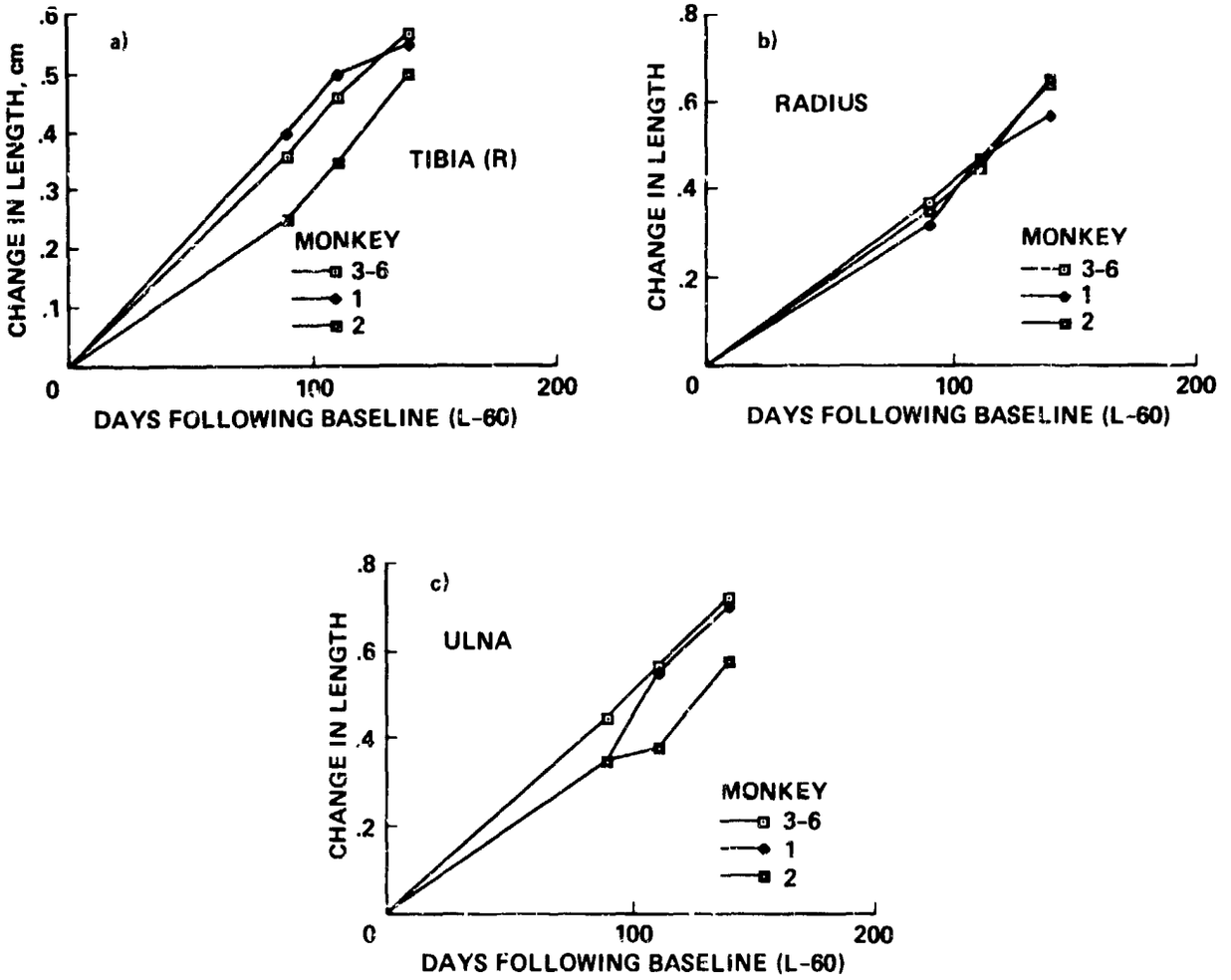

Figure 1. Indicate the cumulative change in length (i.e. growth) from the baseline x-ray at L-60 through the end of the postflight control experiment. For the control monkeys, all three bones are growing at a linear rate, 0.041 ± 0.017, 0.045 ± 0.020, 0,51 ± 0.019 mm/day for the tibia (a), radius (b) and ulna (c). respectively (mean ± SD). For flight monkey 1 (Drema), longitudinal growth was similar in tibia and radius, with a suggestion that ulnar growth might have been slowed by flight but then increased again so that by the end of the experiment it had reached the same level as the controls.

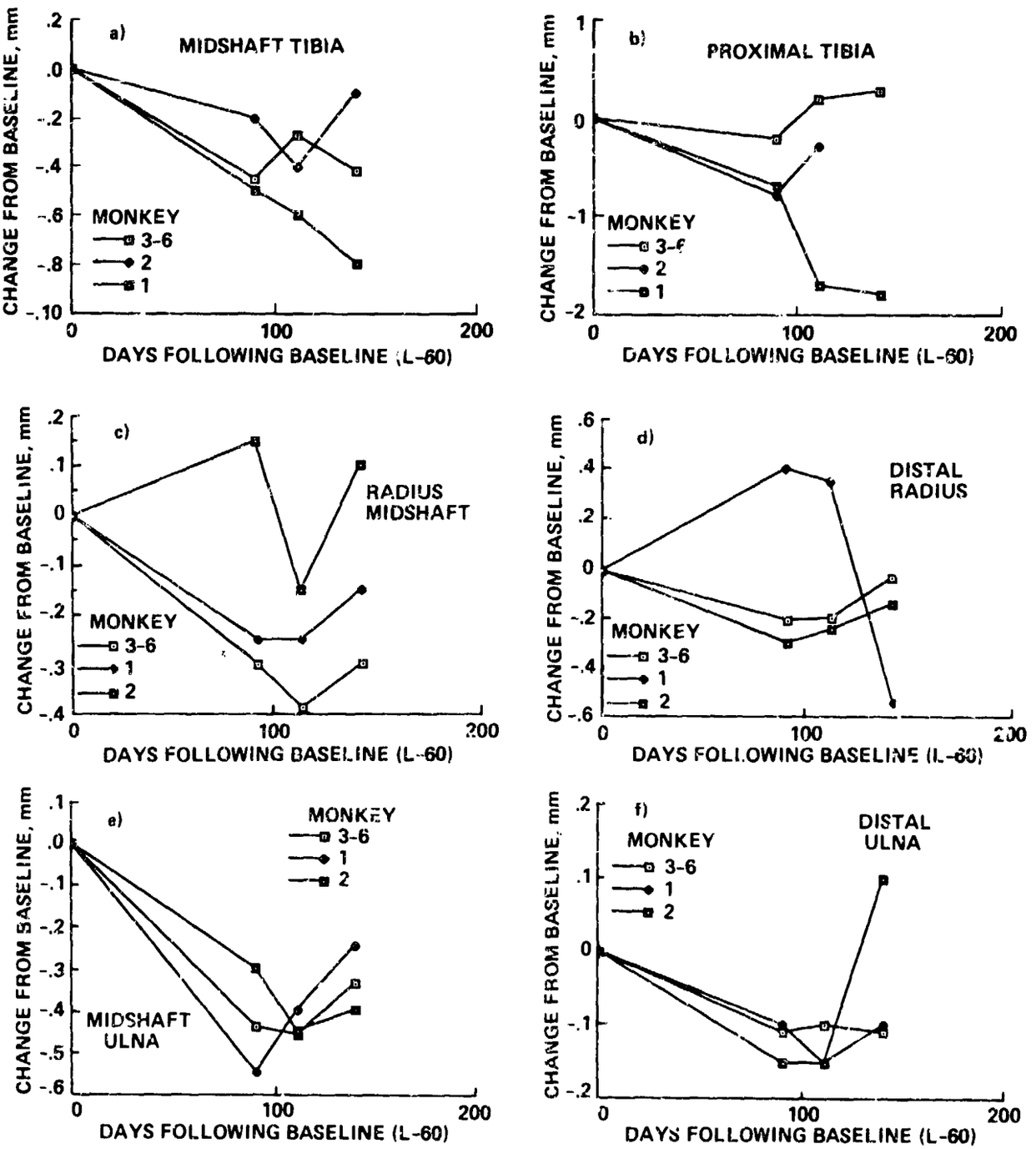

Figure 2. Indicate the change in cortical thickness due to the normal modeling process: (a) midshaft tibia; (b) proximal tibia; (c) radius midshaft; (d) distal radius; e) midshaft ulna; and (f) distal ulna. In the control monkeys, periosteal expansion at the midshaft is 0.2 - 0.4 mm over the experimental period, and the flight monkeys are not different. In general, there is a slight thinning of the cortices as the bones grow and expand, but the changes are quite small. Monkey 2 again shows a distinctly different pattern, especially in the tibia.

NASA

Report Documentation Page

1. Report No.	2. Government Accession No.	3. Recipient's Catalog No.
NASA TM-102254		

4. Title and Subtitle	5. Report Date
Final Reports of the U.S. Experiments Flown on the Soviet Biosatellite Cosmos 1887	February 1990
	6. Performing Organization Code

7. Author(s)	8. Performing Organization Report No.
Editors: James P. Connolly, Richard E. Grindeland, and Rodney W. Ballard	A-90013
	10. Work Unit No. 199-08-12
9. Performing Organization Name and Address	11. Contract or Grant No
Ames Research Center Moffett Field, CA 94035-1000	
	13. Type of Report and Period Covered Technical Memorandum
12. Sponsoring Agency Name and Address	14. Sponsoring Agency Code
National Aeronautics and Space Administration Washington, DC 20546-0001	

15. Supplementary Notes

Point of Contact: James P. Connolly, Ames Research Center, MS 240A-3, Moffett Field, CA 94035-1000
(415) 694-6483 or FTS 464-6483

16. Abstract

Cosmos 1887, a biosatellite containing biological and radiation experiments from the Soviet Union, the United States and seven other countries, was launched on September 29, 1987. One Rhesus monkey's feeder stopped working two days into the flight and a decision was made to terminate the mission after 12 1/2 days. The biosatellite returned to Earth on October 12, 1987. A system malfunction, during the reentry procedure, caused the Cosmos 1887 spacecraft to land approximately 1800 miles beyond the intended landing site and delayed the start of the postflight procedures by approximately 44 hours. Further information on the conditions at landing and postflight activities is included in the Mission Operations portion of this document.

U.S. and U.S.S.R. specialists jointly conducted 26 experiments on this mission, including the postflight transfer of data, hardware and biosamples to the U.S. The U.S. experiments examined the effect of spaceflight on adaptation of the musculoskeletal, nervous, immune, cardiovascular, hepatic and endocrine systems. In addition to the biological experiments, the U.S. placed eight radiation detector packages inside and outside the spacecraft to measure total radiation doses during the flight and to evaluate spacecraft shielding. A description of the Cosmos 1887 mission is presented in this document including preflight, on-orbit, and postflight activities, and Final Science Reports for each of the U.S./U.S.S.R. joint experiments.

17. Key Words (Suggested by Author(s))	18. Distribution Statement
Space biology Microgravity Soviet biosatellite Cosmos 1887 satellite	Unclassified-Unlimited Subject Category - 51

19. Security Classif. (of this report)	20. Security Classif. (of this page)	21. No. of Pages	22 Price
Unclassified	Unclassified	529	A23

NASA FORM 1626 OCT 86

For sale by the National Technical Information Service, Springfield, Virginia 22161